

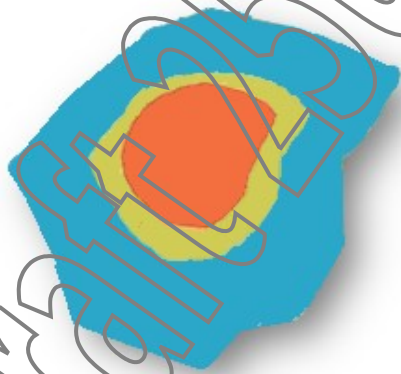
1

2

International Handbook on the Assessment of Odour Exposure using Dispersion Modelling

3

4



Handbook Odour Exposure Modelling

5

6

Olgres.org

7

2023

Public Release

Due date for comments 9th July 2023

Link to send your comments [here](#).

AMIGO

1

11 International Handbook on the Assessment of Odour Exposure using Dispersion Modelling,
12 2023.

14 An initiative of the *International Environmental Society of Odour Managers*, AMIGO (for its
15 acronym in Spanish) and *olores.org*.

16 AMIGO is a non-profit entity dedicated to promoting and disseminating the importance of
17 proper odour management.

18 *Olores.org* is a website owned by *Ambiente et Odora S.A.*, focusing on odour management.

20 **Legal notice**

22 The contents of this publication do not necessarily reflect the official opinions of AMIGO or
23 Olores.org. Neither AMIGO / Olores.org nor any person or company acting on behalf of
24 AMIGO / Olores.org is responsible for the use that may be made of the information
25 contained in this handbook.

27 **Copyright notice**



30 Except where otherwise noted, the content on this document is licensed under a Creative
31 Commons Attribution 4.0 International Public License.

33 Read a summary of the licence here <https://creativecommons.org/licenses/by/4.0/> or access
34 the full licence legal code here <https://creativecommons.org/licenses/by/4.0/legalcode>.

35 Reproduction is authorised, provided the source is acknowledged.

37 Graphics and figures taken from other publications are subject to the copyright of those
38 publications.

40 **Published by:**

41 Asociación Medioambiental Internacional de Gestores del Olor (AMIGO)

42 Uribitarte, 6, 48001, Bilbao, Spain

43 Email: info@gestoresdelolor.org

44 Website: <https://gestoresdelolor.org/index.php/en/>

46 **Citation:**

47 AMIGO & Olores.org (2023) International Handbook on the Assessment of Odour Exposure
48 using Dispersion Modelling. **URL here.**

50 ISBN **XXXXXXXX**

51 ISSN **XXXXXXXX**

52 doi:**XXXXXXXX**

53 Contents

54

55 International Handbook on the Assessment of Odour 56 Exposure using Dispersion Modelling

57

58	Contents	1
59	Acknowledgements	7
60	Foreword	10
61	Introduction	11
62	1. Scope	13
63	2. Terms, Definitions, Abbreviations and Symbols	14
64	2.1 Terms and Definitions	14
65	2.2. Abbreviations and Acronyms	22
66	2.3. Symbols and Units	24
67	3. Meteorology	26
68	3.1 Introduction	26
69	3.2 Meteorological conditions	26
70	3.2.1 Introduction	26
71	3.2.2 Insolation, Surface Heating, and the Energy Budget	27
72	3.2.3 Wind, Turbulence, and Buoyancy	29
73	3.2.4 Development of the Planetary Boundary Layer (PBL)	30
74	3.2.4.1 Mixed (Convective) Layer	31
75	3.2.4.2 The Neutral PBL	32
76	3.2.4.3 Residual Layer	32
77	3.2.4.4 Stable Boundary Layer	32
78	3.2.5 The Concept of Stability Classes	32
79	3.2.6 Time Scale / Meteorological Data Resolution	33
80	3.3 Types of Meteorological Data Sets	34
81	3.3.1. Screening meteorological data	37
82	3.3.2. Observations data sets - ready-made data	37
83	3.3.3. Observations data sets - developing site-specific data sets	38
84	3.3.3.1. Selecting a representative weather station	39
85	3.3.3.2. Selecting a representative vertical profile	39
86	3.3.4. Diagnostic models meteorological data	39
87	3.3.5. Prognostic models meteorological data	40
88	3.4 Meteorological data requirements for key dispersion models used in odour	
89	assessments	42
90	3.4.1. Prognostic Meteorological Models – WRF	44
91	3.4.2. Prognostic Meteorological Model Data – Mesoscale Model Interface Program	
92	(MMIF)	46
93	3.4.3. Screening Meteorological Models – MAKEMET (for AERSCREEN) and ADMS-	

94	SCREEN	47
95	3.4.3.1. MAKEMET	47
96	3.4.3.2. ADMS-SCREEN	48
97	3.4.4. Gaussian Plume Models – AERMOD, ADMS, AODM, ARIA Impact	49
98	3.4.4.1. AERMET for AERMOD	49
99	3.4.4.2. ADMS	53
100	3.4.4.3. AODM	54
101	3.4.4.4. ARIA Impact	55
102	3.4.5. Lagrangian Puff Models – CALPUFF, SCIPUFF	56
103	3.4.5.1. CALMET for CALPUFF	56
104	3.4.5.2. SCIPUFF	58
105	3.4.6. Lagrangian Particle-Puff Model – TAPM	60
106	3.4.7. Lagrangian Particle Models – SPRAY, AUSTAL (LASAT), LAPMOD and	
107	GRAL	60
108	3.4.7.1. SPRAY	60
109	3.4.7.2. AUSTAL / LASAT	61
110	3.4.7.3. LAPMOD	61
111	3.4.7.4. GRAL – The GRAZ Lagrangian Model	62
112	3.5. Meteorological Data Evaluation and Reporting	64
113	3.5.1. Single-Population Data Evaluation	64
114	3.5.2. Technical Approach to Prognostic Model Evaluation	69
115	3.5.3. Operational Evaluation of Surface Fields	70
116	3.5.3.1. Mean Statistics	70
117	3.5.3.2. Difference Statistics	70
118	3.5.3.3. Skill Measures	71
119	3.5.3.4. Benchmarks	72
120	3.5.4. Graphical Evaluation Tools	72
121	3.5.4.1. Time series Plots	73
122	3.5.4.2. Spatial Distribution Plots	73
123	3.5.4.3. Correlation Analysis	75
124	3.5.4.4. Wind Roses	76
125	3.5.4.5. Scatter Plots	77
126	3.5.4.6. Quantile-Quantile Plots	78
127	3.5.4.7. Taylor Diagram	79
128	3.5.5. Conclusion	80
129	3.6. References	81
130	4. Sources and emissions characterisation	87
131	4.1 Introduction	87
132	4.2 Measuring odour emissions	88
133	4.2.1 Point sources	88
134	4.2.1.1. Synthetic description of sampling techniques for point sources	90
135	4.2.2 Active area sources	91
136	4.2.2.1. Synthetic description of sampling techniques for active area sources	91
137	4.2.3 Passive area sources	93
138	4.2.3.1. Synthetic description of sampling techniques for passive area sources	93

139	4.2.4 Volume sources	98
140	4.2.4.1. Synthetic description of estimation techniques for volume sources	99
141	4.2.5 Gas detector tubes	100
142	4.2.6 Emerging methodologies	101
143	4.3 Modelling odour emissions	101
144	4.3.1 Point sources	102
145	4.3.2 Active area sources	104
146	4.3.3 Passive area sources	104
147	4.3.4 Volume sources	106
148	4.3.4.1. Geometrical parameters	106
149	4.3.4.2. Estimation of OER and SOER	107
150	Example 1: Fugitive emissions from refineries or chemical plants	108
151	Example 2: Emissions from livestock buildings	108
152	4.3.5. Temporal variation of emissions	109
153	4.3.6. Future industrial plants	110
154	4.3.7. Uncertainties	110
155	4.4 Ambient air measurements: EN 16841	111
156	4.4.1. Ambient air measurement to characterise odour exposure: grid method	112
157	4.4.2. Ambient air measurement of odours by using the plume method	113
158	4.5 The need for odour emission factors	116
159	4.6 Conclusions	116
160	4.7 References	118
161	5. Dispersion Algorithms	123
162	5.1. Introduction	123
163	5.2. The role of dispersion models in the frame of odour applications	125
164	5.3. General synthetic description of the dispersion algorithms	128
165	5.3.1. Introduction	128
166	5.3.2. Evolution of basic models	128
167	5.3.3. Current form of Gaussian plume models	131
168	5.3.4. Lagrangian models	132
169	5.3.4.1. Overview	132
170	5.3.4.2. Particle vs Puff Lagrangian approach	133
171	5.3.4.3. Particle-Puff Lagrangian approach	136
172	5.3.4.3. Lagrangian models and odour	137
173	5.3.4. Eulerian models	137
174	5.3.5. Computational Fluid Dynamic (CFD) Models	138
175	5.4. Operational existing models	140
176	5.4.1. Introduction	140
177	5.4.2. Screening models – simple models and empirical equations	141
178	5.4.2.1. Screening Models	141
179	5.4.2.2. Empirical Equations for assessing separation distances	145
180	5.4.2.3. Summary	151
181	5.4.3. Steady State Gaussian Plume Models	151
182	5.4.3.1. ARIA Impact	151

183	5.4.3.2. ADMS	152
184	5.4.3.3. AERMOD	154
185	5.4.3.6. Summary	157
186	5.4.4. Lagrangian Puff Models	160
187	5.4.4.1. CALPUFF	160
188	5.4.4.2. SCIPUFF	163
189	5.4.5. Lagrangian Particle Models	163
190	5.4.5.1. AUSTAL	164
191	5.4.5.2. LAPMOD	165
192	5.4.5.3. GRAL	167
193	5.4.5.4. SPRAY	169
194	5.4.5.5. QUIC	169
195	5.4.6. Summary of Lagrangian Puff and Particle Models	170
196	5.4.7. Particle-puff Lagrangian models	173
197	5.4.7.1 TAPM	173
198	5.5. General well-known problems/limitations/solutions	174
199	5.5.1 General introduction	174
200	5.5.2 Gaussian models	174
201	5.5.2.1 Overview	174
202	5.5.2.2 Complex environments where the Gaussian plume model is not	
203	applicable	175
204	5.5.2.2 Light winds, calms and lateral plume meander	177
205	5.5.3 Lagrangian models	182
206	5.5.3.1 Lagrangian puff models	182
207	5.5.3.2 Lagrangian particle models	186
208	5.5.4 Eulerian models	187
209	5.5.4.1 Eulerian grid models	187
210	5.5.4.2 CFD models	187
211	5.6. Which model or type of model is suitable for odours?	188
212	5.6.1 General Introduction	188
213	5.6.2 Key features affecting odour dispersion and model types	188
214	5.6.2.1 Time and space causality effects due to the meteorology, including land	
215	use effects, recirculations, coastal or mount/valley breeze	188
216	5.6.2.2 Spatial characteristics of the surface	188
217	5.6.2.3 Calm winds and mass accumulations	189
218	5.6.2.4 Obstacles/buildings (explicitly simulated or parameterised)	189
219	5.6.2.5 Short-range/ Long range Simulations	189
220	5.7. Model validation in the frame of odour applications	190
221	5.7.1. Examples of validation with odour measurements	192
222	5.7.2. Data from physical modelling experiments	194
223	5.7.3. Data from social participation	194
224	5.7.4. Evaluation of model performances	195
225	5.7.5. Final remarks	196
226	5.8. A window open on the research	196
227	5.8.1. Dissipation of the concentration variance	197

228	5.8.2. Fluctuating plume	198
229	5.8.3. Micromixing model	200
230	5.8.4. Two-Particles Lagrangian Dispersion models	201
231	5.9. A bridge towards the stakeholders	202
232	5.10. References	204
233	6. Output dose-response	221
234	6.1. Introduction	221
235	6.2. The FIDOS factors	222
236	6.2.1 Frequency	222
237	6.2.2 Intensity	224
238	6.2.3. Duration	226
239	6.2.3.1 Fundamentals	226
240	6.2.3.2. Methods for assessing peak concentrations	227
241	6.2.3.3. Methods additionally accounting for the sensitivity of persons	231
242	6.2.4 Offensiveness	232
243	6.2.5. Sensitivity	233
244	6.2.5.1 Measuring sensitivity with Interviews	235
245	6.2.5.2 Measuring sensitivity with Surveys/Questionnaires.	236
246	6.2.5.3 Measuring sensitivity with odour diaries	238
247	6.2.5.4 Measuring sensitivity with an analysis of records of complaints	238
248	6.2.5.5 Measuring sensitivity with citizen science	239
249	6.3. Limitations on dose-response curves	239
250	6.4. A window open to research	240
251	6.5. Conclusions	241
252	6.6. References	241
253	7. Other approaches	247
254	7.1. Introduction	247
255	7.2. Calculating odour emission rate using reverse modelling	247
256	7.2.1 EN 16841 part 2	248
257	7.2.2 EN 17628	251
258	7.2.3 EN 15445	251
259	7.2.4 VDI 3788 part 2	251
260	7.3. Calculating the origin and type of odour sources	252
261	7.3.1 Use of wind data to get preliminary information on the origin and type of a	
262	source	252
263	7.3.1.1 Wind direction	252
264	7.3.1.2 Pollution Roses	253
265	7.3.1.3 Wind speed	256
266	7.3.1.4 Three-variable plots (Ternary plots)	257
267	7.3.1.5 Non-parametric analysis	258
268	7.3.2 Numerical modelling approaches for back-trajectories and backward plumes.	
269		259
270	7.3.3 Source Term Estimation Methods using backward modelling approaches	260
271	7.3.4 Tracing the origin of odour nuisance by integrating citizen-science and	
272	modelling approaches	261

273	7.3.4.1 Tarragona (Spain).	262
274	7.3.4.2. Sicily (Italy)	263
275	7.3.4.3. Israel	264
276	7.4. Calculating odour impact by balancing the hedonic tone of multiple sources	267
277	7.4.1 Example of hedonic tone weighting	270
278	7.5. Calculating odour impact from intermittent sources and non-static receptors	271
279	7.5.1 Calculation of odour exposure by intermittent / discontinuous / seasonal	
280	sources.	271
281	7.7. Online calculation of odour impact	275
282	7.7.1 Real time odour plumes	275
283	7.7.2 Forecasting odour impact	276
284	7.8. Role of electronic olfaction devices to test the performance of odour dispersion	
285	models.	277
286	7.8.1 Evaluation of performance according to EN 16841 part 1	277
287	7.8.2 Evaluation of performance according to EN 16841 part 2	278
288	7.9. References	278
289	8. Reporting	285
290	8.1. Introduction	285
291	8.2. Report structure	285
292	8.2.1 Cover Page	285
293	8.2.2 Introduction	286
294	8.2.3. Regulatory requirements	287
295	8.2.4. Project description	287
296	8.2.4.1. Site location and affected area	288
297	8.2.4.2. Facility, plant, and process description	288
298	8.2.5. Model selection and setup	289
299	8.2.5.1. Dispersion model selection and assumptions	290
300	8.2.5.2. Dispersion model application	290
301	8.2.6. Presentation of the odour impact assessment results	291
302	8.2.6.1. Odour impact assessment criteria - Data elaboration criteria	293
303	8.2.6.2. Criteria for odour exposure maps	294
304	8.2.6.3. Criteria for quantification of odour exposure at receptors	296
305	8.3. References	299
306	Appendix A	301
307	A. Raw meteorological data	301
308	B. AERMOD-ready meteorological data	307
309	C. Geophysical data	310
310	D. Tools	312
311	E. Prognostic Model Information	315
312		
313		

314 Acknowledgements

315 This document was possible thanks to the contribution of over 50 volunteers from all over the world.
316 This work was initially coordinated by Jennifer Barclay (New Zealand) and Günther Schaubberger
317 (Austria), who acted as convenors during the first part of development. Then Jennifer Barclay took the
318 role of the sole convenor.

319 In addition, seven *Task Groups* (TG) were created. Each was assigned a leader/leaders:

- 320 • TG1: Definitions (Imelda Shanahan)
- 321 • TG2: Meteorology (Christelle Escoffier / Jennifer Barclay/ Loren Trick)
- 322 • TG3: Emissions and source characterisation (Andrew Balch / Roberto Bellasio)
- 323 • TG4: Dispersion algorithm (Giuseppe Brusasca / Gianni Tinarelli)
- 324 • TG5: Output dose-response (Rodrigo Rosales)
- 325 • TG6: Reporting (initially Tiziano Zarra / Giusy Oliva, later replaced by Silvia Trini Castelli/
326 Geordie Galvin)
- 327 • TG7: Other approaches (Carlos Nietzsche Diaz)

328 Monthly meetings were held online on the last Thursday of each month at alternative times separated
329 by 12 hours to have a more equitable distribution of time slots for volunteers from different time zones.
330 The first meeting took place on the 27th of August, 2020. The first draft was ready for comments on
331 the 30th of June, 2022. The second draft was prepared for comments on the 25th of May, 2023 The
332 final version was released on **XX/XX/XXXX**.

333 This handbook is here thanks to the active contributions of these volunteers (in alphabetic order):

Name	Company \ Research Institute	Country
Andrew Balch	Air Environment	Australia
Carlos Nietzsche Diaz	Ambiente et Odora	Spain
Christelle Escoffier	Wood Environment & Infrastructure Solutions the United Kingdom,	UK
Dietmar Öttl	Dept Housing, Energy, Tech.of the Gov. Styria	Austria
Emmanuelle Duthier	Numtech France,	France
Eva Berbekar	Uppenkamp + Partner, Germany	Germany
Geordie Galvin	Astute Environmental Consulting Pty Ltd	Australia
Gianni Tinarelli	Arianet	Italy

18 *Leave your comments on this draft [here](#). Due date 9th July 2023*

Giuseppe Brusasca	Arianet	Italy
Giusy Oliva	University of Salerno	Italy
Günther Schauburger	University of Veterinary Medicine	Austria
Heike Hauschildt	Olfasense GmbH	Germany
Helga Lauerbach	Lohmeyer	Germany
Hellen Arichábala	IKANI S.A.	Ecuador
Imelda Shanahan	TMS Environment Ltd	Ireland
Jean-Michel Guillot	IMT Mines Ales France	France
Jennifer Barclay	Atmospheric Science Global Ltd	New Zealand
Laura Hinderink	Uppenkamp + Partner, Germany	Germany
Loren Trick	LT Environmental LLC	USA
Osnat Yosef	Ministry of Environment of Israel	Israel
Phyllis Diosey	Hazen and Sawyer United States of America,	USA
Roberto Bellasio	Enviroware srl	Italy
Rodrigo Rosales	Environmental Assessment Service of Chile,	Chile
Rossella Prandi	Simularia	Italy
Silvia Trini Castelli	CNR-ISAC (National Council for Research)	Italy
Tiziano Zarra	Università degli Studi di Salerno	Italy

334

335 Other experts and consultants that were part of this group, and who participated in
336 meetings and discussions during the preparation of the Handbook included the following:

Andrea Peña	Environmental Assessment Service of Chile	Chile
Andrea Rossi	Progress SRL.	Italy
Angie Wanger	Trinity Consultants	USA

20 *Leave your comments on this draft [here](#). Due date 9th July 2023*

Catalina Pérez	Environmental Assessment Service of Chile,	Chile
Claudio Dipietro	Progress SRL	Italy
Constanza Fariña	Variable Ambiental	Chile
Débora Lia Perazzoli	Envex	Brazil
Dov Skibin	Ministry of Environment	Israel
Eric Concepción	Ceimic	Peru
Hélène Piet Sarnet	Egis Group France,	France
Hugo van Belois	NEN Commission on odour	Netherlands
Jerome Godart	Atmo Normandie France,	France
Kenny K M Lok	EnviPro Technology Company Limited, China,	China
Laura Capelli	University Politecnico di Milano, Italy,	Italy
Luis Diaz	Particulas Chile,	Chile
Manuel Santiago	Advisian Spain,	Spain
Martí de Riquer	Meteosim	Spain
Nick Jones	Olfasense	UK
Oliver Olang	Element Qatar,	Qatar
Rafael Geha	Ambiental RB,	Brazil
Rebecca Kavanagh	Ambiente et Odora	Spain
Roberto Sozzi	Independent Scientific Consultant	Italy
Sarveshkumar Sharma	Indian Institute of Technology Bombay,	India
Valérie Nastasi	Suez	France

337

338

339 Foreword

340 This document has been prepared by a group of experts under the umbrella of the website olores.org
341 and the *International Environmental Society of Odour Managers* (AMIGO, for its acronym in Spanish).

342 This handbook shall be given the status of an international document. That means that the authors
343 have tried to include as many international references as possible while striving to create a valuable
344 worldwide handbook.

345

346 Introduction

347 Odour issues are currently one of the major causes of environmental grievances worldwide and, in
348 some countries, are routinely the cause of most environmental complaints to regulatory authorities
349 (Schusterman, 1992; Kaye & Jiang, 2000). There continue to be multiple reasons for the prominence
350 of odour complaints, including an unrelenting urban expansion of residential areas into land-use areas
351 once predominantly agricultural with few largely isolated facilities; increases in facility operations and
352 their size; increasingly higher aesthetic, and environmental expectations of citizens, who are less
353 familiar and tolerant of odours than in the past, and concerns over potential health risks from airborne
354 odorous substances.

355 In most countries, environmental regulations cover the most common air pollutants, including NO₂ or
356 SO₂. The criterion is based on the occurrence of health effects following short- and/or long-term
357 exposure to the contaminants. There is slight health risk variation between jurisdictions, states, and
358 countries. However, odour regulation tends to be much more varied across a broad spectrum: from
359 having little to no specific mention in environmental legislation to extensive and rigid requirements that
360 include a combination of odour source testing, odour dispersion modelling, ambient odour monitoring,
361 setback distances, process operations, and odour control procedures. Odour legislation can be highly
362 variable from one country to the next, and it can also be highly variable from one jurisdiction to the
363 next within the same country (Bokowa et al., 2021).

364 For regulatory purposes, much of the focus of attention in the last couple of decades has been on
365 establishing odour guidelines in the hope of bringing consistency to the control and regulation of
366 odours. With the focus on setting rules, less effort has been spent in a variety of jurisdictions on
367 assessing the best tools suited for the computation of odour impacts concerning accurate emission
368 rates, source characterisation, and the critical role of local meteorology, interpretation of modelled
369 results, or the suitability and applicability of one dispersion model over another. The handbook
370 addresses several key issues central to the theme of effective management and odour regulation.

371 This handbook is a collaborative work by more than 50 international odour experts from seventeen
372 countries, including; Australia, Austria, Belgium, Brazil, Chile, China, Ecuador, France, Germany,
373 Ireland, Italy, New Zealand, Peru, Qatar, Spain, United Kingdom and the United States of America.

374 Experts within this group met monthly in 2020, 2021, 2022 and 2023 via teleconference to discuss
375 different aspects of this work. Six special Task Groups (TGs) were initially created. Later a further TG
376 was also created to deal with all aspects not included in previous chapters. Each task group had
377 between 5 and 10 members responsible for writing and reviewing individual sections within each task
378 group. The task groups were the following:

- 379 ● TG1 - Definitions;
- 380 ● TG2 - Meteorology;
- 381 ● TG3 - Emissions and Source characterisation;
- 382 ● TG4 - Dispersion Algorithms;

26 *Leave your comments on this draft [here](#). Due date 9th July 2023*

- 383 • TG5 - Output dose-response;
- 384 • TG6 - Reporting;
- 385 • TG7 - Other approaches.

386 The structure of this handbook follows more or less the division of TGs. The exception is TG7, which
387 has been located after TG5, leaving TG6 reporting as the last.

388

389 This handbook on odour dispersion modelling aims to guide the use of dispersion modelling of
390 odours.

391 1. Scope

392 This handbook presents different aspects needed for evaluating odour exposure by using
393 dispersion modelling to help the final user. This handbook applies to

394

- 395 ● calculating the odour/odorant level in ambient air from odour emission sources;
- 396 ● choosing appropriate odour models depending on a project's specific conditions, in
397 particular, dealing with complex situations;
- 398 ● selecting appropriate meteorology.
- 399 ● understanding the dose-response criteria and how the Frequency-Intensity-Duration-
400 Offensiveness-Sensitivity scheme fits in a result; and
- 401 ● the preparation of an odour report based on the results of a model.

402 2. Terms, Definitions, Abbreviations and Symbols

403 2.1 Terms and Definitions

404

405 **ADMS**

406 Atmospheric Dispersion Modelling System developed by Cambridge Environmental
407 Research Consultants (CERC) in the United Kingdom and approved as the regulatory model
408 in some countries.

409

410 **AERMAP**

411 AERMOD program geophysical processor.

412

413 **AERMET**

414 AERMOD program meteorological processor.

415

416 **AERMIC**

417 American Meteorological Society Environmental Protection Agency Regulatory Model
418 Improvement Committee.

419

420 **AERMINUTE**

421 Meteorological processor to re-process the ASOS 1 and 5-minute data.

422

423 **AERMOD**

424 A steady state Gaussian US EPA regulatory plume dispersion model.

425

426 **AERSCREEN**

427 US EPA guideline model for screening applications. Includes many of the AERMOD
428 algorithms.

429

430 **Albedo**

431 is the amount of solar radiation reflected by some surface and is often expressed as a
432 percentage or a decimal value. Overall, albedo is a measure of the reflectivity of the surface
433 of the Earth.

434

435 **AMS**

436 Measuring system permanently installed on-site for continuous monitoring of emissions or
437 measurement of peripheral parameters.

438

439 **Annoyance**

440 The complex human reactions that occur as a result of immediate exposure to an ambient
441 stressor (odour) that, once perceived, causes negative cognitive appraisal that requires a
442 degree of coping.

443 NOTE: Annoyance may or may not lead to 'nuisance' and a complaint action.

444

445 **AODM**

446 Gaussian plume model. Austrian regulatory odour model.

447

448 **AQMG**

449 US Air Quality Management Group.

450

451 **ARIA Impact**

452 Gaussian plume model developed by ARIA Technologies, France and also used in other
453 countries.

454
455 **ARW**

456 Advanced Research Weather and Forecast Model.

457
458 **Atmospheric Stability**

459 Atmospheric stability is a measure of the tendency for air to move vertically. The dominant
460 influences on this vertical movement are atmospheric temperature and pressure.

461
462 **AUSPLUME**

463 Gaussian plume model developed by EPA of the Australian State of Victoria. AERMOD
464 replaced AUSPLUME in January 2014.

465
466 **AUSTAL**

467 The official German Federal Environmental Agency regulatory model. AUSTAL (formerly
468 AUSTAL2000 or AUSTAL2000g) is a Lagrangian particle model. Based on the LASAT
469 model.

470
471 **Back-trajectory**

472 Back-in-time trajectory of an airborne parcel.

473
474 **Bowen Ratio**

475 The ratio of sensible heat flux to latent heat flux densities.

476
477 **BPIPPRM**

478 BPIPPRM is a standalone program that should be used to prepare Building Downwash data
479 for dispersion models.

480
481 **CALMET**

482 Diagnostic Meteorological Model.

483
484 **CALPUFF**

485 Lagrangian Puff Dispersion Model.

486
487 **CALPOST**

488 Post processing program of CALPUFF.

489
490 **CFD**

491 Computational Fluid Dynamic Models (example models are WRF-CFD, OpenFOAM,
492 Code_Saturne, FLOW-3D, FLUENT).

493
494 **Copernicus**

495 The European Union's Earth Observation Programme implemented by ECMWF

496
497 **COSMO**

498 A group of meteorological and military services within Europe and Russia who have
499 developed and maintain the NWP model COSMO

500
501 **CTDMPLUS**

502 A US EPA Complex Terrain steady-state Gaussian plume model. Developed for convective
503 conditions. It is a refined Gaussian plume model.

504
505 **CTSCREEN**

506 Screening version model of CTDMPPLUS.

507

508 **Duration**

509 The duration of the odour occurrence is how long an individual is exposed to odour in the
510 ambient environment.

511

512 **ECMWF**

513 ECMWF is the European Centre for Medium-Range Weather Forecasts, producing global
514 numerical weather predictions and other data for their Member and Co-operating States and
515 the broader community. ECMWF is an independent intergovernmental organisation
516 supported by 35 states.

517

518 **EQs**

519 Empirical Equations. Screening methods with regulatory status used in Europe to determine
520 separation distances.

521

522 **EPA**

523 Environmental Protection Authority. Used in the general term to apply to more than one
524 country.

525

526 **ETA levels**

527 ETA (greek letter η) is a vertical coordinate for atmospheric models, defined with a steplike
528 representation of topography, with mountains formed of the model's grid boxes. The vertical
529 coordinate surfaces are quasi-horizontal, intersecting model mountains or forming their
530 nearly horizontal upper sides.

531

532 **Eulerian Models**

533 Eulerian models are based on the observation of the atmospheric motion at a specific
534 location in space while time passes. "Location" must not be intended as a point but as a
535 volume of the atmosphere. Eulerian models discretise the simulation domain with volume
536 grids and solve the conservation equations within each volume.

537

538 **European odour unit**

539 The amount of odorant(s) that, when evaporated into one cubic metre of neutral gas at
540 standard conditions, elicits a physiological response from a panel (detection threshold)
541 equivalent to that elicited by one European Reference Odour Mass (EROM), evaporated in
542 $1 \text{ m}^{\text{Acce}}$ of neutral gas at standard conditions.

543

544 **FLEXPART**

545 Lagrangian particle model used in Austria / Germany / Norway. Developed at BOKU Vienna,
546 the Technical University of Munich and NILU.

547

548 **Frequency**

549 The frequency of the odour occurrence is how often an individual is exposed to odour in the
550 ambient environment.

551

552 **Gas Detector Tube**

553 Gas detector tubes are sealed glass tubes containing reactive chemicals coated onto solid
554 materials. The chemicals change colour when the target substances are present in the test
555 gases and the extent of the colour change is proportional to the concentration of the target
556 analyte.

557

558 **Gaussian Models**

559 Under certain idealised conditions (homogeneous turbulence, constant wind direction and
560 speed), the mean concentration of a pollutant emitted by a point source has a Gaussian
561 distribution. The atmospheric dispersion models based on this approach are called Gaussian
562 models.

563

564 **GFS**

565 GFS (Global Forecasting System) is a global numerical weather prediction system
566 containing a global computer model and variational analysis run by the United States
567 National Weather Service (NWS).

568

569 **GRAL**

570 The GRAZ Lagrangian particle model. Developed at GRAZ University of Technology and the
571 Regional Governments of Styria and Tyrol, Austria.

572

573 **GRAMM**

574 Prognostic mesoscale model used as a wind field model in GRAL.

575 **Harmonie**

576 A NWP forecast system operated at 2.5km horizontal resolution over a domain that covers
577 Iceland and the surrounding seas. HARMONIE is the abbreviation from HIRLAM-ALADIN
578 Research on Mesoscale Operational NWP In Europmed (in this case Euromed is itself an
579 abbreviation of European-Mediterranean, and ALADIN is A Limited Area Dynamic
580 International model)

581 **Hedonic (odour) tone**

582 Hedonic tone is a property of an odour related to its pleasantness. It is assessed in a
583 classificatory testing process and usually varies between “extremely pleasant” and
584 “extremely unpleasant”.

585

586 **HIRLAM**

587 A NWP forecast system developed by the international HIRLAM programme, a cooperation
588 of European meteorological services.

589

590 **HRRR**

591 A NWP model operated by NCEP over North America with a 3km resolution, radar data
592 assimilation every 15 minutes and a complete data refresh every hour.

593

594 **Humidity**

595 General term related to the amount of water vapour in the air.

596

597 **IFS**

598 A global numerical weather prediction system developed and maintained by ECMWF

599

600 **Intensity**

601 How strong an odour is perceived to be. Odour intensity describes the relative magnitude of
602 an odour sensation as experienced by a person.

603

604 **Intermittent sources**

605 Sources that produce short-term peaks in odorant emissions at a particular time of the day
606 (for example, because of loading/unloading or cleaning operations).

607

608 **Instrumental Odour Monitoring Systems (IOMS)**

609 Instrumental Odour Monitoring Systems (also known as e-noses) are electronic devices with
610 different types of sensors that can carry out either of the three necessary functions to identify
611 odour in ambient air: presence-absence, classification and measurement.

612

613 **ISCST3**

614 Industrial Source Complex Short-Term Model. Steady State Gaussian plume model that was
615 the US EPA near field regulatory model until it was superseded by AERMOD and phased
616 out in 2006.

617

618 **Klug-Manier**

619 A German stability classification system based on wind speed and cloud cover.

620

621 **LAPMOD**

622 Lagrangian Particle Model developed by Enviroware. The model is part of ARIES, the official
623 Italian modelling system for nuclear emergencies operated by ISPRA and the EPA of Emilia-
624 Romagna, Italy.

625

626 **LASAT**

627 Lagrangian particle model, developed by Ingenieurburo Janicke Gesellschaft fur
628 Umweltphysik.

629

630 **Lagrangian Model**

631 Lagrangian models are based on tracking each small portion (e.g., particles) of the
632 atmospheric flow as it moves while time passes. Atmospheric Lagrangian models determine
633 the position of each particle and its properties (e.g., associated mass) as a function of time.

634

635 **Leak Detection and Repair (LDAR)**

636 Leak detection and repair is the process of identifying leaking equipment and repairing
637 it to minimise emissions.

638

639 **LOWWIND**

640 AERMOD low wind options.

641

642 **MAKEMET**

643 A program that interfaces with AERSCREEN to generate a site-specific matrix of screening
644 meteorological conditions for input into AERMOD.

645

646 **MMIF**

647 Mesoscale Model Interface Program developed by US EPA that converts prognostic
648 meteorological model output fields to the parameters and formats required for direct input
649 into dispersion models.

650

651 **MM5**

652 Penn State University (PSU) / National Centre for Atmospheric Research (NCAR)
653 Mesoscale Model, now superseded by Weather Research and Forecasting (WRF) Model.

654

655 **Mixing height**

656 Height of the layer adjacent to the ground over which an emitted or entrained inert non-
657 buoyant tracer will be mixed (by turbulence) within a time scale of about one hour or less.

658

659 **NAM**

660 A NWP model operated by NCEP that generates multiple grids over North America.

661

662 **Non-static receptors**

663 Receptors that are not continuously at a certain point. For example, people returning from
664 work at a particular hour or tourist locations that get occupied during a certain period of the
665 year.

666
667 **Nuisance**

668 Nuisance is the cumulative effect on a person or group of people caused by repeated events
669 of annoyance over an extended period, leading to modified or altered behaviour.

670
671 Definition adapted from *Van Harreveld, A.P.: From odourant formation to nuisance: new*
672 *definitions for discussing a complex process, Water Science & Technology 44:9-15 (2001)*

673
674 **Odour Concentration**

675 The concentration of an odourant mixture is defined as the dilution factor to be applied to an
676 effluent to be no longer perceived as odourant by 50% of people in a population sample. By
677 definition, the odour concentration at the detection limit is 1 ou_E/m³.

678
679 **Odour Impact Assessment (OIA)**

680 Odour impact assessment is the process of qualitatively and / or quantitatively assessing the
681 impact of odour emissions on a neighbourhood or receptor.

682
683 **Odour unit**

684 Odour concentration of an odorous sample at the odour threshold. Any odour unit measured
685 outside of the scope of EN 13725.

686
687 Note: Any measurement carried out in Europe before 2002 (date of first EN 13725) measured “odour units”
688 instead of “European odour units”. p.e with a different flow and velocity of odorous air emanating from the ports,
689 with a number lower than four assessors, or with no methodology to evaluate the performance of assessors
690 before a measurement.

691
692 **Odour emission rate (OER) / Odour flow rate**

693 Quantity of odour units which cross a given surface per unit of time.

694
695 **ÖNORM**

696 A standard published by Austrian Standards International, the Austrian member of the
697 European Committee for Standardisation (CEN) and the International Organisation for
698 Standardisation (ISO).

699
700 **Offensiveness**

701 The character relates to the ‘hedonic tone’ of the odour, which may be pleasant, neutral or
702 unpleasant.

703
704 **PMSS**

705 PMSS (Parallel Micro Swift and Spray) is the parallel version of the SPRAY Lagrangian
706 Particle Dispersion Model, able to run also at the microscale at the level of street canyons,
707 explicitly considering the presence of buildings and their effects on the mean flow,
708 turbulence and dispersion”

709
710 **Particle-puff Approach**

711 A simplification of a three dimensional Lagrangian Particle method mixing a Puff approach
712 (typically in the horizontal) and the solution of a Langevin equation (typically in the vertical)
713 to describe the dispersion of a plume

714
715 **Pasquill-Gifford**

716 A stability classification system based on wind speed, cloud cover, and ceiling height.

717

718 **Peak-to-Mean**

719 Is the ratio between the short-term and long-term odour concentration. Short-term usually
720 refers to a few seconds up to a few minutes, while long-term refers mostly to one hour.

721

722 **PRIME**

723 Building downwash algorithm whose development was funded by EPRI, the US Electric
724 Power Research Institute.

725

726 **Receptor**

727 Location where odour concentration is measured or computed.

728

729 **QUIC**

730 The QUIC (Quick Urban & Industrial Complex) dispersion modelling system is a fast
731 response urban dispersion model including a 3D wind field model called QUIC-URB, a
732 transport and dispersion Lagrangian particle model called QUIC-PLUME, a pressure solver,
733 QUIC-PRESSURE, and a graphical user interface called QUIC-GUI. QUIC is developed by
734 the Lawrence Livermore National Laboratory, USA.

735

736 **RASS**

737 A radio acoustic sounding system which remotely measures temperature profiles in the
738 atmosphere up to an average altitude of 1,000 metres.

739

740 **Sensitive receptor**

741 Sensitive receptors are receptor locations in the odour study area where routine or normal
742 activities could experience adverse effect(s) from odour discharges from a facility. They
743 include private residences, apartment houses, and other distinct residential areas, hospitals,
744 nursing homes, rehabilitation facilities, schools and daycare facilities; public gathering
745 centres, including public plazas and shopping centres; outdoor recreational public places,
746 such as parks, playgrounds, campgrounds, and trailer parks. Office spaces and other
747 external workspaces may also be considered sensitive receptors. Professional judgement
748 should be applied to assess which receptors are the most sensitive for a specific study.

749

750 **Sensitivity**

751 Sensation and emotional responses by individuals to an odorous atmosphere at one time of
752 their daylife/life and the location where the odour is perceived.

753

754 **SODAR**

755 A sonic distance and ranging system which remotely measures a vertical profile of wind
756 speed, direction, thermal stratification and turbulence parameters up to an average altitude
757 of 3,000 metres.

758

759 **Sonic anemometer**

760 Instrument that measures components of the wind vector by determining the effect of the
761 wind on transit times of acoustic pulses transmitted in opposite directions across known
762 paths. Wind speed will increase or decrease the speed of sound depending on whether it is
763 a tailwind or a headwind. Measuring the speed of sound in both directions along that one
764 axis allows the wind speed to be calculated. A two-axis or three-axis sensor can then be
765 used to calculate horizontal or horizontal plus vertical wind speed and wind direction.

766

767 **SCICHEM**

768 The SCIPUFF model expanded to include the treatment of gas- and aqueous-phase
769 chemical reactions and aerosol thermodynamics.

770

771 **SCIPUFF**

772 SCIPUFF (Second-order Closure Integrated PUFF model) is a time-dependent Gaussian

773 puff dispersion model that employs second-order closure turbulence modelling techniques to
774 relate the dispersion rate to velocity fluctuation statistics.

775

776 **SPRAY**

777 Lagrangian Particle Dispersion Model distributed by ARIANET and ARIA Technologies and
778 developed by an Italian / French research group involving the CNR (Italian National
779 Research Council) and other Universities.

780

781 **Source Term Estimation**

782 Source Term Estimation (STE) algorithms are methods used to reconstruct the source of an
783 atmospheric release, namely its location, time of emission and strength, starting from
784 concentrations observed by sensors. STE methods include using a dispersion model, often
785 in its backward or time-reversed configuration starting from measuring points, coupled to
786 optimisation or probabilistic methods to infer the source parameters.

787

788 **Stack Tip Downwash**

789 Stack tip downwash is the capture of the plume in the downwind side of a stack close to it. It
790 happens when the ratio between exit speed and wind speed at the height of the stack is
791 smaller than 1.5. STD is more pronounced for large-diameter stacks.

792

793 **TA Luft**

794 German Air Quality control regulation, titled: "Technical Instructions on Air Quality Control"
795 (*Technische Anleitung zur Reinhaltung der Luft*) and commonly referred to as TA Luft.

796

797 **TAPM**

798 TAPM (The Air Pollution Model) PC-based, nestable, prognostic meteorological and air
799 pollution model driven by a Graphical User Interface, developed and maintained by The
800 Commonwealth Science and Industrial Research Organisation (CSIRO), Australia.

801

802 **STAGMAP**

803 Stagnation Model Analysis, Medford, Oregon, SF6 tracer release under calm conditions.

804

805 **Topography**

806 Representation of surface features such as mountains, hills, rivers, and valleys.

807

808 **Unified Model (UM)**

809 A NWP and climate modelling software suite developed by the United Kingdom Met Office.

810

811 **Wind direction**

812 Orientation of the wind vector in the horizontal direction. Wind direction for meteorological
813 purposes is defined as the direction from which the wind is blowing and is measured in
814 degrees clockwise from true north. Wind direction determines the transport direction of a
815 plume or puff in air quality modelling applications.

816

817 **WRF**

818 A public domain mesoscale NWP system designed for both atmospheric research and
819 operational forecasting applications,

820

821

822 2.2. Abbreviations and Acronyms

ADMS	Atmospheric Dispersion Modelling System
AFWA	Air Force Weather Agency (US)
ARW	Advanced Research Weather and Forecast Model
AQ	Air Quality
AQMG	Air Quality Management Group (US)
ASOS	Automated Surface Observing Systems
BT	Back-Trajectory
CCCS	Copernicus Climate Change Service
CERC	Cambridge Environmental Research Consultants
CFD	Computational Fluid Dynamics
COSMO	Consortium for Small-Scale Modelling
DWM	Diagnostic Wind Models
ECMWF	European Centre for Medium-Range Weather Forecasts
EPA	Environmental Protection Authority
EPRI	Electric Power Research Institute (US)
FAA	Federal Aviation Authority
FSL	Forecast Systems Laboratory
FDDA	Four-dimensional Data Assimilation
GDT	Gas Detector Tube
GFS	Global Forecast System
GUI	Graphical User Interface
HARMONIE	HIRLAM-ALADIN Research on Mesoscale Operational NWP In Europmed. ALADIN is A Limited Area Dynamic International model).
HIRLAM	High-Resolution Limited Area Model
HRRR	High-Resolution Rapid Refresh model
HYSPLIT	Hybrid Single-Particle Lagrangian Integrated Trajectory model
ISCST3	Industrial Source Complex Short Term Model

IFS	Integrated Forecasting System
IOMS	Instrumental Odour Monitoring Systems
LCP	Lambert Conformal Projection
LDAR	Leak Detection and Repair
LPDM	Lagrangian Particle Dispersion Models
MM5	Penn State University (PSU) / National Centre for Atmospheric Research (NCAR) Mesoscale Model, now superseded by WRF
MMIF	Mesoscale Model Interface Programme
NAAQS	National Ambient Air Quality Standards
NAM	North American Mesoscale Forecast System
NCAR	National Centre for Atmospheric Research
NCEP	National Centre for Environmental Prediction
NES	National Environmental Standards
NILU	Norsk Institut for Luftforskning (Norwegian Institute for Air Research)
NOAA	National Oceanic and Atmospheric Administration
NWP	Numerical Weather Prediction
NWS	National Weather Service
OAQPS	Office Of Air Quality Planning and Standards
OCD	Offshore and Coastal Dispersion Model
OIA	Odour Impact Assessment
OIC	Odour Impact Criteria
OER	Odour Emission Rate
PtMR	Peak-to-Mean Ratio
PBL	Planetary Boundary Layer
PDF	Probability Density Function
P&ID	Piping and Instrumentation Diagram
RAP	Rapid refresh numerical weather model
RASS	Radio Acoustic Sounding System
RDM	Reverse Dispersion Modelling

SMOD	Screening Model for Odour Dispersion
SODAR	Sonic Detection And Ranging
SOER	Specific Odour Emission Rate
STD	Stack Tip Downwash
STE	Source Term Estimation
TAPM	The Air Pollution Model
TIBL	Thermal Internal Boundary Layer
UM	Unified Model
US EPA	United States Environmental Protection Agency
VOC	Volatile Organic Compound
WWTP	Waste Water Treatment Plant
WRF	Weather Research and Forecast Model

823 **2.3. Symbols and Units**

824

Symbol	Description	Unit
<i>A</i>	Area	m ²
<i>c_{od}</i>	Odour concentration	ou _E /m ³
<i>EROM</i>	European Reference Odour Mass	µg n-butanol
<i>ou</i>	Odour unit	
<i>ou_E</i>	European odour unit	
<i>p_s</i>	Absolute pressure in stack	kPa
<i>q_{od}</i>	Odour flow rate	ou _E /s
<i>V</i>	Volume	m ³
\dot{V}	Volume Flow Rate	m ³ /s
<i>Z</i>	Dilution factor	
η_{od}	Odour abatement efficiency	%

825

826

827 3. Meteorology

828 3.1 Introduction

829 In science, engineering, and even social science disciplines, a model consists of equations
830 defining individual processes. A model must be constructed or written and then calibrated
831 by observation and sampling to have a predictive value.

832 A traditional mathematical model contains the following elements:

- 833 ● assumptions and constraints;
- 834 ● governing equations; and
- 835 ● initial and boundary conditions.

836 Within the context of odour modelling, a model must describe how the vertical wind profile
837 will develop as an air mass moves across the surface of the earth based on friction forces
838 caused by land use. In addition, a model should deal with how the temperature profile of a
839 column of air will develop throughout the day based on parameters like latitude, surface
840 characteristics, cloud cover, and moisture. Last but not least, a model should address the
841 variation in odour concentration downwind from a source based on the chaotic motions of
842 odorants.

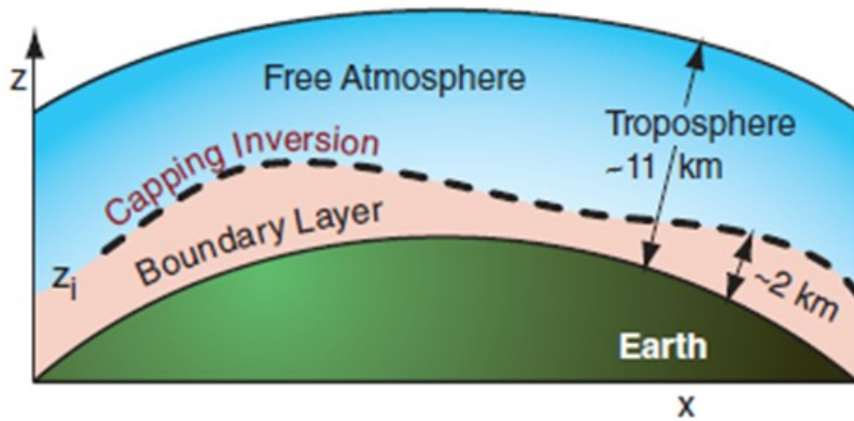
843 There are a number of different approaches to solving these questions. These separate
844 approaches involve different equations, which are called algorithms. One approach is
845 neither "correct" nor "incorrect" but may be described as yielding a better prediction of reality
846 under certain conditions. Numerous varieties of models have evolved for specific uses, and
847 today there are perhaps 100 atmospheric dispersion models mentioned in the literature.

848 In all cases, accurate inputs to the model are required to achieve reliable results.
849 Meteorological parameters constitute an essential set of inputs to an odour model, along
850 with information about the source(s) and the land surface above which the interactions
851 between these inputs play out. This chapter discusses these meteorological parameters and
852 their use within the various models.

853 3.2 Meteorological conditions

854 3.2.1 Introduction

855 A basic understanding of the motions and characteristics of the atmosphere is a prerequisite
856 to assessing odour impacts using dispersion modelling. Therefore it is necessary to review
857 some pertinent details about the layer of air within which we live and work (Stull, 2017). The
858 atmosphere of Earth extends hundreds of kilometres from the surface before vanishing into
859 space. However, most of the atmosphere's mass is located within the troposphere. The
860 term troposphere derives from the Greek words *tropos* (rotating) and *sphaira* (sphere),
861 indicating that rotational turbulence mixes the layers of air and so determines the structure
862 and the phenomena of the troposphere. The troposphere extends from the ground surface
863 up to an average altitude of about 11 kilometres (see Figure 3-1).



864

865 **Figure 3-1** Layers within the troposphere (Stull, 2017)

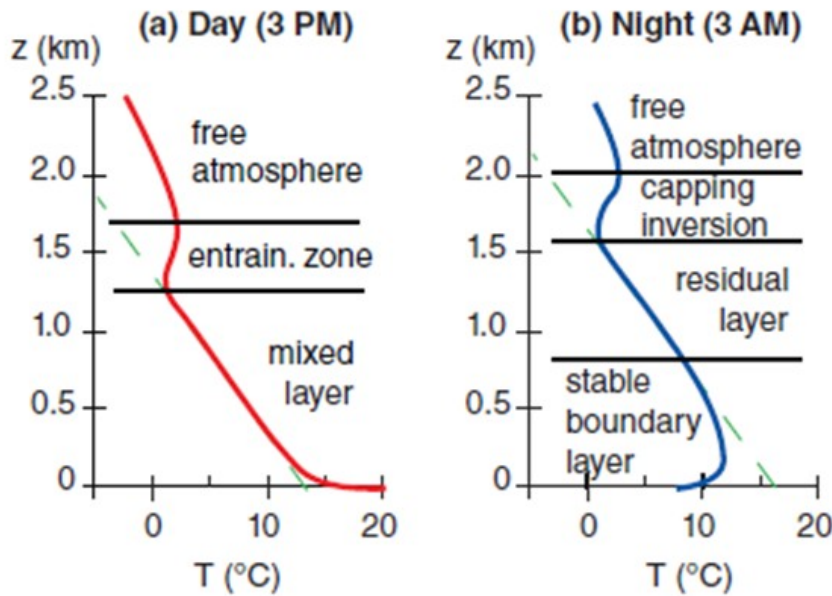
866 Within the troposphere, the layer closest to the Earth's surface is the Planetary Boundary
867 Layer (PBL) or Atmospheric Boundary Layer (ABL). The PBL varies from a few hundred to
868 perhaps a few thousand metres thick. The remainder of the air in the troposphere above the
869 PBL is called the free atmosphere. All conditions within the PBL derive from solar radiation
870 that reaches the ground surface and is absorbed. As the ground warms and cools in
871 response to this incoming solar energy (insolation), the meteorological conditions of wind
872 direction and speed, air temperature and humidity, air pressure, and atmospheric stability
873 (the vertical temperature gradient) constantly change.

874 These meteorological conditions within the PBL create the weather people experience daily
875 as hot/cold, wet/dry, windy/calm, and sunny/cloudy. The same meteorological conditions
876 that create the weather are essential within the context of odour transport and modelling.
877 However, the conditions are interrelated, and it is impossible to completely separate their
878 meaning and impact into individual discussions. The following sections, therefore, provide a
879 general discussion with brief details of each condition to help understand the challenges
880 associated with dispersion modelling. This chapter is not meant to be a complete treatise on
881 meteorology; the interested reader is encouraged to seek additional details in the reference
882 material.

883 3.2.2 Insolation, Surface Heating, and the Energy Budget

884 The Sun drives all energy processes within the atmosphere. At the Earth's surface, a
885 balance exists between insolation, sensible heating (during which a temperature change
886 occurs between the surface and atmosphere), latent heating (during which a phase change
887 occurs between the surface and atmosphere), and heat transport from the surface to the
888 sub-surface. However, not all the solar radiation that reaches the Earth's surface is
889 absorbed by it, since a part of the radiation is reflected back to space by what is known as
890 the Earth's surface albedo. The albedo is defined as the fraction of the incident radiation that
891 is reflected by the surface. Since the Earth's surface is not uniform everywhere, the albedo
892 varies widely from place to place depending upon the nature and composition of the
893 underlying surface. For example, the albedo of a dense forest is very different from that of a
894 freshly covered snow surface.

895 Sensible heat flux is related to atmospheric heating from below. The atmosphere is nearly
896 transparent to incoming shortwave radiation from the sun. Daytime heating of the PBL is
897 then accomplished by sensible heating from the underlying surface, which has absorbed a
898 fraction of the incoming shortwave radiation. At night, the flux reverses direction as the
899 surface loses sensible heat to the air above as illustrated in Figure 3-2.



900

901 **Figure 3-2** Examples of boundary-layer temperature profiles during the day (left) and night
902 (right) during fair weather over land. The adiabatic lapse rate is dashed. The heights shown
903 here are illustrative only. (Stull, 2017)

904 This diurnal cycle varies by latitude and season. Cloud cover affects the daily energy budget
905 at the surface, so cloud cover is an essential meteorological condition. Latent heat flux is
906 related to phase changes of water: evaporation of soil moisture or surface water;
907 transpiration by vegetation; or melting and sublimation of frozen surfaces. Where there is
908 little surface water, the latent heat flux is near-zero (or even negative), and it has large
909 positive values over warm bodies of water or hot, wet soils. It is generally negative over land
910 during the local night time hours.

911 The Bowen ratio is the ratio between the sensible and latent heat fluxes. The Bowen ratio is
912 smallest over oceans and wet land surfaces such as marshes and jungles. It is largest in
913 deserts and drought-ridden locations. The Bowen ratio is related to the strength of vertical
914 mixing within the PBL: larger Bowen ratios are associated with stronger, deeper vertical
915 mixing.

916 3.2.3 Wind, Turbulence, and Buoyancy

917 When the air in direct contact with a warmed surface undergoes sensible heating, the air
918 becomes less dense and begins to rise, and that vertical motion is called convection.
919 Cooler and dense surrounding air moves to replace the warmer, less dense air. That lateral
920 air motion is called advection, or wind. As the air mass moves along the ground surface, it
921 interacts with surface features through friction, imparting a turbulent motion to the air by a
922 process called mechanical mixing. The friction is quantified in terms of a roughness length
923 that depends on the nature of the surface. This roughness length varies by nearly four
924 orders of magnitude depending on whether the surface is open water, grass prairie,
925 cultivated farm fields, mature forests, or dense urban areas. The result of this friction and
926 mechanical mixing is to slow the horizontal movement of the air mass. The rising air mass
927 also experiences turbulence, but it is associated with vertical motion due to the temperature
928 gradient, and that turbulence is called convective mixing.

929 These mixing phenomena are important to our understanding of dispersion modelling since

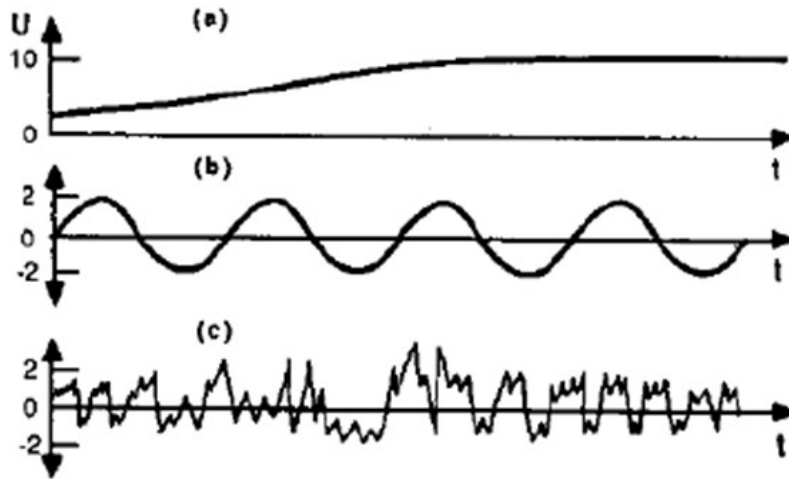
930 entrainment of the surrounding air during that mixing will cause dilution of any contaminants,
931 including odour. The depth of air within the PBL in which mixing occurs is called the mixing
932 height. Moving air masses at distances above the surface experience less interaction with
933 surface features but are still subject to frictional forces, which cause turbulence and mixing.

934 Consider a mass of air moving horizontally and smoothly (laminar flow) over a stationary
935 mass of air. Even though the molecules in the stationary air are not moving horizontally, they
936 move about and collide. At the boundary separating the air layers, there is a constant
937 exchange of molecules between the stationary air and the flowing air. The overall effect of
938 this molecular exchange is to slow down the moving air (Ahrens, 2018). If molecular
939 viscosity were the only type of friction acting on moving air, the effect of friction would
940 disappear in a thin layer just above the surface. There is, however, another frictional effect
941 that is far more important in reducing wind speeds.

942 When laminar flow gives way to irregular turbulent motion, there is an effect similar to
943 molecular viscosity, which occurs throughout a much larger portion of the moving air. Near
944 the Earth's surface, it is related to the roughness of the ground. As the wind blows over a
945 landscape dotted with trees and buildings, it breaks into a series of irregular, twisting eddies
946 that can influence the airflow for hundreds of metres above the surface. The wind speed
947 and direction fluctuate rapidly within each eddy, producing the irregular air motion we know
948 as wind gusts. These eddy motions create a drag on the flow of air far greater than that
949 caused by molecular viscosity.

950 Besides the mean horizontal wind speed and eddies, there is one more motion within the
951 atmosphere, called wave motion. Unlike the turbulent ones, these oscillations move in a
952 pseudo-harmonic way and have a substantially deterministic character. The presence in the
953 atmosphere of these non-turbulent movements, with a characteristic time between an hour
954 and a minute, are collectively referred to as "submeso motions". Waves (vertical oscillations
955 propagating horizontally on a density interface) can exist in the air and behave similarly to
956 water waves. These waves are frequently observed in the night-time boundary layer where
957 stable air is overridden by a warmer residual layer, transporting little heat, humidity, and
958 other scalars such as pollutants. They are, however, effective at transporting momentum and
959 energy. Waves can be generated locally by mean-wind shears and by wind flow over
960 obstacles. Waves can also propagate from distant sources, such as thunderstorms or
961 explosions. One classic waveform is a mountain wave where stable air flows over a ridge or
962 mountain setting up a downwind oscillation.

963
964 The total airflow, or wind, is the sum of these three motions, as depicted in Figure 3-3.
965 Figure 3-3 (a) displays mean wind, which is relatively constant, but varying slowly over the
966 course of hours. Figure 3-3 (b) displays waves in the air flow which represent regular (linear)
967 oscillations of the wind, often with periods of ten minutes or longer. Figure 3-3 (c) displays
968 the turbulence, irregular, quasi-random, non-linear variations with durations of seconds to
969 minutes.



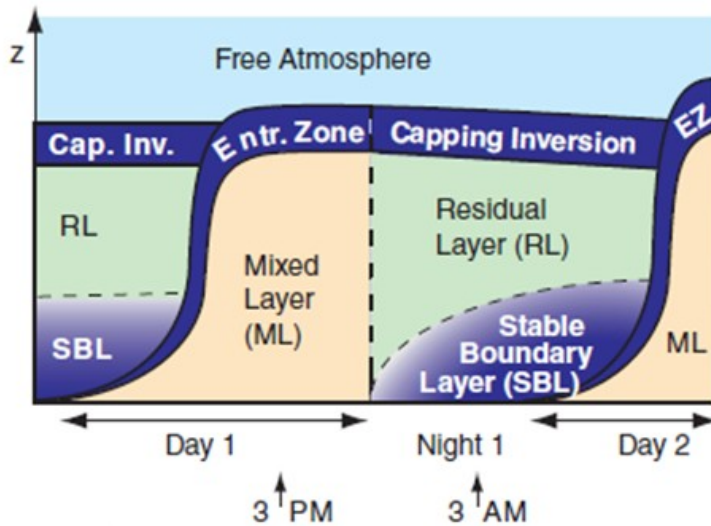
970

971 **Figure 3-3** Diagram showing the three motions of airflow (Stull, 2017)

972 3.2.4 Development of the Planetary Boundary Layer (PBL)

973 The usual classification of the PBL is based on buoyancy effects. Consider a package
974 (parcel, particle) of air, like the air within a balloon but without the membrane. If a parcel of
975 air is displaced upward adiabatically (no heat enters or leaves the parcel), it will expand
976 because of the reduced pressure aloft; hence, its temperature will decrease. The resulting
977 temperature profile for dry air is called the adiabatic temperature profile. Under this ideal
978 condition, displaced parcels have precisely the density of their surroundings and thus
979 experience no net buoyant force or tendency to return to their original position. We call this
980 neutral stratification. Should the mean temperature decrease with height more slowly than
981 the adiabatic profile, a vertically displaced parcel will experience a force tending to restore it
982 to its original position. This situation is called stable stratification. The final case where the
983 decrease of temperature with height exceeds the adiabatic lapse rate is called unstable
984 stratification; here, displaced parcels tend to be vertically accelerated away from their
985 original positions. These tendencies define what is called atmospheric stability.

986 The PBL has pronounced structural differences between day and night. The surface energy
987 budget drives this diurnal cycle. After sunrise, the depth of the PBL increases with time as
988 surface heating drives buoyant convection. The depth typically reaches a maximum in mid
989 to late afternoon (Figure 3-4). On a clear night, a much shallower, stably-stratified boundary
990 layer develops at the surface in response to the surface cooling through emitted radiation. In
991 clear weather over land, the mean wind speed in the surface layer can have a diurnal cycle
992 of substantial amplitude, with higher speeds in unstable daytime conditions and lower
993 speeds in stable conditions at night.



994

995 **Figure 3-4** Components of the boundary layer during fair weather in summer over land
 996 (Stull, 2017)
 997

998 Note: Pink indicates non-locally statically unstable air, light blue (as in the RL) is neutral
 999 stability, and darker blues indicate stronger static stability.

1000 The PBL is constantly evolving in response to both the diurnal heating cycle and changing
 1001 synoptic (large-scale) weather conditions. As a result, its structure and depth can vary
 1002 considerably over space and time. However, it typically has distinct states that we can
 1003 idealise somewhat and discuss in fairly simple terms (Stull, 2017).

1004 3.2.4.1 Mixed (Convective) Layer

1005 During clear days, a land surface is normally warmer than the air aloft because of heating by
 1006 incoming solar radiation. This warmer, near-surface air is buoyant and establishes
 1007 convective, turbulent motions. In some situations, over water, for instance, near-surface air
 1008 becomes buoyant because it contains more water vapour (less dense than air) than the air
 1009 at upper levels. Density changes at constant pressure can thus be caused either by actual
 1010 temperature changes or changes in the specific humidity; in other words, buoyant air is
 1011 either warmer or more humid, or both, than its surroundings. At the top of the convective
 1012 boundary layer there may be an overlying layer of stably stratified air which typically ranges
 1013 from a few hundred metres to a few kilometres thick, as schematically shown by the capping
 1014 inversion in Figure 3-4.

1015 This "inversion" layer acts as a lid for the convection by damping vertical motions and
 1016 establishes the depth of the convective PBL.

1017 This inversion lid can be eroded from below by turbulence and displaced vertically by a
 1018 motion such as that induced by convergence or divergence in the horizontal wind field.
 1019 Therefore, the convective PBL normally becomes deeper as the day progresses because of
 1020 turbulent entrainment of air down into the PBL; however, in some instances, its depth can be
 1021 held stationary or even lowered by subsidence. The latter situation can cause air pollution
 1022 episodes by trapping pollutants in an abnormally thin PBL.

1023 3.2.4.2 The Neutral PBL

1024 If the PBL has an adiabatic lapse rate throughout, which can happen if the surface moisture
 1025 and heat fluxes are negligible and there is no inversion aloft, we have the neutral case. Here

1026 turbulence is due entirely to the wind shear (the change in wind velocity with height), and
 1027 there are no buoyancy effects. Although it is possible that a truly neutral PBL can occur if
 1028 only briefly before some change in heat flux occurs, there is no persistent neutral PBL in the
 1029 real world. It has been widely studied theoretically, and we mention it here to be complete
 1030 but will not discuss it further.

1031 3.2.4.3 Residual Layer

1032 About a half hour before sunset, the thermals cease to form (in the absence of cold air
 1033 advection), allowing turbulence to decay in the formerly well-mixed layer. The resulting layer
 1034 of air is sometimes called the Residual Layer because its initial mean state variables and
 1035 concentration variables are the same as those of the recently-decayed mixed layer. The
 1036 Residual Layer contains the pollutants and moisture from the previous mixed layer but is not
 1037 very turbulent. The Residual Layer is considered to be neutrally stratified, resulting in
 1038 turbulence that is nearly of equal intensity in all directions.

1039 3.2.4.4 Stable Boundary Layer

1040 At night, a land surface typically cools because of radiative heat loss to space. The near-
 1041 surface air cools and creates a positive (stable) temperature gradient in the PBL. This has
 1042 strong dynamic effects on turbulence and hence on the structure of the layer. Energy must
 1043 be expended to maintain vertical velocity fluctuations in the presence of the stable lapse
 1044 rate; since turbulence is inherently three-dimensional, with energy exchanges taking place
 1045 among all three velocity components, the effect of extraction of energy from the vertical
 1046 motions is transmitted to the horizontal components as well.

1047 3.2.5 The Concept of Stability Classes

1048 Frank Pasquill (Pasquill, 1961) defined a method for describing atmospheric stability based
 1049 on his observations of the surface parameters like wind speed, cloudiness, and solar
 1050 irradiance. Pasquill defined six categories of stability ranging from very unstable to stable,
 1051 as follows:

- 1052 A. Very Unstable
- 1053 B. Unstable
- 1054 C. Slightly Unstable
- 1055 D. Neutral
- 1056 E. Slightly Stable
- 1057 F. Stable

1058 The dispersion parameters (the standard deviation of plume concentration in the lateral (σ_y)
 1059 and vertical (σ_z) associated with this method) are used by default in most of the EPA
 1060 recommended Gaussian dispersion models. These parameters are often referred to as the
 1061 Pasquill-Gifford (P-G) sigma curves. For routine applications using the P-G sigma curves,
 1062 the Pasquill stability category (hereafter referred to as the P-G stability category) is
 1063 calculated using the method developed by Turner (1964) which uses actual data provided by
 1064 the National Weather Service (NWS). The Turner method expands the wind speed scale
 1065 slightly, uses numerical categories 1 through 7, and in essence includes an additional P-G
 1066 stability category 'G', Extremely Stable. For US EPA regulatory modelling applications,
 1067 stability categories 6 and 7 (F and G) are combined and considered category 6. Table 3-1
 1068 provides a key to the Pasquill stability categories as originally defined.

1070 **Table 3-1** Meteorological conditions that define the Pasquill Stability Classes

Surface wind speed	Daytime incoming solar radiation	Night-time cloud cover
--------------------	----------------------------------	------------------------

m/s	miles/hr	Strong	Moderate	Slight	≥ 4/8	≤ 3/8
< 2	< 5	A	A – B	B	E	F
2 – 3	5 – 7	A – B	B	C	E	F
3 – 5	7 – 11	B	B – C	C	D	E
5 – 6	11 – 13	C	C – D	D	D	D
> 6	> 13	C	D	D	D	D

Class D applies to heavily overcast skies, at any windspeed day or night

1071 Incoming solar radiation is based on the following: strong ($> 700 \text{ W m}^{-2}$), moderate ($350 - 700 \text{ W m}^{-2}$), slight ($<$
1072 350 W m^{-2})

1073 In terms of odour dispersion, the more unstable the atmospheric conditions are, the greater
1074 the dilution effect. Under atmospheric instability (Class A and B) conditions, odours are
1075 transported over shorter distances before being diluted below the odour threshold, while
1076 under stable conditions (Class E and F), odours travel undiluted for longer distances.

1077 3.2.6 Time Scale / Meteorological Data Resolution

1078 Frequent and accurate updates to meteorological data are necessary and demanded by
1079 many technical fields, including odour modelling. In recent years, numerous key
1080 developments in data forecasting and recording methods have led to long-term and more
1081 reliable data availability. This has also allowed for more frequent data updates. For example,
1082 the atmosphere satellite remote sensing refreshes and provides crucial data multiple times
1083 per day (Emery, 2017).

1084 The major importance of meteorological data calls not only for more frequent updates but
1085 also for high-resolution data. Resolution is a significant factor for advancing the data
1086 forecasting capability as more information and details are available in high-resolution data.
1087 Increased computer capacity and speed have led to smaller grid cell sizes which means
1088 higher data resolution. This provides more accurate forecasts and reliable data to study
1089 atmospheric dynamics. High-resolution data helps predict large-scale changes in the data
1090 patterns, such as topographic effects and small disturbances.

1091 Even more so than in the study of atmospheric pollution, where the hourly average is the
1092 reference parameter for air quality control, the dispersion of odorous substances requires
1093 greater detail since the perception of annoyance occurs over a time order of seconds. This is
1094 the time scale in which the human olfactory system detects the odorants in the inhaled air
1095 during a single breath. Consequently, the modelling process must determine the peak
1096 values generated around the odorous sources. For this, it is necessary to know the
1097 meteorological variables of the site with the best possible temporal detail, compatible with
1098 the parameters that the dispersion models will be able to use.

1099 In any case, the experimental observations must provide the meteorological input to the
1100 models and indicate the degree of uncertainty with which the real situation is described. It is
1101 thus possible to highlight meteorological situations that well represent the dynamics of the
1102 atmosphere from more uncertain situations in which the approximation of the meteorological
1103 description can generate only a limited adherence to the real expected concentrations.

1104 3.3 Types of Meteorological Data Sets

1105 Meteorological data are one of the most important inputs into any air dispersion model. Two
 1106 meteorological elements primarily control ground-level concentrations of contaminants: wind
 1107 direction and speed (for transport); and turbulence, buoyancy, and mixing height of the
 1108 boundary layer (for dispersion). There is a choice between meteorological data sets derived
 1109 from internationally accepted observation techniques (WMO, 2021), (US EPA, 2000), (US
 1110 EPA, 2017) measured at specific sites, or from prognostic models or forecast data run in
 1111 hindcast mode.

1112 The meteorological data requirements for steady-state Gaussian plume models and
 1113 advanced dispersion models vary considerably. Empirical equations, screening models, and
 1114 simple Gaussian plume models typically require 1-dimensional meteorological data (wind
 1115 speed, wind direction and temperature) from a single surface station. These models assume
 1116 the single surface station data apply to the whole modelling domain, both spatially and
 1117 vertically. From the surface to the top of the boundary layer, meteorological conditions are
 1118 assumed to not vary with height.

1119 More advanced Gaussian plume models require 2-dimensional meteorological data from a
 1120 single surface and upper air station. These models also assume the meteorological data
 1121 applies to the whole modelling domain; however, conditions can vary with height according
 1122 to the upper air profile. There are several international repositories of surface and upper air
 1123 raw data; Appendix A contains links to these data, and more information about the data
 1124 variables and formats can be obtained from these data sources. The hourly raw surface
 1125 data typically consists of a record for each date/time of observation. Each record is of
 1126 variable length and consists of a control and mandatory data section and may also contain
 1127 additional, remarks, and element quality data sections. This data is usually compressed to
 1128 minimise file size. Upper air data which consists of fewer variables is organised such that it
 1129 can be viewed in fixed-width columns. Figure 3-5 shows a portion of a surface data file, and
 1130 Figure 3-6 shows upper air data.

```
1131 0127082210999992022010100004+40500-003583FM-12+063399999V0:
9+00301+00201999999ADDMA1103001999999REMMET051METAR LEMD 0:
A103000091GA1001+999999999GE19AGL +99999+99999GF19999900:
0494-003567FM-15+061099999V0203201N001012200019N009999199+
A1240N+00001MA1999999096101MD1710041+99999REMSYN09408221 02:
203501N001519999999Y009900599+00001+00001999999ADDMA110300:
1 20011 39621 40335 52011 80000 333 60007=0078082210999992
LEMD 011030Z VRB02KT CAVOK 07/03 Q1030 NOSIG=0178082210999:
000519999999Y009900599+01201+00601999999ADDMA1103001999999:
19999999N030000199+01501+00551102771ADDGA1999+9999999021GE1:
R LEMD 011500Z 00000KT CAVOK 17/03 Q1028 NOSIG=00780822109:
+99999GF102991001999999999999999MA1999999095971MD1610021+9:
Q1028 NOSIG=0078082210999992022010118304+40494-003567FM-15-
```

1132 **Figure 3-5** Example surface data from Madrid-Barajas (USAF 082210) for January 2022
 1133 (ISD Format)

254	0	1	JAN	2022		
1	99999	8221	40.47N	3.58W	638	2315
2	100	116	99	61	32767	0
3		LEMD			32767	kt
9	956	638	76	45	325	4
4	1000	266	32767	32767	32767	32767
5	950	690	84	46	32767	32767
5	947	716	110	50	32767	32767
4	925	904	134	44	15	4
5	896	1172	156	-174	32767	32767
6	878	1343	32767	32767	210	10
5	870	1420	138	-42	32767	32767
4	850	1617	130	-70	215	13
1134	5	798	2141	94	-106	32767 32767

1135 **Figure 3-6** Example upper air data from Madrid-Barajas (USAF 082210) for January 2022
 1136 (FSL Format)

1137 Advanced Lagrangian puff and particle dispersion models require 3-dimensional data for
 1138 analysis. Because there will not be meteorological sites at every point on the ground in the
 1139 modelling domain, and monitoring in the upper air (anything above the height of a tower) is
 1140 normally very sparse, meteorological models must be used to provide this 'missing data'.
 1141 These models use data from all relevant surface networks (land and sea) and upper air
 1142 stations in conjunction with atmospheric physics to interpolate and develop a matrix of
 1143 meteorological variables across the modelling domain. The advanced dispersion models
 1144 then use this spatially and vertically varying pre-processed meteorological data.

1145 Two types of meteorological models can be used to provide a 3-dimensional grid of
 1146 meteorological data:

- 1147 • Diagnostic Wind Models (DWM), which interpolate and/or extrapolate
 1148 meteorological observations; and
- 1149 • Numerical prognostic models, also known as mesoscale models or Numerical
 1150 Weather Prediction (NWP) models.

1151 The unaltered meteorological model outputs of these two types of models are typically used
 1152 to drive advanced dispersion models. Prognostic and diagnostic meteorological models can
 1153 either form part of an air dispersion modelling system, such as CALMET which is part of the
 1154 CALPUFF modelling system, or they can stand alone entirely like the Weather and Research
 1155 Forecast system, commonly known as WRF.

1156 The biggest concern with using prognostic data directly is related to the horizontal grid
 1157 resolution of the modelling domain. Typically, prognostic models are run on multiple nested
 1158 domains where the innermost nest has a grid of 1 km to 4 km. If the resolution is fine
 1159 enough to resolve important meteorological features such as the sea and land breezes,
 1160 developing cyclones and fronts, terrain, and non-homogeneous land uses, then it is
 1161 appropriate to use prognostic gridded data directly in a dispersion model. However,
 1162 sometimes these features cannot be resolved, and it is not computationally practical to run
 1163 the prognostic model at much finer grid resolutions. Combining gridded coarse prognostic
 1164 model data into a fine-scale diagnostic model is far less computationally demanding than
 1165 running a prognostic meteorological model at less than 1 km resolution. In addition, the
 1166 diagnostic model can also incorporate observational data.

1167 In that case, the diagnostic meteorological model can be used at a much higher spatial
 1168 resolution of, for example, 150 m, with no computational inefficiencies. The prognostic model
 1169 provides a 'first-guess field', which the diagnostic model then modifies to take into account

1170 terrain and land-use features at a finer spatial scale than the prognostic model. The output of
 1171 the diagnostic model is then passed to the dispersion model, which will assess the odour
 1172 dispersion at the same fine-scale as the diagnostic model. The sampling grid used in the
 1173 CALPUFF model may be set even finer. For example, considering 150 m for the CALMET
 1174 grid, CALPUFF may be used with the nesting factor MESH DN=3, which means dividing the
 1175 CALMET grid by 3. Therefore the CALPUFF sampling grid would be 50 m, a grid size that is
 1176 not uncommon in odour applications.

1177 Combining prognostic model output data as input to a diagnostic meteorological model is
 1178 being used in many odour assessments worldwide today and has become the preferred
 1179 approach for obtaining representative on-site data if no measurements are available. The
 1180 US EPA (2017) has stated that "For a near-field dispersion modelling application where
 1181 there is no representative NWS station, and it is prohibitive or not feasible to collect
 1182 adequately representative site-specific data, it may be necessary to use prognostic
 1183 meteorological data for the application" (p. 5200).

1184 Some well-known prognostic meteorological models produce output data in a format that can
 1185 be used by plume models. Prognostic model results may be extracted at a single location
 1186 (the site of pollution emissions) in a format compatible with the plume model, and it is then
 1187 considered a pseudo-observation for input to the dispersion model. The practical advantage
 1188 of extracting single-point meteorological data for a plume model is that there is no missing
 1189 data. In addition to providing surface data, the prognostic model will also provide a vertical
 1190 profile of temperature, wind direction, and wind speed. This is a significant advantage to
 1191 those plume models which can use 2-dimensional meteorology.

1192 3.3.1. Screening meteorological data

1193 Screening meteorological data sets have been developed using idealised hourly standard
 1194 combinations of wind speed, stability class and mixing heights, aiming to mimic the range of
 1195 atmospheric conditions that are likely to occur in any given location. A sample of a screening
 1196 meteorological data file is displayed in Table 3-2. The screening data sets provide a simple
 1197 option to run air dispersion models and can be applied in most locations. The maximum
 1198 ground level concentration predicted using a screening data set is considered conservative.
 1199 This means that the model likely over-predicts concentrations expected to occur in reality,
 1200 assuming that other input data are of good quality.

1201 Idealised meteorological data sets of a few hundred hours can only model one-hour
 1202 averages, and they cannot provide an indication of how frequently an event might occur.
 1203 These data sets should only be used to gain a 'first cut' estimate of the magnitude of the
 1204 maximum ground-level odour concentration for a particular source.

1205 **Table 3-2** METSAMP.MET – An example of a screening meteorological data file
 1206

Date	Temp.	W. Speed	W. Dir.	Stability	Mix. Ht.
00010101	25	0.5	270	A	100
00010102	25	1.0	270	A	100
00010103	25	1.5	270	A	100
00010104	25	2.0	270	A	100
00010105	25	2.5	270	A	100
00010106	25	3.0	270	A	100
00010107	25	0.5	270	B	100

00010108	25	1.0	270	B	100
00010109	25	1.5	270	B	100
00010110	25	2.0	270	B	100
00010111	25	3.0	270	B	100
00010112	25	4.0	270	B	100

1207 3.3.2. Observations data sets - ready-made data

1208 Urban and regional ready-made meteorological data sets derived from measurements are
 1209 sometimes available from local and regional regulatory authorities worldwide. The benefit of
 1210 'ready' prepared single station data sets is;

- 1211 ● they are sequential hourly datasets;
- 1212 ● they are often representative of at least one or more years;
- 1213 ● they meet the criteria of the ambient air quality requirements of the local regulatory
 1214 authority in that they have been properly evaluated;
- 1215 ● they are sufficiently accurate;
- 1216 ● they can be used directly into screening models and empirical equations; and
- 1217 ● they resolve the need for a complex, expensive and timely component of
 1218 meteorological data sets processing.

1219 These data sets, if available, are usually stored by the local authority and can be easily
 1220 obtained. Normally, they would be in a spreadsheet format or simple ASCII format. Ordering
 1221 the data into the format required for the model is normally straightforward. Normally, these
 1222 data are simple one-dimensional data with an emphasis on wind speed, wind direction,
 1223 atmospheric stability and temperature. Appendix A includes a table with links to US State
 1224 and Canadian Provincial authorities that maintain AERMOD-ready data sets, plus links to
 1225 authorities in other countries that maintain similar data.

1226 3.3.3. Observations data sets - developing site-specific data sets

1227 Provided it is of good quality, on-site measured data are always the preferred source of
 1228 meteorological input data. A distinct advantage of having on-site data is that they can also
 1229 be used for dispersion model evaluation studies, and it greatly improves the accuracy of the
 1230 dispersion model results, especially when making decisions about separation distances.

1231 However, developing a meteorological data set can be expensive and time-consuming.
 1232 Depending on the complexity of the site, a degree of meteorological expertise may be
 1233 required to ensure the data accurately represent the conditions experienced at the site.
 1234 Further, for any odour assessment, the data needs to be assessed for quality assurance.

1235 The collection of site-specific meteorological data is fully covered in documents such as the
 1236 'Guide to Instruments and Methods of Observation: Volume I - Measurement of
 1237 Meteorological Variables, WMO-No. 8 (WMO, 2021) and 'Meteorological Monitoring
 1238 Guidance for Regulatory Modelling Applications' (US EPA, 2000). These documents provide
 1239 details on site location, recording mechanisms, data communication, sampling rates, system
 1240 accuracies, data handling, quality control and treatment of missing data. It is recommended
 1241 that this guidance be adopted as best practice for the collection and processing of
 1242 meteorological data for use in dispersion modelling applications.

1243 In general, a meteorological station should be located away from the influences of
 1244 obstructions such as buildings and trees to ensure that the general state of the environment
 1245 (wind direction and temperature) is best represented. A 10 m high mast for measuring wind

1246 direction and speed and temperature differentials is recommended. However, where the
1247 mast is located in good free-flow conditions, and there are height restrictions from local
1248 council bylaws, a 6m high mast can be used instead.

1249 For major industrial sources with tall stacks, or a site within a complex terrain environment,
1250 higher monitoring masts (30 m and higher) are recommended to monitor lower boundary-
1251 layer wind and temperature profiles adequately. It may be necessary for these situations to
1252 supplement such data with monitoring via remote sensing instruments such as SODAR /
1253 RASS or tethered-sonde systems.

1254 The following parameters need to be monitored at the site: surface temperature; temperature
1255 profile (between 1.5 m and 10 m or higher); relative humidity (%); wind speed (m/s); wind
1256 direction (degrees); solar radiation or cloud cover; and cloud ceiling height.

1257 While all the above variables provide valuable information for modelling, the most important
1258 variables are wind speed and direction, and temperature. Cloud cover information, pressure
1259 and relative humidity can usually be obtained from a nearby airport or automatic weather
1260 station. The costs for setting up a 10 m meteorological station to record and log these three
1261 parameters are modest and within reasonable budgets for most projects, with small
1262 additional costs associated with site maintenance and data management.

1263 When developing a meteorological data set, the representativeness of the data set must be
1264 assessed and demonstrated in terms of climatic means and extremes. This can essentially
1265 be established in two ways: by undertaking long-term (three to five years) monitoring of on-
1266 site data collection or by establishing correlations between on-site data, climatic averages
1267 and regional extremes.

1268 3.3.3.1. Selecting a representative weather station

1269 As a rule, site-specific data are always preferred when developing a meteorological data set
1270 for a specific source. However, sometimes this is not possible. Under situations like this,
1271 when there is no on-site data, usually the nearest suitable station to the source is allowed to
1272 be used, as long as it is in a similar meteorological regime as the source or within 5 km of
1273 the source, a recommendation from Victoria EPA in Australia.

1274 For simple single-station plume modelling, off-site data should only be used if the weather
1275 station site has similar topographic characteristics, likely to result in similar meteorological
1276 conditions for the site concerned. For example, when the source and weather station are
1277 located in the same valley or are located at a similar distance to a coastline. The
1278 representativeness of off-site data must be established before being used in any dispersion
1279 modelling study. Appendix A includes links to repositories of global surface hourly data.

1280 3.3.3.2. Selecting a representative vertical profile

1281 More advanced Gaussian dispersion models require a single vertical profile of upper air
1282 data. This data can be obtained from airports that routinely measure the upper air
1283 temperature, pressure, geopotential height, wind speed and wind direction at a minimum
1284 once or twice daily. For example, vertical distributions of temperature, humidity and winds
1285 also called upper-air datasets were developed originally for North America (Schwartz and
1286 Goyett, 2005) but have been extended worldwide and are usually measured at airport
1287 locations. Radiosonde are instruments which are sent airborne on weather balloons to
1288 sample data as they move upwards. Appendix A includes links to this type of data.

1289 Other instruments can be used to measure vertical profiles of temperature, humidity and
1290 winds. Remote sensing instruments like SODAR/ RASS or tethered-sonde systems can

1291 provide this information.

1292 3.3.4. Diagnostic models meteorological data

1293 Diagnostic meteorological models use data from all available locations and assign values to
1294 the meteorological variables throughout a three-dimensional grid by interpolation,
1295 extrapolation and objective analyses. The conservation of mass principle is applied
1296 throughout the process. The term 'diagnostic' is used because the input data and model
1297 results are for the same time period. Diagnostic models are not predictive, and their
1298 calculated fields for each time interval do not depend on fields at previous times. The
1299 model's output is a data file in a format required by a particular air dispersion model.

1300 Diagnostic models need meteorological data to run, they can incorporate available
1301 measurements, and some can directly incorporate the data output of prognostic models.
1302 They can provide meteorology through interpolation and objective analysis in regions with
1303 little data. Diagnostic models are usually run at a horizontal grid resolution varying from 250
1304 m to 4 km.

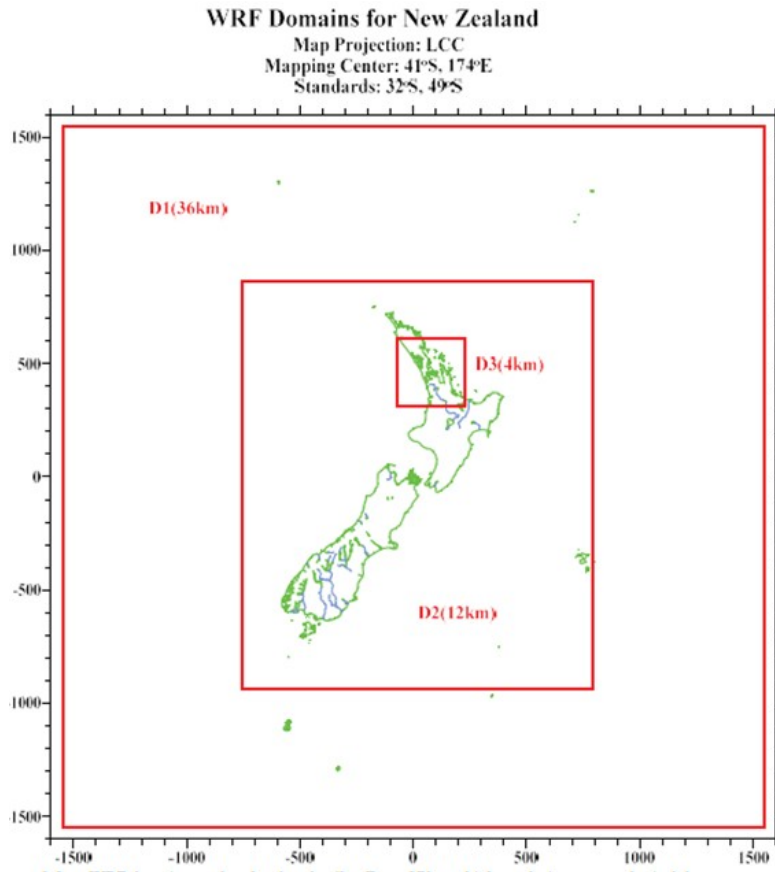
1305 The outputs of these models typically provide three-dimensional data sets as required by
1306 more complex dispersion models. The output of these models can also provide datasets for
1307 gaussian plume models, the data sets are extracted as a single surface station and vertical
1308 profile at a given location.

1309 3.3.5. Prognostic models meteorological data

1310 Prognostic models are driven by large-scale synoptic analyses and numerically solve the
1311 equations of atmospheric dynamics to determine local meteorological conditions. They do
1312 not require local meteorological data to run. However, if data are available in hindcast model
1313 runs (as opposed to forecasting), prognostic models use this historical data to assist in
1314 nudging the numerical solution toward the observation. Prognostic models run in hindcast
1315 mode can assimilate local meteorological data through a process known as 'nudging'.
1316 Essentially, the prognostic model solution is forced towards the observations during the
1317 model run. At best, the model solution is already close, so the forcing is small - hence the
1318 term 'nudging'. Nudging can benefit the model solution but must be used carefully. For
1319 example, nudging will not help with a poor prognostic model set-up, and can produce
1320 numerical instabilities when the model dynamics oppose the observation.

1321 Prognostic models can represent all scales, from global down to features on scales in the
1322 range 1-10 km. Most are run in a nested format with the outer domain covering distances in
1323 the order of 500-1000 km - the regional scale, and at least three inner nests.

1324 Figure 3-7 shows a numerical model setup over New Zealand, consisting of three nests of
1325 increasing spatial resolution.



1326

1327 **Figure 3-7** Three nested model domains (36 km, 12 km and 4 km) for a numerical
1328 prognostic model (courtesy of Atmospheric Science Global)

1329 All model domains are initialised using coarse analyses from global or limited-area models,
1330 usually run by national weather services. These are provided by many forecasting agencies
1331 or similar institutions, such as the US National Meteorological Center for Atmospheric
1332 Research, the European Centre for Medium-Range Weather Forecasts, the UK
1333 Meteorological Office, or the Australian Bureau of Meteorology. The outer domain is also
1334 driven at its boundaries by the global or limited-area models as the run progresses - this
1335 feeds into weather systems' effects on the domain of interest. The prognostic models
1336 describe the three-dimensional fields of temperature, wind speed and direction, and moisture
1337 through the region at a much higher spatial resolution than the initial analysis provided to the
1338 model.

1339 Prognostic models contain realistic dynamical and physical formulations and potentially
1340 produce the most realistic meteorological simulations for regions where data are sparse or
1341 non-existent. The extracted output of prognostic meteorological models can be used in
1342 dispersion models:

- 1343 • as a surface and upper air station at a single location;
1344 • as 3-dimensional gridded data; and
1345 • as 3-dimensional gridded data into a diagnostic meteorological model at a much finer
1346 resolution.

1347 Prognostic model data are now routinely used in odour assessments, usually as the provider
1348 of meteorological weather data in regions with sparse meteorological data. The data are
1349 usually of high quality, with little or no missing values.

1350 Prognostic models do not need local meteorological observations to run, so they can
1351 simulate the meteorology through physics and ‘observational nudging’ in regions where little
1352 data are available. The innermost horizontal grid spacing for a prognostic model varies
1353 widely from a resolution of 1000 m to 12 km.

1354 The output of prognostic models can be extracted at a single location to provide surface data
1355 and vertical profile data sets at that location for gaussian plume models but also provides
1356 three-dimensional data sets for more complex dispersion models as required. Appendix A
1357 includes links to data generated by the global prognostic model WRF.

1358 3.4 Meteorological data requirements for key dispersion models 1359 used in odour assessments

1360 This section focuses on key meteorological models routinely used in odour assessments
1361 worldwide and their meteorological data requirements. Some models, such as WRF, stand
1362 alone and are not attached to any dispersion model; this means that the meteorological
1363 output data from WRF can be transformed into any format for input to dispersion models.
1364 Other models, such as AERMET, the meteorological processor for the dispersion model
1365 AERMOD, only prepare meteorological data for AERMOD. This section is broken up into
1366 five different types of models; meteorological models, screening models, advanced
1367 Gaussian Plume models, and Lagrangian models. They are briefly discussed below.

1368 • **Meteorological models** – particularly WRF, the Weather and Research Forecast
1369 model. WRF is a primary mesoscale numerical prognostic model whose data are
1370 used to routinely drive air pollution dispersion models. In addition to WRF, the
1371 *Mesoscale Model Interface Program* (MMIF), which converts prognostic
1372 meteorological model output fields to the parameters and formats required for direct
1373 input into dispersion models, is also discussed.

1374 • **Screening models** - in particular AERSCREEN and ADMS-SCREEN, which are the
1375 screening models of two of the most well-used Gaussian plume models today,
1376 AERMOD and ADMS, which are used in odour assessments all over the world.

1377 • **Advanced Gaussian plume models** – particularly, AERMOD, ADMS, AODM and
1378 ARIA Impact. AERMOD and ADMS are widely known, advanced models. AERMOD
1379 and AODM enjoy regulatory status in the US and the UK, and AERMOD is also
1380 widely regulated worldwide. AODM is the Austrian Odour Dispersion Model
1381 developed specifically for odour assessments. ARIA Impact is a Gaussian model
1382 that enjoys widespread use throughout Europe and South America.

1383 • **Lagrangian Puff Models** – in particular CALPUFF and SCIPUFF. CALPUFF is a
1384 widely known favourite for odour applications due to its ability to handle complex
1385 atmospheric environments and calm conditions and its long history as a US
1386 regulatory model. SCIPUFF is a new generational second-order closure model. The
1387 sophisticated approach of the new turbulence model is exciting for odour
1388 applications.

1389 • **Lagrangian Particle-Puff models** – in particular, CSIRO’s TAPM. TAPM is widely
1390 used throughout Australia and New Zealand and overseas. The model enjoys a
1391 Particle-puff approach whereby it uses a Gaussian puff model in the horizontal and
1392 regular particle model to describe the vertical dispersion. TAPM is primarily used in
1393 Australia and New Zealand to develop upper air meteorological data in data-sparse
1394 regions.

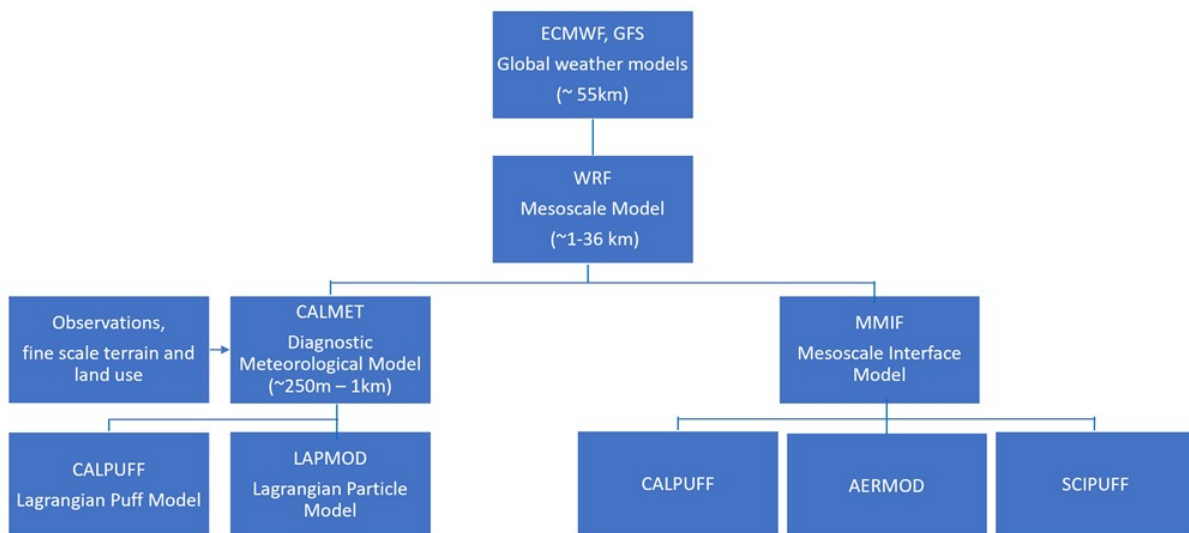
1395 • **Lagrangian Particle models** - specifically, SPRAY, AUSTAL (LASAT), LAPMOD

1396 and GRAL. This suite of dispersion models is developed in Europe. It is connected
 1397 to different meteorological data processors, including both prognostic and diagnostic
 1398 models able to reconstruct flow over complex terrain. These models are routinely
 1399 used in odour applications and assessments.

1400 Figure 3-8 shows a flow chart showing how meteorological data are developed from global
 1401 weather models such as ECMWF and GFS, which are run at a coarse resolution of
 1402 approximately 0.25 to 0.50 degrees over the entire world. These models provide the initial
 1403 data necessary to drive a mesoscale model such as WRF, which is typically run for multiple
 1404 nests of increasing grid resolution. The US EPA's MMIF interface model can translate the
 1405 WRF data directly into the correct format for CALPUFF, AERMOD and SCIFPUFF,
 1406 essentially by-passing those models' meteorological processors. In addition, the WRF
 1407 model output data can also be passed directly to a diagnostic meteorological model (such as
 1408 CALMET), which then uses the data to determine the initial guess wind field, and applies
 1409 fine-scale terrain adjustments as well as user-determined distance weightings to
 1410 observations at a much finer resolution than that from WRF. The output of the diagnostic
 1411 meteorological model is 3D gridded data at a fine resolution, which can then be used to drive
 1412 advanced Lagrangian dispersion models such as CALPUFF and LAPMOD.

1413

1414



1415

1416 **Figure 3-8** Development of meteorological data from global forecast models (courtesy of
 1417 Atmospheric Science Global)

1418 Note: ECMWF and GFS data can be processed through the mesoscale model WRF, and
 1419 transformed via the MMIF interface into dispersion model-ready data, or be passed to a
 1420 diagnostic meteorological model like CALMET which is executed on a much finer resolution
 1421 than the prognostic data to provide a 3D gridded data set for dispersion modelling purposes

1422 3.4.1. Prognostic Meteorological Models – WRF

1423 There are multiple mesoscale meteorological models whose data are used in air quality
 1424 applications worldwide today. Some of these in the USA include: North American
 1425 Mesoscale Forecast System (NAM); High Resolution Rapid Refresh (HRRR); and the Rapid
 1426 Update Cycle (RUC) weather forecast model developed by National Centers for
 1427 Environmental Prediction (NCEP). Similar models in Europe include the ECMWF IFS

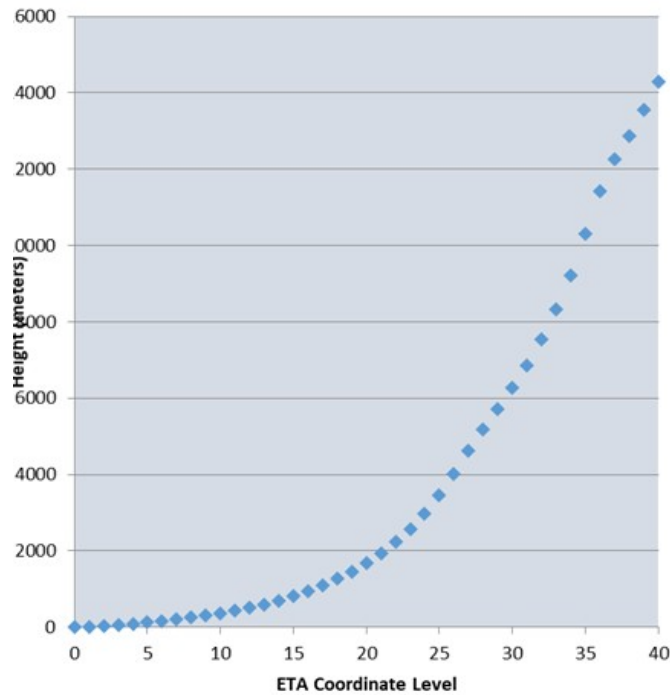
1428 model, developed by the European Centre for Medium-Range Weather Forecasts, the
1429 Consortium for Small-Scale Modelling (COSMO) led by the Deutscher Wetterdienst, the
1430 HIRLAM and HARMONIE developed by a consortium of meteorological institutes from
1431 Sweden, Norway, Denmark, Iceland, the Netherlands, Ireland, Spain, Estonia and Lithuania,
1432 and the Unified Model (UM), developed by Met Office UK. For information about these
1433 models, see Appendix A which contains links to each modelling system home page.

1434 Of these models, one of the most popular is the Weather Research and Forecast Model
1435 (WRF). WRF is a next-generation mesoscale numerical weather prediction model designed
1436 to serve operational forecasting and atmospheric research needs. The development of WRF
1437 has been a collaborative partnership, principally among the National Centre for Atmospheric
1438 Research (NCAR), the National Oceanic and Atmospheric Administration (NCEP), the
1439 Forecast Systems Laboratory (FSL), the Air Force Weather Agency (AFWA), the Naval
1440 Research Laboratory, University of Oklahoma, and the Federal Aviation Administration
1441 (FAA). WRF is a state-of-science three-dimensional numerical weather prediction model
1442 maintained at the National Centre for Atmospheric Research (NCAR) in collaboration with
1443 several governmental agencies (Skamarock et al. 2008, NCAR 2011). In 2004, WRF
1444 officially replaced MM5 (which is short for the Fifth Generation Penn State / NCAR
1445 Mesoscale Model) as the forecast engine. WRF includes much more recent technology and
1446 techniques in its system than MM5. MM5 was a regional mesoscale model used for creating
1447 weather forecasts and climate projections. It was a community model maintained by Penn
1448 State University and the National Centre for Atmospheric Research and was widely used in
1449 air quality applications. Over the last decade, there has been a switch from using MM5 to
1450 the more sophisticated WRF model, especially as the development of MM5 has ceased and
1451 the model is no longer being maintained as a workhorse model.

1452 WRF is a three-dimensional weather prediction model with non-hydrostatic dynamics, a
1453 variety of physics options and the capability to perform Four-Dimensional Data Assimilation
1454 (FDDA). The model can simulate meteorological phenomena such as tropical cyclones,
1455 severe convective storms, sea-land breezes and terrain-forced flows such as mountain
1456 valley wind systems. The Advanced Research WRF (ARW) can be used in applications
1457 ranging from horizontal scales of metres to thousands of kilometres. The model can be run
1458 over multiple nested grids. WRF is well suited for performing retrospective FDDA
1459 simulations to develop a three-dimensional high-resolution meteorological data set to
1460 support air quality modelling.

1461 WRF is routinely used to generate meteorological data either as a single surface station and\
1462 or a single vertical profile of data or as gridded 3D data in data-sparse regions. The model is
1463 typically initialised with a global forecast model such as ECMWF (European Centre for
1464 Medium-Range Forecasts), or the Global Forecast System (GFS) at a resolution of
1465 approximately 0.5°. The first coarse domain is typically at a grid size of 36 km, followed by
1466 two or three nested domains within grid resolutions close to the ratio of 3:1. WRF is routinely
1467 run with 30 – 40 vertical layers from the surface to 100 hPa. Figure 3-9 shows the vertical
1468 distribution of layers. The layer thickness increases from the surface to the upper
1469 atmosphere.

1470

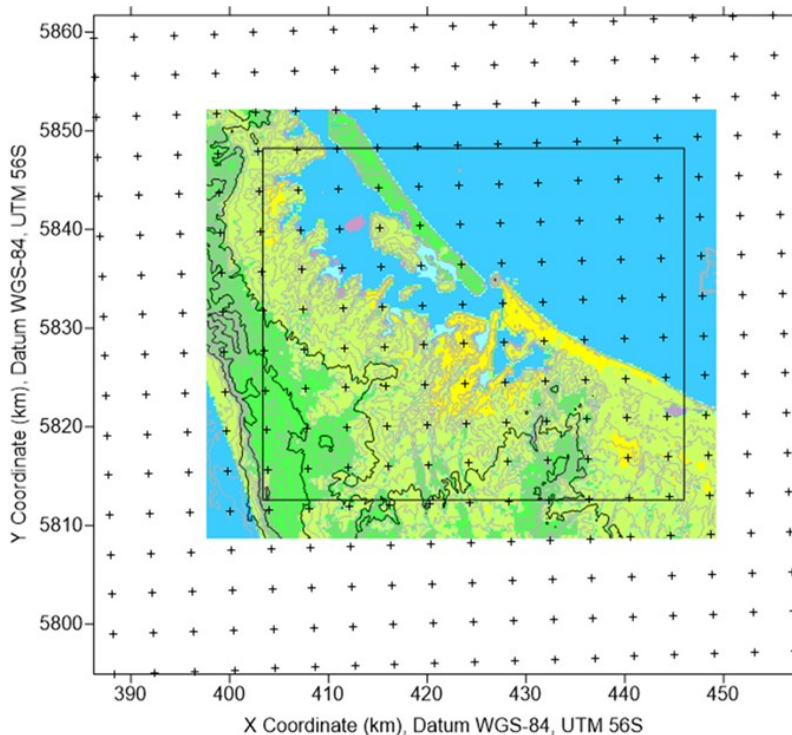


1471

1472 **Figure 3-9** Typical vertical layer structure and levels of WRF (courtesy of Atmospheric
1473 Science Global)

1474 Figure 3-10 shows crosshair cursors, each representing a vertical profile of 40 levels of
1475 meteorological data (wind speed, wind direction, temperature and moisture parameters)
1476 which combined represent a gridded hourly 3D WRF data set. This gridded data can then
1477 be used to represent the 'Initial Guess wind field' of a diagnostic meteorological model,
1478 which is run at a much finer spatial resolution than the WRF model.

1479



1480

1481 **Figure 3-10** WRF grid points used as gridded data encompass the meteorological model
1482 domain of a diagnostic meteorological model (courtesy of Atmospheric Science Global)

1483 Some models contain software that will allow the transformation of the numerical model data
1484 into a format that either the dispersion model or the meteorological processor of the
1485 dispersion model can read directly. Usually, this software is independent, short and
1486 straightforward and must be executed on the same computer that created the meteorological
1487 data. The extracted output of such software is usually a large ASCII-format data set of a
1488 specific period in time, which may be a few months or a year-long data set, and may be a
1489 subset of the original model domain at either the innermost nest or outer nests. The output
1490 data can be a single point or multiple points. Multiple gridded data points can generate huge
1491 files, so they must be split up by month. It should be noted that WRF is typically run under
1492 Linux servers and is highly computational demanding. Other tools which run easily on a PC,
1493 such as the MMIF, convert prognostic meteorological model output files to the parameters
1494 and formats required for direct input into dispersion models, including AERMOD,
1495 SCHICHEM and CALPUFF. MMIF is briefly discussed below.

1496 3.4.2. Prognostic Meteorological Model Data – Mesoscale Model 1497 Interface Program (MMIF)

1498 The Mesoscale Model Interface Program (User Manual, 2021) was developed by Ramboll
1499 US Consulting, Inc. (formerly ENVIRON) on behalf of the US EPA, Office of Air Quality
1500 Planning and Standards (OAQPS).

1501 MMIF is an interface program developed to convert prognostic meteorological output fields
1502 to the parameters and formats required for direct input into dispersion models. MMIF
1503 specifically processes geophysical and meteorological output fields from the Fifth Generation
1504 Mesoscale Model (MM5, Version 3) and the Weather Research and Forecasting (WRF)
1505 model.

1506 Many models now support output data from prognostic meteorological models, particularly
1507 MM5 and WRF; this capability has proven very useful in data-sparse areas. With the
1508 advancement of prognostic meteorological output quality, prognostic data are increasingly
1509 used in air quality modelling. Key features of the MMIF program include:

- 1510 ● applicability on either Linux or Windows platforms;
- 1511 ● a simple text-based user interface control file;
- 1512 ● options to re-diagnose or pass through Planetary Boundary Layer depth;
- 1513 ● an option to generate output on a subset of the meteorological modelling grid;
- 1514 ● an optional mass-weighted vertical aggregation of multiple MM5/WRF layers; and
- 1515 ● an optional mass-weighted vertical interpolation from MM5/WRF layers to a fixed
1516 height above ground layer structure.

1517 The MMIF program supports AERMOD, CALPUFF and SCIPUFF.

1518 In summary, there are advantages of running MMIF to transform prognostic data directly to a
1519 form that dispersion models can use; these typically include:

- 1520 ● removing the need for significant decisions by the modeller concerning
1521 meteorological data switches and choices;
- 1522 ● providing uniformity of meteorological data for review;
- 1523 ● no missing data; and
- 1524 ● providing data over data-sparse regions.

1525 However, there are also significant disadvantages, the most prominent being that the
1526 prognostic model output is often too coarse (12 - 36 km) and will not represent the fine-scale
1527 topography and inhomogeneous land use types surrounding the location of odour emissions.
1528 In addition, numerical model data are known to be primarily responsible for the positive wind
1529 speed biases seen at the surface (Jimenez & Dudhia, 2013).

1530 3.4.3. Screening Meteorological Models – MAKEMET (for 1531 AERSCREEN) and ADMS-SCREEN

1532 3.4.3.1. MAKEMET

1533 The AERSCREEN model employs MAKEMET, a program that generates a matrix of
1534 meteorological conditions in the form of AERMOD-ready surface and profile files based on
1535 user-specified surface characteristics, ambient temperatures, minimum wind speed and
1536 anemometer height (Figure 3-11). Recommended default values for routine MAKEMET are
1537 0.5 m/s for the minimum wind speed and 10 m for the anemometer height. MAKEMET
1538 allows the user to specify more than one set of surface characteristics and ambient
1539 temperature, such as for seasonal or monthly variations in surface characteristics and will
1540 concatenate the resulting meteorological matrices into single surface and profile files.
1541 MAKEMET will also allow the user to specify a single or range of wind directions – useful for
1542 assessing building downwash. However, AERSCREEN will set the wind direction to a single
1543 direction of 270 degrees.

1544

```
ENTER SFC MET FILE NAME
ENTER PFL MET FILE NAME
ENTER MIN. WS (M/S)
ENTER ANEM HT (M)
ENTER OPTION TO ADJUST U* (Y=adjust,N=no adjustment)
ENTER NUMBER OF WIND DIRECTIONS
If the user enters one for the number of wind directions
ENTER WIND DIRECTION
Otherwise
ENTER STARTING WIND DIRECTION
ENTER CLOCKWISE WIND DIRECTION INCREMENT
ENTER MIN AND MAX AMBIENT TEMPS IN KELVIN
ENTER ALBEDO
ENTER BOWEN RATIO
ENTER SURFACE ROUGHNESS LENGTH IN METERS
DO YOU WANT TO GENERATE ANOTHER MET SET THAT WILL BE
APPENDED TO CURRENT FILE?
[TYPE EITHER "Y" OR "y" FOR YES; OR HIT "ENTER" TO EXIT]
If ("Y" or "y") then the program loops through prompts 7 through 10 for each additional data set (e.g. seasonal).
```

1545

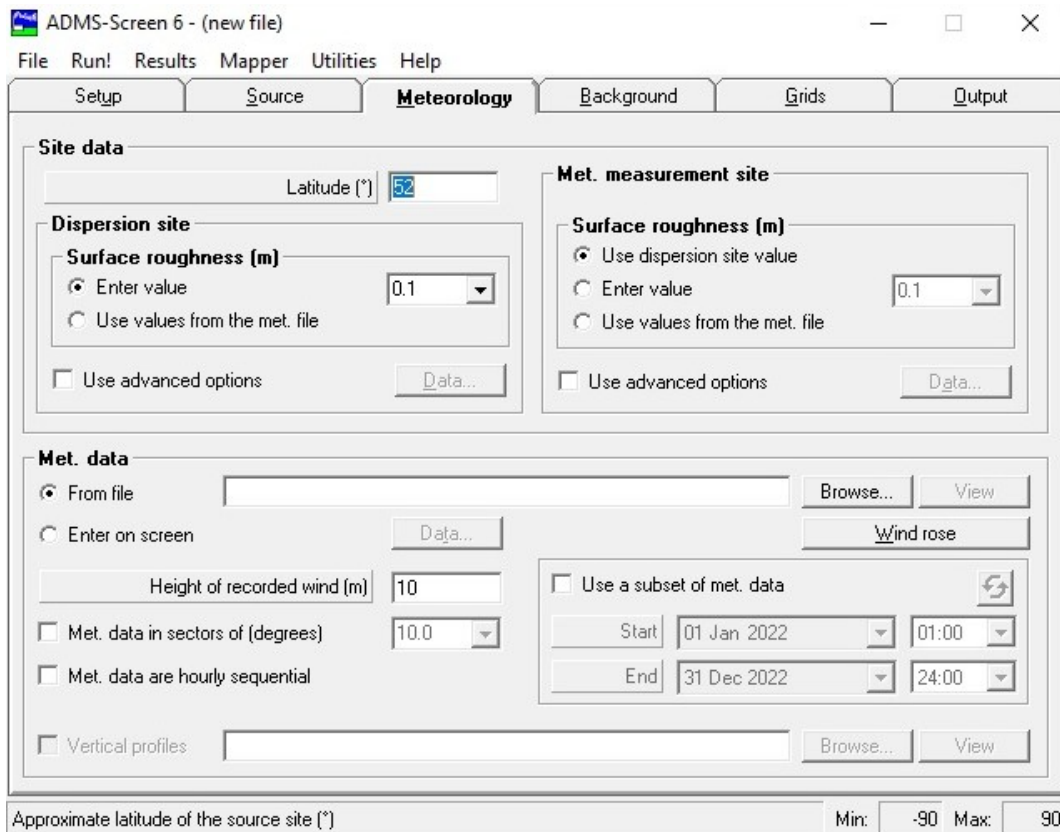
1546 **Figure 3-11** User Prompts for MAKEMET

1547 MAKEMET calculates friction velocity (m/s), Monin-Obukhov length (m), and mechanical
1548 mixing height (m). MAKEMET also calculates the convective mixing height (m) for

1549 convective cases and computes the matrix's boundary layer parameters for each
 1550 combination. MAKEMET typically generates around 300-400 hours of meteorological data.

1551 3.4.3.2. ADMS-SCREEN

1552 The ADMS-SCREEN model uses either standard ADMS format meteorological files or on-
 1553 screen meteorological input. Figure 3-12 shows the ADMS-SCREEN Graphical User
 1554 Interface Page for user-defined meteorological input data. The user is required to enter a
 1555 value for the surface roughness both at the site of emission release and at the site of the
 1556 meteorological station. Meteorological data can either be entered from an external file or
 1557 directly into the screen. Unlike MAKEMET, the model does not create a range of
 1558 combinations of meteorological data. The model will require essential input such as wind
 1559 speed, wind direction, temperature and cloud cover or solar radiation and will then compute
 1560 the boundary parameters for each given meteorological hour. However, ADMS-SCREEN
 1561 can utilise statistical meteorological data from the UK Cambridge Environmental Research
 1562 Centre (CERC), which is free for ADMS-Screen users. This data would be input into ADMS-
 1563 SCREEN as an external file.



1564
 1565 **Figure 3-12** Graphical User Interface for entering meteorological data into ADMS-SCREEN

1566 3.4.4. Gaussian Plume Models – AERMOD, ADMS, AODM, ARIA
 1567 Impact

1568 3.4.4.1. AERMET for AERMOD

1569 AERMOD¹ is supported by a meteorological preprocessor, AERMET, which organises the
 1570 available meteorological data into a format suitable for use by the dispersion model.
 1571 AERMET is programmed to read US National Weather Service hourly surface observations
 1572 and US National Weather Service twice-daily upper air soundings. In addition, the program
 1573 can read on-site specific meteorological data, and, beginning with AERMET Version 22112
 1574 (April 2022) can read prognostic meteorological data processed through MMIF.

1575 There are two stages of data processing with AERMET. The first stage extracts
 1576 meteorological data from archive data files and processes the data through various quality
 1577 assessment checks. The second stage estimates the necessary boundary layer parameters
 1578 for use by AERMOD. The processor writes two files for AERMOD. The first is the hourly
 1579 boundary layer parameter estimates, and the second is a file of multi-level observations of
 1580 wind speed and direction, temperature and standard deviation of the fluctuating wind
 1581 components.

1582 There is no standard format for site-specific meteorological data, allowing multiple levels of
 1583 data from a tower or remote sensing instrumentation to be easily included in the model. In
 1584 addition, the model allows near-surface measurements such as insolation, net radiation and
 1585 temperature difference to be included in the database.

1586 The output data from AERMET for AERMOD consists of two files, one a surface file that
 1587 includes all the surface parameters listed in Figure 3-13 and a vertical profile file of
 1588 meteorological data, Figure 3-14, which is usually from the nearest relevant airport where
 1589 twice daily radiosonde soundings are normal.

27.330S	152.975E	UA_ID:	SF_ID:	OS_ID: 00011111	VERSION: 19191	ADJ_U*															
18 7 1 182 1	-6.6	0.060	-9.000	-9.000	-999.	50.	4.0	1.0000	1.62	1.00	1.45	232.8	10.0	288.5	10.0	9999	-9.00	94.	1025.	2	NAD-OS
18 7 1 182 2	-5.6	0.050	-9.000	-9.000	-999.	50.	2.8	1.0000	1.62	1.00	0.93	229.6	10.0	288.6	10.0	9999	-9.00	94.	1025.	0	NAD-OS
18 7 1 182 3	-5.6	0.050	-9.000	-9.000	-999.	50.	2.8	1.0000	1.62	1.00	1.00	238.6	10.0	288.1	10.0	9999	-9.00	95.	1025.	0	NAD-OS
18 7 1 182 4	-6.7	0.060	-9.000	-9.000	-999.	51.	4.0	1.0000	1.62	1.00	1.62	238.4	10.0	288.4	10.0	9999	-9.00	95.	1025.	0	NAD-OS
18 7 1 182 5	-8.8	0.080	-9.000	-9.000	-999.	57.	7.8	1.0000	1.62	1.00	2.00	232.3	10.0	288.8	10.0	9999	-9.00	94.	1024.	2	NAD-OS
18 7 1 182 6	-8.8	0.080	-9.000	-9.000	-999.	65.	7.8	1.0000	1.62	1.00	2.11	231.8	10.0	288.9	10.0	9999	-9.00	94.	1024.	2	NAD-OS
18 7 1 182 7	-7.8	0.080	-9.000	-9.000	-999.	65.	7.0	1.0000	1.62	1.00	2.09	229.7	10.0	289.2	10.0	9999	-9.00	93.	1025.	5	NAD-OS
18 7 1 182 8	4.4	0.200	0.308	0.005	242.	215.	-165.8	1.0000	1.62	0.44	2.41	222.9	10.0	289.9	10.0	9999	-9.00	92.	1025.	8	NAD-OS
18 7 1 182 9	70.1	0.210	0.827	0.005	295.	231.	-12.1	1.0000	1.62	0.29	2.34	223.0	10.0	290.9	10.0	9999	-9.00	88.	1026.	6	NAD-OS
18 7 1 182 10	132.6	0.200	1.360	0.005	695.	215.	-5.5	1.0000	1.62	0.24	1.97	206.8	10.0	292.1	10.0	9999	-9.00	83.	1026.	2	NAD-OS
18 7 1 182 11	120.8	0.180	1.403	0.005	838.	183.	-4.4	1.0000	1.62	0.22	1.71	203.9	10.0	293.4	10.0	9999	-9.00	77.	1026.	8	NAD-OS
18 7 1 182 12	160.6	0.170	1.617	0.005	965.	168.	-2.8	1.0000	1.62	0.22	1.49	187.9	10.0	294.1	10.0	9999	-9.00	76.	1026.	7	NAD-OS

1590

1591 **Figure 3-13** Format of hourly surface data developed by AERMET for AERMOD

1592 The header record for a surface parameter file contains: the longitude and latitude of the
 1593 surface station; the IDs of the upper air (UA), surface (SF) and on site (OS) stations; the
 1594 AERMET version used for preparing the file; a flag indicating if the surface friction velocity
 1595 has been adjusted for low wind speed stable conditions; the threshold applied for 1-minute
 1596 winds; and flags for substitution of missing cloud cover or temperature.

1597 The data records in columns from left to right stand for;

1598 *year, month, day, j_day, hour, H, u*, w*, VPTG, Zi_c, Zi_m, L, Z_o, B_o, r, W_s, W_d, Z_{ref}, temp,*
 1599 *ztemp, ipcode, pamt, rh, pres, ccvr, WSADJ*

1600 *and where*

j_day = Julian day

W_s = reference wind speed (m/s)

99 1The US EPA in conjunction with the American Meteorological Society are the main
 100 developers of the AERMOD modelling system.
 101

- H = sensible heat flux (W/m²)
- u^* = surface friction velocity (m/s)
- w^* = convective velocity scale (m/s)
- VPTG = vertical potential temperature gradient above Z_{ic} (K/m)
- Z_{ic} = convective boundary layer height (m)
- Z_m = mechanical boundary layer height (m)
- L = Monin-Obukhov length (m)
- Z_o = surface roughness length (m)
- B_o = Bowen ratio
- r = albedo
- W_d = reference wind direction (degrees)
- Z_{ref} = reference height for temperature (m)
- lpcode = precipitation code (0=none, 11=liquid, 22=frozen, 99=missing)
- Pamt = precipitation amount (mm/hr)
- Rh = relative humidity (percent)
- Pres = station pressure (mb)
- Ccvr = cloud cover (tenths)
- WSADJ = wind speed adjustment and data source flag.

18	7	1	1	10.0	0	244.97	1.37	15.37	99.00	99.00
18	7	1	1	30.0	0	203.25	2.35	19.08	99.00	99.00
18	7	1	1	60.0	0	209.38	2.57	19.16	99.00	99.00
18	7	1	1	100.0	0	204.91	3.19	19.21	99.00	99.00
18	7	1	1	140.0	0	199.19	3.68	19.09	99.00	99.00
18	7	1	1	240.0	0	84.61	2.94	18.52	99.00	99.00
18	7	1	1	480.0	0	75.35	2.61	17.22	99.00	99.00
18	7	1	1	820.0	0	74.82	2.13	15.25	99.00	99.00
18	7	1	1	1250.0	1	35.09	6.01	9.54	99.00	99.00
18	7	1	2	10.0	0	232.43	0.78	15.47	99.00	99.00
18	7	1	2	30.0	0	178.96	1.47	18.84	99.00	99.00
18	7	1	2	60.0	0	131.74	1.82	18.90	99.00	99.00
18	7	1	2	100.0	0	115.58	2.24	18.93	99.00	99.00
18	7	1	2	140.0	0	103.25	2.75	18.82	99.00	99.00
18	7	1	2	240.0	0	86.04	2.97	18.27	99.00	99.00
18	7	1	2	480.0	0	70.79	3.07	17.07	99.00	99.00
18	7	1	2	820.0	0	68.37	2.65	15.21	99.00	99.00

1601

1602 **Figure 3-14** Format of an hourly vertical upper profile developed by AERMET from twice
 1603 daily radiosonde soundings for AERMOD

1604 There is no header row in a profile data file. The data records in columns from left to right
 1605 stand for;

1606 *year, month, day, hour, height, top, WDnn, WSnn, TTnn, Sann, SWnn*

1607 *where*

height = measurement height (m)

top = 1, if highest level, else 0

WDnn = wind direction at current level (deg)

WSnn = wind speed at current level (m/s)

TTnn = temperature at the current level (°C)

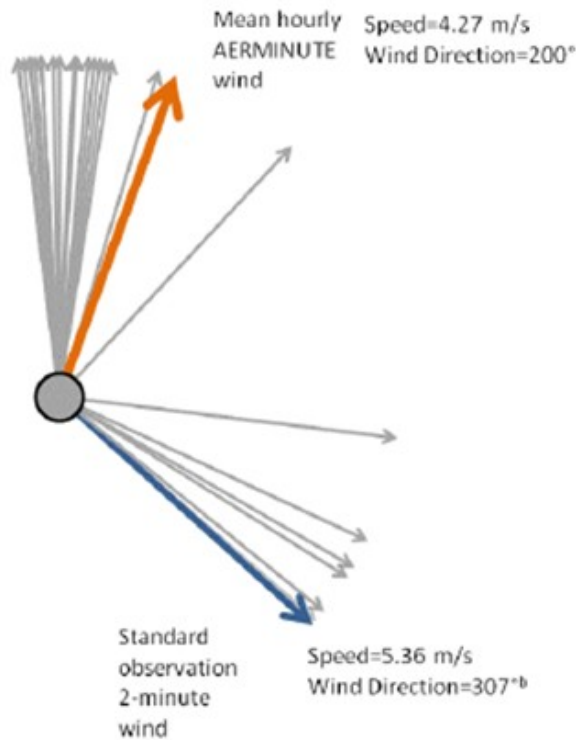
SAnn = sigma theta (degrees)

SWnn = sigma w (m/s)

1608 Where turbulence values of sigma theta and sigma w are not measured these values are
1609 represented in the file as missing value indicator '99.00'. The model then computes the
1610 turbulence using similarity theory.

1611 In addition to AERMET, which outputs hourly data from NWS data (where the hourly
1612 averaged wind speed and wind direction are represented by the average of the last two
1613 minutes before each hour), there is another US EPA-developed meteorological preprocessor
1614 called AERMINUTE which reads 1-minute and optionally 5-minute ASOS data to calculate
1615 hourly average winds for input into AERMET.

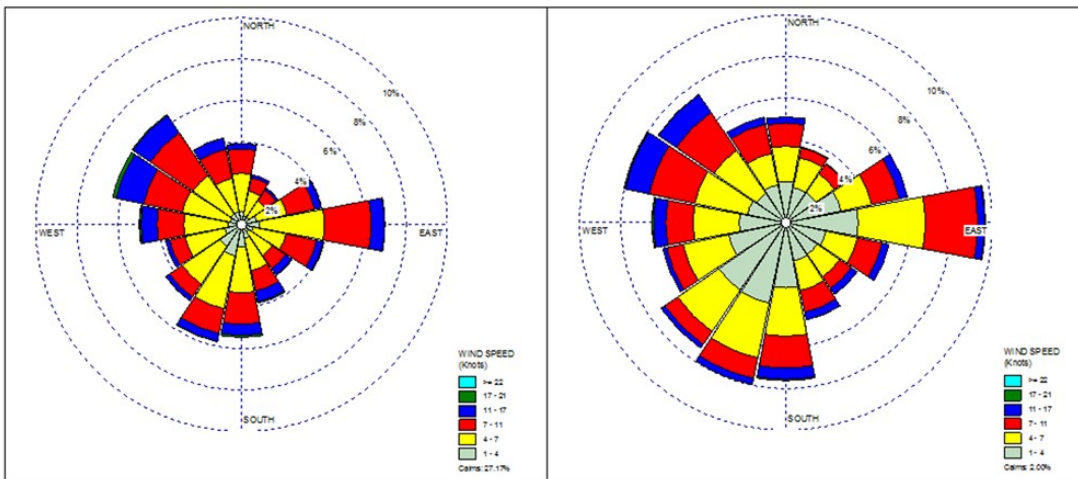
1616 AERMINUTE was developed as there were several concerns related to the use of NWS
1617 meteorological data especially if there was a high incidence of calms and variable winds
1618 reported from the automatic stations (ASOS). AERMINUTE was developed to reduce the
1619 number of calms and missing winds in the surface data file as AERMOD cannot simulate
1620 dispersion under either calm or missing wind conditions. The effect of using AERMINUTE
1621 can be significant. Figure 3-15 shows (as grey arrows) the 1-minute wind direction as
1622 recorded. The blue arrow represents the hourly average wind represented by the final 2
1623 minutes before the hour as done by AERMET. In contrast, the orange wind arrow represents
1624 the mean hourly AERMINUTE wind direction. In addition to computing a new, more
1625 accurate and representative one-hour average wind speed and wind direction, AERMINUTE
1626 also decreases the number of calms by increasing the number of very light winds in the
1627 range 0.1 – 0.5 m/s. Figure 3-16 provides a wind rose with and without the use of
1628 AERMINUTE. For this example, the number of calms was reduced from 27% to 2%.



1629

1630 **Figure 3-15** AERMINUTE recomputes the hourly average wind speed and wind direction
1631 from 1 and 5-minute ASOS data (courtesy of Atmospheric Science Global)

1632



1633

1634 **Figure 3-16** Annual wind rose with (right) and without AERMINUTE (left) (courtesy of J.
1635 Barclay)

1636 3.4.4.2. ADMS

1637 ADMS 5 has a built-in meteorological preprocessor that allows both standard and more
1638 specialist input of flexible input meteorological data. Hourly sequential and statistical data
1639 can be processed, and all input and output meteorological variables are written to a file after
1640 processing. The ADMS meteorological processor is similar to AERMET in that the user
1641 must provide basic surface input data such as wind speed, wind direction, temperature,
1642 pressure, cloud cover, and cloud ceiling height. In addition, twice daily upper air data must

1643 also be provided as well as surface characteristics such as surface roughness length, albedo
1644 and Bowen ratio. The meteorological processor then computes the boundary layer
1645 parameters similarly to AERMET.

1646 The WRF-to-Met utility (Cambridge Environmental Research Consultants, 2016) is a
1647 command line application which extracts meteorological data from WRF netCDF files and
1648 creates ADMS format *.met files. For the purposes of using WRF data in ADMS, it is
1649 assumed to represent the overall meteorological conditions for the previous hour, thus
1650 matching the hour-ending ADMS convention. The WRF-to-Met utility always extracts data
1651 from the lowest grid layer, except if the U10, V10 option for wind speed is selected, in which
1652 case the wind speed and direction will be extracted from the values at 10 metres. The utility
1653 does not create a profile file containing meteorological data at multiple heights. The utility
1654 extracts most WRF variables with the assumption that their units in WRF are the same as
1655 those required in ADMS, so it does not perform any unit conversions except for temperature,
1656 where a conversion from Kelvin to Celsius is required.

1657 An example output file created by the WRF-to-Met utility is shown below as Figure 3-17,
1658 viewed in Notepad.

```
File created by WRFtoMet.exe
Date/time created: 14/8/2014 19:20:30
Model version: 1
Location input for met data extraction (x, y): (13500.00,-668000.00)
Met. data created for location with WRF index (34,25)
Data created from WRF directory: P:\WRF\OUTPUT
The height of the recorded wind is 10.0 m.
The met. data are hourly sequential.

VARIABLES:
S
YEAR
DAY
HOUR
U
PHI
T0C
SOLAR RAD
FTHTAO

DATA:
2010, 1, 9, 5.24, 78.6, 16.28, 334.8, 107.1
2010, 1, 10, 4.95, 75.9, 17.24, 522.6, 186.3
2010, 1, 11, 4.89, 83.4, 18.76, 656.9, 246.8
2010, 1, 12, 5.41, 94.1, 19.28, 725.9, 316.3
2010, 1, 13, 4.79, 107.8, 20.31, 723.5, 311.7
2010, 1, 14, 5.67, 107.4, 19.82, 650.3, 337.8
```

1659
1660 **Figure 3-17** Example WRF-to-Met Utility output file

1661 3.4.4.3. AODM

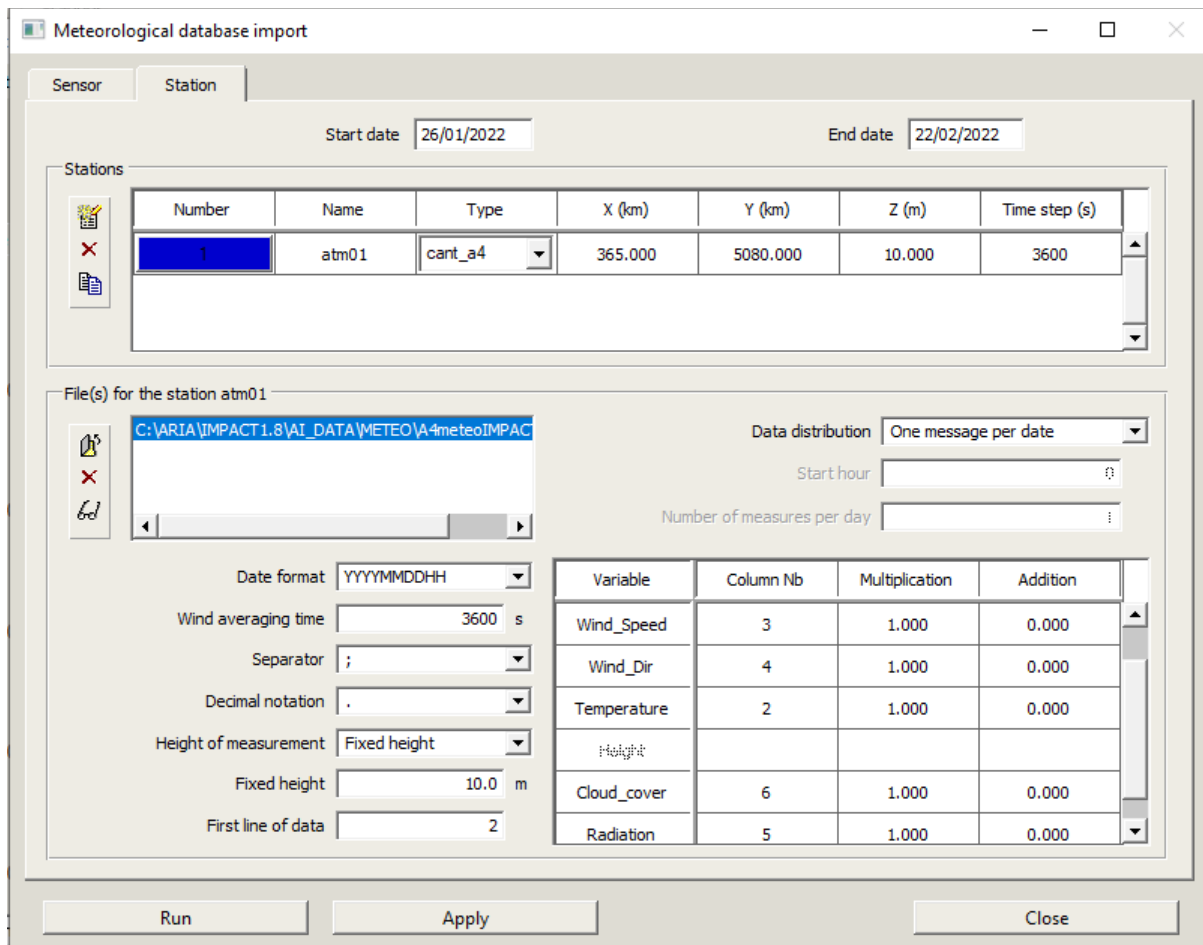
1662 The Austrian Odour Dispersion Model, AODM (Shaubberger, 2000), is a Gaussian model
1663 adapted to predict odour sensation. It estimates the daily and seasonal variation of the
1664 odour emission, the average ambient odour concentration and the momentary (peak)
1665 concentration for the time interval of a single human breath (approximately 5 seconds).
1666 Peak concentrations further downwind are modified by an exponential attenuation function
1667 for which the ratios of the standard deviations of the wind components to the average wind
1668 speed (σ/u) must either be taken from the literature or calculated from ultrasonic
1669 anemometer data.

1670 AODM estimates mean ambient concentrations by the Austrian regulatory dispersion model
1671 (ÖNorm M 9440, 1992/96; Kolb, 1981) and transforms these to instantaneous values
1672 depending on the atmosphere's stability. ÖNorm M 9440 is a Gaussian dispersion model for
1673 continuous, buoyant plumes from stationary sources for use in flat terrain areas. The odour
1674 concentration of the plume's centre line is calculated using statistics of stability classes
1675 representative of the Austrian flatlands north of the Alps. The model is applied for single-
1676 stack emissions and distances from 100 metres to 15 kilometres. Plume rise formulae used
1677 in the model are a combination of formulas suggested by Carson & Moses (1969) and Briggs
1678 (1975). The model uses a traditional discrete stability classification scheme with dispersion
1679 parameters developed by Reuter (1970). AODM was developed in cooperation with the
1680 University of Veterinary Medicine Vienna and has been used mainly to determine adequate
1681 separation distances to populated areas from livestock buildings.

1682 3.4.4.4. ARIA Impact

1683 ARIA Impact has a built-in meteorological preprocessor that allows the user to define or
1684 import a time series of real meteorological data conforming to one of the available formats
1685 and to create an internal meteorological database. The user must provide basic input data
1686 by choosing from a list of available meteorological parameters (such as wind speed,
1687 pressure or cloud cover), defining a sensor type and then associating one or more stations.
1688 At least wind speed, direction and temperature parameters are necessary to import in order
1689 to be able to carry out dispersion simulations later on. The position (x, y, height) and sensor
1690 type are required for each station. It is possible to choose different time resolutions of the
1691 meteorological data in relation to the statistical calculation time step. The user interface has
1692 a wizard for importing data and parameters, with buttons and tables of all available options
1693 and variables, as in the following example (Figure 3-18).

1694
1695



1696
1697

1698 **Figure 3-18** Example of the ARIA Impact Graphical User Interface to import / generate
1699 meteorological data (courtesy of ARIANET)

1700

1701 All meteorological parameters are categorised into different classes, which allow the
1702 calculation of frequency distributions and serve as a basis for the statistical analysis and
1703 calculation of wind roses based on the meteorological data available. The user can select
1704 the formula for stability class computation from the option list according to the parameters
1705 found in the meteorological database.

1706

1707 In order to consider the vertical variation of meteorological variables, ARIA Impact can
1708 compute vertical profiles of both wind speed and temperature based on measurements
1709 made at ground level as well as on atmospheric turbulence, in order to calculate their values
1710 at the stack height and to use them in the dispersion calculation.

1711 3.4.5. Lagrangian Puff Models – CALPUFF, SCIPUFF

1712 3.4.5.1. CALMET for CALPUFF

1713 In its simplest terms, CALMET (Scire et al., 2000) is a meteorological model that develops
1714 hourly wind and temperature fields on a three-dimensional gridded modelling domain.
1715 CALMET can read both numerical weather data output from the WRF model and surface
1716 observation data to assist in the development of three-dimensional wind fields. Associated
1717 two-dimensional fields such as mixing height, surface characteristics, and dispersion

1718 properties are also included in the file produced by CALMET. CALPUFF, CALMET's
1719 dispersion model, is a transport model that reads the output of the CALMET model to advect
1720 'puffs' of material emitted from modelled sources, simulating dispersion and transformation
1721 processes along the way.

1722 The CALMET meteorological model consists of a diagnostic wind field module and
1723 micrometeorological modules for over-water and over-land boundary layers. The diagnostic
1724 wind field module uses a two-step approach to the computation of the wind fields (Douglas &
1725 Kessler, 1988). In the first step, an initial-guess wind field is adjusted for kinematic effects of
1726 terrain, slope flows, and terrain blocking effects to produce a Step 1 wind field. The second
1727 step consists of an objective analysis procedure to introduce observational data into the Step
1728 1 wind field to produce a final wind field.

1729 The CALMET model contains two boundary layer models for application to over-land and
1730 over-water grid cells. Over land surfaces, the energy balance method of Holtslag and van
1731 Ulden (1983) is used to compute hourly gridded fields of the sensible heat flux, surface
1732 friction velocity, Monin-Obukhov length, and convective velocity scale. Mixing heights are
1733 determined from the computed hourly surface heat fluxes and observed temperature
1734 soundings using a modified Carson (1973) method based on Maul (1980). The model also
1735 determines the gridded fields of Pasquill-Gifford-Turner (PGT) stability class and optional
1736 hourly precipitation rates. Over water, the model uses a profiling technique, using the air-sea
1737 temperature difference to determine the micrometeorological parameters in the marine
1738 boundary layer.

1739 The CALPUFF model can be run in several modes, where each mode requires a different
1740 type of meteorological data. The following lists three modes to run CALMET and a fourth
1741 mode using other meteorological processors.

- 1742 ● **CALMET No-Observations (NOOBS) Mode.** CALMET using gridded numerical
1743 model output (e.g., from the MM5, WRF, RAMS, RUC, Eta or TAPM models). No
1744 surface, upper air or buoy observations are used in No-Obs mode.
- 1745 ● **CALMET Hybrid Mode (HYBRID).** CALMET using a combination of gridded
1746 numerical meteorological data supplemented by surface and optional over-water
1747 buoy data.
- 1748 ● **CALMET Observations-Only (OBS) Mode.** – CALMET using observed surface and
1749 upper air data, plus optional buoy data.
- 1750 ● **Single meteorological station dataset.** CALMET is not used, but single station
1751 meteorological data in the form of AERMOD, AUSPLUME, CTDMPPLUS and ISCST3
1752 may all be passed directly into CALPUFF.

1753 If good quality gridded, prognostic meteorological data are available. CALMET NOOBS
1754 mode is recommended as the preferred method for regulatory screen modelling. When run
1755 this way, CALMET uses gridded wind fields generated by one of the numerical prognostic
1756 models. The procedure permits the prognostic model to run with a significantly larger
1757 horizontal grid spacing than the diagnostic model. The 3D gridded data typically contains
1758 winds, vertical velocity, pressure, temperature and moisture parameters.

1759 The essential benefits of running the model in NOOBS mode are:

- 1760 ● CALMET can be run on a much finer horizontal resolution than the prognostic model.
1761 The model will adjust the winds for the fine-scale terrain, and Land use of the
1762 CALMET model domain;
- 1763 ● Spatial variability in the horizontal and the vertical;
- 1764 ● Simplicity of the NOOBS run, fast and efficient;
- 1765 ● No additional data are required;

- 1766 ● Most of the decision-making by the user is eliminated; and
- 1767 ● No over-water data required to invoke the over-water boundary layer algorithm.

1768 The HYBRID mode is considered an ‘advanced simulation’ since it combines the numerical
1769 prognostic model data in a gridded 3D format in conjunction with surface observation data.
1770 More work is required by the user to collect, format and quality control-check the data. In
1771 addition, the user must make specific model choices over various critical parameters
1772 pertaining to the distance weighting factors of the surface observations.

1773 Finally, CALMET can be run in OBS-only mode. At a minimum CALMET must be provided
1774 hourly surface data from one or many stations as well as radiosonde data at intervals no
1775 more than 14 hours apart. This run requires significant effort by the modeller who needs to
1776 decide multiple choices pertaining to the station data, as well as managing the quality of the
1777 data and missing data.

1778 There is a final choice to run CALPUFF with single-station meteorology of the form used to
1779 run AERMOD, ISCST3, AUSPLUME and CTDMPLUS. There are significant benefits of
1780 running CALPUFF with single-station meteorology compared to running a steady-state
1781 Gaussian model with the same meteorology. These are as follows;

- 1782 ● The time required for a plume material to reach a receptor (the causality effect) is
1783 accounted for in the puff transport, unlike the plume models where the plume extends
1784 to infinity even after 1 hour with a 1 m/s wind;
- 1785 ● CALPUFF has memory in that each hours emissions and meteorology are retained
1786 and may impact the concentrations during a subsequent hour; and
- 1787 ● CALPUFF is able to model calms, unlike regular plume models.

1788 3.4.5.2. SCIPUFF

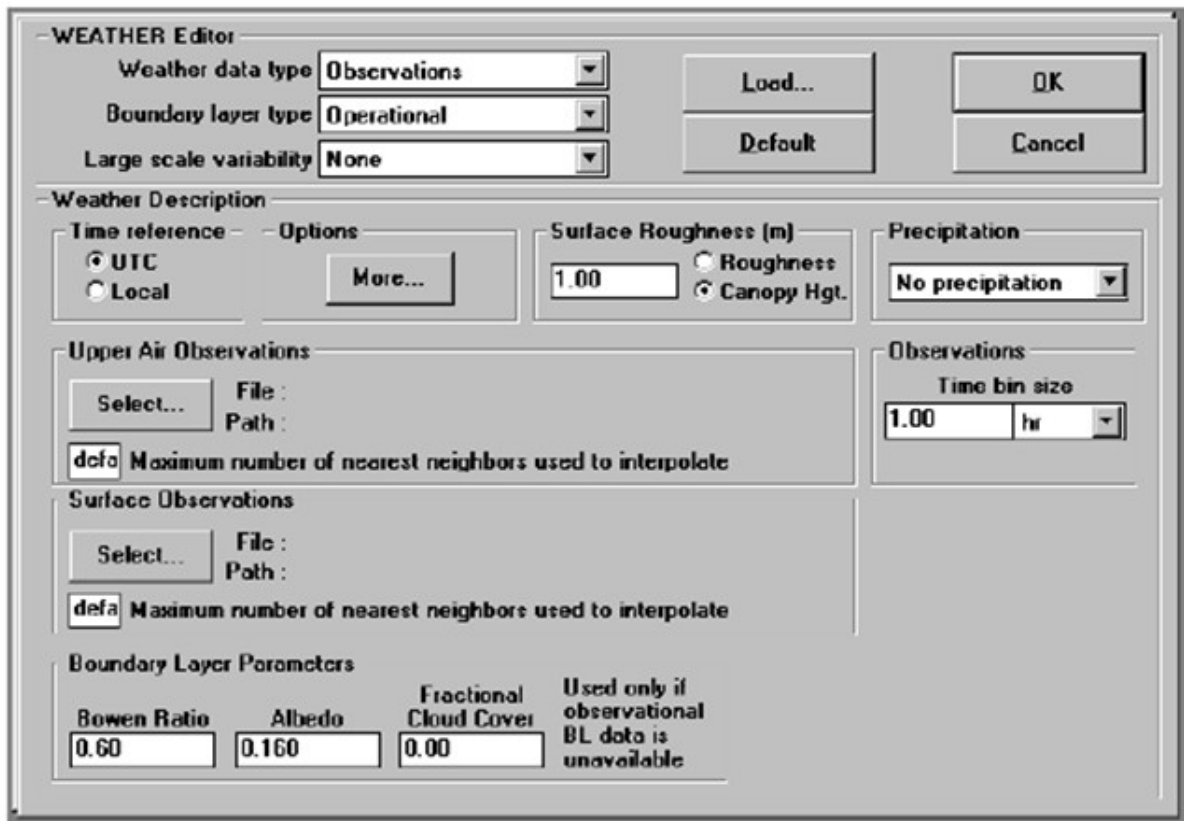
1789 SCIPUFF is a Lagrangian puff dispersion model that uses a collection of Gaussian puffs to
1790 represent an arbitrary, three-dimensional, time-dependent concentration field. The turbulent
1791 diffusion parameterisation is based on modern turbulence closure theory (Sykes, 1998).
1792 SCIPUFF can use several types of meteorological data for input, including

- 1793 ● Fixed winds where wind speed and direction are assumed constant;
- 1794 ● Observational input where time-dependent observations are combined from multiple
1795 surface stations and/or upper-air profiles; and
- 1796 ● Time-dependent 3-dimensional gridded input.

1797 Planetary boundary layer turbulence is represented explicitly in terms of surface heat flux
1798 and shear stress using parameterised profile shapes. Turbulence data may be optionally
1799 specified as follows:

- 1800 1. Planetary boundary layer - Vertical profiles of the boundary layer scale turbulent
1801 velocity fluctuations, heat flux and turbulence length scales can be provided as input
1802 by the user, or may be modelled based on boundary layer characteristics. Options for
1803 treatment of the boundary layer include “calculated”, “observed” or “simple diurnal”.
1804 Input requirements depend on the boundary layer treatment type.
- 1805 2. Large-scale variability - For long-range transport, the mesoscale horizontal velocity
1806 fluctuations and turbulence length scale may be specified by the user, computed
1807 from a theoretical model or read from a meteorological observation file.

1808 A Graphical User Interface (GUI) shown in Figure 3-19 assists SCIPUFF users in setting up
1809 the required meteorological inputs for the model.



1810

1811 **Figure 3-19** SCIPUFF Graphical User Interface

1812 Observational weather data files must follow formatting specific to SCIPUFF. Fixed wind
 1813 information (10 metres above the surface) may be input directly. Gridded meteorology
 1814 output from the WRF model can be read directly by SCIPUFF without the need for pre-
 1815 processing with the MMIF program.

1816 SCIPUFF calculates surface heat flux using a surface energy balance model. Boundary
 1817 layer height is estimated from an evolution equation that models growth from convectively
 1818 and mechanically-driven entrainment into the overlying stable air. The Bowen ratio, Albedo,
 1819 and Cloud Cover parameters may be selected for use when observational boundary layer
 1820 data are unavailable. Alternately, the daytime and nighttime inversion heights and sensible
 1821 flux may be input directly. The surface roughness length and canopy height may also be
 1822 selected by the user.

1823 3.4.6. Lagrangian Particle-Puff Model – TAPM

1824 The meteorological component of TAPM is an incompressible, non-hydrostatic, primitive
 1825 equation model with a terrain-following vertical coordinate for three-dimensional simulations.
 1826 The model solves the momentum equations for horizontal wind components, the
 1827 incompressible continuity equation for vertical velocity, and scalar equations for potential
 1828 virtual temperature and specific humidity of water vapour, cloud water/ice, rainwater and
 1829 snow. The Exner pressure function is split into hydrostatic and non-hydrostatic components,
 1830 and a Poisson equation is solved for the non-hydrostatic component. Explicit cloud
 1831 microphysical processes are included. The turbulence terms in these equations have been
 1832 determined by solving equations for turbulence kinetic energy and eddy dissipation rate, and
 1833 then using these values in representing the vertical fluxes by a gradient diffusion approach,
 1834 including a counter-gradient term for heat flux. A vegetative canopy, soil scheme, and urban

1835 scheme are used at the surface, while radiative fluxes, both at the surface and at upper
1836 levels, are also included.

1837 3.4.7. Lagrangian Particle Models – SPRAY, AUSTAL (LASAT), 1838 LAPMOD and GRAL

1839 3.4.7.1. SPRAY

1840 SPRAY can be connected to different meteorological processors to acquire the three-
1841 dimensional fields of the average wind and air temperature and the variables related to
1842 particle dispersion. In particular, the most natural meteorological preprocessor for SPRAY is
1843 the mass-consistent diagnostic code SWIFT (Finardi et al. 1998), able to reconstruct, directly
1844 on the 3D grid needed by the dispersion code, wind and temperature fields over complex
1845 topography minimising the divergence of the flow. SWIFT considers data at discrete time
1846 steps, derived either from ground-level and vertical profiles measured at any point inside the
1847 computational domain, or considering a 3D grid of modelled data simulated at a coarser
1848 resolution. The code performs an initial interpolation phase in which all the available data are
1849 considered together and put on the target grid, followed by an adjustment phase during
1850 which the mass-conservation equation is applied to minimise the divergence field. During the
1851 adjustment phase, vertical velocities coupled with the underlying orographic profile are
1852 generated. This allows the SPRAY code to use wind fields generated at a relatively high
1853 resolution, down to less than a hundred metres, to describe meteorological fields in the
1854 presence of complex topographies. SWIFT can generate also 2D horizontal fields of the
1855 scaling variables describing the turbulence characteristics (such as the friction velocity u_* ,
1856 the Monin-Obukhov length L , the convective velocity scale w_* and the mixing-layer or stable-
1857 layer height) which depend on the horizontal structure of the land-use at the target
1858 resolution. These fields are then directly considered by the SPRAY code to generate the 3D
1859 fields of the variables related to the random particle movements through some embedded
1860 parameterisations. For the same purpose, the SPRAY code can be also coupled with the
1861 turbulence parameterisation code SurfPro (Silibello et al. 2006), which can also derive 2D
1862 time-dependent deposition velocities for the gaseous species or particulate matter to be
1863 considered in the dispersion simulation. SPRAY can be also connected with the output of the
1864 meteorological prognostic code RAMS (Pielke et al. 1992), using the preprocessing system
1865 named MIRS (Method for Interfacing Rams and Spray, Trini Castelli et al., 2000, 2014,
1866 2017). This interfacing code generates directly the 3D fields of the variables related to the
1867 random particle movements on the target grid using the data generated by RAMS and
1868 applying some different parameterisations.

1869 3.4.7.2. AUSTAL / LASAT

1870 The German regulatory model AUSTAL, formerly known as AUSTAL2000, Federal
1871 Environment Agency, 2014) is designed to work in two modes: statistical calculations and
1872 “time series” calculations. In the second case, AUSTAL needs hourly data for wind speed,
1873 wind direction in 10-degree sectors and stability class according to Klug/Manier (or,
1874 alternately, Obukhov length scale). Meteorological data are usually provided in the form of
1875 an AKTerm file (meteorological time series in the format used by the German Weather
1876 Service). An AKTerm is a text file with one line of data for each successive hour of the year.

1877 The internal boundary layer of AUSTAL is set up to assume a wind shear (Ekman spiral)
1878 with a height typical for central Europe. This must be considered when using AUSTAL in
1879 other countries. The wind shear can be switched off with the NOSTANDARD option
1880 NOSHEAR.

1881 Klug / Manier is the default German classification scheme for atmospheric stability. The Klug

1882 / Manier Class ID is specified as: 1: Klug / Manier I (very stable), 2: Klug/Manier II (stable), 3:
1883 Klug / Manier III/1 (stable to neutral), 4: Klug / Manier III/2 (neutral to unstable), 5: Klug /
1884 Manier IV (unstable), 6: Klug / Manier V (very unstable). The Klug / Manier stability classes 1
1885 to 6 correspond approximately to the Pasquill-Gifford classes F to A. In the time series file,
1886 the Monin-Obukhov length is specified as a more direct and detailed measure of the stability.

1887 A diagnostic wind field model (TALdia) is integrated in the meteorological preprocessor and
1888 allows dispersion calculations in inhomogeneous terrain or in the presence of buildings. In
1889 articulated terrain, wind field libraries from prognostic models can be integrated into
1890 AUSTAL. In steep terrain, the limits of the diagnostic wind field model (TALdia) are reached.
1891 Flows around buildings can also be taken into account via the integrated diagnostic wind
1892 field model. However, if an assessment in the recirculation zone in the lee of buildings is
1893 necessary, prognostic wind field modelling has to be implemented in advance outside the
1894 model system AUSTAL.

1895 3.4.7.3. LAPMOD

1896 The meteorological input of LAPMOD consists of three dimensional fields of wind and
1897 temperature and two dimensional fields of turbulent parameters as Monin Obukhov length,
1898 friction velocity, convective scale velocity, mixing layer height, etc. (Enviroware, 2022)
1899 LAPMOD reads directly the meteorological fields generated with CALMET (Scire et al.,
1900 2000), the diagnostic meteorological model also used in input by the CALPUFF dispersion
1901 model. LAPMOD is fully coupled with CALMET, up to version 6.5.0. CALMET also provides
1902 the geophysical variables required by LAPMOD, including terrain elevation, needed to
1903 calculate the concentration values, and roughness or the land use category, used to
1904 estimate deposition fluxes. LAPMOD can interpolate in time the meteorological output fields
1905 of CALMET with frequency specified in input by the user. For example, if the meteorological
1906 fields are provided with 1-hour time resolution, the user can specify to interpolate those fields
1907 every 10 minutes. Of course, LAPMOD can directly use high frequency time resolution when
1908 they are available (for example using CALMET 6.5.0). LAPMOD requires CALMET to be
1909 used with UTM (Universal Transverse Mercator) map projection, and all the “entities”
1910 (sources, receptors, etc.) in LAPMOD must be defined with those coordinates. The
1911 meteorological data needed by LAPMOD to perform a simulation may be within a single
1912 CALMET file, or within a series of files specified in chronological order (it may be useful, for
1913 example, to split the CALMET output over all the months of a year, when a single file could
1914 be too big).

1915 CALMET is the preferred tool to provide meteorological data to LAPMOD because, for
1916 example, it is 3-dimensional and allows the use of high space resolution for the geophysical
1917 features. However, other two options are possible.

1918 The first one consists in preparing the meteorological fields with a prognostic meteorological
1919 model such as MM5 or WRF, and then to post-process their output with the MMIF
1920 (Mesoscale Model Interface Program processor, US-EPA, 2021). LAPMOD reads directly
1921 the output of the MMIF processor, which can be contained in a single file or in a series of
1922 files specified in chronological order (as for CALMET). Since the map projection of MMIF is
1923 Lambert Conformal Conic (LCC), all the LAPMOD coordinates (domain, receptors,
1924 emissions) must be expressed with the same projection. MMIF, as CALMET, is 3-
1925 dimensional, but it typically does not provide information with the same spatial resolution,
1926 because it is based on the output of prognostic models.

1927 Finally, the meteorological input file of LAPMOD may also be prepared with the LAPMET
1928 processor, which reads the AERMOD meteorological files and writes its output in CALMET
1929 format. The meteorological file prepared in this way derives from a single meteorological
1930 station, therefore it is not 3-dimensional as those prepared with CALMET or MMIF. In other

1931 words, for a specific time, the meteorological field is homogeneous along the horizontal
1932 direction. The variation along the vertical direction is determined using the information within
1933 the vertical profile input file of AERMOD and with the similarity theory. LAPMET is currently
1934 used for debugging purposes and for comparing LAPMOD and AERMOD results using the
1935 same meteorological data.

1936 3.4.7.4. GRAL – The GRAZ Lagrangian Model

1937 In flat terrain, GRAL requires at a minimum the wind speed, wind direction, and stability
1938 class at a single point at any height. A power law as a function of the Obukhov length
1939 provides the vertical wind profile. The latter is derived from the stability class and the
1940 roughness length, which needs to be specified by the user and shall be representative for
1941 the whole modelling domain. Additional turbulence quantities, e.g. friction velocity or profiles
1942 of the standard deviation of wind velocity fluctuations, are mostly based on the well-known
1943 Monin-Obukhov similarity theory. GRAL also offers the possibility of using observed
1944 turbulent quantities (e.g. sonic anemometer observations) at a single location at multiple
1945 heights. In both cases, the input format is a simple text file.

1946 Time series of meteorological data can either be used without any further data processing,
1947 or - in case that wind and stability data are used – can be binned into user-defined classes in
1948 order to enhance computational efficiency. In this way, simulations for an entire year can be
1949 sped up by about a factor of 10 in most cases. GRAL comes with its own graphical user
1950 interface (GUI) which is recommended for preparing and processing all of the model input
1951 data.

1952 In the presence of either buildings or vegetation, GRAL automatically invokes a prognostic
1953 microscale wind-field model, which has been validated according to the German guideline
1954 VDI 3783-9 (Oettl, 2015a). Currently, only the 3D wind fields are used in the Lagrangian
1955 dispersion algorithm, because it was found that the usage of the turbulent kinetic energy
1956 does not improve results (Oettl, 2015b). The required input data for meteorology remains
1957 unchanged in the presence of buildings or vegetation.

1958 In complex terrain, 3D wind fields are provided by the prognostic mesoscale model GRAMM
1959 (Oettl, 2020). In the simplest mode, GRAMM can use the same meteorological data as
1960 GRAL in flat terrain, namely a single point observation of wind speed, direction, and stability
1961 class. The initial wind profile in GRAMM is obtained in the same manner as for GRAL in flat
1962 terrain, while the initial temperature stratification is assumed to be neutral. The incoming
1963 solar radiation is directly linked to the stability class and wind speed. All initial meteorological
1964 fields are assumed to be horizontally homogeneous in GRAMM. Lateral boundary conditions
1965 are kept constant, while the surface energy balance is computed continuously by taking into
1966 account shading effects of the surrounding topography and by utilising a soil model with
1967 seven layers. The soil and land use properties, such as roughness length or thermal
1968 conductivity, are parameterised by using the CORINE land use classification scheme. With
1969 this methodology, quasi steady-state wind fields are simulated with GRAMM that can be
1970 used as input for GRAL.

1971 Over the years, the methodology has been refined in order to improve the quality of the 3D
1972 wind fields. By developing the so-called ‘match-to-observation’ algorithm (MTO), the model’s
1973 performance could be greatly enhanced (e.g. Berchet et al., 2017). The basic principle of the
1974 MTO is the following: in a first step a large number (>2.000) of quasi steady-state wind fields
1975 for the domain of interest are computed with GRAMM using any possible combination of
1976 classified wind speed, direction, and stability. In a second step, the MTO selects for each
1977 hour of the year the best fitting 3D wind field comparing simulated and observed winds and
1978 stabilities at all available monitoring stations within the modelling domain. Note, that the
1979 MTO as well as GRAMM are fully integrated in the GUI. As the calculation of the wind fields

1980 can be very time consuming for large modelling domains (> 100 km x 100 km), specifically
1981 when using a high horizontal grid resolution (100 - 500 m), it is recommended to pre-
1982 compute such wind fields only once for a representative reference year.

1983 Recent research focuses on coupling GRAMM with global reanalysis data such as ERA5
1984 (Copernicus Climate Change Service, 2017). The main motivation is to improve the
1985 interaction of synoptic-scale flows with thermally-driven local flows (e.g. mountain-valley
1986 winds) in highly complex terrain such as the alps (e.g. Oettl and Veratti, 2021a; Oettl,
1987 2021b).

1988

1989 3.5. Meteorological Data Evaluation and Reporting

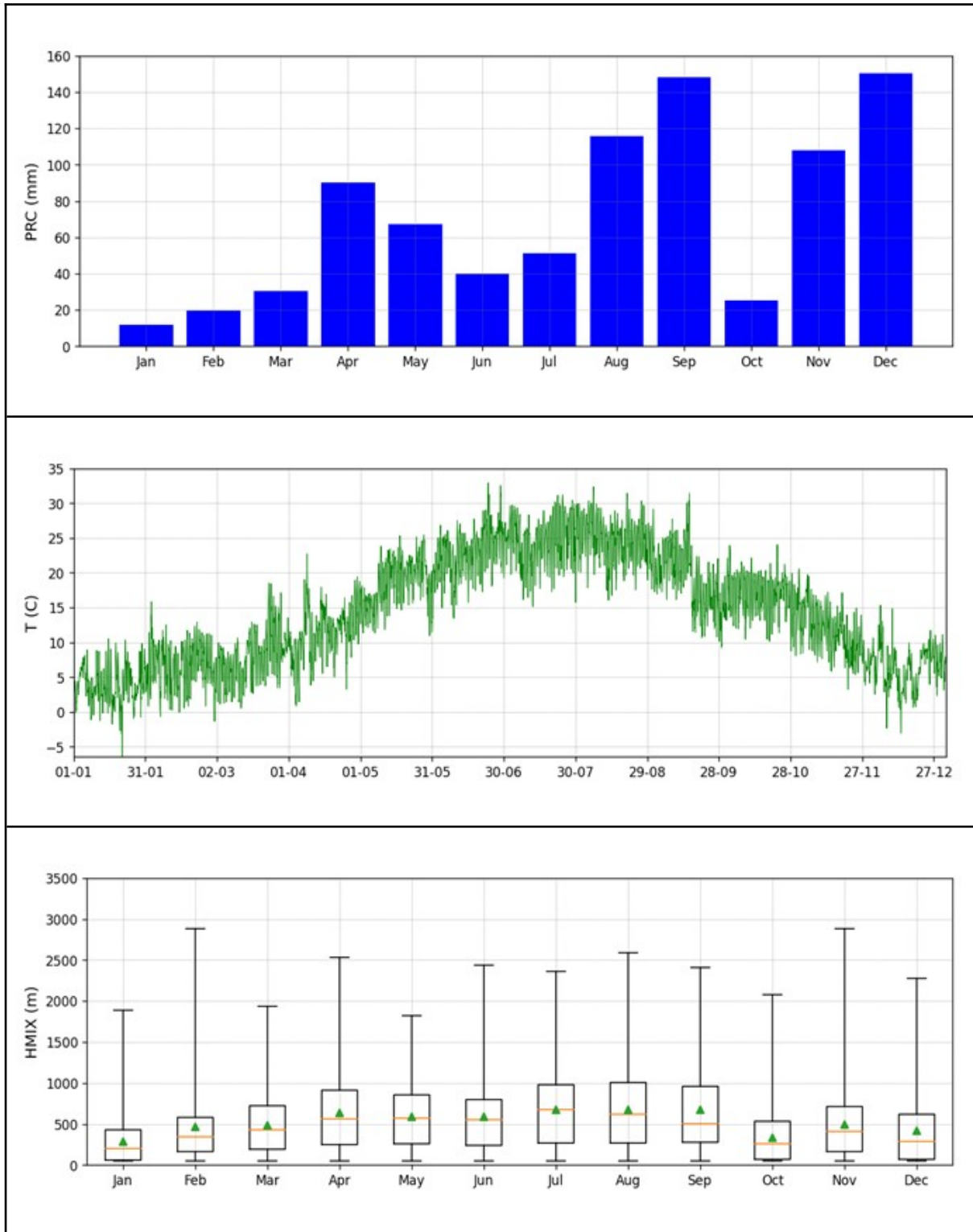
1990 Once the meteorological data set required for an odour dispersion analysis has been
1991 assembled, it is reasonable and proper to perform a few simple analyses of the data to be
1992 sure it is representative of the project site. These analyses may include: a determination of
1993 annual and monthly means of critical parameters; construction of annual and monthly wind
1994 rose plots; construction of simple plots or diagrams of atmospheric stability, mixing height,
1995 temperature, and precipitation over time; and perhaps an analysis of average vector wind
1996 speed and direction. This type of analysis and presentation of single-variable data can be
1997 included in the final modelling report and adds a level of confidence to any such report.

1998 When meteorological data is extracted from a numerical model such as WRF, some
1999 additional statistical analysis of the data is required; the modelled data should be compared
2000 to observational data collected during the simulation period. This analysis will provide
2001 inferences about the differences between the two populations, that is, the modelled data
2002 versus observations data. These analyses typically will include: differences of the means of
2003 the populations; differences of the variances; the mean bias error; the root mean square
2004 error; the index of agreement; and other measures.

2005 3.5.1. Single-Population Data Evaluation

2006 As a first step, summarise the data fields to be used in the dispersion model by calculating
2007 the monthly means and standard deviations of scalar quantities such as surface
2008 temperature, mechanical and convective mixing height, precipitation, and sensible heat flux.
2009 These calculated values should be compared to long-term averages for the modelling
2010 domain to determine if the selected meteorology can be considered sufficiently
2011 representative. A few simple graphs such as given in Figure 3-20 can help to visualise the
2012 data over the modelling period.

2013



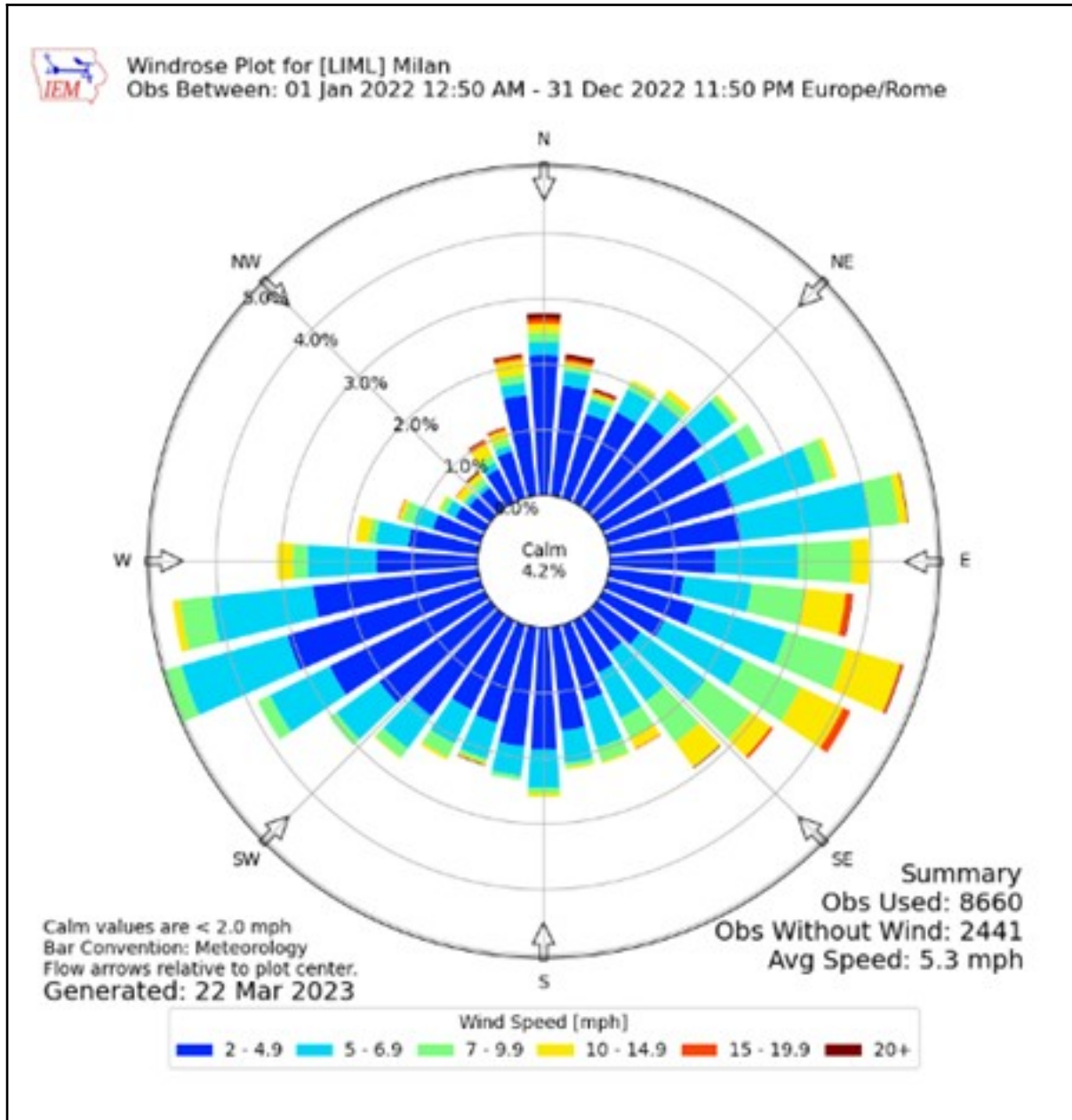
2014

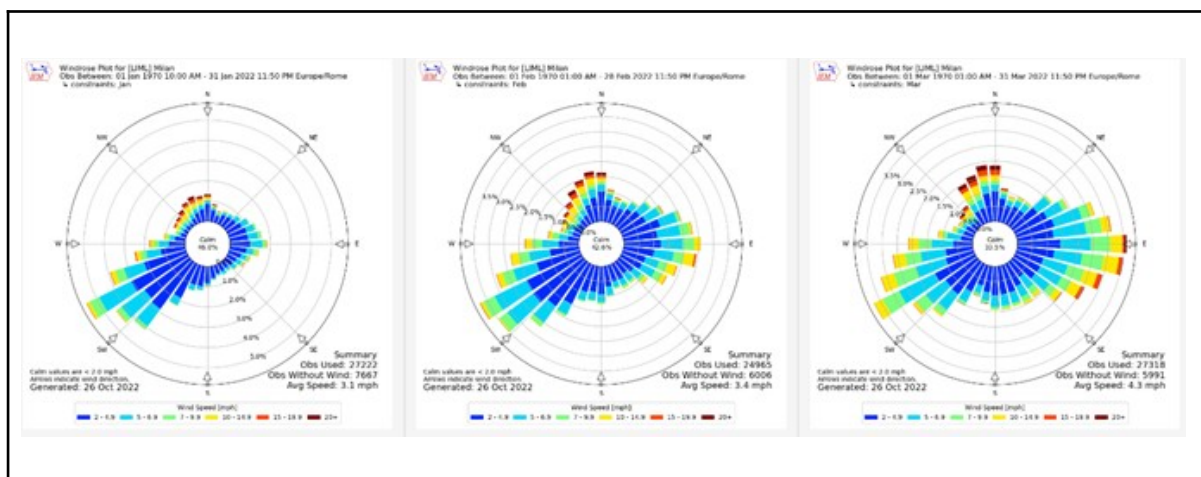
2015 **Figure 3-20** Precipitation (top), Temperature (centre), and Mixing Height (bottom) plots
 2016 (Courtesy of Enviroware)

2017 Next create annual and monthly wind rose diagrams. Wind roses are graphical charts that
 2018 characterise the speed and direction of winds at a location. Presented in a circular format,
 2019 the length of each 'spoke' or 'petal' around the circle indicates the amount of time that the
 2020 wind blows from a particular direction. Colours along the spokes indicate categories of wind

2021 speed. Wind roses are a very important evaluation method as they provide an easy-to-
2022 understand graphical output of many hundreds of hours of varying wind speed and wind
2023 direction. Figure 3-21 depicts example annual and monthly wind rose diagrams.

2024





2025

2026 **Figure 3-21** Example Annual (top) and Monthly (bottom) Wind Rose Diagrams (Source:
2027 Iowa Environmental Mesonet, <https://mesonet.agron.iastate.edu/>)

2028 Within the context of odour modelling, the monthly wind roses provide additional insight into
2029 critical periods of the year for receptors located across the modelling domain. Finally, daily
2030 wind roses can provide an additional check that any sea-land breeze is correctly reproduced
2031 by the meteorological data set. Appendix A includes links to several useful Tools including
2032 those which offer wind rose generators.

2033 Conduct additional analyses for winds. Wind speed and direction are two components of the
2034 same quantity, i.e., wind is a vector with both magnitude and direction. While it is acceptable
2035 for a data user to calculate the arithmetic mean of wind speed (as a scalar quantity), this
2036 cannot be done for wind direction. The main issue arises because wind direction is usually
2037 reported as an angle in degrees, 0–360 (or 0-359) where 0 or 360 represents a wind blowing
2038 from a northerly direction. If the wind direction is blowing from the north and traverses the
2039 discontinuity at the beginning/end of the circular scale, and then the arithmetic mean is
2040 calculated, this will result in the average wind direction to be somewhere in the southern
2041 quadrant. This is clearly incorrect. To correctly deal with this scale discontinuity,
2042 trigonometric functions must be used to handle the angles (US EPA, 2000), (Grange, 2014).

2043 Wind speed is expressed as the ratio of two different measures: distance and time. The
2044 harmonic mean is generally more appropriate than the arithmetic mean if the data values are
2045 ratios of two variables with different measures. For general wind analysis, however, the
2046 harmonic mean is rarely used. Both methods of calculation are shown here for
2047 completeness.

2048 The scalar mean wind speed is:

2049
$$\bar{u} = \frac{1}{N} \sum_{i=1}^N u_i \quad (\text{Equation 3-1})$$

2050 and the harmonic mean wind speed is:

2051
$$\bar{u}_h = \frac{1}{\sum_{i=1}^N \frac{1}{u_i}} \quad (\text{Equation 3-2})$$

2052 where u_i is the wind speed at each time of observation. Note that the harmonic mean is not
2053 defined when the wind is null. This statistic is very sensitive to low winds.

2054 These scalar wind speed calculations are quite simple to perform since the meteorological
 2055 data set consists of columns of the various parameters which can easily be imported into a
 2056 worksheet for manipulation.

2057 Vector functions are used to average wind direction and can be used to compute a type of
 2058 average wind speed which is different from the scalar average discussed above. The wind
 2059 components V_e and V_n must be calculated as:

$$2060 \quad V_e = \frac{-1}{N} \sum_{i=1}^N u_i \left[2\pi \times \frac{\theta_i}{360} \right] \quad (\text{Equation 3-3a})$$

$$2061 \quad V_n = \frac{-1}{N} \sum_{i=1}^N u_i \left[2\pi \times \frac{\theta_i}{360} \right] \quad (\text{Equation 3-3b})$$

2062 Where:

2063 V_e = east-west component of the wind direction

2064 V_n = north-south component of the wind direction.

2065 u_i is the wind speed at each time of observation, and

2066 θ is the wind direction in degrees.

2067 Since wind direction (θ) is in degrees, the units for the components are radians. There are
 2068 two other things to note: (i) the wind components here are calculated along with wind speed
 2069 (u_i), that is, the vectors are weighted by their magnitude, and (ii) the negative sign negates
 2070 the direction. This negation is because wind direction, by meteorological convention, is
 2071 defined from where the wind is blowing from, while the vectors define the direction where the
 2072 flow is heading to.

2073 The vector average wind speed is then calculated as:

$$2074 \quad \underline{U}_{RV} = (V_e^2 + V_n^2)^{1/2} \quad (\text{Equation 3-4})$$

2075 And the vector average wind direction as:

$$2076 \quad \theta_{RV} = \arctan\left(\frac{V_e}{V_n}\right) + \text{FLOW} \quad (\text{Equation 3-5})$$

2077 Where if:

2078 $\text{ArcTan}(V_e/V_n) < 180$ then $\text{FLOW} = 180$

2079 $\text{ArcTan}(V_e/V_n) > 180$ then $\text{FLOW} = -180$

2080 One can easily use a worksheet to perform these calculations as shown in Figure 3-22. Note
 2081 that in many programming languages the ArcTan function is available in two different forms,
 2082 $\text{ATAN}(V_e/V_n)$ or $\text{ATAN2}(V_e, V_n)$.

Date/Time (LST)	WD(deg)	WS(m/s)	1/WS	<u>i</u>	<u>V_i</u>	<u>V_i</u>
07/12/2019 01:00	189	6.2	0.161	1	0.970	6.124
07/12/2019 02:00	186	5.7	0.175	2	0.596	5.669
07/12/2019 03:00	195	5.7	0.175	3	1.475	5.506
07/12/2019 04:00	202	6.7	0.149	4	2.510	6.212
07/12/2019 05:00	171	4.6	0.217	5	-0.720	4.543
07/12/2019 06:00	215	6.2	0.161	6	3.556	5.079
07/12/2019 07:00	227	6.2	0.161	7	4.534	4.228
07/12/2019 08:00	205	5.7	0.175	8	2.409	5.166
07/12/2019 09:00	193	7.2	0.139	9	1.620	7.015
07/12/2019 10:00	198	7.7	0.130	10	2.379	7.323
07/12/2019 11:00	195	7.7	0.130	11	1.993	7.438
07/12/2019 12:00	176	9.3	0.108	12	-0.649	9.277
07/12/2019 13:00	169	8.8	0.114	13	-1.679	8.638
07/12/2019 14:00	156	9.3	0.108	14	-3.783	8.496
07/12/2019 15:00	152	7.2	0.139	15	-3.380	6.357
07/12/2019 16:00	173	7.7	0.130	16	-0.938	7.643
07/12/2019 17:00	195	7.7	0.130	17	1.993	7.438
07/12/2019 18:00	199	7.7	0.130	18	2.507	7.280
07/12/2019 19:00	226	7.2	0.139	19	5.179	5.002
07/12/2019 20:00	246	6.2	0.161	20	5.664	2.522
07/12/2019 21:00	201	6.7	0.149	21	2.401	6.255
07/12/2019 22:00	195	5.7	0.175	22	1.475	5.506
07/12/2019 23:00	193	5.7	0.175	23	1.282	5.554
07/13/2019 00:00	197	5.1	0.196	24	1.491	4.877
	Scalar	6.8			1.370	6.214
	Harmonic	6.6		ArcTan	12.4	
	Vector	6.4		Vector	192	

2083

2084 **Figure 3-22** Worksheet calculation for vector wind quantities

2085 3.5.2. Technical Approach to Prognostic Model Evaluation

2086 For both episodic and annual simulations, it is important that the observational databases to
 2087 which the model outputs will be compared consist purely of routine surface and aloft
 2088 measurements performed by individual countries' National Weather Service and other State
 2089 agencies. The evaluation must focus on the ability of the meteorological prognostic model to
 2090 correctly estimate surface and upper air wind speed, wind direction, temperature, mixing
 2091 height and precipitation at pertinent time and space scales. All of the same parameters must
 2092 be analysed as above, except that instead of using single population data, these statistics
 2093 compare the two data populations: the prognostic model data versus observations.

2094 Statistical procedures include scalar and vector mean wind speeds, standard deviations in
 2095 measured and observed winds, errors of difference (total plus systematic and unsystematic
 2096 components), two model skill measures, plus the Index of Agreement. Statistical measures
 2097 for temperature, mixing height, and precipitation should include means, biases, gross errors,
 2098 and the index of agreement.

2099 Complementing the statistical measures are a variety of graphical displays which include
 2100 state-variable time series plots, two-dimensional parameter fields, vertical profiles of
 2101 predicted and observed variables, skew-T plots, scatter plots and wind roses.

2102 For gridded 3-dimensional meteorological model predictions, evaluations could be both (a)
 2103 subregional evaluations, and (b) limited time-period evaluations (e.g., monthly and
 2104 seasonal). These evaluations are aimed at elucidating the model's ability to predict key
 2105 processes at smaller time scales (e.g. coastal circulation regimes) as well as defining the
 2106 model's ability to produce reliable air quality inputs at scales appropriate to odours from tall

2107 stacks that might disperse a reasonable distance.

2108 All of the techniques in this Chapter have been employed extensively in other prognostic
2109 model performance testing after Doty et al (2002), Tesche and McNally (2001), Tesche et al
2110 (2002), Emery et al (2001). These evaluation procedures are endorsed by the US EPA (US
2111 EPA, 2000). A brief description of each statistic is given here; the reader is directed to the
2112 references and to general statistics texts for more detailed information.

2113 3.5.3. Operational Evaluation of Surface Fields

2114 3.5.3.1. Mean Statistics

2115 Begin the evaluation by determining annual and monthly means and standard deviations of
2116 scalar variables in both populations as described earlier. For winds, follow the techniques
2117 for vector calculations.

2118 3.5.3.2. Difference Statistics

2119 Now begin the process of determining how similar the two populations are. For quantities
2120 that are continuous in space and time (i.e., wind speed, temperature, pressure, odour
2121 concentrations), difference statistics provide considerable insight into the model's
2122 performance, temporally and spatially. Difference statistics are based on the definition of a
2123 residual quantity, d_i . For instance a temperature residual, for example, is defined as:

$$2124 \quad d_i = c_e(x_i, t) - c_o(x_i, t) \quad (\text{Equation 3-6})$$

2125 Where d_i is the i -th residual based on the difference between model-estimated (c_e) and
2126 observed (c_o) temperature at location x and time i . In the definitions that follow below, the
2127 letter c has been used to denote any continuous atmospheric variable (e.g., temperature,
2128 precipitation, etc).

2129 Standard deviation of residual distribution (SD_r). The standard deviation of the residual
2130 distribution is given by:

$$2131 \quad SD_r = \left\{ \frac{1}{N-1} \sum_{i=1}^N (d_i - MBE)^2 \right\}^{\frac{1}{2}} \quad (\text{Equation 3-7})$$

2132 Where

2133 Mean Bias Error (MBE) is the first moment, defined below. This statistic describes the
2134 dispersion or spread of the residual distribution about the estimate of the mean. The
2135 standard deviation is calculated using all estimation-observation pairs above the cut-off level.
2136 The second moment of the residual distribution is the variance, the square of the standard
2137 deviation. Since the standard deviation has the same units of measure as the variable (e.g.,
2138 m/s for wind) it is used here as the metric for dispersion. The standard deviation and
2139 variance measure the average spread of the residuals, independent of any systematic bias
2140 in the estimates. No direct information is provided concerning sub-regional errors or about
2141 large discrepancies occurring within portions of the diurnal cycle although in principle these,
2142 too, could be estimated.

2143 Mean Bias Error (MBE). The mean bias error is given by:

2144
$$MBE = \frac{1}{N} \sum_{i=1}^N (c_e(x_i, t) - c_{o(x_i, t)}) \quad (\text{Equation 3-8})$$

2145 Where N equals the number of hourly estimate-observation pairs drawn from all valid
 2146 monitoring station data on the simulation period of interest. This is simply the average of the
 2147 sum of the residuals. MBE is not a good estimator because MBE=0 does not necessarily
 2148 indicate a good model, since many overestimations may be compensated by many
 2149 underestimations.

2150 There are other measures of error and all are based on this Mean Bias Error. They include:

- 2151 ● Mean Normalised Bias Error (MNBE), often just called the bias
- 2152 ● Mean Absolute Gross Error (MAGE)
- 2153 ● Mean Absolute Normalised Gross Error (MANGE)
- 2154 ● Root Mean Square Error (RMSE)
- 2155 ● Systematic Root Mean Square Error (RMSEs)
- 2156 ● Unsystematic Root Mean Square Error (RMSEu)

2157 It is important that RMSE, RMSEs and RMSEu are all analysed. For example, if only RMSE
 2158 is estimated (and it appears acceptable) it can consist largely of the systematic component.
 2159 This bias might be removed, thereby reducing the bias transferred to the dispersion model.
 2160 On the other hand, if the RMSE consists largely of the unsystematic component (RMSEu),
 2161 this indicates further error reduction may require model refinement and/or data acquisition. It
 2162 also provides error bars that may be used with the inputs in subsequent sensitivity analyses.

2163 3.5.3.3. Skill Measures

2164 Index of Agreement (I). Following Willmott (1981, 1984) and Pereira et al. (2018), one index
 2165 of agreement is given by:

2166
$$I = 1 - \frac{\sum_{i=1}^N (P_i - O_i)^2}{\square} \quad (\text{Equation 3-9})$$

2167 Where *P* and *O* are, respectively, the predicted and observed values

2168 The Index of Agreement (I or sometimes IOA) condenses all the differences between the
 2169 model estimates and observations into one statistical quantity. It is the ratio of the
 2170 cumulative difference between the model estimates and the corresponding observations and
 2171 the observed mean. Viewed from another perspective, the Index of Agreement is a measure
 2172 of how well the model estimates departure from the observed mean matches, case by case,
 2173 the observations' departure from the observed mean. Thus, the correspondence between
 2174 estimated and observed values across the domain at a given time may be quantified in a
 2175 single metric and displayed as a time series. The Index of Agreement has a theoretical
 2176 range of 0 to 1, the latter score suggesting perfect agreement.

2177 RMS Skill Error (Skille). The root mean square skill error is defined as:

2178
$$Skill_e = \frac{RMSE_u}{SD_o} \quad (\text{Equation 3-10})$$

2179 Variance Skill Ratio (Skillvar). The variance ratio skill is given by:

2180
$$Skill_{var} = \frac{SD_e}{SD_o} \quad \text{(Equation 3-11)}$$

2181 Where SDe and SDo are the standard deviations of the model estimated parameter and the
 2182 observed parameter, respectively.

2183 There are several free software tools that can perform the statistical analyses described in
 2184 this Section related to comparison of modelled data versus observational data. See
 2185 Appendix A for more information.

2186 3.5.3.4. Benchmarks

2187 There is a need for some benchmarks against which to compare new prognostic model
 2188 simulations. In three studies (Tesche et al 2001, 2001b; Emery et al 2001), an attempt was
 2189 made to formulate a set of mesoscale model evaluation benchmarks based on the most
 2190 recent performance evaluation literature at the time. The purpose of the benchmarks is not
 2191 to assign a passing or failing grade to a particular model application, but rather to put its
 2192 results into a useful context. The following benchmarks listed in Table 3-3 may be helpful to
 2193 modellers and model users in understanding how poor or good their results are relative to
 2194 the range of other model applications.

2195 **Table 3.3** Meteorological benchmarks

	Wind speed	Wind direction	Temperature	Humidity
IOA	≥ 0.6	--	≥ 0.8	≥ 0.6
RMSE	≤ 2 m/s	--	--	--
Mean Bias	≤ ±0.5 m/s	≤ ±10°	≤ ±0.5 K	≤ ±1 g/kg
Gross Error	--	≤ 30°	≤ 2 K	≤ 2 g/kg

2196 3.5.4. Graphical Evaluation Tools

2197 Over the years a rich variety of graphical analysis and display methods have been
 2198 developed to evaluate the performance of meteorological models. There are a number of
 2199 procedures for graphically representing model results and observations that allow for direct
 2200 comparison between them. In many instances, the differences in how modelled and
 2201 measured quantities are treated in certain of these graphical techniques are more a matter
 2202 of preference than correctness. Each graphical technique requires some assumptions that
 2203 influence the outcome. However, by using a variety of graphical approaches it is possible to
 2204 examine a model performance from different viewpoints and thus gain a clearer
 2205 understanding of the results. Some of the well-known graphical displays include;

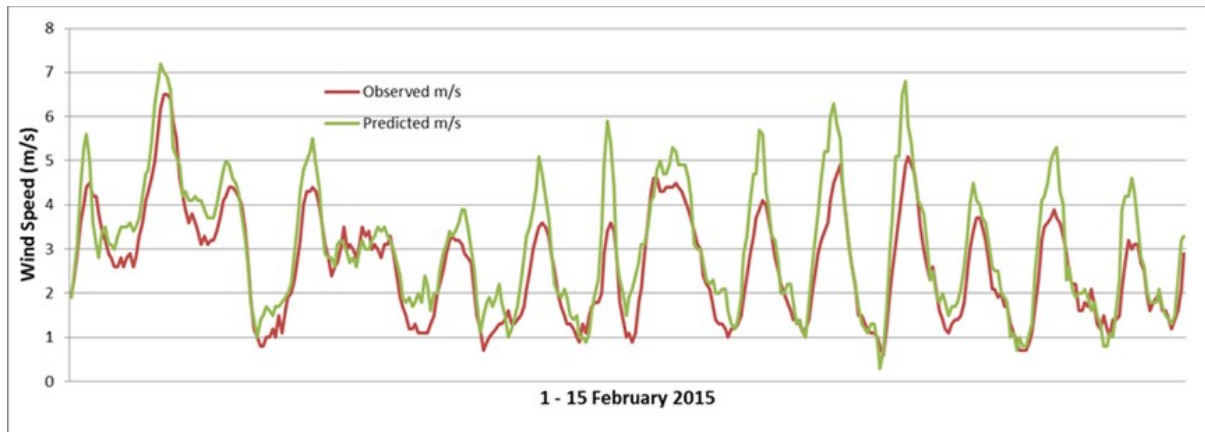
- 2206 ● the temporal correlation (time series) between point estimates and
- 2207 observations;
- 2208 ● the spatial distribution (gridded fields) of estimated quantities;
- 2209 ● the correlation among hourly pairs of estimates, observations, residuals and
- 2210 distributions;
- 2211 ● the variation in spatial mean, bias and error estimates as functions of time
- 2212 and space; and
- 2213 ● the degree of mismatch between volume-averaged model estimates and point

2214 measurements.

2215 3.5.4.1. Time series Plots

2216 Time series analysis is extremely useful to observe how a given variable behaves / changes
2217 over time. For example, the plot below (Figure 3-23) shows the observed and predicted
2218 wind speed over a two week period in February 2015. In this example, the plot shows that
2219 the two time series are very well correlated, but that the predictions have a slight tendency to
2220 overestimate the observations.

2221



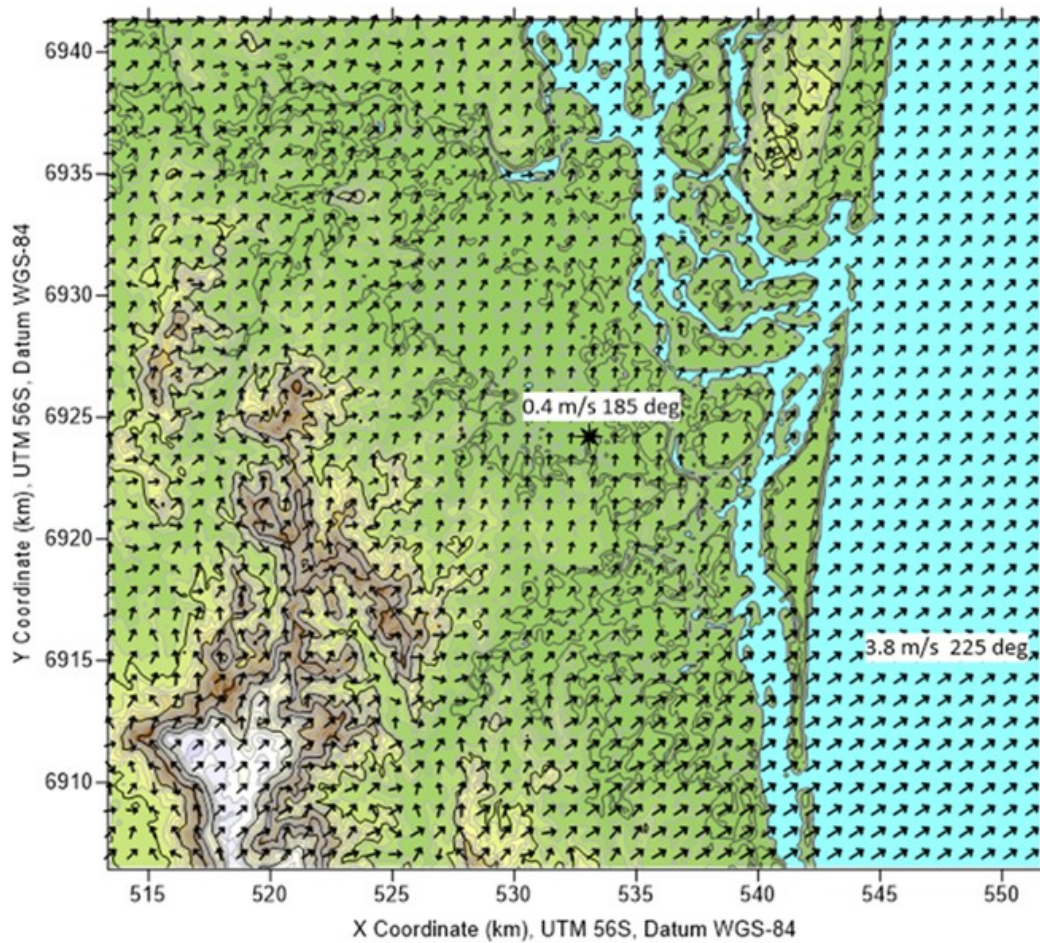
2222

2223 **Figure 3-23** Time series plot of observed and predicted wind speed over a two-week period
2224 from 1 - 15 February 2015 (courtesy of Atmospheric Science Global)

2225 3.5.4.2. Spatial Distribution Plots

2226 A spatial distribution in statistics is the arrangement of phenomenon across a portion of the
2227 earth's surface. A graphical display of such an arrangement is an important tool in
2228 environmental statistics. A spatial distribution map of winds, as shown in Figure 3-24,
2229 provides information on the spread of winds across a region whose effects might influence a
2230 location of key interest. Spatial distribution plots can be generated for most meteorological
2231 phenomena, such as temperature, wind speed and direction, mixing height, atmospheric
2232 stability etc. Spatial distribution plots provide information far beyond a single point of
2233 interest, and they can help validate the meteorology at a single point.

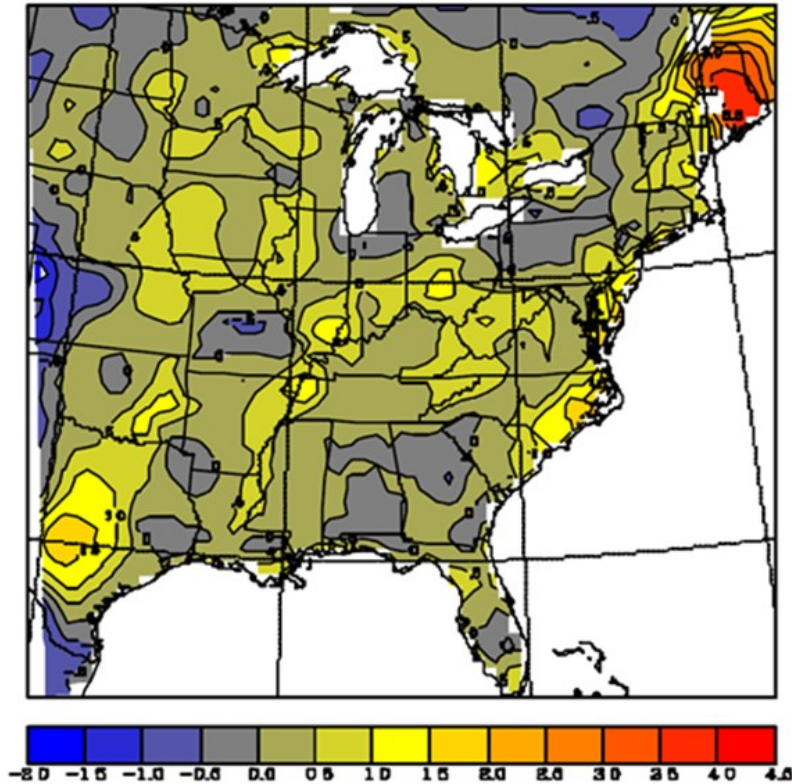
2234



2235

2236 **Figure 3-24** Spatial distribution plot of wind field representing a snapshot of a single hour.
2237 (courtesy of Atmospheric Science Global)

2238 Another type of spatial distribution plot is shown in Figure 3-25, which shows a spatial
2239 difference field of Bias in modelled minus observed surface wind fields over a 48 km grid
2240 domain.



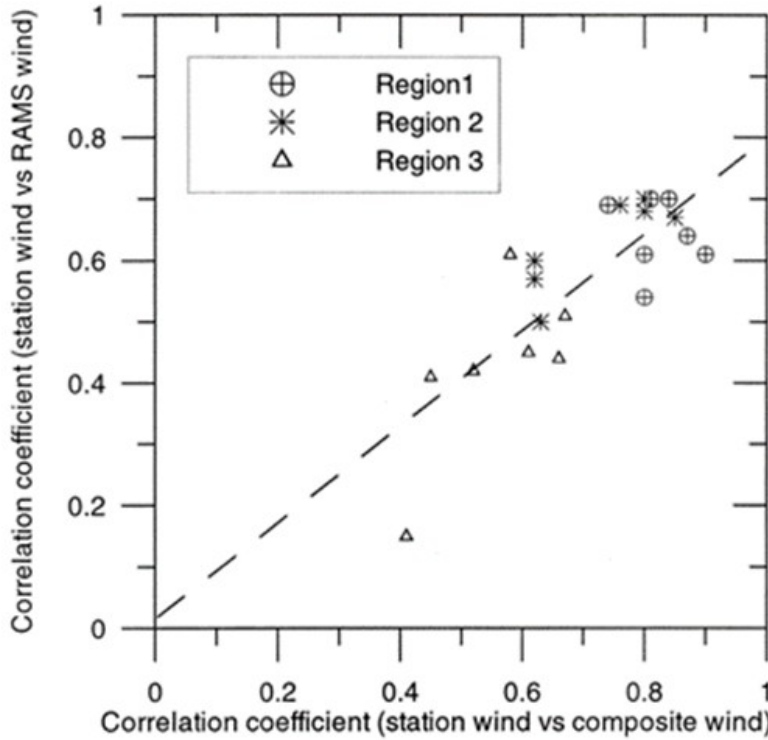
2241

2242 **Figure 3-25** Spatial distribution plot showing the model bias of wind fields over the eastern
2243 US during July 1995 (Doty et al., 2002).

2244 3.5.4.3. Correlation Analysis

2245 Correlation analysis is a useful technique in meteorology as it helps us determine the degree
2246 of relationship between variables. Correlations between variables indicate that changes in
2247 one variable are associated with changes in other variables, but this does not mean that the
2248 changes in one variable actually cause the changes in the other variable. Sometimes it is
2249 clear that there is a causal relationship.

2250 Correlations are a useful evaluation tool as they can tell if two variables have a linear
2251 relationship, and the strength of that relationship. Figure 3-26 shows the graphical
2252 correlation relationship between observed and modelled winds. It is a simple measure to
2253 show the strength of a linear relationship between two meteorological variables.

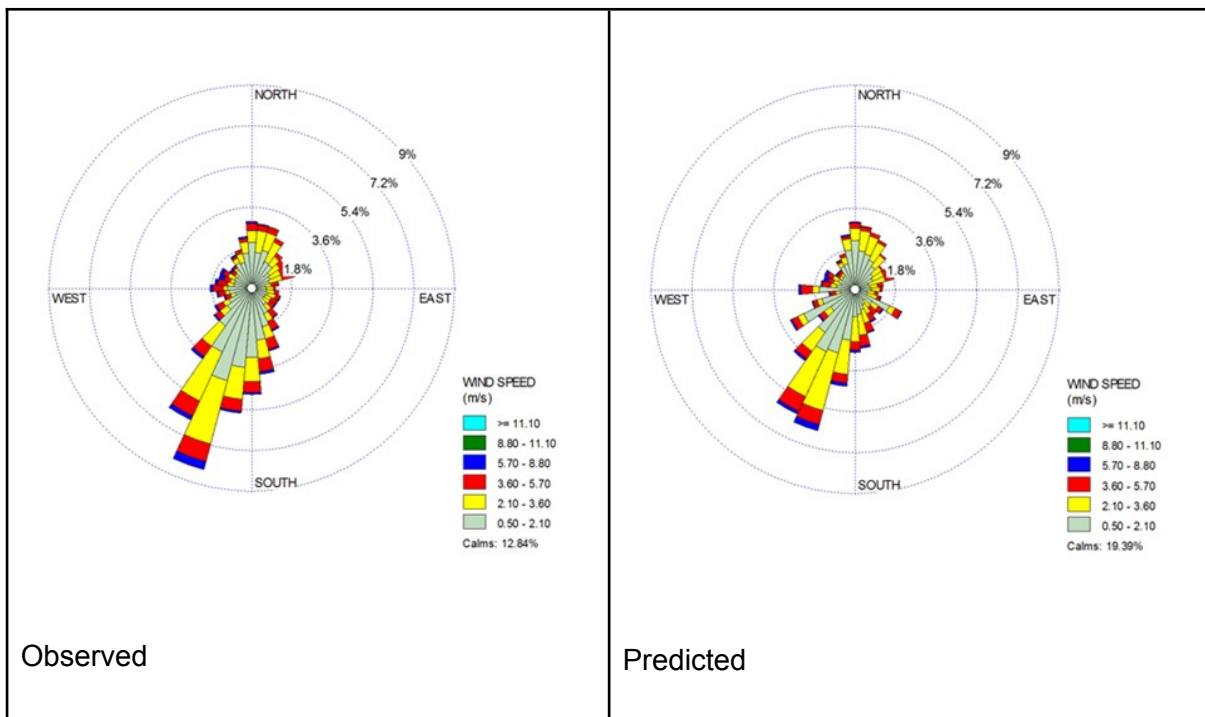


2254

2255 **Figure 3-26** Schematic plot showing the strong correlation relationship between observed
 2256 and modelled winds (Weather and Forecasting 16, 5)

2257 3.5.4.4. Wind Roses

2258 Wind roses (discussed earlier) that are prepared from the modelled and observed data can
 2259 be placed side-by-side for an easy graphical comparison of the two data sets. Figure 3-27
 2260 shows this technique.



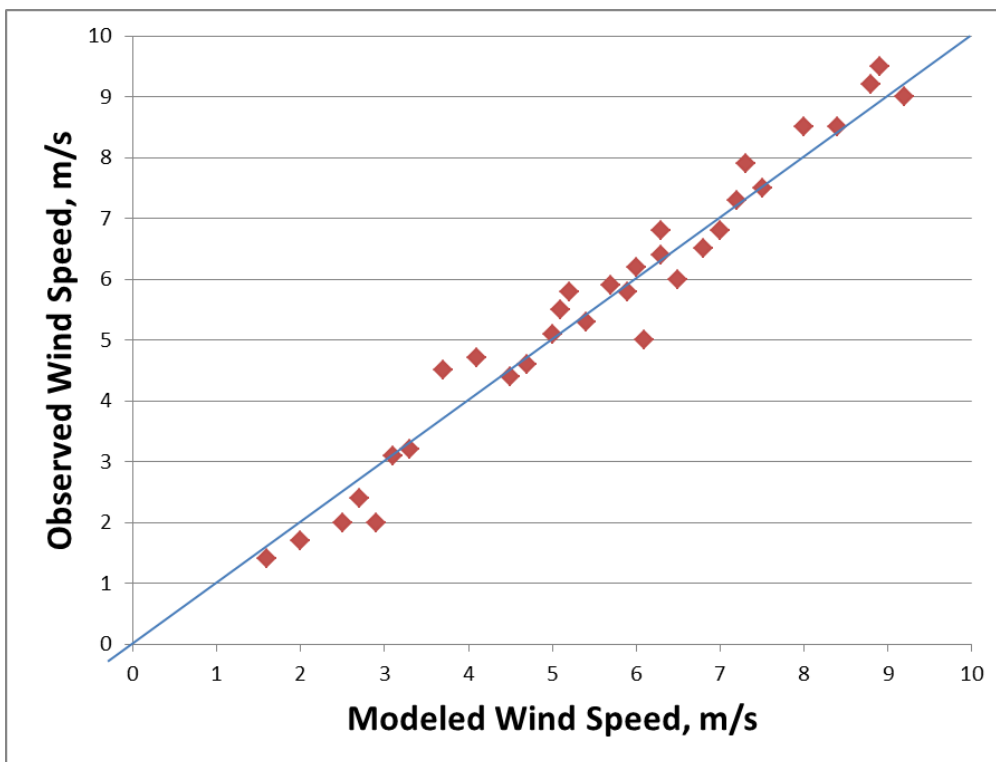
2261 **Figure 3-27** Wind roses of observed and predicted winds (courtesy of Atmospheric Science
2262 Global)

2263 3.5.4.5. Scatter Plots

2264 Scatter plots are a type of data visualisation that shows the relationship between different
2265 variables. The data are typically shown by placing various data points between the x and y-
2266 axis. The scatter plot's primary uses are to observe and show relationships between two
2267 numeric variables. They can also show if there are any unexpected gaps in the data and if
2268 there are any outlier points. Scatter plots offer the following advantages:

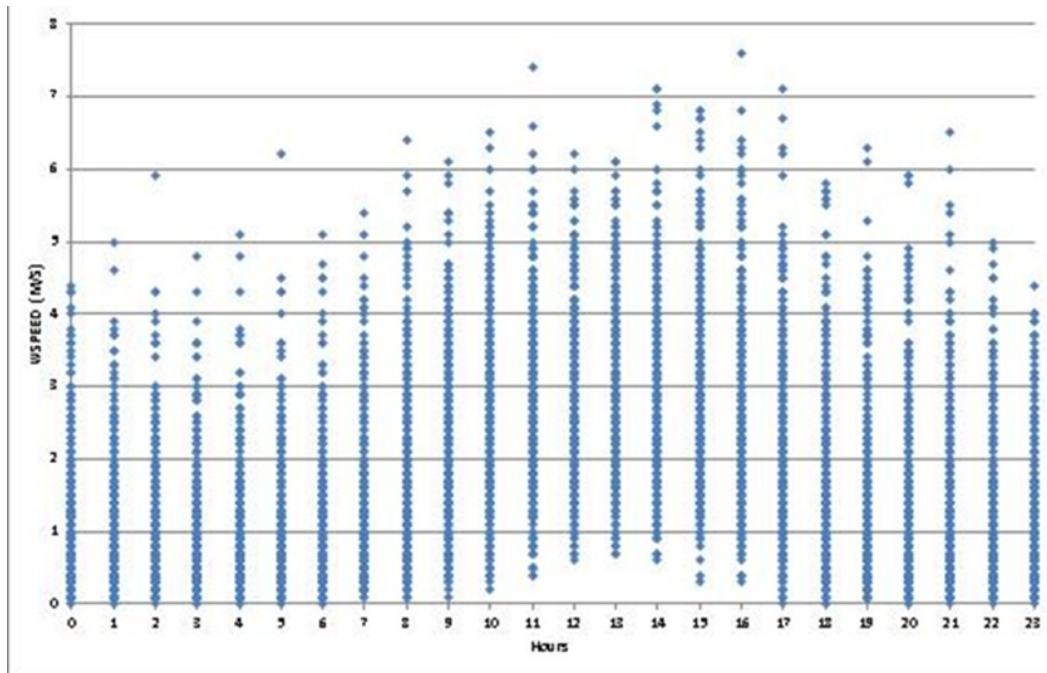
- 2269 • They identify correlation – they allow the comparison between two different
2270 variables
- 2271 • They are nonlinear, easy to read and easy to create

2272 Scatter diagrams do not measure the precise extent of the correlation and will only give an
2273 approximate idea of the relationship, they are a qualitative expression of the quantitative
2274 change. Figure 3-28 is an example of a scatter plot.



2275
2276 **Figure 3-28** Example scatter plot to compare observed versus modelled wind speed
2277 (courtesy of Atmospheric Science Global)

2278 The following Figure 3-29 is a variation of a scatter plot which depicts all measured wind
2279 speeds by hour over the course of a one-year modelling period.

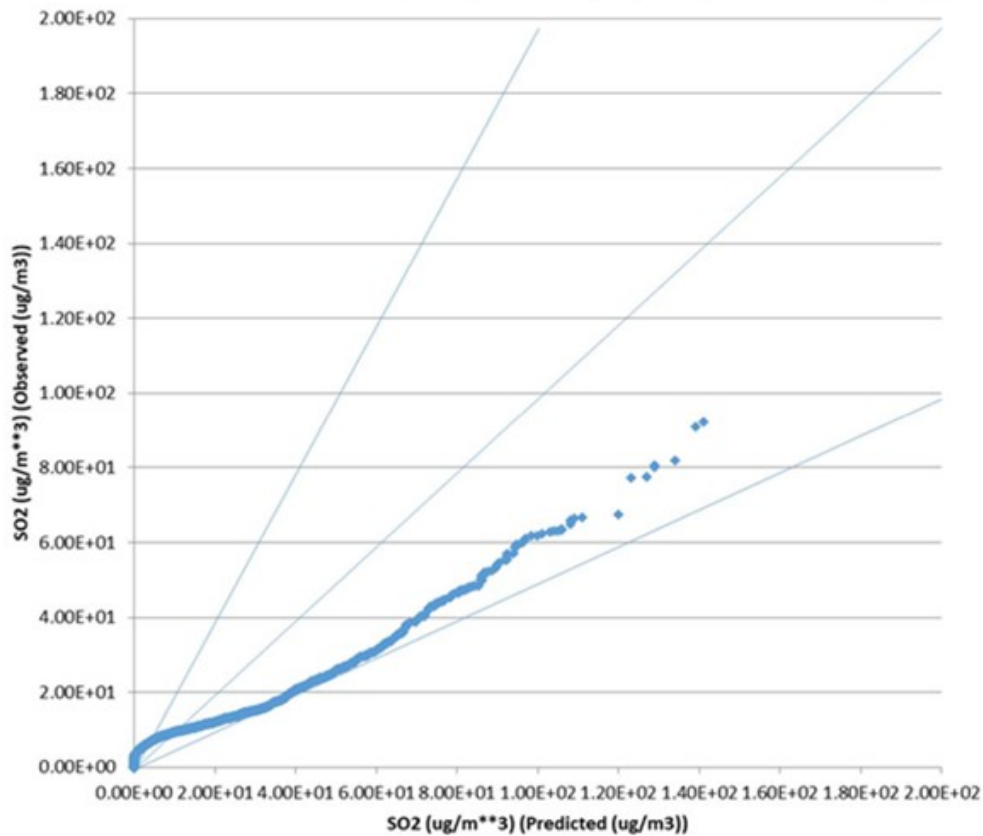


2280

2281 **Figure 3-29** A diurnal scatter plot of wind speed by hour over a full year (courtesy of
2282 Atmospheric Science Global)

2283 3.5.4.6. Quantile-Quantile Plots

2284 A QQ plot is a probability statistic graph, which is a graphical method for comparing two
2285 probability distributions. The purpose of a QQ plot is to show if two data sets come from the
2286 same distribution. Plotting the first data set's quantiles along the x-axis and plotting the
2287 second data set of quantiles along the y-axis is how the plot is constructed. Figure 3-30
2288 shows a QQ plot typically used to compare observed vs predicted distributions.



2289

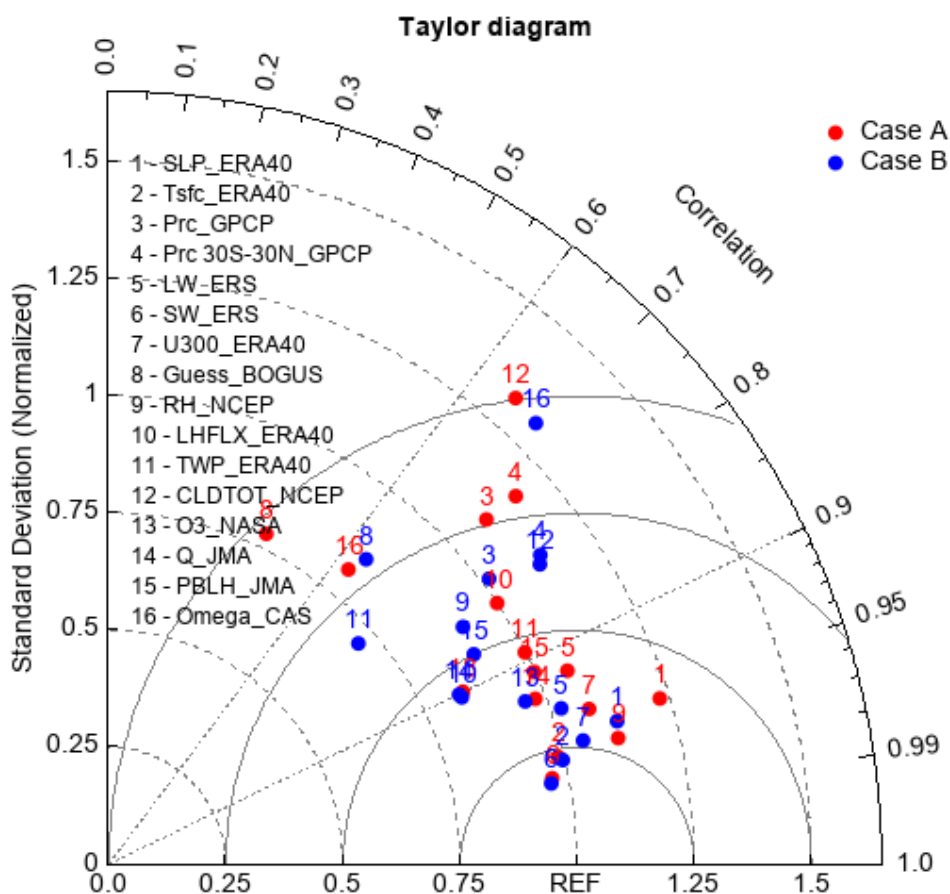
2290 **Figure 3-30** Quantile-Quantile probability plot comparing observed (y-axis) vs predicted (x-
2291 axis) SO₂ concentrations (µg/m³) (courtesy of Atmospheric Science Global)

2292 3.5.4.7. Taylor Diagram

2293 The Taylor diagram uses the law of cosines to represent in a single graph how the three
2294 most representative statistics of the performance of a model vary simultaneously, such as:

- 2295 1. The mean square error, without taking into account the effect of the sign of
2296 the error (RMSE), which is very useful for checking the accuracy of the
2297 model.
- 2298 2. The standard deviation (SD) makes it possible to check the variability in both
2299 data samples and see whether this variability is conserved or varies in the
2300 model concerning what is observed for the real data.
- 2301 3. The Pearson Correlation Coefficient, r , which shows how close the linear
2302 relationship is between the pairs of data formed by the model and the real
2303 determinations.

2304 It is challenging to measure odour in ambient air. Therefore, this kind of diagram is rarely
2305 used in odour modelling. The following Figure 3-31 shows an example comparing standard
2306 deviations.



2307

2308 **Figure 3-31** Taylor Diagram for comparison of standard deviations (MeteoInfo,
2309 <http://meteothink.org/>)

2310 3.5.5. Conclusion

2311 A plausibility check of the meteorological simulation is recommended. This plausibility check
2312 should be performed with independent observations, that is observations not used in the
2313 meteorological assessment. These observations should be close to the location of the
2314 emission source and/or those most representative of the meteorology of the plant
2315 environment. It is recommended that, at least one of the series of observations used in the
2316 plausibility check, should contain data from vertical wind profiles.

2317 The Guideline of good practices in the elaboration of dispersion models of the Basque
2318 Country, Spain, 2012 mentions that a meteorological plausibility check should include:

- 2319 ● A topographic map with the location of the meteorological stations used and the
2320 emission source(s).
- 2321 ● The wind roses estimated by the modelling at the location points of the selected
2322 meteorological stations and those obtained with the observations.
- 2323 ● Statistical metrics of at least wind, temperature and precipitation differences between
2324 observations and simulations (scatter plots of points, correlation coefficients, Taylors
2325 diagrams, etc.).
- 2326 ● Temporal wind sequences measured-simulated in selected periods (one or several
2327 weeks) within the year in question, coinciding with selected episodes of odour impact
2328 by one or several chemical species (subject to monitoring in the local network). The
2329 selected episodes and chemical species are at the discretion of the person in charge

- 2330 of the evaluation, but must be justified.
2331 • Discussion of the differences found, both in episodes and in statistics and wind
2332 roses, and how they might affect the dispersion calculations.

2333 Taking into account the interannual meteorological variability, it would be ideal to use a
2334 temporal sequence of 5 complete years (not necessarily consecutive) to estimate the
2335 dispersion of the outbreak under evaluation. However, due to the difficulties associated with
2336 the preparation of a complete annual sequence of the non-stationary and three-dimensional
2337 meteorological fields of the target area, duly validated and with the necessary spatial and
2338 temporal resolution, the use of a 1-year time series is considered sufficient. According to the
2339 same guideline commented before, the choice of year should be adequately justified, in
2340 relation to at least two criteria:

- 2341 1. Priority should be given to temporal proximity (recent years), normally better
2342 documented.
2343 2. Representativeness in terms of intensity-frequency of pollution episodes in the
2344 selected simulation domain and year should be examined. A wet year (with many
2345 days with precipitation) or low frequency of pollution episodes (e.g. few situations
2346 with anticyclonic blockages) cannot be selected, with the sole justification of data
2347 availability.

2348 In addition to justifying the selection made, it is recommended that the evaluation includes a
2349 discussion of what variations in impact estimates would be expected in those years with
2350 more adverse meteorology.

2351 3.6. References

2352
2353 Ahrens, C. D., & Henson, R. (2016). Essentials of meteorology: An invitation to the
2354 atmosphere. Cengage Learning.
2355

2356 Berchet, A., K. Zink, C. Müller, D. Oetli, J. Brunner, L. Emmenegger, and D. Brunner (2017)
2357 A cost-effective method for simulation city-wide air flow and pollutant dispersion at building
2358 resolving scale. Atmos Environ, 158, 181-196
2359

2360 Marlon Brancher, K. David Griffiths, Davide Franco, Henrique de Melo Lisboa, A review of
2361 odour impact criteria in selected countries around the world, Chemosphere, Volume 168,
2362 2017, Pages 1531-1570, ISSN 0045-6535. Available online:
2363 <<https://doi.org/10.1016/j.chemosphere.2016.11.160>>. (Accessed Nov 2022).
2364

2365 Briggs, G.A. (1975). Plume Rise Predictions. Lectures on Air Pollution and Environmental
2366 Impact Analyses, Workshop Proceedings, American Meteorological Society, 59-111.
2367

2368 Cambridge Environmental Research Consultants. (2016) WRF to Met Utility, User Guide
2369 Version 1.4.
2370

2371 Carson, D. J. (1973). The development of a dry inversion-capped convectively unstable
2372 boundary layer. Quarterly Journal of the Royal Meteorological Society, 99(421), 450-467.
2373 doi:10.1002/qj.49709942105.
2374

2375 Chang, J., Hanna, S. (2004). Air quality model performance evaluation. In Meteorology and

- 2376 Atmospheric Physics, Vol. 87, Iss. 1-3, 167-196. DOI:10.1007/s00703-003-0070-7
2377
- 2378 Copernicus Climate Change Service (C3S) (2017) ERA5: Fifth generation of ECMWF
2379 atmospheric reanalyses of the global climate. Copernicus Climate Change Service Climate
2380 Data Store (CDS). Available online: <https://cds.climate.copernicus.eu/cdsapp#!/home>.
2381 (Accessed Nov 2022).
2382
- 2383 Dennis, R., Fox, T., Fuentes, M. et al. A framework for evaluating regional-scale numerical
2384 photochemical modelling systems. Environ Fluid Mech 10, 471–489 (2010).
2385 DOI:10.1007/s10652-009-9163-2
- 2386 Departamento de Medio Ambiente, Planificación Territorial, Agricultura y Pesca. Gobierno
2387 Vasco. Guideline of good practices in the elaboration of dispersion models (Guía de Buenas
2388 Prácticas para la elaboración de modelos de dispersión). (2012). Available online:
2389 https://www.euskadi.eus/contenidos/documentacion/guia_modelos_dispersion/es_doc/adjuntos/guia_modelos_dispersion.pdf >. (Accessed Nov 2022).
2390
- 2391 Doty, K., T. W. Tesche, D. E. McNally, B. Timin, and S. F. Mueller, 2002. Meteorological
2392 Modelling for the Southern Appalachian Mountains Initiative (SAMI), Final Report to the
2393 Southern Appalachian Mountains Initiative, prepared by the University of Alabama,
2394 Huntsville, Alpine Geophysics, LLC, U.S. EPA/OAQPS, and the Tennessee Valley Authority.
2395
- 2396 Douglas S and R. Kessler (1999) Users Guide to the Diagnostic Wind Field Model (Version
2397 1.0), Systems Application, Inc. San Rafael, CA.
- 2398 Emery, C., E. Tai, and G. Yarwood, 2001. Enhanced Meteorological Modelling and
2399 Performance Evaluation for Two Texas Ozone Episodes”, Prepared for the Texas Natural
2400 Resources Conservation Commission, prepared by ENVIRON, International Corp, Novato,
2401 CA.
2402
- 2403 Emery, B., & Camps, A. (2017). Introduction to satellite remote sensing: atmosphere, ocean,
2404 land and cryosphere applications. Elsevier.
2405
- 2406 Environmental Protection Agency. Ireland, 2019. Odour Emissions Guidance Note Air
2407 Guidance Note AG9. Available online:
2408 https://www.epa.ie/publications/compliance--enforcement/air/air-guidance-notes/AG9_Odour-Emissions-Guidance-Note_Sep2019_v1.pdf >. (Accessed Nov 2022).
2409
2410
- 2411 Enviroware srl, (2022). Available online: <https://www.enviroware.com/lapmod/>>. (Accessed
2412 Nov 2022).
2413
- 2414 EPA Victoria (2013). Construction of input meteorological data files for EPA Victoria’s
2415 regulatory air pollution model (AERMOD), Publication 1550. Available online
2416 <https://www.epa.vic.gov.au/-/media/epa/files/publications/1550.pdf>. (Accessed Feb 2023).
2417
- 2418 EPRI, SCICHEM Version 3.2.2 Users Guide, Technical Update December 2019
2419
- 2420 Federal Environment Agency (UBA), Germany. (2014) AUSTAL2000, Program

- 2421 Documentation of Version 2.6. Available online: <http://austal.de/de/home.html> (accessed
2422 Nov 2022).
- 2423
- 2424 Finardi, S., Tinarelli, G., Faggian, P., & Brusasca, G. (1998). Evaluation of different wind field
2425 modelling techniques for wind energy applications over complex topography. *Journal of*
2426 *Wind Engineering and Industrial Aerodynamics*, 74, 283-294.
- 2427
- 2428 Grange, S. (2014). Technical note: Averaging wind speeds and directions.
2429 10.13140/RG.2.1.3349.2006. DOI:10.13140/RG.2.1.3349.2006
- 2430
- 2431 Holtslag, A. A. M., & Van Ulden, A. P. (1983). A simple scheme for daytime estimates of the
2432 surface fluxes from routine weather data. *Journal of Applied Meteorology and Climatology*,
2433 22(4), 517-529.
- 2434
- 2435 Jiménez, P.A. and Dudhia, J. (2013). On the Ability of the WRF Model to Reproduce Surface
2436 Wind Direction over Complex Terrain. *Journal of Applied Meteorology and Climatology*, 52,
2437 1610-1617. doi:10.1175/JAMC-D-12-0266.1
- 2438
- 2439 Maul, P.R (1980) Atmospheric transport of sulfur compound pollutants. Central Electricity
2440 Generating Bureau MID/SSD/80/0026/R. Nottingham, England
- 2441
- 2442 Nappo, C. (2002) An Introduction to Atmospheric Gravity Waves. Elsevier, Inc., First Edition
- 2443 Pasquill, F. (1961) Atmospheric Diffusion. Van Nostrand Go. Published online by Cambridge
2444 University Press, (2006). Available online: <[https://www.cambridge.org/core/journals/journal-](https://www.cambridge.org/core/journals/journal-of-fluid-mechanics/article/abs/atmospheric-diffusion-by-f-pasquill-van-nostrand-go-1961-297pp-60s/38E8CD2705AFA216F5C482472BB6112D)
2445 [of-fluid-mechanics/article/abs/atmospheric-diffusion-by-f-pasquill-van-nostrand-go-1961-](https://www.cambridge.org/core/journals/journal-of-fluid-mechanics/article/abs/atmospheric-diffusion-by-f-pasquill-van-nostrand-go-1961-297pp-60s/38E8CD2705AFA216F5C482472BB6112D)
2446 [297pp-60s/38E8CD2705AFA216F5C482472BB6112D](https://www.cambridge.org/core/journals/journal-of-fluid-mechanics/article/abs/atmospheric-diffusion-by-f-pasquill-van-nostrand-go-1961-297pp-60s/38E8CD2705AFA216F5C482472BB6112D)>.
- 2447
- 2448 National Center for Atmospheric Research (2022). User's Guide for the Advanced Research
2449 WRF (ARW) Modelling System, Version 4.4. Available online
2450 https://www2.mmm.ucar.edu/wrf/users/docs/user_guide_v4/contents.html. (Accessed Feb
2451 2023).
- 2452
- 2453 Oetl, D. (2015a) Quality assurance of the prognostic, microscale wind-field model GRAL
2454 14.8 using wind-tunnel data provided by the German VDI guideline 3783-9. *Journal of Wind*
2455 *Engineering & Industrial Aerodynamics*, 142, 104-110
- 2456
- 2457 Oetl, D. (2015b) Evaluation of the revised Lagrangian particle model GRAL against wind-
2458 tunnel and field experiments in the presence of obstacles. *Boundary Layer Meteorol*, 155,
2459 271-287
- 2460
- 2461 Oetl, D. (2020) Documentation of the prognostic mesoscale Model GRAMM Version 22.09.
2462 Institute of Thermodynamics and Sustainable Propulsion Systems, Graz University of
2463 Technology. Available online: <https://gral.tugraz.at/>. (Accessed Feb 2023).
- 2464
- 2465 Oetl, D., and G. Veratti (2021a) A comparative study of mesoscale flow-field modelling in an
2466 Eastern Alpine region using WRF and GRAMM-SCI. *Atmospheric Research*, 249, 105288
- 2467
- 2468 Oetl, D. (2021b) Development of the mesoscale model GRAMM-SCI: Evaluation of

- 2469 simulated highly-resolved flow fields in an Alpine and Pre-Alpine region. *Atmosphere*, 12,
2470 298. Available online: < <https://doi.org/10.3390/atmos12030298>>. (Accessed Nov 2022).
2471
- 2472 Olesen, H. and Chang, J. (2010). Consolidating tools for model evaluation, *International*
2473 *Journal of Environment and Pollution*, Vol. 40, Nos. 1/2/3, pp.175–183a
2474
- 2475 Pereira, H. R., Meschiatti, M. C., Pires, R. C. de M., & Blain, G. C.. (2018). On the
2476 performance of three indices of agreement: an easy-to-use r-code for calculating the
2477 Willmott indices. *Bragantia*, 2018 77(2), 394–403. DOI:10.1590/1678-4499.2017054.
- 2478 Pielke, R. A., Cotton, W. R., Walko, R. E. A., Tremback, C. J., Lyons, W. A., Grasso, L.
2479 D., ... & Copeland, J. H. (1992). A comprehensive meteorological modelling system—RAMS.
2480 *Meteorology and atmospheric Physics*, 49(1), 69-91.
- 2481 Reuter, H. (1970). The dependency of the diffusion conditions of air pollutants on
2482 meteorological parameters. *Archiv für Meteorologie, Geophysik und Bioklimatologie, Serie A*,
2483 19, 173-186.
2484
- 2485 Schauburger G. et al. (2000) Diurnal and annual variation of the sensation distance of odour
2486 emitted by livestock buildings calculated by the Austrian odour dispersion model (AODM).
2487 *Atmospheric Environment* 34(2000)28: 4839-4851. Available online: <[http://i115srv2.vu-](http://i115srv2.vu-wien.ac.at/bm/AODM/AODM1.html)
2488 [wien.ac.at/bm/AODM/AODM1.html](http://i115srv2.vu-wien.ac.at/bm/AODM/AODM1.html)>. (Accessed Nov 2022).
2489
- 2490 Scire, J. S., Robe, F. R., Fernau, M. E., & Yamartino, R. J. (2000). A user's guide for the
2491 CALMET Meteorological Model. *Earth Tech, USA*, 37.
2492
- 2493 Silibello C. (2006) "SURFPRO (SURface-atmosphere interFace PROcessor) User's guide",
2494 Rapporto ARIANET R2006.06.
2495
- 2496 Skamarock, W. C., Klemp, J. B., Dudhia, J., et al. (2008). A Description of the Advanced
2497 Research WRF Version 3, Report No. NCAR/TN-475+STR, U.S. National Center for
2498 Atmospheric Research. doi:10.5065/D68S4MVH.
2499
- 2500 Stull, R. (2017). *Practical Meteorology: An Algebra-based Survey of Atmospheric Science*.
2501 The University of British Columbia. ISBN 978-0-88865-283-6. Available online:
2502 <https://www.eoas.ubc.ca/books/Practical_Meteorology>. (Accessed Nov 2022).
2503
- 2504 Sykes, R.I., Parker, S.F., Henn, D.S., Cerasoli, C.P., and Santos, L.P. (1998). Second-order
2505 Closure Integrated PUFF Model (SCIPUFF), PC-SCIPUFF Version 1.2PD Technical
2506 Documentation, ARAP Report No. 718, Titan Corporation. Available online
2507 <https://gaftp.epa.gov/Air/aqmg/SCRAM/models/nonepa/scipuff/scipuff.pdf>. (Accessed Feb
2508 2023).
- 2509 Tesche, T. W., and D. E. McNally. (2001a). Evaluation of CAMx and Models-3/CMAQ over
2510 the Lower Lake Michigan Region with Inputs from the RAMS3c and MM5 Models, prepared
2511 for the Coordinating Research Council, prepared by Alpine Geophysics, LLC, Ft. Wright, KY.
- 2512 Tesche, T. W., D. E. McNally, C. A. Emery, and E. Tai. (2001b). Evaluation of the MM5
2513 Model Over the Midwestern U.S. for Three 8-Hr Oxidant Episodes, prepared for the Kansas

- 2514 City Ozone Technical Work Group, prepared by Alpine Geophysics, LLC, Ft. Wright, KY and
2515 ENVIRON International Corp., Novato, CA.
- 2516 Tesche, T. W., and D. E. McNally. (2002). Evaluation of the RAMS Meteorological Fields for
2517 Seven SAMI Modelling Episodes”, prepared for the Tennessee Valley Authority and the
2518 Southern Appalachian Mountains Initiative, prepared by Alpine Geophysics, LLC, Ft. Wright,
2519 KY.
- 2520 Tesche, T.W., D. E., McNally and C. Tremback. (2002). Operational Evaluation of the MM5
2521 Meteorological Model over the Continental United States. Protocol for Annual and Episodic
2522 Evaluation. US EPA Task Order 4TCG-68027015. Office of Air Quality Planning and
2523 Standards. Available online
2524 [https://www.epa.gov/sites/default/files/2020-10/documents/tesche_2002_evaluation_protocol](https://www.epa.gov/sites/default/files/2020-10/documents/tesche_2002_evaluation_protocol.pdf)
2525 [.pdf](https://www.epa.gov/sites/default/files/2020-10/documents/tesche_2002_evaluation_protocol.pdf). (Accessed Feb 2023)
- 2526 Tesche, T. W., D. E. McNally, C. F. Loomis, and J. G. Wilkinson. (2002). Regional
2527 Photochemical Modelling over Central Florida for Nine 8-hr Ozone Episodes, Final Report
2528 prepared for the Florida Department of Environmental Protection, prepared by Alpine
2529 Geophysics, LLC, Ft. Wright, KY.
- 2530 Trini Castelli S. (2000). MIRS: a turbulence parameterisation model interfacing RAMS and
2531 SPRAY in a transport and diffusion modelling system. Internal Report. ICGF/CNR No
2532 412/2000 T
- 2533 Trini Castelli, S., Falabino, S., Tinarelli, G., & Anfossi, D. (2014). Effect of the turbulence
2534 parameterisations on the simulation of pollutant dispersion with the RMS modelling system.
2535 In Air pollution modelling and its application XXII, 529-534. Springer Netherlands.
2536 doi:10.1007/978-94-007-5577-2_89.
- 2537 Trini Castelli S., Tinarelli G., Reisin T.G.. (2017). Comparison of atmospheric modelling
2538 systems simulating the flow, turbulence and dispersion at the microscale within obstacles.
2539 Environmental Fluid Mechanics, 17, 879-901.
- 2540 Turner, D.B., (1964). A diffusion model for an urban area. Jour. Appl. Meteor., Vol. 3. pp.
2541 83-91.
2542
- 2543 US Environmental Protection Agency (2017). Guideline on Air Quality Models - Appendix W.
2544 Available online https://www.epa.gov/sites/production/files/2020-09/documents/appw_17.pdf.
2545 (accessed Feb 2023).
2546
- 2547 US Environmental Protection Agency Office of Air Quality (2000). Meteorological Monitoring
2548 Guidance for Regulatory Modeling Application. Available online:
2549 https://www.epa.gov/sites/production/files/2020-10/documents/mmgrma_0.pdf. (Accessed
2550 Nov 2022).
2551
- 2552 US Environmental Protection Agency (2022). Guidance on the Use of the Mesoscale Model
2553 Interface Program (MMIF) for AERMOD Applications, EPA-454/B-22-011. Available online
2554 https://gaftp.epa.gov/Air/aqmg/SCRAM/models/related/mmif/MMIF_Guidance.pdf.
2555 (Accessed Feb 2023).

171 *Leave your comments on this draft [here](#). Due date 9th July 2023*

2556 Willmott, C. J. (1981). On the validation of models. *Physical Geography*, 2(2), 184-194.
2557 doi:10.1080/02723646.1981.10642213.

2558 Willmott, C. J. (1984). On the evaluation of model performance in physical geography. In G.
2559 L. Gaile and C. J. Willmott (Eds.). *Spatial Statistics and Models*, (p.443-460). Springer,
2560 Dordrecht. DOI:10.1007/978-94-017-3048-8_23.

2561 World Meteorological Organisation (2021). Guide to Instruments and Methods of
2562 Observation: Volume I - Measurement of Meteorological Variables, WMO-No. 8. Available
2563 online https://library.wmo.int/doc_num.php?explnum_id=11386. (Accessed Feb 2023).

2564 Yamartino, R.J. (1984). A Comparison of Several "Single-Pass" Estimators of the Standard
2565 Deviation of Wind Direction, *Journal of Applied Meteorology and Climatology*, 23(9), 1362-
2566 1366.

2567

2568 4. Sources and emissions characterisation

2569 4.1 Introduction

2570 Odour sources can be classified from a geometrical point of view according to how they are
2571 treated within atmospheric dispersion models. In this classification, odour emissions may
2572 come from point, area, line or volume sources.

2573 Odour annoyance may be due to the simultaneous emissions from multiple sources. For
2574 instance, a municipal waste treatment centre is characterised by several types of sources:
2575 area/volume sources (e.g., compost piles, waste stocks), point sources (e.g., biogas
2576 exhaust), and diffuse sources (e.g., leakage from buildings). Sources are often static but
2577 also in motion (e.g., trucks turning a compost pile over).

2578 Special requirements for the modelling techniques are necessary to consider the interaction
2579 of different emission sources like point sources (e.g. stacks, exhaust air ducts), line sources
2580 (e.g. ventilation belts, roadways), area sources (e.g. slag beds, biofilters, clarifiers,
2581 manoeuvring areas) and volume sources (windows and gates distributed over an operation
2582 building, stockpiles).

2583 In principle, all sources have to be specified, but sometimes criteria are introduced to neglect
2584 sources with odour emission rates or odour concentrations below specific thresholds. If there
2585 are many homogeneous sources, these are sometimes combined into a sort of equivalent
2586 source.

2587 Another approach is to determine the odour flow rate after performing a field inspection (EN
2588 16841 part 2) followed by a backpropagation use of the odour dispersion modelling (reverse
2589 modelling).

2590 One important input variable of odour dispersion models is the *Odour Emission Rate* (OER),
2591 expressed in ou/s, or the *Specific Odour Emission Rate* (SOER), expressed in ou/m²/s. The
2592 OER calculation needs first to collect and analyse the air sample to estimate its odour
2593 concentration and second to determine the air flow rate. Sometimes, the OER is not
2594 available, and the emission rate of odorants (e.g., H₂S) is expressed in mass per unit time
2595 (e.g., g/s). In these situations, the resulting concentration of each released odorant must be
2596 compared with its odour threshold to determine if it has been exceeded.

2597 The characterisation of odour emissions is closely related to the type of source, in particular
2598 the geometry, whether passive or active areas or point (e.g. stacks) or fugitive (e.g. stockpile
2599 or building) sources. The specific objective of a study may also influence the method of
2600 sampling emissions from a source.

2601 The sampling method will strongly influence the characterisation of the odour, and it is
2602 important to link the source parameters with the proposed sampling protocol. According to
2603 the applied technique, there are different ways to estimate the OER. The obtained value is
2604 strictly related to the specific technical details of the sampling and must be considered as a
2605 “relative” value. It means that another sampling protocol may give other values. Therefore,
2606 an OER of a source may be different due to the sampling method adopted. This will, in turn,
2607 affect the emission rate input and model predictions. For example, in [paragraph 4.2.3.1](#), it is
2608 mentioned that using wind tunnels or flow chambers will condition the odour rate obtained.

2609 Other important source data are needed for dispersion modelling, such as release height,
2610 exhaust gas temperature, exhaust gas velocity and surface area. This chapter aims to
2611 describe the inputs to the dispersion model that relate to the source characteristics and rate
2612 of odour emission.

2613 4.2 Measuring odour emissions

2614 4.2.1 Point sources

2615 A point source, as defined in EN 13725, is a discrete stationary source releasing waste gas
2616 to the atmosphere via ducts of defined dimensions with a controlled or controllable volume
2617 flow rate. Stacks and vents are the most common examples of point sources.

2618 The following geometrical and emission information defines a point source:

- 2619 ● Coordinates;
- 2620 ● Height above the ground of the release point;
- 2621 ● Cross-sectional area of the stack/duct at exit plane;
- 2622 ● Exit type (e.g., vertical, horizontal, tilted, with or without rain cap, ...);
- 2623 ● Exit velocity of the effluent;
- 2624 ● Temperature of the effluent;
- 2625 ● Volume flow rate;
- 2626 ● Odour concentration within the flue gas.

2627 Point sources vary in configuration and include simple stacks that discharge vertically to the
2628 atmosphere at various heights above the ground or surrounding buildings, and complex
2629 discharge arrangements such as goose-neck downward discharges, horizontal discharges
2630 and capped vertical discharges. Some representative examples of point source discharge
2631 configurations are shown in Figure 4-1, while Figure 4-2 represents an example of emission
2632 extraction from a piggery. The discharge geometry is an essential factor defining the point
2633 source as it may exert a controlling influence on the source's effective release height of
2634 odours.

2635 According to EN 13725:2022, the OER is the number of odour units which crosses a given
2636 surface per unit of time. The OER is typically expressed in ou_E/s , but other units are
2637 sometimes used, for example, ou_E/min or ou_E/h . The OER is a quantity equivalent to the
2638 emission rate - typically expressed in g/s - in dispersion models used for air quality impact
2639 assessments.

2640

2641



2642 **Figure 4-1** Examples of point sources. Vertical stack with free discharge (top left); vertical
2643 stack with rain-cap (top right); Y-shaped vertical stack with internal rain cap (bottom left);
2644 Horizontal stack (Bottom right). (Courtesy of Enviroware)

2645



2646

2647 **Figure 4-2** Example of emission extraction from a piggery. (Courtesy of Air Environment)

2648

2649

2650

2651 4.2.1.1. Synthetic description of sampling techniques for point sources

2652 The odour concentration determined by olfactometry is the result of sensory measurements
2653 by selected panel members according to EN 13725:2022. The odorous gas is sampled in
2654 polymer bags at the source, and then the bag is connected to an olfactometer, where panel
2655 members conduct a sensorial analysis. Sampling introduces an additional uncertainty to that
2656 associated with dynamic olfactometry.

2657 Different steps are taken to ensure the sampling is carried out correctly. For instance, the
2658 bag and the sampling line are verified to be odourless; the sampling line is connected to the
2659 exhaust gas to sample, and the bag is placed in a vacuum box / chamber. The exhaust gas
2660 is drawn into the bag by the vacuum in the box / chamber. The sample must have minimum
2661 contact with sampling materials. In some cases, a sample must be diluted in order to avoid
2662 condensation, or simply because the odour concentration is too high.

2663 It is necessary to check if the gas contains particulates, and, if yes, it needs to be filtered
2664 because particulates are incompatible with olfactometer use. Temperature and humidity are
2665 also checked because the gas cannot be too hot, or too humid. A dilution probe with dry air
2666 or dry nitrogen can decrease humidity and then avoid condensation in the bag. Using
2667 nitrogen, the dilution rate can be easily verified by measuring oxygen level in the sample. Of

2668 course the dilution factor (generally between 5 to 10) at this sampling step must be included
2669 in the determination of the final olfactometry analysis results, also based on a dilution
2670 (dilution of the sample to determine its limit of perception). A pre-dilution of the sample can
2671 be carried out in the laboratory for highly concentrated samples. This action is necessary if
2672 the concentration of the sample is potentially higher than the dilution range of the
2673 olfactometer.

2674 According to EN 13725, storage time between sampling and olfactory analysis should
2675 usually be at most 30 hours by convention. However, there needs to be more clarity in the
2676 literature to substantiate that degradation, adsorption and diffusion phenomena will be
2677 insignificant below certain storage times. Significant degradation of odour concentration in
2678 samples within 30 hours after sampling has been reported, for example, for odorants emitted
2679 from foundries and tobacco leaf processing. That is one of the reasons why the German
2680 standard on olfactometry VDI 3880 allows a maximum time of 6 hours between sampling
2681 and analysis.

2682 4.2.2 Active area sources

2683 These sources are characterised by odour emission from a surface with a volumetric flow or
2684 exit velocity greater than specific thresholds. According to EN 13725, active area sources
2685 are “*aerated with air gas that is driven through the matrix underneath the surface by*
2686 *mechanical ventilation*” such as, aerated composting. A typical example of an active area
2687 source is a biofilter, as shown in Figure 4-3.

2688 EN 13725:2022 classifies active area sources as *sources with an exit velocity $v > 0.008$*
2689 *$m^3/s/m^2$. Area sources with lower exit speeds are passive area sources.*



2690

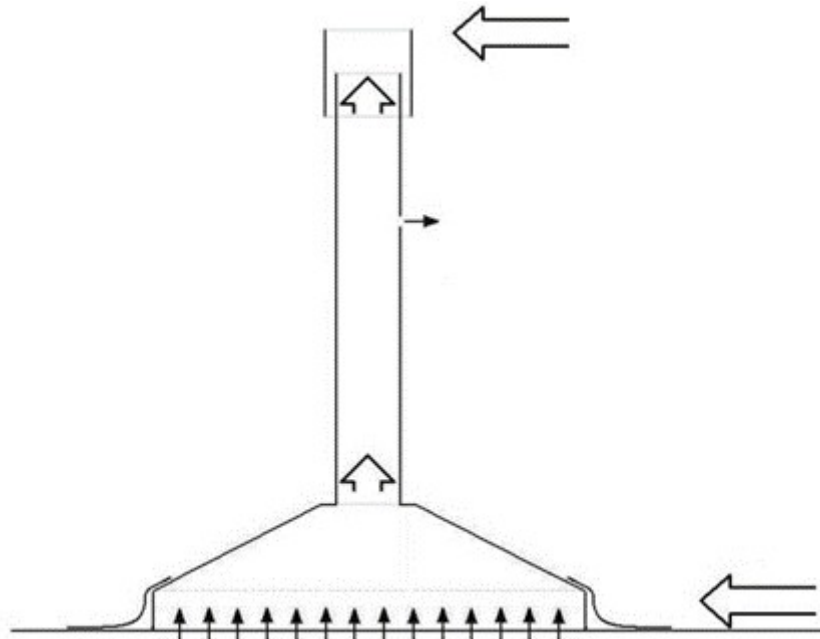
2691 **Figure 4-3** Example of active source: biofilter surface (left panel); biofilter container open on
2692 the top (right panel) (Courtesy of Olfasense)

2693

2694

2695 4.2.2.1. Synthetic description of sampling techniques for active area sources

2696 For the measurement of active area sources with a minimum discharge velocity (e.g.,
2697 biofilters, aerated compost heaps), a sampling hood with one m^2 surface is used to avoid
2698 disturbances of the air discharge with the atmosphere (Figure 4-4). Sampling takes place in
2699 the chimney of the sampling hood.



2700

2701 **Figure 4-4** Sampling hood, as defined in EN 13725:2022 and VDI 3880:2015 for active area
2702 sources.

2703

2704 Usually, due to the extent of the area sources, inhomogeneities must be checked and a
2705 sampling strategy must be defined. Sampling points are selected on the basis of
2706 representative source flow rates. Alternatively, a complete coverage of the area
2707 could be considered, as shown in Figure 4-5.

2708



2709

2710 **Figure 4-5** Complete coverage of an active area source.

2711

2712

2713

2714 The product of the odour concentration of the sample bag (ou_E/m^3) and air velocity through
2715 the device (m/sec) gives the specific odour emission rate (SOER, $ou_E/m^2/s$). It is observed
2716 that the air velocity through the device is the ratio between the air flow rate (m^3/s) and the
2717 specific area A_d (m^2) of the device. The odour emission rate (OER) is the product between
2718 the SOER and the area A_s of the emitting surface.

2719 4.2.3 Passive area sources

2720 According to EN 13725:2022, passive area sources are areas with an exit velocity $v < 0.008$
2721 $m^3/s/m^2$. Passive area sources include waste landfills, fields after manure spreading,
2722 compost piles and open wastewater tanks. They emit through diffusion at the boundary layer
2723 between the source surface and the air. The emission depends on multiple variables, such
2724 as the material's humidity, atmospheric temperature and wind speed. Examples of area
2725 sources are shown in Figure 4-6.

2726



2727

2728 **Figure 4-6** Different area sources: compost pile (left panel); aeration basin (right panel).
2729 (Courtesy of Olfasense)

2730

2731 4.2.3.1. Synthetic description of sampling techniques for passive area sources

2732 For the passive area sources, the emission rate is estimated by simulating the flow through a
2733 ventilated hood (such as flux hoods and wind tunnels). The emission flow rate is then the
2734 hood's ventilation rate and is typically dependent on sampling conditions.

2735 The SOER is estimated by covering a part of the surface with a ventilated hood with a
2736 defined flow rate, which can then be measured in the exit stack (VDI 3880:2015). The
2737 sampling plan shall ensure that the area sampled is representative of the total emission from
2738 the area source.

2739

2740 Different methods exist to measure the odour emission rate of these sources. The most
2741 common are wind tunnels (Figure 4-7) and flux hoods (Figures 4-8 and 4-9).

2742

2743 EN 13725:2022 recommends considering the following aspects when using a wind tunnel:

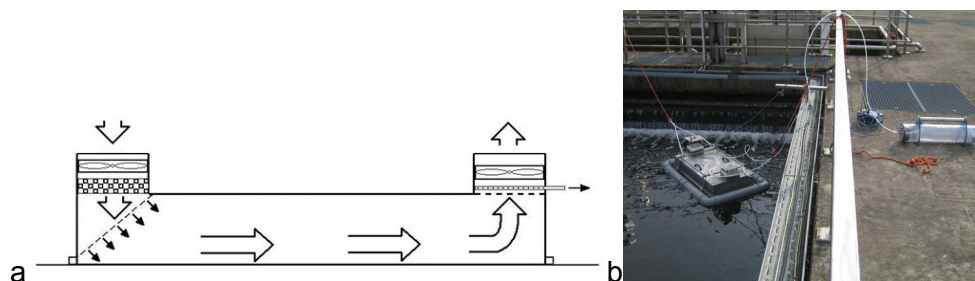
2744

- 2745 1. Sweep air fed into the inlet of the wind tunnel shall be odourless.

2746

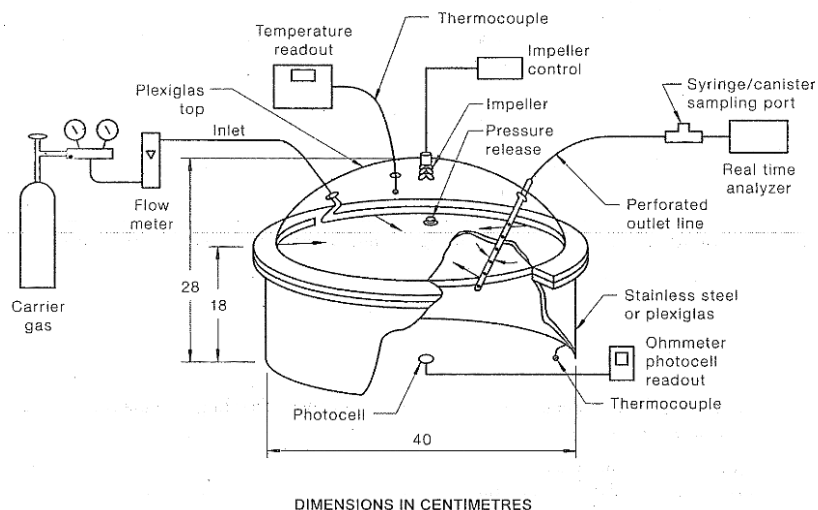
- 2747 2. The flow regime of the sweep air inside the wind tunnel shall be laminar, not
2748 turbulent.
2749
- 2750 3. Since an increase in the sweep air flow rate produces a dilution effect that reduces
2751 the outlet odour concentration, in field conditions, the sweep air flow rate should be
2752 chosen low enough to get an outlet odour concentration higher than the field blank
2753 value. For this reason, a low sweep air velocity in the ventilation chamber is
2754 recommended.
2755
- 2756 4. To get a laminar flow regime of sweep air in the ventilation chamber and as much
2757 homogeneous air velocity as possible, air velocity in any point of the ventilation
2758 chamber, the design of the wind tunnel device upstream of the ventilation chamber is
2759 fundamental. Upstream of the ventilation chamber, a divergent and a parallel flow are
2760 recommended.
2761
- 2762 5. Design and materials of wind tunnel devices should prevent solar radiation from
2763 unnaturally increasing the air temperature in the ventilation chamber and the
2764 temperature of the emitting surface.
2765
- 2766 6. The above-listed parameters mainly affecting the mass transfer rate (in particular
2767 source temperature, sweep air humidity, and sweep air velocity) should be
2768 determined, recorded and reported.

2769



2770

2771 **Figure 4-7** Example of a wind tunnel: ventilated sampling hood, as defined in VDI
2772 3880:2015. Schematic view (left panel); floating on a basin (right panel).(Courtesy of
2773 Olfasense)



2774

2775 **Figure 4-8** Flux Chamber: Set up of the emission isolation according to US EPA 1986



2776

2777 **Figure 4-9** Flux chamber on a liquid source (left panel) and on a solid source (right panel)

2778

2779 Over the last 30 years, there has been a long-standing debate about the appropriateness
 2780 and accuracy of wind tunnels versus flux chambers for quantifying area source emissions as
 2781 the sampling devices give quite different results compared to each other and emission
 2782 theory (e.g., Smith & Watts, 1994a; Smith & Watts, 1994b; Jiang & Kaye, 1996; Parker et al.,
 2783 2013; Prata et al., 2018; Lucernoni et al., 2016). Therefore, verifying that they were collected
 2784 using the same sampling method is essential when comparing emission data from different
 2785 measurements.

2786

2787 An extensive comparison study was conducted in October 2013 in France (Guillot et al.,
 2788 2014) to understand the differences in the results of the odour emission rates calculated
 2789 from different sampling devices. The project aimed to test two types of devices: flux
 2790 chambers (with low sweeping flows) and wind tunnels (with high sweeping flows). Liquid
 2791 area sources and solid area sources were tested. Figure 4-10 shows the experiment's
 2792 setting for a solid area source (composting pile), while Figure 4-11 shows the experiment's
 2793 setting for a liquid area source (pond).



2794
2795 **Figure 4-10** Sampling flux chambers and wind tunnels in a composting pile. (Courtesy of
2796 JM. Guillot)
2797



2798
2799 **Figure 4-11** Sampling flux chambers and wind tunnels in a pond (Courtesy of JM. Guillot)
2800

2801 Some of the devices tested with a low sweeping flow (flux chambers) are shown in Figure 4-
2802 12, while some of the devices tested with a high sweeping flow (wind tunnels) are presented
2803 in Figure 4-13.
2804

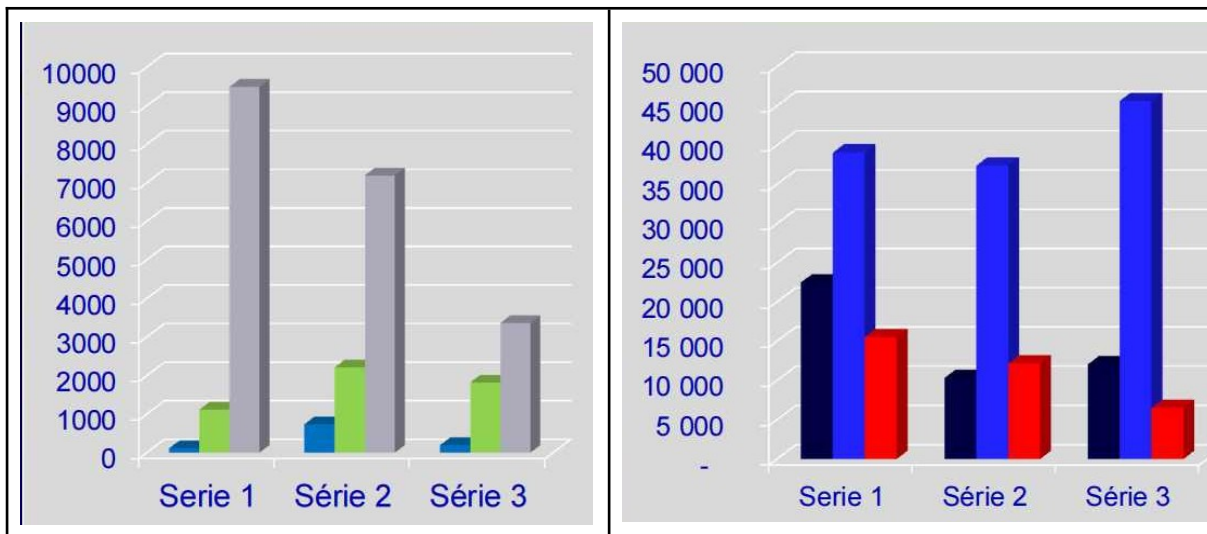


2805
2806 **Figure 4-12** Devices with a low sweeping flow. (Courtesy of JM. Guillot)
2807



2808
2809 **Figure 4-13** Devices with a high sweeping flow. (Courtesy of JM. Guillot)

2810
2811 The graphs in Figure 4-14 show the results for both types of devices.
2812



2813 **Figure 4-14** Left panel: SOER in $ou_E/h/m^2$ for three different flux chambers (blue, green and
2814 grey) at different measurement periods. Right panel: SOER in $ou_E/h/m^2$ for three different
2815 wind tunnels (colours dark blue, blue and red) at different measurement periods. (Courtesy
2816 of JM. Guillot)

2817
2818
2819 The project results showed that, for example, for measurement day 1 (Serie 1), flux
2820 chambers (left panel) showed significantly different SOERs between each other with
2821 differences of several orders of magnitude. Moreover, for the same measurement period
2822 (Serie 1), wind tunnels showed a much higher SOER, sometimes four times higher than the
2823 highest SOER obtained by a flux chamber. In the case of wind tunnels, the variability of the
2824 results was also relevant. This result demonstrates that odour emission from a static area
2825 source can only be compared to another if sampling conditions are similar.
2826

2827 Both methods lead to emissions at the boundary of the source. The link from odour
2828 concentration to emission rates is the diffusion coefficient. This factor might vary with
2829 different parameters such as atmospheric conditions.

2830

2831 A way to verify the impact of passive area sources is by performing a plume inspection. EN
2832 16841-2:2017 describes two ways of measuring the impact of a source. With the impact
2833 measurements, the model results can be validated. The effective emission rate can be
2834 determined by using reverse modelling, see [paragraph 4.4.2](#).

2835 4.2.4 Volume sources

2836 When the emissions are immediately spread over a 3D region, they can be modelled
2837 through volume sources. Examples of this type of source are industrial buildings with high
2838 gates and windows, open stall barns with natural ventilation, or portions of plants with
2839 fugitive emissions (i.e., unintentional losses) from items that are designed to be sealed (e.g.,
2840 valves, flanges), passive ventilation apertures, leakage through building cladding (e.g.,
2841 Figure 4-15).

2842 These sources have no defined dimensions and no defined volume flow rate. Their
2843 description in an air dispersion model is challenging and highly dependent on every specific
2844 case.

2845



2846

2847 **Figure 4-15** Example of diffuse emissions from an industrial building.

2848

2849 4.2.4.1. Synthetic description of estimation techniques for volume sources

2850 In the absence of a defined volume flow, sampling in a bag to estimate the emission rate
2851 (like for the point source) is not applicable. Moreover, it is challenging to sample due to the
2852 influence of weather on the source parameters (mainly temperature, humidity and flow). In
2853 some cases, emission rates could be derived using a source apportionment approach if a
2854 known indicator related to odour is available. For instance, Invernizzi et al. (2021) described
2855 a series of approximations to determine VOC emission rates.

2856 When dealing with fugitive emissions, odour measurements must be performed at the
2857 receptor site (ambient air). Field inspection and *Reverse Dispersion Modelling* (RDM) is an
2858 appropriate and highly recommended approach.

2859 Another methodology to measure diffuse / fugitive sources is the one proposed by *EN 17628*
2860 (Fugitive and diffuse emissions of common concern to industry sectors - Standard method to
2861 determine diffuse emissions of VOCs into the atmosphere), see [paragraph 7.2.2](#). This
2862 standard specifies an array of methods to detect and / or identify and / or quantify VOC
2863 emissions from industrial sources. These methods include *Optical Gas Imaging* (OGI),
2864 *Differential Absorption Lidar* (DIAL), *Solar Occultation Flux* (SOF), *Tracer Correlation* (TC)
2865 and RDM. Additionally, the EN 15446:2008 standard includes guidance on how to perform a
2866 measurement for different specific items (e.g., valves, flanges, pump seals, compressor
2867 seals, ...). It also specifies how to estimate the emission rates starting from the VOC
2868 concentration measurements in ppm.

2869 An additional method to estimate the fugitive emissions of VOC is to make an inventory of
2870 the equipment (e.g., valves, flanges, etc.) by reading the P&IDs (Piping and Instrumentation
2871 Diagrams) of a plant, then applying the relevant emission factors for each item of equipment
2872 (e.g., Ng et al., 2017). The emissions depend on the equipment and on the characteristics of
2873 the flow through it, both in terms of composition and of phase (gas, liquid, 2-phase). This
2874 method is complex and time-consuming because some plants (e.g., refineries) may have
2875 hundreds of P&IDs describing thousands of pieces of equipment. For example, US-EPA
2876 (2005) reports an average number of valves greater than 7000 and an average number of
2877 over 12000 connectors for a typical refinery or chemical plant. Leak detection and repair
2878 (LDAR) programs have been promoted to reduce fugitive emissions (US-EPA, 2022a). VOC
2879 emission factors for many items are available, for example, from US-EPA (1995a).

2880 As for the passive area sources, ambient air measurement may be used to derive emission
2881 rates for modelling (EN 16841). Additional details are given in [paragraph 4.4.2](#).

2882

2883 4.2.5 Gas detector tubes

2884 Gas detector tubes (GDTs), also called colour indicator tubes, are relatively simple tools to
2885 detect the presence of a specific chemical species or class of species in the atmosphere and
2886 their concentration. They are thin glass tubes containing a reagent powder that reacts with
2887 the specific gas generating a coloured stain. The length of the stain is read against a
2888 calibrated scale on the tube, indicating the concentration level. A hand pump - or an
2889 electronic pump - is used to draw the air sample into the tube. The volume amount of the air
2890 sample is typically 100 cm³, but it may also be half of it (50 cm³), and sampling usually takes
2891 less than one minute to complete. The datasheets of each tube contain tables with
2892 temperature correction factors to adjust the resulting concentration to the ambient
2893 temperature. Other adjustments may also be made for pressure.

2894 The main advantage of the gas detector tubes is that they are very inexpensive compared to
2895 other measurement techniques (the cost of each measurement is approximately 10-15
2896 USD). They are also simple to use and give immediate results. The disadvantage is that they
2897 are less accurate than other measurement techniques and indicate the concentration of
2898 odorants, not odour units of the composite gas, which may contain numerous odorants; they
2899 may also be relatively insensitive and not detect substances at levels close to the odour
2900 thresholds of the species present. However, in the odour field, odorant concentrations at
2901 emission sources are sometimes completely unknown, and gas detector tubes may be very
2902 useful to get initial indications. The use of GDTs for odour pollution studies is also described
2903 in the scientific literature (e.g, Tanaka et al., 2004; Ninh et al., 2007; Schmitt, 2017).

2904

2905 Each gas detector tube is specific for a gas or a class of compounds, and a given
2906 concentration range. Therefore the user must know the chemical species expected in their
2907 emissions and the order of magnitude of their concentrations. However, some tubes are
2908 capable of simultaneously determining multiple unknown substances in the sample.

2909

2910 GDTs are a useful method that could be easily employed at point and active area sources
2911 but probably less useful at the more difficult to characterise passive area sources and
2912 volume sources. Additional information about gas detector tubes can be found in Kawamura
2913 et al. (2021). Gas detector tubes are available from different brands worldwide, such as
2914 Dräger, Uniphos, Gastec, Sensidyne, RAE and Kitagawa.

2915

2916 4.2.6 Emerging methodologies

2917 New methodologies for measuring odour emissions are emerging that are based on the
2918 simultaneous use of drones and Instrumental Odour Monitoring Systems (IOMS). For
2919 example, Burgués et al. (2022) present the results of a study that aimed to characterise and
2920 monitor odour emissions from a WWTP using a drone-based chemical sensor system. The
2921 study was conducted over a period of several weeks, during which time the researchers
2922 used a drone equipped with a chemical sensor to collect air samples at different locations
2923 within the plant. The results show that the airborne IOMS was able to detect and quantify
2924 different odorous compounds emitted from the WWTP.

2925 According to the authors, the use of a drone-based IOMS provided several advantages over
2926 the gold standard odour monitoring method (dynamic olfactometry). The drone was able to
2927 collect air samples from hard-to-reach locations, which are not accessible by ground-based
2928 monitoring systems. Additionally, the drone-based system was cheaper, and was able to
2929 collect real-time data, providing a more accurate and comprehensive understanding of odour
2930 emissions from the wastewater treatment plant.

2931

2932 4.3 Modelling odour emissions

2933 One of the first steps to be performed when dealing with complex plants, that may be
2934 characterised by the presence of tens of odour-emitting sources of any type (stacks, diffuse
2935 sources and fugitive sources), is to decide if all of them must be considered. The magnitude
2936 of the odour emissions from these sources may be very different, with some of them being
2937 important emitters, and some others being less important or even negligible. Since the
2938 preparation of data for all the sources within the dispersion model is a time-consuming

2939 process, it is important to understand if and when a source can be considered negligible.
 2940 These considerations are typically based on specific thresholds on the OER and the odour
 2941 concentration. For example, the odour guidelines of Region Lombardy (Italy), as described in
 2942 DGR 3018/2012, state that all the sources characterised by an OER greater than 500 ou_E/s
 2943 must be considered in a study, excluding those characterised by a maximum odour
 2944 concentration below 80 ou_E/m³. In other words, sources characterised by OER below 500
 2945 ou_E/s or concentration below 80 ou_E/m³ can be neglected. A source with a variable OER, for
 2946 example because it depends on meteorological variables, can be neglected only if the OER
 2947 remains below 500 ou_E/s for each time of simulation interval. Of course, there are no
 2948 particular contraindications - excluding the additional time required for the study - to use all
 2949 the sources in view of a conservative principle. Most importantly, other factors should be
 2950 considered before excluding a source from a simulation, for example its proximity to a
 2951 sensitive receptor or the particularly offensive hedonic tone of its emissions.

2952 4.3.1 Point sources

2953 Point sources are usually identified as vertical stacks that emit freely into the atmosphere.
 2954 Stacks are characterised by a well-defined volume flow expressed in volume per unit time at
 2955 a specific temperature. Typically volume flow is given at a temperature of 0°C, and is
 2956 expressed in Nm³/h (normal cubic metres per hour).

2957
 2958 The OER is calculated from the product of odour concentration (C_{od}) and volumetric flow on
 2959 wet basis at a temperature of 20°C and pressure of 101.3kPa (EN 13725:2004). Then, if the
 2960 volumetric flow of the stack Q_s (m³/h) is given at a different temperature T_s (°C) and pressure
 2961 P_s (kPa), it must be transformed with the following equation:

$$2963 \quad Q = Q_s \frac{273.15 + 20}{273.15 + T_s} \frac{P_s}{101.3}$$

2964
 2965 For example, if a stack has $Q_s = 20000$ m³/h at $T_s = 130$ °C and $P_s = 105$ kPa, the volumetric
 2966 flow at 20°C and 101.3 kPa is 15074 m³/h, or 4.18 m³/s. Therefore, if the flue gas of the
 2967 same stack has an odour concentration $C_{od} = 5000$ ou_E/m³, the resulting OER is 20936 ou_E/s.

2968
 2969 From a practical point of view, the emission temperature T_s is always known because it is
 2970 needed by the atmospheric dispersion models for calculating the plume rise parameters. On
 2971 the contrary, the pressure P_s within the stack is almost never known, therefore, in the above
 2972 equation, the correction for pressure is often neglected (i.e., it is assumed that
 2973 $P_s = 101.3$ kPa).

2974
 2975 When exit velocity is not measured, it can be estimated by calculating the volume flow at the
 2976 emission temperature and dividing by the exit area and by 3600 s/h. For example,
 2977 considering again the stack described above, and assuming a diameter of 1.1 m (i.e., an
 2978 area of 0.950m²), the exit velocity is 5.85 m/s.

2979
 2980 Temperature and exit velocity are important variables for calculating the plume rise. In some
 2981 cases plume rise may be reduced due to the presence of a rain cap or due to the horizontal
 2982 direction of the stack, as shown in the previous Figure 4.1. In these situations the vertical
 2983 velocity of the plume is null, and the plume rise is due only to thermal buoyancy if the exit

2984 temperature exceeds the ambient temperature. Some atmospheric dispersion models
2985 contain algorithms to simulate this kind of emissions. For example, as reported in the 2021
2986 British Columbia Dispersion Modelling Guideline (BC, 2021):

2987
2988 *“AERSCREEN and AERMOD can handle this situation explicitly through the selection of*
2989 *options, POINTCAP and POINTHOR for treating capped and horizontal plumes,*
2990 *respectively. The source parameters are input as if it were a vertically oriented stack and the*
2991 *model applies adjustments internally to account for these types of orientations. For plumes*
2992 *with little or no buoyancy, users can specify a stack gas exit temperature = 0.0 K,*
2993 *automatically setting the exit temperature to the ambient temperature.*

2994
2995 *CALPUFF can also handle these sources through the use of the adjustable vertical*
2996 *momentum flux factor (FMFAC) for point sources with constant emissions which can assume*
2997 *only the values 1 (corresponding to a vertically oriented stack) and 0 (corresponding to a*
2998 *horizontal or capped stack with no vertical momentum). If time-varying point source*
2999 *emissions are applied, in the PTEMARB.DAT file, set TIDATA(7) (the vertical momentum*
3000 *flux) = 0”.*

3001
3002 Other modern dispersion models may have algorithms to simulate releases from horizontal
3003 stacks or rain-capped stacks, and the users should adopt these algorithms when present.
3004 When the simulation is carried out with a dispersion model without specific algorithms for
3005 rain caps and horizontal stacks, the user may force the exit velocity to 0.001 m/s. It must be
3006 observed that higher emission velocities (e.g., 0.1 m/s) are not suggested because they may
3007 still result in significant momentum plume rise being calculated, as pointed out by the US-
3008 EPA Model Clearinghouse Memorandum dated July 9, 1993.

3009
3010 For vertical stacks with rain caps the stack tip downwash must not be activated, but their
3011 height must be reduced by three times their actual diameter, which means assuming the
3012 maximum effect of the stack tip downwash. If the atmospheric dispersion model adopts a
3013 parametric algorithm for the plume rise (e.g., the Briggs equations), an effective diameter
3014 must be calculated to maintain the volume flow and buoyancy. The equivalent diameter d_E
3015 can be calculated as

3016
3017
$$d_E = d \sqrt{v}$$

3018
3019 Where d (m) is the actual stack diameter, and v (m/s) is the actual exit velocity. For example,
3020 a capped stack with a diameter of 0.2 m and exit velocity 3m/s would have an equivalent
3021 diameter $d_E = 11.0\text{m}$.

3022
3023 If the atmospheric dispersion model adopts a numerical algorithm for the plume rise, it
3024 solves a set of differential equations and needs the stack diameter as one of the initial
3025 conditions. The previous numerical example shows that the equivalent diameter may be -
3026 and often is - very large with respect to the actual diameter, therefore using the equivalent
3027 diameter in a numerical algorithm for the plume rise may give unrealistic results. In these
3028 cases, the actual stack diameter must be used, as suggested for example by the Iowa
3029 Department of Natural Resources (IDNR, 2014), or - as suggested by the AERMOD user
3030 guide (US-EPA, 2022b) - the initial radius must be assumed two times the actual stack
3031 diameter (i.e., the diameter must be multiplied by 4) to account for the interaction of the

3032 existing plume with the cap.

3033

3034 When dealing with horizontal stacks in dispersion models without specific algorithms to treat
3035 them, the stack tip downwash algorithm (if present) must not be activated, the exit velocity
3036 may be set to 0.001 m/s, and their actual height must be used.

3037

3038 Rarely, the stack tip is tilted and unobstructed. In these cases, the actual stack diameter and
3039 height must be given as input to the dispersion model, while the vertical component of the
3040 exit velocity must be used (IDNR, 2014). Unless the dispersion model has its own algorithm
3041 to simulate tilted stacks, the vertical component is calculated by multiplying the exit velocity
3042 and the cosine of the angle between the stack and the vertical. If the tilted stack is
3043 obstructed by a rain cap or any other equipment that suppresses the vertical momentum, the
3044 exit velocity may be set to 0.001 m/s as described previously.

3045

3046 Point sources may be affected by building downwash, which means that their plume can be
3047 captured in the building wake, increasing the ground-level concentration. As a general rule, a
3048 building may cause downwash to the stacks located within a distance of $5L$, with L the
3049 minimum between the height and the width of the building. Sources within this distance
3050 lower than 2.5 the building height are subject to building downwash.

3051 Some hybrid models, such as Eulerian/Lagrangian models or microscale Eulerian CFD
3052 models, can simulate building downwash without the need for any empirical methodology
3053 (Flassak et al., 2010; Oettl, 2015). However, for most atmospheric dispersion models used
3054 for regulatory purposes, the building downwash parameters to include in the input data may
3055 be determined with the Building Profile Input Program, BPIP (US-EPA, 1995c). Among the
3056 input data required by BPIP there are coordinates and the height of the buildings. These
3057 data may be obtained from plot plans of the industrial plant or, for some locations where the
3058 “3D Buildings” feature is available, from Google Earth with a good approximation.

3059

3060

3061 4.3.2 Active area sources

3062 As shown in Chapter [4.2.2](#), active area sources are characterised by their volumetric flow by
3063 unit of area. Therefore, their OER may be calculated by multiplying the volume flow at 20°C
3064 (m^3/hm^2) and the odour concentration (ou_E/m^3) by the total area of the source.

3065

3066 Within the dispersion model, an active area source can be simulated through an equivalent
3067 point source, which means a point source with equivalent area and the same volumetric
3068 flow. They typically emit at ambient temperature. Other times they are simulated through a
3069 series of point sources, for example, one in each vertex of the active area source (assuming,
3070 for instance, a rectangular shape). The sum of the volumetric flows of the point sources must
3071 be the total volumetric flow of the active area source.

3072

3073 According to EN 13725:2022, area sources with an exit velocity $v > 0,008$ m/s are, by
3074 consensus, active area sources and shall be sampled accordingly. Area sources with lower
3075 exit speeds are considered to be passive area sources.

3076

3077 4.3.3 Passive area sources

3078 Emissions from passive area sources are typically governed by evaporation and diffusion.
 3079 The concentration gradient provides the driving force for the transfer of odorants from solid
 3080 or liquid surfaces to the air (Laor et al., 2014).

3081
 3082 As discussed in [paragraph 4.2.3](#), the specific odour emission rate (SOER) of passive area
 3083 sources is determined by wind tunnels, or similar instruments, in which air flows with a
 3084 known velocity (typically of the order of 0.3 m/s), and the SOER value depends on the flow
 3085 velocity. This means that the actual emission from the source depends on the wind speed
 3086 close to its surface. The OER due to a specific wind speed v_s close to the emitting surface is
 3087 calculated as (e.g., Lucernoni et al., 2016):

3088
 3089
$$OER = A SOER \left(\frac{v_s}{v_R} \right)^k$$

3090
 3091 where A (m²) is the area of the passive source, v_R (m/s) is the reference air speed within the
 3092 wind tunnel during the measurement (e.g., 0.3 m/s) and k is a constant typically equal to 0.5.
 3093 It is observed that Jiang and Kaye (1996) suggested k=0.63, but k=0.5 is most often used.

3094
 3095 The wind speed over the emitting surface (v_s) can be calculated with a power law relation,
 3096 even though other equations can be used, as described for example, by Ravina et al. (2020).
 3097 The power law equation is:

3098
 3099
$$v_s = v_h \left(\frac{z + z_{wt}}{h} \right)^p$$

3100
 3101 Where h (m) is the height at which the wind speed v_h (m/s) is known, z (m) is the height
 3102 above the ground of the area source, z_{wt} (m) is the half height of the wind tunnel, and p
 3103 (unitless) is a power coefficient depending on the atmospheric stability and land use type
 3104 (rural or urban). The values of the power coefficient p are shown in Table 4-1 (US-EPA,
 3105 1995b), even though different values have also been proposed (e.g., Arya, 1999; Scire et al.,
 3106 2000).

3107
 3108 **Table 4-1** Values of the power coefficient p

Stability	Rural	Urban
A	0.07	0.15
B	0.07	0.15
C	0.10	0.20
D	0.15	0.25
E	0.35	0.30
F	0.55	0.30

3109

3110
3111 Considering the special case of emissions from liquid surfaces within tanks (e.g., wastewater
3112 tanks), the tank height above the ground is often used for z in the power law equation. When
3113 the tank is almost full, this approach is correct, while it can cause overestimated emissions
3114 when the tank is not completely full, because the wind speed at the tank top is higher than
3115 the wind speed close to the emitting surface, which may be well below the tank top. Bellasio
3116 and Bianconi (2022) proposed a possible solution to this problem with new equations in
3117 which emissions depend on the distance between the tank top and the emitting surface, the
3118 wind direction and the tank orientation (for rectangular tanks).

3119
3120 When the odour source is placed in a location partially protected from the wind (e.g., the
3121 presence of buildings and other structures), using the above equation for getting the OER as
3122 a function of wind speed may give overestimated emissions. However, even in those
3123 situations, the odour emission is related to the atmospheric motion close to the emitting
3124 surface. A possible treatment of these situations involves using an indicator of the
3125 mechanical turbulence in place of the wind speed v_s close to the emitting surface. Therefore,
3126 the OER may be estimated as

3127
3128
$$OER = A SOER \left(\frac{u_*}{v_R} \right)^{0.5}$$

3129
3130 Where u^* is the friction velocity (m/s), which may be obtained from the meteorological model.

3131
3132 The above equations apply to situations when the emissions depend on the “stripping” of
3133 odorous molecules from the surface. There are situations in which the emissions do not
3134 depend on wind speed. For example, the odour emissions from cultivated landfill areas
3135 (permanently covered waste) do not depend on wind speed because they are related to the
3136 biogas production from the old waste within the landfill. Capelli et al. (2018) pointed out that
3137 a variable SOER proportional to the square root of the wind speed results in an
3138 overestimation of about one order of magnitude of the landfill odour impact. Therefore, the
3139 landfill surfaces must be treated as a particular type of passive area source, not depending
3140 on the wind speed. On the contrary, the odour emissions from fresh waste within the front of
3141 the landfill may depend on wind speed and must be treated as described above.

3142

3143 4.3.4 Volume sources

3144 4.3.4.1. Geometrical parameters

3145 Three-dimensional sources such as the one shown in Figure 4-16 are typically described as
3146 volume sources within atmospheric dispersion models. These sources are used for
3147 simulating non-buoyant emissions from buildings or fugitive emissions from valves, flanges
3148 and other items.

3149
3150 The geometrical parameters needed to define a volume source within a Gaussian dispersion
3151 model (e.g., AERMOD) or a Lagrangian puff model (e.g., CALPUFF) are the height of the
3152 centre of the plume (h_e), the initial lateral dimension (S_{y0}), and the initial vertical dimension
3153 (S_{z0}). The initial dimensions can be determined as summarised in Table 4-2 (US-EPA, 1992)

3154
3155
3156
3157
3158
3159
3160
3161
3162
3163
3164
3165
3166

Table 4-2 Initial lateral and vertical dimensions of a volume source (US-EPA, 1992)

Type of source	S_{y0}	S_{z0}
Surface-based ($h_e \sim 0$)	Side length / 4.3	Vertical dimension / 2.15
Elevated source ($h_e > 0$) on or adjacent to building		Building height / 2.15
Elevated source ($h_e > 0$) not on or adjacent to building		Vertical dimension / 4.3

3167
3168
3169
3170
3171
3172
3173
3174
3175
3176
3177
3178
3179
3180
3181
3182
3183
3184
3185
3186
3187
3188
3189
3190
3191
3192

As an alternative, when the volume source is used for simulating fugitive emissions from a building, the New Zealand Ministry of Environment (2004) states that the initial vertical dimension (S_{z0}) may be estimated as a quarter of the building height. The initial lateral dimension (S_{y0}) may be estimated as a quarter of the building width (i.e., the minimum of the horizontal building dimensions).

In AERMOD, the initial lateral and vertical dimensions are used to reconstruct the volume source through two virtual point sources placed at an upwind distance such that at the volume source position, they have those horizontal and vertical dispersions. The positions of the two virtual point sources vary at each simulation time according to the wind speed and wind direction values.

When using volume sources in AERMOD, it is important to remember that receptors cannot be placed within the “exclusion zone”, defined as a circle of radius R (m) equal to $R=2.15S_{y0}+1$. Since AERMOD sets to zero the concentration values within the exclusion zone, it must be verified that the exclusion zone of each source does not extend outside the plant perimeter.

In a Lagrangian particle model, a volume source can be defined more precisely with the shape of the region characterised by the emissions, for example, a parallelepiped, a sphere or a hemisphere. The computational particles are released in random positions within the specified volume during the emissions. Then, particles released at higher levels of the volume source are transported and dispersed more effectively than those released at lower levels with weak wind.

3193 4.3.4.2. Estimation of OER and SOER

3194 When dealing with volume sources, both OER and SOER may be difficult to define.
3195 Typically, what is available is a measure or an estimation of the odour concentration within
3196 the building or the region of interest. Then, there may be two alternatives: 1) the OER is
3197 calculated as the product between the concentration value and the volume flow rate through
3198 the building, or 2) the SOER is calculated as the product between the concentration value
3199 and a representative air speed over the area of interest. It is challenging to give specific
3200 universal equations to treat these situations because any case may require specific
3201 assumptions. Therefore, two examples are described below to illustrate the possible
3202 situations. They are only a starting point to elaborate on other situations.

3203 Example 1: Fugitive emissions from refineries or chemical plants

3204 Fugitive emissions may be simulated with volume sources because they affect large areas of
3205 the plant, both along the horizontal and vertical planes. Those emissions happen in areas
3206 with many obstacles, such as pipelines, buildings, racks, tanks and other structures.
3207 Therefore, wind speed cannot fully act within this industrial environment. However, it is
3208 reasonable to assume that the OER varies as a function of meteorological variables because
3209 both mechanical and convective parameters affect the emissions. For this reason, an
3210 equation for the OER variability should include the dependence on the friction velocity u^*
3211 (representing the mechanical turbulence) and the convective velocity w^* (representing the
3212 convective turbulence). If a representative odour concentration C_{od} may be defined for the
3213 region of area A affected by fugitive emissions (e.g., with dynamic olfactometry, from
3214 scientific literature, from similar plants), the OER for each hour of simulation could be
3215 estimated as

$$3216$$
$$3217 OER = A C_{od} \text{Max}(u_i, w_i)$$

3218 Example 2: Emissions from livestock buildings

3219 These buildings can be considered volume sources. When the odour concentration within a
3220 building has been measured or estimated, the OER can be calculated by multiplying it and
3221 the volumetric flow. For each hour of the simulation period, the volumetric flow Q (m^3/s) can
3222 be estimated considering a contribution due to the wind force (Q_{wf}) and a contribution due to
3223 the thermal buoyancy (Q_{tb}) as described, for example, by Angrecka and Herbut (2014):

$$3224$$
$$3225 Q = \sqrt{\square}$$

3226

3227 The contribution of the wind force (Q_{wf}) is calculated as:

$$3228$$
$$3229 Q_{wf} = E A v$$

3230

3231 Where E is a constant ($E=0.35$), A is the inlet area (m^2), and v is the wind speed (m/s) at a
3232 height above the ground representative for the inlet area, for example, half the opening
3233 height. The wind speed at the representative height can be estimated starting from the
3234 measurements at the anemometer height using the power law equation described in
3235 [paragraph 4.3.3](#) about passive area sources or other tools (e.g., CFD models, when they are
3236 available). Of course, the measurements can be substituted by the
3237 predictions/reconstructions of meteorological models at the first level above the ground.

3238 The contribution of the thermal buoyancy (Q_{tb}) is calculated as
3239

$$3240 \quad Q_{tb} = \frac{C_d A}{3} \sqrt{g H (T_i - T_e)}$$

3241

3242 Where C_d is a constant ($C_d=0.86$), g is the acceleration due to gravity (9.81 m/s^2), H is the
3243 height of the openings (m), T_i is the livestock building internal temperature (K) and T_e is the
3244 external temperature (K). The internal temperature may vary over time and can be a function
3245 of the number and age of cattle within the barn.

3246

3247 During winter, curtains or other equipment may be used to protect the animals from
3248 excessive cooling. The presence of the curtains can be simulated, for example, by reducing
3249 the inlet area during the winter months.

3250 Another example of estimating odour from livestock buildings is described by Rzeźnik and
3251 Mielcarek-Bocheńska (2022). In this publication, the volumetric flow, or ventilation rate, is
3252 calculated as a function of the number of cows, the amount of CO_2 produced by each cow,
3253 and the difference between the internal and external CO_2 concentrations. Additionally, the
3254 amount of CO_2 produced by each cow is calculated based on the heat flux needed to
3255 maintain vital functions, pregnancy and milk production. The final value is then corrected
3256 according to the internal temperature.

3257 The OER resulting from the described procedures is time-dependent and varies for each
3258 hour of the simulation period. These examples may be applied, with due modifications, to
3259 other types of odour emissions from a building.

3260

3261 4.3.5. Temporal variation of emissions

3262 The temporal variation of the odour emissions must be described as precisely as possible
3263 within the dispersion models. These variations may be due to the meteorological
3264 dependence of the odour emissions, for example, in wastewater tanks. They may also be
3265 due to the normal working processes, for instance, in the uncovered landfill front tip during
3266 the day hours and working days, and temporary cover during the closing hours and
3267 weekends.

3268 Brancher et al. (2021) simulated the odour emission from a livestock building, assuming
3269 constant OER and hourly-varying OERs under different assumptions. Their results show that
3270 hourly OERs can improve the confidence in impact assessments compared to simulations
3271 driven by constant emissions.

3272 In some situations, the odour emissions are regular over time, for example, when they
3273 happen N hours of the day every day. In other situations, for instance, when considering
3274 discharges from leachate vessels, the release is short and may happen at any time within
3275 the day when the pressure reaches a specific level. It is typically known, for example, that
3276 the release happens one hour a day, but not exactly when. For example, this kind of release
3277 must be simulated by activating it for a random hour each day.

3278 Similarly, if the odour emission happens for N hours within a working interval of M hours
3279 ($M > N$), with the N hours unknown, they must vary randomly or cyclically within the
3280 dispersion model. In fact, considering the same N hours for all the days of the simulation

3281 may give unrealistic results, for example, because the wind always blows along a specific
3282 direction in those hours (e.g., sea/land breeze) or because the N hours are always within a
3283 time interval with maximum mixing height (e.g., close to noon), or minimum mixing height
3284 (e.g., early morning).

3285 All the most advanced atmospheric dispersion models can define an emission time trend in
3286 their main input file when the trend is cyclic or by external files when variations are
3287 complicated or arbitrary.

3288 When defining a precise time dependence of the odour emissions is impossible, the most
3289 unfavourable conditions must be considered in the atmospheric dispersion model (i.e., the
3290 highest OER must be used).

3291

3292 4.3.6. Future industrial plants

3293 While for existing plants odour impact assessment (OIA) studies can be done using emission
3294 observations (e.g., volumetric flow, odour concentration, SOER), for future plants OIAs can
3295 only be done using the maximum authorised volumetric flow, and the odour concentration or
3296 SOER of similar plants or from the bibliography. Alternatively, the assessment might be
3297 based on a regulatory permit using the maximum allowable SOER as input data. This
3298 approach for future plants may not reflect the reality, but it typically gives overestimations.
3299

3300 Care must be taken when comparing the results of a study where a current scenario and a
3301 future scenario are analysed. Indeed, if the current scenario is simulated starting from the
3302 odour emission observations and the future scenario is simulated with the maximum
3303 authorised values, the difference between the results of the two scenarios will be
3304 unrealistically large.

3305

3306

3307 4.3.7. Uncertainties

3308 In atmospheric modelling, emission estimation is a complex process that involves many
3309 uncertainties. In odour modelling, these uncertainties are possibly even larger.

3310

3311 For example, the simplest situation would be the calculation of the OER of a stack, by the
3312 multiplication of the odour emission concentration and the volume flow rate corrected by
3313 temperature. However, the odour concentration within the stack is typically measured once
3314 and used for a long period of time, but the odour concentration may be a function of the level
3315 of production, which is not constant in time. In air quality studies, on the contrary, particularly
3316 in large plants, major stacks are often equipped with CEMSs, which measure pollutant
3317 concentration, temperature, flow rate and other variables in nearly real-time. Very different
3318 results have been obtained by using a constant OER or hourly-varying OERs with the same
3319 median value (Brancher et al., 2021).

3320

3321 Uncertainties in weather data, such as wind speed, temperature, and atmospheric stability,
3322 can significantly impact odour emission estimation. In fact, as seen in the previous
3323 paragraphs, excluding the conveyed sources (stacks), the meteorological variables play an

3324 important role in estimating the OER.

3325

3326 When emission factors are used for estimating the odour emissions, their inaccuracy reflects
3327 on the final calculations. The same is true when for a specific source there are no
3328 measurements or emission factors, and the emissions are estimated on the basis of similar
3329 sources.

3330

3331 Another source of uncertainty is related to the assumptions and the input values of the
3332 algorithm used to estimate odour emissions. For example, the calculation of the volumetric
3333 flow from a livestock building may be based on the internal temperature, which depends on
3334 the number of animals, their age, physical state and other variables. All these variables have
3335 their own uncertainties, as well as the algorithm that uses them to give the internal
3336 temperature of the building.

3337

3338 As commented in the previous paragraphs, different measurement techniques can lead to
3339 varying degrees of uncertainty in odour emission estimation. These uncertainties can also
3340 arise from inadequate sampling and analysis techniques, such as sampling duration or
3341 frequency.

3342

3343 Finally, odour assessment by panellists is subjective by its nature. Odour concentration
3344 results can be affected by the limited number of trained panellists available, the repeatability
3345 and reliability of their assessments.

3346

3347 It is important to keep in mind all these uncertainties - and possibly others not mentioned
3348 here but described in the scientific literature (e.g., Laor et al., 2014) - when carrying out
3349 OIAs.

3350

3351 **4.4 Ambient air measurements: EN 16841**

3352 Odour flow rate may be determined after performing a field inspection (EN 16841) followed
3353 by a backpropagation use of the odour dispersion modelling (reverse modelling).

3354 With the plume method according to EN 16841-2 (dynamic or stationary), one sniffing unit
3355 per cubic metre (su/m^3) is defined by panel members to express the odour concentration at
3356 the border of the plume (i.e., at a transition point). The sniffing unit is based on the
3357 recognition of the specific odour under analysis, not to the detection of any odour. It means
3358 that one sniffing unit ($1 \text{ su}/\text{m}^3$) corresponds to an odour concentration from 1 to $5 \text{ ou}/\text{m}^3$.
3359 With this approach, the odour flow rate is usually expressed in su/s .

3360 With the grid approach (EN 16841-1), no odour flow rate is estimated. This approach
3361 characterises odour exposure in a defined assessment area.

3362 The plume (stationary and dynamic) method and the grid one (stationary) are briefly
3363 described in the following section. For a detailed presentation, reading EN 16841 standard
3364 and related papers is recommended.

3365

3366 4.4.1. Ambient air measurement to characterise odour exposure: grid
3367 method

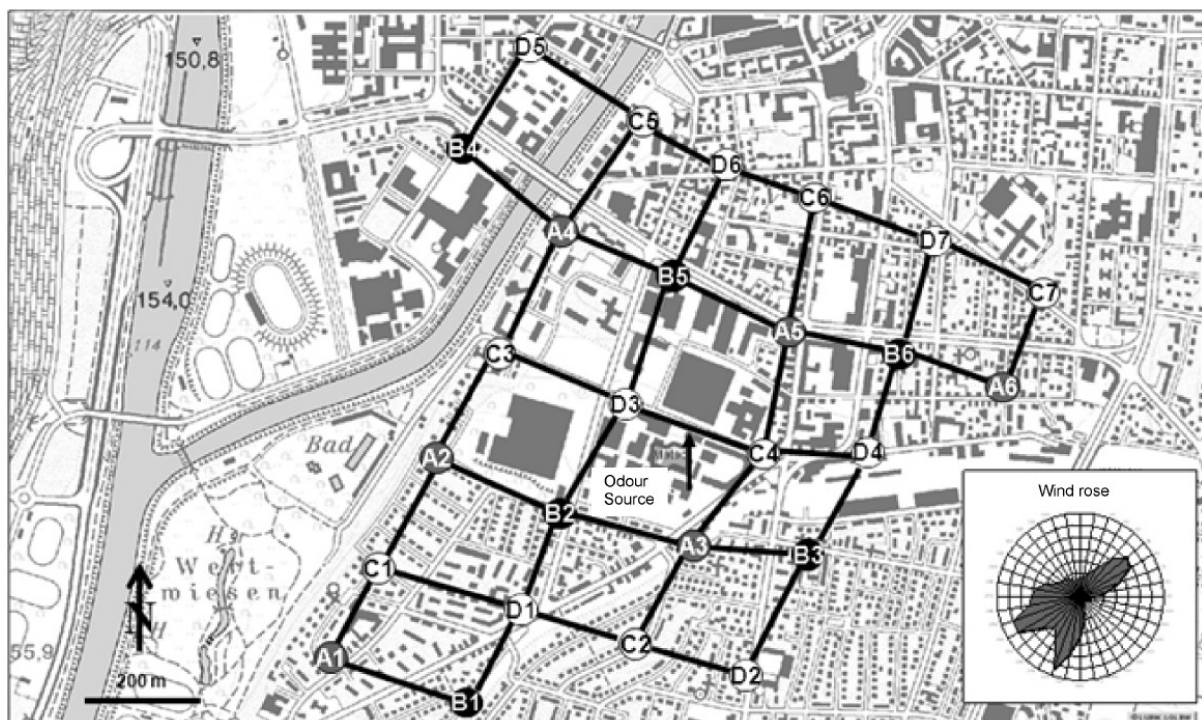
3368 **Grid inspection according to EN 16841-1** is used to derive the odour impact as the odour
3369 hour frequency of all emitting sources with detectable impact. This method is an efficient way
3370 to measure the impact in an odour-affected environment.

3371 The grid method is a statistical survey method which is applied over a sufficiently long period
3372 of time, to provide a representative map of the exposure to recognisable odour and its
3373 spatial distribution over the assessment area. These grid measurements are used to
3374 determine the distribution of odour hour frequency for recognisable odour in ambient air, in
3375 an assessment area, under meteorological conditions that are assumed to be representative
3376 of local meteorology of about the last 10 years.

3377 The odour hour frequency is an odour exposure indicator, and can be used to assess the
3378 exposure to recognisable odours originating from one or many specific odorant source(s)
3379 emitting in a particular area of study.

3380 The odour hour frequency is determined for one or more “assessment squares”, configured
3381 as grid measurement points. The assessment area is defined as a known impact distance or
3382 minimum radius of a circle from the highest stack which equals 30 times the highest stack
3383 height. In the case of several installations, the area is combined from the circles from each
3384 source.

3385 The assessment area is covered with a grid of equidistant points. The squares resulting from
3386 the joining of four measurement points are the assessment squares. A square size of 250 m
3387 should be initially chosen. Depending on the needs and the scope of the study, larger
3388 (maximum of 500 m) or smaller squares (e.g. 125 m, 100 m, 50 m) are possible. To reflect
3389 the decrease in odour exposure with increasing distance, adjacent assessment squares at
3390 different distances from the emitter should always be defined. An example is given in Figure
3391 4-16.



3392

3393 **Figure 4-16** Example for an assessment area in the vicinity of an odour source with
3394 assessment squares and measurement points (literature source: EN 16841-1:2017)

3395 The measurement points are divided into four routes (A, B, C and D in Figure 4-17). Each
3396 square is represented in a route with one point. The assessment takes place on 104 days in
3397 a year. Each day one of the routes is chosen, and after four measurements all four routes
3398 are performed. After 26 single measurements for each measurement point, the sum of all
3399 single measurements gives the result for the square.

3400 A shorter survey duration can be planned for practical reasons, but the survey shall be at
3401 least six months, with a minimum scale of 52 single measurements for each assessment
3402 square. In this case, colder and warmer months shall be equally represented to denote an
3403 entire year.

3404 The starting time varies from one measurement to the next. The measurement days should
3405 not be on consecutive days.

3406 For statistical purposes, throughout the survey, all days of a week shall be roughly equally
3407 represented in the survey plan. The daily start of a survey should be changed and after four
3408 measurements all times of the day (morning, afternoon, evening and night) are covered.

3409 The measurement is performed by a panel of at least 8 trained odour assessors.

3410

3411 4.4.2. Ambient air measurement of odours by using the plume method

3412 EN 16841-2:2017 distinguishes two ways of capturing the outline of a plume: *stationary*
3413 method and *dynamic* method. The plume extent is determined with trained odour panellists.

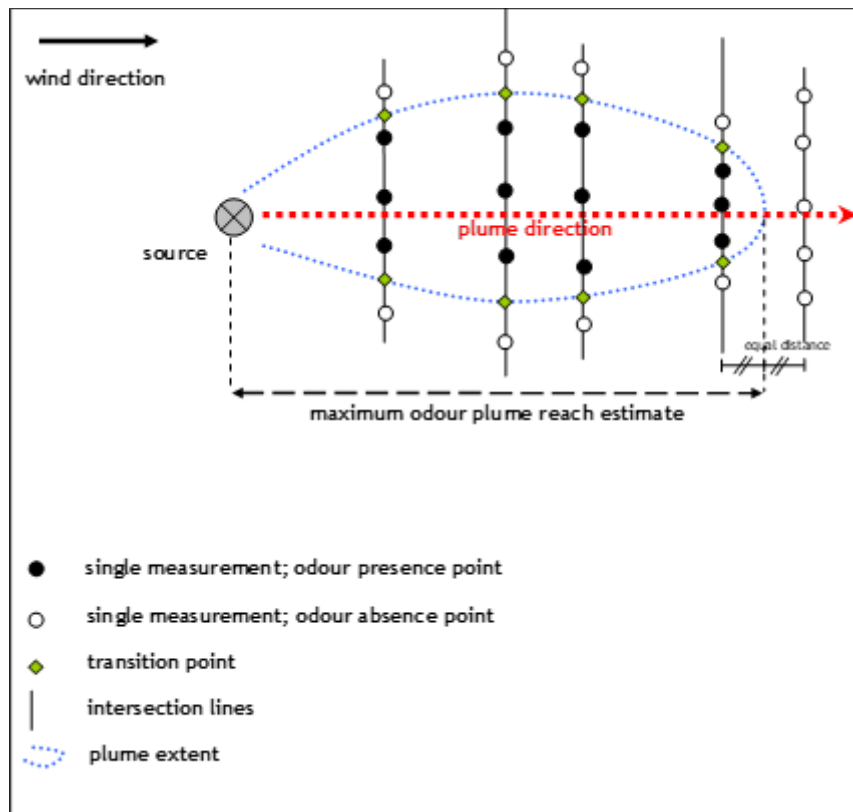
3414 Using the **stationary method**, the panel members are located at specific intervals along
3415 intersection lines perpendicular to the plume direction. Several panel members (minimum 5-
3416 panel members) are positioned at intervals along each intersection line to cover the
3417 estimated width of the recognisable plume.

3418 At each measurement point, the panellists stay for 10 minutes. During this time, the panel
3419 member evaluates the perceived smell from the source every 10 seconds. So, each panel
3420 member determines the percentage odour time in the course of one single measurement.

3421 If the result of a single measurement reaches a percentage odour time less than 10%, the
3422 odour is considered as being absent, while at higher values the odour is present. Single
3423 measurements at one intersection line are conducted simultaneously. Intersection lines at
3424 different distances from the source are assessed subsequently assuming that the relevant
3425 meteorological conditions remain the same.

3426 At least one intersection line has to be at a sufficient distance to ensure that no recognisable
3427 odour is present at any measurement point to be able to determine the maximum plume
3428 reach estimate (Figure 4-17).

3429 Parallel to the plume measurements the meteorological conditions such as wind direction,
3430 wind speed and parameters to determine turbulence are measured. This can be done for
3431 example with 3D-like ultrasonic devices.



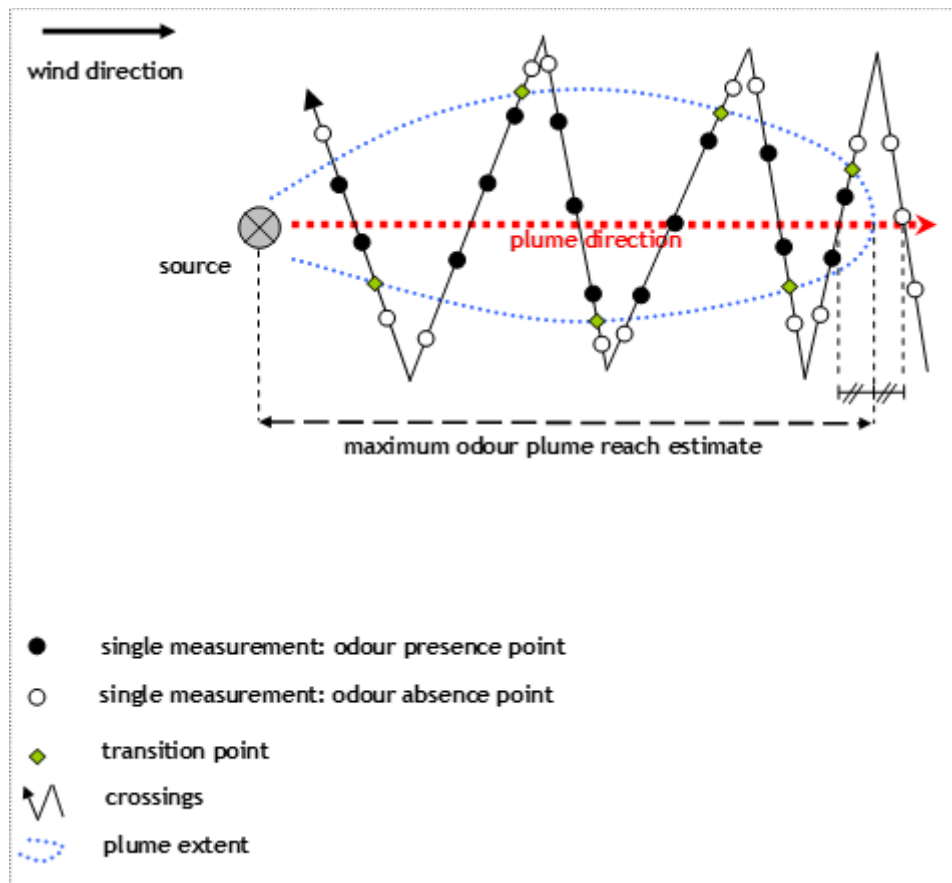
3432

3433 **Figure 4-17** Schematic diagram of an example of stationary plume measurement (EN
3434 16841-2)

3435 Using the **dynamic method**, the panel members cross the plume, while conducting single
3436 measurements at frequent intervals. At a minimum, two panel members are needed.

3437 By successively entering and exiting the plume and in this way determining the transition
3438 between the absence and presence of recognisable odour, the extent of the plume is
3439 defined. This approach helps to avoid addiction to the recognisable odour. The plume
3440 direction is crossed at different distances from the source. This includes crossings at
3441 distances where no recognisable odour is detected. One measurement consists of two
3442 crossings: one moving toward the plume, and one moving away from the plume.

3443 The maximum plume reach estimate is defined as the distance along the plume direction
3444 between the source and the point halfway from the furthest intersection line or crossing
3445 where odour presence points were recorded, and the first intersection line or crossing
3446 where only odour absence points were recorded. This equal distance between the two intersection
3447 lines/crossings is indicated as a green circle on the schematic Figure 4-18.



3448

3449 **Figure 4-18** Schematic diagram of an example of dynamic plume measurement (EN 16841-
3450 2)

3451 Measurements with both methods are repeated several times, minimum of 10 plumes, with
3452 different meteorological conditions. Meteorological conditions characterised by variable wind
3453 direction should be avoided.

3454 The plume extent derived from both methods can be used to validate model results. For this,
3455 the model is set up with the meteorological situation and an assumed emission rate. The
3456 plume extent for the situation is compared. From this comparison a suitable emission rate for
3457 the source can be determined. The methodology to calculate the odour emission rate of a
3458 source is described in [paragraph 7.2.1](#).

3459

3460 4.5 The need for odour emission factors

3461 The emissions of many air pollutants (e.g., NO_x, SO₂, PM₁₀, ...) can be calculated starting
3462 from the knowledge of specific process or activity indicators, such as for example the
3463 amount of fuel used or the number of km travelled for a given vehicle. Many methodologies
3464 and collections of emission factors exist, for instance the European CORINAIR (EEA, 2019)
3465 or the US AP42 (US-EPA, 2023).

3466

3467 Concerning odour, many papers reporting emission factors or SOER for specific productions
3468 have been published (e.g., Frechen, 2004; Sironi et al., 2005; Sironi et al., 2007; Capelli et
3469 al., 2014; Mielcarek and Rzeźnik, 2015; Davoli et al., 2021), but they have not been

3470 homogenised and organised in a single collection.

3471

3472 For odour emissions, the use of a single activity indicator is not sufficient. For example,
3473 emissions from animal housing facilities show great variability over the course of the day and
3474 the year, which depends on the size of growth of the animals, the fluctuations of the ambient
3475 air temperature, animal activities, the housing system, and the management (Brancher et al.,
3476 2021). For modelling of livestock farms the use of emission factors is suitable (for instance
3477 emission factors per animal), which can be defined specifically for piggeries as the odour
3478 emission rate (ou/s) released to the atmosphere by a pig (Romain et al., 2013).

3479

3480 The emission factor method is the only one applicable for future projects but, even for
3481 existing livestock buildings, it is a convenient way of avoiding expensive measurements
3482 which could only be afforded for large units or production systems (Van Harreveld et al.,
3483 2001).

3484

3485 A comprehensive methodology to estimate odour emissions and a large collection of odour
3486 emission factors do not exist and should be developed. Such a methodology would be an
3487 important tool for atmospheric modellers to carry out odour impact assessments (OIA) when
3488 emission measurements are not readily available.

3489

3490 4.6 Conclusions

3491 Sampling odours is challenging and it accounts for a large part of the uncertainties
3492 associated with the results of an air dispersion model.

3493

3494 OERs from point sources are reasonably well characterised, while those of area sources
3495 may vary depending on the device used for sampling and depending on the flow rate used.
3496 That means that, for the same area source, two different OERs can be obtained depending
3497 on the sampling device used. The most challenging activity is the characterisation of diffuse
3498 emissions. Field inspection is an appropriate approach, and it is highly recommended.
3499 Another possible way is to consider VOCs as odour proxy, and to use diffuse/fugitive VOCs
3500 measurement techniques as, for example, those proposed by *EN 17628*. Also, emissions
3501 factors for compounds related to odour (e.g., NH₃, VOC) exist for waste treatment activities
3502 (ADEME, 2012).

3503

3504 Depending on the kind of source that needs to be investigated, specific equipment is
3505 required and this investigation needs to be carried out according to specific measurement
3506 guidelines. This chapter did not detail these techniques: the reader should consider existing
3507 standards and reference works.

3508

3509 When the object of the odour impact assessment (OIA) is a future plant, dispersion models
3510 are the only tool that can be used. The OER or SOER can be obtained from similar existing
3511 plants or from the scientific literature. In these situations, a database of odour emission
3512 factors and a detailed methodology explaining their applicability would be very useful. A
3513 comprehensive database of odour emission factors nowadays does not exist.

3514

3515 Besides odour emission data, additional information is needed to assess odour exposure by

3516 means of air dispersion models. For example, when dealing with stacks, it is important to
3517 know the exit direction (vertical, horizontal, or tilted with a specific angle) and if a rain hat is
3518 present or not. The exit temperature is also important, both to determine the exit velocity and
3519 to calculate the volumetric flow at the same temperature at which odour concentration is
3520 specified. Additionally, when considering passive area sources, the OER is determined at
3521 every simulation hour starting from the measured SOER and evaluating how it varies
3522 according to the airspeed close to its surface. In order to determine this speed, the wind
3523 speed at the anemometer height (or first vertical model level), the atmospheric stability and
3524 the roughness length must be known.

3525
3526 This chapter did not consider the qualitative dimension of the odour. Indeed, in dispersion
3527 models, the main variable introduced into the software is the emission of odour whatever its
3528 nature (e.g., compost, chemical farm, coffee roasting, bakery, carcass rendering). There are
3529 many situations, especially in the case of multiple sources, where the character of the odour
3530 is important, but it is typically not considered when carrying out an OIA. The global odour
3531 emission rate cannot be determined by simple emission sampling and olfactometric
3532 measurements in the laboratory. This is particularly true for complex sites like, for example,
3533 landfills (e.g., Belgiorno et al., 2012), where odour is due to multiple sources, such as
3534 windrows turning, fugitive emissions, vehicles gas emissions and heterogeneous emissions
3535 surface. However, in recent years there have been some approaches to include the hedonic
3536 tone in the evaluations, as discussed in [paragraph 7.4](#).

3537
3538 In order to approach the notion of nuisance (remembering the meaning of FIDOS), for which
3539 the hedonic tone is essential, it is ideally necessary to involve the residents in the evaluation,
3540 and to increase citizen participation. A resident-watchman survey becomes more accepted
3541 by the authorities and offers several advantages. The most important advantage is probably
3542 the restoration of the dialogue between the stakeholders ([paragraph 5.9](#)).

3543
3544 The correct characterisation of odour emissions and sources is an important step in OIAs
3545 carried out with modelling techniques. It requires time and may be expensive when
3546 samplings are required, but if it is not done with due diligence and following specific
3547 guidelines, the model results may be imprecise when not completely wrong.

3548

3549 4.7 References

3550 ADEME (2012). Programme de recherche de l'ADEME sur les émissions atmosphériques du
3551 compostage. Juillet 2012. [https://bibliothèque.ademe.fr/air-et-bruit/3505-programme-de-](https://bibliothèque.ademe.fr/air-et-bruit/3505-programme-de-recherche-de-l-ademe-sur-les-emissions-atmospheriques-du-compostage.html)
3552 [recherche-de-l-ademe-sur-les-emissions-atmospheriques-du-compostage.html](https://bibliothèque.ademe.fr/air-et-bruit/3505-programme-de-recherche-de-l-ademe-sur-les-emissions-atmospheriques-du-compostage.html) (Accessed
3553 Apr 2023).

3554

3555 Angrecka, S., & Herbut, P. (2014). The impact of natural ventilation on ammonia emissions
3556 from free stall barns. Polish Journal of Environmental Studies, 23(6), 2303-2307.

3557

3558 Arya, S. P. (1999). Air pollution meteorology and dispersion (Vol. 310). New York: Oxford
3559 University Press.

3560

3561 BC 2021. British Columbia Dispersion Modelling Guideline

- 3562 [https://www2.gov.bc.ca/assets/gov/environment/air-land-water/air/reports-pub/](https://www2.gov.bc.ca/assets/gov/environment/air-land-water/air/reports-pub/bc_dispersion_modelling_guideline_2021.pdf)
3563 [bc_dispersion_modelling_guideline_2021.pdf](https://www2.gov.bc.ca/assets/gov/environment/air-land-water/air/reports-pub/bc_dispersion_modelling_guideline_2021.pdf) (Accessed Apr 2023).
3564
3565 Belgiorno, V., Naddeo, V., & Zarra, T. (Eds.). (2012). Odour impact assessment handbook.
3566 John Wiley & Sons. ISBN: 9781119969280
3567
3568 Bellasio, R., & Bianconi, R. (2022). A Heuristic Method for Modelling Odour Emissions from
3569 Open Roof Rectangular Tanks. *Atmosphere*, 13(3), 367.
3570
3571 Brancher, M., Hoinaski, L., Piringer, M., Prata, A. A., & Schauburger, G. (2021). Dispersion
3572 modelling of environmental odours using hourly-resolved emission scenarios: Implications
3573 for impact assessments. *Atmospheric Environment: X*, 12, 100124.
3574
3575 Burgués, J., Doñate, S., Esclapez, M. D., Saúco, L., & Marco, S. (2022). Characterisation of
3576 odour emissions in a wastewater treatment plant using a drone-based chemical sensor
3577 system. *Science of The Total Environment*, 846, 157290.
3578
3579 Brancher, M., Hoinaski, L., Piringer, M., Prata, A. A., & Schauburger, G. (2021). Dispersion
3580 modelling of environmental odours using hourly-resolved emission scenarios: Implications
3581 for impact assessments. *Atmospheric Environment: X*, 12, 100124.
3582
3583 Capelli, L., Sironi, S., & Del Rosso, R. (2014). Odour emission factors: Fundamental tools for
3584 air quality management. *Chemical Engineering Transactions*, 40, 193-198.
3585
3586 Capelli, L., Grande, M., Intini, G., & Sironi, S. (2018). Comparison of field inspections and
3587 dispersion modelling as a tool to estimate odour emission rates from landfill surfaces.
3588 *Chemical Engineering Transactions*, 68, 187-192.
3589 <https://re.public.polimi.it/retrieve/handle/11311/1125626/480100/LC142.pdf> (Accessed Mar
3590 2023).
3591
3592 CEN, EN 15446:2008. Fugitive and diffuse emissions of common concern to industry sectors
3593 - Measurement of fugitive emission of vapours generating from equipment and piping leaks.
3594 (European Standard EN 15446:2008). European Committee for Standardisation, 2008.
3595
3596 CEN, EN 13725:2022. Stationary source emissions. Determination of odour concentration by
3597 dynamic olfactometry and odour emission rate. (European Standard EN 13725:2022).
3598 European Committee for Standardisation, 2022.
3599
3600 CEN, EN 17628:2022. Fugitive and diffuse emissions of common concern to industry sectors
3601 - Standard method to determine diffuse emissions of volatile organic compounds into the
3602 atmosphere. (European Standard EN 17628:2022). European Committee for
3603 Standardisation, 2022
3604
3605 Davoli, E., Bianchi, G., Bonura, A., Invernizzi, M., & Sironi, S. (2021). Odor Emissions
3606 Factors for Bitumen-Related Production Sites. *Applied Sciences*, 11(8), 3700.
3607
3608 DGR 3018/2012. D.g.r. 15 febbraio 2012 - n. IX/3018 Determinazioni generali in merito alla
3609 caratterizzazione delle emissioni gassose in atmosfera derivanti da attività a forte impatto

- 3610 odorigeno (In Italian). [https://www.regione.lombardia.it/wps/wcm/connect/8c3b2bab-5c37-4a55-8397-b0a9d684f094/DGR+3018_2012.pdf?MOD=AJPERES&CACHEID=8c3b2bab-](https://www.regione.lombardia.it/wps/wcm/connect/8c3b2bab-5c37-4a55-8397-b0a9d684f094/DGR+3018_2012.pdf?MOD=AJPERES&CACHEID=8c3b2bab-5c37-4a55-8397-b0a9d684f094)
3611 [5c37-4a55-8397-b0a9d684f094](https://www.regione.lombardia.it/wps/wcm/connect/8c3b2bab-5c37-4a55-8397-b0a9d684f094/DGR+3018_2012.pdf?MOD=AJPERES&CACHEID=8c3b2bab-5c37-4a55-8397-b0a9d684f094) (Accessed Feb 2022).
3612
3613
3614 EEA (1999) EMEP/EEA air pollutant emission inventory guidebook 2019.
3615 <https://www.eea.europa.eu/publications/emep-eea-guidebook-2019> (Accessed Feb 2022).
3616
3617 Flassak, Th., Janicke U., Ketzl M. (2010). Comparison of ground-level centreline
3618 concentrations calculated with the models OML, AERMOD/PRIME, MISKAM and
3619 AUSTAL2000 against the Thompson wind tunnel data set for simple stack-building
3620 configurations. 13th Int. Conf. On Harmonisation within Atmospheric Dispersion Modelling for
3621 Regulatory Purposes, 1-4 June 2010, Paris, France, 171-175
3622
3623 Frechen, F. B. (2004). Odour emission inventory of German wastewater treatment plants-
3624 odour flow rates and odour emission capacity. Water Science and Technology, 50(4), 139-
3625 146.
3626
3627 M. Guillot (2012) Presentation on results of CODEPISO, conference on odour, organised by
3628 KTT-iMA Sarl, Strasbourg.
3629
3630 Guillot, J. M., Clincke, A. S., & Guilleman, M. (2014). Odour emission from liquid and solid
3631 area sources: a large intercomparison of sampling devices. CHEMICAL ENGINEERING, 40.
3632
3633 IDNR (2014). Iowa Department of Natural Resources. Rain Caps and Horizontal Stacks.
3634 [https://www.iowadnr.gov/portals/idnr/uploads/air/insidednr/dispmodel/](https://www.iowadnr.gov/portals/idnr/uploads/air/insidednr/dispmodel/rain_caps_and_horizontal_stacks.pdf)
3635 [rain_caps_and_horizontal_stacks.pdf](https://www.iowadnr.gov/portals/idnr/uploads/air/insidednr/dispmodel/rain_caps_and_horizontal_stacks.pdf) (Accessed Feb 2022).
3636
3637 Invernizzi, M., Roveda, L., Polvara, E., & Sironi, S. (2021). Lights and shadows of the voc
3638 emission quantification. Chemical Engineering Transactions, 85, 109-114.
3639
3640 IPPC (2002). Horizontal Guidance for Odour Part 2 – Assessment and Control. Technical
3641 Guidance Note IPPC H4. Environment Agency, United Kingdom, 2002.
3642 <https://www.sepa.org.uk/media/61338/ippc-h4-2-odour-pt-2-draft-for-consultation-2002.pdf>
3643 (Accessed Feb 2022).
3644
3645 Jiang, K., & Kaye, R. (1996). Comparison study on portable wind tunnel system and isolation
3646 chamber for determination of VOCs from areal sources. Water Science and Technology,
3647 34(3-4), 583-589.
3648
3649 Kawamura, K., Miyazawa, K., & Kent, L. (2021). The past, present and future in tube-and
3650 paper-based colorimetric gas detectors. AppliedChem, 1(1), 14-40.
3651
3652 Laor, Y., Parker, D., & Pagé, T. (2014). Measurement, prediction, and monitoring of odours
3653 in the environment: a critical review. Reviews in Chemical Engineering, 30(2), 139-166.
3654
3655 Lucernoni, F., Capelli, L., & Sironi, S. (2016). Odour sampling on passive area sources:
3656 Principles and methods. Chemical Engineering Transactions, 55-60.
3657

- 3658 Mielcarek, P., & Rzeźnik, W. (2015). Odor emission factors from livestock production. Polish
3659 Journal of Environmental Studies, 24(1), 27-35.
3660
- 3661 New Zealand Ministry for the Environment (2004). Good practice guide for atmospheric
3662 dispersion modelling. ISBN: 0-478-18941-9.
3663 [http://tools.envirolink.govt.nz/assets/Uploads/Good-Practice-Guide-MFE-atmospheric-
3665 dispersion-modelling-jun04.pdf](http://tools.envirolink.govt.nz/assets/Uploads/Good-Practice-Guide-MFE-atmospheric-
3664 dispersion-modelling-jun04.pdf) (Accessed Mar 2023).
- 3666 Ng, R. T., Hassim, M. H., & Hurme, M. (2017). A hybrid approach for estimating fugitive
3667 emission rates in process development and design under incomplete knowledge. Process
3668 Safety and Environmental Protection, 109, 365-373.
3669
- 3670 Nicolas, J., Delva, J., Cobut, P., & Romain, A. C. (2008). Development and validating
3671 procedure of a formula to calculate a minimum separation distance from piggeries and
3672 poultry facilities to sensitive receptors. Atmospheric Environment, 42(30), 7087-7095.
3673
- 3674 Ninh, H. P., Tanaka, Y., Nakamoto, T., & Hamada, K. (2007). A bad-smell sensing network
3675 using gas detector tubes and mobile phone cameras. Sensors and Actuators B: Chemical,
3676 125(1), 138-143.
3677
- 3678 Oetli, D. (2015) Evaluation of the revised Lagrangian particle model GRAL against wind-
3679 tunnel and field experiments in the presence of obstacles. Boundary Layer Meteorol, 155(2),
3680 271-287.
3681
- 3682 Parker, D. B., Gilley, J., Woodbury, B., Kim, K. H., Galvin, G., Bartelt-Hunt, S. L., ... & Snow,
3683 D. D. (2013). Odorous VOC emission following land application of swine manure slurry.
3684 Atmospheric Environment, 66, 91-100.
3685
- 3686 Prata Jr, A. A., Santos, J. M., Timchenko, V., & Stuetz, R. M. (2018). A critical review on
3687 liquid-gas mass transfer models for estimating gaseous emissions from passive liquid
3688 surfaces in wastewater treatment plants. Water Research, 130, 388-406.
3689
- 3690 Ravina, M., Bruzzese, S., Panepinto, D., & Zanetti, M. (2020). Analysis of separation
3691 distances under varying odour emission rates and meteorology: A WWTP case study.
3692 *Atmosphere*, 11(9), 962.
3693
- 3694 Romain, A. C., Nicolas, J., Cobut, P., Delva, J., Nicks, B., & Philippe, F. X. (2013).
3695 Continuous odour measurement from fattening pig units. Atmospheric Environment, 77, 935-
3696 942.
3697
- 3698 Rzeźnik, W., & Mielcarek-Bocheńska, P. (2022). Odour emissions from livestock buildings.
3699 *Atmosphere*, 13(2), 254.
3700
- 3701 Scire, J. S., Robe, F. R., Fernau, M. E., & Yamartino, R. J. (2000). A user's guide for the
3702 CALMET Meteorological Model. *Earth Tech, USA*, 37.
3703
- 3704 Sironi, S., Capelli, L., Céntola, P., Del Rosso, R., & Grande, M. I. (2005). Odour emission
3705 factors for assessment and prediction of Italian MSW landfills odour impact. Atmospheric

- 3706 Environment, 39(29), 5387-5394.
3707
- 3708 Sironi, S., Capelli, L., Céntola, P., Del Rosso, R., & Grande, M. I. (2007). Odour emission
3709 factors for assessment and prediction of Italian rendering plants odour impact. Chemical
3710 Engineering Journal, 131(1-3), 225-231.
3711
- 3712 Schmitt, K., Tarantik, K., Pannek, C., Benito-Altamirano, I., Casals, O., Fabrega, C., ... &
3713 Prades, J. D. (2017). Colorimetric sensor for bad odor detection using automated colour
3714 correction. In Smart Sensors, Actuators, and MEMS VIII (Vol. 10246, pp. 348-357). SPIE.
3715
- 3716 Smith, R. J., & Watts, P. J. (1994a). Determination of odour emission rates from cattle
3717 feedlots: Part 1, a review. Journal of Agricultural Engineering Research, 57(3), 145-155.
3718
- 3719 Smith, R. J., & Watts, P. J. (1994b). Determination of odour emission rates from cattle
3720 feedlots: Part 2, evaluation of two wind tunnels of different size. Journal of Agricultural
3721 Engineering Research, 58(4), 231-240.
- 3722 Tanaka, Y., Yoshioka, M., Nakamoto, T., & Moriizumi, T. (2004). Study of bad-smell sensing
3723 using gas detector tube. IEEJ Transactions on Sensors and Micromachines, 124(9), 321-
3724 326.
3725
- 3726 US-EPA (1992) Screening procedures for estimating the air quality impact of stationary
3727 sources. EPA-454r-92-019. October 1992.
3728 https://www.epa.gov/sites/default/files/2020-09/documents/epa-454r-92-019_ocr.pdf
3729 (Accessed Feb 2023).
3730
- 3731 US-EPA (1993) Model Clearinghouse Memorandum, dated July 9, 1993, "Proposal for
3732 Calculating Plume Rise for Stacks with Horizontal Releases or Rain Caps for Cookson
3733 Pigment.
3734
- 3735 US-EPA (1995a) Protocol for equipment leak emission estimates. EPA 453/R-95-017.
3736 [https://www.epa.gov/sites/default/files/2020-09/documents/protocol_for_equipment_leak_em](https://www.epa.gov/sites/default/files/2020-09/documents/protocol_for_equipment_leak_emission_estimates.pdf)
3737 [ission_estimates.pdf](https://www.epa.gov/sites/default/files/2020-09/documents/protocol_for_equipment_leak_emission_estimates.pdf) (Accessed Apr 2023)
3738
- 3739 US-EPA (1995b) User's Guide for the Industrial Source Complex (ISC3) Dispersion Model;
3740 Description of Model Algorithms; Report EPA-454/B-95-003b; US-EPA: Research Triangle
3741 Park, NC, USA, 1995; Volume II.
3742
- 3743 US-EPA (1995c) User's Guide to the Building Profile Input Program, Revised February 1995,
3744 PA-454/R-93-038, United States Environmental Protection Agency, Washington DC, USA
3745
- 3746 US-EPA (2005) Cost and Emission Reductions for Meeting Percent Leaker Requirements
3747 for HON Sources. Memorandum to Hazardous Organic NESHAP Residual Risk and Review
3748 of Technology Standard Rulemaking docket. Docket ID EPA-HQ-OAR-2005-0475-0105.
3749
- 3750 US-EPA (2022a). Leak Detection and Repair: A Best Practices Guide
3751 (<https://www.epa.gov/compliance/leak-detection-and-repair-best-practices-guide>). (Accessed
3752 Feb 2023).
3753

241 *Leave your comments on this draft [here](#). Due date 9th July 2023*

- 3754 US-EPA (2022b). User's Guide for the AMS/EPA Regulatory Model (AERMOD). EPA-454/B-
3755 22-007. June 2022.
3756 https://gaftp.epa.gov/Air/aqmg/SCRAM/models/preferred/aermod/aermod_userguide.pdf
3757 (Accessed Feb 2023).
3758
3759 US-EPA (2023) AP-42: Compilation of Air Emissions Factors. [https://www.epa.gov/air-](https://www.epa.gov/air-emissions-factors-and-quantification/ap-42-compilation-air-emissions-factors)
3760 [emissions-factors-and-quantification/ap-42-compilation-air-emissions-factors](https://www.epa.gov/air-emissions-factors-and-quantification/ap-42-compilation-air-emissions-factors) (Accessed Feb
3761 2023).
3762
3763 Van Harreveld, A. P., Jones, N., & Stoaling, M. (2001). Assessment of community response
3764 to odorous emissions. Environment Agency UK-R&D Technical Report P4-095.
3765
3766 VDI 3880:2011-10. Olfactometry; Static sampling (Olfaktometrie – Statische Probenahme),
3767 Berlin, Beuth Verlag. 2011.
3768
3769 Zarra, T., Belgiorno, V., & Naddeo, V. (2021). Environmental odour nuisance assessment in
3770 urbanized area: Analysis and comparison of different and integrated approaches.
3771 *Atmosphere*, 12(6), 690.
3772
3773

3774 5. Dispersion Algorithms

3775 5.1. Introduction

3776 In everyday life, there are many contexts (industrial, agricultural, energy production, waste
3777 management, water treatment) in which the release of odorous substances into the
3778 atmosphere and the related nuisance that they can cause on the population play a very
3779 important role. Since the behaviour of odours depends crucially on the characteristics of the
3780 atmosphere, this is treated, similarly to what is supposed for other air quality issues, as a
3781 problem related to the transport and dispersion of gaseous substances in the turbulent
3782 atmospheric boundary layer. Atmospheric Dispersion Modelling is therefore considered, for
3783 various reasons, a fundamental support tool for the study and reconstruction of the odour
3784 impact. The knowledge of the characteristics of the available modelling technologies, or
3785 “Dispersion Algorithms”, of their related advantages and limitations, allows a better choice
3786 among the different approaches and guarantees a better correspondence between the
3787 results of their application and the expectations of potential users.

3788 In general, there are several reasons why dispersion modelling techniques are used in the
3789 field of odour impact assessment. Models are used to quantitatively predict the impact of
3790 pollution on air quality over relatively large geographical areas, potentially extending the
3791 information to a very high number of points compared to what is typically available from
3792 existing measurement systems, hence constituting a network of receptors at substantially
3793 zero cost. They are also necessary for the impact assessment of future plants or pollutant
3794 sources and allow, through source apportionment procedures, the separation of the
3795 contributions generated by different emission sources located in a certain area. They allow
3796 studying the effects of any mitigation measures on the emission sources, through a
3797 quantitative analysis of engineering solutions and the application of cost-benefit procedures.
3798 They are an essential part in the site planning process, as tools to minimise the impact of the
3799 emissions on the population. In fact, model simulations allow optimising the design of
3800 emission sources for a least-impact result, defining the possible insertion and correct
3801 localisation of buffer zones and fence lines, arranging any monitoring networks and
3802 designing the land use to minimise the pollutant exposure to the population.

3803 They make it possible to objectify the impacts of odorous sources, helping to remove the
3804 "emotional" effect which is often associated with odorous nuisance. Models can directly
3805 address different aspects of the FIDOS process (Frequency, Intensity, Duration,
3806 Offensiveness and Sensitivity) and finally, they are the only tool capable of simultaneously
3807 taking into account aspects such as emissions, meteorology, and land use which are
3808 responsible, through a mutual and complex interaction, of the effects of odour annoyance on
3809 the population.

3810 For all the reasons listed above, the use of dispersion modelling technologies is suggested,
3811 or in several cases explicitly required, by many guidelines or odour regulations/legislations in
3812 different countries around the world (see for example Bokowa et al. 2021), representing a
3813 widespread practice connected to the management of odour problems.

3814 The purpose of this chapter is, therefore, to describe the dispersion algorithms and the
3815 available model implementations with sufficient details to support the choice of the various
3816 possible approaches that are offered and that are typically used in the field of odour
3817 applications. Given that the main objective of the document is to constitute a handbook, an
3818 attempt was made to orient the content of the chapter to a wide range of possible model
3819 users. In this sense, the chapter does not constitute an extremely detailed and completely
3820 exhaustive description from a technical point of view, which is possibly referred to both
3821 specific texts on dispersion modelling (e.g. Arya, 1998; Barrat, 2001; Zannetti, 2010), and on
3822 the dispersive structure of the Atmospheric Boundary Layer (e.g. Garratt, 1994; Stull, 1988).
3823 The topic covered in this chapter will be hence addressed taking into account many aspects
3824 of the modelling approach to odours, including a critical analysis of some well-known
3825 problems related to the use of the models in this field, which has distinctive characteristics
3826 posing some specific critical issues.

3827 In particular, the chapter deals, in Section 2, with the topic of the role of the dispersion
3828 models in the specific field of odour applications, detailing the different aspects of the
3829 possible implementations and use related to the different phases of the planning or control of
3830 emitting sources.

3831 Section 3 is devoted to a concise description of the various available modelling
3832 methodologies, starting from the simpler screening formulas, moving to stationary and
3833 homogeneous Gaussian formulations, the Lagrangian Puff/Segment or Stochastic Particle
3834 approaches and the Eulerian approach. Both the main theoretical and practical aspects of
3835 the different methodologies are described in order to give a general view of the topic.

3836 These different methodologies for dispersion modelling represent a theoretical framework
3837 that has already been put into practice and implemented in modelling tools all over the world.
3838 They have a recognised name, often sponsored by national or worldwide recognised
3839 organisations as a possible standard or directly developed by private institutions and
3840 consequently present on the market. These models are, in the end, the tools to be applied
3841 by final users such as consultants or public agencies. Section 4 is hence devoted to
3842 describing a reasoned list of the dispersion modelling operational tools available and
3843 currently used in different parts of the world for odour applications. The list separates
3844 different models depending on the considered methodologies and gives the main
3845 characteristics and peculiarities of each model.

3846 The adaptation of the use of the standard atmospheric dispersion models for the
3847 characterisation of odour impacts poses some specific problems compared to a more
3848 standard use related to air pollution simulations. In particular, it is well known that olfactory-
3849 related problems are perceived during short time intervals and in this respect it is necessary
3850 to model the “instantaneous” concentrations instead of time-averaged concentrations on
3851 time scales of the order of one hour, one day or one year as in a typical air quality
3852 framework. Since dispersion models are often developed to simulate concentrations
3853 averaged in time (typically of the order of one hour) or ensembles (over many realisations of
3854 the same statistical ensemble), some specific corrections have to be taken into account,
3855 such as the introduction of the Peak-to-Mean Ratio concept or the direct simulation of
3856 higher-order momentum for the statistical distribution of the concentration. Other problems
3857 are connected to the meteorological input that should be in principle able to reproduce this
3858 specific time variability particularly evident in low wind stable conditions, or connected to the

3859 description of the emissions, for example in the presence of diffuse, meteorology-driven
3860 sources. Section 5 is devoted to these issues, describing the current limits of each model
3861 technology and in some cases the way used to overcome them.

3862 Once a categorisation of the different available models is given, Section 6 addresses the
3863 problem of the model suitability. Different complexities of the models must meet with
3864 different complexities of the faced problems. This section aims at giving support in choosing
3865 the different modelling technologies available, according to the different characteristics of the
3866 problems, such as the presence of homogeneous/non-homogeneous and/or stationary/non-
3867 stationary weather conditions, the presence or absence of complex topography, the spatial
3868 scale etc.

3869 Section 7 is dedicated to the problem of model validation. Considering the use of the
3870 dispersion models in the frame of odour applications, there is a need for a specific validation
3871 framework and protocol, in order to verify the methodologies adopted to solve some of the
3872 existing problems such as, for example, the reproduction of peak concentrations. An
3873 overview of the available datasets and methods fitting this purpose is given.

3874 A bridge towards the stakeholders is discussed in Section 8, in order both to address their
3875 needs in dealing with odour nuisance and to raise their awareness about the usefulness and
3876 necessity of using dispersion models, by widening their knowledge of the advantages offered
3877 by these technologies.

3878 Finally, Section 9 contains a window opened on the current research regarding the
3879 atmospheric dispersion modelling approaches, particularly related to the scientifically
3880 advanced ways considered to overcome some of the problems cited above. These activities,
3881 including for example LES/DNS methods, PDF methods, two-particle Lagrangian Stochastic
3882 models, and Fluctuating Plume models, have not yet been able to provide standardised or
3883 commercially ready-to-use products, but contain many new helpful ideas that will lead to
3884 even more advanced modelling systems in the next future. This, even considering the
3885 development and diffusion of the High Performance Computing that is often required, is
3886 available in a form usable to produce simulations in a relatively standard way and in a
3887 reasonable time.

3888 **5.2. The role of dispersion models in the frame of odour** 3889 **applications**

3890 Atmospheric dispersion models are a useful mathematical tool for connecting an emission
3891 source to a receptor, simulating the behaviour of the substance (gas or aerosol) and
3892 predicting its fate. This is achieved by using a set of differential equations that describe the
3893 mechanisms of transport, turbulent diffusion, chemical transformation, and soil deposition
3894 (dry and wet) involving the substances emitted into the atmosphere. By integrating these
3895 equations numerically (or analytically in the simplest cases) in time and space, it is possible
3896 to quantify the concentrations that are generated around and away from the emitter source /
3897 s.

3898 The difficulty of solving this process completely and correctly is well known due to the
3899 uncertainties and approximations present in the input data (acquisition of three-dimensional

3900 fields of meteorological variables, definition of source terms, characterisation of the territory)
3901 and to the intrinsic stochastic variability of the turbulent dispersion processes that typify the
3902 atmospheric medium. However, this "dynamic" method of calculating the impact of a source
3903 is the only one that can guarantee a valid result (given a correct description of the variables
3904 involved): simplified statistical methods of correlation between concentration measurements
3905 and polluting sources are not able to take into account the atmospheric non-linearity, such
3906 as the variation of the wind direction, the sudden transition from stable to unstable
3907 conditions, chemical transformations involving different substances, etc...

3908 For the study of odour emissions, we currently have models with different levels of
3909 complexity, which provide simulations that can be used to ensure control of their dispersion
3910 and impact on the territory. The validation and routine use of these models is possible
3911 thanks to the availability of adequate computing resources and three-dimensional
3912 meteorological data with increasingly higher spatial and temporal resolution.

3913 In detail, dispersion models can be applied in many contexts:

- 3914 > they are indispensable tools of knowledge to predict the impact for project not yet
3915 built: according to the emissions generated, it is possible to calculate the
3916 concentrations at the ground, to study the spatial distribution around the plant and
3917 their temporal variation (day / night, weekday / holiday, seasonal, climatic trend); with
3918 these studies it is possible:
- 3919 ● to verify compliance with the parameters and / or thresholds imposed by
3920 current legislation, if existing;
 - 3921 ● to predict possible nuisances for the resident population in the vicinity of the
3922 plant in critical meteorological / emission situations;
 - 3923 ● if the project is not acceptable, solutions can be simulated that involve a
3924 different configuration of emissions;
 - 3925 ● to define the optimal configuration for the system (height of chimneys,
3926 dimensions of area sources, fugitive, etc.);
- 3927
- 3928 > for a plant or emitting source already present and functioning, the use of the models
3929 can provide an estimate of their impact on the territory, continuously (hour by hour) or
3930 at fixed times (monthly or annual evaluations), using adequate meteorological data
3931 (from measurements or 3D modelled field) and available emission estimates; in this
3932 way it is possible to:
- 3933 ● verify compliance with the legislation according to the variation in emissions
3934 that occur in the management of the plant or during the occurrence of
3935 meteorological situations not foreseen in the preliminary impact assessment
3936 phase;
 - 3937 ● in the event of odour nuisance, help to understand its origin: if it is due to high
3938 emissions, to unfavourable dispersion conditions, to a complex flow field
3939 generated by buildings for example, etc...
 - 3940 ● simulate the changes in the impacts as a consequence of necessary or
3941 required evolutions to the plant structure;
 - 3942 ● having weather forecasts available, a modelling system can be usefully
3943 exploited to predict in advance critical situations for the dispersion of odours:
3944 this allows optimal management of the system through the activation of

3945 containment measures (if possible) or the displacement of planned works,
3946 particularly critical for odour emissions, in the most favourable hours from a
3947 dispersive point of view, so as to guarantee the least possible disturbance for
3948 the workers and the resident population;
3949 • use the system also in accidental situations and provide impact maps in a
3950 short time, useful during emergency interventions.
3951

3952 The direct "dynamic" simulation of the evolution of odour emissions makes it possible to
3953 separate the contributions of the different sources on the territory and to evaluate their
3954 differentiated impact over time and space; in the event that an emission includes several
3955 odorous substances, the separation of the effects can be calculated immediately in the case
3956 of chemically non-interacting substances (at least over a short time); in the presence of
3957 significant chemical reactions it is necessary to use models with source apportionment
3958 algorithms. In the case of simulations referring to the odour unit, the separation of
3959 contributions is not easily derivable.

3960 The dispersion models can also be used for the estimation of the source term, in case this is
3961 difficult to quantify or even unknown: using meteorological and concentration measurements
3962 of a tracer distributed on a territory, it is possible to invert the integration and estimate the
3963 quantity that generated these concentrations; the procedure, like all inverse operations, is
3964 very critical (in particular in the absence of information on the location of the source) and
3965 sensitive to uncertainties in the initial measurements (meteorological and chemical), but can
3966 give important indications in dangerous situations (e.g. reports of intense and unexpected
3967 odours by the population).

3968 The use of models to support experimental campaigns to verify the environmental
3969 compatibility of a plant should be noted: in fact, some measurement techniques relating to
3970 odorous substances (electronic noses) are still uncertain and subject to debate; furthermore,
3971 the measurements refer to a point and the sensors are often expensive and cannot be
3972 distributed in large numbers on the territory, so the impact maps obtainable with the models
3973 can be used in synergy with the measurements (and with assimilation techniques for
3974 example) to obtain spatialised information on the whole territory.

3975 The flexibility of the models allows exploratory analyses to evaluate the stability of the results
3976 as a function of the approximations of the input variables, it is possible to perform
3977 comparative studies between different emission scenarios or even change the expected site
3978 of the plant under study to optimise its position to obtain the least foreseeable impact.

3979 The distinctive characteristic of the use of dispersion models for odorous substances
3980 basically lies in the need to have an assessment of the peak concentration, unlike
3981 atmospheric pollution where the preferred scale is the hour: in the case of olfactory
3982 disturbance, the time scale of interest is considerably lower, essentially on the order of the
3983 duration of a respiratory act.

3984 It is, therefore, necessary to have models capable of determining not only the average odour
3985 concentrations, but also the concentration fluctuations.

3986

3987 5.3. General synthetic description of the dispersion algorithms

3988 5.3.1. Introduction

3989 The dispersion of air pollution both in urban areas and rural areas is of great concern to the
3990 scientific community. In the last few decades, normal levels of air pollution and odour have
3991 increased and many countries have started to focus on regulation and monitoring. Air quality
3992 models are an important management tool as they are able to predict pollutants (gases and
3993 particles) in the atmosphere. There are many different types of models and their
3994 performance depends on many different variables. The classification of models may refer to
3995 the source type (point, line, area, volume), the adopted scale (small or large), the input type
3996 (deterministic or stochastic), the dynamic conditions (steady or unsteady state), and the
3997 pollutant sources (gases or particles).

3998 Dispersion models vary on the mathematics used, but they all require the same input data
3999 that include:

- 4000 ● meteorological conditions such as wind speed and wind direction, the amount of
4001 atmospheric turbulence, the ambient temperature, mixing height, cloud cover and
4002 solar radiation;
- 4003 ● source term – the emission rate of the pollutant being released;
- 4004 ● source characteristics such as the source location, height, type of source, exit
4005 velocity and temperature;
- 4006 ● terrain elevations and land use type; and
- 4007 ● the location, geometry (mainly height and width) of any obstructions in the path of the
4008 emitted plume.

4009 Many of the modern, advanced dispersion model programs include pre- and post-processors
4010 for the input of meteorological and geophysical data as well as statistical modules for the
4011 plotting and tabulating of the pollutant's impact over a geographical area.

4012 Among the models used in the world today for odour assessments Gaussian plume models
4013 are largely used together with Lagrangian puff and particle models. Both are able to
4014 estimate the downwind ambient concentrations of air pollutants from different source types.
4015 Lagrangian models work well for both homogenous and stationary conditions over flat
4016 terrain, and inhomogeneous and non-steady state conditions over complex terrain, while
4017 Gaussian models are ideally suited for homogenous conditions in flat terrain. Despite their
4018 simplicity, Gaussian plume models are still widely used in atmospheric dispersion modelling
4019 around the world, and most often for regulatory purposes because of their easy
4020 implementation and their near real-time response.

4021 The technical literature on air pollution dispersion is quite extensive and dates back to the
4022 1930s and earlier. The basic formulations are discussed below.

4023 5.3.2. Evolution of basic models

4024 Because computational power was low, early air pollution models were simplifications which
4025 could only solve first approximations, and could only simplistically describe the dispersion of

4026 chemically unreactive substances from a point source in a time-stationary and horizontally
 4027 homogeneous meteorological and turbulent environment. In the last decade of the last
 4028 century, it became evident that the passive scalar assumptions of the early simplistic models
 4029 were not representative of the convective planetary boundary layer (PBL) (daytime and
 4030 sunny hours with low/moderate wind). This led to the development of semi-empirical, Hybrid
 4031 models in which the main elements that characterise the convective PBL were introduced.
 4032 This allowed a more realistic reproduction of dispersion in these situations. However, the
 4033 complex characteristics of nocturnal and highly stable situations in which turbulence coexists
 4034 and interacts with a myriad of wave motions and meandering was totally ignored in these
 4035 early models.

4036 A common feature of the early Gaussian plume and Hybrid models is that they both
 4037 assumed quasi-stationary situations and horizontally homogeneous computational domains,
 4038 and were a gross simplification of reality. It was inevitable that the simulations they produced
 4039 were nothing more than a rough estimate of the mean concentration fields downwind of ideal
 4040 sources that were essentially point-like in conditions far from high convectivity, and of
 4041 medium-high stability. Today, these models are considered screening models and are
 4042 suitable for providing the order of magnitude of the impact of a given source.

4043 One of the early air pollutant dispersion equations was derived by Bosanquet, 1936. This
 4044 early formulation did not assume a Gaussian distribution nor did it include the effect of
 4045 ground reflection of the pollutant plume. However, by 1947, Sir Graham Sutton derived an
 4046 air pollution plume dispersion equation (Sutton, 1947) which did include the Gaussian
 4047 distribution assumption for the vertical and crosswind dispersion of the plume and also
 4048 included the effect of ground reflection of the plume. This early Gaussian equation came at
 4049 the time of the industrial revolution when there was a need to have numerical tools to
 4050 simulate the dispersion of pollutants emitted in the PBL from industrial sources. Under the
 4051 stimulus provided by the advent of stringent environment control regulations, there was a
 4052 growth in the use of air pollutant plume dispersion calculations and early models from the
 4053 late 1960s until today. The basis for most of these early models was the Gaussian equation
 4054 which was considered the complete equation for Gaussian dispersion modelling of
 4055 continuous, buoyant air pollution plumes provided in two well-known publications, (Turner,
 4056 1994) and (Beychok, 2005). The equation is:

$$4057 \quad C = \frac{Q}{u} \frac{f}{\sigma_y \sqrt{g}}$$

4058 where

$$4059 \quad f = \exp\left(\frac{-y^2}{2\sigma_y^2}\right) \text{ is the crosswind dispersion parameter}$$

4060 $g = g_1 + g_2 + g_3$ is the vertical dispersion parameter

$$4061 \quad g_1 = \exp\left[\frac{-(z - H_e)^2}{2\sigma_z^2}\right] \text{ is the vertical dispersion with no reflections}$$

4062 $g_2 = \exp\left[\frac{-(z+H_e)^2}{2\sigma_z^2}\right]$ is the vertical dispersion for reflection from the ground

4063 $g_3 = \sum_{m=1}^{\infty} \exp\left[\frac{-(z-H_e-2mL)^2}{2\sigma_z^2}\right]$ is the vertical dispersion for reflection from an inversion aloft

4064 C is the concentration of pollutant, in g/m^3 , at any receptor located:

- 4065 • X metres downwind from the emission source point
- 4066 • Y metres crosswind from the emission plume centerline
- 4067 • Z metres above the ground level

4068 Q is the pollutant emission rate, in g/s

4069 u is the horizontal wind velocity along the plume centreline, in m/s

4070 H_e is the height of the emission plume centerline above ground level, in m

4071 σ_z is the vertical standard deviation of the emission distribution, in m

4072 σ_y is the horizontal standard deviation of the emission distribution, in m

4073 L is the height from the ground level to the bottom of the inversion aloft, in m

4074 $\exp()$ is the exponential function

4075 The above equation includes the upward reflection from the ground and the downward
4076 reflection from the bottom of the inversion lid present in the atmosphere.

4077 The sum of the four exponential terms in g_3 converges to a final value quite rapidly. For
4078 most cases, the summation of the series with $m=1$, $m=2$ and $m=3$ provided an adequate
4079 solution.

4080 σ_z and σ_y are functions of the atmospheric stability class, i.e., a measure of the turbulence in
4081 the atmosphere and of the downwind distance to the receptor. The classification of
4082 atmospheric stability was first presented by Pasquill (Klug, 1984) who proposed 6
4083 atmospheric stability classes (describing atmospheric conditions from the most to the least
4084 dispersive) which are referred to as:

- 4085 • A – extremely unstable
- 4086 • B – moderately unstable
- 4087 • C – slightly unstable
- 4088 • D – neutral
- 4089 • E – slightly stable
- 4090 • F – moderately stable

4091 The above Gaussian plume equation required the input of the pollutant plume centreline
4092 height above ground level H_e , which is the sum of H_s (the actual physical height of the
4093 emission point) plus Δh , the plume rise due to the plume's buoyancy, if any. To determine

4094 Δh many of the dispersion models developed between the late 1960s and the early 2000s
4095 used the 'Briggs equations' (Briggs, 1965). (Briggs, 1968) compared many of the plume rise
4096 models that were available at that time and in that same year he wrote a comparative
4097 analysis of plume rise algorithms in a publication published by the US Air Resources
4098 Laboratory (Slade, 1968). (Briggs, 1969) wrote a critical review of all the available plume rise
4099 literature. In this review Briggs proposed a set of plume rise equations which have become
4100 widely known as the 'Briggs' equations; these equations were subsequently modified by the
4101 same author (Briggs, 1971) and (Briggs, 1972). The 'modified' Briggs plume rise equations
4102 are still employed in many popular worldwide regulatory air pollution models.

4103 5.3.3. Current form of Gaussian plume models

4104 The current form of the standard Gaussian plume model is based on a simple formula that
4105 describes the three-dimensional concentration field generated by a point, volume or area
4106 source under stationary meteorological and emission conditions, and for concentrations on
4107 the ground is expressed by (e.g., (Zannetti, 1990), (Turner, 2020)).

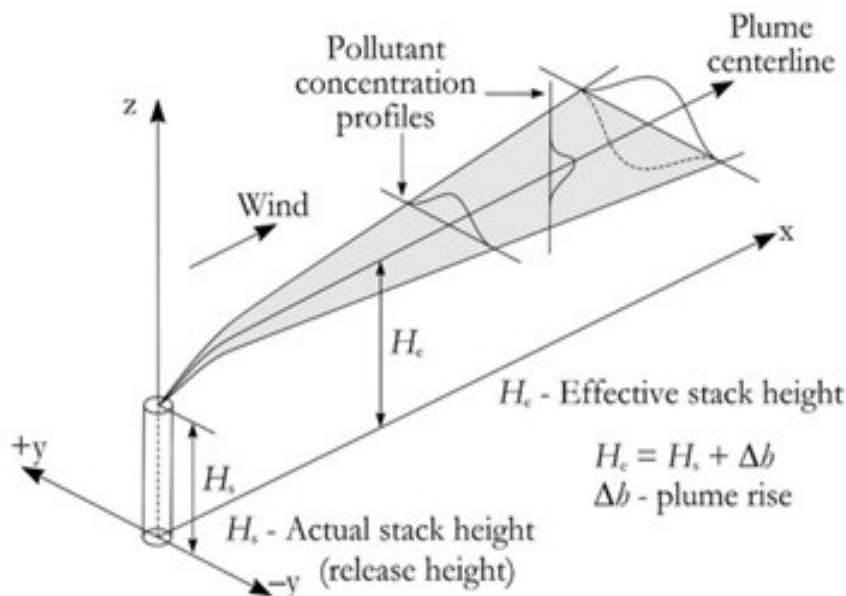
$$4108 \quad C(x, y, 0) = \frac{Q}{\pi \sigma_y \sigma_z u} \exp\left[-\frac{1}{2} \left(\frac{y}{\sigma_y}\right)^2\right] \exp\left[-\frac{1}{2} \left(\frac{H_e}{\sigma_z}\right)^2\right]$$

4109 Where C is the concentration of gas or aerosols (generally particles less than about 20
4110 microns) at x, y, z=0 due to a continuous emission with an effective emission rate Q. H_e is
4111 the height of the plume centreline when it becomes level, and is the sum of the physical
4112 stack height H_s and the plume rise Δh . The following assumptions are made:

- 4113 ● The plume spread has a Gaussian distribution in both the horizontal and vertical
4114 planes with a standard deviation of plume concentration distribution in the horizontal
4115 and vertical of σ_y and σ_z , respectively.
- 4116 ● The mean wind speed affecting the plume is u.
- 4117 ● The uniform pollutant emission rate is Q.
- 4118 ● The total reflection of the plume takes place at the earth's surface, i.e., there is no
4119 deposition or reaction at the surface.

4120 [Figure 5-1](#) shows a schematic figure of a Gaussian plume. The effective stack height H_e and
4121 the crosswind (σ_y) and vertical (σ_z) deviation of the profile are the key parameters of the
4122 model.

4123



4124

4125 **Figure 5-1** Schematic figure of a Gaussian plume (Leelossy et al. 2014)

4126

4127 The main important assumptions of Gaussian plume models are:

- 4128 ● The horizontal meteorological conditions are homogenous over the space modelled.
- 4129 For each step modelled, the wind speed and wind direction, temperature and mixing
- 4130 height is constant.
- 4131 ● There is no wind shear in the horizontal or vertical plane.
- 4132 ● The pollutants are non-reactive gases or aerosols.
- 4133 ● The plume is reflected at the surface and aloft with no deposition or reaction with the
- 4134 surface.

4135 5.3.4. Lagrangian models

4136 5.3.4.1. Overview

4137 Lagrangian models provide an alternative method for simulating atmospheric diffusion. They
 4138 are called Lagrangian because they describe the fluid elements that follow the instantaneous
 4139 flow. According to (Zannetti, 1990) the 'Lagrangian' term was initially used to distinguish
 4140 between the Lagrangian box models that follow the average wind trajectory, from the
 4141 Eulerian box models which do not move. Today, however, the term Lagrangian has been
 4142 extended to describe all models in which plumes are broken up into segments, puffs or
 4143 fictitious particles whose behaviour is followed along the mean flow.

4144
$$C(r, t) = \int_{-\infty}^t \int_{\square} p(r, t \vee r', t') S(r', t') dx' dt'$$

4145 Where the integration in space is performed over the entire atmospheric domain, and

4146 $C(r,t)$ is the ensemble average² concentration at r at time t ;
 4147 $S(r',t')$ is the source term (mass volume⁻¹ time⁻¹);
 4148 $p(r,t|r',t')$ is the probability density function (volume⁻¹) that an air parcel moves from r' at t' to r
 4149 at t , where for any r' and t' ,

$$\int_{\Omega} p(r,t|r',t') dr \leq 1$$

4151 The expression above can be less than one when chemical or depositional phenomena are
 4152 considered; otherwise, mass conservation always requires the value to be equal to one. For
 4153 a primary pollutant, (pollutant emitted directly from a source), $S(r',t')$ is greater than zero only
 4154 at points where the pollutant is released (e.g., exit points of stacks). For a secondary
 4155 pollutant (pollutant formed when primary pollutants react in the atmosphere), $S(r',t')$ can be
 4156 non-zero virtually anywhere. For both primary and secondary pollutants, however, the
 4157 equation above which represents mass conservation must be satisfied.

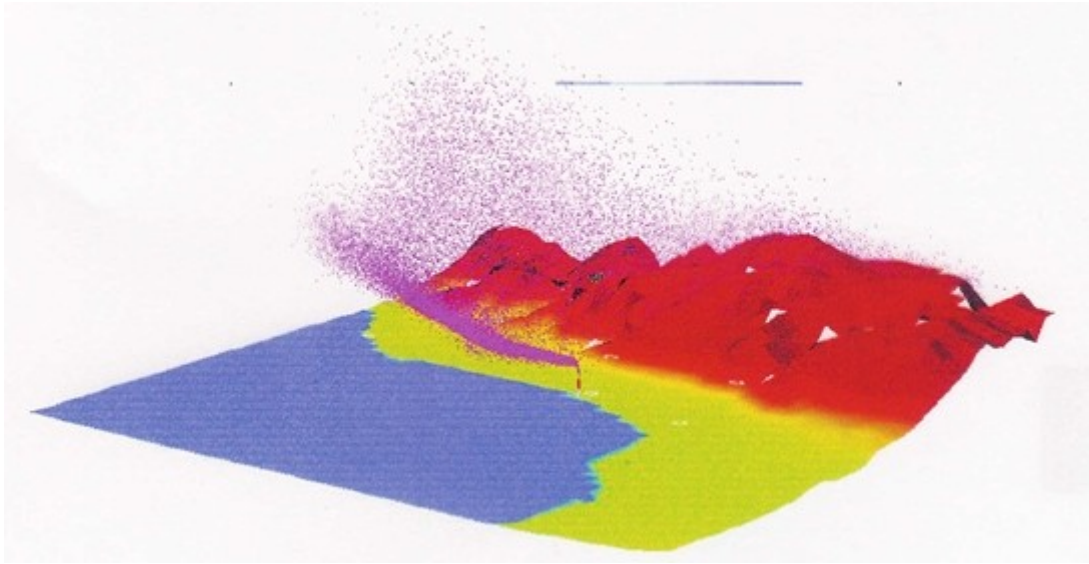
4158
 4159 The Lagrangian approach is more ideally suited to simulating diffusion and chemical
 4160 reactions over short distances, e.g., tens of metres, (Scire, 2000b) from all source types, to
 4161 very far downwind distances, e.g., hundreds of kilometres, (Lamb, 1979). Lagrangian
 4162 models require no grid network, and can have as few or as many receptor points as required
 4163 which can be arbitrarily distributed in any configuration over the area of interest. The
 4164 absence of a grid network and of finite differencing schemes makes the computational
 4165 process of modelling dispersion over elevated and complex terrain relatively simple. In
 4166 addition, the Lagrangian approach is essentially free of the assumptions that hinder the
 4167 plume model and they can explicitly account for wind shear, particle settling, deposition and
 4168 resuspension, calm winds, and time and space variability in the meteorology or source
 4169 emission conditions. The temporal evolution of the dispersion is also properly simulated, and
 4170 complex Lagrangian models can treat chemical transformations. In addition, Lagrangian
 4171 models can employ readily measurable Eulerian turbulence statistics such as the variances
 4172 of the velocity fluctuations, or, use more common Lagrangian statistics like the sigma (σ)
 4173 parameter.

4174 5.3.4.2. Particle vs Puff Lagrangian approach

4175 Compared to Eulerian models discussed below, the Lagrangian approach is grid-free, and it
 4176 follows at all scales, the motion of individual plume parcels, whose paths are modelled
 4177 based on a random walk process. The Lagrangian approach describes all phases of
 4178 dispersion with the same accuracy, and very importantly the near-field or near-source
 4179 region, where most odour complaints generally occur. In Lagrangian particle models, the
 4180 dispersion of the airborne pollutants is simulated through fictitious particles, each containing
 4181 a small amount of the emitted tracer mass. These particles are small enough to move
 4182 according to the smallest eddies and are also large enough not to be influenced by the
 4183 viscosity. The local wind drives their mean motion and the diffusion is determined by
 4184 velocities obtained as the solution of Lagrangian stochastic differential equations, providing
 4185 the statistical characteristic of turbulent flows. Different portions of the emitted plumes can

264 ²The ensemble average of a stochastic process (random variable) is analogous to an
 265 expected value. That is, given a large number of trials, it is the 'average' waveform that
 266 would result from a stochastic process. This means that an ensemble average is a function
 267 of the same variable that the stochastic process is.

4186 experience different atmospheric conditions, allowing a realistic reproduction of the complex
 4187 atmospheric phenomena that can occur in coastal and mountainous areas. The
 4188 concentration is calculated by counting particles in a box. The Lagrangian particle model
 4189 releases for each iteration a number of fictitious particles from any source within a model
 4190 domain (see for example [Figure 5-2](#)). The particles on the domain statistically represent the
 4191 turbulent transport and simulate the pollutants' plume growth.
 4192
 4193



4194
 4195 **Figure 5-2** Schematic figure of a Lagrangian particle dispersion model (courtesy of
 4196 ARIANET).

4197
 4198 Lagrangian puff models, on the other hand, represent a continuous plume as a number of
 4199 discrete packets of pollutant material (see [Figure 5-3](#)). Most puff models (e.g. : (Ludwig,
 4200 1977), (van Egmond, 1983), (Peterson, 1986)) evaluate the contribution of a puff to the
 4201 concentration at a receptor by a 'snapshot' approach. Each puff is 'frozen' at a particular
 4202 time interval (sampling step). The concentration due to the 'frozen' puff at that time is
 4203 computed (or sampled). The puff is then allowed to move, evolving in size, strength, etc, until
 4204 the next sampling step. The total concentration at a receptor is the sum of the contributions
 4205 of all nearby puffs averaged for all sampling steps within the basic time step, which is usually
 4206 an hour.

4207
 4208 The basic formulation for modern-day puff models which use an integrated puff sampling
 4209 function can be explained in the equations below for the contribution of a puff at a receptor
 4210 is:

4211
$$C = \frac{Q}{\pi \sigma_x \sigma_y} g \exp\left(\frac{-d_a^2}{2\sigma_x^2}\right) \exp\left(\frac{-d_c^2}{2\sigma_z^2}\right)$$

4212
$$g = \frac{2}{\sqrt{\pi}}$$

4213 Where

4214 C is the ground-level concentration (g/m³)

4215 Q is the pollutant mass (g) in the puff,

4216 σ_x is the standard deviation (m) of the Gaussian distribution in the along-wind direction,

4217 σ_y is the standard deviation (m) of the Gaussian distribution in the cross-wind direction

4218 σ_z is the standard deviation (m) of the Gaussian distribution in the vertical direction

4219 d_a is the distance (m) from the puff centre to the receptor in the along-wind direction,

4220 d_c is the distance (m) from the puff centre to the receptor in the cross-wind direction,

4221 H_e is the effective height (m) above the ground of the puff centre,

4222 g is the vertical term (m) of the Gaussian equation, and

4223 h is the mixed-layer height (m).

4224 The summation in the vertical term g accounts for multiple reflections off the mixing lid and

4225 the ground. It reduces to the uniformly mixed limit of 1/h for $\sigma_z > 1.6 h$. In general, puffs

4226 within the convective boundary layer meet this criterion within a few hours after release.

4227 Therefore, for a horizontally symmetric puff with $\sigma_x = \sigma_y$, the equation reduces to:

$$4228 \quad C(s) = \frac{Q(s)}{2\pi\sigma_y^2(s)} g(s) \exp\left[\frac{-R^2(s)}{2\sigma_y^2(s)}\right]$$

4229 Where R is the distance (m) from the centre of the puff to the receptor and s is the distance

4230 (m) travelled by the puff. The distance dependence of the variables is indicated, e.g., C(s),

4231 $\sigma_z(s)$ etc. Integrating this equation of the distance of puff travel, ds, during the sampling

4232 step, dt, yields the time-averaged concentration, \underline{C} described below as

$$4233 \quad \underline{C} = \frac{1}{ds} \int_{s_0}^{s_0+ds} \frac{Q(s)}{2\pi\sigma_y^2(s)} g(s) \exp\left[\frac{-R^2(s)}{2\sigma_y^2(s)}\right] ds$$

4234 Where s_0 is the value of s at the beginning of the sampling step. An analytical solution to

4235 this integral can be obtained if it is assumed that the most significant s-dependencies during

4236 the sampling step are in the R(s) and Q(s) terms.

4237

4238 The horizontal dispersion coefficient, σ_y and the vertical term, g, are evaluated and held

4239 constant throughout the trajectory segment. At mesoscale distances, the fractional change in

4240 puff size during each sampling step is usually small, and the use of the midpoint values of σ_y

4241 and g is adequate. This assumption reduces the number of times that the dispersion

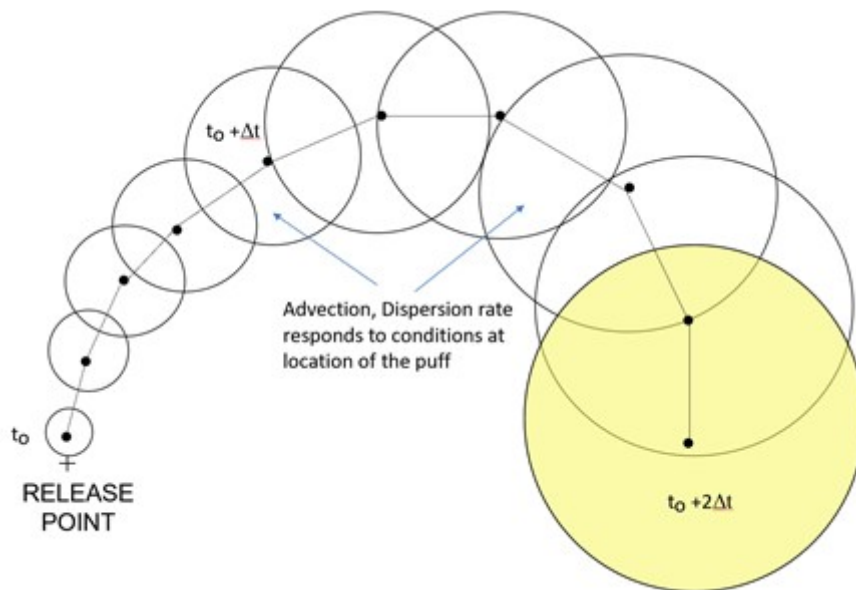
4242 coefficients and vertical reflection terms need to be computed to one sampling step, but may

4243 not be appropriate in the near-field where the fractional puff growth rate can be rapid. These

4244 models have gotten around this by integrating the sampling function with receptor-specific

4245 values of σ_y and g, evaluated at the point of closest approach of the puff to each receptor.

4246



4247

4248 **Figure 5-3** Schematic figure of a Lagrangian puff dispersion model (Courtesy of
4249 Atmospheric Science Global).

4250 5.3.4.3. Particle-Puff Lagrangian approach

4251 This approach typically uses a Gaussian puff solution in the terrain following horizontal
4252 direction and a particle solution for the vertical coordinate. The method allows a particle/puff
4253 to influence more than one horizontal grid point and so the total number of particles needed
4254 for a model run is reduced. The dispersion simulation still accounts for height-varying values
4255 of winds and turbulence in the same way as conventional particle models. There are not
4256 many models of this type and there is very little in the literature on their use in odour
4257 modelling. The main aim of these models was to reduce the number of particles, memory
4258 and computer time when compared to a regular particle model. It is understood that models
4259 of this type typically use an analytic puff solution of the Langevin equation for stationary,
4260 homogeneous, Gaussian turbulence, which agrees exactly with the full Langevin equation
4261 solution when these conditions on the turbulence are satisfied in the horizontal directions.
4262 The puff centroid is advected by the mean winds and is acted upon by the wind shear and
4263 turbulence in the vertical direction, but horizontal diffusion is included by assuming a lateral
4264 Gaussian concentration distribution with standard deviation σ_y . The approximation assumes
4265 horizontal wind shear is negligible, which is acceptable when the puffs are small, but is likely
4266 to break down as puffs increase in horizontal extent. Generally, these models do well in
4267 reproducing normal particle models in the convective boundary layer, except for where there
4268 is significant horizontal wind shear. In addition, (Hurley, 1994) found the Particle-puff
4269 approach has an advantage over puff models in that it can realistically handle the vertical
4270 structure of the atmosphere through the Langevin equation for the vertical coordinate, and
4271 does not require the complex vertical boundary conditions used by puff models to account
4272 for reflection at the ground and the mixing height. In particular, skewed turbulence can
4273 easily be accounted for in the convective boundary layer and well-mixed conditions in the
4274 vertical can be represented without complex Gaussian puff image sources. In addition, the
4275 particle/puff is able to handle vertical variations of wind and turbulence in the same way as
4276 existing particle models.

4277 5.3.4.3. Lagrangian models and odour

4278 The Lagrangian approach is much more ideally suited to modelling odours than steady-state
 4279 Gaussian plume models. They are ideally suited for modelling the very near field from a few
 4280 tens of metres out to hundreds of kilometres. In addition, modelling dispersion around
 4281 elevated and complex terrain is relatively simple, and they can model calm events which are
 4282 usually the worst-case odour conditions. When linked to diagnostic and or numerical model-
 4283 derived 3-dimensional meteorology they can produce very reliable model results for odour
 4284 assessments.

4285
 4286 Lagrangian particle models have been successfully used to calculate direction-dependent
 4287 separation distances to avoid odour annoyance (Piringer, 2016) and to perform better in
 4288 complex terrain environments (Baumann-Stanzer, 2015). The Lagrangian approach did
 4289 much better reproducing the physical processes and generally calculated larger separation
 4290 distances compared to the Gaussian model applied in their study. The Lagrangian approach
 4291 is also routinely and successfully used for most odour assessments in Australia and New
 4292 Zealand and is the preferred regulatory odour model in those countries, as limitations of the
 4293 Gaussian plume model for odour assessments are generally well recognised.

4294 Currently, Lagrangian models like Gaussian plume models also assume a 1-hour time-
 4295 averaged distribution in the plume, which does not fully account for the turbulent odour
 4296 concentration fluctuations, which is on the order of seconds, nor the meander of the plume
 4297 from the mean direction. Similarly to Gaussian plume models, it has been normal practice
 4298 around the world in odour assessments using Lagrangian models to apply Peak-to-Mean
 4299 Ratios to try and account for the short-scale concentration fluctuations. Peak-to-Mean
 4300 Ratios are a simple 'stand-alone' formula to estimate the concentration fluctuation intensity.
 4301 They assume that the concentration fluctuation intensity completely defines a probability
 4302 density function. Their use is required in different parts of the world (see for example
 4303 Brancher et al., 2017), considering concentrations at different averaging time intervals
 4304 from 1 hour to 1 second as in the assessment criterion in in New South Wales, Australia
 4305 (NSW Approved Methods, 2022)

4306
 4307 However, recent research by (Ferrero & Öttl, 2019) and (Ferrero et al., 2020) show that
 4308 concentration fluctuation can be obtained directly from the Lagrangian approach. This new
 4309 research is discussed in [Section 7.8 \(A window open on the research\)](#).

4310 5.3.4. Eulerian models

4311 Eulerian models ([Figure 5-4](#)) utilise a fixed reference grid, as opposed to the moving grid of
 4312 the Lagrangian model, to describe the dispersion of emitting sources. The Eulerian models
 4313 integrate the general form of the advection-diffusion equation following (Collett, 1997) and
 4314 (Reed, 2005):

4315
$$\delta \langle c_i \rangle \frac{dt}{dt} = -U \nabla \cdot \langle c_i \rangle - \nabla \cdot \langle c_i U' \rangle + D \nabla^2 \langle c_i \rangle + \dot{c}_i S_i \dot{c}_i$$

4316 Where:

4317 U = Windfield vector U(x,y,z), U = U_i + U'

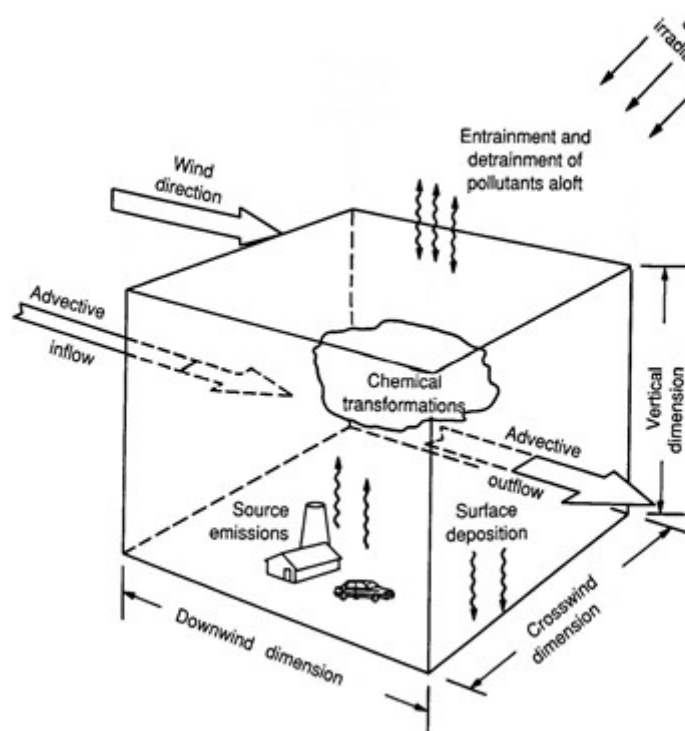
4318 U_i = average wind field vector

4319 U' = fluctuating wind field vector

4320 c_i = concentration of pollutant for i^{th} species, $c = \langle c \rangle + c'$
 4321 $\langle c \rangle$ = average pollutant concentration, where $\langle \rangle$ denotes average
 4322 c' = fluctuating pollutant concentration
 4323 D = molecular diffusivity
 4324 S_i = source or sink term (chemical reactions should be taken into account)
 4325

4326 The terms $U \cdot \nabla \langle c_i \rangle$, $\nabla \cdot \langle c'_i U \rangle$, and $D \nabla^2 \langle c_i \rangle$ represent the rates of advection, turbulent
 4327 diffusion, and molecular diffusion, respectively. For most cases, the wind field vector U is
 4328 considered turbulent and requires average and fluctuating wind field vector components.
 4329 The previous equation is numerically solved on a fixed grid at discrete time steps to give the
 4330 behaviour in time and space of the concentration of the i^{th} species. Eulerian models can
 4331 describe the fate of any pollutant, even if this is not directly emitted into the computational
 4332 domain, considering the intrusion through the upper and lateral boundaries. Once the initial
 4333 and boundary conditions are given, Eulerian models can describe the time and space
 4334 behaviour of the air quality inside a certain volume, allowing in a relatively natural way to
 4335 implement also chemical transformations involving all the species considered in a simulation.
 4336 For this reason, Eulerian models are more often used as the computing core of air quality
 4337 forecasting systems at a regional scale.
 4338

4339 The difficulty of Eulerian models to describe the dispersion in the near field makes this
 4340 approach not very suitable for odour assessments. In practice, this method is rarely used in
 4341 this field.
 4342



4343
 4344 **Figure 5-4** Schematic figure of an Eulerian dispersion model (source: (NOAA, 2008)).

4345 5.3.5. Computational Fluid Dynamic (CFD) Models

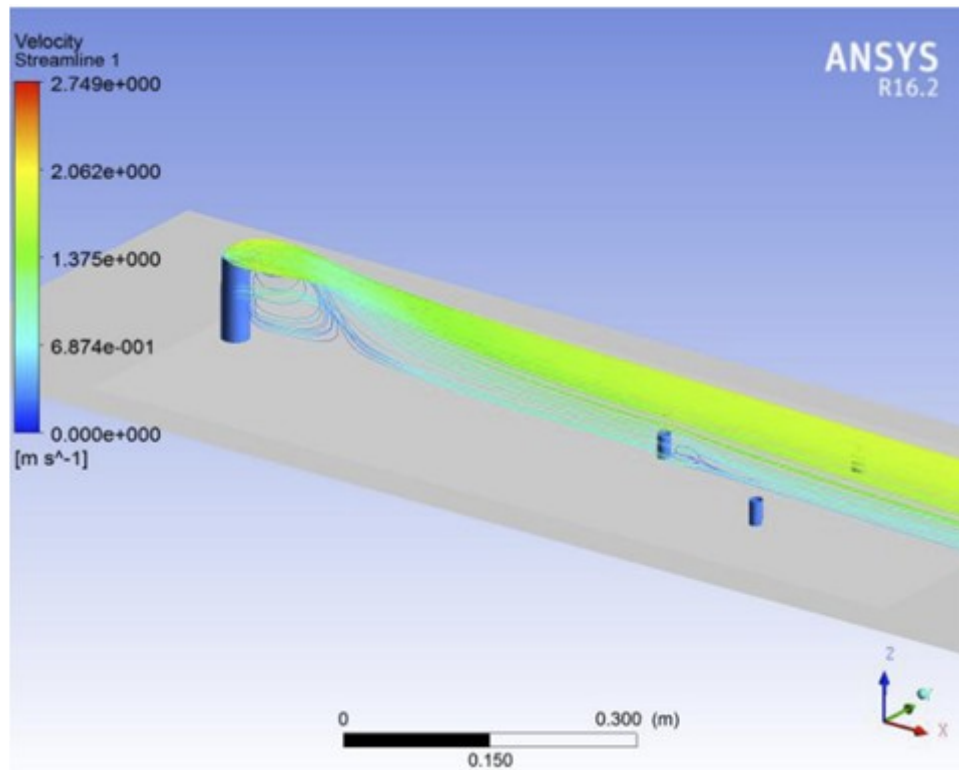
4346 Computational fluid dynamic (CFD) models are becoming increasingly useful in the field of
4347 odour assessments (Lin, 2009). CFD models can predict how a fluid will flow in a given
4348 situation and can model airflow and pollutant dispersion in unstable and stable atmospheric
4349 conditions or where nearby structures cause localised turbulence. Odour facilities are
4350 frequently located in industrial areas or are themselves surrounded by structures, trees and
4351 commonly, hedges, popular with animal husbandry facilities. CFD models can calculate the
4352 properties such as flow patterns, pressure losses and temperature distribution, which are
4353 then used to predict how air pollutants will behave. CFD models are also becoming
4354 increasingly popular with complicated odour-producing facilities as they are ideally suited to
4355 very near-field modelling in adverse situations (Lin, 2007a). These models are especially
4356 useful in designing and optimising heating, ventilating and industrial extraction systems from
4357 large poultry and piggery barns. In addition, windbreaks have been found to improve odour
4358 dispersion and help reduce setback distances (Panofsky, 1984). According to (Lin, 2006)
4359 (Lin 2007b), a natural windbreak with an optical porosity of 35% reduced, on average, the
4360 maximum odour dispersion distance by 20% compared to a site without a windbreak.

4361
4362 CFD models ([Figure 5-5](#)) have advanced significantly in the last decade, primarily due to the
4363 advancing power of computational hardware and software. CFD simulations have the
4364 potential to yield more accurate solutions than other methodologies because they are a
4365 solution of the fundamental physics equations and include the effects of detailed three-
4366 dimensional geometry and local environmental conditions.

4367
4368 According to the US EPA (Huber, 2004), one of the key roles of CFD simulations for all air
4369 quality applications, including odour, is that CFD simulations should be shown to be
4370 comparable with simple proven air dispersion models which are being reliably applied today
4371 in routine air quality studies. (Huber, 2004) consider this critical to demonstrate that the
4372 complex numerical techniques part of CFD software are well-behaved under simple
4373 conditions. The US-EPA encourages users not to use CFD software to support studies
4374 where simple analytical studies are possible and instead to use CFD applications for
4375 complex conditions where the simple analytical solutions are not appropriate.

4376
4377 For odour applications, CFD models cannot be used as regulatory tools. These models are
4378 complex, easily influenced by user choice of boundary conditions, grid resolution and
4379 structure and can simulate just one atmospheric condition at a time.

4380



4381

4382

Figure 5-5 Schematic figure of a CFD model (source: Brusca, 2008).

4383 5.4. Operational existing models

4384 5.4.1. Introduction

4385 It is typical for the US, Europe and other countries to have preferred and/or recommended
4386 dispersion models for regulatory air quality assessments. These ‘preferred’ models are
4387 primarily used to determine compliance with a state or countries’ National Ambient Air
4388 Quality Standards (NAAQS). It is normal for these air quality models to be used on both
4389 existing sources and new sources. These models are often associated with strict guidelines
4390 such as the ‘Guideline on Air Quality Models’ (US-EPA, 2017) in the US and the European
4391 Air Quality Directive (Denby, 2010). The guidelines themselves are periodically revised to
4392 ensure that any new model developments or expanded regulatory requirements are
4393 incorporated. These models are normally available from the regulatory site website or the
4394 developers’ home website. Some of these models are open-source (users can view and
4395 access the code), and others are closed-source. In the US, ‘open source’ models are
4396 usually guideline models that have undergone a lengthy third-party review process.
4397 Typically, US guideline models:

4398

4399

4400

4401

4402

4403

4404

- are pre-approved for designated uses in regulatory applications,
- have undergone an extensive, multi-year model assessment and evaluation process,
- have been evaluated relative to observations,
- are associated with free user access to all model documentation and codes,
- have undergone significant public review process at public hearings
- are associated with formal peer review committees created by the US EPA and other professional organisations such as AWMA, and private industry groups API and

4405 EPRI

4406 Because of this lengthy, costly and thorough process to become a guideline model, US EPA
4407 endorsed dispersion models quickly find themselves regulatory models in other countries
4408 who are comfortable with the significant effort put in by the US, where it can often take 20 or
4409 more years for a model to reach guideline status. In the US and in countries that employ US
4410 guideline models as their own tend to use these 'preferred' regulatory models regardless of
4411 whether they are inherently suitable for modelling odours or not. It is important that for
4412 regulatory applications in the US, there is a balance between the technology employed by
4413 the model and its ability to be utilised efficiently, cost-effectively, and be readily reviewed by
4414 the local authority. Many countries have followed this approach and as a result, the US
4415 regulatory models are routinely and much more frequently used for odour modelling all over
4416 the world, than any other model, regardless of their suitability. In Europe, Australia and New
4417 Zealand US guideline models do not carry as much weight in odour modelling where users
4418 are able to apply more sophisticated Lagrangian puff and particle models. In Europe, this
4419 might be multiple advanced country-specific developed particle models. A consequence of
4420 this is that these sophisticated 'odour' models are not as well known outside of Europe, and
4421 therefore are not widely used amongst the international odour community.

4422
4423 The following sections below discuss those dispersion models that are commonly used for
4424 odour assessments. These models range from simple screening models (AERSCREEN,
4425 ADMS-SCREEN, SMOD) to advanced Gaussian plume models (ADMS, AERMOD, ARIA
4426 Impact, AODM), to Lagrangian particle (SPRAY, AUSTAL, LAPMOD, GRAL, QUIC) and puff
4427 models (CALPUFF, SCIPUFF) and finally Eulerian and CFD models (CODE_SATURNE,
4428 FLOW 3D). Eulerian models are discussed, but in a limited sense, as there is little literature
4429 on their use in odour modelling. Discussion on CFD models is included as they have been
4430 very beneficial in assessing the impact of odours in adverse environments, such as
4431 complicated building structures (Tomasello, 2019), or in considering the effect of natural
4432 vegetation boundaries on odour (Jin, 2007a) and pollution (Santiago, 2019) dispersion.

4433
4434 Commonly used odour dispersion models are discussed in this next Section. For each
4435 model, there is a brief discussion provided on the evolution, development and key algorithms
4436 of the model, plus whether the model is regulated for odour assessments and who is using it.
4437 In addition, whether the model can manage odour units, concentration fluctuations,
4438 treatment of calms and odour concentration outputs, in so far as percentiles, exceedances,
4439 and comparison to odour criteria, is also considered.

4440 5.4.2. Screening models – simple models and empirical equations

4441 5.4.2.1. Screening Models

4442 Screening models will typically produce estimates of 'worst-case' 1- hour concentrations for
4443 a single source without the need for an hourly year-long meteorological data set, detailed
4444 terrain or land use. Simple conversion factors usually allow estimation of 3-hour, 8-hour, 24-
4445 hour and annual concentrations. A principle key aim of screening models is that they are
4446 intended to produce concentration estimates equal to or greater than the estimates by a
4447 regulatory model with a fully developed set of meteorological and terrain data.

4448
4449 Typically, in the US, it is typical for a screening model to be a 'lighter' version of the main

4450 regulatory model. Examples of this are:

- 4451 ● AERSCREEN, the screening version of AERMOD
- 4452 ● CTSCREEN, the screening version of CTDMPLUS
- 4453 ● SCREEN3, the screening version of ISCST3

4454

4455 While the European Union (van Aalst, 1998) does not list a set of screening models, it does
4456 endorse the use of screening methods and says:

4457

4458 *“Particularly for first screening purposes, or in case of limited input information, the use of*
4459 *simple models may be appropriate... If initial screening leads to the conclusion that levels*
4460 *may be of the order of the limit values, more sophisticated models should be selected”*.

4461

4462 In Annex 5.1 ‘Urban Dispersion models’ found in the European Air Quality Directive, the EU
4463 provides a list of hand calculations to estimate: A. Area source model, B. Elevated point
4464 source, C. Street Canyon, and D a Highway. For each source type of A, B or C, the EU
4465 provides the equations for estimating the 1-hour average air concentrations at an arbitrary
4466 receptor using simplified expressions of the ATDL urban diffusion model after (Hanna, 1972)
4467 and (Gifford, 1973) for A and a simplified Gaussian relationship for B. These equations are
4468 to be used anywhere in Europe and are not site or country specific.

4469

4470 In addition, the EU has examples where local environmental agencies have recommended
4471 locally adapted dispersion tools in some geographical areas in combination with
4472 meteorological data for calculating odour concentration. This simplifies the application of
4473 advanced dispersion modelling because no specific meteorological knowledge is needed to
4474 run them. Examples of these simplified screening models include SMOD (Screening model
4475 for odour dispersion) used for planning and informative purposes of licencing procedures in
4476 the German province of North Rhine (Hartmann, 2007; Janicke, 2007). Another European
4477 screening model is the Gaussian plume model, V-STACKS (Steyn, 1978) model in the
4478 Netherlands, and in Manitoba, Canada (Manitoba, 2008) look-up tables have been recently
4479 developed based on AERMOD simulations. These screening methods are examples of an
4480 integral part of locally adapted solutions and are not easily transferred to other regions.

4481

4482 The US EPA currently supports several screening models; AERSCREEN, CAL3QCH,
4483 COMPLEX1, CTSCREEN, RTDM3.2, SCREEN3, TSCREEN, VALLEY and VISCREEN, but
4484 only one or two of these is of any use for odour assessments. Of these models, SCREEN3 is
4485 one of the oldest and most well-known screening models, written in 1995 and updated in
4486 2013. Like other screening models, SCREEN can simulate a single source in short-term
4487 calculations. The model includes the effects of downwash and can estimate concentrations
4488 due to inversion break-up and incorporate the effects of simple terrain. SCREEN examines
4489 various meteorological conditions, including all stability classes and wind speeds. SCREEN
4490 is seldom used in the field, and there is no history or literature on its use in odour
4491 assessments. Many algorithms (building downwash and dispersion coefficients) have been
4492 superseded in advanced Gaussian models such as AERMOD. Therefore there is more
4493 likelihood that AERSCREEN will be used for odour assessments.

4494

4495 AERSCREEN (US-EPA, 2021), like SCREEN, is an interactive command-prompt application
4496 that interfaces with MAKEMET, which is a processor for generating a meteorological matrix,
4497 as well as interfaces to AERMOD’s AERMAP (terrain processor) and BPIPPRM for

4498 processing building information. AERSCREEN will use user-defined single values for
4499 albedo, Bowen ratio and surface roughness and can model inversion break-up fumigation
4500 and shoreline fumigation. Like SCREEN3, the model does not contain input and output
4501 odour-specific information. AERSCREEN will build a matrix of meteorological hours based
4502 on the minimum wind speed and ambient minimum and maximum temperatures. This
4503 approach ensures that the model captures poor dispersion. The benefits of a screening
4504 model like AERSCREEN are that it can assess the potential worst-case impact of a known
4505 odour, such as naphthalene (ORION, 2019), where the emission rate is known. The model
4506 will compute the odour concentration at various discrete distances downwind, for instance, at
4507 the property boundary, the nearest off-site sensitive receptor, and the nearest residence.
4508 The model uses local terrain information and generated meteorological data to compute
4509 worst-case conditions. The model also assumes continuous emissions. If these results are
4510 generally below the appropriate short-term odour criteria levels, then no more work is usually
4511 needed. This saves time and money for a full-blow dispersion model assessment, likely
4512 producing lower results. However, screening models are unsuitable for complex odour
4513 emission scenarios, typical of most activities.

4514

4515 Another well-known Gaussian screening model is ADMS-Screen (CERC, 2021). ADMS-
4516 Screen models' dispersion from a single stack to calculate ground-level concentrations,
4517 providing rapid assessments of stack height. The model can compare predicted
4518 concentrations with air quality strategy objectives. The model has the option to include the
4519 effects of a single building. ADMS-Screen uses the ADMS dispersion code, including the
4520 ADMS Mapper, for GIS visualisation and editing. ADMS-Screen is used to assess the impact
4521 of point source emissions quickly.

4522

4523 A summary of AERSCREEN and ADMS-Screen is provided in Table 5-1. Both these
4524 models, whilst screening models, still require substantial input and are unsuitable for use in
4525 the field. These models are only recommended for a quick, 1-hour, worst-case assessment
4526 of a known odorant. They are not suitable for assessing a complex mix of odour compounds
4527 where the emission rate is largely unknown; they are also inappropriate for comparing the
4528 model output with odour criteria using percentiles. They are also not fit to assess
4529 exceedances of an odour impact criteria. They cannot assess concentration fluctuation
4530 internally and would require external processing to apply a PtMR, hedonic tone, or to
4531 compute a < 1-hour average. In addition, neither model allows odour-specific emission
4532 inputs and output odour concentration. In addition, there is little information in the literature
4533 concerning the use of screening models for odour assessments.

4534

4535

4536

4537

4538

4539

4540

4541

4542

4543

4544

4545

4546 **Table 5-1** Well-known screening dispersion models, AERSCREEN and ADMS-SCREEN,
 4547 used for odour applications

Parameter	AERSCREEN	ADMS-SCREEN
Meteorology	Non-sequential meteorological data file representing a matrix of conditions derived from specific details concerning ambient minimum and maximum temperature, min wind speed (default 0.5 m/s) and anemometer height. Processor will generate approximately 300-400 hours. Wind direction is set at 270°.	Standard ADMS format meteorological files or on-screen meteorological input. UK statistical met data suitable for screening modelling is available from CERC
Pre-processor	AERMINUTE, AERMET and AERMAP for terrain elevations	ADMS meteorological processors
Terrain and Land use	Interface to AERMAP for source and receptor heights, single value to characterise dominant land use	No land use inputs and assumes flat terrain
Surface characteristics	Single value for Bowen ratio, surface roughness, seasonal tables	None
Building downwash	Interface to BPIPPRM	Single building effects are considered
Receptors	Flagpole receptors, up to 10 discrete receptors in a user file, use terrain heights from AERMAP	Cartesian grid, specified discrete receptors
Dispersion	Turbulence based dispersion coefficients, urban/rural dispersion option	Turbulence based dispersion coefficients, urban/rural dispersion option
Boundary layer structure	h, L _{MO} scaling	h, L _{MO} scaling
Plume Rise	Briggs empirical equation	Briggs empirical equation
Concentration distribution	Gaussian	Gaussian
Partial Penetration	Plume fumigation due to inversion break-up	Plume fumigation due to inversion break-up
Coastal effects	Shoreline fumigation of plume	none
Source type	Point, area and volume source	Point source only
Odour unit inputs and outputs	no	no
Emission rate	Only in lb/hr or g/s. Odour emission rate will need to be modified to comply with model input requirements	Only in g/s. Odour emission rate will need to be modified to comply with model input requirements

Parameter	AERSCREEN	ADMS-SCREEN
Output	Plume centreline maximum ground level concentrations. Not suitable to compute percentiles or exceedance data	Not suitable to compute percentiles or exceedance data
Averaging period	1hr, 3hr, 8hr, 24 hr and annual	1hr, 24hr, annual and percentiles
Concentration fluctuation	No	No
Pollutant type	Ideally suited to computing worst case concentrations from a known measurable odour such as H ₂ S, or a single odour chemical compound such as naphthalene	Ideally suited to computing worst case concentrations from a known measurable odour such as H ₂ S, or a single odour chemical compound such as naphthalene

4548

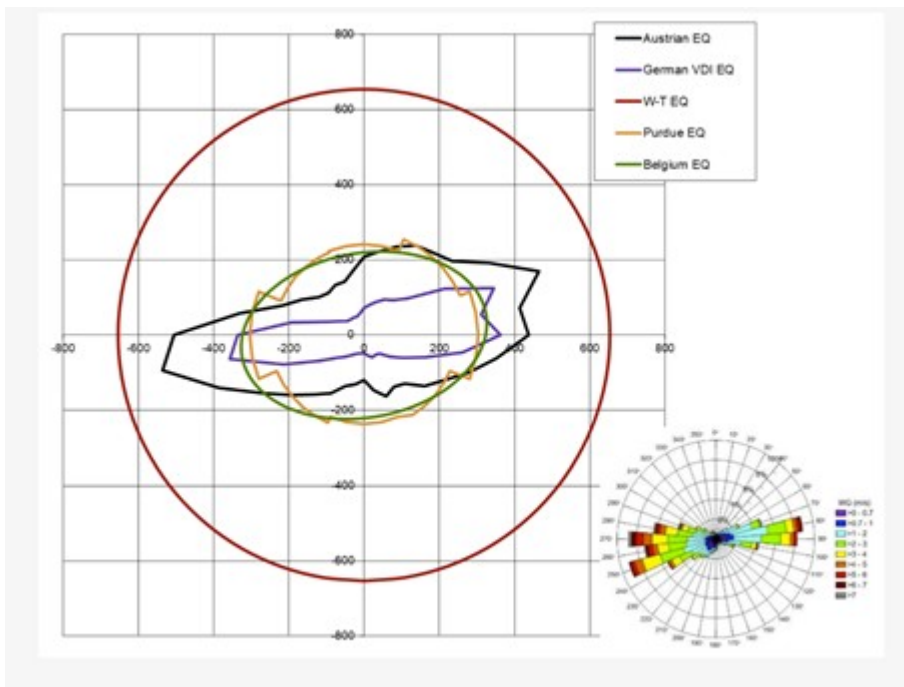
4549 5.4.2.2. Empirical Equations for assessing separation distances

4550 There are other screening tools such as empirical equations (EQs) that are frequently used
 4551 in Europe (e.g., Brancher, 2020a; Schaubberger, 2012a) primarily for livestock buildings to
 4552 determine separation distances between an odorous facility and nearby sensitive receptors.
 4553 In Europe and elsewhere, separation distances are generally determined by two steps:

- 4554 1. calculation of the odour exposure as a timeseries of odour concentrations using
 4555 dispersion models, and
- 4556 2. determining the separation distances through the evolution of the odour exposure by
 4557 the odour impact criteria.

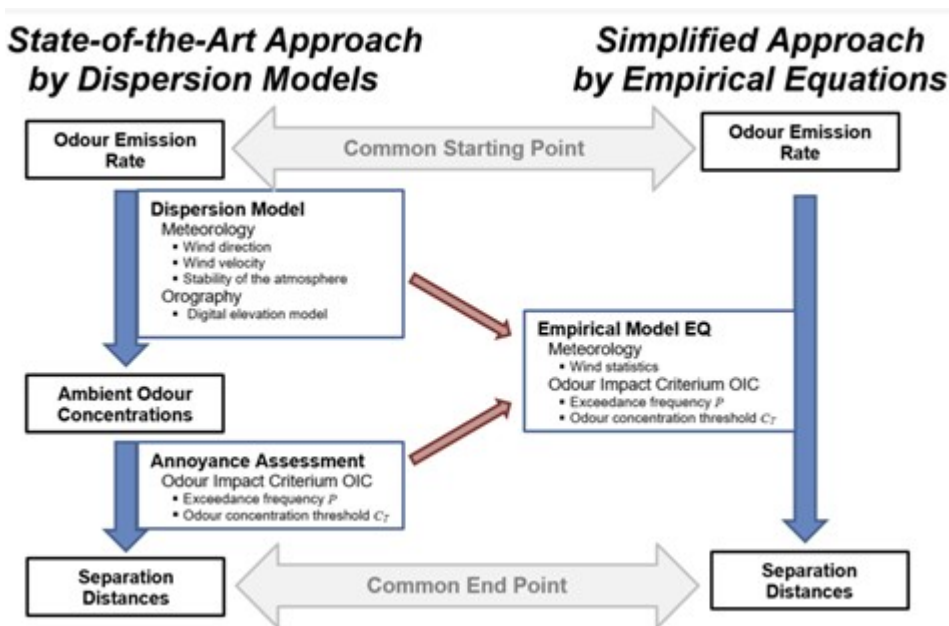
4558 (Brancher, 2020a) noted that simple EQs deliver a unique, fixed distance circle around the
 4559 source, while advanced EQs which include meteorological predictors such a wind
 4560 frequencies and mean wind velocities within direction sectors, result in separation distance
 4561 shapes that have been derived from regression analyses of dispersion model equations.
 4562 (Brancher, 2020a) showed the difference between the German VDI (Schaubberger, 2012a;
 4563 VDI 3984, 2012) and Austrian (Schaubberger, 2012b) shapes where the meteorology of the
 4564 site is defined by wind statistics as determined by the frequency of wind direction for each
 4565 10-degree sector, compared to simpler EQs. Another comparative analysis between the
 4566 German and the Austrian empirical equations has been described by (Wu, 2019). Figure 5-6
 4567 shows the shapes of separation from five EQs for a livestock building of 22,500 ouE/s. The
 4568 prevailing wind direction at the site was from the WSW and ENE. The comparison shows the
 4569 impact of meteorology on the separation distances calculated by the EQs. The German and
 4570 the Austrian EQs, include the wind statistics from the site, the Belgian EQ (Nicolas, 2008)
 4571 uses a rough parameterisation for the prevailing wind direction, the Purdue EQ (Lim, 2000)
 4572 uses the wind frequency of 45-degree sectors, and the W-T EQ (Williams, 1986) does not
 4573 consider the wind frequency as a predictor. Australia (State of Victoria) (EPA Victoria, 2013)
 4574 and New Zealand (Auckland City Council, 2012), set a minimum distance criterion for certain
 4575 industry types. This has the same effect as the W-T EQ which sets a circle around the site.
 4576 Figure 5-6 shows that the W-T EQ is unsuitable to describe the meteorological situation of

4577 the dilution and overestimates the separation distance for several wind directions.
 4578



4579 **Figure 5-6** Separation distances computed from empirical equations which are used as
 4580 screening tools. The Austrian and German VDI EQs use 10-degree meteorological statistics
 4581 whilst the Belgian and Purdue EQs use more coarse meteorological data. The W-T Scheme
 4582 uses no meteorology. (Brancher, 2020a).
 4583
 4584

4585 Figure 5-7 shows a schematic diagram that compares a full dispersion model simulation to
 4586 calculate separation distances versus that of the screening tool empirical equations. The
 4587 dispersion model can simulate many more physical processes than EQs and must be run
 4588 with more complex input data. In the simplified scheme, both procedures begin with the
 4589 odour emission rate and end with the direction-dependent separation distance. The red
 4590 arrows show the simplification of the input parameters in the EQs.
 4591



4592

4593 **Figure 5-7** Schematic diagram comparing screening empirical equations alongside
4594 dispersion modelling (Brancher, 2020a).

4595

4596 A major advantage of empirical equations lies in their simplified handling of the influence of
4597 meteorological input on separation distances. Separation distances from EQs are
4598 determined by the equation coefficient values which are derived from a statistical analysis of
4599 the time series of modelled ambient odour concentrations by the odour impact criteria. The
4600 EQ procedure includes implicit input of the exceedance probability to the empirical
4601 equations. This means that the two-step procedure of the state-of-the-art modelling
4602 methodology is reduced to a single step for EQs.

4603

4604 Table 5-2 shows some commonly used EQs employed internationally from livestock
4605 buildings and used primarily to determine separation distance. Note, Table 5-2 is not
4606 inclusive of all the empirical equations currently in use in odour assessments around the
4607 world. There are many that have not been included. Australia for example has several
4608 empirical equations for computing the separation distance required from livestock facilities.
4609 Western Australia has one such equation (Griffiths, 2013), while a second screening tool
4610 equation (Dairy Australia, 2008) is for estimating the separation distance for the pig and beef
4611 industries which takes into account the number of animals, site management practice,
4612 receptor type, local terrain and vegetation. Many screening methods like these are loosely
4613 employed and many do not have any local or regulatory status.

4614

4615

4616 **Table 5-2** Odour-specific empirical equations used for computing separation distances

	German VDI	Austria	Belgium	USA (Minnesota)	Purdue Setback Model	Australia (Victoria), New Zealand	Canada (Ontario)	Australia
Reference	Schauberger, 2012a; VDI 3984, 2012	Schauberger, 2012b	Nicolas., 2008	Jacobson, 2005	Lim, 2000	EPA Victoria, 2013; Auckland City Council, 2012	Guo, 1998	Meat and Livestock Australia Ltd 2012
Meteorology	Wind direction frequency, exceedance probability	Mean wind velocity for each 10 degrees of wind direction, exceedance probability	Rough parameterisation for the prevailing wind direction Surface roughness protection level (zoning)	Not taken into consideration	Wind frequency for 45 degrees of wind direction, zoning, topography,	Not taken into consideration	Not taken into consideration	Not taken into consideration
Building downwash	no	no	no	no	Orientation and shape of building	na	na	no

	German VDI	Austria	Belgium	USA (Minnesota)	Purdue Setback Model	Australia (Victoria), New Zealand	Canada (Ontario)	Australia
Terrain and Land use	Flat terrain	Flat terrain	Surface roughness	no	Land Use factor for agricultural and pure residential areas Topography factor for good ventilated area (flat terrain) and narrow valleys	na	na	Simple topography and land use factor
Emission	Odour emission rate ($\text{ou}_E \text{ s}^{-1}$) (500 - 50,000)	Odour emission rate ($\text{ou}_E \text{ s}^{-1}$)	Number of animals, species, ventilation system, manure, feeding	All potential sources assigned an odour emission rate. OFFSET model can account for size, nature and range of odour	Odour emission rate ($\text{ou}_E \text{ s}^{-1}$)	na	Species, number of animals, zoning, manure	Stocking intensity and management of beef feedlots

	German VDI	Austria	Belgium	USA (Minnesota)	Purdue Setback Model	Australia (Victoria), New Zealand	Canada (Ontario)	Australia
Evolution of empirical equation	Derived from dispersion modelling of 23 sites using (AUSTAL2000) Single point source from 5m	Derived from regression equations from dispersion models with minimum distance of 100m. Single point source from 6 sites		Derived from dispersion modelling over 4 years and 85 farms		Derived from review of empirical evidence of the performance of the recommended separation distances		Derived from model predicted odour concentrations calibrated by receptor impacts
Outcome	Worst case outcome Shape determined by meteorology	Best fit approach Shape determined by meteorology		Worst-case		Worst case	Worst case	Worst case
Separation Distance Shape	Shape corresponds to wind frequency of 10 deg sectors	Shape corresponds to wind frequency of 10 deg sectors	Ellipse orientated in prevailing wind direction	circle	Shape corresponds to frequency of the wind direction for 45 deg sectors	circle	circle	circle

4617
4618
4619

4620 5.4.2.3. Summary

4621 Screening tools are only useful if they greatly simplify the process of full dispersion
4622 modelling, provide reasonable yet conservative results and are fast and low cost to use. It is
4623 also important that they meet the requirements that the odour emission rate is quantitated in
4624 the same way as it is done for dispersion models and that separation distances are
4625 determined for odour impact criteria the same as for dispersion models. These constraints
4626 ensure a meaningful comparison of empirical equation separation distances against
4627 modelled separation distances. If the screening tools and models meet these criteria then
4628 there is no reason that they should not be usefully incorporated as screening level analysis
4629 tools in tiered regulatory odour assessment frameworks. A tiered framework recognises
4630 that tools such as simple power function-based equations may be sufficient to demonstrate
4631 that a proposal presents a low risk of impacting on amenities at nearby sensitive receptors
4632 and that if the criteria of the tier is met, then no more advanced work is necessary. But
4633 conversely if the screening level assessment does not pass then a more refined tool using
4634 dispersion modelling may be necessary. For some geographical areas local environmental
4635 agencies recommended locally adapted dispersion screening methods in combination with
4636 meteorological data for calculating such things as separation distances, this further simplifies
4637 the application of such tools as no specific meteorological information is compulsory to run
4638 them. These screening tools can work very well at the local level of regulatory control.

4639 5.4.3. Steady State Gaussian Plume Models

4640 There are multiple steady-state Gaussian models that are currently being used to model
4641 odours around the world. The most well-known and advanced model is the US EPA,
4642 regulatory model, AERMOD and the less used UK regulatory model, ADMS. Other
4643 Gaussian plume models used in odour assessments include: AODM, the Austrian odour
4644 regulatory model, and ARIA Impact, a widely used model in France, Italy and Brazil. Older
4645 Gaussian plume models, ISCST3, CTDMPLUS, AUSPLUME have been superseded by
4646 AERMOD, and are therefore not discussed further. Commonly used Gaussian plume
4647 models are discussed below.

4648 5.4.3.1. ARIA Impact

4649 ARIA Impact is a simple and user-friendly modelling suite including CALPACT, a Gaussian
4650 plume/puff model, and AERMOD. It is developed and maintained by the French ARIA
4651 Technologies company and used in different countries. It can simulate the long-term
4652 dispersion of atmospheric pollutants (gaseous or particulate) from all types of emitting
4653 sources (point, surface, linear) in a simplified moderate topographic environment and
4654 calculate concentrations, and depositions (dry and wet) expressed as annual average or
4655 percentiles. The built-in Gaussian model switches from the plume dispersion algorithm to the
4656 puff algorithm in case of calm wind conditions, thus overcoming the inherent 1 m/s limitation
4657 of the plume approach. The software was developed to be used as a regulatory model to
4658 meet air quality criteria and can be used to evaluate the odour impact of a facility.

4660 The software comes with a graphical user interface (GUI), allowing an easy import of both
4661 meteorological and topographic data and the definition of atmospheric emissions sources
4662 (constant, with cyclical temporal variation, or fully variable) with no limitation of the number of
4663 species or sources. A meteorological preprocessor helps calculating some needed derived

4664 variables such as stability categories, mixing height and surface layer parameters (u^* , L , w^*).
4665 The model is able to perform simple NO_x to NO and NO₂ conversions. It can take into
4666 account background pollution and includes a dust extraction module. The model can
4667 manage an extended range of deposition and concentration model output results such as
4668 percentiles, frequency of exceedance thresholds, values at specific points and output in
4669 multiple formats for further plotting. ARIA Impact can simultaneously treat multiple gas and
4670 particulate chemical species, radioactive pollutants as well as manage an odorous mix of
4671 chemicals expressed as an odour unit. Typical spatial scales of model application range
4672 from 5 x 5 km² to 30 x 30 km². Inputs also include hourly meteorological data from a single
4673 weather station and terrain data with knowledge of the dominant land use types.
4674

4675 Since the model is suitable in the near field, it may be a useful tool to assess the odour
4676 impact from the accidental releases of some species such as H₂S and HCl. Although ARIA
4677 Impact can be strictly considered only partially as a regulatory tool, thanks to its simplicity of
4678 use and the presence of an efficient GUI it has found over time and still finds several
4679 applications in impact studies in France, Italy and Brazil, for both air quality and odour
4680 applications.

4681 5.4.3.2. ADMS

4682 The ADMS model (Atmospheric Dispersion Modelling System) is an advanced steady-state
4683 Gaussian plume model for calculating ground level concentrations emitted from both
4684 continuous point, line, volume and area sources, or intermittent point sources. ADMS was
4685 developed by Cambridge Environmental Research Consultants (CERC, 2021b) of the UK in
4686 collaboration with the UK Meteorological Office, National Power plc (now INNOGY Holdings
4687 plc) and the University of Surrey. The first version of ADMS was released in 1993. Version 3
4688 of the model was released in 1999, Version 5 was released in 2013, with a number of
4689 additional features and Version 6 was released in 2023. ADMS Version 6 contains a number
4690 of enhancements compared to ADMS Version 5, particularly in respect of modelling the
4691 effects of buildings, and modelling of time varying emissions factors.
4692

4693 ADMS includes algorithms which take into account: downwash effects of nearby buildings
4694 within the path of the dispersing pollution plume; effects of complex terrain; effects of
4695 coastline locations; wet deposition, gravitational settling and dry deposition; short term
4696 fluctuations in pollutant concentration; chemical reactions; radioactive decay and gamma-
4697 dose; pollution plume rise as a function of distance; jets and directional releases; averaging
4698 time ranging from very short to annual; and condensed plume visibility. The system also
4699 includes a meteorological data input pre-processor.
4700

4701 The model is capable of simulating passive or buoyant continuous plumes as well as short
4702 duration puff releases. It characterises atmospheric turbulence by two parameters, the depth
4703 of the boundary layer and the Monin-Obukhov length rather than the single parameter
4704 Pasquill Gifford classes.

4705 The performance of the model has been evaluated against various measured dispersion
4706 data sets.
4707

4708 Users of ADMS include:

- 4709 • Governmental regulatory authorities including the UK Health and Safety Executive
4710 (HSE)

- 4711 ● Environmental Agency of England and Wales
- 4712 ● Over 130 individual company licence holders in the UK
- 4713 ● Scottish Environmental Protection Agency (SEPA) in Scotland
- 4714 ● Northern Ireland Environment Agency
- 4715 ● Governmental organisations including the Food Standards Agency (UK)
- 4716 ● Users in other European countries, Asia, Australia and the Middle East

4717
4718 ADMS Version 3 is accepted by the US Environmental Protection Agency as an "Alternative"
4719 model (US-EPA, 2021b).

4720
4721 ADMS is used widely in odour assessments in the UK and uses the odour unit (ouE) as
4722 defined in the CEN standard (EN 13725:2003). One ouE is the mass of a pollutant that,
4723 when evaporated into 1 m³ of odourless gas at standard conditions, is at the detection limit.
4724 The model allows the following odour release rates; ouE/s for point sources, ouE/m/s for line
4725 sources, ouE/m²/s for area sources and ouE/m³/s for volume sources. Output odour
4726 concentrations are in odour units (ou) defined as a ratio, and ou_E, as a mass measure.

4727
4728 Within the same modelling framework ADMS 5 includes a 'fluctuations' option. This option
4729 allows the user to take account of the variations in concentration caused by the 'short' time
4730 scale turbulence in the lower atmosphere and changes in meteorology. The technical
4731 formulation of the fluctuation module is described in depth in (Thomson, 1992; Thomson,
4732 2017). The fluctuations module uses a probability distribution function (PDF) of
4733 concentrations and considers variations due to turbulence and changes in meteorology.

4734
4735 ADMS 5, like all steady-state Gaussian models, does not model calm wind events, which are
4736 often worst-case dispersion events for odours. By default, the model does not model hours
4737 when the wind speed is less than 0.75 m/s. However, the model has an optional capability
4738 for treating very low wind speeds via an 'additional input file' that allows lower wind speeds
4739 to be modelled. Since a key feature of low winds is that the wind direction is highly variable,
4740 ADMS 5 splits the dispersion into two types of plumes, the usual Gaussian plume aligned in
4741 the direction of the wind, and a radially-symmetric plume, with concentrations calculated as a
4742 weighted average of the two. The radially symmetric plume is modelled as a passive
4743 source with a source height equal to the maximum plume height from the standard plume
4744 rise calculations, and assumes an equal probability of all wind directions.

4745
4746 This scheme is similar to that used in AERMOD, which splits the plume into a coherent and
4747 radial plume for all wind speeds and is controlled through various LOWWIND options.

4748
4749 While ADMS is the default regulatory model in the UK, the Environmental Agency (UKEA)
4750 appears to be less strict regarding odour modelling (Pullen, 2007). The UKEA makes it clear
4751 that various models may be used in applications for authorisation and that the applicant must
4752 demonstrate that the model is fit for purpose. Although the UK Institute of Air Quality
4753 Management (Bull, 2014) says that odour assessments in the UK are almost exclusively
4754 undertaken using AERMOD and ADMS.

4755 5.4.3.3. AERMOD

4756 AERMOD was established in 1991 through AERMIC, the American Meteorological
4757 Society/Environmental Protection Agency Regulatory Model Improvement Committee

4758 (AERMIC), to introduce state-of-the-art modelling concepts into the EPA's own developed air
4759 quality models. AERMOD was developed to incorporate air dispersion based on planetary
4760 boundary layer turbulence structure and scaling concepts, including treatment of surface and
4761 elevated sources and simple and complex terrain. On November 9 of 2005, AERMOD was
4762 adopted by the EPA and promulgated as their preferred regulatory model, effective as of
4763 December 9 of 2005 (Federal Register, 2005). The developmental and adoption process
4764 took 14 years (from 1991 to 2005).

4765
4766 AERMOD is a steady-state plume model incorporating air dispersion based on planetary
4767 boundary layer turbulence structure and scaling concepts. AERMOD supports two input data
4768 processors; AERMET, a meteorological data pre-processor incorporating air dispersion
4769 based on planetary boundary layer turbulence structure and scaling concepts, and
4770 AERMAP, a terrain data preprocessor incorporating complex terrain.

4771
4772 The AERMOD model is an integrated system that includes three modules:

- 4773 ● A steady-state dispersion model designed for short-range (up to 50 kilometres)
4774 dispersion of air pollutant emissions from stationary industrial sources.
- 4775 ● A meteorological data pre-processor (AERMET) that accepts surface meteorological
4776 data, upper air soundings, and optionally, data from on-site instrument towers. It then
4777 calculates atmospheric parameters needed by the dispersion model, such as
4778 atmospheric turbulence characteristics, mixing heights, friction velocity, Monin-
4779 Obukhov length and surface heat flux.
- 4780 ● A terrain pre-processor (AERMAP) whose main purpose is to provide a physical
4781 relationship between terrain features and the behaviour of air pollution plumes. It
4782 generates location and height data for each receptor location. It also provides
4783 information that allows the dispersion model to simulate the effects of air flowing over
4784 hills or splitting to flow around hills

4785
4786 AERMOD is an advanced steady-state Gaussian plume model for calculating ground-level
4787 concentrations of pollutants emitted from both intermittent and continuous point, line, volume
4788 and area sources.

4789
4790 AERMOD includes new and improved algorithms (over ISC3, which it replaced) which take
4791 into account: the downwash effects of nearby buildings within the path of the dispersing
4792 pollution plume; effects of moderate terrain; dispersion in both the convective and stable
4793 boundary layers; plume rise and buoyancy; plume penetration into elevated inversions;
4794 computation of vertical profiles of wind, turbulence, and temperature; the urban night-time
4795 boundary layer, treatment of plume meander.

4796
4797 The model is capable of simulating passive or buoyant continuous plumes, and it
4798 characterises atmospheric turbulence by two parameters, the depth of the boundary layer
4799 and the Monin-Obukhov length rather than the single parameter Pasquill Gifford classes of
4800 the ISCST3 model.

4801
4802 AERMOD is the most widely used model in the world today, and is the US EPA
4803 recommended dispersion model for predicting air quality in the near field (up to 50 km).
4804 However, it is important to point out that in the United States, odour assessments are not
4805 limited by the requirements of 40 CFR 51, Appendix W rules and regulations. These

4806 guidelines only apply to criteria air pollutants (air pollutants with established air quality
 4807 standards). Odours do not have federally enforceable air quality standards and are not
 4808 regulated through the preparation of State Implementation Plans, New Source Review or
 4809 Prevention of Significant Deterioration permit requirements (Barclay, 2019). However,
 4810 despite the fact that odour assessments are not limited to the current US EPA model
 4811 guidelines AERMOD's status as a guideline model means that most odour assessments are
 4812 undertaken using AERMOD, regardless of whether it is suitable or not. Outside the US,
 4813 many countries (Australia, Canada, New Zealand, Southern Africa) regulate odours where
 4814 dispersion modelling is often a requirement. Many of these countries look to the US for
 4815 regulatory models and guidance.

4816

4817 For modelling odours, AERMOD includes no option to input and output odour emission
 4818 rates. The default emission rate units for AERMOD are g/s for point and volume sources
 4819 and g/s/m² for area sources. By default, the model converts these input units to output units
 4820 of micrograms per cubic metre ($\mu\text{g}/\text{m}^3$) for concentration.

4821

4822 Similarly to ADMS, AERMOD is unable to model calms (0.0 m/s) and will simply skip over
 4823 these hours. The minimum allowable wind speed to define the boundary layer parameters is
 4824 defined as $2^{1/2} * \sigma_{vmin}$ where $\sigma_{vmin} = 0.2$ m/s or wind speed_{min} = 0.28 m/s. This minimum is
 4825 independent of the threshold wind speed which is 0.51 m/s. The restriction is based on the
 4826 accuracy of the instruments. Sonic anemometers have no threshold limitations and therefore
 4827 no wind speed threshold is imposed and the output AERMINUTE file can have winds lower
 4828 than 0.28 m/s. By US EPA (and Australia) regulatory requirements, any data set that does
 4829 not meet the 90% data coverage must use AERMINUTE which is a meteorological
 4830 processor (or other method) to re-process the 1-10 minute automatic weather station
 4831 readings to produce a new 1-hour average wind speed and wind direction which is different
 4832 than the regular standard archived hourly data. The result of AERMINUTE is to generate a
 4833 new meteorological data set that has fewer calm periods and more winds in the range 0.1
 4834 m/s to 1 m/s. The effect of AERMINUTE is shown in Table 5-3 which shows the number of
 4835 calms for Danelly Fields met station in Alabama (US) with and without the use of
 4836 AERMINUTE. The percentage of calms reduces from 27% of the data set to just 2% with its
 4837 use, and the number of wind speeds increased from 0% in the range 0.28 – 1 m/s to 9.73%.
 4838 Just how much AERMINUTE changes the 1-hour wind speed and wind direction pattern is
 4839 shown in the annual wind rose (Figure 5-8) with and without the inclusion of AERMINUTE.
 4840 However, it is observed that the ASOS 1-minute and ASOS 5-minute data needed to feed
 4841 AERMINUTE may not be available in many countries outside of the US.

4842

4843

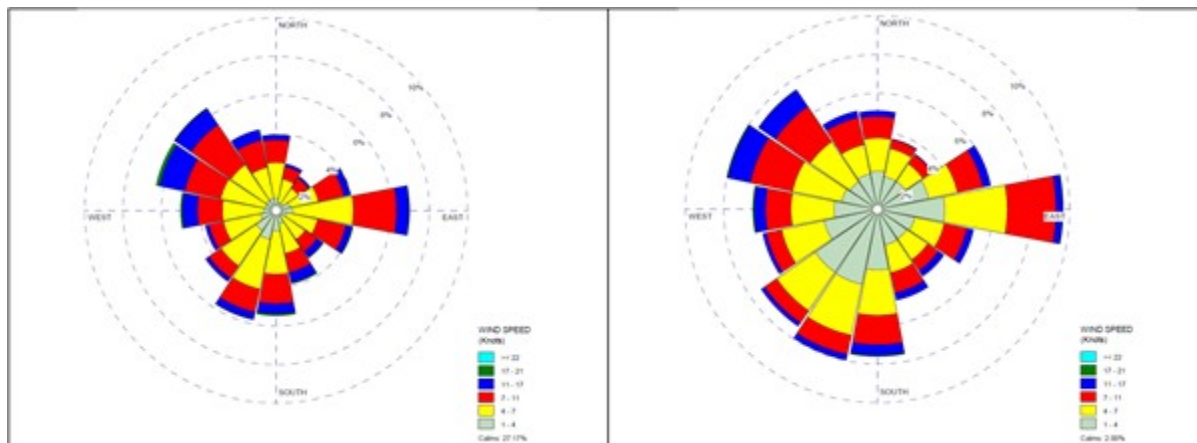
4844 **Table 5-3** Wind speed statistics for Danelly Field, AL for 2011 with and without AERMINUTE

Year	AERMET %	AERMET average wind speed (m/s)	AERMINUTE /AERMET (%)	AERMINUTE /AERMET average wind speed (m/s)
Danelly Field	Calms [†] = 27.2	5.02	Calms [†] = 2.0	5.43

2011	0.28 – 1 m/s = 0 1 – 2 m/s = 12	0.28 – 1 m/s = 9.7 1 – 2 m/s = 27.9
------	------------------------------------	--

4845 *Percentage calm based on threshold wind speed = 0.5 m/s

4846



4847

4848

4849

4850

4851

4852

4853

4854

4855

4856

4857

4858

Figure 5-8 Annual wind roses showing the effects of AERMET using hourly data and AERMET including a re-analysis of the 1-minute ASOS data using AERMINUTE (Barclay and Borissova, 2019)

4859

4860

4861

4862

However, while AERMINUTE solved one problem (i.e., reduced the number of calms in a data set and thereby increased the number of hours modelled to > 90%), increasing the number of very light winds created other problems such as AERMOD tendency to over predict in light winds (Connors, 2013), and its treatment of lateral plume meander, which is responsible for most of the horizontal plume dispersion in stable atmospheric conditions.

4863

4864

4865

4866

4867

4868

4869

4870

4871

4872

4873

4874

4875

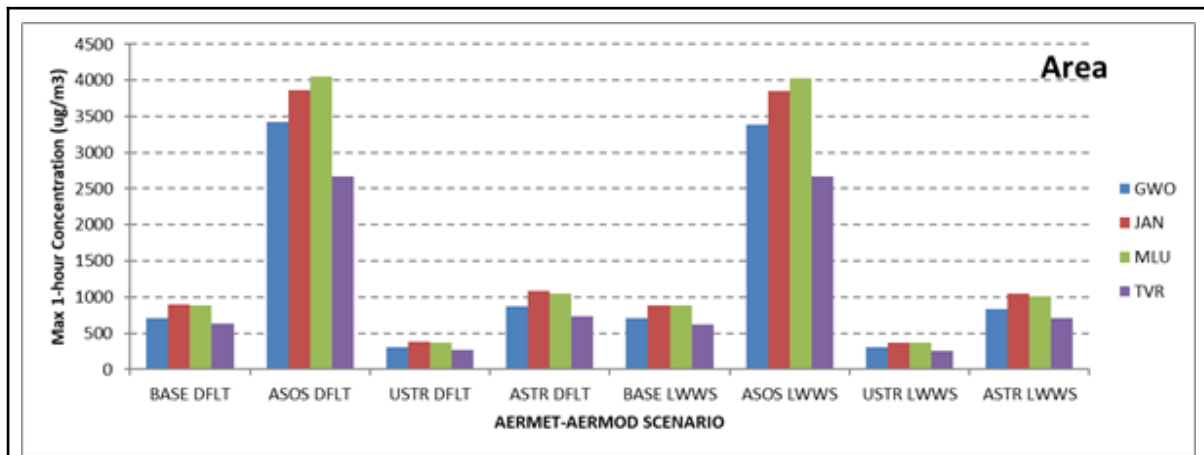
4876

4877

4878

The US-EPA is continuously working on AERMOD and AERMET to improve their algorithms, for example those related to a better calculation of the friction velocity, or the treatments of calms.

The effect of these changes to AERMET and AERMOD from 2012 until the latest version of the model (ASTR LWWS) is significant for an area source as shown in Figure 5-9 for four nearby meteorological stations (GWO, JAN, MLU, TVR). AERMOD is especially sensitive to the re-analysis of 1 and 5 minute ASOS winds (ASOS DFLT, ASOS LWWS), where there is an order of magnitude difference from the pre 2012 (BASE DFLT) model. The most likely options for AERMOD outside of the US where 1-10 minute ASOS data may not be available is likely to be USTR LWWS, which takes into account the default Adj_u^* option, default LOWWIND values and uses regular saved hourly data, which in the US, is representative of the last two minutes of wind speed and wind direction of each hour, and in Australia and New Zealand, the last ten minutes of the hour is the hour. As can be seen from Figure 5-9, USTR LWWS significantly underpredicts all the other combinations, including the pre 2012 BASE model. This will always be the case as long as there are 10% or more of the data set that contains calm winds. For odour assessments this is a significant concern. Odours will tend to accumulate and stagnate under calm conditions, but AERMOD will not model these conditions and therefore will most likely underpredict these worst-case episodes.



AERMET

BASE – hourly data, pre 2012 (before adj_u* and LOWWIND changes)

ASOS – re-analysis of < 1 hour data (AERMINUTE), no adj_u* (2012)

USTR – hourly data (no AERMINUTE), adj_u*

ASTR - re-analysis of < 1 hour data (AERMINUTE), adj_u*

AERMOD

DFLT – Default, no LOWWIND

LWWS – LOWWIND (since 2015)

4880 **Figure 5-9** Ground level concentrations reflecting major US EPA changes for 4
 4881 meteorological stations for a single area source (Barclay and Borissova 2019)

4882

4883 It is important to note that AERMOD was not developed for odour modelling or accidental
 4884 releases of pollutants, and therefore does not make allowance for modelling concentration
 4885 fluctuations within the hour. Scaling of concentrations by a constant Peak-to-Mean Ratio or
 4886 hedonic tone must be applied directly to the emission rate or the output concentration. The
 4887 model will allow cyclical scaling of emission rates which are suitable for those peaks to mean
 4888 ratios that might vary with stability and source type. AERMOD like most other advanced
 4889 models will allow the computation of percentiles, a necessary criterion of most odour
 4890 assessment criteria around the world, as well as provide plot files of ranked odour
 4891 concentrations and number of hours exceeding such an odour criterion.

4892

4893 AERMOD has been used in odour studies all over the world, both in experimental capacity
 4894 and regulatory assessments. The model's use and application in odour assessments is
 4895 likely to grow.

4896 5.4.3.6. Summary

4897 Table 5-4 is a summary of the most well-known, regulatory Gaussian plume models used in
 4898 odour applications today.

4899

4900

4901 **Table 5-4** Summary of key features of well known, regulatory steady-state Gaussian plume models used in odour assessments around the
 4902 world today

	ADMS-5	AERMOD	ARIA Impact
Regulatory status for modelling odours	United Kingdom, Northern Ireland, Scotland	United States, Australia, New Zealand, Canada, Countries in Africa and Middle East	The suite includes two models: CALPACT, which is a non-regulatory model and AERMOD, whose regulatory status is described in the previous column. Normally accepted in Italy, France, Brazil and everywhere as a derivation of the models suggested by US-EPA
Meteorology			
Pre-processor	In-built processors, allows flexible input met. data. Model also allows a user input file of light winds < 0.75 m/s	External processors. AERMET and AERMINUTE. AERMINUTE to be used if >10% of data is calm. It is used to recompute the 1-hour average winds from 1–5-minute ASOS met data. AERMET then computes surface parameters (h, w*, u*, L) from measured observations of cloud cover, wind speed and direction, temperature.	Internal meteorological processor computing surface parameters (h, w*, u*, L) and stability classes from measured observations of cloud cover and/or global and/or net radiation, wind speed and direction, temperature.
Dispersion			
Boundary layer structure	h, L _{MO} scaling	h, L _{MO} scaling	h, L _{MO} , stability categories
Plume Rise	Advanced integral model using Runge-Kutta method	Briggs empirical equations	Briggs, Briggs small stacks, Anfossi equations and empirical equations.
Concentration distribution	Advanced Gaussian (PDF)	Advanced Gaussian (PDF)	Classical and Advanced Gaussian (PDF)
Complex Effects			
Buildings	ADMS building module	PRIME building module	

	ADMS-5	AERMOD	ARIA Impact
Complex Terrain	Based on calculation of flow field and turbulence field by FLOWSTAR model	Interpolation between plume displaced by terrain height (neutral) and plume impaction (no vertical displacement, stable)	Use of a simplified terrain module
Calm winds	By default, does not model winds <0.75 m/s. 'Calms option' will allow additional input file for winds < 0.75 m/s, this invokes plume split into Gaussian plume aligned along wind and radially-symmetric plume to account for plume meander	Default low wind speed is 0.2828 m/s consistent with sigma v of 0.2. Users now have an option to set minimum wind speed, minimum sigma v and plume meander using alpha LOWWIND option. Model will skip over 'zero winds'. AERMINUTE recomputes the 1-hour average from ASOS stations	CALPACT with a Gaussian puff internally driven scheme during hours of "low wind speed" (wind speed < 1 m/s)
Plume Meander		AERMOD plume meander is invoked for all wind speeds, not just when wind tending to 0.0 No plume meander for area sources	
Odour Input and Output units	yes	Input emission rate is g/s, output concentration is ug/m ³ . For odours use emission factor of 1 that assumes input is ou/s and output odour concentration is ou/m ³	Input emission rate in ou/s and output concentrations in ou/m ³
Concentration fluctuations (built in Peak-to-Mean Ratio)	yes	No, must apply PtMR by scaling concentrations or emission rates	No, must apply PtMR by scaling concentrations or emission rates
Compute averaging times < 1-hour	No	No	Yes, with limitations
User-defined outputs	1-hour to annual averaging Percentiles Exceedances	1-hour to annual averaging Percentiles Exceedances	1-hour to annual averaging Percentiles Exceedances

4903
4904

4905 5.4.4. Lagrangian Puff Models

4906 5.4.4.1. CALPUFF

4907 The CALPUFF model was developed by (Scire, 2000) using an integrated puff approach
4908 based on the MESOPUFF II model (Scire, 1984a; Scire, 1984b) with modifications for near-
4909 field applications.

4910
4911 The CALPUFF modelling system includes three main components: CALMET, CALPUFF and
4912 CALPOST and a large set of pre-processing programs designed to interface the model to
4913 standard, routinely-available meteorological and geophysical datasets. In simple terms,
4914 CALMET is a meteorological model that develops wind and temperature fields on a three-
4915 dimensional gridded modelling domain. Associated two-dimensional fields such as mixing
4916 height, surface characteristics, and dispersion properties are also included in the file
4917 produced by CALMET. CALPUFF is a Lagrangian puff dispersion model that advects ‘puffs’
4918 of material emitted from modelled sources, simulating dispersion and transformation
4919 processes along the way. In doing so it typically uses the fields generated by CALMET, or as
4920 an option, it may use simpler non-gridded meteorological data from existing plume models
4921 such as ISCST3, CTDMPPLUS, AUSPLUME and AERMOD. Temporal and spatial variations
4922 in the meteorological fields selected are explicitly incorporated in the resulting distribution of
4923 puffs throughout a simulation period. The primary output files from CALPUFF contain either
4924 concentrations or deposition fluxes evaluated at selected receptor locations. CALPOST is
4925 used to process these files, producing tabulations summarising the simulation results, and
4926 identifying the highest and second-highest 3-hour average concentrations at each receptor,
4927 for example. Any percentile or exceedance level can be obtained through its external post-
4928 processing tools.

4929
4930 CALPUFF was designated a US EPA Appendix A Guideline model in 2003 (Federal
4931 Register, 2003). Prior to the model promulgation to an Appendix A guideline model,
4932 CALPUFF, like the ISCST3 (US-EPA, 1995) model before it underwent rigorous testing,
4933 model evaluations and multiple peer reviews over more than a decade. This lengthy,
4934 dedicated, state-of-science and transparent process occurred under the scrutiny of the then
4935 Air Quality Management Group (AQMG) within the US EPA. In January 2017, CALPUFF
4936 was removed from the US EPA Appendix A as the preferred long-range transport model with
4937 no replacement (Federal Register, 2017), (Barclay, 2018). In the US, AERMOD is now the
4938 only dispersion model with guideline status and is the recommended US EPA dispersion
4939 model for use for all near-field applications out to 50 km (Federal Register, 2017). The US
4940 EPA-approved version of CALPUFF, Version 5.85 of the model (equivalent to the 2008
4941 version with bug fixes, can still be found on the ‘Alternative Models’ web page. The model is
4942 now Version 7. The new wording in (Federal Register, 2017) points out that removing
4943 CALPUFF as a preferred model does not affect its use under the Federal Land Managers
4944 guidance regarding Air Quality assessments in National Parks, nor any previous use of the
4945 model as part of regulatory applications requiring Civil Aviation Authority. (Federal Register,
4946 2017) also states that the use of CALPUFF in the near field as an alternative model for
4947 situations involving complex terrain and complex winds has not changed by removing
4948 CALPUFF as a preferred model. The US EPA further points out that it recognises that
4949 “AERMOD is limited” and that CALPUFF or another Lagrangian model may be more suitable

4950 in complex environments. Therefore, they have continued to provide the flexibility to use it.
 4951 This last point is important as the EPA recognises that AERMOD is limited in complex, non-
 4952 steady-state environments. This is especially important for odour assessments which are
 4953 often located in complex meteorological environments, i.e., close to water bodies, such as
 4954 WWTPs and in complex terrain environments such as Pulp and Paper Mills.

4955
 4956 Unlike Gaussian plume models, Lagrangian models can model calm events. Calm periods
 4957 in CALPUFF are determined when the puff transport speed is less than the user-supplied
 4958 threshold wind speed of 0.5m/s. While CALPUFF has no special calm module, several
 4959 adjustments are made to the normal algorithms. These adjustments alter how slugs are
 4960 released, how gradual rise is addressed, how near-source effects are simulated, and how
 4961 the puff size changes during each sampling step. These adjustments are consistent with the
 4962 conceptual model in which fresh releases rise virtually straight up from a source and
 4963 disperse as a function of time due to wind fluctuations about a mean of zero, while existing
 4964 emission stagnate, and disperse as a function of time due to wind fluctuations about a mean
 4965 of zero. Adjustments made to puffs that are released into a calm period include:

- 4966 ● Slugs are released as puffs
- 4967 ● All mass for the period is placed into one puff
- 4968 ● Distance to final rise is set to zero
- 4969 ● No building downwash effects are included
- 4970 ● Growth of σ_y and σ_z is based on time (not distance travelled) during the sampling
 4971 step
- 4972 ● Minimum values of the turbulence velocities σ_v and σ_w are imposed

4973 It is acknowledged that during calm conditions, estimates of the turbulence velocities σ_v and
 4974 σ_w can be indeterminate, and CALPUFF relies on these velocities to grow puffs. Calm
 4975 periods can be associated with very stable and convective boundary layers, with their
 4976 distinctly different turbulent properties. Given these concerns, CALPUFF allows the use of
 4977 stability-dependent minimum turbulence velocities.

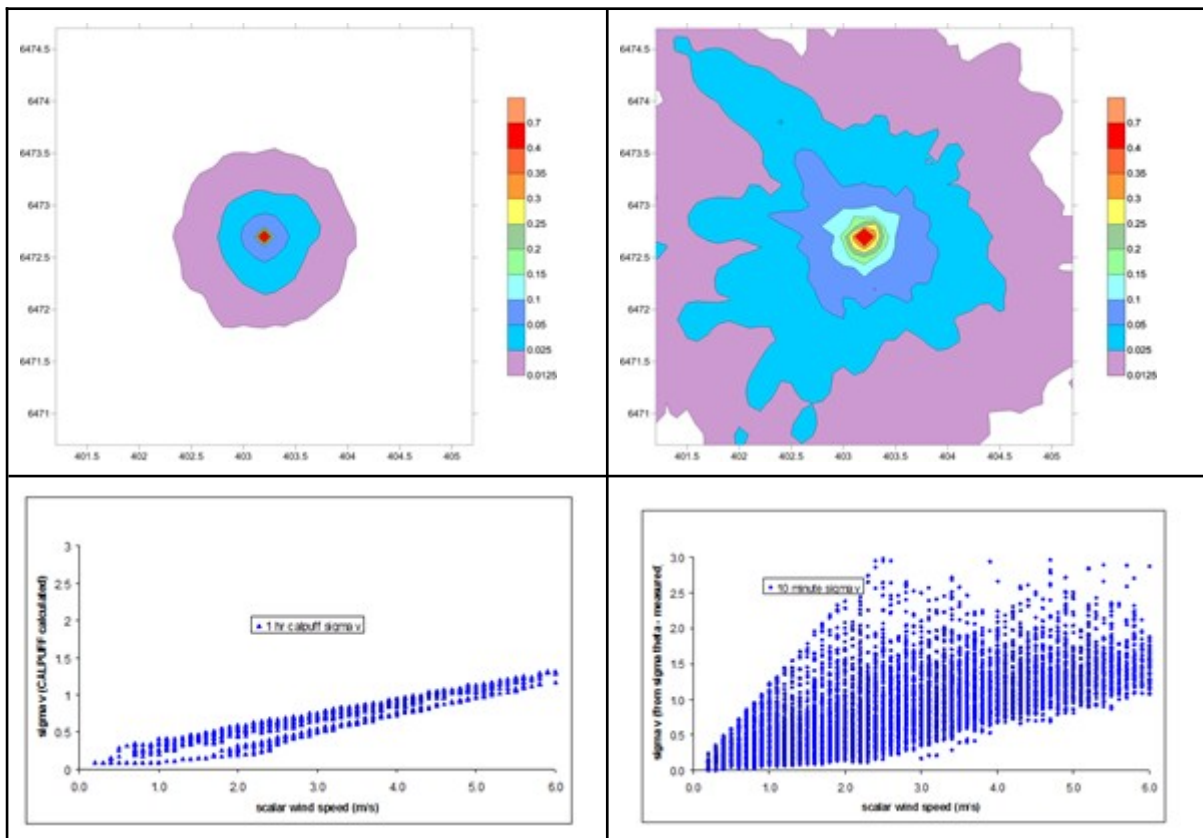
4978
 4979 A recent (2011) modification to CALPUFF, important for odour assessments over short time
 4980 scales, was the capability of Version 6 of the model to allow sub-hourly temporal resolution
 4981 of both source characteristics, input meteorological fields and output sub-hourly temporal
 4982 resolution of modelled output fields. This included the introduction of sub-hourly time-
 4983 varying structures that were designed and then implemented into CALMET Version 6. This
 4984 included the introduction of a sub-hourly time step within the model for purposes of
 4985 computing solar radiation, wind fields and boundary layer parameters and the modification of
 4986 the structure of the output data file produced by CALMET to allow for hourly or sub-hourly
 4987 time steps. This version of the model can accommodate input meteorological and overwater
 4988 data with an arbitrary time resolution. This includes sub-hourly measurements of turbulence
 4989 parameters (σ_v , σ_w) which are readily available from modern ultrasonic anemometers.

4990
 4991 Figure 5-10 shows the difference in predicted ground level concentrations from CALPUFF
 4992 using default hourly meteorology and computed dispersion coefficients under calm
 4993 conditions compared to using 10-minute meteorology and measured 10-minute turbulence
 4994 parameters. The first plot (lhs), when using model default options (minimum wind speed
 4995 threshold of 0.5 m/s, hourly meteorology, computed turbulence coefficients) shows a typical
 4996 'bull's-eye' of ground level concentrations where the concentrations at the source are very
 4997 high and plume dilution is a function of time. The second plot (rhs) shows the predicted

4998 ground concentrations for 10-minute meteorology and real measured 10-minute turbulence
 4999 parameters σ_v and σ_w . The computed 1-hour turbulent dispersion coefficient (σ_v) and
 5000 10-minute measured σ_v corresponding to each isopleth plot is also shown.

5001
 5002 The implications of directly using sonic anemometer data for local scale odour dispersion in
 5003 a model equipped to use the data are apparent. Using site-specific winds and turbulent data
 5004 on small temporal time scales may alleviate the need to apply any additional Peak-to-Mean
 5005 Ratio. CALPUFF was compared using 15-minute meteorology and real measured turbulence
 5006 parameters with the STAGMAP data set (Stagnation Model Analysis, Medford, Oregon
 5007 1991). In this study, SF_6 was released under true calm conditions. CALPUFF showed very
 5008 good agreement with this data set (Barclay, 2008).

5009



5010 **Figure 5-10** Predicted ground level concentrations under calm conditions using model
 5011 defaults (1-hour meteorology, calm wind speed threshold 0.5 m/s, minimum σ_v 0.5 m/s,
 5012 computed turbulence parameters) on lhs, compared to 10-minute meteorology and
 5013 measured 10-minute turbulence parameters (rhs). (Barclay and Scire 2011).

5014

5015 In 2014, CALPUFF Version 7.2.1 was updated to allow users to apply an averaging time
 5016 factor to the lateral turbulence. This approach is suitable when sub-hourly meteorological
 5017 data are available but no measured turbulence parameters. This allows users to apply an
 5018 equivalent sub-hourly σ_v value when using the default hourly turbulence dispersion
 5019 coefficients or PG curves.

5020

5021 CALPUFF will directly allow the user to input odour emission rates into the model in the form
 5022 of:

5023

- Point, volume and line sources - Odour Unit * m^3/s (vol. flux of odour compound),

5024 and

5025 • Area sources - Odour Unit * m/s (vol. flux/m² of odour compound)

5026 The model will output odour concentrations in odour units. The model will allow any
5027 percentile to be computed and will compute odour criteria exceedances.

5028

5029 Application of constant Peak-to-Mean Ratios can easily be applied to the model either
5030 through scaling the emission rate within the model control file, or in the post processing
5031 phase. In addition, scaling according to source type and stability category can also be done
5032 readily through the CALPUFF control file.

5033

5034 5.4.4.2. SCIPUFF

5035 SCIPUFF (Sykes, 1998) is a Lagrangian puff dispersion model that uses a collection of
5036 Gaussian puffs to represent an arbitrary, three-dimensional, time-dependent concentration
5037 field. The turbulent diffusion parameterisation is based on modern turbulence closure theory,
5038 specifically, the second-order closure model of (Donaldson, 1973) and (Lewellen, 1977),
5039 which provides a direct relationship between the predicted dispersion rates and the
5040 measurable turbulent velocity statistics of the wind field. In addition to the average
5041 concentration value, the closure model also provides a prediction of the statistical variance in
5042 the concentration field resulting from the random fluctuations in the wind field. The closure
5043 approach also provides a direct representation for the effect of averaging time (Sykes,
5044 1997).

5045

5046 Shear distortion is accurately represented using the full Gaussian spatial moment tensor,
5047 rather than simply the diagonal moments, and an efficient puff splitting/merging algorithm
5048 minimises the number of puffs required for a calculation. In order to increase calculation
5049 efficiency, SCIPUFF uses a multi-level time-stepping scheme with an appropriately sized
5050 time-step for each puff. An adaptive multi-grid is used to identify neighbouring puffs in the
5051 spatial domain, which greatly reduces the search time for overlapping puffs in the interaction
5052 calculation and puff-merging algorithm. Static puffs are used to represent the steady-state
5053 phase of the plume near the source and are updated only with meteorology, also decreasing
5054 the number of puffs needed for the calculation.

5055

5056 SCIPUFF can model many types of source geometries and material properties. It can use
5057 several types of meteorological input, including surface and upper-air observations or three-
5058 dimensional gridded data. Planetary boundary layer turbulence is represented explicitly in
5059 terms of surface heat flux and shear stress using parameterised profile shapes. A Graphical
5060 User Interface (GUI) that runs on a PC is used to define the problem scenario, run the
5061 dispersion calculation and produce colour contour plots of resulting concentrations. The GUI
5062 also includes an online 'Help'.

5063 5.4.5. Lagrangian Particle Models

5064

5065 5.4.5.1. AUSTAL

5066 AUSTAL (previously known as AUSTAL2000 and AUSTAL2000g) is an atmospheric
5067 dispersion model for simulating the dispersion of air pollutants in the ambient atmosphere. It

5068 was developed by Ingenieurbüro Janicke under contract to the Federal Ministry for
5069 Environment, Nature Conservation and Nuclear Safety. AUSTAL was initially published in
5070 1986 as a Gaussian Plume model (AUSTAL86), in 2002, the Lagrangian dispersion was
5071 implemented in AUSTAL2000, odour dispersion was added in 2004. It was recently modified
5072 primarily regarding boundary layer parameterisation, plume rise and wet deposition in
5073 accordance with the TA Luft 2021, resulting in the program AUSTAL.

5074 Although not named in the TA Luft (Air Quality regulation in Germany), AUSTAL is the
5075 reference dispersion model accepted as being in compliance with the requirements of Annex
5076 2 of the TA Luft and the pertinent VDI Guidelines. The program AUSTAL (starting with
5077 version 3) refers to the TA Luft 2021 and is the successor of the program AUSTAL2000
5078 (ending with version 2), which refers to the TA Luft 2002. AUSTAL is provided by the Federal
5079 Environmental Agency as a free reference implementation.

5080 AUSTAL is in compliance with the German guideline VDI 3945/3. For any model to be used
5081 under the TA Luft, it must follow this German Guideline. To date, there is no other model that
5082 follows the VDI 3945/3.

5083 The dispersion model AUSTAL can be used to model the transport of passive trace
5084 substances in the lower atmosphere on a local and regional scale. The vertical dimension is
5085 up to about 2000 m with a maximum of 100 layers, the horizontal scale can reach tens of
5086 kilometers, with a maximum of 300 by 300 grid points. To cover larger areas, up to 6 nested
5087 calculation grids can be used (the grid resolution has to increase by factor 2 from one grid to
5088 the next). AUSTAL is a Lagrangian particle model, the dispersion of trace substances in the
5089 atmosphere is simulated utilising a random walk process. The physical processes that can
5090 be simulated include transport by the mean wind field, dispersion in the atmosphere,
5091 sedimentation of heavy aerosols, deposition on the ground (dry deposition) as well as
5092 washout of trace substances by rain and wet deposition. Thermal and mechanical plume rise
5093 is covered parametrically based on the German guidelines VDI 3782/3, or utilising the three-
5094 dimensional plume rise model PLURIS. For odorants, odour hour frequencies can be
5095 determined, with or without weighting factors based on hedonic tone. In flat and
5096 homogeneous terrain, the time dependent meteorological parameters are described by
5097 means of a one-dimensional boundary layer model that is based on simple parameters that
5098 characterise the weather situation. The sampling error can be reduced by increasing the
5099 number of particles released by the model. Emission sources of any number can be defined
5100 in form of point, line, area or volume sources. Most of the source parameters, especially
5101 emission rates, exhaust velocity, exhaust temperature and plume humidity can be specified
5102 as independent time series. The result of the dispersion simulation is the three-dimensional
5103 concentration field of the emitted trace substances averaged over successive time intervals,
5104 and the mass flow density of deposition into the ground. All substances regulated in the TA
5105 Luft (2021) are preprogrammed and the modelling results for each substance are post-
5106 processed, so that for each substance the respective impact values (daily average, yearly
5107 average, e.g.) can easily be assessed. In addition to that, inert substances or particles can
5108 be implemented to model missing substances in the default selection.

5109

5110

5111 5.4.5.2. LAPMOD

5112 LAPMOD is a Lagrangian particle model whose development started more than 20 years
5113 ago (e.g., Bianconi, 1999). The model had different names in the course of its development,
5114 and for a short period it included a photochemical module (Zanini, 2002). During the years

5115 the model has been improved, validated (e.g., Bellasio, 2017; Bellasio, 2018; Haq, 2019)
 5116 and enriched with some pre- and post-processors. According to the performance evaluation
 5117 criteria proposed by (Chang, 2004) - based on FA2, NMSE and fractional bias - LAPMOD
 5118 can be defined as a “good” model both in rural (Kincaid) and urban (Indianapolis) terrain.
 5119 Anyway, model validation is a continuous process, and other tests are underway.

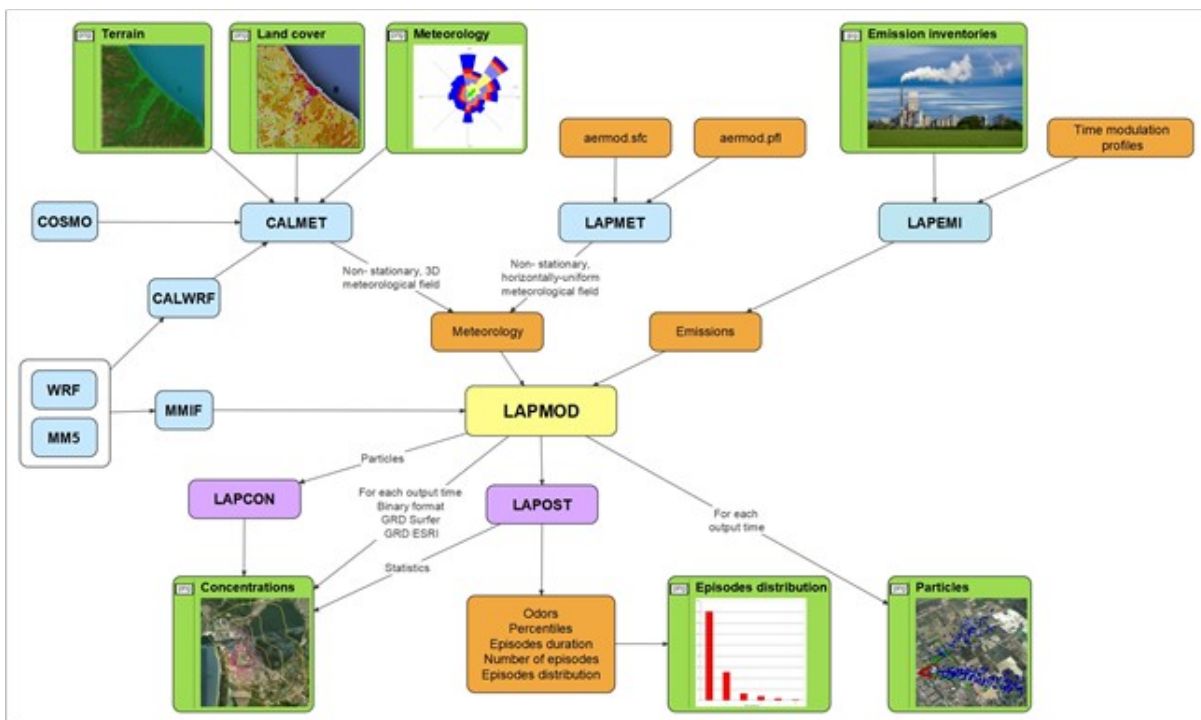
5120

5121 LAPMOD is not only a model but a modelling system, whose structure is summarised in
 5122 Figure 5-11. The modelling system is open-source, its Fortran code and documentation can
 5123 be downloaded at <https://www.envioware.com/lapmod/>.

5124

5125 LAPMOD is used in Italy and Europe both for air quality (e.g., Ugolini, 2013) and odour (e.g.,
 5126 Pollini, 2015) applications. Moreover, LAPMOD is integrated into ARIES (Accidental Release
 5127 Impact Evaluation System), the official Italian modelling system for nuclear emergencies
 5128 (e.g., Bellasio, 2012), and in the AQWeb modelling system of the EPA of Emilia Romagna
 5129 (one of the Italian regions). A recent paper (Bellasio and Bianconi, 2022) used LAPMOD to
 5130 evaluate the results of different odour emission scenarios generated by a new method for
 5131 calculating odour emissions from open-roof rectangular tanks. Finally, it has also been
 5132 mentioned by the (US-EPA, 2020) among the models available for homeland security.

5133



5134

5135 **Figure 5-11** Schematic Representation of the LAPMOD Modelling system (Courtesy of
 5136 Envioware)

5137

5138 Being a 3D non-stationary model, the most appropriate meteorological data should be
 5139 prepared with the CALMET diagnostic meteorological model, which can be used with high
 5140 spatial resolution. However, LAPMOD can also use the 3D meteorological data prepared
 5141 with WRF and MMIF, typically with a lower grid resolution.

5142

5143 Many features of LAPMOD make it suitable for odour applications, as described for example
 5144 in (Bianconi, 2011). For example, it allows simulating releases with arbitrarily time variable

5145 emission rates (up to a resolution of one second) from a number of source types: point
5146 sources without plume rise (e.g., stacks with rain caps), buoyant point sources (e.g., stacks),
5147 linear sources (e.g., road traffic), circular sources (e.g., tanks), spherical sources (e.g., dirty
5148 bomb), parallelepipedal sources (e.g., buildings) and area sources of arbitrary shape (e.g.,
5149 any area source). Independently of the source type, LAPMOD requires the emission rates in
5150 terms of a specific variable X per unit of time, which means g/s for “classic” pollutants (e.g.,
5151 NOX, PM10, ...), Bq/s for radionuclides, and ouE/s for odour. The output unit is controlled by
5152 the user through a multiplication factor, for example, when the release rate is in g/s and the
5153 multiplication factor is 1, the output concentration is in g/m^3 ; on the contrary, if the
5154 multiplication factor is 10^6 , the output concentrations are in $\mu\text{g}/\text{m}^3$. The release units are not
5155 explicitly required by LAPMOD, but the user needs to know them in order to obtain correct
5156 results.

5157
5158 In a Lagrangian particle model each particle moves due to deterministic (mean wind field)
5159 and stochastic (turbulence) effects. Therefore, even in calm wind conditions, which are the
5160 worst situations for the dispersion of odour and any other pollutant, the model continues to
5161 work because the particles move according to the stochastic part of the trajectory equation.
5162 Numerical plume rise can be simulated for buoyant point sources with two different
5163 algorithms: JJ (Janicke and Janicke), and WT (Webster and Thomson). The main difference
5164 between the two algorithms is that JJ considers the presence of water vapour within the
5165 released plume (important for example for modelling emissions from dryers). Specific
5166 algorithms as stack tip downwash (i.e., the capture of the plume in the stack wake, resulting
5167 in an increase of the concentration values immediately downwind of the stack), partial plume
5168 penetration of elevated inversions (which depends on the combined effects of plume
5169 buoyancy, wind speed at stack height, difference between mixing height and stack height
5170 and strength of the inversion) and plume induced turbulence during plume rise (large close
5171 to the release, when the entrainment activity is maximum and the plume radius grows very
5172 quickly, while it reduces moving away from the source) are also available for buoyant point
5173 sources. Building downwash, which may be important when stacks are involved, is still under
5174 implementation. For many odour applications involving area or volume sources this is not an
5175 issue.

5176
5177 Atmospheric concentrations over regular and sensitive (discrete) receptors are calculated by
5178 LAPMOD starting from particle masses and the relative positions of particles and receptors
5179 by means of a kernel method (Vitali., 2006). Concentration fields calculated with kernel
5180 methods are less noisy than those calculated with the “classical” counting box method,
5181 based on the computation of the total mass within a specific volume of atmosphere.
5182 Moreover, kernel estimators require less particles.

5183
5184 Odour concentrations can be determined in two ways in LAPMOD. The first, is the
5185 calculation of the hourly concentrations and the application of a constant Peak-to-Mean
5186 Ratio (e.g., 2.3 as indicated by the Lombardy Region, Italy) in order to compute the peak
5187 concentration. The second, and most interesting way, to calculate the peak concentration is
5188 by determining the Peak-to-Mean Ratio dynamically as a function of atmospheric stability,
5189 distance from sources and age of the particle (e.g., Schauburger, 2000; Mylne, 1992a;
5190 Mylne, 1992b; Smith, 1973). An example of application of LAPMOD with this second method
5191 for calculating odour concentrations has been described by (Invernizzi, 2020). The same
5192 paper contains an intercomparison against the results of two other atmospheric dispersion

5193 models.

5194

5195 The LAPOST processor can be used to estimate some of the FIDOS parameters
 5196 (Frequency, Intensity, Duration, Offensiveness and Location), except offensiveness which
 5197 depends on the odour mixture and has subjective characteristics. Concerning frequency (F)
 5198 for example, LAPOST calculates the number of exceedances of an odour threshold specified
 5199 by the user. Intensity (I) is represented by means of the maximum hourly concentration or
 5200 with the 98th percentile of the peak concentration. Duration (D) is calculated by LAPOST for
 5201 each point and each odour episode. The episode indicates the time for which concentration
 5202 remains consecutively above the odour threshold. LAPOST also determines the number of
 5203 exceedance episodes, which coincides with the number of exceedances only when each
 5204 exceedance lasts for a single hour. A specified percentile of episode durations can also be
 5205 calculated for each output receptor. The location (L) is automatically determined by LAPOST
 5206 because all the results are associated with precise coordinates.

5207 5.4.5.3. GRAL

5208 The Graz Lagrangian Model – GRAL (Oetl, 2020a) - was initially developed in 1999, and
 5209 has been used extensively in regulatory assessments and scientific studies. The model is
 5210 used worldwide by more than 1,000 authorities and research institutes. Over the years the
 5211 capabilities of GRAL have been extended, and the current version of the model can simulate
 5212 the following:

- 5213 ● Dispersion of chemically non-reactive pollutants.
- 5214 ● Computation of odour-hours based on a concentration-variance model (e.g., Oetl
 5215 and Ferrero, 2017).
- 5216 ● Dry and wet (only in transient mode) deposition and sedimentation.
- 5217 ● Dispersion from road tunnel portals. GRAL fulfils the requirements of the Technical
 5218 Guideline RVS 04.02.12 in Austria (e.g., Oetl, 2002).
- 5219 ● Dispersion over the full range of wind speeds, in particular low-wind-speeds (e.g.,
 5220 Oetl, 2005; Anfossi, 2006), and for all stability conditions.
- 5221 ● Dispersion in built-up areas, including building downwash effects (e.g., Oetl, 2015a;
 5222 Oetl, 2015b).
- 5223 ● Dispersion of stack emissions, taking into account temperature and exit velocity (e.g.
 5224 Oetl, 2020a).
- 5225 ● Dispersion in complex terrain, allowing for the effects of buildings (e.g., Oetl 2015c).
- 5226 ● Decay rates (e.g. bacteria die off, radioactive decay)
- 5227 ● Flow and dispersion within vegetation layers
- 5228 ● The model can handle steady-state (standard mode) as well as transient simulations
 5229 (e.g. puff releases) (e.g., Petrov, 2019)

5230 The effect of buildings and vegetation on dispersion is taken into account using a micro-
 5231 scale flow-field model. This is fully integrated into the GRAL code and is automatically
 5232 launched whenever buildings or vegetation layers are added to the model domain. In the
 5233 case of complex terrain, GRAL can be coupled with the prognostic, meso-scale wind field
 5234 model GRAMM ('Graz Mesoscale Model'; (Oetl, 2020b)). Both GRAL and GRAMM are
 5235 parallelised and can be run on both Windows and Linux operating systems. The models can
 5236 be operated through a graphical user interface (GUI) which has been thoroughly tested for
 5237 Windows operating systems. Since 2017 a LINUX version for the GUI is available, though it
 5238 is not as intensively tested as the Windows version. There is no limit to the number of
 5239 separate emission sources that can be included in a GRAL simulation. The lower bound for

5240 the horizontal grid size is 2 m, and there is no upper bound. The scale of application ranges
 5241 from individual streets (e.g. street canyons) to urban agglomerations that are several tens of
 5242 kilometres across. At all scales the effects of buildings and/or topography (e.g. cold air
 5243 drainage flows) on dispersion are taken into account.

5244
 5245 GRAL allows the usage of odour emission rates in M OU/h and offers two different methods
 5246 for odour impact assessments. The first, is the calculation of user-defined percentiles (e.g.
 5247 98 percentile of mean-hourly odour concentrations at a receptor). In this case, the model
 5248 outputs are odour-concentration maps for the specified percentile. The second, is based on
 5249 the computation of odour hours, whereby the Peak-to-Mean Ratio can either be calculated
 5250 by a spatially and temporal constant value (adjustable by the user), or by using the
 5251 concentration-variance model by (Oettl, 2017). The concentration-variance model simulates
 5252 the Peak-to-Mean Ratio (i.e. the ratio of the 90th percentile to mean) in dependence on the
 5253 three-dimensional structure of the plume(s) and spatially inhomogeneous atmospheric
 5254 turbulence. The model outputs when using this assessment method are maps showing the
 5255 frequencies of odour hours. The contribution of each odour source can be assessed by
 5256 defining source groups in GRAL. For each source group, individual temporal varying
 5257 emission rates can be defined. An evaluation of GRAL regarding odour assessments has
 5258 been carried out in, for example, Oettl (2020a), Invernizzi (2020), Brancher (2020a).

5259
 5260 Quality assurance is central to the ongoing development of GRAL, based on these
 5261 fundamentals:

- 5262 • Regular reports detailing the model physics, and the publication of results in
 5263 international peer-reviewed scientific journals.
- 5264 • Comprehensive documentation of the software, with version control.
- 5265 • A handbook for the GUI that includes hints and recommendations for good practice.
- 5266 • Validation of every update using 30 different data sets (field experiments, wind tunnel
 5267 experiments, air quality measurements), as published in the GRAL documentation.

5268 The model (binaries) and the complete documentation is available via: <https://gral.tugraz.at/>.
 5269 The GRAL code is available under the GNU/GPL 3 licence:
 5270 <https://github.com/GralDispersionModel>.

5271

5272 5.4.5.4. SPRAY

5273 SPRAY is a Lagrangian stochastic particle model designed to perform dispersion simulations
 5274 in complex terrain (Tinarelli, 2000). The early Version 1 of the code was based on a three-
 5275 dimensional form of the Langevin equation for the random velocity with coupled non-
 5276 gaussian random forcing following (Thomson, 1984) which was subsequently improved by
 5277 (Tinarelli, 1994), was able to satisfactorily reproduce locally to regional scale dispersion both
 5278 over flat (Brusasca, 1989) and complex terrain (Nanni, 1996) taking into account the
 5279 emission from single or multiple sources, and low-wind stable conditions (Brusasca, 1992).
 5280 Version 2 introduced a better-based theory (Thomson, 1987) covering the further demand of
 5281 more complex regional scale simulations taking into account longer periods (of the order of
 5282 entire years) with a variety of emissions of different kinds (i.e., main roads, industrial or
 5283 urban areas). Version 3 of the SPRAY code currently released includes some
 5284 improvements, enhancing the description of turbulence parameterisations, introducing
 5285 building downwash effects and improving the time response characteristics for long
 5286 simulations. In addition, specific developments for odour applications have been introduced,

5287 allowing the calculation of a longitudinal Peak-to-Mean Ratio, based on the original work of
5288 (Mylne, 1991) and (Mylne, 1992). Two more recent developments have been recently
5289 released, allowing more advanced calculations of the Peak-to-Mean Ratio considering
5290 respectively a simplified form of the variance transport equation and a Micromixing Model.
5291 (Tinarelli et al.,2022).

5292

5293 SPRAY can be linked to the output of different meteorological models able to reconstruct 3D
5294 fields of the meteorological flow over complex terrains, such as the diagnostic code SWIFT
5295 or the prognostic codes RAMS or WRF.

5296

5297 A more comprehensive version of the SPRAY code, allowing simulations at the microscale
5298 (horizontal resolution of the order of 1 m, explicitly considering the effects of buildings or
5299 obstacles to the atmospheric flow) and implementing a sophisticated MPI parallelisation
5300 scheme has been introduced. This version, named PSPRAY, is part of the PMSS modelling
5301 suite (Oldrini, 2017), maintained by ARIA Technologies and ARIANET, including the
5302 PSWIFT diagnostic meteorological code, working at the microscale.

5303 5.4.5.5. QUIC

5304 The QUIC fast-response urban dispersion modelling system computes the three-dimensional
5305 wind patterns and dispersion of airborne contaminants around clusters of buildings. The
5306 system is comprised of a wind model, QUIC-URB; a Lagrangian dispersion model,
5307 QUICPLUME; and a graphical user interface, QUIC-GUI.

5308 QUIC-URB uses empirical algorithms and mass conservation to estimate the wind velocities
5309 around buildings.

5310

5311 The QUIC-PLUME dispersion model is Lagrangian, that is, it tracks the movement of
5312 particles as they disperse through the air. QUIC-PLUME utilises the mean wind fields
5313 computed by QUIC-URB and produces the turbulent dispersion of the airborne contaminant
5314 using random walk equations. QUIC-PLUME has been specially adapted to account for
5315 particle reflection on building surfaces and for the additional dispersion due to horizontal
5316 inhomogeneities in the turbulence field. QUIC has been also used for applications involving
5317 odours, see for example, Pettarin et al. (2015) and source location, see Gunawardena et al.
5318 (2021).

5319

5320 5.4.6. Summary of Lagrangian Puff and Particle Models

5321 Table 5-5 summarises the key features of Lagrangian puff and particle models.

5322 **Table 5-5** Summary of key features of well-known regulatory Lagrangian Puff and Particle models used in odour assessments around the world
 5323 today

Description	CALPUFF	SCIPUFF	SPRAY	AUSTAL LASAT	GRAL	LAPMOD
Dispersion						
Dispersion coefficient (σ_y , σ_z) options	-direct measurements of σ_v and σ_w -estimated values of σ_v and σ_w based on similarity theory -PG dispersion (rural areas) -McElroy-Pooler (urban areas) -CTDM (neutral/stable)	Employs second-order closure turbulence schemes				Hanna et al. (1982) for stable and neutral conditions. Hurley and Physik (1993) for convective (i.e. unstable) conditions.
Special features for odour modelling						
Odour input and output units	Input -point and volume sources $ou \cdot m^3/s$ Input – area sources $ou \cdot m/s$ Output units in odour units (ou/m^3)					Suitable multiplication factors in LAPMOD or its post processor allow to use any emission unit
Output statistics for odour	Percentiles, exceedances, ranked, isopleth, exceedance plots	Percentiles, exceedances, ranked, isopleth, exceedance plots	Percentiles, exceedances, ranked, isopleth, exceedance plots	Percentiles, exceedances, ranked, isopleth, exceedance plots	Percentiles, exceedances, ranked, isopleth, exceedance plots	Percentiles, exceedances, ranked, isopleth, exceedance plots
Sub-hour capability	Version 6 of the model allows sub-hour meteorology including measured sub-hour turbulence coefficients	1-hour time step	1-hour time step	1-hour time step	1-hour time step	Theoretically up to 1 second

Description	CALPUFF	SCIPUFF	SPRAY	AUSTAL \ LASAT	GRAL	LAPMOD
Adjustments to <1-hour averaging periods	1-hour averaging period is minimum with 1-hour meteorological data, which means <1-hour assessment criteria must apply external power law equation. Otherwise, averaging time will be same as meteorology time step, i.e., 10-minute meteorology means a 10-minute averaging time					The best option is to use a high frequency meteorological field (e.g., CALMET output with 10-minute time step).
Concentration fluctuations (built in Peak-to-Mean Ratio)	CALPUFF 1 st -order closure integrated puff model User must apply PtM factor when using 1-hour meteorology. Otherwise use sub-hour meteorology and turbulence parameters in place of PtM factor.	SCIPUFF is a 2 nd -order closure integrated puff model. Velocity fluctuations might be obtained without external application of PtMR, but requires modelling the turbulence				Possibility to use a constant PtMR, or a dynamic PtMR based on stability conditions and time from release
Treatment of calms	Yes, user-defined min wind speed (def 0.5 m/s). Model switch from distance to time dependent sigma's, no downwash, slug model, no gradual plume rise. Puff will diffuse with time but not be advected anywhere	Yes	Yes	Yes	Yes	Yes

5324 5.4.7. Particle-puff Lagrangian models

5325 Some Lagrangian models employ a Particle-puff approach, described in 5.3.4.3.

5326 Hurley (1994) found that particle numbers, memory and computer time requirements were
5327 significantly reduced compared to a regular particle model. This is because fewer particles
5328 were needed as turbulence only needs to be resolved vertically, and each particle influences
5329 any concentration grid points horizontally. There is little literature on applying Particle-Puff
5330 models and their use or evaluation in odour assessments. However, these models are
5331 expected to return similar results to standard Lagrangian particle and puff models and are
5332 more computationally efficient than full particle models.

5333 5.4.7.1 TAPM

5334 Australia's Lagrangian model, The Air Pollution Model (TAPM) (Hurley, 1994; Hurley, 2002),
5335 is different to typical air pollution models that rely on semi-empirical/analytic approaches
5336 based on Gaussian plumes or puffs. TAPM solves approximations to the fundamental fluid
5337 dynamics and scalar transport equations to predict meteorology and pollutant concentration
5338 for a range of pollutants important for air pollution applications. TAPM consists of coupled
5339 prognostic meteorological and air pollution concentration components, eliminating the need
5340 for site-specific meteorological observations. Instead, the model predicts the flows important
5341 to local-scale air pollution, such as sea breezes and terrain-induced flows, against a
5342 background of larger-scale meteorology provided by synoptic analyses.

5343
5344 The meteorological component of TAPM is an incompressible, non-hydrostatic, primitive
5345 equation model with a terrain-following vertical coordinate for three-dimensional simulations.
5346 The model includes cloud microphysics. The model includes a vegetative canopy, soil
5347 scheme and urban scheme, which are used at the surface, while radiative fluxes at the
5348 surface and at upper levels are also included. The air pollution component of TAPM, which
5349 uses the predicted meteorology and turbulence from the meteorological component, consists
5350 of four modules. The Eulerian Grid Module solves prognostic equations for the mean and
5351 variance of concentration and the cross-correlation of concentration and virtual potential
5352 temperature. The Lagrangian Particle Module can accurately represent the near-source
5353 dispersion model (Physick, 1994). The plume rise module (Hurley, 1995) accounts for
5354 plume momentum and buoyancy effects for point sources. The building wake module is
5355 based on PRIME (Schulman, 2000) and allows plume rise and dispersion to include wake
5356 effects on meteorology and turbulence. TAPM also includes gas-phase photochemical
5357 reactions based on the Generic Reaction Set, gas- and aqueous-phase chemical reactions
5358 for sulphur dioxide and particles, and a dust mode for total suspended particles (PM_{2.5},
5359 PM₁₀ and PM₂₀). Wet and dry deposition effects are also included. The output of TAPM
5360 will allow the extraction of time series, profiles and summary statistics of pollution. A built-in
5361 graphical user interface allows the user to see colour-shaded maps of concentration
5362 statistics, which are also easily exported into a spreadsheet. Time series of pollution can be
5363 easily viewed. TAPM does not allow odour input emission units or output in odour units.
5364 The model will output concentration as either $\mu\text{g}/\text{m}^3$ or ppb for all model heights. The model
5365 will also process the percentiles (90th – 99.9th) level. Scaling factors, such as a 3-minute
5366 averaging time or PtM factors, would need to be applied to the predicted ground-level
5367 concentrations after TAPM has been executed in a spreadsheet.

5368

5369 TAPM is widely used in Australia and New Zealand, primarily to develop upper air data as
 5370 single or multiple vertical profiles or as gridded data. This data is commonly used as input to
 5371 the CALMET diagnostic meteorological model, on which CALPUFF is then executed.
 5372 TAPM includes routines to single output 1-dimension meteorological data for AUSPLUME
 5373 and/or 2-dimensional meteorological data in AERMOD and CALMET format for any location
 5374 over its model domain. In addition, TAPM can output gridded 3D data at typically 1 km
 5375 resolution or larger.

5376
 5377 In summary, although TAPM is not used exclusively in odour applications within Australia
 5378 and New Zealand, it is an essential and frequently used model in most odour assessments
 5379 that require dispersion modelling.

5380 5.5. General well-known problems/limitations/solutions

5381 5.5.1 General introduction

5382 This section aims to give a general picture of the main problems presented using the
 5383 different model types described in the previous paragraphs, both in general terms and
 5384 specifically for the odour assessment applications. Different descriptions are reported for
 5385 each model type, even though some problems may be familiar to different models.

5386 5.5.2 Gaussian models

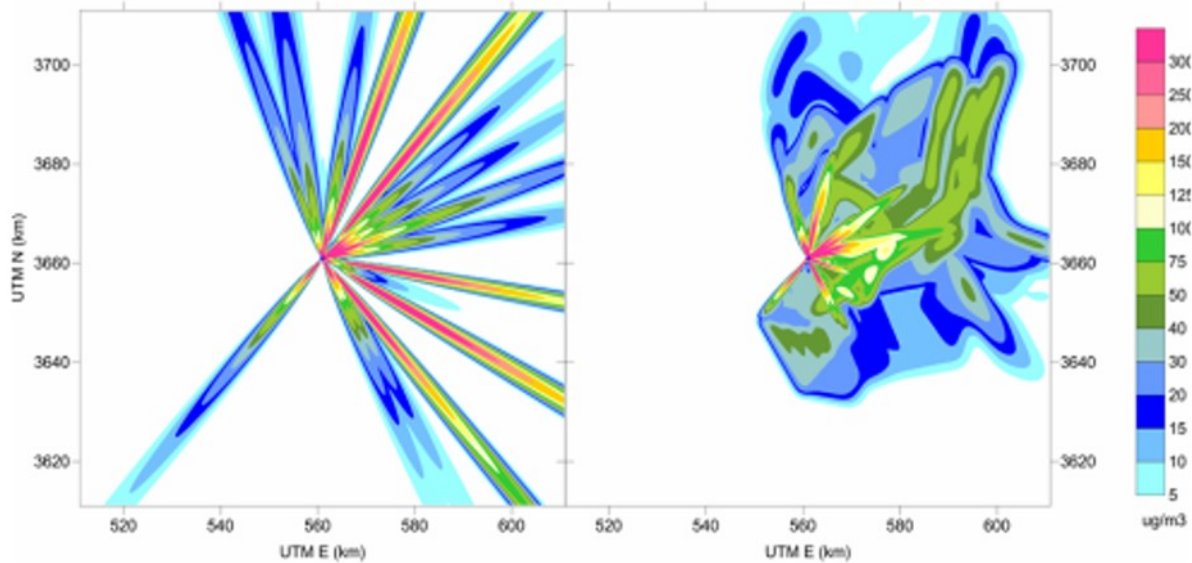
5387 5.5.2.1 Overview

5388 Meteorological conditions are horizontally homogeneous within the modelling domain. This
 5389 means that meteorological variables such as wind speed and direction, mixing height,
 5390 temperature, humidity, and turbulence variables such as surface friction velocity (u^*),
 5391 convective velocity scale (w^*), Monin-Obukhov length (L), have the same value at a specific
 5392 time over the domain.

5393
 5394 Meteorological conditions are assumed constant over the time needed for the plume to
 5395 reach each receptor; also, source characteristics, including emission rates, are constant.

5396
 5397 Finally, each hour is separate and independent of other hours: there is no memory of
 5398 pollutant location or emissions from other hours (see Figure 5-12).

5399



5400
 5401 **Figure 5-12** Comparison of Steady-state Gaussian plume model (left) vs Lagrangian puff
 5402 model (right) for 24-hour simulation over flat terrain (Courtesy of Atmospheric Science
 5403 Global)

5404 5.5.2.2 Complex environments where the Gaussian plume model is not applicable

5405 Sea breezes, thermal internal boundary layer (TIBL) fumigation, inversion break-up
 5406 fumigation, terrain channelling effects, stagnation and retention events, causality effects,
 5407 horizontal and vertical wind shear effects are all complicated 3-dimensional features that
 5408 require sophisticated meteorological models in order to simulate these events realistically.
 5409 These phenomena are significant everyday occurrences affecting all source types, from
 5410 ground-level-based odour sources to those released from tall point sources such as pulp and
 5411 paper mill factories.

5412
 5413 The only way to capture these phenomena is to use sophisticated diagnostic and numerical
 5414 meteorological models. Interfacing gridded 3D wind fields from traditional weather-type
 5415 models with a fine resolution diagnostic meteorological model such as CALMET allows
 5416 regional flows to be captured with the added benefit of including multiple observation
 5417 stations. In many instances, gridded 3D numerical model data (e.g., WRF and ECMWF) is
 5418 more useful than a single observation site typical of Gaussian plume models which:

- 5419 A. tend to be representative of conditions in their immediate vicinity,
- 5420 B. frequently suffer from missing or loss of data and,
- 5421 C. are limited to just the surface.
- 5422 D. unable to capture the 3D signal in the atmosphere.

5423 Precipitation, gridded cloud cover and detailed sea surface temperatures are additional
 5424 significant advantages of using numerical meteorological data in regulatory modelling.

5425
 5426 The procedure of combining sophisticated numerical 3D gridded data into a diagnostic
 5427 meteorological model permits the prognostic model to be run with a significantly larger
 5428 horizontal grid spacing and different vertical grid resolution than that used in the diagnostic
 5429 model, which can then be run at a much finer resolution (< 250m) incorporating fine-scale
 5430 terrain and Land Use data. This allows the three-dimensional features of the flow field, such

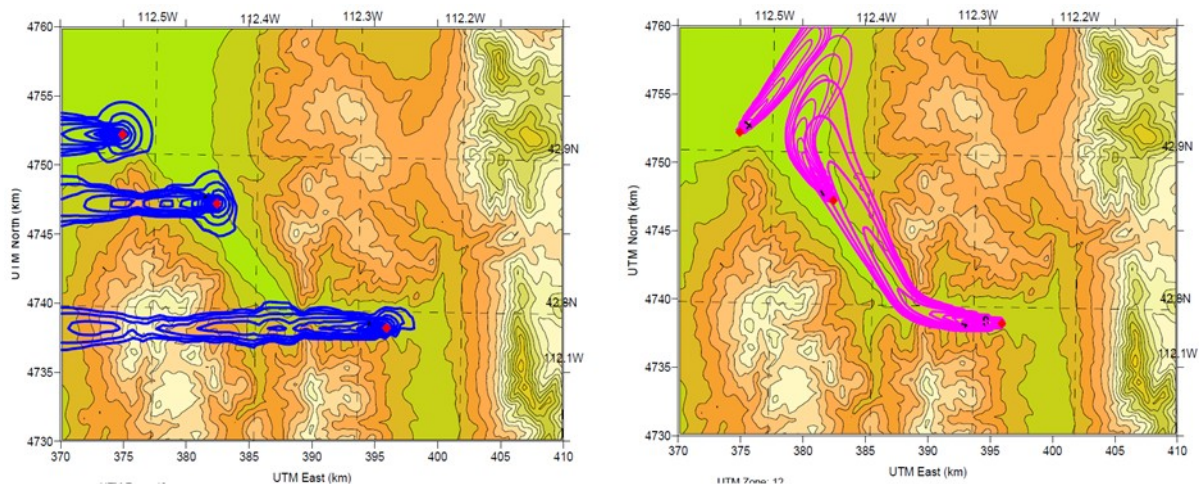
5431 as the sea breeze circulation with return flow aloft, which may not be captured in the surface
5432 observational data, to be introduced into the diagnostic wind field results.

5433 Gaussian plume models such as AERMOD and ADMS, which are limited to one surface
5434 meteorological site and an upper air profile, do not know the three-dimensional flow and
5435 therefore produce spatially uniform meteorology across all receptors. This is a major
5436 drawback of the steady-state assumption. Usually, the winds are derived from a single point
5437 measurement from a nearby site, such as an airport which does not necessarily reflect the
5438 flow in the valleys. Steady-state models do not adjust the winds to reflect the terrain effects,
5439 and the net effect is that the steady-state flow field does not reproduce the terrain-induced
5440 spatial variability in the wind fields. In addition, the plume model's straight-line trajectory
5441 assumption cannot handle the curved flow associated with terrain-induced deflection of
5442 channelling.

5443
5444 Figure 5-13 shows the results of 3 individual sources and their related plumes from
5445 AERMOD vs that from a Lagrangian puff model, CALPUFF. In a complex terrain simulation,
5446 the plumes from the simple plume model blow directly across the valley, regardless of the
5447 terrain. In this scenario as well as the plumes going in the wrong direction, they also give
5448 unrealistically high concentrations on the terrain features, and they do not model the
5449 cumulative impact as they do not overlap.

5450
5451 Gaussian models should not be used in complex flow situations (i.e., conditions where
5452 steady-state criteria are not met). Examples of complex flow situations are:

- 5453 ● Complex terrain
- 5454 ● Coastal regions/ land-water boundaries
- 5455 ● Overwater transport
- 5456 ● Inhomogeneous dispersion conditions
- 5457 ● Land use/land cover variation
- 5458 ● Distance (> 10 - 20 km)
- 5459 ● Stagnation
- 5460 ● Light wind speed dispersion, calm conditions
- 5461 ● Flow reversals
- 5462 ● Land-sea breeze
- 5463 ● Upslope/downslope, valley flows
- 5464 ● Recirculation
- 5465



5466
5467

5468 **Figure 5-13** Cumulative impacts and terrain channelling effects from three sources using
5469 AERMOD (left) vs CALPUFF (right). The spatially varying wind flow produced by CALPUFF
5470 is shown in the figure on the right, where winds are channelled through the main valley,
5471 generating a cumulative impact. AERMOD on the other hand has a uniform wind field and is
5472 unable to produce terrain channelled effects, hence the three sources do not overlap
5473 (Barclay and Borissova 2013).

5474 5.5.2.2 Light winds, calms and lateral plume meander

5475 Light winds, calms and lateral plume meander are important because:

- 5476 ● Odours can reach their highest levels
- 5477 ● They are difficult to model – models struggle to capture the generation of turbulence
5478 by mesoscale motions
- 5479 ● All models rely on advection
- 5480 ● Plume models (e.g., AERMOD, ADMS) have inverse wind speed dependency
5481 therefore cannot handle calms
- 5482 ● Turbulence diffusion never completely vanishes (never strictly laminar), but the
5483 turbulence diffusion can be extremely slow
- 5484 ● Flow tends to be terrain driven, in combination with heating and cooling of near-
5485 surface air
- 5486 ● Very strong inversions develop under clear skies
- 5487 ● Flow in stable hours usually downslope but can be multi-layered due to different
5488 potential temperatures of different contributory flows
- 5489 ● Cloud shadow – immediate negative heat flux which sets up turbulence suppressing
5490 stratification near the ground

5491

5492 Gaussian plume models, such as ADMS and AERMOD, are unable to model calm winds
5493 and will simply skip over these hours. In AERMOD, the minimum allowable wind speed to
5494 define the boundary layer parameters is defined as $2^{1/2} * \sigma_{vmin}$ where $\sigma_{vmin} = 0.2$ m/s (then the
5495 minimum wind speed is about 0.28 m/s). This minimum is independent of the threshold wind
5496 speed, which is 0.51 m/s. The restriction is based on the accuracy of the instruments. Sonic
5497 anemometers have no threshold limitations; therefore, no wind speed threshold is imposed,
5498 and the output AERMINUTE file can have winds lower than 0.28 m/s. ADMS has a low wind
5499 speed threshold similar to AERMOD and is currently set at 0.3 m/s. If the wind speed is

5500 lower than 0.3 m/s (including 0.0 m/s), ADMS will increase the wind speed to 0.3 m/s and
5501 adjust the friction velocity and surface heat flux. However, it is essential to note that the
5502 minimum wind speed at 10 m is 0.75 m/s.

5503

5504 By US-EPA (and Australia) regulatory requirements, any data set that does not meet the
5505 90% data coverage must use AERMINUTE, which is a meteorological processor (or another
5506 method) to re-process the 1-10 minute automatic weather station readings to produce a new
5507 1-hour average wind speed and wind direction which is different than the regular standard
5508 archived hourly data. AERMINUTE generates a new meteorological data set with fewer calm
5509 periods and much more wind in the range of 0.1 m/s to 1 m/s. However, while AERMINUTE
5510 solved one problem (i.e., reduced the number of calms in a data set and thereby increased
5511 the number of hours modelled to > 90%), increasing the number of very light winds created
5512 other problems, such as AERMODs tendency to over-predict in light winds, and its treatment
5513 of lateral plume meander, which is responsible for most of the horizontal plume dispersion in
5514 stable atmospheric conditions. AERMOD, similarly to ADMS, accounts for the lateral
5515 meander of plumes in the stable boundary layer by interpolating between two concentration
5516 limits, the coherent (wind direction determined) plume limit, and the random plume limit
5517 which assumes an equal probability of any wind direction.

5518

5519 As the wind speed approaches zero, plume transport and dispersion changes from a
5520 "coherent" plume (Gaussian shape) advected in a single direction to a random or "pancake"
5521 plume dispersing radially in all directions.

5522

5523 This scheme in AERMOD was understood to apply to situations when the wind speed was
5524 near zero, but it actually applies to all wind speeds. AERMOD concentrations are thus a sum
5525 of the Coherent Plume and Random Plume (see Figure 5-14) according to

5526

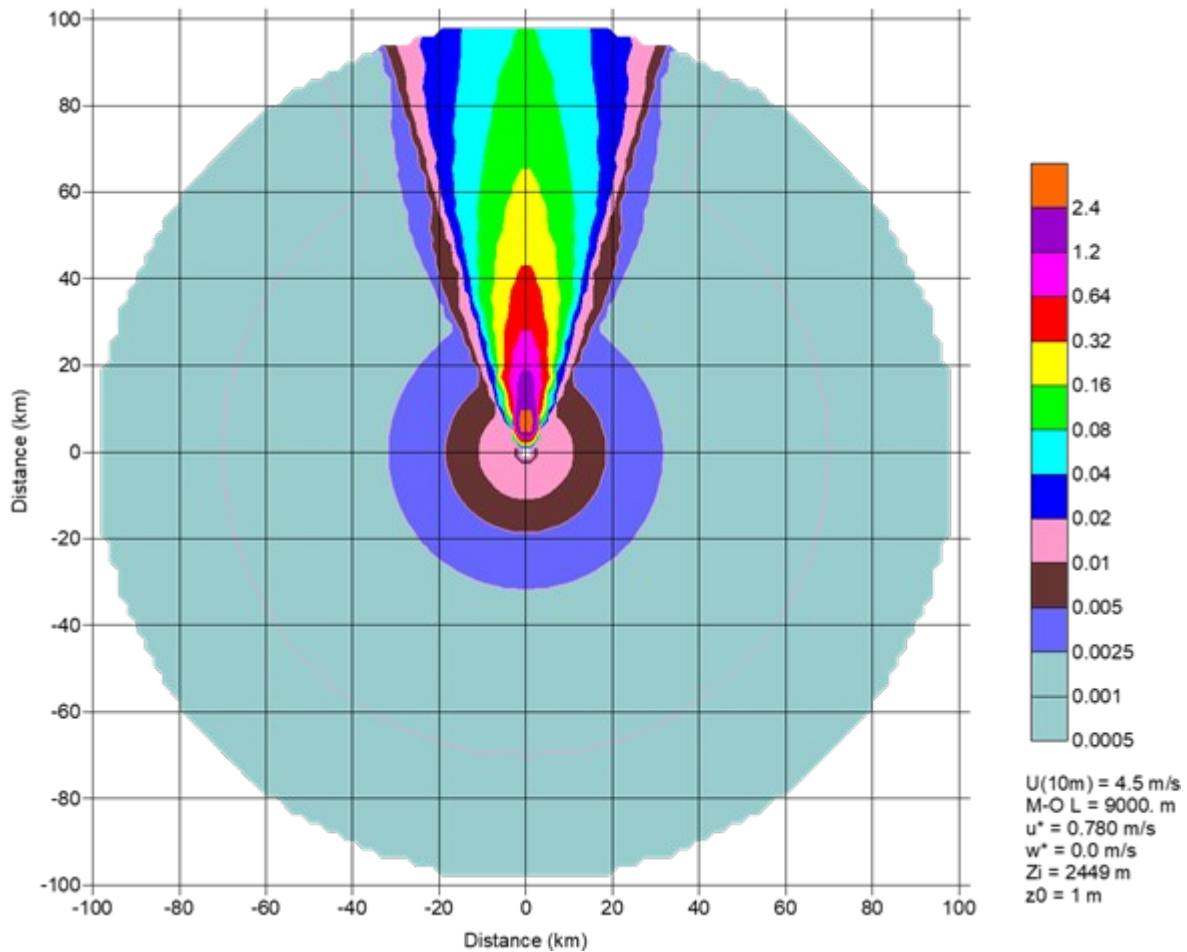
5527
$$\text{Conc (final)} = F(\text{Random}) * \text{Conc}(\text{Random}) + (1 - F(\text{Random})) * \text{Conc}(\text{Coherent})$$

5528

5529 Where $F(\text{Random})$ is the fraction of plume removed from the main (coherent) plume and
5530 distributed in circular 360-degree rings around the source, including upwind of the source.

5531

5532 Mass is removed in all conditions, not just light wind speeds. Under some convective
5533 conditions, a large amount of mass (40 to 67%) is removed from the main plume, which is
5534 thus depleted. The effect of the random plume is potentially large concentrations located
5535 upwind of each source that may even exceed plume concentration downwind under some
5536 conditions, such as hilly terrain upwind of the source.



5537

5538

Figure 5-14 AERMOD predicted concentrations for steady 4.5 m/s wind and neutral stability. Concentrations occur upwind due to the random plume effect (Courtesy of Atmospheric Science Global)

5540

5541

5542

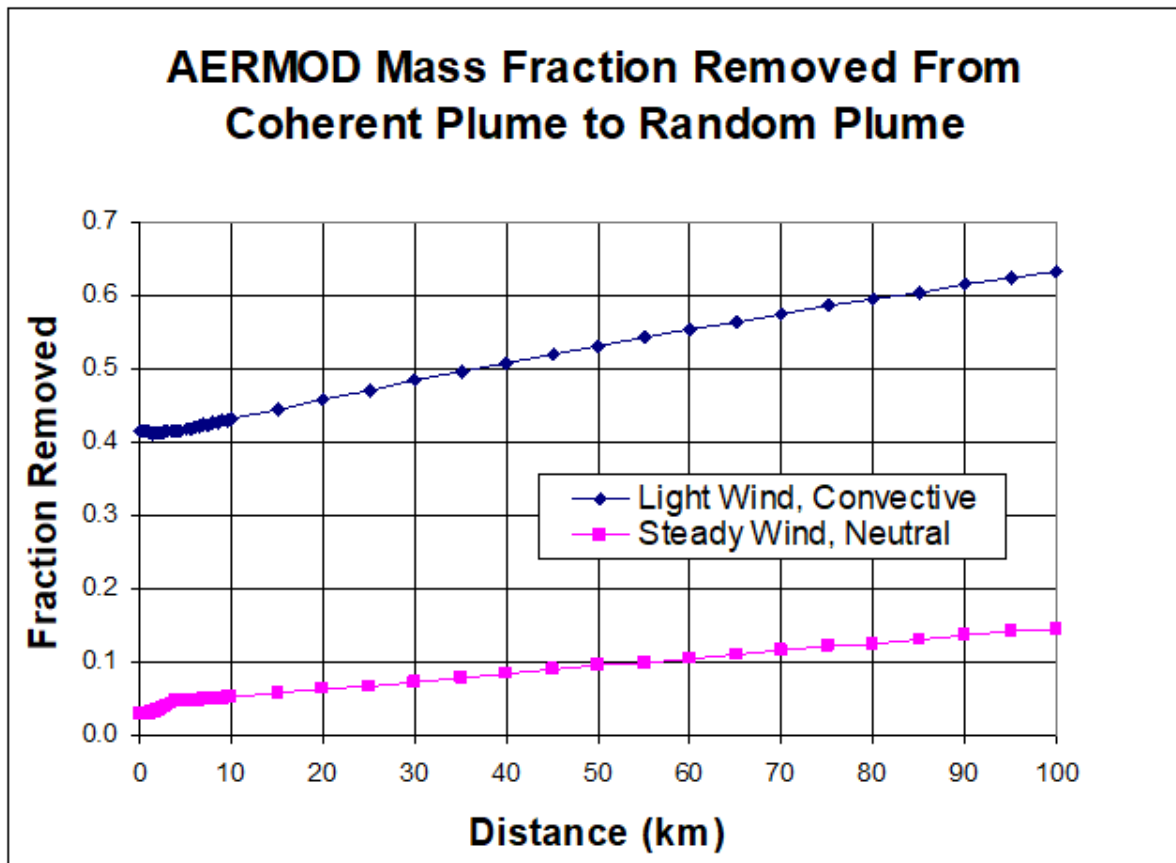
Figure 5-15 shows the significant amount of mass removed from the main coherent plume and placed into the random plume for a light wind situation in convective conditions (40% to 65%) and under a steady wind in neutral conditions (6% - 16%). In moderate terrain applications, the concentration can be higher upwind of the source than downwind, and in many instances, this has led to concentration under predictions downwind. As a result, major changes have been made to AERMET and AERMOD since 2012 to try and improve AERMOD's predictions in light winds. These changes are still ongoing today. These modifications, which affected both AERMET and AERMOD, are summarised below.

5548

5549

5550

5551



5552

5553

5554 **Figure 5-15** AERMOD Mass fraction removed from coherent plume to random plume
 5555 (Courtesy of Atmospheric Science Global)

5556

5557 Since 2012 until 2018, the US EPA underwent significant major changes to AERMET (points
 5558 1, 2 below) and AERMOD (points 3, 4, 5 below) which included:

5559

5560

5561

5562

5563

5564

5565

5566

5567

5568

5569

5570

5571

5572

5573

5574

5575

5576

5577

1. Development of AERMINUTE in order to recompute the hourly average from 1 and 5-minute ASOS data. The effect of this was to increase the number of light winds in the category 0.1 – 0.5 m/s and increase the number of modelled hours to 90% or more.
2. Adjustment to the friction velocity (Adj_u^*)
3. Introduction of 4 LOWWIND options
4. FRAN (adjustments to the random\pancake plume)
5. Adjustments to the minimum value of σ_v

At the 2012 10th EPA Modelling Conference, modifications were made to AERMOD V12345 called the 'beta Adj_u^* ' option for a revised u^* formulation under stable conditions and two different low wind speed options in AERMOD (Jeffrey et al., 2013). It was found that AERMOD was routinely under-predicting u^* during stable boundary layer conditions under low wind speeds. This had the effect of underestimating the mixed layer height, leading to the overestimation of concentrations trapped within the mixed layer. However, the effect of Adj_u^* sent the model back to under-predicted concentrations. Therefore, it was realised that changes were needed for AERMOD and AERMET.

Between 2012 and 2018, the US EPA developed 4 LOWWIND (US EPA LOWWIND White

5578 Paper) options; each option was mutually exclusive, non-default beta options focused on the
5579 minimum value of sigma-v (lateral turbulence intensity). Further, each of these options
5580 included changes to the default plume meander. The LOWWIND options were briefly;

5581
5582 LOWWIND1 (V12345) increased minimum σ_v of 0.2 m/s to 0.5 m/s; turned off the horizontal
5583 meander component altogether, and eliminated upwind dispersion, whereas;

5584
5585 LOWWIND2 (V12345) increased the minimum σ_v of 0.2 m/s to 0.3 m/s, incorporated
5586 meander with an adjustment on the default upper limit of the meander factor (FRAN) from
5587 1.0 to 0.95. It included upwind concentrations due to horizontal meander and an adjustment
5588 to the meander component, e.g., 12 hours is used for BIGT (time scale where mean wind
5589 information at source is no longer correlated with plume location) instead of 24 hrs).

5590
5591 LOWWIND3 (V16216) increased the minimum σ_v of 0.2 m/s to 0.3 m/s, consistent with
5592 LOWWIND1, but used the FASTALL approach that matches centreline concentration for
5593 LOWWIND2, based on an effective σ_y . This scheme eliminated upwind dispersion – the
5594 effect of this is to potentially cause higher concentrations for receptors near the plume
5595 centreline than LOWWIND2.

5596
5597 Alpha LOWWIND (V18081) allowed the user to adjust the minimum σ_v (default 0.2m/s)
5598 within the range 0.01 - 1.0 m/s, the min wind speed value from 0.01 - 1.0 m/s (default 0.2828
5599 m/s) and, the meander factor within the range of 0.0 - 1.0 (default 1.0). [Note. Alpha options
5600 are for 'experimental' use only and are not to be used for regulatory applications].

5601
5602 The US EPA subsequently then removed the LOWIND1, LOWIND2 and LOWWIND3
5603 options. The current version of the model now includes the adjust u^* option (ADJ_ u^*) and
5604 the alpha LOWWIND option, which was designed to aid in further exploring potential
5605 improvements in model predictions under low wind conditions. However, since there is
5606 virtually no literature on how variations of these parameters perform, plus alpha options are
5607 experimental only, most users worldwide continue to use the model default options.

5608
5609 ADMS, similarly to AERMOD, treats the plume's lateral meander in light wind conditions
5610 through a radial solution. The default wind speed is 0.5 m/s (unless specified in an external
5611 input file), and when the wind speed data is below this, the model will calculate the radial
5612 plume only and not the coherent plume. The approach used for calm conditions > 0.5 m/s is
5613 to calculate the concentration as a weighted average of a normal Gaussian-type plume (C_g)
5614 and a radially symmetric plume (C_r), where the weighting depends on the wind speed at 10
5615 m. The radially symmetric plume is modelled as a passive source with a source height equal
5616 to the maximum plume height from the standard plume rise calculations. It assumes an
5617 equal probability of all wind directions. The model calculates C_r only for winds less than the
5618 threshold (0.5 m/s or as specified in an external file).

5619
5620 In addition, area sources in AERMOD currently do not experience any lateral meander. In
5621 the latest US-EPA (2021) LOWWIND White Paper, the EPA looks for “considerations for
5622 updates in the AERMOD model system” and “welcomes input from the community on the
5623 possible implementations of meander for area sources”. The lack of plume meander for area
5624 sources means that area sources will most likely be significantly under or over-predicting
5625 ground-level concentrations. This has serious consequences for many odour sources, which

5626 are largely ground-based area sources, such as, for example, evaporating and wastewater
5627 ponds, clarifiers, composting, and biofilters.

5628 5.5.3 Lagrangian models

5629 5.5.3.1 Lagrangian puff models

5630 Lagrangian puff models describe a continuous emission as a series of discrete packets (i.e.,
5631 puffs) of pollutant material which move independently (Scire et al., 2000). The centre of each
5632 puff moves by advection according to the “local” wind field. The “local” wind field may be, for
5633 example, the wind at the height where the larger puff mass is located or the average wind
5634 speed and direction along the vertical size of the puff.

5635

5636 The effect of atmospheric turbulence is to increase the puff size as it moves. Some
5637 formulations are available to describe the puff growth; they depend typically on the standard
5638 deviation of the wind components, the travel time of the puff and the Lagrangian time scales.
5639 The standard deviation of the wind components may be estimated in different ways
5640 depending on the atmospheric stability conditions.

5641

5642 Puffs are typically spherical; however, sometimes, they may be stretched along the wind
5643 direction. They are named “slugs” in those cases. In near-field applications, when the wind
5644 field is rapidly varying, using slugs is important because it assures the correct calculation of
5645 the concentration fields.

5646

5647 The vertical wind shear across a single puff, when significantly extended along the vertical,
5648 is typically managed by splitting the original puff into smaller puffs by conserving the mass.
5649 This procedure is called “puff-splitting”. Actually, puff splitting may be both along the vertical
5650 and along the horizontal direction (<http://www.src.com/calpuff/FAQ-answers.htm>). Horizontal
5651 puff splitting is needed when the puff becomes very large and covers several meteorological
5652 grid cells. In such a case, a single huge puff would not respond correctly to the cell-to-cell
5653 meteorological variability; therefore, it must be divided into more small puffs. The application
5654 of this procedure is important both in long-range simulations and in simulations over smaller
5655 domains, typical for odour impact studies when the meteorological grid size is kept small to
5656 reconstruct terrain features as precisely as possible. Applying the puff splitting procedure
5657 increases the number of puffs and, therefore, the computational resources required for the
5658 simulation.

5659

5660 Lagrangian puff models have many advantages with respect to the Gaussian plume models.
5661 The main one is the possibility of using three-dimensional time-varying meteorological data
5662 to obtain more realistic concentration fields. Additionally, these models can handle calm or
5663 low-wind conditions, which are important while evaluating odour pollution. For example,
5664 considering the Lagrangian puff model CALPUFF, puffs are not advected by the model
5665 during calm hours. However, they continue to increase their size due to atmospheric
5666 turbulence.

5667 Puff models can simulate a large variety of sources. Considering the sources of interest in
5668 odour applications, they can simulate point sources (e.g., stacks), area sources (e.g.,
5669 biofilters, tanks, and landfill portions) and line sources (e.g., transportation of malodorous
5670 substances and polluted water channels). When point sources are modelled, plume rise

5671 algorithms are activated.

5672

5673 Concentrations at each receptor are due to the sum of the contributions of each puff (e.g.,
5674 De Visscher, 2013; Zannetti, 2013). CALPUFF (Scire et al., 2000), probably the most used
5675 Lagrangian puff model, includes a simple averaging-time scaling factor to estimate short-
5676 term peak concentrations needed in odour modelling. The first method includes a scaling
5677 factor (through the input variable AVET) to adjust the lateral dispersion coefficient, which
5678 means acting on plume meandering. The second method uses the scaling factor directly on
5679 the output concentrations (in CALPOST or any other post processor). In both cases, the
5680 scaling factor used in CALPUFF is constant, depending on a 1/5 power law of the time ratios
5681 (e.g., 60 minute of the output concentration or the Pasquill Gifford averaging time of the
5682 lateral dispersion coefficient, and 1 minute for the averaging time of interest to get the peak
5683 value). This scaling factor of CALPUFF does not depend on the stability conditions or the
5684 puff travel time.

5685

5686 One of the drawbacks of Lagrangian puff models with respect to Gaussian plume models is
5687 the longer time needed to carry out simulations. These additional computational resources
5688 are due to the inherent complexity of the model and the high number of puffs that must be
5689 released to get good concentration fields. The number of puffs may also increase during the
5690 simulation due to puff-splitting, as mentioned above. Additionally, computational times are
5691 longer when area or line sources are used, with respect to emission scenarios involving only
5692 stacks.

5693

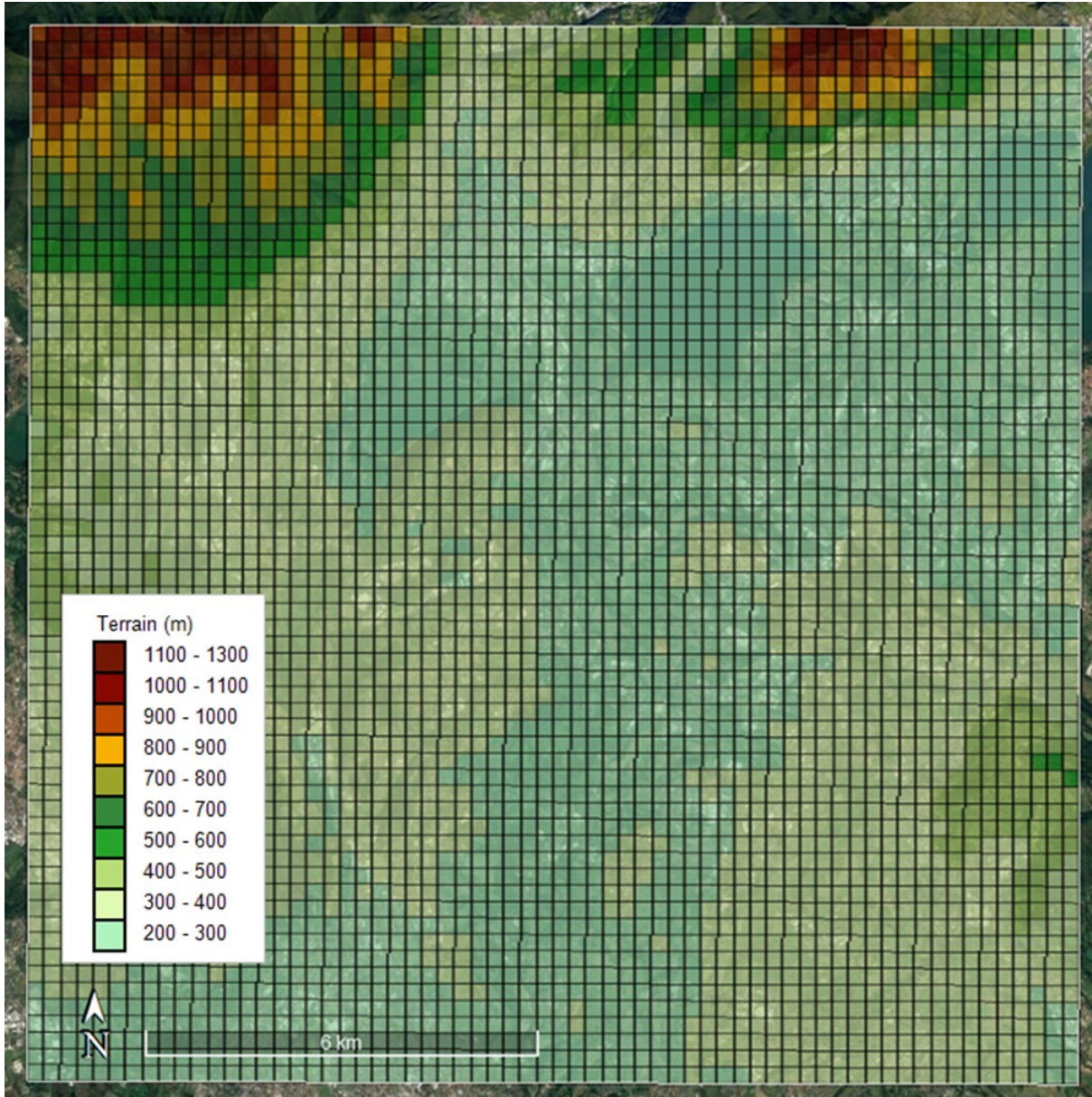
5694 The use of a Lagrangian puff model requires additional resources with respect to a Gaussian
5695 plume model, both in terms of computational time, both in terms of knowledge (more input
5696 data and variables required). Additionally, even though such models can be used with a
5697 single point meteorology as AERMOD or the old ISC3, the best results are obtained only
5698 using a three-dimensional meteorological model (e.g., CALMET), therefore, the user is
5699 required to know how to use it. Also, diagnostic models as CALMET may be fed by the
5700 output of complex prognostic meteorological models (e.g., WRF), which are very difficult to
5701 use, and require huge computational resources (indeed they often require to hire cloud
5702 computational resources, as for example AWS, Amazon Web Services). All this additional
5703 complexity must be justified. Using a Gaussian plume model may be a reasonable choice
5704 when the simulation must be carried out over an almost flat domain with practically no calms.

5705

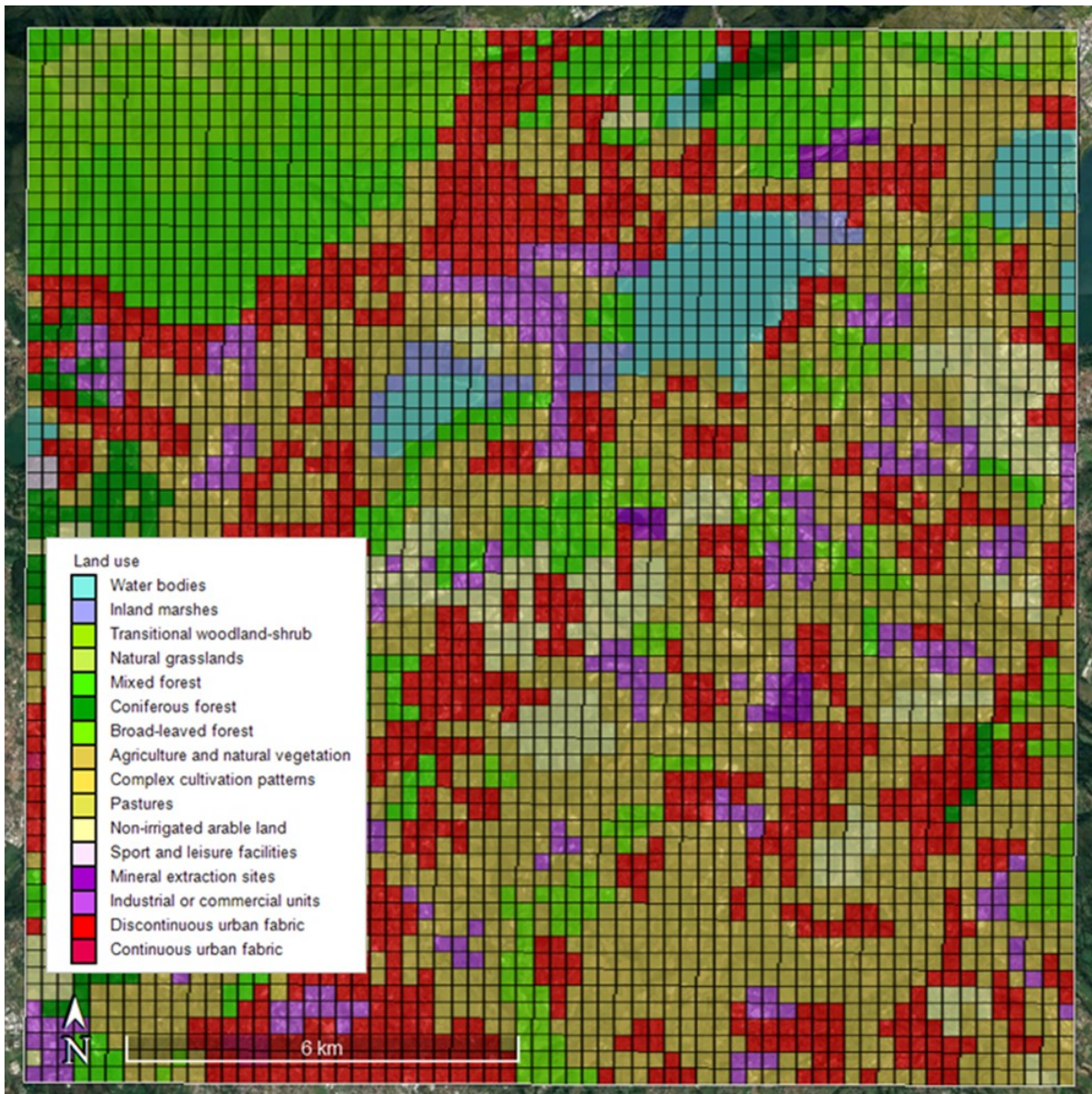
5706 As mentioned, an additional difficulty in using Lagrangian puff (and particle) models is
5707 related to preparing the meteorological field. Practical problems must be faced and solved.
5708 For example, the user must decide which grid resolution can describe the terrain features
5709 within a complex terrain domain without requiring many computational points. A practical
5710 suggestion in these cases is to describe each terrain feature with 5/10 grids (e.g.,
5711 <http://www.src.com/calpuff/FAQ-answers.htm>). For example, if the width of a valley is 2 km,
5712 the user should use a meteorological grid size ranging from 400 m to 200 m.

5713 Of course, once the domain and grids of the meteorological model are defined, the average
5714 terrain elevation over each grid must be determined. The original (raw) terrain data must
5715 have a spatial resolution equal to or higher than the grid resolution. For example, the SRTM
5716 (*Shuttle Radar Topography Mission*) data may be used for practically any domain in the
5717 world (<https://srtm.csi.cgiar.org/srtmdata/>). The same operation must be performed for the
5718 land use data. The land use over each grid must be defined as the prevailing one, not the

5719 average one as for terrain. For example, the original (raw) land use data for the European
5720 territory may derive from the CORINE Land Cover project ([https://land.copernicus.eu/pan-](https://land.copernicus.eu/pan-european/corine-land-cover)
5721 [european/corine-land-cover](https://land.copernicus.eu/pan-european/corine-land-cover)). A final check must be done to evaluate the correctness of the
5722 gridded values of terrain and land use, for example, using tools such as Google Earth. An
5723 example of a terrain map averaged over the grids of a simulation domain and superimposed
5724 on Google Earth is shown in Figure 5-16. Similarly, Figure 5-17 shows the general land use
5725 over the same domain.
5726



5727 **Figure 5-16** Example of average terrain elevation over a 16x16 km² domain with 250 m grid
5728 size (Courtesy of Enviroware).
5729
5730
5731



5732
5733 **Figure 5-17** Example of prevailing land use over a 16x16 km² domain with 250 m grid size
5734 (Courtesy of Enviroware).

5735
5736 When preparing the meteorological field with a diagnostic model such as CALMET,
5737 particular attention must be paid to the quality of the surface and upper air input data quality.
5738 For each hour of simulation (assuming for simplicity simulations with 1-hour resolution), each
5739 meteorological variable must have a valid value at least in one surface station; otherwise,
5740 the model stops the simulation with an error message. This means that the user must check
5741 the quality and validity of the input data and, if needed, define a procedure to recover the
5742 missing values. When missing values are sparse, scalar variables (e.g., temperature,
5743 precipitation, relative humidity) may be recovered simply by averaging the values containing
5744 the missing data, or by repeating the last valid value.

5745
5746 The same procedure may be adopted for wind speed and direction, even though the
5747 situation is a bit more complicated (for example, it must be decided if a scalar or a vector
5748 average must be performed). When the missing values are continuous for a relatively long
5749 time, if there are no other stations with valid data for that period, a possible option is to

5750 create a pseudo station, possibly close to the borders of the simulation domain, starting from
5751 the output of a prognostic model such as WRF.

5752

5753 The situation is even more difficult when the missing data involve vertical profiles. Vertical
5754 profiles are typically available twice daily, and a single upper air station is often used in
5755 simulations. Sometimes a full vertical profile is missing, and it could be replaced, for
5756 example, by the vertical profile of the same time of the previous day. When the output of a
5757 prognostic model is used in the input, the vertical profile issue is automatically solved.

5758 5.5.3.2 Lagrangian particle models

5759 Lagrangian Particle Dispersion Models (LPDMs) offer some general advantages compared
5760 to Gaussian Plume and Puff models but show at the same time some specific shortcomings
5761 that should be taken into account. The main advantages are related to their intrinsic
5762 capability to describe pollutant dispersion three-dimensionally. Particles can move with
5763 continuity throughout the computational domain, and the three-dimensional distribution of the
5764 particles allows, in principle, a detailed description of the dispersion phenomena everywhere
5765 in the PBL. This capability overcomes all previously described spatial problems for the
5766 Gaussian Plume and Puff Models (e.g., the need to activate puff splitting procedures when
5767 the puff becomes too big).

5768

5769 On the other hand, this evident advantage requires a detailed description of the
5770 meteorological conditions necessary to drive a dispersion simulation, particularly turbulence.
5771 The difficulties related to preparing three-dimensional non-stationary meteorological fields
5772 are the same described for the Lagrangian puff models in the previous paragraph.

5773

5774 Some of the turbulence variables required by LPDMs, such as Lagrangian time scales, are
5775 difficult to measure and are not directly calculated by the closure schemes of the turbulence
5776 used by the meteorological driving models. Another critical point of LPDMs is related to the
5777 statistical dependence of their results. The implementation of the stochastic differential
5778 equations inside such models implies the use of random numbers and the use of discrete
5779 numerical samples from theoretical distributions. This sampling methodology, typical of all
5780 the Monte-Carlo methods, tends to generate final results in terms of concentration fields that
5781 are not strictly unique. A different sequence of numbers extracted from the same distribution
5782 generates different results in a way that could be erroneously assimilated to the statistical
5783 behaviour of the atmospheric turbulence, being instead a consequence of the numerical
5784 sampling. This implies a greater difficulty in the operations of a simulation setup to minimise
5785 this problem with respect to simpler models involving analytical formulations. This implies
5786 finding a tradeoff between the number of particles used to discretise the source emissions
5787 and the quality of the simulation. Sometimes, this can be in contrast with the available
5788 computational tools. Nowadays, this problem is minimised by the wide availability of parallel
5789 computers and the possibility of finding parallel operational LPDMs easily.

5790

5791 Finally, LPDMs share the same problem with other modelling methodologies. Being only
5792 able to describe the trajectories of independent particles, they can only deal with average
5793 ensemble concentrations, showing an intrinsic difficulty in describing peak values. Ad-hoc
5794 algorithms need to be added as post-processing tools to compute Peak-to-Mean Ratios to
5795 be applied to the expected results of such models.

5796

5797 5.5.4 Eulerian models

5798 5.5.4.1 Eulerian grid models

5799 Eulerian grid models suffer the disadvantage that their resolution is confined by the spatial
5800 discretisation of the mesh on which they are solved. The use of the mesh is computationally
5801 expensive and requires some form of optimisation to achieve any degree of efficiency. As
5802 the focus of odour analysis is mainly in the near-field of the source, this approach is not
5803 generally applied for odour modelling purposes.

5804
5805 Eulerian grid models have the following limitations for odour assessments:

- 5806 ● Odour sources cannot be adequately described due to their mesh size. The pollutant
5807 is immediately spread in the whole grid containing the source, and this is not
5808 acceptable for odour, which is typically a short-range problem.
- 5809 ● Due to the typical size of their grid cells, Eulerian models struggle to form a
5810 continuous plume in the near field, and odour assessments are mostly near-field
5811 issues.
- 5812 ● They do not include near-field algorithms like building downwash or stack tip
5813 downwash.
- 5814 ● They are computationally inefficient and slow, especially in complex terrain areas
5815 where small grid cells are required to capture the resolution of the terrain.
- 5816 ● They only provide mean concentrations and cannot consider concentration
5817 fluctuations, which is important for odour.

5818 5.5.4.2 CFD models

5819 In principle, CFD models could be reliable tools to assess odour pollution due to the ability to
5820 take into account the impact of many types of obstacles such as buildings, plant structures,
5821 and trees on a micro-scale explicitly. However, due to the following drawbacks, CFD models
5822 are more commonly used in research rather than for regulatory purposes:

- 5823 ● The preparation of the computational grid can be challenging and requires
5824 considerable time.
- 5825 ● The computational time of the simulation is significantly higher than for other, less
5826 complex models.
- 5827 ● They are typically used to assess a specific meteorological situation (e.g. neutral
5828 atmospheric conditions, a specific wind direction, or a given temperature value).
- 5829 ● The application of a modelling tool is finalised to calculate concentration percentiles
5830 over a whole year.
- 5831 ● The model set-up is complex, and the user choice of boundary conditions and grid
5832 resolution can easily influence the outcome.

5833
5834 In some cases, the wind field near the source is modelled using CFD. This micro-scale wind
5835 field is then inserted into a Lagrangian model to assess the odour dispersion in the impact
5836 area. This has the advantage of short computational time, and the meteorological conditions
5837 can be better estimated by a specific situation for a small area compared to modelling the
5838 whole impact area.

5839

5840 5.6. Which model or type of model is suitable for odours?

5841 5.6.1 General Introduction

5842 This paragraph briefly summarises the types of air dispersion models which are more
 5843 suitable for odour assessment. According to what has been written, Eulerian grid models are
 5844 not commonly used and suitable for odour assessment in few situations. Additionally, while
 5845 on the one hand, CFD models are a powerful tool to describe odour dispersion in a complex
 5846 environment for a specific meteorological situation, on the other hand, they cannot be
 5847 applied for regulatory purposes (i.e., a minimum of a 1-year long simulation) due to their
 5848 high-demanding computational resources. Therefore, only Gaussian models (e.g.,
 5849 AERMOD, ADMS, ISCST3, CTDMPPLUS, AUSPLUME, SCREEN) and Lagrangian models
 5850 (e.g., CALPUFF, SCIPUFF, SPRAY, AUSTAL, LAPMOD) will be considered in this
 5851 paragraph.

5852 5.6.2 Key features affecting odour dispersion and model types

5853 A summary of the key features affecting odour dispersion for each model type (Gaussian
 5854 and Lagrangian) is reported in Table 5-6.

5855 5.6.2.1 Time and space causality effects due to the meteorology, including land use 5856 effects, recirculations, coastal or mount/valley breeze

5857 Gaussian plume models do not consider causality effects, and their plumes immediately
 5858 extend in a straight line to infinity (see, for example, Figure 5-1). Lagrangian puff and particle
 5859 models allow full causality effects; they allow curved and variable trajectories. In principle,
 5860 Lagrangian particle models are even better than Lagrangian puff models because they do
 5861 not need the activation of particular algorithms (e.g., puff splitting) to follow precisely the
 5862 atmospheric flow along the vertical or the horizontal direction.

5863 5.6.2.2 Spatial characteristics of the surface

5864 Gaussian models can partially consider the surface variability of the domain. For example,
 5865 AERMET, the meteorological processor of AERMOD, uses values of geophysical variables
 5866 averaged along different directions up to a certain distance from the surface meteorological
 5867 station. The AERSURFACE processor determines these average values.

5868
 5869 Additionally, AERMOD can carry out simulations in moderately complex terrain but can only
 5870 simulate the impingement of the plume on the ground. At the same time, the flow is not
 5871 affected by the terrain features.

5872
 5873 On the contrary, the meteorological processor of the three-dimensional Lagrangian models
 5874 contains information about terrain elevation and land use (then geophysical variables) in
 5875 each grid cell (as shown, for example, in Figure 5-16 and Figure 5-17).

5876 5.6.2.3 Calm winds and mass accumulations

5877 Odour nuisance may be maximum under calm wind conditions; therefore, it is essential to
 5878 describe those situations as precisely as possible. Gaussian models cannot handle wind
 5879 speeds tending to zero because, as previously shown, they have wind speed at the

5880 denominator in their basic formulation.

5881

5882 Lagrangian puff and particle models can handle calm wind situations. For example,
5883 CALPUFF switches from distance-dependent to time-dependent sigmas at user-defined
5884 minimum wind speed.

5885 5.6.2.4 Obstacles/buildings (explicitly simulated or parameterised)

5886 CFDs can treat the presence of obstacles explicitly and modify the atmospheric flow.
5887 However, as written above, they are not suitable for regulatory purposes.

5888

5889 Gaussian models can treat obstacles (buildings and other structures opaque to the wind) in
5890 a parameterised way. This is the case, for example, of the building downwash algorithms.
5891 Some Lagrangian particle dispersion models have been developed to work at the
5892 microscale, considering a horizontal resolution of a few metres and explicitly treating the
5893 presence of obstacles. This is the case, for example, of PMSS, QUIC, GRAL and LASAT.

5894 5.6.2.5 Short-range/ Long range Simulations

5895 Odour assessment is typically a short-range issue. Both Gaussian and Lagrangian models
5896 have features capable of describing short-range effects, such as, for example, building
5897 downwash, stack tip downwash and plume-induced turbulence.

5898

5899

5900 **Table 5-6** Key features which affect odour dispersion by model type

Feature	Gaussian Plume Models	Lagrangian Puff and Particle Models
Causality effects considered	No causality effects, plumes extend in a straight line to infinity immediately	Full causality effects, allows curved and variable trajectories
Spatial variability of surface characteristics (land use)	Land use variability allowed in wind sectors centred over the met station	Land use and parameters (Bowen Ratio, Z_0 , albedo) vary with each grid cell across model domain
Spatial variability of meteorological variables (wind speed, wind direction, temperature)	None, single station and uniform meteorological variables	Full spatial variability of meteorological and turbulence variables
Ability to treat calm winds	Cannot handle a zero-wind speed, minimum wind speed must be set else model will skip over calm hours	Models can handle calms. [e.g., CALPUFF switches from distance-dependent sigmas to time-dependent sigmas at user-defined minimum wind speed]
Mass accumulation under stagnation conditions	Unable to handle stagnation or accumulation of pollutant mass	Retains previous hours emissions and will allow accumulation under stagnation events

Memory of previous hours emissions or meteorology

No memory, each hour and emission rate are treated independently of previous hour

Full memory

Coastal effects, and recirculation

None, or very limited

These more advanced models are linked to advanced 3D diagnostic and prognostic meteorological models so include the ability for TIBL calculations and 3D sea and land breeze

5901

5902

5903

5904

5905 5.7. Model validation in the frame of odour applications

5906 Model validation is a fundamental phase in developing and using mathematical models –
5907 both analytical and numerical - because it allows for determining the model's reliability. In
5908 principle, validation can be divided into three steps:

- 5909 • Theoretical validation, which means to verify if all the physical and chemical
5910 equations needed to describe a specific problem have been considered in the
5911 mathematical model.
- 5912 • Validation of the implementation phase (or code verification), which means verifying if
5913 possible approximations or simplifications introduced in the original equations to
5914 solve them (analytically or numerically) are acceptable. In the case of a non-
5915 analytical solution, the numerical method must guarantee accuracy and a reduced
5916 numerical error. Finally, the correct implementation of the resulting model into a
5917 computer code must be evaluated and tested. The correct implementation can be
5918 verified by accessing the code and checking how the model algorithms are written
5919 (for open-source models). Testing can be done by applying the so-called sensitivity
5920 analysis, which evaluates if model output varies in agreement with model input.
5921 Sensitivity analysis can also be used to implicitly verify the model implementation
5922 when its code is not accessible.
- 5923 • Comparison of model predictions against observations. Typically, the term
5924 “validation” or “plausibility check” is used only for this phase, even though – strictly
5925 speaking - it must include the previous two.

5926 Validating an atmospheric dispersion model requires handling at least three sets of data:

- 5927 1. concentration and deposition time series at specific receptors of known coordinates,
- 5928 2. source and emission characteristics and
- 5929 3. meteorological fields.

5930 For air quality (AQ) applications, many datasets are available for validating models in
5931 different conditions: almost flat terrain (e.g., Kincaid, 1983), complex terrain (e.g., Martin's
5932 Creek, (Dresser, 2011)), and urban environment (e.g., Indianapolis, (Murray, 1988)).

5933 Datasets that provide information on varying source terms (e.g., Oklahoma City, (Allwine,
5934 2004) and the case studies of (COST ES1006, 2015a) to validate time-dependent features
5935 are also available for AQ models. These datasets for validating the AQ models are often
5936 based on the release of SF₆ (sulfur hexafluoride), as in the Kincaid and Indianapolis
5937 experiments. The SF₆ environmental background is very low because it is produced
5938 industrially; it does not exist in nature. For those field experiments, concentration time series
5939 at several receptors are available. On the contrary, when the pollutant of interest is odour –
5940 not an odorous pollutant such as H₂S, but the odour – concentration time series are not
5941 available since odour measurement in the field is a complicated task (e.g., Bax, 2020; Conti,
5942 2020; Capelli, 2013), and detailed emissions are practically never available. An additional
5943 problem with the validation of odour dispersion models is that odour is ubiquitous (e.g.,
5944 Chacko, 2020), and its measurement at a specific position cannot be associated with the
5945 emission of interest, particularly when the distance from it increases. Another challenge is
5946 that odour at the emission level is typically measured using human panel members, and
5947 therefore the measurement is associated with great variation (e.g., Klarenbeek, 2014;
5948 Hansen, 2016). Indeed, due to the physiological nature of odour measurements with
5949 dynamic olfactometry, even with trained panel members, the results are not as precise (i.e.,
5950 repeatable) and reproducible (i.e., they may have high inter-laboratory variance) as they
5951 would be with an analytical measurement technique. A great help in odour field
5952 measurements could arrive from IOMSs (e.g., Borowik, 2020), but additional work must be
5953 done to consider them reliable operational devices.

5954 Concerning the second point (emissions), validation data for AQ models are often related to
5955 a stack's emissions, and source characteristics and emissions variables are precisely
5956 measured, even for relatively long periods. For example, emission rates, exit temperature
5957 and exit velocity may be available with a 1-hour time resolution for several days. On the
5958 contrary, odour concentrations (in terms of ou_E/m³) within a stack are not measured
5959 continuously; in practical applications, a single observation must be used for emissions
5960 related to relatively long periods. Additionally, quite often, the odour source is not a stack but
5961 (e.g.) a pond, a tank, or a building (e.g., a stable), and the emission rate is a function of
5962 meteorological variables as well as other variables (e.g., the internal temperature of the
5963 stable, see for example (Angrecka, 2014).

5964 Further general difficulties of field experiments include obtaining data that characterise the
5965 site's meteorological conditions and the results' limited statistical representativeness due to
5966 the changing boundary conditions, such as wind speed and direction. On the other hand,
5967 nowadays, the meteorological data needed to feed a dispersion model should not be a
5968 problem. In urban areas, where odour-related problems may be important due to their impact
5969 on many inhabitants, weather stations are often available (even if not always representative).
5970 In any case, even in rural areas and without weather stations, the meteorological fields
5971 needed to validate the model can be reconstructed with great accuracy using modelling
5972 chains, such as, for example, WRF-CALMET (e.g., Skamarock, 2008; Scire, 2000a). Even
5973 the (US-EPA, 2017) recognises the possibility of the “use of prognostic meteorological data
5974 for areas where there is no representative NWS (National Weather Service) data, and it is
5975 infeasible or prohibitive to collect site-specific data”.

5976 Considering what has been reported above, and adding that the time interval of odour
5977 concentrations is very short (i.e., the time of a single breath, about 10 s) when compared to

5978 AQ concentrations (typically 1 hour), it is clear that validating an odour dispersion model is
5979 quite complicated and presents several uncertainties. However, validation remains a task to
5980 be done in many cases.

5981 Datasets based exclusively on the release of inert tracers (e.g., SF₆) will not be discussed in
5982 the following chapters because they are essentially those used for AQ model validation,
5983 briefly mentioned above. Additional information about those experiments can be found in
5984 (Capelli, 2013) and (Onofrio, 2020).

5985 5.7.1. Examples of validation with odour measurements

5986 A dataset available for validating odour models is the one related to the Uttenweiler
5987 (Germany) field experiment (Bächlin, 2002; Bächlin, 2003; Aubrun et al., 2004; Souza et al.,
5988 2014; Oetli, 2020a). The dataset has been used by Brancher et al. (2020b) to evaluate three
5989 approaches to predict sub-hourly odour peak concentrations, from a simple constant Peak-
5990 to-Mean Ratio to more complex ones. As Brancher et al. (2020b) described, the dataset has
5991 been obtained by releasing odour and SF₆ from a point source within a pig farm. The site is
5992 almost flat, with cultivated fields surrounding the farm and a small forest north of the barn.
5993 The barn comprised two buildings, respectively, 7.65 and 10.65 metres high. The smaller
5994 one had two stacks of 8.5 metres of height connected to the internal ventilation systems.
5995 Only one of the stacks was used in the experiment. Two releases have been carried out, one
5996 in December 2000, and one in October 2001, for 14 valid trials. Small volumes of SF₆ tracer
5997 and odorant gas were released in parallel during each experiment. Odour levels were
5998 measured with a 10-minute sampling time by up to 12 persons with certified odour
5999 perception capabilities positioned in one or two lines perpendicular to the wind direction. At
6000 the same time, 10-minute SF₆ concentrations were measured. Moreover, fast response
6001 concentration measurements (0.1 Hz) of SF₆ were performed at two receptors at the
6002 position of two persons breathing odour. A sonic thermo-anemometer made measurements
6003 of temperature, wind speed and direction every 10 seconds. All experiments had enough
6004 cloud coverage to prevent turbulent conditions, and the wind speeds were sufficiently high.

6005 (Hoff, 2006) performed a field experiment by measuring the odour released from a deep-pit
6006 swine finishing facility located in Iowa (USA) in a rural environment characterised by flat
6007 terrain. Meteorological variables were simultaneously measured using an on-site weather
6008 station. From June to November 2004, odour emission and concentration data downwind
6009 from the source were collected in three intensive sessions characterised by twelve
6010 atmospheric conditions. They placed two panel members at the four grid points at different
6011 downwind distances. Each panellist used a Nasal Ranger field olfactometer. Moreover, both
6012 at source and at grid points, two 10-litre Tedlar bags were collected for dynamic dilution
6013 olfactometry. Each measure was characterised by two 10-minute samplings 15 minutes
6014 apart.

6015 (Yu, 2011) described the application of a *Livestock Odour Dispersion Model* (LODM) and its
6016 comparison against field measurements collected by the University of Manitoba (Zhang,
6017 2005) from June to August 2004. The measurements were performed around two swine
6018 farms in Manitoba (Canada) in a flat cropland with a roughness length of 0.1 m. Both two
6019 farms were characterised by ventilated barns. Along with the odour field measurements,
6020 odour emission rates were also measured. The field measurements were done by fifteen

6021 trained sniffers positioned on a three-row grid at 100 m, 500 m and 1000 m downwind from a
6022 fixed point. Measurement sessions were 10 minutes long, and the odour was sniffed for 10
6023 seconds. A total of 129 measurement sessions were conducted, 100 during the daytime.
6024 During each session, weather data were also collected at 2 m above ground level with a time
6025 resolution of one minute.

6026 (Ranzato, 2012) used the CALPUFF dispersion model and the field inspection technique
6027 (VDI 3940, 2006) to quantify the odour impact due to the operation of a municipal solid
6028 waste (MSW) plant located in northeastern Italy. Even though their intention was not to
6029 validate the model but to highlight the differences between the two methods to evaluate
6030 odour impact, their results gave useful information about the model's performance. The
6031 frequency of odour episodes was evaluated over the same 6-month period (July 2009 -
6032 January 2010) with the model and field inspection. An inspection grid was defined starting
6033 from citizen complaints and prevailing wind; it was composed of 48 measurement points with
6034 a distance of about 250 m, one from the other. Fourteen trained assessors conducted a
6035 series of visits to the inspection grid, and each grid point was visited 26 times by different
6036 assessors. At each point, the assessor sniffed the ambient air every 10 s over 10 min and
6037 recorded the perceived odour. In this way, odour hours (when the odour is perceived for at
6038 least 10% of its duration according to (VDI 3788, 2000) were defined with field inspection.
6039 With CALPUFF, odour hours were determined as those where the peak concentration (i.e.,
6040 the value obtained by multiplying the 1-hour average concentration by the Peak-to-Mean
6041 Ratio) was higher than one ou_E/m^3 . The frequencies of odour hours were then compared
6042 both qualitatively and quantitatively. The qualitative comparison was made by observing the
6043 frequency isolines obtained with the two methods. In contrast, the quantitative comparison
6044 was made at the discrete receptors (i.e., field inspection points) through different statistical
6045 parameters (Nash-Sutcliffe model efficiency, mean absolute error, root mean square error,
6046 mean absolute relative error). The authors found a satisfying agreement between model
6047 results and field inspection data. However, while the spatial extension of the odour was
6048 similar according to the model and observations (qualitative comparison), the frequency of
6049 odour episodes was sometimes different (quantitative comparison). For example, CALPUFF
6050 underestimated the peak concentrations close to the plant, possibly due to missing fugitive
6051 emissions among its sources.

6052 (Yeo, 2020) simulated with a CFD (computational fluid dynamics) the odour emitted by a pig
6053 farm in South Korea within an area of complex terrain. Odour samples were conducted
6054 simultaneously at different locations using a portable air sampler inside and outside the pig
6055 houses. All measuring devices were located 1.5 m high from the ground surface. Four
6056 sampling locations were used outside the pig houses, the first one positioned at the farm's
6057 boundary and the farther one at 140 m from it. The distance between each sampling location
6058 was about 40/50 m. Odour sources (ventilation from the pig houses) and emissions are
6059 described in the paper; therefore the data could be used for model validation.

6060 5.7.2. Data from physical modelling experiments

6061 Data obtained from physical experiments, such as from wind tunnels, may be important to
6062 create datasets for odour model validation. Data obtained from those experiments must be
6063 converted to full scale in order to be used. The advantages of physical experiments are the
6064 controllable boundary conditions and the statistical representativeness of the results. For

6065 example, (Aubrun, 2002) replicated the work of (Bächlin, 2002) (Bächlin, 2003) with neutral
6066 tracer gas experiments within a 1:400 scale physical model in a wind tunnel. Several
6067 parameters influencing odour dispersion were varied during the experiment:
6068 presence/absence of terrain, different wind directions, different ratios between the velocity of
6069 the ventilation stack and reference wind speed, and two stacks working independently or
6070 simultaneously. Concentrations were measured at a height corresponding to 1.6 m full scale.
6071 Time series were collected for over 33 hours with a frequency of 1.25 Hz (both full-scale).
6072 The objective of these researchers was to generate a dataset that should be now available
6073 on the website of Hamburg University. These data have been used by de (Melo, 2012) to
6074 compare CALPUFF and AERMOD results.

6075 5.7.3. Data from social participation

6076 The validation of odour dispersion models can also be done using odour observations
6077 recorded by residents about a specific plant, and the odour emissions estimated for such a
6078 plant. As a minimum, this type of validation allows the evaluation of the ability of a model to
6079 predict odour in specific locations and at specific times, although the evaluation of odour
6080 intensity could be more difficult. An example of this kind of validation is described in (Sironi,
6081 2010).

6082 (Nimmermark, 2005) considered seven livestock farms (swine, cows, turkeys) located in
6083 Minnesota (USA) and compared the predictions of the Gaussian puff model INPUFF2 and
6084 the observations of odour intensities at twenty neighbourhood residences. In order to
6085 characterise the emissions, odour samples were collected from each animal housing facility
6086 and each manure storage unit at each farm. The neighbourhoods were trained to identify
6087 odour intensity on a 5-level intensity scale, from “none” to “extreme”. After removing the
6088 odour observations not in agreement with wind direction, 309 valid observations remained.
6089 There was a good agreement between predicted and observed odour intensity. The
6090 frequency of odour episodes was not considered in this study.

6091 (Haeger-Eugensson, 2014) evaluated allergens and odours emitted by horse stables with
6092 forced ventilation in Sweden. 102 persons of different ages were randomly selected near the
6093 riding school stable to evaluate the presence of odour. They simulated the ammonia
6094 emissions from the stable using the ADMS model (Carruthers, 1993), where ammonia was
6095 used as a tracer for odour. The authors found that the ammonia concentration was well
6096 below its odour detection threshold at all distances where people sensed odour. They
6097 concluded that odour could be due not only to ammonia but also to the presence and
6098 combination with other odorous species.

6099 More recently, (Zhang, 2021) described the application of the CALPUFF model (Scire,
6100 2000b) for simulating odour emissions from a Waste Water Treatment Plant (WWTP)
6101 located in the region of Tianjin (China). A total of 126 persons randomly selected from the
6102 residential areas around the plant were interviewed to gather information about the influence
6103 of the WWTP odour emissions on their life. They were asked questions about the degree of
6104 perceived odour intensity, degree of perceived odour annoyance, time of occurrence, and
6105 season. The questionnaires provided discrete results. For example, odour intensity was on a
6106 6-point scale (0 for no odour, 1 for very faint strength, ..., 5 for very strong strength), while
6107 annoyance was on a 5-point scale (0 for not annoyed, ..., 4 for extremely annoyed). The

6108 results of the questionnaires were related to the CALPUFF odour estimations through
 6109 binomial logistic regression models, and statistical parameters evaluated the predictive
 6110 ability.

6111 Diaz et al. (2016) compared the results of the odour impact of an animal by-product
 6112 rendering plant predicted with CALPUFF using WRF meteorology forecast data with those of
 6113 real citizen observations. Previous data analysis of this plant using this technology did not
 6114 show a good agreement (Cartelle et al. 2014). Therefore, the aim was to examine different
 6115 approaches to improve the results. After 10 months, the results showed that the optimum
 6116 level to consider a forecasted result as an odour incident was 2.1 ou_E/m³. The system was
 6117 able to adequately forecast only 41.2% of the incidents. The use of peak-to-mean ratios
 6118 improved the results. The use of a higher WRF resolution did not have any effect on the
 6119 results.

6120

6121 5.7.4. Evaluation of model performances

6122 The model results and the evaluation measures selected for model validation depend on the
 6123 investigated model and the available validation data set. Various modelling results, such as
 6124 odour concentration, various percentiles, frequency, duration, and separation distances, can
 6125 be considered for model validation.

6126 Commonly used performance measures and acceptance criteria for AQ models are
 6127 described, for example, in (Chang, 2004) and (Mosca, 1998). The comparisons apply
 6128 qualitative as well as quantitative methods to evaluate the ability of AQ models to reproduce
 6129 the observations. A scatter plot of the measured vs modelled results is a common qualitative
 6130 comparison to evaluate model performance. The following primary quantitative measures
 6131 are typically applied for model evaluation:

6132 Fractional mean bias:

$$6133 \quad FB = \frac{2(C_o - C_p)}{C_o + C_p}$$

6134 Normalised mean-square error:

$$6135 \quad NMSE = \frac{(C_o - C_p)^2}{C_o C_p}$$

6136 Geometric mean:

$$6137 \quad GM = \exp\left(\frac{\ln(C_o) + \ln(C_p)}{2}\right)$$

6138 Geometric variance:

$$6139 \quad GV = \exp\left(\frac{\ln(C_o) - \ln(C_p)}{2}\right)^2$$

6140 Fractions within a factor of two:

6141 fraction where $0.5 < \frac{C_p}{C_o} < 2$.

6142 In the formulae above C_p represents the model predictions and C_o the observations. (Hanna,
6143 2012) provide separate acceptance criteria for AQ models for rural and urban settings.
6144 Further, less commonly applied model evaluation measures for AQ models, such as the
6145 correlation coefficient, factor of exceedance, index of agreement, normalised absolute
6146 difference and figure of merit in space, can be found, for example, in (COST ES1006,
6147 2015b). These performance measures and their criteria can be applied to time-averaged and
6148 time-dependent dispersion characteristics.

6149 Many of the above-mentioned and further statistical parameters used for AQ models can
6150 also be applied to odour models when both estimated and observed values are available.
6151 For example, (Wu, 2019) applied root mean square error, relative absolute error (Benett,
6152 2013) and the Nash-Sutcliffe model efficiency (Nash, 1970) to evaluate the performance of
6153 AERMOD (Cimorelli, 2003) and (VDI 3894-2, 2012) to predict separation distances.

6154

6155 5.7.5. Final remarks

6156 Validation is a fundamental phase to estimate an atmospheric dispersion model's reliability
6157 and gain confidence in it. It is a complicated task for air quality dispersion models and, for
6158 the reasons explained in this paragraph, an enormous effort for odour models.
6159 Notwithstanding its complexity and cost, preparing reliable datasets, including
6160 meteorological data, emission characterisation, and ambient odour concentrations, would be
6161 important for odour modelling science. As mentioned at the beginning of the paragraph,
6162 many such datasets are freely available for validating air quality models, but no datasets are
6163 available for validating odour models. Two noticeable exceptions are the datasets of
6164 (Bächlin, 2002) and (Aubrun, 2002), but the datasets are not openly available and accessible
6165 on the Internet.

6166 5.8. A window open on the research

6167 One of the main problems connected with using dispersion models to describe the odour
6168 impact is related to the intrinsic characteristic of the odour itself. The sensation of olfactory
6169 nuisance occurs during normal respiratory activity. Without going into details, the respiratory
6170 act of an individual periodically conveys air taken from the external environment into his
6171 respiratory system and puts it in contact with the human olfactory system. The latter
6172 analyses the air from the external environment and determines its hedonic degree, which
6173 can be pleasant or unpleasant. In the latter case, we are faced with a sensation of smell
6174 sensation, an olfactory nuisance. Since any human respiratory act occurs at a relatively high
6175 frequency, approximately every less than 5 seconds, it follows that the sensation of olfactory
6176 nuisance represents an event that needs, in principle, to be described at such a high
6177 frequency. It is hence necessary to have available dispersion algorithms able to describe
6178 events occurring in a way close to being "instantaneous" or, in other words, representing the

6179 peak events represented by peak concentrations.

6180

6181 All the dispersion algorithms and models previously described in this chapter and currently
 6182 used for odour applications have mainly been derived and designed for their application in
 6183 the frame of air quality. For this purpose, the request to describe peak concentrations was
 6184 not very stringent except for specific cases (dispersion of toxic or potentially explosive
 6185 substances, for example). On the other hand, standard dispersion models are built to obtain
 6186 average concentrations. To tackle this issue, some ad-hoc algorithms have been developed
 6187 to parameterise or derive from the average concentration the peak values needed to better
 6188 describe the odour impact. These parameterisations are often part of the dispersion tools
 6189 used for odour applications and justify their use in this framework. At the same time, the
 6190 research is currently moving to study and develop new tools to address the problem more
 6191 directly and physically better. The scope of this section is to give a general description of the
 6192 new methods under development, opening a window on what could be the core of the new
 6193 dispersion algorithms that could be adopted in the future. This is not meant to be a detailed
 6194 description but only a general touch to solicit the possible interest of the reader and to give
 6195 the flavour of each new modelling approach, leaving the details inside the associated cited
 6196 bibliography. Although in many cases well developed and accompanied by a substantial
 6197 bibliography, all these new methods do not yet find direct applications and development in
 6198 widely used and consolidated models.

6199

6200 The following four different approaches are taken into account:

- 6201 1. Dissipation of the concentration variance
- 6202 2. Fluctuating plume
- 6203 3. Micromixing model
- 6204 4. Two Particles Lagrangian Dispersion Models

6205

6206 Each method describes concentration peaks, either directly calculated or statistically derived
 6207 from the moments of the concentration distribution simulated by the equation of the adopted
 6208 scheme. What follows is a general description of each approach, together with some useful
 6209 references to get all the related details.

6210 5.8.1. Dissipation of the concentration variance

6211 Supposing that the instantaneous concentration C can be described as:

6212

$$6213 C = \underline{C} + c$$

6214

6215 Where \underline{C} represent any possible average (time or ensemble) value and c a fluctuation, it is
 6216 possible (Stull, 1988; Sorbjan, 1989; Tampieri, 2017) to write an Eulerian differential
 6217 equation for the conservation of the average concentration

6218

$$6219 \frac{\partial \underline{C}}{\partial t} + \underline{U}_j \frac{\partial \underline{C}}{\partial x_j} = S_c - \frac{\partial \underline{U}_j C}{\partial x_j}$$

6220 where S_c represents the source term for the concentrations.

6221 From this differential equation and other considerations related to a Reynolds decomposition
 6222 for both the flow and concentrations, the following differential equation, which describes the
 6223 spatial distribution and temporal evolution of the variance of the concentration fluctuation,

6224 can be written
6225

$$6226 \quad \frac{\partial c^2}{\partial t} + U_j \frac{\partial c^2}{\partial x_j} = \dot{c} - 2u_j c \frac{\partial C}{\partial x_j} - \frac{\partial u_j c^2}{\partial x_j} - 2\epsilon_c \dot{c}$$

6227

6228 This last equation could be, like the previous one, directly numerically solved considering
6229 both specific methods for the closure and appropriate initial and boundary conditions,
6230 leading to a complex model that is requiring a too big computational effort in the typical
6231 simulation conditions required for odour applications. The idea is to find suitable
6232 approximations of the equations to be adapted inside relatively standard modelling tools
6233 such as Gaussian plume and Lagrangian Particle dispersion models. Once a simplified
6234 solution for c^2 is given, it is possible, supposing a given form of a statistical distribution for C
6235 described by the first two moments (such as a Gamma or Weibull), to estimate any other
6236 moment or percentile. A definition of the peak concentration can be derived from the higher
6237 percentiles of the distribution, such as the 95th or 98th.

6238 References for the application of such methods inside Gaussian plume models can be found
6239 in Wilson et al. (1982a,b, 1985) and in Lofstrom et al. (1995). In these works, the spatial and
6240 temporal distribution of the concentration variance for a gaseous substance is represented
6241 as an equivalent diffusion process from the “source of variance” characterised by a certain
6242 emission rate.

6243

6244 The implementation inside a Lagrangian Particle Dispersion model of the computation of the
6245 concentration variance can be found in Manor (2014), Ferrero et al. (2017) and Oettl and
6246 Ferrero (2017). More recently, this methodology has also been implemented into the SPRAY
6247 Lagrangian Particle Dispersion Model, as presented at the NOSE 2020 international
6248 conference.

6249

6250 5.8.2. Fluctuating plume

6251 Suppose to consider the emission of a passive substance, in this case coloured in violet, as
6252 documented in the photographic sequence reproduced in Figure 5.18.

6253



6254



Figure 5-18 Emission of a passive substance 15 s (left) and 55 s (right) after the release. Side view (above) and view from behind (below) (from Long et al., 2010)

6255

6256

6257

6258

6259

6260

6261

6262

6263

6264

6265

6266

6267

6268

6269

6270

6271

6272

6273

6274

6275

6276

6277

6278

6279

6280

6281

6282

6283

6284

6285

6286

6287

6288

6289

6290

6291

6292

6293

As can be seen, when a passive substance is emitted from a source (for example a point source), instantaneous plumes are generated in succession, different from each other and having an irregular shape that, only on average, can be described as the usual regular plume characterised by a progressive widening with the distance downwind, proportional to the turbulence present in the air. If we focus our attention on a single instantaneous plume, we notice that in the first phase of dispersion, close to the source, the plume is coherent and relatively narrow and meanders from one side to the other, mainly horizontally but also vertically, even if to a lesser extent. The meandering of the plume is more pronounced near the source, progressively reducing with the distance, until it disappears. As we know, this is due to the fact that the meandering of the plume is inversely proportional to its characteristic size. This phenomenological evidence inspired the Fluctuating Plume Model proposed by Gifford (1959), which was originally formulated more as a conceptual way than a quantitative model. With this conceptual model, the dispersion is described by the superposition of independent Gaussian plumes characterised by dispersion parameters describing the "instantaneous dispersion". Each Gaussian plume considers a different position of its centroid, described by a stochastic variable given that the coordinates of the position of the centroid derived from the stochastic nature of the turbulent vortices present in the PBL. These vortices have a characteristic dimension not less than the dimension characteristic of the entire plume at the considered leeward distance. In practice, if one samples at the receiving point of coordinates (x, y, z) with a high frequency (i.e. at successive instants very close to each other), what would be obtained is a sequence of instantaneous concentration values c_i , each corresponding to a very precise position of the centroid i . Since the meandering of the centroid is a stochastic process driven by turbulent vortices present in the PBL and larger than the characteristic dimension of the instantaneous plume, the instantaneous concentration values c_i will be realisations of the stochastic process "concentration at the point (x, y, z) ".

After a period of a few decades in which the Gifford model constituted only a conceptual method useful for interpreting the experimental evidence, some works describing an implementation into modelling realisations appeared in the scientific literature, such as Högström (1972), Mussio et al. (2001) and Yu et al. (2011). More recently, the work of Marro et al. (2015), on the basis of the availability of measurements systematically collected in the wind tunnel (Sironi et al. 2015) must be cited. The intrinsic limit of this type of realisation lies in the fact that the Gaussian Plume modelling can be considered sufficiently realistic only in situations in which there are no orographic problems and in which the meteorology is

6294 relatively homogeneous and not highly convective.

6295

6296 To overcome these problems, the most natural way to concretise Gifford's conceptual model
 6297 is to formulate it in a completely Lagrangian context, as was done in part in the work of
 6298 Marro et al. (2015) subject of the previous point. The description of some Lagrangian
 6299 implementations can be found in Luhar et al. (2000), Cassiani and Giostra (2002), Franzese
 6300 (2003) and Mortarini et al. (2009), in addition to the clear synthesis made on this subject by
 6301 Ferrero and Mortarini (2014).

6302 5.8.3. Micromixing model

6303 A micromixing model (or PDF model) views the intrinsically continuous PBL as a geometric
 6304 space in which a very large number of air particles, each fully detectable, are uniformly
 6305 distributed. Each of them is completely characterised at a generic instant t by:

- 6306 • a position in space $\mathbf{X}(t)$,
- 6307 • a velocity fluctuation $\mathbf{u}(\mathbf{X},t)$ with respect to a mean (Eulerian) field of motion $\mathbf{U}(\mathbf{X},t)$;
- 6308 • by a concentration of the interested pollutant $C(\mathbf{X},t)$

6309 At each instant t prior to an initial instant t_0 all particles (initially uniformly distributed in
 6310 space) possess a concentration $C(t < t_0) = 0$. At a given initial time t_0 , some of these particles
 6311 will transit through the source (e.g. a point source) and will acquire mass from it and,
 6312 therefore an initial concentration of $C_0(t_0)$ while all the others will continue to keep zero
 6313 concentration. From the instant t_0 onwards, the model will begin to simulate the dispersion
 6314 of all the particles (both those with non-zero concentration and those with zero
 6315 concentration), that is, both all their different stochastic trajectories and their mutual
 6316 interaction. This interaction is constituted by a mass exchange of the pollutant between a
 6317 generic particle and the adjacent particles, a mass exchange induced by molecular diffusivity
 6318 and driven by the turbulence that is present locally in the PBL. In practice, the model will
 6319 simulate the trajectory of all particles using the laws of a normal Lagrangian one-particle
 6320 model with the practical problem related to the huge number of particles whose trajectory
 6321 and mass exchange must be simulated.

6322

6323 In a micromixing model, the pollutant exchange among close particles is modelled, for
 6324 simplicity, through a bulk law describing, for each particle, such mass exchange with the
 6325 adjacent external environment, seen as a continuous fluid characterised by an average
 6326 concentration C . In practice, for the p -th particle, this exchange is described by the
 6327 micromixing relation that simulates the action of molecular diffusivity:

6328

$$6329 \frac{dC^p(X_p, t)}{dt} = \frac{-C^p(X_p, t) - \underline{C^p(X_p, t)}}{\tau_m}$$

6330

6331 Where τ_m represents the so-called micromixing time scale. Some particles will decrease in
 6332 concentration (those passing through the source) while others (those that constitute the
 6333 surrounding air) will increase it.

6334 Assuming to divide the entire computational domain into cells, at the end of the time step,
 6335 there will be N_k particles in the k -th cell, each with its own concentration. The average
 6336 characteristic concentration of the cell can be computed as

6337

$$6338 \quad \underline{C}_k(t) = \frac{1}{N_k} \sum_{p=1}^{N_k} C^p(t)$$

6339

6340 while the second moment can be computed as

6341

$$6342 \quad \underline{C}_{k\Box}^2(t) = \frac{1}{N_k} \sum_{p=1}^{N_k} \dot{c} \dot{c}$$

6343

6344 and finally, the concentration variance can be computed as

6345

$$6346 \quad (\sigma_c^2)_k = \underline{C}_{k\Box}^2(t) - \dot{c}$$

6347

6348 To overcome the problem of simulating a huge number of particles, Cassiani (2013)
 6349 proposed the Volumetric Particle Approach (VPA), a model that can initially be seen as a
 6350 drastic simplification of a generic micromixing model. However, as pointed out by Ferrero et
 6351 al. (2020) and Cassiani et al. (2020), the simplified two-particle model proposed
 6352 independently by Kaplan (2014) coincides exactly with the VPA model, which, therefore, can
 6353 also be considered a simplified Lagrangian two-particle model (described in the following
 6354 section). Some of the practical aspects related to this model, in particular, the derivation of
 6355 the micromixing time scale τ_m , are described in Dixon and Tomlin (2007), Cassiani (2013)
 6356 and Marro et al. (2018).

6357 5.8.4. Two-Particles Lagrangian Dispersion models

6358 As already seen in this chapter, a Lagrangian Particle Model can be used to describe
 6359 operationally the average dispersion of a passive substance (chemically non-reactive)
 6360 emitted in the turbulent PBL. Basically, this consists in assuming that portions of fluid which
 6361 are emitted from the source move independently, each constituting a distinct and
 6362 independent statistical realisation. The velocity u and the position x of each particle together
 6363 constitute a continuous Markov process and will be obtained by integrating a system of
 6364 stochastic Langevin differential equations. The ensemble mean concentration field is
 6365 obtained from the set of trajectories of the different particles. A model that operates in this
 6366 manner is called the One Particle Lagrangian Model.

6367

6368 The independence among emitted particles prevents us from describing the concentration
 6369 fluctuations. In order to describe this last, it is, in fact, necessary to take into account the
 6370 correlation between the various emitted particles conditioning their motion. Basically, the
 6371 movement of an emitted particle is not independent of the motion of the other particles. In
 6372 principle, the correlation between particles decreases with time until it disappears at great
 6373 distances from the emission point. By taking this effect into account, it is possible to
 6374 reconstruct the statistics of the motion of the particles and, therefore, the concentration
 6375 statistics, including the concentration variance.

6376

6377 Thomson (1990) has formulated a method, named Lagrangian Two-Particle Model,
 6378 considering the emission not only of independent single particles, but of pairs of particles in
 6379 which each of the two particles is conditioned by the presence of the other one. The

6380 proposed model, together with the reconstruction of the average concentration substance, is
 6381 also able to determine the concentration variance. The limitation of this model lies in the fact
 6382 that it is valid only in homogeneous and isotropic conditions. To try to extend the model to
 6383 situations characterised by non-stationary, non-homogeneous and non-isotropic turbulence,
 6384 Du (2001) has proposed a heuristic and reasonable extension. One of the main difficulties
 6385 that this approach is still having resides in the difficulty to find good parameterisations of the
 6386 statistical properties of the turbulent atmosphere related to the movements of coupled
 6387 particles in order to feed the model operationally in a way similarly adopted by commonly
 6388 used One Particle Lagrangian Models.

6389 5.9. A bridge towards the stakeholders

6390 The concern about the odour nuisance is increasing in the population and among
 6391 stakeholders. The first questions they ask for answers are: From where does such
 6392 'disgusting' odour come? Is it dangerous for health?

6393 As described in previous sections, numerical models can certainly support tracking and
 6394 detecting the possible sources of odour nuisance. To contribute to responding to these
 6395 specific questions, their development and improvement should be *application-oriented*, and
 6396 in this context, the interaction with decision-makers and stakeholders and with their needs
 6397 becomes a fundamental aspect.

6398 It is thus important to address some basic issues, such as the following ones, which can
 6399 drive the integration of numerical models in nuisance-response procedures and protocols.

- 6400 ● *What do the stakeholders need and desire to know for handling the problem of odour*
 6401 *nuisance*
- 6402 ● *What scientists are nowadays able to provide, what is yet unknown*
- 6403 ● *What is the gap between science and response and what can be done to fill it*
- 6404 ● *What is the meeting point between scientists and stakeholders in dealing with odour*
 6405 *problems*

6406 Environmental protection agencies and decision makers need tools that may support them in
 6407 identifying the source of the odour nuisance, possibly during its occurrence, in order to
 6408 collect measurements timely and in the right place, then to analyse the samplers in a
 6409 convenient time frame. As a follow-up, tracking the origin of the emission allows taking the
 6410 needed countermeasures to avoid further releases from the same source.

6411 Alert systems, also involving citizens who may send complaints about odour nuisance
 6412 episodes, are increasingly developed nowadays. Numerical models may be integrated into
 6413 the response system to track back the possible odour source using the alerts' distribution as
 6414 receptors. The main open issues related to the appropriate modelling of the odour dispersion
 6415 in the air have been discussed in previous sections, and they represent the actual scientific
 6416 limits that still need to be overcome. Traditional dispersion models need to be modified to
 6417 adapt their application for the simulation and prediction of atmospheric transport of odours
 6418 and the characterisation of their nuisance. Atmospheric dispersion modelling systems can
 6419 also be used to define regulatory frameworks for odour emissions from industrial, agricultural
 6420 and sanitary activities. The assessment of the impact of odour emissions may support the
 6421 definition of the criteria and measures to control and regulate the releases.

6422 In this context, the dialogue and cooperation between scientists, stakeholders and decision-
 6423 makers is essential. The practical problems that responders have to face and the final goals
 6424 they need to achieve should be part of the guidelines for model development and
 6425 improvement. A proper balance between the complexity, efficacy and usability of models is
 6426 to be pursued to guarantee their applicability in alert systems. Based on odour reporting
 6427 provided by the stakeholders, a comprehensive analysis framework beyond the model
 6428 simulation, has to be established to identify the odour source, to assess the impacted areas
 6429 and provide useful indications for the protection intervention. The *citizen-science* approach
 6430 should be promoted and sustained, involving and training the population, since it is a unique
 6431 opportunity to get distributed information in space and time, which can be fruitfully used as
 6432 input for the model simulations.

6433 The cooperation between scientists, stakeholders and decision makers should thus entangle
 6434 all aspects, from the modelling system conceptual approach, to its development,
 6435 implementation and maintenance, from the training of the operators to the design of the
 6436 guidelines for the use of the results and outputs.

6437 Responding to the above questions - as in the following - clarifies that air quality experts
 6438 may be ascribed to be the bridge between the scientific community developing the models
 6439 and the final decision makers. Air quality experts are expected to have a good knowledge
 6440 about running dispersion models for odour assessments, even when not directly involved in
 6441 the scientific development of the models themselves.

6442 • *What the stakeholders need and desire to know for handling the problem of odour*
 6443 *nuisance*

6444 In general, air quality experts working for the local authorities would need information about
 6445 available modelling tools and corresponding training. The establishment of national
 6446 guidelines on odour assessment is a key element for developing harmonised and
 6447 comprehensible methods. Assembling working groups where scientists are involved in the
 6448 development of guidelines would be indeed extremely valuable.

6449 • *What scientists are nowadays able to provide, what is yet unknown*

6450 Great advances have been accomplished in the field of applicable complex numerical
 6451 models for regulatory purposes. Nowadays, it is possible to account for buildings, vegetation,
 6452 topography and complex odour sources using coupled Lagrangian dispersion models and
 6453 Eulerian flow field models. Two major issues for which scientific progress remains to be
 6454 pursued are: (i) the establishment of dose-response relationships between odour annoyance
 6455 and any kind of odour impact criteria (e.g. odour hours, concentrations), and (ii) the
 6456 development of flow-field models that are able to account for the interaction between
 6457 synoptic flows and local thermal flows at high horizontal resolutions (< 500m).

6458 • *What is the gap between science and response, and what can be done to fill it*

6459 The air quality experts must possess a good knowledge about the legislative requirements
 6460 for odour assessments. In most Countries, the legislation stays quite vague in this regard.
 6461 Therefore, legislative terms like “a neighbour must not be annoyed in an unacceptable
 6462 manner” or “any health risk is unacceptable” need to be rendered into quantifiable terms

6463 such as limit values that can be assessed by dispersion models or field inspections (e.g. EN
6464 16841).

6465 • *What is the meeting point between scientists and stakeholders in dealing with odour*
6466 *problems*

6467 The meeting point between scientists and stakeholders are likely the air quality experts
6468 employed at the regional and national governments. Fostering the interaction between air
6469 quality experts and the scientific community by establishing e.g. conferences,
6470 communication platforms would be a step forward for harmonising and accelerating the
6471 development of applicable guidelines and models.

6472 In conclusion, promoting the cooperation between model developers, model users,
6473 stakeholders and decision makers is the most efficient pathway to provide fit-for-purpose
6474 modelling tools also in the framework of odour nuisance assessment and response.

6475 5.10. References

6476 Allwine, K. J., & Flaherty, J. E. (2006). Joint Urban 2003: Study overview and instrument
6477 locations (No. PNNL-15967). Pacific Northwest National Lab.(PNNL), Richland, WA (United
6478 States).

6479 Anfossi, D., S. Alessandrini, S. Trini Castelli, E. Ferrero, D. Oetl, G. Degrazia (2006) Tracer
6480 dispersion simulation in low wind speed conditions with a new 2-D Langevin equation
6481 system. Atmos. Environ., 40, 7234-7245

6482 Angrecka, S., & Herbut, P. (2014). The impact of natural ventilation on ammonia emissions
6483 from free stall barns. Polish Journal of Environmental Studies, 23(6), 2303-2307.

6484 Arya, S. P. (1998). Air Pollution Meteorology and Dispersion, 1st Edition, Oxford University
6485 Press. ISBN 0195073983.

6486 Aubrun, S., Leitl, B., & Schatzmann, M. (2002). Validation Data for Odour Dispersion
6487 Models. In 8th International Conference on Harmonisation within Atmospheric Dispersion
6488 Modelling for Regulatory Purposes.

6489 Aubrun, S.; Leitl, B. 2004. Unsteady characteristics of the dispersion process in the vicinity
6490 of a pig barn. Wind tunnel experiments and comparison with field data. Atmospheric
6491 Environment, v. 38, n. 1, p. 81–93.

6492 Auckland City Council (2012) Separation Distances for Industry. A Discussion document.
6493 Available online: <[https://www.aucklandcouncil.govt.nz/plans-projects-policies-reports-
6494 bylaws/our-plans-strategies/unitary-plan/history-unitary-plan/
6495 docs345airqualitybuffersheavyindustry/Appendix-3.45.2.pdf](https://www.aucklandcouncil.govt.nz/plans-projects-policies-reports-bylaws/our-plans-strategies/unitary-plan/history-unitary-plan/docs345airqualitybuffersheavyindustry/Appendix-3.45.2.pdf)> (accessed 2021).

6496 Bächlin, W., Rühling, A., Lohmeyer, A., & Lohmeyer, I. (2002). Bereitstellung von
6497 validierungsdaten Für geruchsausbreitungsmodelle–naturmessungen. Forschungsbericht
6498 FZKA-BWPLUS, Förderkennzeichen BWE, 20003, 183.

- 6499 Bächlin W., Rühling A., Lohmeyer A. Dispersion of odour - A new model validation data set
6500 is available. September 2003, Staub, Reinhaltung der Luft 63(9):387-390.
- 6501 Barclay, J. (2008) Clean Air Society of Australia and New Zealand. Low wind speed
6502 workshop. Queensland, Australia.
- 6503 Barclay J. & Scire J. (2011). Generic Guidance and Optimum Model Settings for the Calpuff
6504 Modelling System for Inclusion into the Approved Methods for the Modelling and
6505 Assessments of Air Pollutants in NSW, Australia. Prepared For: NSW Office of Environment
6506 and Heritage, Sydney Australia.
- 6507 Barclay J. & Borissova M. (2013). Potential Problems Using AERMOD to Implement Current
6508 Odour Regulations for WWTPs. 5th International Water Association (IWA) Conference on
6509 Odours and Air Emissions, March 4-7, 2013. San Francisco, CA, USA.
- 6510
- 6511 Barclay, J. & Borissova, M. (2019) AERMOD concerns for regulatory applications. Clean Air
6512 Society of Australia and New Zealand Conference. Queenstown. New Zealand.
- 6513 Barclay, J. (2019) CALPUFF Model, History and Current Status. Olores.org [Olores.org -](#)
6514 [CALPUFF Model, History and Current Status – Part 1](#)
- 6515 Barclay, J. & Evanson I. (2021) Clean Air Society of Australia and New Zealand (CASANZ) 4-
6516 day Odour Training Course.
- 6517
- 6518 Barrat R. (2001). Atmospheric Dispersion Modelling, 1st Edition, Earthscan Publications.
6519 ISBN 1853836427.
- 6520 Baumann-Stanzer, K., Andronopoulos, S., Armand, P., Berbekar, E., Efthimiou, G., Fuka, V.,
6521 Gariazzo C., Gasparac G., Harms F., Hellsten A., Jurcacova K., Petrov A., Rakai A., Stenzel
6522 S., Tavares R. & Trini Castelli, S. (2015). COST ES1006 Model evaluation case studies:
6523 Approach and results. COST Action ES1006.
- 6524 Bax, C., Sironi, S., & Capelli, L. (2020). How can odors be measured? An overview of
6525 methods and their applications. Atmosphere, 11(1), 92.
- 6526 Bellasio, R., Scarpato, S., Bianconi, R., & Zeppa, P. (2012). APOLLO2, a new long range
6527 Lagrangian particle dispersion model and its evaluation against the first ETEX tracer release.
6528 Atmospheric environment, 57, 244-256.
- 6529 Bellasio, R., Bianconi, R., Mosca, S., & Zannetti, P. (2017). Formulation of the Lagrangian
6530 particle model LAPMOD and its evaluation against Kincaid SF6 and SO2 datasets.
6531 Atmospheric Environment, 163, 87-98.
- 6532 Bellasio, R., Bianconi, R., Mosca, S., & Zannetti, P. (2018). Incorporation of numerical plume
6533 rise algorithms in the Lagrangian particle model LAPMOD and validation against the
6534 Indianapolis and Kincaid datasets. Atmosphere, 9(10), 404.
- 6535 Bellasio, R., & Bianconi, R. (2022). A Heuristic Method for Modeling Odor Emissions from

- 6536 Open Roof Rectangular Tanks. *Atmosphere*, 13(3), 367.
- 6537 Bennett, N. D., Croke, B. F., Guariso, G., Guillaume, J. H., Hamilton, S. H., Jakeman, A.
6538 J., ... & Andreassian, V. (2013). Characterising performance of environmental models.
6539 *Environmental Modelling & Software*, 40, 1-20.
- 6540 Beychok, M. R. (2005). *Fundamentals of stack gas dispersion*. MR Beychok.
- 6541 Bianconi R., Mosca S. and Graziani G. (1999) PDM: A Lagrangian particle model for
6542 atmospheric dispersion. European Commission. EUR 17721 EN, 63 pp.
- 6543 Bianconi R. and R. Bellasio (2011) La modellistica atmosferica dell'inquinamento olfattivo a
6544 fini autorizzativi. Workshop Ecomondo Come gestire il disagio olfattivo: tra le carenze
6545 normative e l'affidabilità dei controlli. Rimini, 9 Novembre 2011. (In Italian).
- 6546 Bokowa A., Diaz C., Koziel J.A., McGinley M., Barclay J., Schauburger G., Guillot J.-M.,
6547 Sneath R., Capelli L., Zorich V., Izquierdo C., Bilsen I., Romain A.-C., del Carmen Cabeza
6548 M., Liu D., Both R., Van Belois H., Higuchi T., Wahe L. (2021). Summary and Overview of
6549 the Odour Regulations Worldwide. *Atmosphere*, 12, 206.
6550 <https://doi.org/10.3390/atmos12020206>
- 6551 Bosanquet, C. H., & Pearson, J. L. (1936). The spread of smoke and gases from chimneys.
6552 *Transactions of the Faraday Society*, 32, 1249-1263.
- 6553 Bowne, N. E., & Londergan, R. J. (1983). Overview, results, and conclusions for the EPRI
6554 Plume-Model Validation and Development Project: plains site. Final report (No. EPRI-EA-
6555 3074). TRC Environmental Consultants, Inc., East Hartford, CT (USA).
- 6556 Brancher, M., Griffiths, K. D., Franco, D., & de Melo Lisboa, H. (2017). A review of odour
6557 impact criteria in selected countries around the world. *Chemosphere*, 168, 1531–1570.
6558 <https://doi.org/10.1016/j.chemosphere.2016.11.160>
- 6559 Brancher, M., Piringier, M., Knauder, W., Wu, C., Griffiths, K. D., & Schauburger, G. (2020a).
6560 Are empirical equations an appropriate tool to assess separation distances to avoid odour
6561 annoyance? *Atmosphere*, 11(7), 678.
- 6562 Brancher, M., Hieden, A., Baumann-Stanzer, K., Schauburger, G., & Piringier, M. (2020b).
6563 Performance evaluation of approaches to predict sub-hourly peak odour concentrations.
6564 *Atmospheric Environment: X*, 7, 100076.
- 6565 Briggs, G. A. (1965). A plume rise model compared with observations. *Journal of the Air
6566 Pollution Control Association*, 15(9), 433-438.
- 6567 Briggs, G. A. (1968). Concawe meeting: Discussion of the comparative consequences of
6568 different plume rise formulas. *Atmospheric Environment* (1967), 2(3), 228-232.
- 6569 Briggs, G. A. (1969). Plume rise. US-AEC critical review series TID-25075. 68-86. National
6570 Technical Information Service, Springfield, Virginia, 22161.
- 6571 Briggs, G. A. (1971). Some recent analyses of plume rise observations. In *Proceedings of
6572 the Second International Clean Air Congress*. Englund, Berry, eds. Academic Press, NY.

- 6573 Briggs, G. A. (1972). Chimney plumes in neutral and stable surroundings. *Atmospheric*
6574 *Environment* (1967), 6(7), 507-510.
- 6575 Brusasca, G., Tinarelli, G., & Anfossi, D. (1992). Particle model simulation of diffusion in low
6576 wind speed stable conditions. *Atmospheric Environment. Part A. General Topics*, 26(4), 707-
6577 723.
- 6578 Brusca, S., Famoso, F., Lanzafame, R., Mauro, S., Messina, M., & Strano, S. (2016). Pm10
6579 dispersion modeling by means of cfd 3d and Eulerian–Lagrangian models: analysis and
6580 comparison with experiments. *Energy Procedia*, 101, 329-336.
- 6581 Bull, M., McIntyre, A., Hall, D., Allison, G., Redmore, J., Pullen, J., ... & Fain, R. (2014).
6582 Guidance on the Assessment of Odour for Planning. Institute of Air Quality Management
6583 (IAQM), London.
- 6584 Capelli, L., Sironi, S., Del Rosso, R., & Guillot, J. M. (2013). Measuring odours in the
6585 environment vs. dispersion modelling: A review. *Atmospheric Environment*, 79, 731-743.
- 6586 Cartelle Fernández D., Díaz Jiménez C., VellónGraña J.M. and Rodríguez López A.,2014,
6587 The New Tool for Prediction of Odour Incidents. A key frame for a better management of an
6588 industrial plant. 4th International Conference on Environmental Odour Monitoring & Control
6589 (NOSE 2014), 14-17 September 2014, Venice, Italy, AIDIC Publications.
- 6590 Carruthers, D. J., McHugh, C. A., Robins, A. G., Thomson, D. J., Davies, B., & Montgomery,
6591 M. (1994). UK Atmospheric Dispersion Modelling System Validation Studies. In *Air Pollution*
6592 *Modeling and Its Application X* (pp. 491-501). Springer, Boston, MA.
- 6593 Cassiani, M., & Giostra, U. (2002). A simple and fast model to compute concentration
6594 moments in a convective boundary layer. *Atmospheric Environment*, 36(30), 4717-4724.
- 6595 Cassiani, M. (2013). The volumetric particle approach for concentration fluctuations and
6596 chemical reactions in Lagrangian particle and particle-grid models. *Boundary-layer*
6597 *meteorology*, 146(2), 207-233.
- 6598 Cassiani, M., Bertagni, M. B., Marro, M., & Salizzoni, P. (2020). Concentration fluctuations
6599 from localised atmospheric releases. *Boundary-Layer Meteorology*, 177(2), 461-510.
- 6600 CERC (2021a) ADMS-Screen. Available online: <[https://www.cerc.co.uk/environmental-](https://www.cerc.co.uk/environmental-software/ADMS-Screen-model.html)
6601 [software/ADMS-Screen-model.html](https://www.cerc.co.uk/environmental-software/ADMS-Screen-model.html)> (accessed 2021).
- 6602 CERC (2021b) ADMS Model. <Available online:
6603 <http://cerc.co.uk/environmental-software/ADMS-model.html>> (accessed 2021).
- 6604 Chacko, R., Jain, D., Patwardhan, M., Puri, A., Karande, S., & Rai, B. (2020). Data based
6605 predictive models for odor perception. *Scientific reports*, 10(1), 1-13.
- 6606 Chang, J. C., & Hanna, S. R. (2004). Air quality model performance evaluation. *Meteorology*
6607 *and Atmospheric Physics*, 87(1), 167-196.
- 6608 Cimorelli A.J., Venkatram A., Weil J.C., Paine R.J., Wilson R.B., Lee R.F., Peters W.D.

- 6609 (2003) AERMOD description of model formulation, US EPA Report 454/R-03-002d, p. 85.
- 6610 Collett, R. S., & Oduyemi, K. (1997). Air quality modelling: a technical review of
6611 mathematical approaches. *Meteorological Applications*, 4(3), 235-246.
- 6612 Connors, J. A., Paine, R. J., & Hanna, A. S. (2013). AERMOD low wind speed issues:
6613 Review of new model release. *Air and Waste Management Association-Guideline on Air*
6614 *Quality Models 2013: The Path Forward*, 1, 213-244. Available online:
6615 <[https://www.researchgate.net/profile/Steven-Hanna/publication/289330686_AERMOD_low](https://www.researchgate.net/profile/Steven-Hanna/publication/289330686_AERMOD_low_wind_speed_issues_Review_of_new_model_release/links/5b47743345851519b4b4543c/AERMOD-low-wind-speed-issues-Review-of-new-model-release.pdf)
6616 [_wind_speed_issues_Review_of_new_model_release/links/5b47743345851519b4b4543c/](https://www.researchgate.net/profile/Steven-Hanna/publication/289330686_AERMOD_low_wind_speed_issues_Review_of_new_model_release/links/5b47743345851519b4b4543c/AERMOD-low-wind-speed-issues-Review-of-new-model-release.pdf)
6617 [AERMOD-low-wind-speed-issues-Review-of-new-model-release.pdf](https://www.researchgate.net/profile/Steven-Hanna/publication/289330686_AERMOD_low_wind_speed_issues_Review_of_new_model_release/links/5b47743345851519b4b4543c/AERMOD-low-wind-speed-issues-Review-of-new-model-release.pdf)> (accessed 2021).
- 6618 Conti, C., Guarino, M., & Bacenetti, J. (2020). Measurements techniques and models to
6619 assess odor annoyance: A review. *Environment international*, 134, 105261.
- 6620 COST ES1006 (2015a): Model Evaluation Case Studies, COST Action ES1006, April 2015.
- 6621 COST ES1006 (2015b): Model evaluation protocol, COST Action ES1006, April 2015.
- 6622 Dairy Australia (2008) Effluent and Manure Management Database for the Australian Dairy
6623 Industry. Chapter 5. Odour emissions and control. Available online:
6624 <<https://www.dairyingfortomorrow.com.au/wp-content/uploads/combined.pdf>> (accessed
6625 2021).
- 6626 de Melo, A. M. V., Santos, J. M., Mavroidis, I., & Junior, N. C. R. (2012). Modelling of odour
6627 dispersion around a pig farm building complex using AERMOD and CALPUFF. Comparison
6628 with wind tunnel results. *Building and Environment*, 56, 8-20.
- 6629 Denby B., Georgieva E., Larssen S., Guerreiro C., Li L., Douros J., Moussiopoulos N.,
6630 Fragkou L., Gauss M., Olesen H., Miranda A.I., Dilara P., Thunis P., Lappi S., Rouil L.,
6631 Lükewille A., Querol X., Martin F., Schaap M., van den Hout D, Kobe A., Silibello C, Vincent
6632 K., Stedman J., Gonçalves M., Pirovano G., Volta L., van Pul A., González Ortiz A., Roberts
6633 P. & Oettl D. (2010). Guidance on the use of models for the European Air Quality Directive.
6634 In A Working Document of the Forum for Air Quality Modelling in Europe. FAIRMODE
6635 Technical Report Version (Vol. 4). Available online:
6636 <<https://citeseerx.ist.psu.edu/viewdoc/download?doi=10.1.1.472.9073&rep=rep1&type=pdf>>
6637 (accessed 2021).
- 6638 De Visscher, A. (2013). Air dispersion modeling: foundations and applications. John Wiley &
6639 Sons.
- 6640 Diaz Jimenez, C., Izquierdo Zamora C., Cartelle Fernandez D., Comparison of Predicted
6641 Versus Real Odour Impacts in a Rendering plant with PrOlor. 5th International Conference
6642 on Environmental Odour Monitoring & Control (NOSE 2016), 14-17 September 2014, Ischia,
6643 Italy, AIDIC Publications.
- 6644 Donaldson, C. D. (1973). Construction of a dynamic model of the production of atmospheric
6645 turbulence and the dispersal of atmospheric pollutants. In *Workshop on Micrometeorology*
6646 (Vol. 313, p. 392). Amer. Meteor. Soc.

- 6647 Dresser, A. L., & Huizer, R. D. (2011). CALPUFF and AERMOD model validation study in
6648 the near field: Martins Creek revisited. *Journal of the Air & Waste Management Association*,
6649 61(6), 647-659.
- 6650 Du, S. (2001). A heuristic Lagrangian stochastic particle model of relative diffusion: model
6651 formulation and preliminary results. *Atmospheric Environment*, 35(9), 1597-1607.
- 6652 EN 16841-1: 2017-03 Ambient air - Determination of odour in ambient air by using field
6653 inspection - Part 1: Grid method; German version EN 16841-1:2016.
- 6654 EPA Victoria (2013) Recommended separation distances for industrial residual air
6655 emissions. Publication no. 1518. Available online:
6656 <<https://www.epa.vic.gov.au/-/media/epa/files/publications/1518.pdf>> (accessed 2021).
- 6657 Federal Register (2005) Revision to the Guideline on Air Quality Models: Adoption of a
6658 Preferred General Purpose (Flat and Complex Terrain) Dispersion Model and Other
6659 Revisions. Vol. 70, N. 216. November 9, 2005. Available online:
6660 <<https://www.govinfo.gov/content/pkg/FR-2005-11-09/pdf/05-21627.pdf>> (accessed 2021).
- 6661 Federal Register (2017) Revisions to the Guideline on Air Quality Models: Enhancements to
6662 the AERMOD Dispersion Modeling System and Incorporation of Approaches To Address
6663 Ozone and Fine Particulate Matter. Vol. 82, N. 10. January 17, 2017. Available online:
6664 <<https://www.govinfo.gov/content/pkg/FR-2017-01-17/pdf/2016-31747.pdf>> (accessed
6665 2021).
- 6666 Ferrero E., Mortarini L. (2014): Turbulence and Dispersion - CNR-ISAC / University of
6667 Eastern Piedmont.
- 6668 Ferrero, E., Mortarini, L., & Purgè, F. (2017). A simple parameterisation for the
6669 concentration variance dissipation in a Lagrangian single-particle model. *Boundary-Layer
6670 Meteorology*, 163(1), 91-101.
- 6671 Ferrero, E., & Oetli, D. (2019). An evaluation of a Lagrangian stochastic model for the
6672 assessment of odours. *Atmospheric Environment*, 206, 237-246.
- 6673 Ferrero, E., Manor, A., Mortarini, L., & Oetli, D. (2020). Concentration fluctuations and odor
6674 dispersion in Lagrangian models. *Atmosphere*, 11(1), 27.
- 6675 Franzese, P. (2003). Lagrangian stochastic modeling of a fluctuating plume in the convective
6676 boundary layer. *Atmospheric Environment*, 37(12), 1691-1701.
- 6677 Garratt J. R. (1994). *The Atmospheric Boundary Layer*. Cambridge Atmospheric and Space
6678 Science Series, ISBN-13 978-0521467452.
- 6679 Gifford, F. A., & Hanna, S. R. (1973). Modelling urban air pollution. *Atmospheric
6680 Environment* (1967), 7(1), 131-136.
- 6681 Gunawardena, N., Leang, K. K., Pardyjak, E. (2015). Particle swarm optimisation for source
6682 localization in realistic complex urban environments. *Atmospheric Environment*, 262,
6683 118636.

- 6684 Griffiths, D. A risk-based procedure for broiler farm separation distance calculations. In
6685 Proceedings of the 21st International Clean Air and Environment Conference, Sydney,
6686 Australia, 7–11 September 2013.
- 6687 Guo, H., Jacobson, L. D., Schmidt, D. R., Nicolai, R. E., & Janni, K. A. (1998). Comparison
6688 of Five Models for Setback Distance Determination. In 2001 ASAE Annual Meeting (p. 1).
6689 American Society of Agricultural and Biological Engineers.
- 6690 Haeger-Eugensson, M., Ferm, M., & Elfman, L. (2014). Use of a 3-D dispersion model for
6691 calculation of distribution of horse allergen and odor around horse facilities. *International
6692 journal of environmental research and public health*, 11(4), 3599-3617.
- 6693 Hanna, S. R. (1972). Description of ATDL computer model for dispersion from multiple
6694 sources. Air Resources Atmospheric Turbulence and Diffusion Laboratory, National Oceanic
6695 and Atmospheric Administration. Oak Ridge, Tennessee, USA.
- 6696 Hanna, S. R., Briggs, G. A., & Hosker Jr, R. P. (1982). Handbook on atmospheric diffusion
6697 (No. DOE/TIC-11223). National Oceanic and Atmospheric Administration, Oak Ridge, TN
6698 (USA). Atmospheric Turbulence and Diffusion Lab..
- 6699 Hanna, S., & Chang, J. (2012). Acceptance criteria for urban dispersion model evaluation.
6700 *Meteorology and Atmospheric Physics*, 116(3), 133-146.
- 6701 Hansen, M. J., Jonassen, K. E., Løkke, M. M., Adamsen, A. P. S., & Feilberg, A. (2016).
6702 Multivariate prediction of odor from pig production based on in-situ measurement of
6703 odorants. *Atmospheric Environment*, 135, 50-58.
- 6704 Hartmann U., Janicke L., Janicke U. & Höscher M. (2007) A Screening Model for Odor
6705 Dispersions (SMOD). In *Gerüche in der Umwelt: Innenraum- und Außenluft; Tagung, Bad
6706 Kissingen, 13. und 14. November 2007; VDI Verl.: Düsseldorf, Germany; pp. 302–312.*
- 6707 Hoff S., Bundy D., Harmon J., Jacobson L., Schulte D., Schmidt D., Henry C. (2006)
6708 Validation of Odor Dispersion Measurements and Modeling. Proceedings: Workshop on
6709 Agricultural Air Quality, Bolger Conference Center, Potomac, MD June 5-8, 2006. pp. 270-
6710 282.
- 6711 Högström, U. (1972). A method for predicting odour frequencies from a point source.
6712 *Atmospheric Environment* (1967), 6(2), 103-121.
- 6713 Huber, A., Tang, W., Flowe, A., Bell, B., Kuehlert, K., & Schwarz, W. (2004, August).
6714 Development and applications of CFD simulations in support of air quality studies involving
6715 buildings. In Proceedings of 13th joint conference on the applications of air pollution
6716 meteorology with the Air & Waste Management Association. Vancouver, British Columbia,
6717 Canada.
- 6718 Hurley, P. (1994). PARTPUFF A Lagrangian Particle-Puff Approach for Plume Dispersion
6719 Modeling Applications. *Journal of Applied Meteorology and Climatology*, 33(2), 285-294.
- 6720 Hurley P.J. & Manins P.C. (1995). Plume rise and enhanced dispersion in LADM. CSIRO
6721 Atmospheric Research, ECRU Technical Note No. 4.

- 6722 Hurley, P., & Physick, W. (1993). A skewed homogeneous Lagrangian particle model for
6723 convective conditions. *Atmospheric Environment. Part A. General Topics*, 27(4), 619-624.
- 6724 Hurley, P., Physick, W., Luhar, A., & Edwards, M. (2002). The Air Pollution Model (TAPM)
6725 Version 2. Part 2: Summary of some verification studies. *CSIRO, Atmos. Res*, 72, 20-36.
- 6726 Invernizzi, M., Brancher, M., Sironi, S., Capelli, L., Piringer, M., & Schaubberger, G. (2020)
6727 Odour impact assessment by considering short-term ambient concentrations: A multi-model
6728 and two-site comparison. *Environment International*, 144, 105990.
- 6729 Jacobson, L. D., Guo, H., Schmidt, D. R., Nicolai, R. E., Zhu, J., & Janni, K. A. (2005).
6730 Development of the OFFSET model for determination of odor-annoyance-free setback
6731 distances from animal production sites: Part I. Review and experiment. *Transactions of the*
6732 *ASAE*, 48(6), 2259-2268.
- 6733 Janicke, L. (2007). SMOD—Erstellung Eines Screening-Modells Für Geruchsimmissionen;
6734 Landesamtes für Natur. Umwelt und Verbraucherschutz NRW: Essen, Germany.
- 6735 Jeffrey, C.A., Paine, R.J, Hanna, S. (2013). AERMOD low wind speed issues. Review of
6736 new model release.
- 6737 Kaplan, H. (2014). An estimation of a passive scalar variances using a one-particle
6738 Lagrangian transport and diffusion model. *Physica A: Statistical Mechanics and its*
6739 *Applications*, 393, 1-9.
- 6740 Klarenbeek, J. V., Ogink, N. W., & van der Voet, H. (2014). Odor measurements according
6741 to EN 13725: A statistical analysis of variance components. *Atmospheric Environment*, 86,
6742 9-15.
- 6743 Klug, W. (1984). *Atmospheric Diffusion*. F. Pasquill and FB Smith. Ellis Horwood, (John
6744 Wiley & Sons) Chichester, 1983. pp. 437. *Quarterly Journal of the Royal Meteorological*
6745 *Society*, 110(464), 565-565.
- 6746 Lamb, R. G., Hogo, H., & Reid, L. E. (1979). A Lagrangian approach to modeling air
6747 pollutant dispersion: Development and testing in the vicinity of a roadway (No. EPA/600/4-
6748 79/023 Final Report).
- 6749 Leelossy, Á., Molnár, Jr. F., Izsák, F. , Havasi, A., Lagzi, I. , Mészáros, R. (2014).
6750 Dispersion modeling of air pollutants in the atmosphere: a review. *Cent. Eur. J. Geosci.* 6(3)
6751 257-278.
- 6752 Lewellen, W.S. (1977). Use of invariant modelling. *Handbook of Turbulence*. W. Frost and
6753 T.H. Moulden (eds). Plenum Press pp. 237-280.
- 6754 Lim, T. T., Heber, A. J., Ni, J. Q., Grant, R., & Sutton, A. L. (2000). Odor impact distance
6755 guideline for swine production systems. *Proceedings of the Water Environment Federation*,
6756 2000(3), 773-788. Available online:
6757 <[https://d1wqtxts1xzle7.cloudfront.net/44534232/ODOR_IMPACT_DISTANCE_GUIDELINE](https://d1wqtxts1xzle7.cloudfront.net/44534232/ODOR_IMPACT_DISTANCE_GUIDELINE_FOR_SWINE20160408-18827-xx0ucp-with-cover-page-v2.pdf?Expires=1633258314&Signature=OIOMH~ag4M-kXNQXhg1yHWPOgh9ysrwF0sOhNpG-)
6758 [_FOR_SWINE20160408-18827-xx0ucp-with-cover-page-v2.pdf?](https://d1wqtxts1xzle7.cloudfront.net/44534232/ODOR_IMPACT_DISTANCE_GUIDELINE_FOR_SWINE20160408-18827-xx0ucp-with-cover-page-v2.pdf?Expires=1633258314&Signature=OIOMH~ag4M-kXNQXhg1yHWPOgh9ysrwF0sOhNpG-)
6759 Expires=1633258314&Signature=OIOMH~ag4M-kXNQXhg1yHWPOgh9ysrwF0sOhNpG-

- 6760 E9HZU3xwyMY4XMMQ2JW2T-
 6761 t0mCBPQWHQKJgq4zYIFatuouqjDi2iPwGX2~ULbvezKsyrJ0w05L1P0G8fBhFqwjTXdCoKd
 6762 pZGt8M0KAXWFCqcGdAIPmUBn602PeckydpmJTJ2WBjYsafS1kshxnBm3VZI4eAsdwAz82
 6763 U1mU8Lih59-
 6764 xFWiMYqV7IUIGwE4nN8rRfexJctMWI4AnhvJ4sls9lp6Flo~mUiAojSclnhPKbbO5exfbxLmfLN
 6765 Y5pbsZzUd5fsTEhnnYRx-DIUNTmA4WJlwBeJ7yLR3ChMTZUMNEhGQ__&Key-Pair-
 6766 Id=APKAJLOHF5GGSLRBV4ZA> (accessed 2021)
- 6767 Lin, X. J., Barrington, S., Nicell, J., Choiniere, D., & Vezina, A. (2006). Influence of
 6768 windbreaks on livestock odour dispersion plume in the field. *Agriculture, ecosystems &*
 6769 *environment*, 116(3-4), 263-272.
- 6770 Lin, X. J., Barrington, S., Choiniere, D., & Prasher, S. (2007a). Simulation of the effect of
 6771 windbreaks on odour dispersion. *Biosystems engineering*, 98(3), 347-363.
- 6772 Lin, X., Barrington, S., Nicell, J., & Choiniere, D. (2007b). Effect of natural windbreaks on
 6773 maximum odour dispersion distance (MODD). *Canadian Biosystems Engineering*, 49, 6.
- 6774 Lin, X. J., Barrington, S., Gong, G., & Choiniere, D. (2009). Simulation of odour dispersion
 6775 downwind from natural windbreaks using the computational fluid dynamics standard k-ε
 6776 model. *Canadian Journal of Civil Engineering*, 36(5), 895-910.
- 6777 Long, K. J., Haupt, S. E., Hendrickson, M., Keay, J. (2010). Applying photogrammetric
 6778 techniques to study smoke plumes. 16th Conference on Air Pollution Meteorology, American
 6779 Meteorological Society, January 16-21 2010, Atlanta.
- 6780 Lofstrom, P., Jorgensen, H., Lyck, E., & Mikkelsen, T. (1970). A concentration fluctuation
 6781 model for decision-makers based on joint tracer and lidar measurements from a non-buoyant
 6782 elevated plume. *WIT Transactions on Ecology and the Environment*, 3.
- 6783 Ludwig, F. L., Gasiorek, L. S., & Ruff, R. E. (1977). Simplification of a Gaussian puff model
 6784 for real-time minicomputer use. *Atmospheric Environment* (1967), 11(5), 431-436.
- 6785 Luhar, A. K., Hibberd, M. F., & Borgas, M. S. (2000). A skewed meandering plume model for
 6786 concentration statistics in the convective boundary layer. *Atmospheric Environment*, 34(21),
 6787 3599-3616.
- 6788 Manor, A. (2014). A stochastic single-particle Lagrangian model for the concentration
 6789 fluctuations in a plume dispersing inside an urban canopy. *Boundary-layer meteorology*,
 6790 150(2), 327-340.
- 6791 Marro, M., Nironi, C., Salizzoni, P., & Soulhac, L. (2015). Dispersion of a passive scalar
 6792 fluctuating plume in a turbulent boundary layer. Part II: analytical modelling. *Boundary-Layer*
 6793 *Meteorology*, 156(3), 447-469.
- 6794 Marro, M., Salizzoni, P., Soulhac, L., & Cassiani, M. (2018). Dispersion of a passive scalar
 6795 fluctuating plume in a turbulent boundary layer. Part III: Stochastic modelling. *Boundary-*
 6796 *layer meteorology*, 167(3), 349-369.
- 6797 Mortarini, L., Franzese, P., & Ferrero, E. (2009). A fluctuating plume model for concentration

- 6798 fluctuations in a plant canopy. *Atmospheric Environment*, 43(4), 921-927.
- 6799 Mosca, S., Graziani, G., Klug, W., Bellasio, R., & Bianconi, R. (1998). A statistical
6800 methodology for the evaluation of long-range dispersion models: an application to the ETEX
6801 exercise. *Atmospheric Environment*, 32(24), 4307-4324.
- 6802 Murray, D. R., & Bowne, N. E. (1988). Urban power plant plume studies (No. EPRI/EA-
6803 5468). TRC Environmental Consultants, Inc., East Hartford, CT (USA).
- 6804 Mussio P., Gnyp A., Henshaw P. (2001): A fluctuating plume dispersion model for prediction
6805 of odor-impact frequencies from continuous stationary sources - *Atmos. Environ.*, 35, 2955-
6806 2962
- 6807 Mylne, K. R., & Mason, P. J. (1991). Concentration fluctuation measurements in a dispersing
6808 plume at a range of up to 1000 m. *Quarterly Journal of the Royal Meteorological Society*,
6809 117(497), 177-206.
- 6810 Mylne, K. R. (1992). Concentration fluctuation measurements in a plume dispersing in a
6811 stable surface layer. *Boundary-Layer Meteorology*, 60(1), 15-48.
- 6812 Naddeo V., Belgiorno V., Zarra T. (2012). Odour characterisation and exposure effects. In:
6813 Belgiorno V., Naddeo V., Zarra T., *Odour Impact Assessment Handbook*. p. 7-30, John
6814 Wiley & Sons, Inc., ISBN: 9781119969280
- 6815 Nanni, A., Riva, G. M., Tinarelli, G., & Brusasca, G. (1996). Particle model simulation of
6816 pollutants dispersion from a line source in complex terrain. *Science of the total environment*,
6817 189, 301-309.
- 6818 Nash, J. E., & Sutcliffe, J. V. (1970). River flow forecasting through conceptual models part I
6819 —A discussion of principles. *Journal of hydrology*, 10(3), 282-290.
- 6820 Nicolas, J., Delva, J., Cobut, P., & Romain, A. C. (2008). Development and validating
6821 procedure of a formula to calculate a minimum separation distance from piggeries and
6822 poultry facilities to sensitive receptors. *Atmospheric Environment*, 42(30), 7087-7095.
- 6823 Nimmermark, S. A., Jacobson, L. D., Schmidt, D. R., & Gay, S. W. (2005). Predictions by the
6824 odor from feedlots, setback estimation tool (OFFSET) compared with observations by
6825 neighborhood monitors. *Journal of the Air & Waste Management Association*, 55(9), 1306-
6826 1314.
- 6827 Nironi, C., Salizzoni, P., Marro, M., Mejean, P., Grosjean, N., & Soulhac, L. (2015).
6828 Dispersion of a passive scalar fluctuating plume in a turbulent boundary layer. Part I:
6829 Velocity and concentration measurements. *Boundary-layer meteorology*, 156(3), 415-446.
- 6830 NOAA (2008). Lecture 13. Mathematical Models. Available online: <
6831 [https://www.gfdl.noaa.gov/wp-content/uploads/files/user_files/pag/lecture2008/
6832 lecture13.pdf](https://www.gfdl.noaa.gov/wp-content/uploads/files/user_files/pag/lecture2008/lecture13.pdf)> (accessed 2021).
- 6833 New South Wales Approved Methods for the modelling and Assessments of Air Pollutants
6834 (2022). [Approved methods for the modelling and assessment of air pollutants \(nsw.gov.au\)](https://www.nsw.gov.au/air-pollution/assessments)

- 6835 Oettl, D. (2015a) Evaluation of the revised Lagrangian particle model GRAL against wind-
6836 tunnel and field experiments in the presence of obstacles. *Boundary Layer Meteorol*, 155,
6837 271-287
- 6838 Oettl, D. (2015b) Quality assurance of the prognostic, microscale wind-field model GRAL
6839 14.8 using wind-tunnel data provided by the German VDI guideline 3783-9. *J. of Wind Eng.*
6840 *& Ind. Aerodynamics*, 142, 104-110
- 6841 Oettl, D. (2015c) A multiscale modelling methodology applicable for regulatory purposes
6842 taking into account effects of complex terrain and buildings on the pollutant dispersion: a
6843 case study for an inner Alpine basin. *Env. Sci. and Poll. Res.*, 22 (22), 17860-17875
- 6844 Oettl, D. (2020a): Documentation of the Lagrangian Particle Model GRAL Vs. 20.1. Amt d.
6845 Stmk. Landesregierung, Graz, 208 pp
- 6846 Oettl, D. (2020b): Documentation of the prognostic mesoscale Model GRAMM Vs. 20.1. Amt
6847 d. Stmk. Landesregierung, Graz, 125 pp
- 6848 Oettl, D., A. Goulart, G. Degrazia, D. Anfossi (2005) A new hypothesis on meandering
6849 atmospheric flows in low wind speed conditions. *Atmos. Environ.*, 39, 1739 – 1748
- 6850 Oettl, D., and E. Ferrero (2017) A simple model to assess odour hours for regulatory
6851 purposes. *Atmos. Environ.*, 155, 162-173
- 6852 Oettl, D., M. Kropsch, and M. Mandl (2018): Odour assessment in the vicinity of a pig-fattening
6853 farm using field inspections (EN 16841-1) and dispersion modelling. *Atmos. Environ.*, 181,
6854 54-60
- 6855 Oettl, D., P. J. Sturm, M. Bacher, G. Pretterhofer, R. A. Almbauer (2002) A simple model for
6856 the dispersion of pollutants from a road tunnel portal. *Atmos. Environ.*, 36, 2943-2953.
- 6857 Oldrini, O., Armand, P., Duchenne, C., Olry, C., Tinarelli, G. (2017). Description and
6858 preliminary validation of the PMSS fast response parallel atmospheric flow and dispersion
6859 solver in complex built-up areas. *J. Environ. Fluid Mech.* 17 (3), 1–18.
- 6860 Onofrio, M., Spataro, R., & Botta, S. (2020). A review on the use of air dispersion models for
6861 odour assessment. *International Journal of Environment and Pollution*, 67(1), 1-21.
- 6862 ORION (2019) Available online:
6863 <[https://www.townofhamburgny.com/wp-content/uploads/2019/08/Odor-Analysis-Letter-](https://www.townofhamburgny.com/wp-content/uploads/2019/08/Odor-Analysis-Letter-1.pdf)
6864 1.pdf> (accessed 2021).
- 6865 Panofsky, H. A. (1984). *Atmospheric turbulence. Models and methods for engineering*
6866 *applications.*, 397.
- 6867 Petersen, W. B. (1986). A demonstration of INPUFF with the MATS database. *Atmospheric*
6868 *Environment* (1967), 20(7), 1341-1346.
- 6869 Pettarin, N., Campolo, M., Soldati, A. (2015). Urban air pollution by odor sources: Short time
6870 prediction. *Atmospheric Environment*, 122, 74-82.

- 6871 Petrov, A. and E. Georgieva (2019) An urban air pollution modelling test: GRAL vs. CUTE
6872 case 1. AIP Conference Proceedings 2075, 120007, <https://doi.org/10.1063/1.5091265>.
- 6873 Physick, W. L., Noonan, J. A., McGregor, J. L., Hurley, P. J., Abbs, D. J., & Manins, P. C.
6874 (1994). LADM: a Lagrangian atmospheric dispersion model.
- 6875 Piringer, M., Knauder, W., Petz, E., & Schaubberger, G. (2016). Factors influencing
6876 separation distances against odour annoyance calculated by Gaussian and Lagrangian
6877 dispersion models. *Atmospheric environment*, 140, 69-83.
- 6878 Pollini E. and Luciali P. (2015) Caratterizzazione delle sorgenti odorigene ed applicazione
6879 modellistica per lo studio della diffusione degli odori. (In Italian) Available online:
6880 <[https://www.chimicifisiciinterprover.it/wp-content/plugins/download-attachments/includes/
6881 download.php?id=2318](https://www.chimicifisiciinterprover.it/wp-content/plugins/download-attachments/includes/download.php?id=2318)> (accessed 2021).
- 6882 Pullen, J., & Vawda, Y. (2007). Review of dispersion modelling for odour predictions.
6883 Environment Agency, United Kingdom.
- 6884 Ranzato, L., Barausse, A., Mantovani, A., Pittarello, A., Benzo, M., & Palmeri, L. (2012). A
6885 comparison of methods for the assessment of odor impacts on air quality: Field inspection
6886 (VDI 3940) and the air dispersion model CALPUFF. *Atmospheric Environment*, 61, 570-579.
- 6887 Reed, W. R., & Centers for Disease Control. (2005). Significant dust dispersion models for
6888 mining operations (Vol. 9478). Createspace Independent Pub.
- 6889 Santiago, J. L., Buccolieri, R., Rivas, E., Calvete-Sogo, H., Sanchez, B., Martilli, A., Alonso
6890 R., Elustondo D., Santamaria J.M. & Martin, F. (2019). CFD modelling of vegetation barrier
6891 effects on the reduction of traffic-related pollutant concentration in an avenue of Pamplona,
6892 Spain. *Sustainable Cities and Society*, 48, 101559.
- 6893 Schaubberger, G., & Piringer, M. (1997, May). Guideline to assess the protection distance to
6894 avoid annoyance by odour sensation caused by livestock husbandry. In *Proc. 5th
6895 International Livestock Environment Symposium* (pp. 170-178).
- 6896 Schaubberger, G., Schmitzer, R., Kamp, M., Sowa, A., Koch, R., Eckhof, W., Eichler, F.,
6897 Grimm, E., Kypke, J., & Hartung, E. (2012a). Empirical model derived from dispersion
6898 calculations to determine separation distances between livestock buildings and residential
6899 areas to avoid odour nuisance. *Atmospheric environment*, 46, 508-515.
- 6900 Schaubberger, G., Piringer, M., Jovanovic, O., & Petz, E. (2012b). A new empirical model to
6901 calculate separation distances between livestock buildings and residential areas applied to
6902 the Austrian guideline to avoid odour nuisance. *Atmospheric environment*, 47, 341-347.
- 6903 Schaubberger, G., Piringer, M., & Petz, E. (2000). Diurnal and annual variation of the
6904 sensation distance of odour emitted by livestock buildings calculated by the Austrian odour
6905 dispersion model (AODM). *Atmospheric Environment*, 34(28), 4839-4851.
- 6906 Schulman, L. L., Strimaitis, D. G., & Scire, J. S. (2000). Development and evaluation of the
6907 PRIME plume rise and building downwash model. *Journal of the Air & Waste Management
6908 Association*, 50(3), 378-390.

- 6909 Scire, J. S., Lurmann, F. W., Bass, A., & Hanna, S. R. (1984a). Development of the
6910 MESOPUFF II dispersion model. Final report (No. PB-84-184753). Environmental Research
6911 and Technology, Inc., Concord, MA (USA).
- 6912 Scire, J. S., Lurmann, F. W., Bass, A., & Hanna, S. R. (1984b). User's guide to the
6913 MESOPUFF II model and related processor programs. NTIS, SPRINGFIELD, VA(USA).
6914 1984.
- 6915 Scire, J. S., Robe, F. R., Fernau, M. E., & Yamartino, R. J. (2000a). A user's guide for the
6916 CALMET Meteorological Model. Earth Tech, USA, 37.
- 6917 Scire, J. S., Strimaitis, D. G., & Yamartino, R. J. (2000b). A user's guide for the CALPUFF
6918 dispersion model. Earth Tech, Inc, 521, 1-521.
- 6919 Sironi, S., Capelli, L., Céntola, P., Del Rosso, R., & Pierucci, S. (2010). Odour impact
6920 assessment by means of dynamic olfactometry, dispersion modelling and social
6921 participation. Atmospheric Environment, 44(3), 354-360.
- 6922 Skamarock, W. C., Klemp, J. B., Dudhia, J., Gill, D. O., Barker, D. M., Wang, W., & Powers,
6923 J. G. (2008). A description of the Advanced Research WRF version 3. NCAR Technical
6924 note-475+ STR.
- 6925 Slade, D. H. (Ed.). (1969). Meteorology and atomic energy, 1968. US Atomic Energy
6926 Commission, Division of Technical Information. Available from Clearinghouse for Federal
6927 Scientific and Technical Information, National Bureau of Standards, US Department of
6928 Commerce, Springfield, VA.
- 6929 Smith, M. (1973). Recommended Guide for the Prediction of the Dispersion of Airborne
6930 Effluents, No, 68-31123, New York. Am. Soc. Tech. Eng.
- 6931 Sorbjan Z. (1989): Structure of the Atmospheric Boundary Layer - Prentice Hall, 317 pp.
- 6932 Souza FC, Hoinaski L., de Melo Lisboa H., Comparison of AERMOD and SYMOS'97 models
6933 for calculating odor dispersion: A study case in Uttenweiler, Ist International Seminar of
6934 Odours in the Environment, Santiago, Chile, 2014, www.olores.org, weblink
- 6935 Stull R.B. (1988). An Introduction to Boundary Layer Meteorology, Springer, ISBN-13 978-
6936 9027727695.
- 6937 Sutton, O. G. (1947). The problem of diffusion in the lower atmosphere. Quarterly Journal of
6938 the Royal Meteorological Society, 73(317-318), 257-281.
- 6939 Sykes, R. I., & Gabruk, R. S. (1997). A second-order closure model for the effect of
6940 averaging time on turbulent plume dispersion. Journal of Applied Meteorology, 36(8), 1038-
6941 1045.
- 6942 Sykes, R. I., Parker, S. F., Henn, D. S., Cerasoli, C. P., & Santos, L. P. (1998). PC-SCIPUFF
6943 version 1.2 PD technical documentation. ARAP Rep, 718(180), 08543-2229.
- 6944 Tampieri, F. (2017). Turbulence and dispersion in the planetary boundary layer. Switzerland:

- 6945 Springer International Publishing.
- 6946 Thomson, D. J. (1984). Random walk modelling of diffusion in inhomogeneous turbulence.
6947 Quarterly Journal of the Royal Meteorological Society, 110(466), 1107-1120.
- 6948 Thomson, D. J. (1987). Criteria for the selection of stochastic models of particle trajectories
6949 in turbulent flows. Journal of fluid mechanics, 180, 529-556.
- 6950 Thomson, D. J. (1990). A stochastic model for the motion of particle pairs in isotropic high-
6951 Reynolds-number turbulence, and its application to the problem of concentration variance.
6952 Journal of fluid mechanics, 210, 113-153.
- 6953 Thomson, D.J. (1992) The fluctuations module. A paper by the Met. Office. P13/01E/92.
6954 Available online: <
6955 https://www.cerc.co.uk/environmental-software/assets/data/doc_techspec/P13_01.pdf>
6956 (accessed 2021).
- 6957 Thomson, D.J. (2017) Concentration fluctuations in ADMS3 onwards, including fluctuations
6958 from anisotropic and multiple sources. A paper by the Met Office and CERC. Available
6959 online: <[https://www.cerc.co.uk/environmental-software/assets/data/doc_techspec/
6960 P13_07.pdf](https://www.cerc.co.uk/environmental-software/assets/data/doc_techspec/P13_07.pdf)> (accessed 2021).
- 6961 Tinarelli, G., Anfossi, D., Brusasca, G., Ferrero, E., Giostra, U., Morselli, M. G., Moussafir J.,
6962 Trombetti F., & Tampieri, F. (1994). Lagrangian particle simulation of tracer dispersion in the
6963 lee of a schematic two-dimensional hill. Journal of Applied Meteorology and Climatology,
6964 33(6), 744-756.
- 6965 Tinarelli, G., Anfossi, D., Castelli, S. T., Bider, M., & Ferrero, E. (2000). A new high
6966 performance version of the Lagrangian particle dispersion model SPRAY, some case
6967 studies. In Air pollution modeling and its application XIII (pp. 499-507). Springer, Boston,
6968 MA.
- 6969 Tinarelli, G., Sozzi, R., Barbero, D. (2022). Implementation of a simplified micromixing model
6970 inside a Lagrangian Particle Dispersion code for the estimation of concentration variances
6971 and peaks. Chemical Engineering Transactions, Vol. 95, ISBN 978-88-95608-94-5; ISSN
6972 2283-9216.
- 6973 Tomasello, N., Valenti, F., Cascone, G., & Porto, S. (2019). Development of a CFD model to
6974 simulate natural ventilation in a semi-open free-stall barn for dairy cows. Buildings, 9(8), 183.
- 6975 Turner, D. B. (2020). Workbook of atmospheric dispersion estimates: an introduction to
6976 dispersion modeling. CRC press.
- 6977 Ugolini, P., Trentini, A., Bonafé, G., & Poluzzi, V. Comparison of the results of two air quality
6978 models in the simulation of a turbogas cogeneration plant PM emissions. Environmental
6979 Sciences, 6, 795-797.
- 6980 ul Haq, A., Nadeem, Q., Farooq, A., Irfan, N., Ahmad, M., & Ali, M. R. (2019). Assessment of
6981 Lagrangian particle dispersion model "LAPMOD" through short range field tracer test in
6982 complex terrain. Journal of environmental radioactivity, 205, 34-41.

- 6983 US-EPA (1995) User's Guide for the Industrial Source Complex Dispersion Models, Volume
6984 1 User Instructions. US EPA -454/B-95-003a. September 1995.
- 6985 US-EPA (2017) Revisions to the Guideline on Air Quality Models: Enhancements to the
6986 AERMOD Dispersion Modeling System and Incorporation of Approaches To Address Ozone
6987 and Fine Particulate Matter. Appendix W. Federal Register, Vol. 82, No. 10, Tuesday,
6988 January 17, 2017. Rules and Regulations. <https://www.epa.gov/sites/production/files/2020-09/documents/appw_17.pdf> (Accessed 2021)
6989
- 6990 US-EPA (2020) Dispersion Modeling Systems Relevant to Homeland Security Preparedness
6991 and Response. EPA/600/R-20/338| October 2020.
- 6992 US-EPA (2021a) AERSCREEN User's Guide. EPA-454/B-21-005. Available online:
6993 <https://gaftp.epa.gov/Air/aqmg/SCRAM/models/screening/aerscreen/aerscreen_userguide.pdf> (accessed 2021).
6994
- 6995 US-EPA (2021b) Alternative dispersion models. Available online:
6996 <<https://www.epa.gov/scram/air-quality-dispersion-modeling-alternative-models#adms>>
6997 (accessed 2021).
- 6998 van Aalst R., Edwards L., Pulles T., De Saeger, E., Tombrou, M. & Tønnesen, D. (1998)
6999 Guidance report on preliminary assessment under EC air quality directives. European
7000 Environment Agency. Technical Report N. 11. Available online:
7001 <<https://www.eea.europa.eu/publications/TEC11a>> (accessed 2021).
- 7002 Van Egmond, N. D., & Kesseboom, H. (1983). Mesoscale air pollution dispersion models—II.
7003 Lagrangian puff model and comparison with Eulerian grid model. Atmospheric Environment
7004 (1967), 17(2), 267-274.
- 7005 Varini D. and Fornaciari S. (2019) Sviluppo delle tecniche di valutazione delle emissioni
7006 odorigene in un'azienda di rendering. (In Italian) Available online:
7007 <http://www.arpa.fvg.it/export/sites/default/tema/aria/stato/Odori/allegati/scuola_odori_2019/Fornaciari_Varini.pdf> (accessed 2021).
7008
- 7009 Vitali, L., Monforti, F., Bellasio, R., Bianconi, R., Sachero, V., Mosca, S., & Zanini, G. (2006).
7010 Validation of a Lagrangian dispersion model implementing different kernel methods for
7011 density reconstruction. Atmospheric Environment, 40(40), 8020-8033.
- 7012 VDI 3894 Part 2, Emissions and their Impact from Livestock Operations. Method to
7013 Determine the Separation Distance for Odour; Verlag des Vereins Deutscher Ingenieure:
7014 Düsseldorf, Germany, 2012
- 7015 VDI 3788, 2000. VDI 3788 Part 1. Environmental Meteorology: Dispersion of Odorants in the
7016 Atmosphere e Fundamentals, vol. 1. VDI (Verein Deutsche Ingenieure), Handbuch
7017 Reinhaltung der Luft.
- 7018 VDI 3940, 2006. VDI 3940 Part 1. Measurement of Odor Impact by Field Inspection and
7019 Measurement of the Impact Frequency of Recognisable Odors Grid Measurement, vol. 1.
7020 VDI (Verein Deutsche Ingenieure), Handbuch Reinhaltung der Luft.

- 7021 Williams, M. L., & Thompson, N. (1986). The effects of weather on odour dispersion from
7022 livestock buildings and from fields. *Odor Prevention and Control of Organic Sludge and*
7023 *Livestock Farming*, 227-233.
- 7024 Wilson, D. J., Robins, A. G., & Fackrell, J. E. (1982a). Predicting the spatial distribution of
7025 concentration fluctuations from a ground level source. *Atmospheric Environment* (1967),
7026 16(3), 497-504.
- 7027 Wilson, D. J., Fackrell, J. E., & Robins, A. G. (1982b). Concentration fluctuations in an
7028 elevated plume: a diffusion-dissipation approximation. *Atmospheric Environment* (1967),
7029 16(11), 2581-2589.
- 7030 Wilson, D. J., Robins, A. G., & Fackrell, J. E. (1985). Intermittency and conditionally-
7031 averaged concentration fluctuation statistics in plumes. *Atmospheric Environment* (1967),
7032 19(7), 1053-1064.
- 7033 Wu, C., Brancher, M., Yang, F., Liu, J., Qu, C., Schauburger, G., & Piringer, M. (2019). A
7034 comparative analysis of methods for determining odour-related separation distances around
7035 a dairy farm in Beijing, China. *Atmosphere*, 10(5), 231.
- 7036 Yeo, U. H., Decano-Valentin, C., Ha, T., Lee, I. B., Kim, R. W., Lee, S. Y., & Kim, J. G.
7037 (2020). Impact Analysis of Environmental Conditions on Odour Dispersion Emitted from Pig
7038 House with Complex Terrain Using CFD. *Agronomy*, 10(11), 1828.
- 7039 Yu, Z., Guo, H., & Laguë, C. (2011). Development of a livestock odor dispersion model: Part
7040 II. Evaluation and validation. *Journal of the Air & Waste Management Association*, 61(3),
7041 277-284.
- 7042 Zanini, G., Bellasio, R., Bianconi, R., Delle Monache, L., Kolarova, M., Lorenzini, R., ... &
7043 Vitali, L. (2002, October). PLPM (Photochemical Lagrangian Particle Model): formulation and
7044 preliminary validation. In *Proceedings of 8th Int. Conf. on Harmoisation within Atmospheric*
7045 *Dispersion Modelling for Regulatory Purposes*.
- 7046 Zannetti, P. (1990). *Air Pollution Modeling. Theories, Computational Methods and Available*
7047 *Software*. Van Nostrand Reinhold, New York. Pp. 444.
- 7048 Zannetti P. (ed.) (2010). *Air Quality Modeling: Theories, Methodologies, Computational*
7049 *Techniques, & Available Databases & Software, Vol. IV, Advances and Updates*, Air and
7050 *Waste Management Association*, ISBN 978-1-9334740-8-3.
- 7051 Zhang, Q., Zhou, X. J., Guo, H. Q., Li, Y. X., & Cicek, N. (2005). Odour and greenhouse gas
7052 emissions from hog operations. Final Report Submitted to Manitoba Livestock Manure
7053 Management Initiative Inc.
- 7054
- 7055
- 7056
- 7057

439

7058

440

215

7059 6. Output dose-response

7060 6.1. Introduction

7061

7062 Of the five senses, the sense of smell is the most complex and unique in structure and
 7063 organisation. While human olfaction supplies 80% of flavour sensations during eating, the
 7064 olfactory system plays a significant role as a defence mechanism by creating a natural
 7065 aversion response to malodours and irritants. Human olfaction protects from potential illness
 7066 or infection caused by tainted food and matter, such as rotting vegetables, decomposing
 7067 meat, and faecal matter.

7068

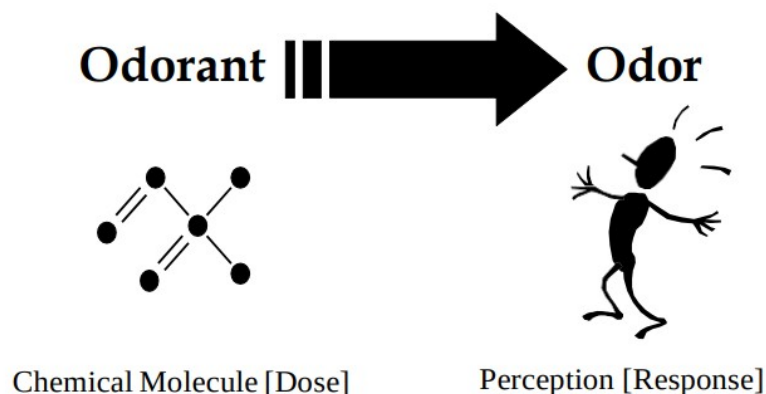
7069 Two concepts are used interchangeably within the odour impact assessment framework and,
 7070 often, incorrectly: odour and odorant. Further, there needs to be clarification between the
 7071 stimulus of odorant(s) concentration and the effect, which is the odour sensation. Further,
 7072 there is a need to link odour sensation to odour nuisance.

7073

7074 Figure 6-1, illustrates how an odorant creates the odour perception. The term odour refers to
 7075 the perception experienced when one or more chemical substances in the air come in
 7076 contact with the various human sensory systems and when the stimuli are sufficient to
 7077 trigger perception.

7078

7079



7080

7081

7082 **Figure 6-1** Chemical Odorant versus Odour Perception (courtesy of St. Croix Sensory)

7083

7084 The term odorant refers to any chemical in the air that is part of the perception of odour by a
 7085 human (odorant is a chemical). Odour perception may occur when one odorant (chemical
 7086 substance) is present or when many odorants (chemical substances) are present.

7087

7088 An analogy that helps to understand what is happening with odour perception in the olfactory
 7089 system is envisioning the receptor nerves like keys on a piano. As a single chemical odorant
 7090 hits the piano keyboard (the olfactory epithelium), a tone is played (odour perception). When
 7091 multiple chemical odorants are present and hit the piano keyboard, the result is a chord
 7092 (odour perception). For example, if keys 1, 3, and 7 are hit by three different odorants, the

7093 brain may perceive earthiness. Likewise, if keys 4, 6, and 12 are hit by three different
 7094 odorants, the brain may perceive sewer. The greater the number of odorant molecules
 7095 present (higher concentrations), the louder the chord is played. The loudness of the chord is
 7096 analogous to the intensity of the odour perception.

7097
 7098 Perception of odours depends not only on the sensitivity of each individual or community but
 7099 also on the number of times this odour occurs, how intense it is, how unpleasant it is, and
 7100 the duration of the odour episodes once they are perceived. Odour perception also varies
 7101 depending on the recipient's experience, expectations, motivation and degree of alertness.

7102

7103 6.2. The FIDOS factors

7104

7105 A range of factors influence the impact of the odour experienced by a community, the most
 7106 relevant being *Frequency, Intensity, Offensiveness, Duration* and *Sensitivity* (FIDOS).

7107

7108 It is possible to find in the literature (Bokowa et al. 2021; H4 Odour Management, 2011) the
 7109 terms FIDO, FIDOL (L stands for Location) and FIDOR (R stands for Receptor). In this text,
 7110 we have preferred to use the term FIDOS to give a more meaningful name to that factor
 7111 related to the odour impact, not covered by frequency, intensity, duration and offensiveness.

7112

7113 The following chapters will describe each of these FIDOS factors in detail.

7114

7115 6.2.1 Frequency

7116

7117 The frequency of odour exposure simply refers to how often odour events occur. It is a
 7118 function of the variations of odour emissions over time and of the meteorological conditions
 7119 in the area around an odour source. The frequency of odour events is generally greatest in
 7120 areas most often downwind of the source, especially under light wind and stable
 7121 atmospheric conditions (provided that the odour is not emitted at a significant height above
 7122 the ground).

7123

7124 Although the frequency of odour events is a prime determinant of the likelihood of nuisance
 7125 occurring, the timing of events can also be important. There are times of the day, for
 7126 example, when there may be a greater likelihood of people being exposed to any ambient
 7127 odour, such as in the morning period around breakfast or around the evening mealtime. At
 7128 other times, the likelihood of being away from the home, or asleep or simply inside with
 7129 windows and doors shut may reduce the likelihood of being affected by odours that are
 7130 present in the ambient air.

7131

7132 The dispersion models are relevant, as they allow the calculation of the odour concentration
 7133 at certain receptor points (immission), allowing estimating the odour supply frequencies as a
 7134 function of the modelled time.

7135

7136 Exposure to odour is usually quantified in terms of a frequency of occurrence of mean hourly
 7137 concentrations of a certain odour above a defined limit concentration. Considering that the

7138 criteria of maximum hourly impact, or most unfavourable condition, are not representative of
 7139 a permanent exposure condition synthesised in a year due to the variation of the seasonal
 7140 meteorological state of a certain place, the use of the percentile criterion is recommended.
 7141 which allows you to view the percentages of hours in which the value defined for the 8,760
 7142 hours of the year is exceeded (this is the relationship between frequency and percentile).

7143

7144 What are Percentiles?

7145

7146 A percentile is a descriptive statistic that can be used to describe the distributional
 7147 characteristics of a dataset. To arrive at percentile values, data must be rank ordered, i.e.
 7148 arrayed in order of decreasing or increasing magnitude, to form a frequency distribution. In
 7149 this case, data would, for example, be hourly odour concentration data for a year and a
 7150 specific location. The 98th percentile represents the concentration value for which 98% of
 7151 the data points are less than or equal to this value. Other percentiles can be used as well.
 7152 For example, the 50th percentile or median is the variable's value that has an equal number
 7153 of data points on either side. The range enclosed by the 1st - percentile and 99th percentile
 7154 provides an indication of the data range. When time series data are used, the nth-percentile
 7155 value may be used as a criterion representing the value that may be exceeded only (100-n)
 7156 % of the time, i.e. $(100-n)\% \times 8760$ hours over a full year.

7157

7158 Why are Percentiles Used in Odour Assessment?

7159

7160 Understanding the reasons for the use of percentiles in odour assessments requires a brief
 7161 discussion of the history of odour research. Early odour research found that measured
 7162 instantaneous odour nuisance and modelled hourly odour concentration are weakly but
 7163 significantly correlated. In other words, the reported nuisance increased with increasing
 7164 odour concentration levels. However, stronger and linear correlations were found between
 7165 (long-term) nuisance surveys and the logarithmic 98th-percentile and 99.99th-percentile (i.e.
 7166 maximum) values of the modelled annual hourly odour concentration (e.g. Verschut et al.,
 7167 1991; Walpot et al., 1991). This relationship was particularly clear for high odour
 7168 concentrations ($C_{98 \text{ 1 hr}}$ exceeding roughly 10 ou/m^3). This better correlation with higher
 7169 percentiles compared to other descriptive statistics (e.g. mean, mode, median, etc.) may be
 7170 explained by the fact that the relatively rare hours with high concentration levels are more
 7171 critical in causing nuisance than the majority of hours when the concentration is relatively
 7172 low (or zero).

7173

7174 Another important finding was that no single unambiguous relationship between nuisance
 7175 and absolute odour concentration level could be established. This means that for one type of
 7176 industry, an odour nuisance threshold in terms of the proportion of people annoyed may be
 7177 significantly higher (e.g. $C_{98 \text{ 1 hr}} = 10 \text{ ou/m}^3$) than for another type of industry (e.g. $C_{98 \text{ 1 hr}} = 3$
 7178 ou/m^3). This is due to the complexity of odour nuisance. The actual odour nuisance that is
 7179 experienced depends on several factors such as type of components (hedonic value), place
 7180 of occurrence, time of occurrence (frequency, time of exposure) and personal experience
 7181 (Australian Pork Limited, 2003).

7182

7183 In subsequent research, Miedema (1992) found a correlation between community odour
 7184 annoyance and percentiles of odour concentration for five different types of odour sources,
 7185 including a pig farm. The 99.5th percentile was found to be a somewhat better indicator of

7186 odour impact across a range of sources than the 98th percentile. It was suggested that this
 7187 is because people base their annoyance judgement on the hours of maximum concentration.
 7188 It was found that a single curve can describe the linear relationship between $\log(C_{99.5 \text{ 1 hr}})$
 7189 and annoyance for all types of odour sources. This research suggested that different
 7190 characters (in terms of “offensiveness” or “pleasantness”) of odour did not play an important
 7191 role with respect to nuisance. The research also found that the level of annoyance in the
 7192 community due to an odour source did not depart from baseline levels until the $C_{99.5 \text{ 1 hr}}$ odour
 7193 level exceeded about 10 ou. In summary, the better correlation between percentiles and
 7194 community nuisance levels compared to other descriptive statistics (e.g. between the mean
 7195 and nuisance levels) explains the use of percentiles in odour assessments. The actual
 7196 relationship between percentiles and community nuisance levels in absolute terms will
 7197 depend on many factors, including odour quality (hedonic value), place of occurrence, time
 7198 of occurrence and personal experience.

7199
 7200 On the other hand, and complementing the aforementioned, Miedema et al. (2000)
 7201 developed a model for predicting the percentage of individuals who are highly annoyed in
 7202 the surrounding community (%HA). This model is expressed as follows:

7203
 7204 **Equation 6-1**
$$\%HA = 9.55 \times C_{98}^2$$

7205
 7206 %HA : the percentage of individuals who are highly annoyed in the surrounding community.
 7207

7208 C_{98} : 98th percentile concentration.
 7209

7210 In addition, it was found that the accuracy of the prediction of the percentage of individuals
 7211 who are highly annoyed in the surrounding community is improved if both the pleasantness
 7212 of odour and odour concentration is taken into account (Miedema et al., 2000).

7213

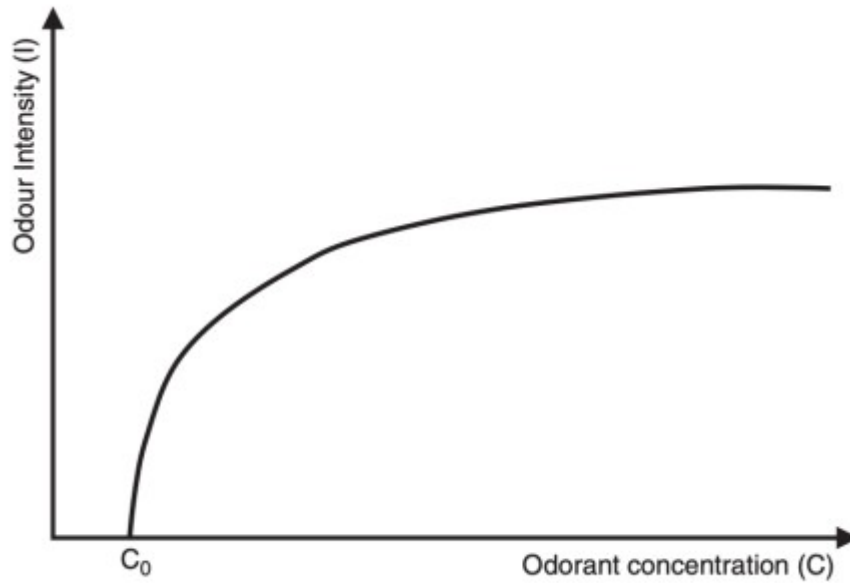
7214 6.2.2 Intensity

7215

7216 The perception of intensity of an odour is how strong an odour is perceived to be. Odour
 7217 intensity describes the relative magnitude of an odour sensation as experienced by a
 7218 person. The perception of intensity of an odour in relation to the odour concentration follows
 7219 a logarithmic relationship (the same relationship occurs for other human senses, such as
 7220 hearing and sensitivity to light). Therefore, to understand the concept of intensity, we must
 7221 first define the concept of odour concentration. According to EN 13725 the odour
 7222 concentration is “the number of European odour units per cubic metre under normal
 7223 conditions”. Odour concentration is measured in European odour units and its symbol is ou_E .

7224

7225 The logarithmic nature of odour perception is important for all odour sources. It means that
 7226 decreasing the concentration of an odour (as determined by olfactometry) by 10-fold will only
 7227 decrease the intensity by a much smaller amount (see Figure 6-2). Intensity can be
 7228 assessed in many ways.
 7229



7230
7231 **Figure 6-2** Logarithmic relationship between intensity and concentration

7232
7233 An assessment of odour impacts from the sources using an odour intensity criterion
7234 approach recognises the fact that the same concentration (stimulus) of different odorants
7235 does not elicit the same perception of intensity (response) in people. This approach may be
7236 advantageous to activities that emit odorous substances that exhibit low intensity at relatively
7237 high concentration.

7238
7239 Odour concentrations above the detection threshold are not direct indicators of perceived
7240 odour intensity. For each odorant, its odour intensity is a non-linear function of its
7241 concentration and the perceived odour intensity can be described using a mathematical
7242 equation (Stevens Law or the Weber-Fechner Law). The Weber Fechner law can be
7243 expressed by the equation:

7244
7245 **Equation 6-2**
$$S = k_w \times \log \frac{I}{I_0}$$

7246
7247 Where,

7248
7249 S = perceived intensity of sensation (theoretically determined).

7250 I = physical intensity (odour concentration).

7251 I_0 = threshold concentration (1 ou_E).

7252 k_w = Weber-Fechner coefficient.

7253
7254 Odour intensity can be categorised according to the German Standard method VDI 3882/1,
7255 Olfactometry - Determination of Odour Intensity, Part 1, 1992, into odour intensity in
7256 categories described as not perceptible, very weak, weak, distinct, strong, very strong and
7257 extremely strong and assigned corresponding numerical values, 0 to 6. The seven-point
7258 intensity scale is defined as shown in Table 6-1.

7259
7260 **Table 6-1** Odour Intensity Categories

Odour Strength	Intensity Level
Extremely strong	6
Very strong	5
Strong	4
Distinct	3
Weak	2
Very weak	1
Not perceptible	0

7261

7262

7263 Solving the experimentally established Stevens Law or Weber-Fechner equations at a
 7264 particular intensity level for odours characteristic of an individual facility yields a
 7265 corresponding odour concentration value. The approach requires a considerable amount of
 7266 initial work by a proponent or industry group to establish the intensity versus concentration
 7267 relationships for a particular odour type.

7268

7269 This method requires an odour intensity study to determine the relationship between odour
 7270 concentration and odour intensity, in order to specify the odour concentration equivalent to
 7271 the intensity level of "weak". The method for determining odour concentration and intensity
 7272 must follow the procedure and standards internationally validated, for example: Australian
 7273 and New Zealand Standard (AS/NZS 4323.3:2001) and the German Standard VDI 3882/1.
 7274 The samples collected from the source will be analysed simultaneously in the laboratory for
 7275 odour concentration and intensity, using odour panels and dynamic olfactometry equipment.
 7276 By doing this, it is possible to develop a relationship between them and determine the odour
 7277 concentration equivalent to the intensity level of "weak" or "strong".

7278

7279 6.2.3. Duration

7280

7281 6.2.3.1 Fundamentals

7282

7283 Odour nuisance is known to be closely linked to short-term odour-concentration peaks, as
 7284 these may reach levels well above the recognition threshold causing immediate annoyance.
 7285 In the past decades, dispersion models have become a standard tool for air quality
 7286 assessments, which are based mostly on the prediction of hourly-mean concentrations.
 7287 Typically, dispersion models are not designed for providing concentrations for time intervals
 7288 well below one hour. Different approaches have been developed for implementation in
 7289 regulatory models. These could be split into two groups: (1) methods providing short-term
 7290 concentrations based on predicted hourly-mean concentrations of a dispersion model, and
 7291 (2) methods that additionally account for the sensitivity of persons. The methods are usually
 7292 strongly related to odour regulations set up by local or national authorities. In the following,
 7293 only approaches are outlined which are in use for regulatory purposes, while

7294 models/methods currently discussed in the scientific literature but are not yet applied in
 7295 practice will not be discussed subsequently.
 7296

7297 6.2.3.2. Methods for assessing peak concentrations

7298

7299 A basic concept relating short-term C_p to long-term concentrations C_m was suggested by
 7300 Smith (1973):

7301 **Equation 6-3**
$$\frac{C_p}{C_m} = \left(\frac{t_m}{t_p}\right)^n$$

7302

7303 $\frac{C_p}{C_m}$: constant Peak-to-Mean Ratio.

7304

7305 $\frac{t_m}{t_p}$: the ratio of the long- and short-term intervals, and n is an empirical exponent.

7306

7307 Often a constant exponent n is used, ranging from 0.18 to 0.68 (Beychock, 1994;
 7308 Venkatram, 2002). For instance, the U.S. EPA regulatory model CALPUFF (Scire et al.,
 7309 2000) as well as the Australian regulatory model AUSPLUME (Lorimer, 1986) set n equal to
 7310 0.2. Table 6-2 lists countries and regions applying a constant Peak-to-Mean Ratio in the
 7311 odour regulations.

7312

7313 **Table 6-2** List of countries using a constant Peak-to-Mean Ratio (Brancher et al. 2017)

Country	Region	t_p	$\frac{C_p}{C_m}$
Canada	Quebec	4 min	1.9
	Ontario	10 min	1.65
	Manitoba	3 min	2.3
Denmark	-	1 min	7.8
Italy	Lombardy, Puglia	Not defined	2.3
Australia	Victoria	3 min	1.82

7314

7315 It can easily be deduced from the widely accepted K-theory

7316

7317

$$\overline{u'c'} = K_i \frac{\partial \bar{c}}{\partial x_i}$$

7318 **Equation 6-4**

7319

7320 $\overline{u'c'}$: the turbulent flux.

7321

7322 $\frac{\partial c}{\partial x_i}$: flow mix in atmosphere

7323

7324 K_i :the exchange coefficient that expresses the turbulent structure of the atmosphere.

7325

7326 that the turbulent flux $u'c'$ of any quantity becomes zero in case that it is well mixed within7327 the atmosphere, i.e. $\frac{\partial c}{\partial x_i}=0$. This is approximately the case far downwind from a source, or

7328 in the case that multiple and/or large extended odour sources cause overlapping plumes. It

7329 follows, as the turbulent velocities $u' \neq 0$ in the atmosphere, that c' must be close to zero, and7330 that the corresponding Peak-to-Mean Ratio $\frac{C_p}{C_m}$ approaches one in such circumstances.

7331 Apparently, besides the distance from the source and the shape of (overlapping) plumes, the

7332 turbulent structure of the atmosphere, expressed by the exchange coefficient K_i , also

7333 exhibits an influence on the turbulent flux, and thus on the Peak-to-Mean Ratio.

7334

7335 The method developed by Piringer et al. (2015) takes into account two of the

7336 aforementioned influences: atmospheric stability and distance from a single point source:

7337

7338

$$\frac{C_p}{C_m} = 1 + \left(\left[\frac{C_p}{C_m} \right]_0 - 1 \right) e^{-0.73 \frac{T}{T_L}}$$

7339 **Equation 6-5**

7340

7341 T : stands for travel time.7342 T_L for the Lagrangian time scale.

7343

7344 $\left[\frac{C_p}{C_m} \right]_0$: the initial Peak-to-Mean Ratio

7345

7346 $\frac{C_p}{C_m}$: Peak-to-Mean Ratio

7347

7348 Both the initial Peak-to-Mean Ratio $\left[\frac{C_p}{C_m} \right]_0$ and T_L depend on atmospheric stability. Brancher

7349 et al. (2020) pointed out that the approach tended to underestimate Peak-to-Mean Ratios

7350 (expressed as the 90th percentile in their study) caused by the rapid exponential decrease of7351 $\frac{C_p}{C_m}$ with a downwind distance.

7352

7353 Table 6-3 lists countries that are using variable Peak-to-Mean Ratios in their regulations. As

7354 can be seen, the majority applies ratios depending on atmospheric stability classes

7355 (Pasquill-Gifford-Turner). However, in some regions in Australia Peak-to-Mean Ratios vary

7356 also with distance from the source as well as inside or outside wake-affected zones.
 7357

7358 **Table 6-3** List of countries using a variable Peak-to-Mean Ratio $\frac{C_p}{C_m}$ (Brancher et al.
 7359 2017)

Country	Region	t_p	$\frac{C_p}{C_m}$	
Israel	-	10 min	PGT stability classes A, B: 2.45 C: 1.82 D: 1.43 E, F: 1.35	
Hong Kong		5 s	PGT stability classes A, B: 45 C: 27 D: 9 E, F: 8	
Australia	New South Wales	1 s	PGT classes A, B, C, D Far field: 2.3 Near field: 2.5 Wake-free Point: 12	PGT classes E, F Far field: 1.9 Near field: 2.3 Wake-free Point: 25
	Queensland	1 s	Volume, wake-affected point: 2.3 Wake-affected point, and all ground-based sources: 2 Wake-free point: 10	

7360
 7361 Oettl and Ferrero (2017) developed the concentration-variance method in which the hourly-
 7362 mean concentration is calculated with any suitable dispersion model, while the concentration
 7363 variance is estimated by neglecting the advection and diffusion terms in the time-dependent
 7364 governing equation for the concentration variance.

7365
 7366
 7367 **Equation 6-6**

$$\frac{\partial \underline{c}'^2}{\partial t} = 2 \sigma_{ui}^2 T_{Li} \left(\frac{\partial \underline{C}}{\partial x_i} \right)^2 - \frac{\underline{c}'^2}{t_d}$$

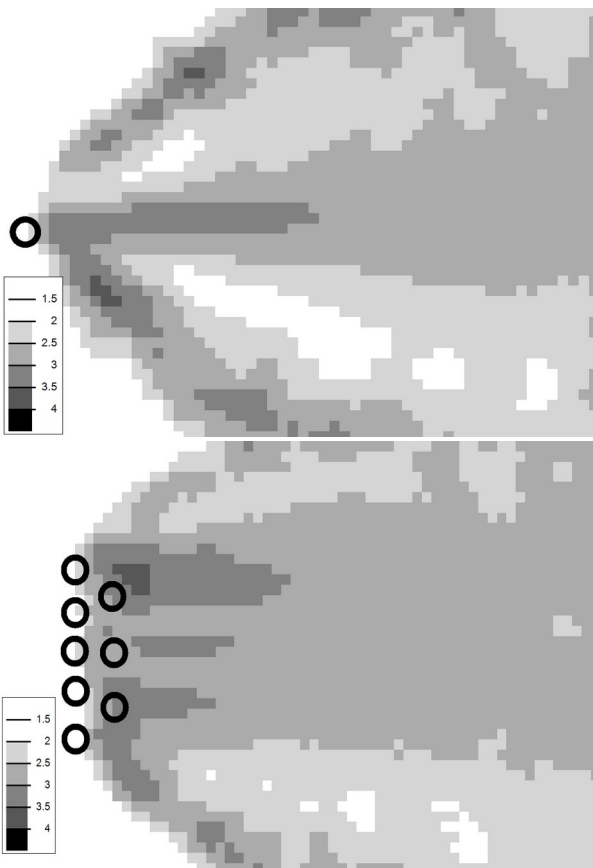
- 7369
 7370 σ_u^2 : variance of wind speed fluctuations
 7371 t_d : dissipation time scale for the concentration variance
 7372 \underline{c} : hourly-mean concentration computed by a dispersion model

7373

7374 One of the main advantages of using Equation 6.6 is that it can be computed in post-
 7375 processing mode, and thus, is independent on the dispersion model applied for calculating
 7376 the mean concentration field. The simulated concentration variances are used in
 7377 combination with a slightly modified two-parameter Weibull probability distribution function to
 7378 get the Peak-to-Mean Ratio expressed as the 90th percentile of the cumulative frequency
 7379 distribution. Figure 6-2 displays modelled Peak-to-Mean Ratios using Equation 6.6 for a
 7380 single point source (upper) and multiple point sources (lower) in neutral atmospheric
 7381 stability. Contrasting the simpler models outlined before, the method suggests strongly
 7382 varying Peak-to-Mean Ratios. While the ratios expectedly decrease with increasing distance
 7383 to the source, secondary maxima are visible at the edge of the plume, which is in agreement
 7384 with observations (e.g. Yee et al., 1994). Overlapping plumes significantly affect Peak-to-
 7385 Mean Ratios as can be seen from the lower frame of Figure 6-2. Recently, Brancher et al.
 7386 (2020) compared the concentration-variance method with the one used in Germany
 7387 (constant factor of 4) and the model suggested by Piringer et al. (2015) outlined before.
 7388 They concluded, by comparing Peak-to-Mean ratios with observations near a pig shed in
 7389 Germany, that the concentration-variance approach provided the most realistic ratios.

7390

7391



7392

7393

7394 **Figure 6-2** Modelled Peak-to-Mean Ratios using Equation 6.6 near a single point source
 7395 (upper) and multiple point sources (lower) indicated by the circle and wind from the left.
 7396 (courtesy of Öttl Dietmar)

7397

7398 6.2.3.3. Methods additionally accounting for the sensitivity of persons

7399

7400 Janicke and Janicke (2004) did not only consider the concentration fluctuations themselves,
 7401 but took into account the probability $P_0(c)$ of qualified panel members to recognise a certain
 7402 type of odour dependent on its concentration. This is expressed in the definition of the so-
 7403 called “odour hour” in the German guideline VDI 3788 (2015) by the following function:
 7404

$$\kappa = \int_0^{\infty} P_0(c) f(c) dc,$$

Equation 6-7

7405

7406 $f(c)$: the probability density function of odour concentrations at some observational point
 7407 for an hourly interval.

7408

7409 $P_0(c)$: the probability of qualified panel members to recognise a certain type of odour
 7410 dependent on its concentration.

7411

7412 $\kappa \geq 0.9$: odour hour

7413

7414 An odour hour is defined by $\kappa \geq 0.9$, i.e., in 10% of the time odour will be detected by the
 7415 qualified panel members. Janicke and Janicke (2004) demonstrated that for an assumed
 7416 log-normal distribution for $P_0(c)$:

$$P_0(c) = 0.5 \left[1 + \operatorname{erf} \left(\frac{\ln \left(\frac{c}{c_{OT}} \right)}{\sqrt{2}\alpha} \right) \right]$$

Equation 6-8

7417 $P_0(c)$: the probability of qualified panel members to recognise a certain type of odour
 7418 dependent on its concentration.

7419 α : scale parameter.

7420 erf : the error function

7421 c : the odour concentration

7422 c_{OT} : the odour concentration detected by 50% of qualified panel members

7423

7424 For $\alpha > 1$ an almost constant Peak-to-Mean Ratio of about 4 is obtained, practically
 7425 independent on the shape of $f(c)$. This is the very reason why in Germany a constant factor
 7426 of four is prescribed as Peak-to-Mean Ratio for computing an odour hour.

7427

7428 The value of α can be determined by means of dynamic olfactometry however. Oettl et al.
 7429 (2021) analysed more than 1000 datasets covering a wide range of odour types, and found
 7430 a median for α of 0.6. In this case, the shape of $f(c)$ becomes important and needs to be
 7431 taken into account in odour assessments. Oettl et al. (2018) implemented the concentration-
 7432 variance model outlined in the previous section in the Lagrangian Particle Model GRAL

7433 (Oettl, 2020), which is widely used in Austria for odour assessment studies though the model
 7434 is not mandatory. It could be demonstrated that computed odour-hour frequencies using
 7435 GRAL, in the vicinity of a pig shed, agreed well with observed frequencies based on the
 7436 European standard EN 16841-1 (2017). It should be emphasised that the main advantage of
 7437 using odour hours in assessment studies over the widely used limit values based on
 7438 percentiles of hourly-mean odour concentrations (e.g. Brancher et al., 2017), is the
 7439 possibility of using either dispersion modelling or field inspections in odour assessments.
 7440 Recently, Brancher et al. (2020) linked the concentration-variance model with the German
 7441 Lagrangian Particle Model LASAT (Janicke Consulting, 2019).
 7442

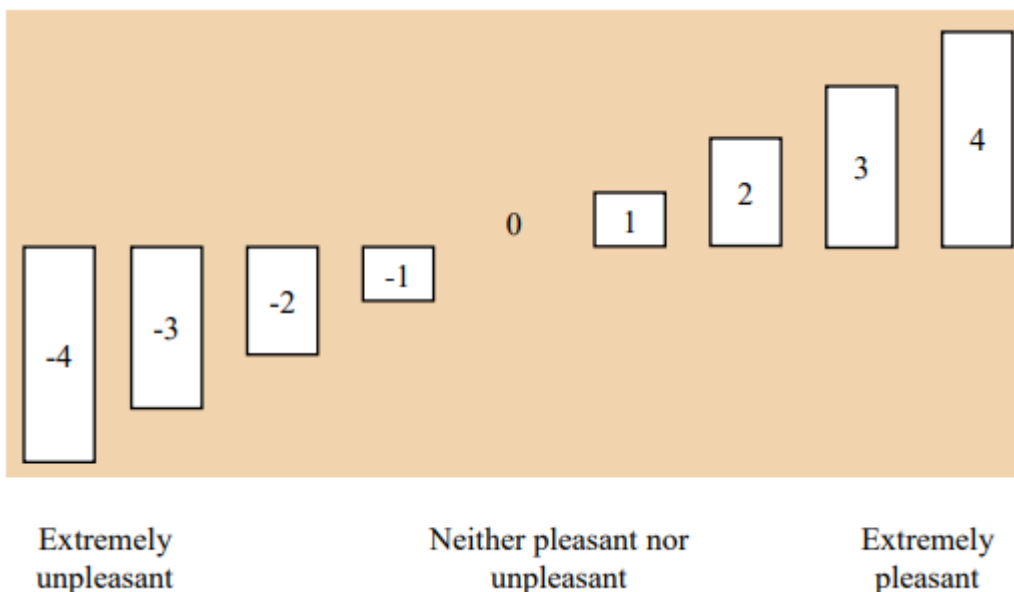
7443 6.2.4 Offensiveness

7444

7445 Offensiveness is the character related to the “hedonic tone” of the odour, which may be
 7446 pleasant, neutral or unpleasant.

7447

7448 According to the German guideline VDI 3882 Part 2, the methodology uses a nine-point
 7449 scale, ranging from -4 (extremely unpleasant) to +4 (extremely pleasant), being 0 an odour
 7450 that is perceived neither as pleasant nor unpleasant (Figure 6-3).
 7451



7464 the NVN.

7465

7466 This parameter is a subjective measure of the acceptability of an odour and a key element
7467 in estimating odour annoyance. As with most parameters, the hedonic tone is not an
7468 independent quality of a volatile compound, and it depends on the intensity, concentration,
7469 duration and frequency of the odour exposure. Moreover, the hedonic tone also differs
7470 widely from person to person, and it is strongly influenced by previous experiences,
7471 emotions and other circumstances.

7472

7473 Odour character is what the substance smells like. However, because individuals perceive
7474 odour individually, the same chemical may be described quite differently among people.
7475 Odour character can also change with concentration. For example, butyl acetate has a
7476 sweet odour at low concentrations but smells like banana at higher concentrations.

7477

7478 With the potential evolution of the odour with the concentration, the hedonic tone itself can
7479 be affected. Even a pleasant odour can become unpleasant if the concentration is too high.
7480 It can be the case for perfumes but also very often with the food industry. So offensiveness
7481 must be considered at the level of odour exposure without extrapolation of potential
7482 evolution for lower or higher concentrations. The global feeling (with all the factors) is for
7483 offensiveness, the perception for one level in the concentration range and this aspect is
7484 covered by intensity description.

7485 6.2.5. Sensitivity

7486

7487 Sensitivity (of individuals to odours in one environment) is individuals' sensation and
7488 emotional responses to an odorous atmosphere at one time of their daylife/life and the
7489 location where the odour is perceived.

7490

7491 Four basic factors affect the sensitivity of individuals:

7492

7493 ● Experience.

7494 ● Expectations.

7495 ● Motivation and

7496 ● Degree of alertness of the receiver.

7497

7498 From this point of view, as none of these parameters is included in the equations of the
7499 dispersion algorithm, it is difficult that just by using dispersion modelling a modeller will be
7500 able to calculate the odour impact of a facility.

7501

7502 When assessing odour impact, and above all when dealing not only with individuals but also
7503 with a group of people, other factors affect the sensitivity of a population. A first approach
7504 was described by (Rossi et al. 2015). This author describes the following factors affecting
7505 sensitivity:

7506

7507 1. The population affected (large city, town, scattered houses, etc.).

7508 2. The use of the land where it is located (industrial, rural, hospital, school, etc.),

7509 3. The housing uses (a continuous, occasional, fortuitous, repeated passage, etc.),

7510 4. Type of protection that the impacted area may have (historical site, natural site, etc.).

7511

7512 The IAQM Guidance on the assessment of odour for planning (Bull et. al. 2018) proposes
7513 another approach. This Guidance differentiates between receptors with high, medium and
7514 low sensitivity according to the following table:

7515

7516

High sensitivity receptor	<p>Surrounding land where:</p> <ul style="list-style-type: none"> • users can reasonably expect enjoyment of a high level of amenity; and • people would reasonably be expected to be present here continuously, or at least regularly for extended periods, as part of the normal pattern of use of the land. <p>Examples may include residential dwellings, hospitals, schools/education and tourist/cultural.</p>
Medium sensitivity receptor	<p>Surrounding land where:</p> <ul style="list-style-type: none"> • users would expect to enjoy a reasonable level of amenity, but wouldn't reasonably expect to enjoy the same level of amenity as in their home; or • people wouldn't reasonably be expected to be present here continuously or regularly for extended periods as part of the normal pattern of use of the land. <p>Examples may include places of work, commercial/retail premises and playing/recreation fields.</p>
Low sensitivity receptor	<p>Surrounding land where:</p> <ul style="list-style-type: none"> • the enjoyment of amenity would not reasonably be expected; or • there is transient exposure, where the people would reasonably be expected to be present only for limited periods of time as part of the normal pattern of use of the land. <p>Examples may include industrial use, farms, footpaths and roads.</p>

7517

7518 The weighting of receptor sensitivity can be carried out using traditional *psychometric tools*.

7519 In this case, values or quantity are attributed to psychological conditions and other

7520 phenomena so that, in this way, it is possible to compare the psychic characteristics of

7521 different people and to work with objective information. An example of such methodology is

7522 the German standard VDI 3883 which to date it is divided into 4 parts. Each of the parts

7523 deals with a different psychometric approach. Part 1 of this standard, for example, describes

7524 a method for assessment of odour nuisance by means of the questionnaire technique as

7525 well as for estimation of whether and to which extent odour nuisance is present in an area.

7526

7527 Other psychometric tools used traditionally are

7528

7529 1. Interviews (telephone, face-to-face)

7530 2. Surveys, Questionnaires

7531 3. Odour diaries

7532 4. Analysis of records of complaints

7533

7534 In addition, there is a fifth psychometric tool being used nowadays:

7535

7536 5. Mapping odours by using citizen science approaches

7537

7538 These psychometric tools are very much used in contexts related to the evaluation of odour
7539 impact.

7540

7541 The following subchapters will deal with each of these psychometric tools.

7542

7543 6.2.5.1 Measuring sensitivity with Interviews

7544

7545 Interviews can be carried out door to door. Another way of carrying out interviews is by
7546 phone, provided that a phone book is provided.

7547

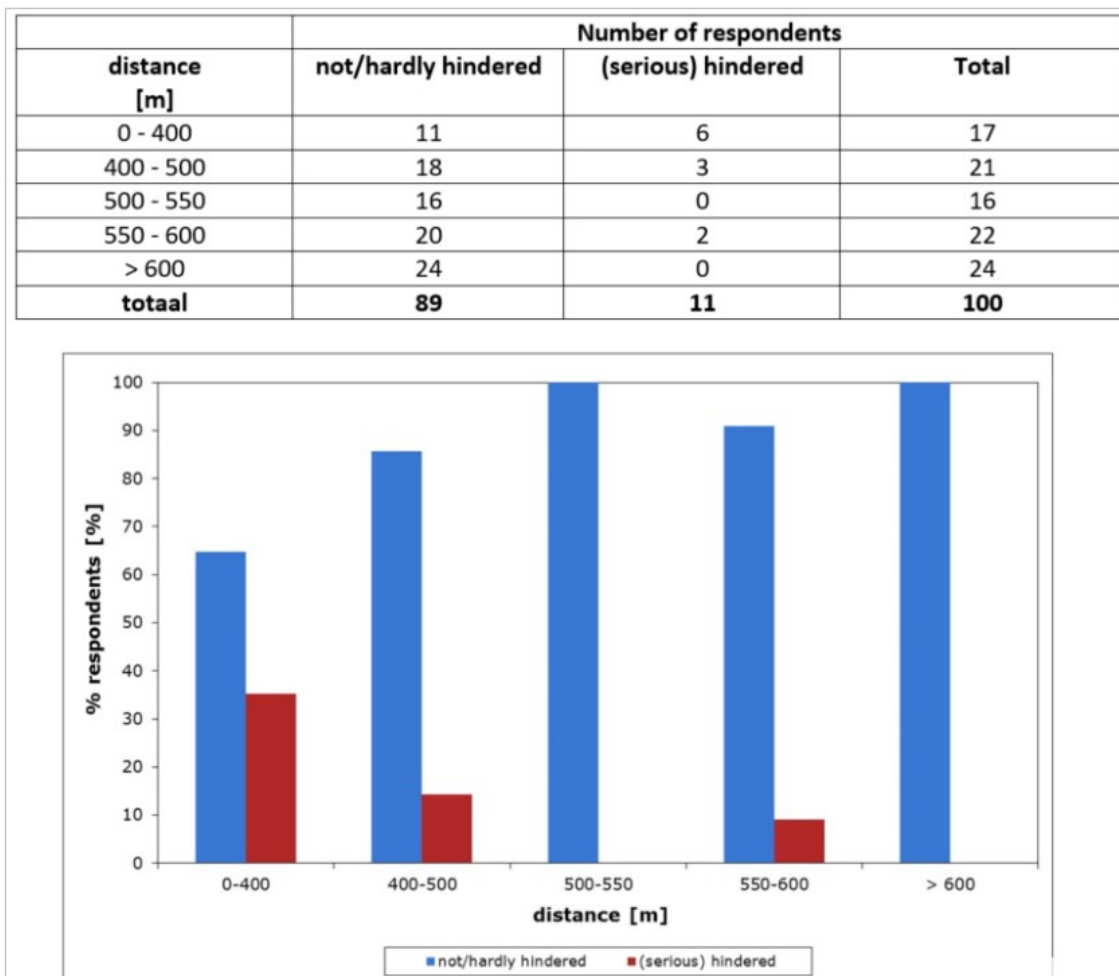
7548 In the following example a telephone survey was carried out by the Belgian company VITO,
7549 after selecting phone numbers corresponding with different addresses, at different distances
7550 from a waste treatment plant.

7551

7552 A total of 17 people living less than 400 metres from the plant answered the phone call. Of
7553 those 17 people, 11 answered that the odour was not annoying, whilst the other 6 answered
7554 that they were seriously annoyed.

7555

7556 Different people at different distances from the plant were also interviewed, the following
7557 Figure 6-4 shows the results of all the people that answered the phone call (100 people in
7558 total).



7559
7560 **Figure 6-4** Comparison of results from interviews by phone to citizens at different
7561 distances from a waste treatment plant. Red bars show the percentage of respondents that
7562 were annoyed and blue bars show the percentage of respondents that were not annoyed
7563 (Courtesy of VITO, Belgium).

7564 6.2.5.2 Measuring sensitivity with Surveys/Questionnaires.

7565
7566 Surveys and questionnaires are very useful for dose-response studies. There are numerous
7567 studies that link health with odour impact in the literature such as Aatamila et al. (2011);
7568 Baldwin et al (2004); Dalton et. al. (1999); Dalton et. al. (2003); Government of Alberta
7569 (2017); Heany et. al. (2011); Helene et. al. (2020); Miedema et. al. (2000); Oiamo et. al.
7570 (2015); Ragoobar et. al. (2016); Rethage et. al. (2007); Schiffman et. al. (1995); Schiffmann
7571 et. al. (2004); Shusterman et. al. (1991); Steinheider et. al. (1993); Sucker et al. (2001); van
7572 Harreveld et al. (2002).

7573
7574 Most of the studies aforementioned relied on surveys and questionnaires in order to find
7575 sensitivity in a population. There are in fact a couple of German standards dealing with the
7576 use of questionnaires. Those are:

- 7577
7578
- VDI 3883 part 1:2015-09 Effects and assessment of odours - Assessment of odour

7579 annoyance - Questionnaires

- 7580 ● VDI 3883 part 2:1993-03 Effects and assessment of odours; determination of
- 7581 annoyance parameters by questioning; repeated brief questioning of neighbour
- 7582 panellists

7583

7584 The difference between these 2 standards is that part one deals with one single
7585 questionnaire and part 2 deals with a questionnaire repeated a few times along the period of
7586 study.

7587

7588 These 2 standards are key, as they can be used when a dispersion model is showing no
7589 impact, but the citizens are still complaining about the situation of a plant. The following
7590 snapshot (Figure 6-5) shows some of the questions asked in part 1.

7591

Questions 1+2: Questions on the general pollution situation and sensation of annoyance

Question 3: The intensity and frequency of odours are graded with verbal descriptions

Question 4: Annoyance reactions to odours and noise are to be given on a so-called thermometer scale. The advantage of this answer scale is that it is non-verbal, i.e. no verbal description of the investigated situation is necessary.

Question 5: As a control, the same situation is recorded as in Question 4 but in this case with a verbal description

Question 6: This is the question on the state of annoyance, i.e. on the emotional assessment, in the extreme range

7592

7593 **Figure 6-5** Example of questions made according to VDI 3883 part 1

7594

7595 Respondents are also asked to mark in a thermometer how much annoyed they are, which
7596 is a very graphic way to measure annoyance.

7597

7598 German standards are not only used in Germany, but in many other parts of the world. For
7599 example, in some parts of Colombia these standards (transposed as the NTC 6012 part 1
7600 and part 2 Colombian standards) are used to take a decision on requiring an odour emitting
7601 activity to take additional measures in order to solve a situation of odour conflict.

7602

7603 For example, the Government of the Colombian region of the Valle del Cauca (CVC) has in
7604 place several protocols to deal with odour impact based on questionnaires.

7605

- 7606 ● Guide: Field planning and data processing - psychometric assessment of odour
- 7607 nuisances of odour nuisance. CVC (2018)

7608

- Guide: Field guide for Interviewer - odour complaints. CVC (2018)

7609

- Technical instructions: methodological route for determining potential nuisance due to intense odorous substances due to intense odorous substances. CVC (2016)

7610

7611

7612 A typical path in Germany and other parts of Europe could be the following.

7613

7614

1. A dispersion model is carried out

7615

2. If there are still complaints, the plant is asked to whether carry out the grid method according to EN 16841 part 1 or to take corrective actions

7616

7617

3. If there are still complaints, the plant is asked to carry out a VDI 3883 or take corrective actions.

7618

7619

4. If the results of the VDI 3883 show that there is impact, then the plant must take corrective actions.

7620

7621

7622 6.2.5.3 Measuring sensitivity with odour diaries

7623

7624

Odour diaries are a very important tool to understand odour impact. When performed correctly, this psychometric technique can deliver very interesting results. For example, on many occasions citizens have some confusion with the type of smells that they perceive, and odour diary may serve to a consultant to check whether it is always the same odour character perceived or not.

7625

7626

7627

7628

7629

7630

Odour diaries are much used all over the world. For example, the Agency for Toxic Substances and Disease Registry of USA has, in its [website](#), very comprehensive information on the topic. EPA Victoria of Australia has also a guideline (2021) dealing with the use of odour diaries.

7631

7632

7633

7634

7635 6.2.5.4 Measuring sensitivity with an analysis of records of complaints

7636

7637

Unfortunately, an unstructured analysis of records of complaints will have several limitations for a consultant. Usually complaints are addressed to several organisms and just a few citizens will be available to carry out this task. That means that complaints are just the tip of an iceberg, as usually there are many citizens who do not complain, but are also impacted by odours.

7638

7639

7640

7641

7642

7643

Better results can be achieved if there is a protocol to deal with complaints with a structured set of questions asked to the citizen who is doing the call. A couple of German standards on the topic are:

7644

7645

7646

7647

- VDI 3883 part 3:2014-06 Effects and assessment of odours - Conflict management in air pollution abatement - Fundamentals and application to ambient odour

7648

7649

- VDI 3883 Blatt 4:2017-06 Effects and assessment of odours - Processing odour complaints

7650

7651

7652

A simple search on the internet will show many guidelines on how to carry out an odour complaint. For example, the Government of the Colombian region of the Valle del Cauca (CVC) has a Guide on recommendations for visit report - odour complaints (2016). Other authorities with protocols for odour complaints are [Metrovancouver](#) (Canada), several

7653

7654

7655

7656 [councils](#) in UK. [NSW EPA](#) (Australia), etc.

7657

7658 6.2.5.5 Measuring sensitivity with citizen science

7659

7660 Citizen science involves the participation of communities in recording the frequency, intensity
7661 and type of the odour. The data obtained from social participation may be associated with
7662 other parameters, such as meteorological data recorded during the same study period,
7663 allowing its integration and comparison to dispersion models.

7664

7665 Citizen science does not provide odour concentration in ou_E/m^3 , which is only measured by
7666 the do at emission-level.

7667

7668 There are two main limitations that affect the traditional four psychometric methodologies
7669 mentioned beforehand. First, the timestamp of the odour complaint is usually not very
7670 accurately recorded. Second, the location of the odour complaint is also usually registered,
7671 but again not very accurately.

7672

7673 Nowadays there are apps in smartphones that are able to register very accurately the time
7674 and location of an odour observation. In fact, these apps are able to, not only register an
7675 odour observation, but also register where the odour came from, by using meteorological
7676 data or even better, reverse modelling. At this stage, a standard on this new methodology is
7677 being prepared by the Spanish Standardisation Agency UNE (Izquierdo et. al. 2021). A large
7678 *Horizon 2020* European Project has been carried out.

7679

7680 Following this new methodology, a better approach could be taken by comparing odour
7681 observations performed by citizens and comparing them with the results of dispersion
7682 models to calculate the correct odour concentration value that triggers an odour observation.

7683

7684 In other words, sensitivity adjustments can be carried out by adding a factor that establishes
7685 the actual odour nuisance of an activity at the closest receptors (Díaz et al. 2021).

7686 6.3. Limitations on dose-response curves

7687

7688 Unfortunately, it is challenging to set a proposal on maximum allowable levels because, as
7689 mentioned before, in the end, it will all depend on the sensitivity of the receptors. A perfectly
7690 fine FIDOS setting might fit in a community, while the same FIDOS levels can fail to prevent
7691 odour impact due to the different degrees of perception of the sensitive receptors.

7692

7693 An odour modeller is supposed to apply best practices, such as the ones proposed in this
7694 handbook. However, the final result will usually not be right or wrong, as it will depend on
7695 many factors, being one of them the sensitivity of the receptors.

7696

7697 Percentiles 98 or 90 and odour concentrations of 1 odour unit or 3 odour units should not be
7698 taken as the absolute truth. In some cases, there will still be odour complaints.

7699

7700 When there is evidence that the odour modelled does not correspond with the real situation
 7701 in the area, other tools can be used. The most common approach is the use of the grid
 7702 method proposed by EN 16841 part 1 (NCh 3533 in Chile). This approach requires six
 7703 months to 1 year of data and involves a number of measurements carried out by a group of
 7704 assessors.

7705
 7706 The grid method described in EN 16841 part 1 is a statistical survey method which is applied
 7707 over a sufficiently long period of time, to provide a representative map of the exposure to
 7708 recognisable odour, spatially distributed over the assessment area. These grid
 7709 measurements are used to determine the distribution of the so-called, '*odour hour*'
 7710 frequency for recognisable odours in ambient air in an assessment area under
 7711 meteorological conditions that are assumed to be representative of the local meteorology
 7712 (e.g. the last ten years). An *odour hour* is obtained by a single measurement when the
 7713 percentage odour time reaches or exceeds 10 % by convention.

7714
 7715 One *odour hour* should not be confused with one ou_E/m^3 . The first one is based on a
 7716 *recognition* threshold (supra-threshold) measurement and the second one is based on a
 7717 *detection* determination (threshold).

7718
 7719 *Odour hours* obtained using EN 16841 part 1 and *odour concentrations* obtained using
 7720 dispersion modelling should not be compared unless any sort of transformation is carried out
 7721 to take into account the differences in the nature of both units.

7722
 7723 The grid method does not measure sensitivity. In cases where EN 16841 part 1 shows that
 7724 there is no impact, but there is still reasonable evidence that odour impact is occurring, other
 7725 methods can be used.

7726
 7727 If there are still odour complaints after carrying out an odour campaign according to EN
 7728 16841 part 1, other approaches can be taken, for example, based on the psychometric tools
 7729 commented in chapter 7.

7730 6.4. A window open to research

7731 For several years, approaches have been based on FIDOS factors (Frequency, Intensity,
 7732 Duration, Offensiveness, Sensitivity). This approach, which shows the multifactorial impact
 7733 of odour complaints, needs to be improved.

7734
 7735 There is a need to identify the subjective parameters linked to odour exposure (and
 7736 nuisance) based on the FIDOSs scheme and to verify that they are sufficient.

7737
 7738 The approach must be validated on the basis of data (experimental). For that, there is a
 7739 clear need for more dose-response studies coupled with modelling in order to evaluate the
 7740 dose appropriately.

7741
 7742 The *International Commission on Biological Effects of Noise* (ICBEN) meets regularly at
 7743 conferences every 3-4 years. In these events, epidemiologists around the globe meet to
 7744 discuss the different impacts that vector noise produces on people (and nature in general).
 7745 Odour is an environmental stressor very similar to noise. Unfortunately, there is not such an

7746 event to study the impact of odours on health, so there is a need for many more dose-
 7747 response studies to understand the effects of this environmental vector better and for an
 7748 organisation similar to IC BEN to take the lead on this topic. Some authors (Guadalupe-
 7749 Fernandez et al., 2021) mention that there is a need for higher quality studies, especially
 7750 concerning study design (e.g., using panel studies), exposure assessment (e.g., using
 7751 dispersion models), and outcome assessment.

7752 6.5. Conclusions

7753
 7754 The FIDOS factors commonly provide the basis for jurisdictional odour criteria. The
 7755 concentration threshold of a standard odour modelling criterion is related to the intensity
 7756 dimension of FIDOS. The percentile compliance parameter may be alternatively expressed
 7757 as a frequency of exceedances or the number of allowed exceedances of the threshold
 7758 within a given period, thus aligning with the frequency factor of FIDOS. These parameter
 7759 values may be adjusted in criterion frameworks to account for variations in the FIDOS
 7760 factors of odour offensiveness and receptor sensitivity.

7761
 7762 It can be noted that all factors strongly influence global perception. However, the way to
 7763 estimate factors can be different. It is possible to just consider qualitative values that
 7764 represent the perception of one factor (for example, Low/high for frequency), or typically, if a
 7765 percentile is defined, the factor is then considered quantitative because a scale with time
 7766 recording is introduced.

7767
 7768 The form of evaluation of the FIDOS protocol is linked to the odour standards or regulations
 7769 established in each country, which vary in compliance values, odour measurement unit,
 7770 methodology to assess nuisance, etc. Therefore, it is challenging to define a single way,
 7771 procedure or criterion in the applicability of the FIDOS protocol.

7772 6.6. References

7773
 7774 Aatamila M., Verkasalo K. Pia, Korhonen J. M., Suominen A.L., Hirvonen M.R., Viluksela K.
 7775 M., Nevalainen A. Odour annoyance and physical symptoms among residents living near
 7776 waste treatment centres. *Environmental Research* 111 (2011) 164–170

7777
 7778 Air Quality Bureau of the Iowa Department of Natural Resources, A Review of The Science
 7779 and Technology of Odor Measurement, 30 December 2005.

7780
 7781 Australian Standard 4323.3:2001 Stationary source emissions - Determination of odour
 7782 concentration by dynamic olfactometry

7783
 7784 Australian Pork Limited, Evaluation of the 98th percentile 1-hour concentration as an
 7785 indicator of odour impact, 30 may 2003.

7786
 7787 Baldwin CM, Bell IR, Guerra S, Quan SF. Association between chemical odor intolerance
 7788 and sleep disturbances in community-living adults. *Sleep Medicine* 5:53-59 (2004).

7789

- 7790 Beychock, M.R. (1994) Fundamentals of Stack Gas Dispersion, 3 ed. M.R. Beychock,
7791 Irvine.
- 7792 Both, R., Kwiatkowski, K. Limit values for odour in ambient air – A legal system applied all
7793 over Germany. 9th IWA Odour & VOC / Air Emission Conference, Bilbao, Spain,
7794 www.olores.org. [Link](#).
- 7795
- 7796 Brancher, M., K.D. Griffiths, D. Franco, H. Melo Lisboa (2017) A review of odour impact
7797 criteria in selected countries around the world. Chemosphere, 168, 1531-1570.
- 7798
- 7799 Brancher, M., A. Hieden, K. Baumann-Stanzer, G. Schauburger, M. Piringer (2020)
7800 Performance evaluation of approaches to predict sub-hourly peak odour concentrations.
7801 Atmos. Environ. X, 7, <https://doi.org/10.1016/j.aeaoa.2020.100076>
- 7802
- 7803 Dalton P. Cognitive Influence on Health Symptoms from Acute Chemical Exposure. Health
7804 Psychology Vol.18 No.6.579-590 (1999)
- 7805
- 7806 Dalton P. Understanding the Human Response. How people sense, perceive and react to
7807 odors. BioCycle, November 2003.
- 7808
- 7809 Díaz C, Izquierdo, C. Antón A, Is it possible to set a universal odour limit? (2021)
7810 NOSE2021.
- 7811
- 7812 EN 16841-1 (2017) Ambient air – Determination of odour in ambient air by using field
7813 inspection – Part 1: Grid method. Draft version. 60 pp
- 7814
- 7815 Guideline: Odour Emissions (In English. Department of Water and Environmental
7816 Regulation, Government Western Australia, 2019, Available online:
7817 <[https://www.der.wa.gov.au/images/documents/our-work/licences-and-works-approvals/
7818 licensing%20guidelines/Guideline%20-%20Odour%20emissions%20v1.0%20FINAL
7819 %20\(June%202019\).pdf](https://www.der.wa.gov.au/images/documents/our-work/licences-and-works-approvals/licensing%20guidelines/Guideline%20-%20Odour%20emissions%20v1.0%20FINAL%20(June%202019).pdf) >.(Accessed 2021)
- 7820
- 7821 Bull M, McIntyre A, Hall D, Allison G, Redmore J, Pullen J, Caird L, Stirling M, Fain R,
7822 (2018) Guidance on the assessment of odour for planning, IAQM. Available online:
7823 <https://www.iaqm.co.uk/text/guidance/odour-guidance-2014.pdf>
- 7824
- 7825 Guide: Field guide for Interviewer - odour complaints. Corporación Autónoma del Valle del
7826 Cauca (2018) [http://cvc.gov.co/sites/default/files/Sistema_Gestion_de_Calidad/Procesos
7827 %20y%20procedimientos%20Vigente/0340_Gestion%20Ambiental%20en%20el
7828 %20Territorio/Guia/GU.0340.04%20Guia%20para%20encuestadores%20-%20Olores
7829 %20ofensivos%20V2.pdf](http://cvc.gov.co/sites/default/files/Sistema_Gestion_de_Calidad/Procesos%20y%20procedimientos%20Vigente/0340_Gestion%20Ambiental%20en%20el%20Territorio/Guia/GU.0340.04%20Guia%20para%20encuestadores%20-%20Olores%20ofensivos%20V2.pdf) (accessed 2022)
- 7830
- 7831 Guide: field planning and data processing - psychometric assessment of odour nuisances of
7832 odour nuisance. Corporación Autónoma del Valle del Cauca (2018)
7833 [http://cvc.gov.co/sites/default/files/Sistema_Gestion_de_Calidad/Procesos%20y
7834 %20procedimientos%20Vigente/0340_Gestion%20Ambiental%20en%20el%20Territorio/
7835 Guia/GU.0340.03%20Guia%20para%20Planificacion%20de%20campo%20y
7836 %20procesamiento%20de%20datos.%20Olores%20ofensivos%20V2.pdf](http://cvc.gov.co/sites/default/files/Sistema_Gestion_de_Calidad/Procesos%20y%20procedimientos%20Vigente/0340_Gestion%20Ambiental%20en%20el%20Territorio/Guia/GU.0340.03%20Guia%20para%20Planificacion%20de%20campo%20y%20procesamiento%20de%20datos.%20Olores%20ofensivos%20V2.pdf) (accessed 2022)
- 7837

- 7838 Guide: recommendations for visit report - odour complaints. Corporación Autónoma del Valle
 7839 del Cauca (2016) http://cvc.gov.co/sites/default/files/Sistema_Gestion_de_Calidad/Procesos
 7840 [%20y%20procedimientos%20Vigente/0340_Gestion%20Ambiental%20en%20el](http://cvc.gov.co/sites/default/files/Sistema_Gestion_de_Calidad/Procesos)
 7841 [%20Territorio/Guia/GU.0340.02%20Guia%20para%20informe%20de%20visita%20-](http://cvc.gov.co/sites/default/files/Sistema_Gestion_de_Calidad/Procesos)
 7842 [%20Queja%20por%20olores.pdf](http://cvc.gov.co/sites/default/files/Sistema_Gestion_de_Calidad/Procesos) (accessed 2022)
 7843
 7844 Government of Alberta. (2017). Odours and Human Health. Environmental Public Health
 7845 Science Unit, Health Protection Branch, Public Health and Compliance Division, Alberta
 7846 Health. Edmonton, Alberta
 7847
 7848 Good Practice Guide for Assessing and Managing Odour. Ministry for the Environment.
 7849 Wellington, 2016. Available online:
 7850 <<https://www.mfe.govt.nz/sites/default/files/media/Air/good-practice-guide-odour.pdf>>.
 7851 (Accessed 2021).
 7852
 7853 Heaney CD., et al. Relation between malodour, ambient hydrogen sulfide, and health in a
 7854 community bordering a landfill. *Environ Res.* Aug;111(6):847-52 (2011).
 7855
 7856 Helene M. Loos, Linda Schreiner, Brid Karacan, A systematic review of physiological
 7857 responses to odours with a focus on current methods used in event-related study designs,
 7858 *International Journal of Psychophysiology*, Volume 158, 2020, Pages 143-157
 7859
 7860 Izquierdo C., Diaz C., Antón A., Andrés F., Felis J.M., Sánchez G., Saúco L., Rodríguez L.;
 7861 Developing of a New Spanish Standard. Building Collaborative Odour Maps through Citizen
 7862 Science. (2021) NOSE 2021.
 7863
 7864 Guadalupe-Fernandez, V., De Sario, M., Vecchi, S. *et al.* Industrial odour pollution and
 7865 human health: a systematic review and meta-analysis. *Environ Health* **20**, 108 (2021).
 7866 <https://doi.org/10.1186/s12940-021-00774-3>
 7867
 7868 Janicke, L., U. Janicke, D. Ahrens, U. Hartmann, W.J. Müller (2004) Development of the
 7869 odour dispersion model AUSTAL2000G in Germany. *Environ. Odour Manage. Vdi-Ber.*,
 7870 1850, 411–417
 7871
 7872 Janicke Consulting (2019) Dispersion Model LASAT Version 3.4. Reference Book
 7873
 7874 Lorimer, G. (1986) The AUSPLUME Gaussian Plume Dispersion Model. Contract EPA/86-
 7875 02, Environment Protection Authority, Melbourne, Victoria, Australia
 7876
 7877 Marzio Invernizzi, Laura Capelli and Selena Sironi., Proposal of Odor Nuisance Index as
 7878 Urban Planning Tool. *Chemical Senses*, 2017, vol 42, 105-110.
 7879
 7880 Miedema, H.M.E., Walpot, J.I., Vos, H., Steunenberg, C.F., 2000. Exposure-annoyance
 7881 relationships for odour from industrial sources. *Atmos. Environ.* 34, 2927e2936.
 7882
 7883 Odour diary. EPA Victoria. Publication F1019 June 2021
 7884
 7885 Oiamo T., Luginaah I, Baxter J.; Cumulative effects of noise and odour annoyances on

- 7886 environmental and health related quality of life. *Social Science & Medicine* 146, 191-203
7887 (2015)
7888
- 7889 Oettl, D., E. Ferrero (2017) A simple model to assess odour hours for regulatory purposes.
7890 *Atmos. Environ.*, 155, 162–173
7891
- 7892 Oettl, D. (2020): Documentation of the Lagrangian Particle Model GRAL Vs. 20.1. Amt d.
7893 Stmk. Landesregierung, Graz, 208 S. <http://lampz.tugraz.at/~gral/>
7894
- 7895 Oettl, D., E. Ferrero, H. Moshhammer, L. Weitensfelder, M. Kropsch, M. Mandl (2021) Recent
7896 developments in odour modelling and assessment in four provinces in Austria. *Int. J.*
7897 *Environ. Poll.* (in print)
7898
- 7899 Oettl, D., M. Kropsch, M. Mandl (2018) Odour assessment in the vicinity of a pig-fattening
7900 farm using field inspections (EN 16841-1) and dispersion modelling. *Atmos. Environ.*, 181,
7901 54–60
7902
- 7903 Piringer, M., W. Knauder, E. Petz, G. Schauburger (2015) A comparison of separation
7904 distances against odour annoyance calculated with two models. *Atmos. Environ.*, 116, 22-35
7905 Rossi A. L'impatto olfattivo delle emissioni in atmosfera: la classificazione dei ricettori
7906 sensibili. ECOMONDO 2015.
7907
- 7908 Ragoobar T., ganpat w., and rocke k.; Physical well-being and malodour exposure: the
7909 impact of an intensive pig farming operation on a community in trinidad. *International Journal*
7910 *of Science, Environment and Technology*, Vol. 5, No 2, (2016)
7911
- 7912 Rethage et. al., Körperliche Beschwerden im zusammenhang mit Geruchsbelästigungen im
7913 Wohnumfeld. Perspektiven für eine systematische, effektive Erfassung, VDI, Gerüche in der
7914 Umwelt (2007).
7915
- 7916 Shiffman S.S., E.A. Sattely Miller et al. The Effect Of Environmental Odors Emanating From
7917 Commercial Swine Operations On The Mood Of Residents Nearby. *Brain Research Bulletin*,
7918 Vol. 37, Pages 369- 375 (1995).
7919
- 7920 Schiffmann SS, et al. Potential health effects of odor from animal operations, wastewater
7921 treatment, and recycling of byproducts. *J Agromedicine*. 9(2):397-403, (2004)
7922
- 7923 Shusterman D, Lipscomb J, Neutra R, Satin K. Symptom prevalence and odor-worry
7924 interaction near hazardous waste sites. *Environmental Health Perspectives*. 1991;94:25.
7925
- 7926 Steinheider. B. Environmental odours and somatic complaints. *Zentralbl Htg Umweltmed*,
7927 1999.
7928
- 7929 Steinheider B, Winneke G. Industrial odours as environmental stressors: Exposure-
7930 annoyance associations and their modification by coping, age and perceived health. *Journal*
7931 *of Environmental Psychology*. 1993;13(4):353-63.
7932
- 7933 Technical instructions: methodological route for determining potential nuisance due to

- 7934 intense odorous substances due to intense odorous substances. Corporación Autónoma del
7935 Valle del Cauca (2016)
7936 http://cvc.gov.co/sites/default/files/Sistema_Gestion_de_Calidad/Procesos%20y%20procedimientos%20Vigente/0350_Atencion%20al%20Ciudadano/Instructivos-0022/IN.0350.01%20Ruta%20metodologica%20para%20determinar%20molestia%20potencial%20por%20olores.pdf (accessed 2022)
7940
7941 Scire, J., D. Strimaitis, R. Yamartino (2000) A User's Guide for the CALPUFF Dispersion
7942 Model; Earth Tech. Inc.: Concord, MA, USA, pp. 1–521
7943
7944 Smith, M.E. (1973) Recommended Guide for the Prediction of the Dispersion of Airborne
7945 Effluents; ASME: New York, NY, USA.
7946
7947 Sucker et al. Adverse effects of environmental odours: Reviewing studies on annoyance
7948 responses and symptom reporting. *Water. Sci. Technol.*, (2001)
7949
7950 VDI 3788-1 (2015) Environmental meteorology—Dispersion of odorants in the atmosphere—
7951 Fundamentals. German Engineering Association VDI, Düsseldorf, 25 pp.
7952
7953 VDI 3882:1997, part 1, Determination of Odour Intensity, Düsseldorf, Germany.
7954
7955 VDI 3882:1997, part 2; Determination of Hedonic Tone, Düsseldorf, Germany.
7956
7957 EN 13725:2003: Air Quality – Determination of Odour Concentration by Dynamic
7958 Olfactometry, Comité Européen de Normalisation (CEN)
7959
7960 Venkatram, A. (2002) Accounting for averaging time in air pollution modelling. *Atmos.*
7961 *Environ.*, 36, 2165-2170.
7962
7963 UNE-EN 16841-1:2017, Ambient air - Determination of odour in ambient air by using field
7964 inspection - Part 1: Grid method.
7965
7966 van Harreveld AP, Jones N, Stoaling M. Environment Agency. Assessment of Community
7967 Response to Odorous Emissions, R&D Technical Report P4-095/TR, ISBN 1 857059 247.
7968 (2002)
7969
7970 Yee, E., R. Chan, P. R. Kosteniuk, G. M. Chandler (1994) Experimental Measurements of
7971 Concentration Fluctuations and Scales in a Dispersing Plume in the Atmospheric Surface
7972 Layer Obtained Using a Very Fast Response Concentration Detector. *J Appl Meteorol*, 33,
7973 996-1016.
7974
7975
7976

7978 7. Other approaches

7979 7.1. Introduction

7980

7981 Using dispersion modelling is not limited to only calculating odour isoconcentration curves at
7982 different percentiles. Dispersion modelling can be used for many other purposes, such as

7983

7984 1. Calculating odour emission rate by using *Reverse Dispersion Modelling* (RDM);

7985 2. Estimating the location of odour sources by using back trajectory analysis;

7986 3. Source Term Estimation (STE);

7987 4. Calculating odour impact by balancing the hedonic tone of multiple sources;

7988 5. Calculating odour impact from intermittent sources and non-static receptors;

7989 6. Calculating odour impact by using tracers; and

7990 7. Forecasting odour impact.

7991

7992 The following sections will present these topics.

7993 7.2. Calculating odour emission rate using reverse modelling

7994

7995 There are a few standards dealing with using RDM to determine the odour emission rate
7996 from an unknown source.

7997

7998 a) Annex G of EN 16841 part 2 that deals with "Calculation of the odour emission rate by
7999 reverse modelling. Dynamic plume measurement"

8000

8001 b) Chapter 8.2.3 of the EN 17628 dealing with "*Reverse Dispersion Modelling* (RDM) to
8002 determine diffuse emissions of VOCs into the atmosphere";

8003

8004 c) EN 15445:2008 fugitive and diffuse emissions of common concern to industry sectors -
8005 qualification of fugitive dust sources by reverse dispersion modelling.

8006

8007 d) VDI 3788 part 2 Environmental meteorology – Dispersion of odorants in the atmosphere -
8008 Reverse modelling.

8009

8010 RDM can be done in any case, provided that there are adequate meteorological "Gaussian-
8011 like" conditions, but there are some main limitations:

8012

8013 ● Calculation of emission rate is not possible when there are multiple odour sources
8014 (except VDI 3788 part 2);

8015 ● Calculation of the relative contribution of different sources with similar odour
8016 character in the same plant is not possible;

8017 ● When the terrain is not accessible for measuring odour or odorants;

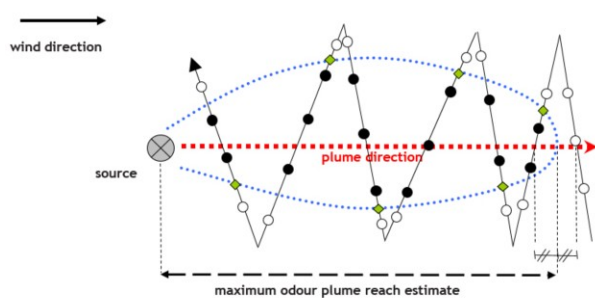
- When the meteorological conditions are not adequate. For example, carrying out RDM during calm winds is not possible.

7.2.1 EN 16841 part 2

As explained in chapter 4.4.2, EN 16841 part 2 is divided into two parts: the *dynamic* and *static plume* methods.

In the *dynamic approach*, the assessors walk (or go by bike) in zigzags through the plume getting either closer or far away from the source, whilst, in the *static method*, the assessors do several transects across the plume. Both techniques should give similar outputs, although, to date, no study has been published comparing the results of both methods.

Figure 7-1 shows a schematic overview of the dynamic plume method and how this method looks in reality (Capelli et al., 2012).



8034

Figure 7-1 Schematic of the dynamic (left) and a real measurement (right) (Capelli et al., 2012)

The natural result of the dynamic plume measurement is the extent of the odour plume. This result can be used to estimate the total odour emission rate using reverse dispersion modelling.

The calculation of the odour emission rate for the dynamic method using RDM is included in one of the annexes of EN 16841 part 2; that is, it is not part of the “normative” part.

The method described in this annexe has been used in Belgium for over 20 years and can easily be applied in other countries. The Flemish odour policy uses these measurements as one of the main techniques to calculate the emission rate and the impact of an odour source (Van Broeck et al., 2001; Van Broeck, 2003; Van Elst, 2016). The method is standardised in a Code of Good Practice (Bilsen et al., 2008; Bilsen & De Fré, 2009).

The odour emission rate of the source under study is calculated based on the recorded plume extent, the source characteristics and the local meteorological conditions during the plume measurement.

8052

8053 The odour emissions calculated based on the plume measurement are expressed as *sniffing*
8054 *units* per second (su/s) instead of *odour units* per second. A fundamental difference with the
8055 European odour unit is that sniffing units are determined by recognising the odour. In
8056 contrast, European odour units are determined by detection, not necessarily by identifying
8057 the odour type. Typically 1 su/m³ corresponds with a concentration of 1 ou_E/m³ to 5 ou_E/m³.

8058

8059 One sniffing unit per cubic metre can be defined as the odour concentration at the border of
8060 the plume. This means the odour concentration can be determined at every transition point
8061 as 1 su/m³. Quantifying higher concentrations (e.g. 5 su/m³) by field observation is not
8062 possible.

8063

8064 The method of reverse modelling is applied as follows: In the first step, the plume extent is
8065 determined as described above. In this step, a sonic anemometer records wind
8066 speed/direction along the process.

8067

8068 In the second step, a dispersion model calculates the average odour concentrations on
8069 ambient air in the surroundings of the odour source under investigation. This is done based
8070 on the source characteristics (emission rate, height, temperature and flow, among others)
8071 and the local meteorological data (wind speed, wind direction and stability class) recorded
8072 during the measurement. Since the odour emission rate is unknown, a fictitious emission
8073 rate of, for example, 5000000 'model units' per second is assumed. The calculated odour
8074 concentrations on ambient air are expressed in model units per m³.

8075

Y/X+	-0,50	0,20	0,10	0,40	0,70	1,00	1,30	1,60	1,90	2,20	2,50	+X/Y (km)
0,90-	- 0,90
0,75-	- 0,75
0,60-	- 0,60
0,45-	- 0,45
0,30-	- 0,30
0,15-	- 0,15
0,00-	.	.	.	35	410	163	87	29	.	.	.	- 0,00
-0,15-	.	.	112	265	266	204	123	88	28	8	.	- -0,15
-0,30-	.	.	21	139	149	124	99	82	49	19	6	- -0,30
-0,45-	.	.	3	75	143	99	80	77	48	34	12	- -0,45
-0,60-	.	.	.	27	95	135	105	70	64	46	22	- -0,60
-0,75-	.	.	.	6	60	95	104	80	60	51	37	- -0,75
-0,90-	.	.	.	1	28	74	85	78	64	47	31	- -0,90
-1,05-	10	51	72	66	51	44	23	- -1,05
-1,20-	3	28	61	59	58	40	37	- -1,20
-1,35-	1	13	45	58	50	44	30	- -1,35
-1,50-	5	27	52	44	36	27	- -1,50
-1,65-	2	14	40	32	32	22	- -1,65
-1,80-	6	25	28	27	21	- -1,80
-1,95-	3	15	22	22	21	- -1,95
-2,10-	1	8	19	18	18	- -2,10
8076 Y/X+	-0,50	0,20	0,10	0,40	0,70	1,00	1,30	1,60	1,90	2,2	2,50	+X/Y (km)

8077

8078 **Figure 7-2** Example of reverse modelling calculation according to EN 16841

8079 After calculating the concentrations in ambient air (in model units per m³), the plume extent
 8080 recorded during the plume measurement is put on the calculated odour distribution grid, and
 8081 the grid points on the edge of the plume are ticked. By definition, the odour concentration at
 8082 these edge points equals one sniffing unit per m³ (su/m³). The average of the concentrations
 8083 in ambient air (in model units per m³) of all edge points is calculated. In this case:

8084 $(117+139+75+95+60+95+74+72+66+51+64+61+64+77+82+99+123+163)/18 = 87.4$.

8085 In this example, the average odour concentration with an emission of 5 000 000 model units
 8086 per second at the edge points is 87,4 model units per m³. Thus, the real odour emission rate
 8087 of the source would be:

8088 $5\ 000\ 000 / 87.4 = 57\ 254$ sniffing units per second.

8089 This type of calculation makes sense when there is just one odour source or when there are
 8090 fugitive emissions all over a building. In complex cases, with multiple sources of odour
 8091 present, assigning the odour emission rate to a specific source is challenging. This is a well-

8092 known limitation, not only using this methodology but for any other reverse modelling
8093 approach.

8094

8095 7.2.2 EN 17628

8096

8097 This standard deals with fugitive and diffuse emissions of common concern to industry
8098 sectors and describes several standard methods to determine diffuse emissions of VOCs
8099 into the atmosphere.

8100 One of the methods proposed in the EN 17628 standard is using RDM to calculate diffuse
8101 emissions of VOC. In this case, a portable VOC monitor (such as FID/PID) is used to
8102 quantify VOC concentration in ambient air. Later, this data is used with meteorological data
8103 to calculate OER at the source.

8104 7.2.3 EN 15445

8105

8106 EN 15445:2008 deals with quantifying dust emissions by using RDM.

8107 The implementation of the procedure involves several steps. First, emissive areas,
8108 measuring points, and receptors are identified and geo-referenced. Then, in the same way
8109 that EN 16841 part 2, a hypothetical value of emission flow is set, and meteorological
8110 parameters are defined.

8111 These data are given as input to an air quality dispersion model that calculates dust
8112 concentration in each receptor. Finally, least squares regression between concentrations
8113 and measured concentrations is applied to obtain an optimised value of dust emission flow.

8114

8115 7.2.4 VDI 3788 part 2

8116 VDI 3788 part 2 is still a draft at the time of writing of this handbook. This standard takes EN
8117 16841 part 2 plume static method and calculates the OER of multiple sources by RDM.

8118 This standard is based on a preprocessing tool named *esofin*, built upon the German
8119 dispersion model *Austal*.

8120 *Esofin* does an interactive run on the emission to retrieve the measured odour frequencies.
8121 The iteration ends when the difference model - measurement at each measurement point in
8122 the plume is at a minimum.

8123 At this stage, the working group dealing with this new standard discusses the limits of the
8124 iteration process and the retrieved emissions. In addition, the group is working on the quality
8125 measures for the plume inspections.

8126 The interesting point of this *esofin* module and the *VDI 3788 part 2* is that, unlike the

8127 previous methodologies, it can calculate the odour emission rate from *multiple* sources. The
8128 iterations are made by testing simultaneously different combinations of OER for different
8129 sources.

8130 For this, all known sources are defined in the model with their emission rates. The unknown
8131 sources are described in the technical parameters as size and location. The iteration
8132 process will find the odour emission rate for the unknown source, which is needed to retrieve
8133 a high correlation to the modelled to the measured impact. The quality of the results
8134 depends on a good knowledge of the investigated site and the situations during the plume
8135 inspection. The meteorological measurements during the field inspection need high-
8136 resolution 3D-turbulence measurements. The measurements should be synchronised with
8137 the odour impact measurements.

8138 The current work of the VDI group is testing with various data sets from plume inspections
8139 with corresponding sampling.

8140

8141 7.3. Calculating the origin and type of odour sources

8142 7.3.1 Use of wind data to get preliminary information on the origin and 8143 type of a source

8144 The correlation of meteorological variables – mostly wind direction and speed - with levels of
8145 air pollution is the most straightforward technique to estimate the potential origin of an odour.
8146 These data can be combined with other data, such as odour concentration, to know where a
8147 source is located. Also, they can be useful in finding out the type of source.

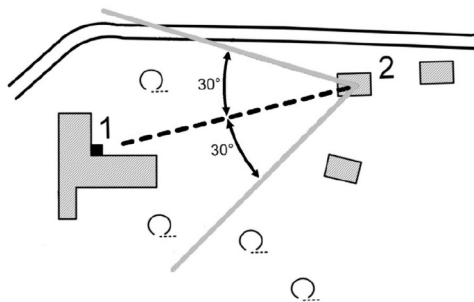
8148 These approaches rely on simple calculations not considering topography or land use. The
8149 methodologies described in this chapter cannot be used when neither of these factors is
8150 important.

8151 7.3.1.1 Wind direction

8152

8153 Meteorology, particularly wind direction and intensity, has been widely used to assess the
8154 source of odour nuisance. A German standard deals with this topic: The *VDI 3883: Part 4*.

8155 VDI 3883 part 4 deals with the effects and assessment of odours, particularly with
8156 processing odour complaints. The following picture shows a scheme of the simplest case
8157 considering only one source of odours.



8158

8159 **Figure 7-3** Schema to identify the origin of an odour source according to the German
8160 standard VDI 3883 part 4

8161 In Figure 7-3, the receptor (2) is exposed to a single-point source (1). The wind direction of
8162 exposure is determined by connecting the two points with a line (dashed line). A 30° angle is
8163 drawn on each side of the connecting line from where the impact occurred.

8164 In this example, the area in between is the exposure sector, which contains wind directions
8165 from 228° to 288° (southwest to west-north-west). If the wind direction is within this range,
8166 the odour observation is plausibly attributed to that source.

8167 More complex cases dealing with *multiple sources*, *area sources* and *fugitive sources* are
8168 addressed in this standard.

8169

8170 7.3.1.2 Pollution Roses

8171 More specifically, this correlation is often carried out using *pollution roses*. These roses are
8172 helpful tools to characterise air masses that represent direct anthropogenic influences
8173 nearby. A pollution rose is similar to a wind rose, but it uses the concentration level of a
8174 specific pollutant in place of the wind speed. It may give important information about the
8175 presence and the approximate position of important emission sources.

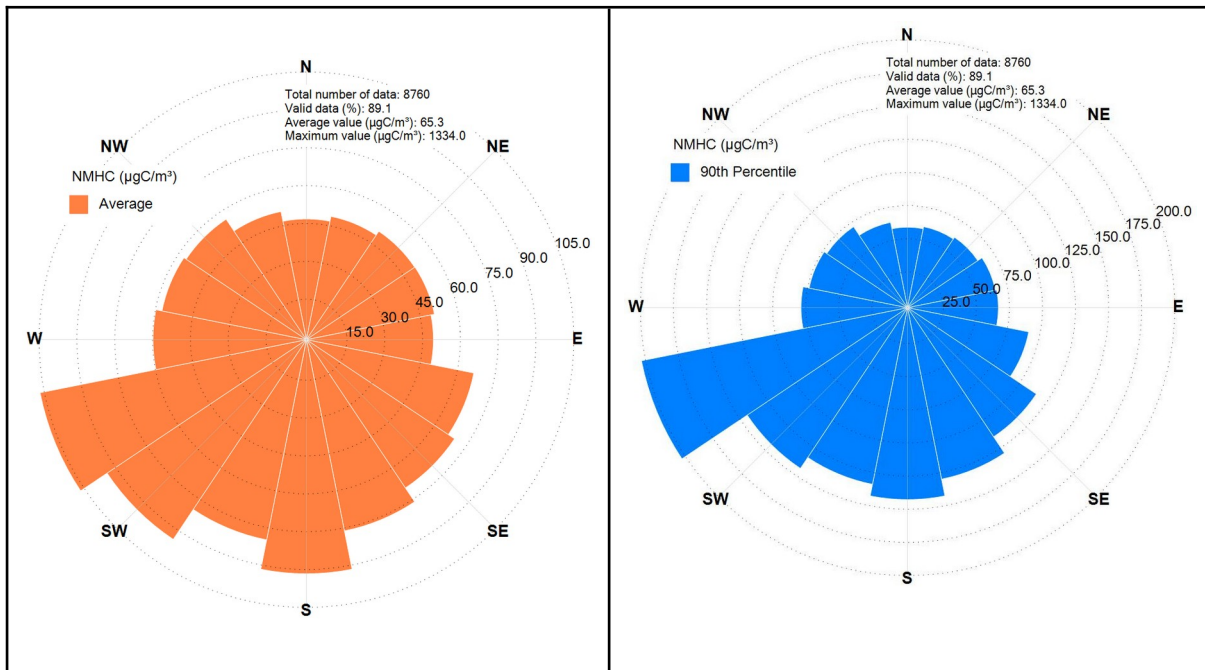
8176 Pollution roses can be misleading in areas where pollution levels are due to the transport
8177 and transformation of pollutants over long distances. However, this is not the case with
8178 odour pollution. Indeed, as pointed out by *Fleming et al. (2012)*, in short-range transport, the
8179 airflow pathway is more influenced by emission source areas than in long-range transport,
8180 where various processes, such as advection, dry and wet deposition, chemical reactions and
8181 physical losses, have more influence on the composition at the receptor location. The wind
8182 rose method often tracks local wind influences (the last 2 or 3 hours before reaching the
8183 station), but it can often be misleading in the longer term.

8184 Two examples of pollution roses are reported below. The graph on the left of Figure 7-4
8185 represents the pollution rose of the average concentration along each wind direction. The
8186 chart has been created starting from a 1-hour time resolution concentration of *non-methane*
8187 *hydrocarbon* available for a whole year. The higher average values are associated with
8188 winds blowing from WSW, SW and S. The graph on the right of Figure 7-4 plots the pollution
8189 of the 90th percentile of concentration values along each direction. This graph shows that

8190 higher values are associated with winds blowing from WSW.

8191 In order to get an idea about the statistical significance of the results, this kind of pollution
 8192 roses must be associated with the information about the number of data used to calculate
 8193 the average, or the percentile, along each direction. For example, the number of data used
 8194 in each direction for the two charts reported below goes from a minimum of 114 (SSE) to a
 8195 maximum of 1117 (W).

8196

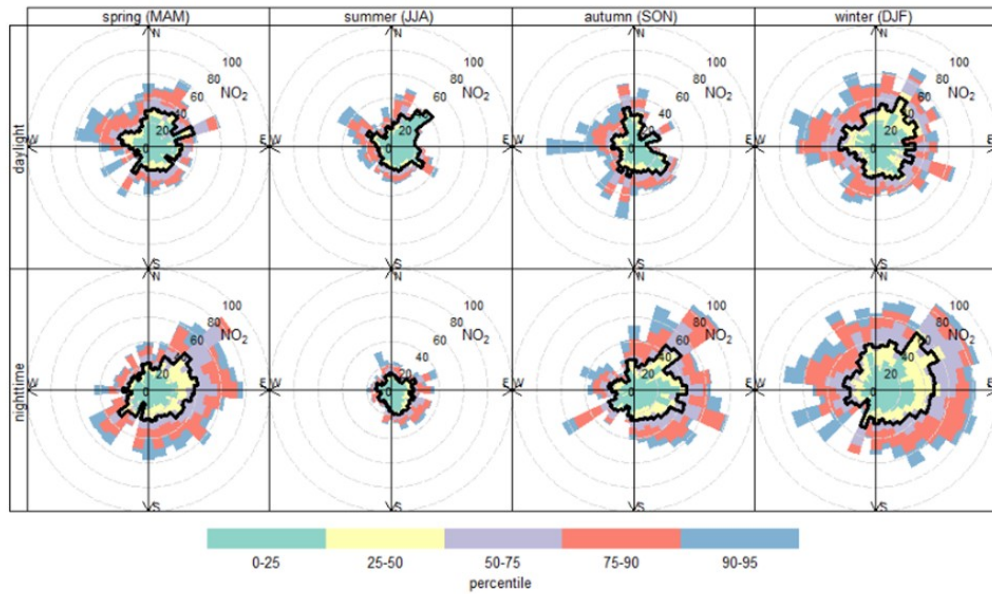


8197 **Figure 7-4** Pollution rose, representing the average concentration along each wind direction
 8198 (left), and Pollution rose, representing the 90th percentile of concentrations along each wind
 8199 direction (right). (courtesy of Enviroware)

8200 Another type of *pollution rose* is the *percentile rose*. The percentile roses are useful for
 8201 showing the distribution of pollutant concentrations related to the wind direction. The
 8202 percentile rose can help to identify different sources, e.g. those that affect high percentile
 8203 concentrations (Carslaw & Ropkins, 2012). Figure 7-5 is an example that explains how
 8204 percentile values vary by season and hour of the day. In this figure, NO₂ concentrations are
 8205 higher in winter and when the wind is from the southeast. NO₂ concentrations are higher
 8206 during nighttime than in winter daylight hours.

8207

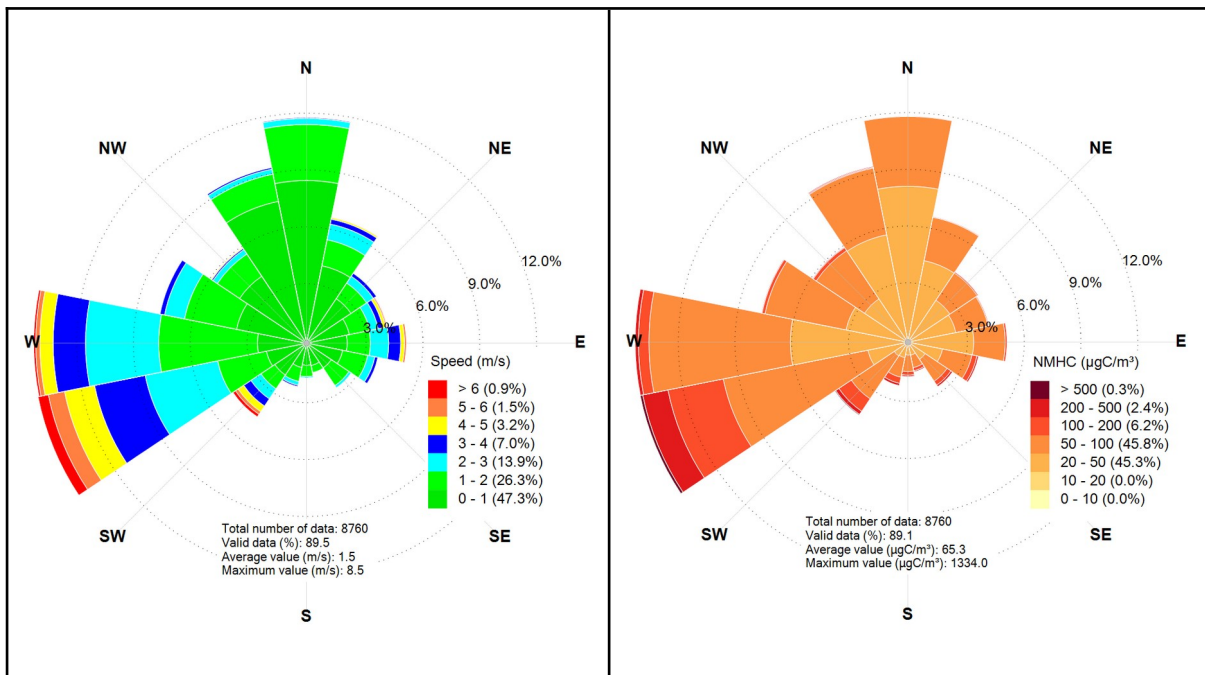
8208



8209

8210 **Figure 7-5** Pollution rose, representing the 90th percentile of concentrations along each
 8211 wind direction (Courtesy of the Israel Ministry of Environment)

8212



8213 **Figure 7-6** A wind rose (left), and concentration rose (right) for the same site (Courtesy of
 8214 Enviroware).

8215 Figure 7-6 shows a wind rose (left) and a pollution rose (right) created from the data of the
 8216 same monitoring station and during the same time interval. These are the same data used
 8217 for preparing the previous Figure 7-6. The pollution rose has been created considering
 8218 concentration intervals along each direction, in the same way, a wind rose is created
 8219 considering speed intervals along each direction. The shape of the two charts is identical:

8220 the longest “arms” of the pollution rose are associated with the prevailing wind direction, not
 8221 with the directions associated with the highest average concentration (or to the highest
 8222 percentile). In this sense, a pollution rose, as shown in Figure 7-6, is not as helpful as one of
 8223 the previous two figures because it gives information already given by the wind rose. Indeed,
 8224 concentrations are also visible by different colours along each direction. However, their role
 8225 is not always well understood (e.g., typically, the highest concentrations are shown by a
 8226 narrow strip).

8227

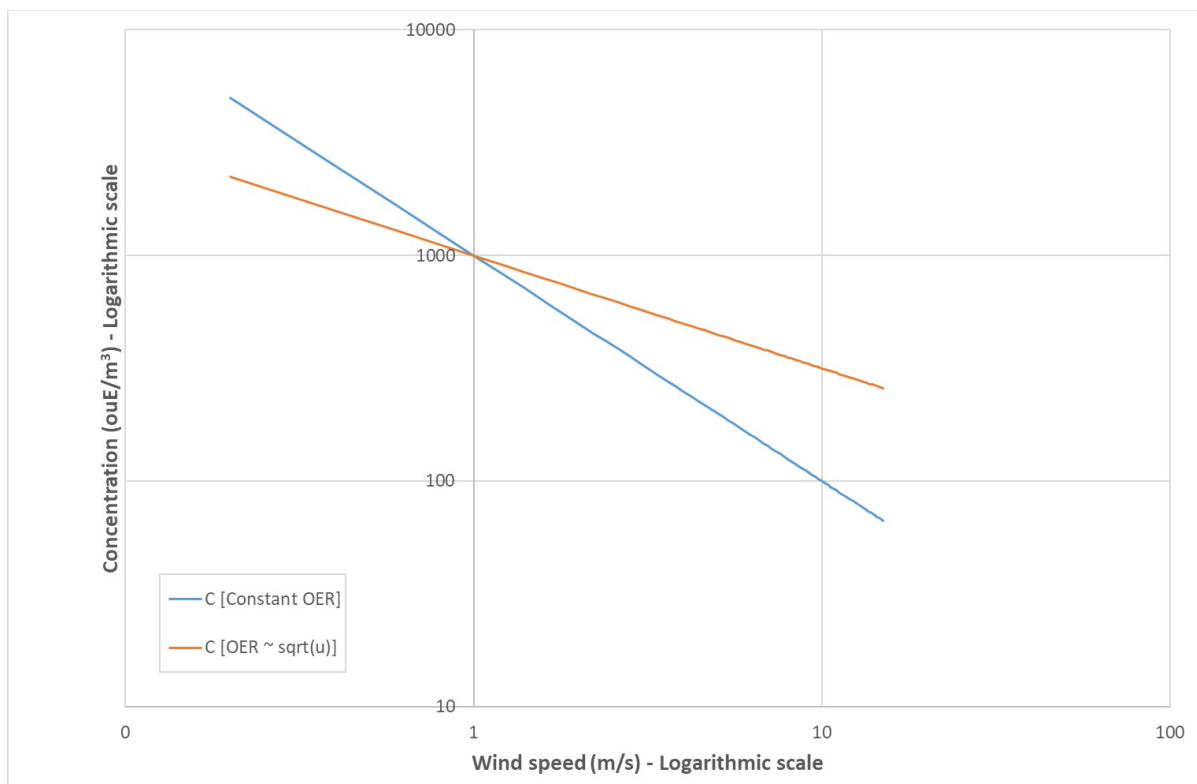
8228 7.3.1.3 Wind speed

8229 Wind speed is important because it gives useful additional information not given by the wind
 8230 direction.

8231 For example, high-level emissions, such as those of a high stack, may be observed near the
 8232 source only for high wind speeds. This happens when *Stack Tip Downwash* (STD) plays a
 8233 role: for large diameter stacks and relatively low momentum releases (i.e., $w_s/U < 1.5$, with
 8234 w_s emission speed and U wind speed at the height of release), the plume is captured within
 8235 the downwind side of the stack, causing high concentration values at the ground. On the
 8236 contrary, the concentration due to low-level emissions decreases while wind speed
 8237 increases.

8238 By applying considerations similar to those reported by Mensink and Cosemans (2005) for
 8239 PM_{2.5}, it is possible to state that the concentration of odour emitted by a source can be
 8240 described by $C = \alpha \text{OER}/U$, where U is the wind speed, OER is the odour emission rate and
 8241 α incorporates the terms of the Gaussian solution. Then, when OER is constant, C
 8242 decreases as U increases. On the contrary, considering, for example, the emissions of a
 8243 passive odour source, OER is proportional to the power of the wind speed (the power is 0.63
 8244 according to Jiang and Kaye, 1996, or 0.5 according to Region Lombardy, 2012). Therefore,
 8245 the odour concentration should go as $C = \beta U^{0.5}/U = \beta/U^{0.5}$, where β incorporates α and other
 8246 constant emission terms. These two different behaviours - qualitatively represented in Figure
 8247 7-7 help in estimating the possible origin of odour:

- 8248 ● If the odour concentration decreases inversely as the wind speed increases, it is
 8249 likely that the source is a stack or any other emitter, not depending on wind speed.
- 8250 ● If odour concentration varies more or less as the inverse of the square root of the
 8251 wind speed, it is likely that odour derives from a passive source whose OER depends
 8252 on the wind speed.



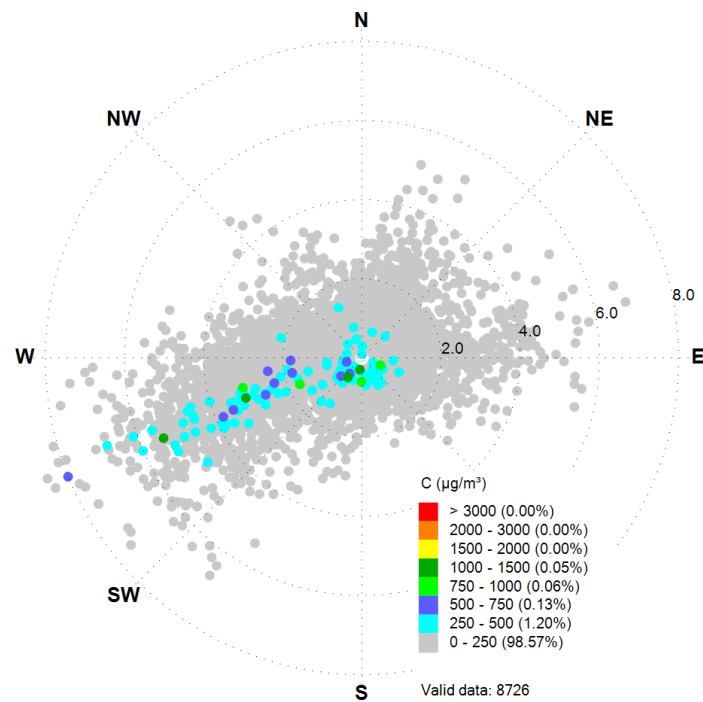
8253

8254 **Figure 7-7** Odour concentration as a function of wind speed for a source with constant OER
 8255 and a source whose OER goes as the square root of wind speed. Both axes are on a
 8256 logarithmic scale. (Courtesy of Enviroware)

8257 7.3.1.4 Three-variable plots (Ternary plots)

8258

8259 When wind data and odour levels, or concentration levels of odorous species, are available
 8260 at the same time, resolution, speed, direction and concentration can be represented in a
 8261 single ternary plot. In this kind of plot, the concentration level is represented by symbols (e.g.
 8262 circles) of different colours and/or sizes, which are placed at a radial distance given by the
 8263 wind speed and at an angular coordinate given by the wind direction. This plot may help in
 8264 estimating the presence of essential sources. The drawback is that many points of different
 8265 colours may be superimposed, and some plot characteristics must be better visible. The
 8266 number of points may be reduced by selecting to show only some values of concentrations,
 8267 for example, the higher ones. An example of a ternary plot is shown in Figure 7-8, which
 8268 indicates the presence of a source WSW from the measuring point.



8269

8270 **Figure 7-8** Example of a ternary plot showing the presence of a source WSW from the
 8271 measuring point (Courtesy of Enviroware)

8272

8273

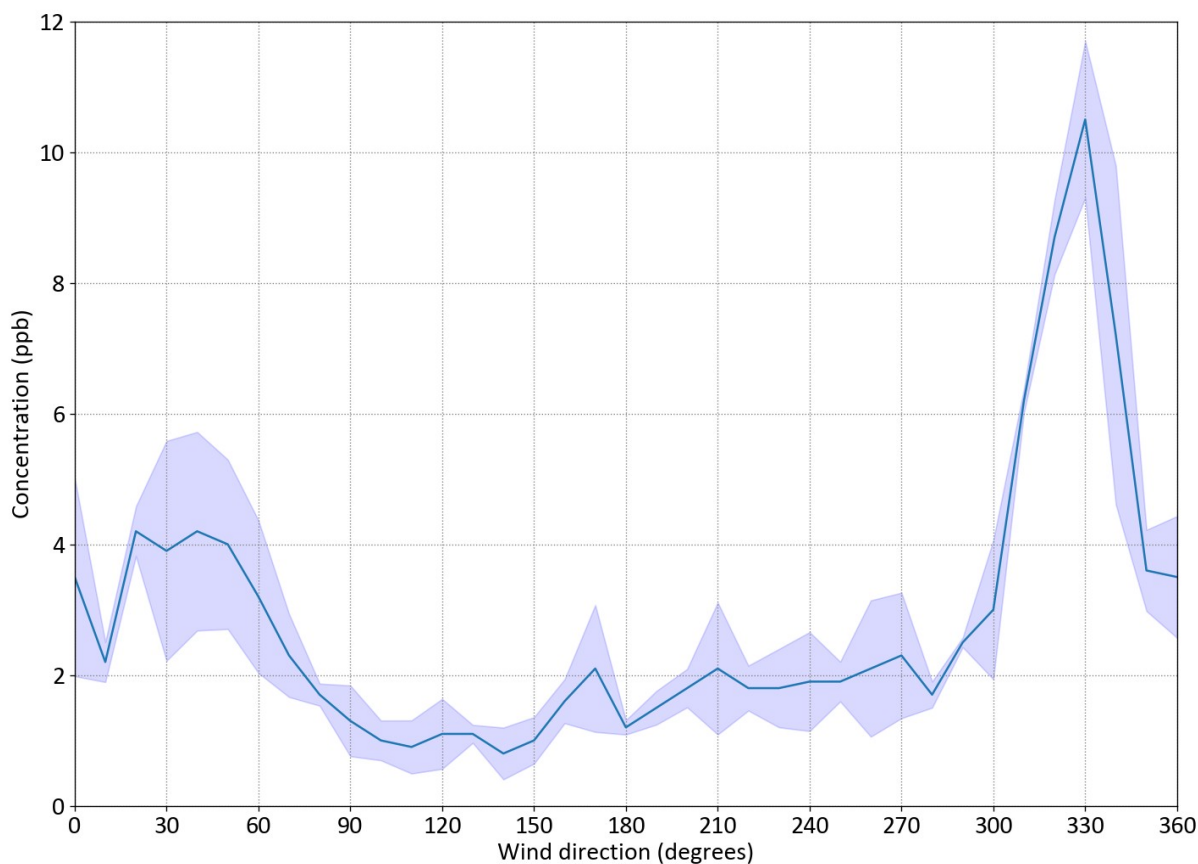
8274 7.3.1.5 Non-parametric analysis

8275

8276 Another useful representation can be obtained by applying the non-parametric regression,
 8277 which is a method to estimate the value of a dependent variable (concentration) starting from
 8278 the values of one or more independent variables (wind speed and direction) without any a
 8279 priori functional relation between the dependent and the independent variables. Examples of
 8280 applications of this analysis are shown in (e.g., *Henry et al., 2002; Yu et al., 2004*). The
 8281 average concentration of a pollutant for a given couple of *wind directions* (wd) and *wind*
 8282 *speed* (ws) is calculated as a weighted mean of the measured concentrations in a window
 8283 centred on (wd, ws). The window size is determined by the *Full Width at Half Maximum*
 8284 (FWHM) of the kernel functions used in the weighted mean. Such size is the unique input
 8285 value of a non-parametric regression. For example, an FWHM of 10 degrees can be used for
 8286 the wind direction, and an FWHM of 2 m/s can be used for the wind speed. Typically, the
 8287 Gaussian kernel is used for the wind direction, and the Epanechnikov kernel is used for the
 8288 wind speed (Yu et al., 2004). For example, Figure 7-9 shows the relation between
 8289 concentration and wind direction.

8290 It is noticed that the considerations reported in this paragraph may be more frequently
 8291 applied to the concentrations of odorous substances than to odour levels.

8292



8293
8294 **Figure 7-9** Example of a chart that can be obtained with the non-parametric analysis
8295 (Courtesy of Enviroware)
8296
8297

8298 7.3.2 Numerical modelling approaches for back-trajectories and 8299 backward plumes.

8300
8301 Numerical models are useful and used tools to trace back in time the trajectories of an
8302 airborne substance released in the atmosphere. As similarly done in forward-mode
8303 applications, they employ meteorological fields to drive the motion of airborne parcels, but
8304 back in time. In the frame of this approach, the determination of the origin of an odour event
8305 can be carried out by using numerical models provided the following information is available:
8306

- 8307 ● Date and time of odour observation of the event
- 8308 ● Location of the odour observation of the event

8309 Starting from such information at the known “receptor”, it is possible to determine the areas
8310 where the potential “source”, originating the odour nuisance, is located. The simplest way to
8311 generate back trajectories consists of calculating the deterministic path of a tracer parcel by
8312 appropriate interpolations of the wind field provided by an atmospheric model. Typically,
8313 Lagrangian models (see Chapter [5.5.3 Lagrangian models](#)) of increasing complexity, from
8314 the mean-trajectory approach to boxes, puffs and particles, can be adopted for more
8315 advanced approaches. Their applicability depends on the time and spatial scales of interest
8316 and the degree of approximation that can be acceptable at such scales. In the simplest
8317 mean-trajectory models, the parcel motion is determined considering only the mean wind

8318 velocity and neglecting the turbulent diffusion. Examples are *FLEXTRA*, (Stohl & Seibert,
 8319 1998), *HYSPLIT* trajectory version (Stein et al., 2015); *TRAJ2D*, (Exponent, 2023) and
 8320 *LAGRANTO*, (Sprenger & Wernli, 2015). Such simplification can be accepted for long-range
 8321 dispersion, which means synoptic and planetary spatial scales from weeks to months. When
 8322 considering the typical scales of the odour dispersion in the atmosphere, from minutes to
 8323 some hours and for distances up to a few km, more advanced models capable of accounting
 8324 for local circulations and turbulence, such as the stochastic Lagrangian particle dispersion
 8325 models, are needed (*FLEXPART*, Pisso et al. 2019; *HYSPLIT*, Stein et al. 2015; *SPRAY*,
 8326 Tinarelli et al., 2000; *LAPMOD*, Bianconi et al. 1999; *LASAT*, Janicke Consulting 2019).
 8327 Here, the local wind determines the mean motion of ‘virtual’ particles containing a mass of
 8328 pollutant or odour units. The diffusion is given by velocities obtained as a Lagrangian
 8329 stochastic differential equations solution. The pathway of the plume or puff of particles is
 8330 thus tracked in backward mode.

8331 Back-trajectory and backwards-plume approaches can be used when only qualitative
 8332 information, such as citizens’ notifications, reveals the odour nuisance occurrence. With this
 8333 method, it is, therefore, possible to trace the atmospheric pathways the parcels followed
 8334 before arriving at the receptor and identify their potential source's origin. Backward
 8335 trajectories were applied to define the origin areas of various types of tracers, not only odour,
 8336 including Saharan dust (Chiapello et al., 1997), radioactive pollutants (Pudykiewicz, 1998;
 8337 Hourdin & Issartel, 2000) and CO₂ peaks (Ferrarese & Trini Castelli, 2019).

8338 In order to identify the origin and the most plausible source of the odour release, in particular
 8339 when a quantitative estimation of the odour event is available, such as measured
 8340 concentration of a substance typifying the odour nuisance, more advanced model
 8341 configurations and additional processing of the model outputs are necessary, in a way
 8342 similar to the reconstruction of the source term and the emission rate based on pollutant
 8343 concentration measurements.

8344

8345 7.3.3 Source Term Estimation Methods using backward modelling 8346 approaches

8347

8348 Identifying the source generating the disturbance can be challenging due to the presence of

8349

8350 ● many potential sources in a complex industrial area

8351 ● unknown sources.

8352 *Source term estimation* (STE) algorithms can predict a possible release location with specific
 8353 emission characteristics, such as the time and amount of release of material or odorous
 8354 emissions. These algorithms are often based on the use of local concentration
 8355 measurements (either chemical species or odour units) given as input to dispersion models
 8356 applied in a configuration capable of solving the inverse problem of the dispersion.

8357 An inverse dispersion model can be derived, in principle, from different standard forward-in-
 8358 time dispersion models, from simple Gaussian, Lagrangian (puff or particles) up to Eulerian
 8359 dispersion models, by appropriately modifying the formulation of the dispersive section and
 8360 considering the advective section backwards in time.

8361 Examples of this modelling approach are retroSPRAY (Armand et al., 2013), the inverse of
8362 the standard Lagrangian particle dispersion model SPRAY, but other examples can be found
8363 in literature, such in Sofiev et al. (2005) and Flesch et al. (1995). Similar techniques can also
8364 be used with the inverse version of Eulerian dispersion models, as in Hourdin and Talagrand
8365 (2006), Elbern et al. (2007), Corazza et al. (2011), and Thompson et al. (2014). Recently,
8366 Hutchinson et al. (2017) published a paper containing a useful and comprehensive review of
8367 STE methods using dispersion models to describe the inverse source-receptor relationship
8368 and considering different types of models. Platt and Deriggi (2012) showed the results from
8369 a comparative activity involving different STE algorithms and backward dispersion models.

8370 Applying a backward dispersion model using the concentration measured at given points as
8371 sources cannot determine all the desired information alone. The backward dispersion
8372 starting at locations and times of observed pollutant concentration values composes 'back-
8373 concentration' fields, which define areas where possible emitting sources reconstruct the
8374 measured concentrations, provided that a good estimate of meteorological fields, particularly
8375 the mean wind, is available. Similarly, in the presence of observations with zero values, back
8376 concentrations starting from those locations (or values compatible with a possible
8377 environmental background) can define exclusion areas and times, identifying where the
8378 pollutant source cannot be located. Due to the intrinsic uncertainty of the dispersion
8379 phenomena, the mean wind reconstruction, the measured concentration data and the model
8380 formulation itself, backward dispersion patterns obtained from different measuring points
8381 may describe relatively large and sometimes non-overlapping or inconsistent areas. In this
8382 respect, a postprocessing phase of the backward simulations is needed to find a statistically
8383 congruent area, integrating all the available information and giving a unique final view of the
8384 emission regions, together with an indication of both the emission rate and time and their
8385 related uncertainties. Different methods are considered to implement these postprocessing
8386 schemes. Among them, a Bayesian approach (Rajaona et al., 2017), statistical approaches
8387 counting the maximum overlap of retro-plumes or applying variational methods to minimise
8388 the values of an objective function (Tinarelli et al., 2018) can be cited.

8389 An approach - which is not backward modelling but can be used as STE - consists of
8390 producing a set of simulations by varying the location and the release duration of a potential
8391 source - placed within a candidate region - and evaluating the concentration at a specific
8392 receptor where concentrations have been measured, or complaints received. The analysis of
8393 the simulation results allows the estimation of the source position and its release duration in
8394 probabilistic terms. The two functionalities, i.e., execution of several simulations and analysis
8395 of their results, have been implemented, for example, in the LAPMOD_SA simulation tool
8396 (Bonafè et al., 2016), which is based on the LAPMOD Lagrangian particle model. The tool
8397 has been applied to understand the origin of a sudden peak of fine particulate matter rich in
8398 ammonium nitrate observed in Bologna (Italy) on February 16, 2012. The candidate
8399 emission area was placed in the northern part of the Po Valley, where manure spreading,
8400 responsible for ammonia emissions, was possible (the southern part was covered by snow).
8401 The result of the application was several areas characterised by specific probabilities to
8402 contribute to the impact at the receptor point.

8403
8404

8405 7.3.4 Tracing the origin of odour nuisance by integrating citizen-
8406 science and modelling approaches

8407

8408 This chapter briefly summarises three examples of applying the back-trajectory technique to
8409 estimate the origin of odour nuisance. The first example is an application in Tarragona
8410 (Spain), the second one is an application in Sicily (Italy), and the third is in operation in Israel
8411 by the Ministry of Environment.

8412 7.3.4.1 Tarragona (Spain).

8413 Tracing the backward course of an air mass is very interesting when using advanced
8414 psychometrics tools, such as citizen science approaches (Gallego et al., 2008; Roca et al.,
8415 2008; Chunrong et al., 2021).

8416

8417 Ramos et al. (2017) presented the case of a small town near Tarragona, Spain, that had
8418 suffered from odour impact from two waste treatment plants. In 2016, the citizen science app
8419 @Nasapp was given to a set of several citizens in this town. As a result, 213 citizen
8420 observations were recorded over six months. Figure 7-10 shows the results obtained.

8421

8422 A close analysis of this figure shows

8423

- 8424 1. Two sets of *Back-Trajectories* (BT) that go through to the plants involved
- 8425 2. Other BTs whose paths do not cross the plants.

8426

8427 In the example above, it was possible to calculate the attribution of the odour observations.
8428 After six months, 63% of the BTs were attributed to one of the plants, 26% to the other plant,
8429 and 11% could not be attributed to any of the plants due to:

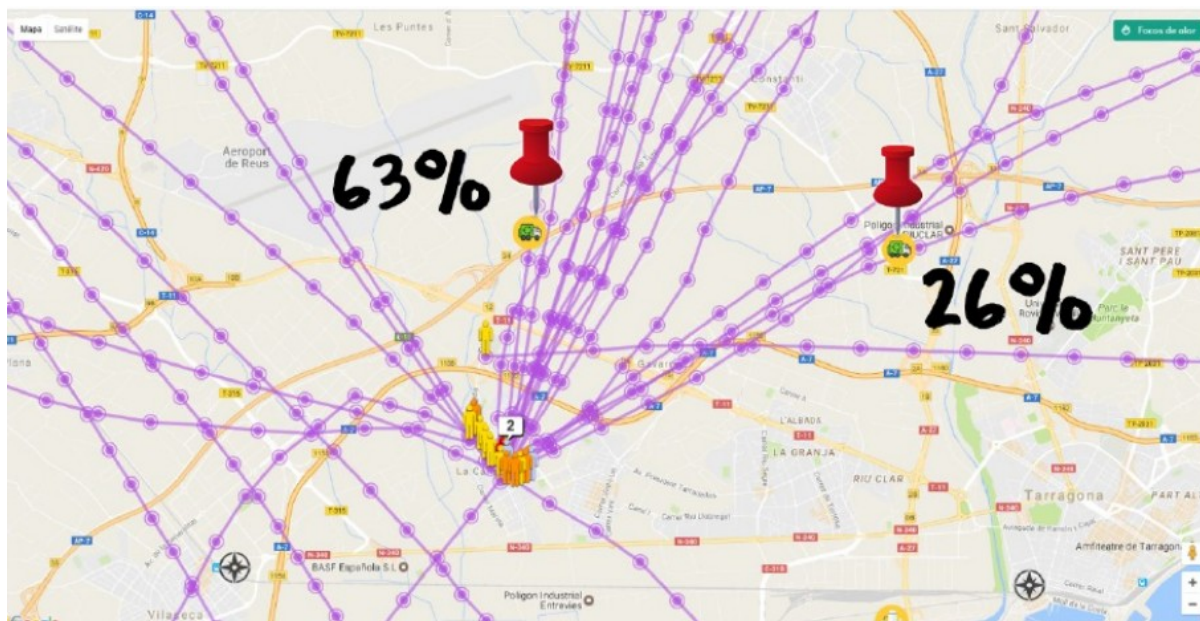
8430

- 8431 1. Errors in the calculation made by the algorithm.
- 8432 2. Odours perceived by the citizens but not attributed to the plants.
- 8433 3. False/biassed observations made by citizens.

8434

8435 In the case of false/biassed observations, using back-trajectories is very useful as citizens
8436 reporting repeated wrong odour observations are very easily detected, and their results can
8437 be automatically discarded.

8438



8439
8440 **Figure 7-10** Results of 6 months of BTs drawn from citizens' observations in a town close to
8441 Tarragona, Spain, impacted by two waste treatment plants (Ramos et al., 2017)

8442
8443 More accurate back-trajectories will be obtained with higher temporal/space resolutions and
8444 at lower altitudes close to the receptor level.

8445
8446 In the example above, BTs were used to identify two sources separated by a distance higher
8447 than that of the spatial resolution of the model. In these cases, an identification between two
8448 sources can usually be carried out. However, for sources very close to each other, BTs will
8449 not be adequate. BTs are not a suitable tool to find out which of the processes of a plant is
8450 responsible for an odour event, as usually, these sources are separated by a distance lower
8451 than the spatial resolution of the model.

8452 7.3.4.2. Sicily (Italy)

8453
8454 Odour nuisances are often a source of justified complaints from the population. Thanks to
8455 the widespread availability of web apps, it is nowadays possible to collect and manage these
8456 complaints in a structured way, allowing a fast visualisation of the areas most affected by
8457 odour nuisance. In this respect, the information collected by such a tool can represent, in
8458 principle, a sort of adaptive receptor network centred on the impact event and moving with it.
8459 Using odour observations as moving “receptor points” and applying a backward dispersion
8460 model can support localising the odorous sources. The idea is to use the STE algorithms
8461 previously described limiting the expected information to identify the emitting area. This, due
8462 to the unavailability, for example, of real observed concentrations, which would give the
8463 necessary input to reconstruct an emitting flow rate. An example of this approach is the
8464 NOSE - *Network for Odours Sensitivity* (<https://nose-cnr.arpa.sicilia.it/>) web application,
8465 developed by CNR-ISAC and ARPA Sicilia and aimed at tracking episodes of odour
8466 nuisance through a citizen-science approach. The meteo-dispersive modelling suite SMART
8467 (Spray-Moloch Atmospheric Regional Tool, Bisignano et al., 2020; Trini Castelli et al., 2021)
8468 is coupled to the NOSE web app. A new and original approach was developed for the
8469 SMART dispersion module, where the SPRAY Lagrangian stochastic particle model was

8470 integrated with the version that includes the backwards-mode option, RetroSPRAY. The
 8471 main challenge lies in using the signals from citizens in place of observed concentrations as
 8472 input receptors for RetroSPRAY. The warnings received through the NOSE Web App are
 8473 sparse in space and time, yet they are considered moving in the space/time receptor grid. A
 8474 three-phase approach was established. A clustering of the warnings is elaborated to
 8475 generate proper 'receptors' for the back-trajectories. Then, simulations with RetroSPRAY are
 8476 performed by releasing a series of retro-puffs from cells containing the identified receptors
 8477 at each time interval, during which a significant number of signals are collected. Finally, the
 8478 back-concentration fields generated by the retro-puffs are statistically combined at emission
 8479 and receptor times. Through such a process, maps are produced, describing the region
 8480 where possible sources can be located. This version of SMART modelling system has been
 8481 applied to different odour nuisance events notified by the NOSE web app, providing reliable
 8482 results in detecting the potential source, in one case identified after a dedicated measuring
 8483 campaign.

8484 7.3.4.3. Israel

8485
 8486 The *Ministry of Environment* of Israel uses an operational web system to identify potential
 8487 sources of odour nuisance in a real-time calculation. The system calculates back trajectories
 8488 and shows the airflow path on a map from the complainer's location (Figure 7-11). The
 8489 system considers all the meteorological data from all stations in the analysis area and
 8490 interpolates the stations' data using Cressman equations. The number of stations
 8491 participating in the analysis is not limited, and their impact varies according to their distance
 8492 from the point of calculation. Forward trajectories can verify a potential pollution source or
 8493 compute an odour nuisance event trajectory in real-time (Figure 7-12). When the system is
 8494 activated for a real-time event persistence or forecast mode, the trajectory can be calculated
 8495 in *perseverance mode* according to the last wind data at each station. This is done using a
 8496 half-hour wind data before the odour event starts and proceeding with the last wind data at
 8497 each station).

8498
 8499 This system helps regulatory authorities and industry plan a response to an air pollution
 8500 event and identify the pollution source (developed by *Meteo-Tech* European Patent
 8501 3339855, Israeli Patent 249780).

8502

8503 **System Components**

8504 To establish the method proposed here, the following infrastructures are required:

- 8505 • meteorological station network
- 8506 • command centre

8507

8508 **Meteorological Network**

- 8509 • The meteorological network enables calculating the wind field at any given time over the
 8510 grid covering the "area of interest".

- 8511 • Analysis and computation of the meteorological grid are done using *Cressman's method*
 8512 (*Cressman, 1959*).

- 8513 • The system computes the meteorological grid values as an average of the last 5
 8514 minutes' data (Wind Speed and Direction).

- 8515 • The wind field calculation is based on data from several available meteorological
 8516 stations in the area of interest

8517

8518 **Methodology for calculation of the airflow trajectories**

8519

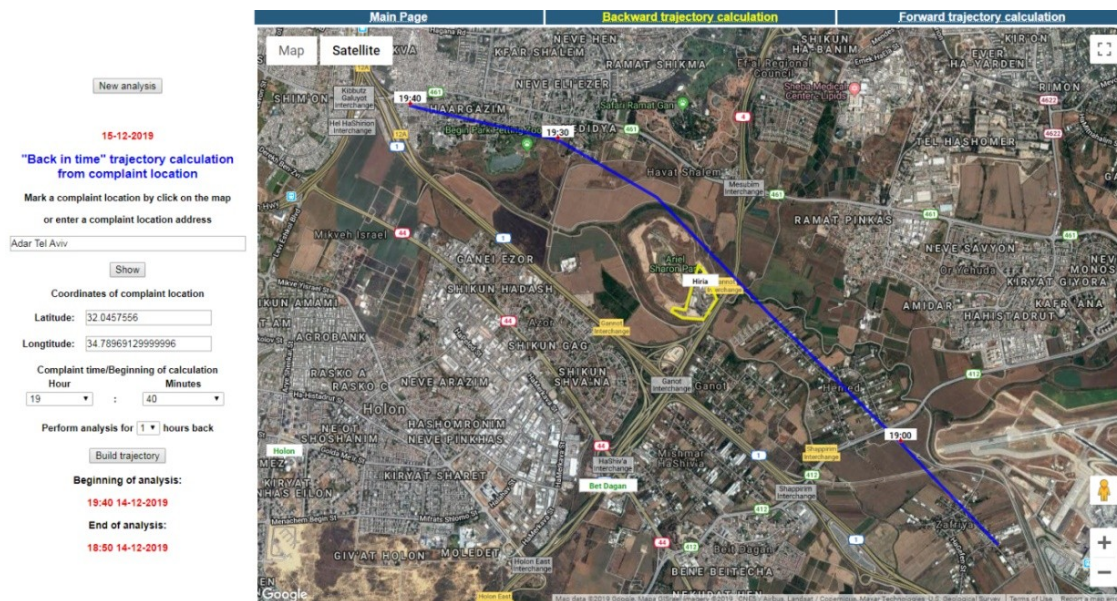
8520 • Meteorological data – the system collects real-time data (wind speed and direction, 5
8521 minutes averages) from available meteorological stations.

8522 • Interpolation – the calculation of the airflow trajectory is based on the data from all
8523 meteorological stations. The closer the station - the greater its influence on the calculated
8524 trajectory.

8525 • The model uses the Cressman algorithm to calculate the wind speed and direction (5
8526 minutes averages) at each grid point, relying on data from the meteorological stations.

8527

8528



8529

8530 **Figure 7-11** Example of backward trajectory from Adar Street Tel Aviv, input data (on the
8531 left side) including the address of the complaint, start hour and date (Courtesy of Israel
8532 Ministry of Environment)

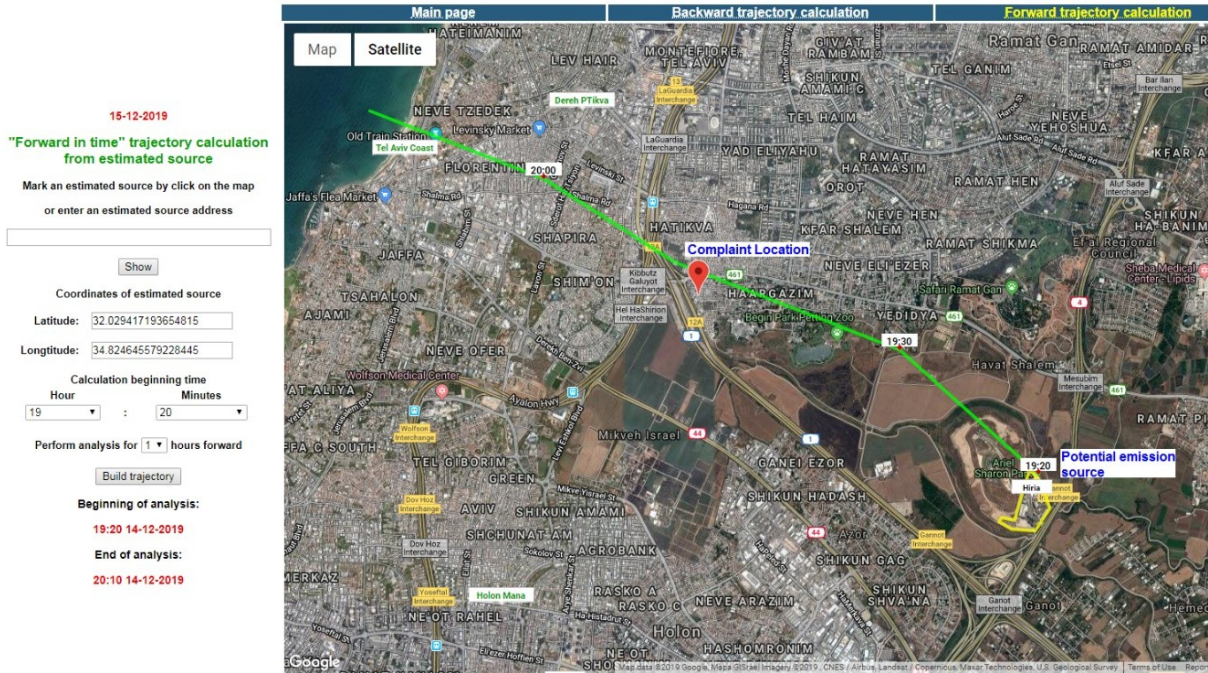
8533

8534

8535

8536

8537

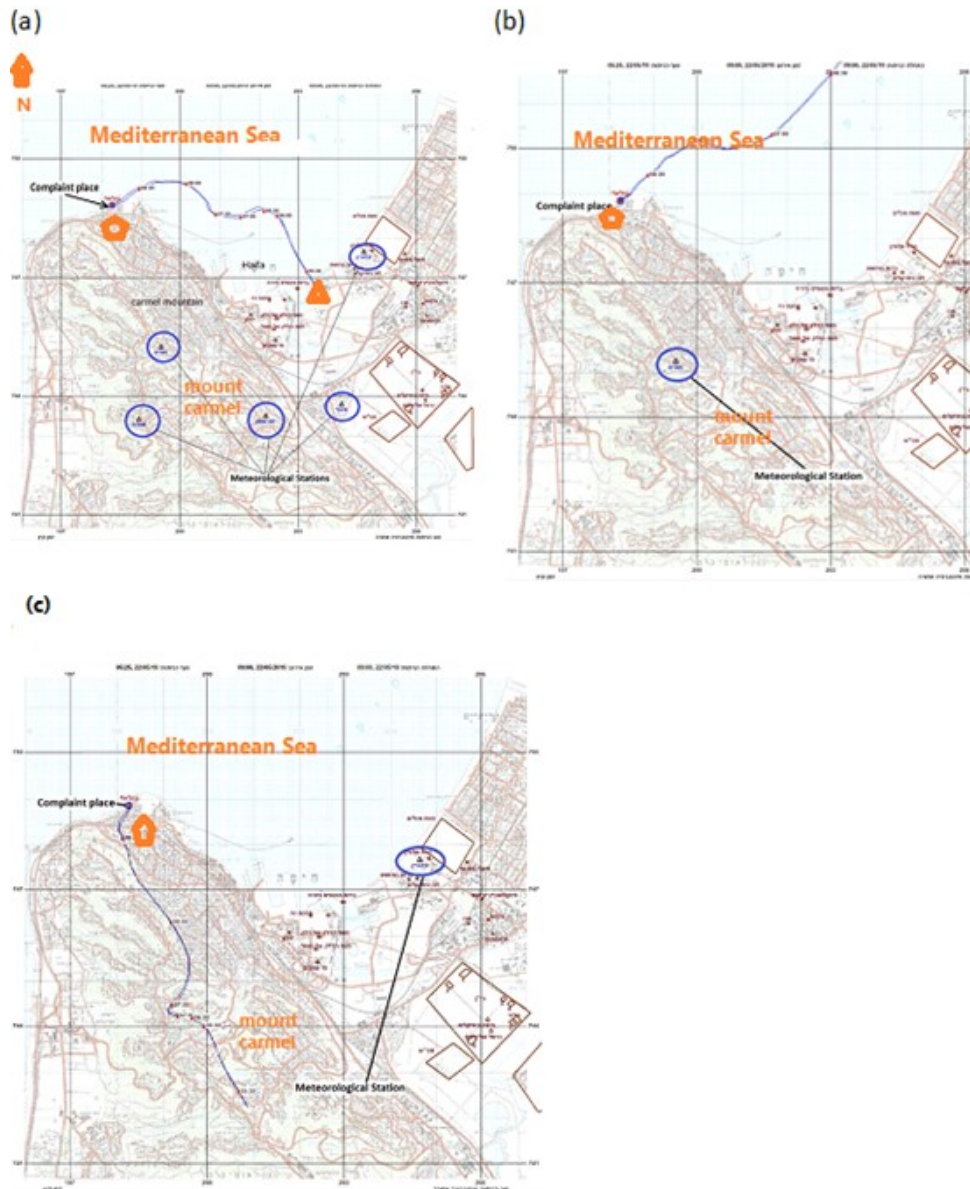


8538
 8539 **Figure 7-12** Example of forward trajectory from Hiriya Recycling Park (Courtesy of Israel
 8540 Ministry of Environment)
 8541

8542 The Haifa Bay industrial area is close to sensitive receptors, characterised by a complex
 8543 topography that includes Mount Carmel (~400 metres), a flat area and the Mediterranean
 8544 Sea. The following example will describe a trajectory analysis of odour nuisances in the
 8545 Haifa area near the shoreline. The complainant's location is marked in Figure 7-13a
 8546 (Complaint place at 9:00 AM) when several met stations are used from different heights
 8547 (marked by a blue circle). The back trajectories (Figure 7-13a) indicated a possible source
 8548 on the coastline (at 5:30 AM, red triangle), and indeed at this time in this area, there were
 8549 unusual emissions from port containers. On the other hand, when one meteorological station
 8550 at Carmel Mountain was used (Figure 7-13b) for the same event, the back trajectory path
 8551 points to a possible source in the sea. When a met station on the coast was chosen (Figure
 8552 7-13c), a possible source of the odour nuisance was in the mountain area.

8553 In this case, identifying the odour nuisance source was incorrect when a single
 8554 meteorological station was used.

8555
 8556
 8557



8558
 8559 **Figure 7-13** Airflow back trajectories calculated from the complaint site at *Bat Galim*
 8560 neighbourhood in *Haifa* from 09:00 AM to 05:25 AM on 22.05.2019. The calculations were
 8561 based on: (a) all the meteorological stations in the area, (b) the mountain meteorological
 8562 station, and (c) the coast meteorological station. (Courtesy of Israel Ministry of Environment).

8563 7.4. Calculating odour impact by balancing the hedonic tone of 8564 multiple sources

8565
 8566 Source apportionment of odour rate from multiple sources is traditionally addressed by
 8567 calculating the contribution of different odour emission rates of each source. Usually, this
 8568 contribution is measured by calculating the number of odour units released per unit of time
 8569 for each source.
 8570

8571 This approach is correct when the odour sources have a similar hedonic tone. However, the
 8572 calculated contribution of each source to the overall odour impact can be challenging when
 8573 different hedonics are involved.

8574
 8575 Whilst calculating the odour concentration in a lab is a *threshold* measurement, the hedonic
 8576 tone is considered a *suprathreshold* measurement. In addition, the calculation of odour
 8577 concentration usually involves four assessors and sometimes up to 8-10, whilst calculating
 8578 the hedonic tone involves a larger group of assessors.

8579
 8580 That said, evaluating the hedonic tone is a valuable tool to calculate the contribution of each
 8581 odour source to the overall odour impact. Sources with an equal odour concentration but
 8582 with different hedonics will impact differently.

8583
 8584 The hedonic tone is usually measured in the lab with scales, such as the one indicated in
 8585 Chapter [6.2.4](#) based on the German Standard VDI 3882 part 2. The Dutch standard NVN
 8586 2818:2019 details the same scale.

8587

8588 **Table 7-1** Scale for the hedonic tone of the Dutch standard NVN 2818:2019

8589

Hedonic Tone	Verbal description
-4	Extremely unpleasant
-3	Moderate unpleasant
-2	Unpleasant
-1	Slightly unpleasant
0	Neutral
1	Slightly pleasant
2	Pleasant
3	Moderate pleasant
4	Extremely pleasant

8590

8591

8592 Hedonic tone can also be measured on the field (*VDI 3940 part 5*).

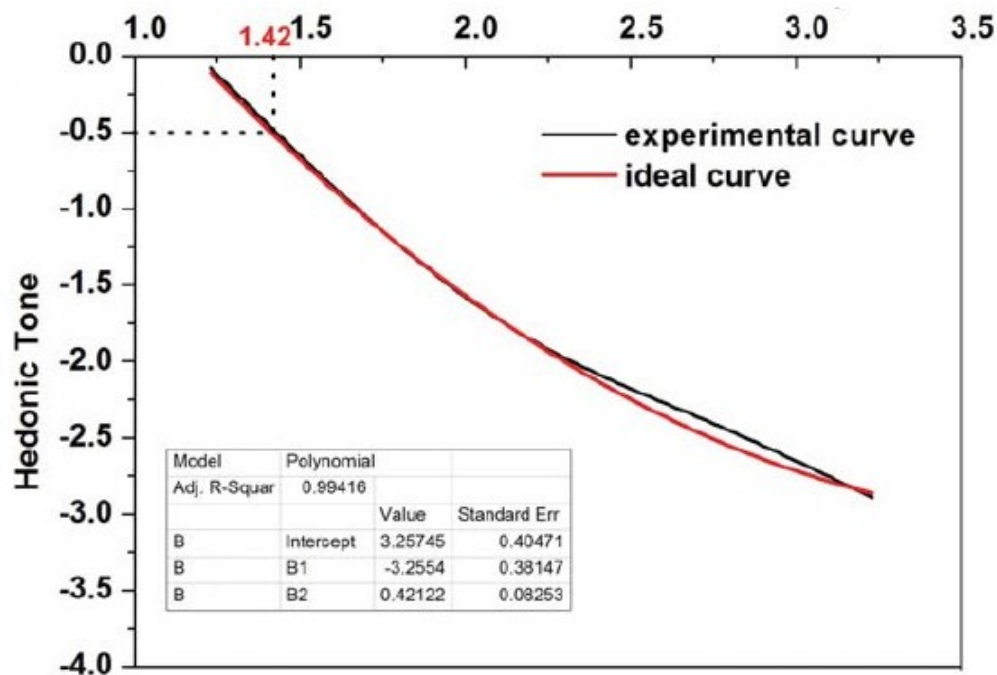
8593

8594 A different measurement of the hedonic tone of an odour sample can be carried out using
 8595 the so-called polarity profiles (Kwiatkowski et al., 2021).

8596

8597 There is a relationship between the odour concentration and the hedonic tone. For example,
 8598 the following graph extracted from *Li et al. (2017)* shows the variation of the hedonic tone
 8599 with the odour index for the case of ammonia. The odour index is directly related to the
 8600 odour concentration.

8601



8602
8603 **Figure 7-14** Relationship between odour concentration index (X) and hedonic tone (Y) for
8604 ammonia (Li et al., 2017)
8605

8606 The behaviour curve of the hedonic tone as a function of *odour concentration index*³ for
8607 ammonia was studied by Li et al., 2017. These authors observed a significant decrease in
8608 the hedonic tone when the odour concentration index increased. When the absolute value of
8609 the hedonic tone was lower than 0.5, the odour was considered neutral, neither pleasant nor
8610 unpleasant. Figure 7-14 above shows that when the hedonic tone is -0.5, the corresponding
8611 concentration index is 1.42 (odour concentration approximately 26 ou/m³). For concentration
8612 indexes lower than 1.42, the ammonia smell will not be unpleasant.
8613

8614 The odour threshold value of ammonia is 1062 µg/m³ at 20°C
8615 (<https://www.odourthreshold.com/>). That means that ammonia odour will be unpleasant at
8616 concentrations of 1062 X 26 = 27612 µg m⁻³.
8617

8618 However, the hedonic tone is not consistently decreasing with increasing odour
8619 concentrations. The following graph shows a concentration-hedonics relationship for several
8620 chemicals (Li et al., 2019). In this case, dimethyl sulfide and butyl acetate follow the same
8621 pattern. However, in the case of limonene, the hedonic tone increases when the
8622 concentration increases and then decreases sharply. Figure 7-15 below shows three distinct
8623 categories of odorants concerning hedonic tone:
8624

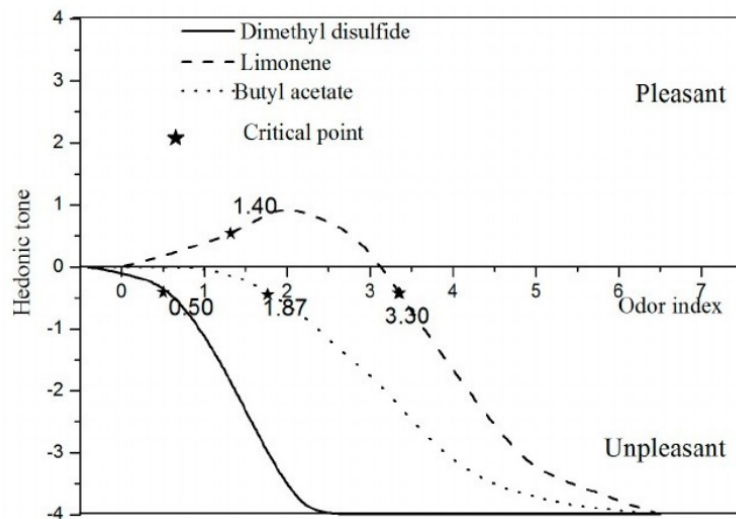
- 8625 ● *Unpleasant odorants* (e.g., dimethyl disulfide, hydrogen sulfide, ammonia, methyl
8626 mercaptan): the odour at each dilution factor is unpleasant to all the assessors, and
8627 the aversion gradually diminishes as the dilution increases.
- 8628 ● *Divergent odorants* (e.g., butyl acetate, methyl isobutane, propionaldehyde): At the

536 ³The odour concentration index is a measurement of odour concentration used in Japan, China and
537 Korea to measure odours. It is numerically equal to the Log of the odour concentration. For example,
538 with reference to Figure XX, 10^{1.42} = 26.3.

8629 same odour concentration, a minority of the assessors find the odour pleasant, while
 8630 the remaining find it unpleasant. The resulting hedonic tone remains negative at all
 8631 the concentration values.

- 8632 • *Pleasant odorants* (e.g., limonene, ethyl acetate, vanillin): The odour is pleasant at
 8633 lower concentration values but becomes unpleasant when the concentration values
 8634 increase.

8635
 8636



8637

8638 **Figure 7-15** Relationship between odour concentration index and hedonic tone for dimethyl
 8639 disulfide, limonene and butyl acetate (Li et al., 2019)

8640

8641

8642 7.4.1 Example of hedonic tone weighting

8643

8644 The hedonic tone is used in many provinces of the *Netherlands* to balance odour impact
 8645 following the Dutch standard NVN 2818. *Brancher et al. 2017*, mention a practical example
 8646 of the legislation in the province of *North Brabant*.

8647

8648 The regulation of *North Brabant* uses the hedonic value $H = -1$ (slightly unpleasant, see
 8649 previous Table 7-1). Before the ambient air level is calculated using a dispersion model, the
 8650 odour emission rates first need to be corrected numerically by the hedonic value associated
 8651 with the source. Calculations are based on a "*hedonic weighted ou_E per unit of time*",
 8652 expressed as $ou_E(H) h^{-1}$. For instance, if a source has an odour emission rate of $630 \text{ Mou}_E h^{-1}$
 8653 and an odour concentration of $7 \text{ ou}_E m^{-3}$ at $H = -1$, then the *hedonic weighted odour*
 8654 *emission rate* is $90 \text{ Mou}_E h^{-1}$ (as a result of dividing $630 \text{ Mou}_E h^{-1}$ by $7 \text{ ou}_E m^{-3}$). Therefore,
 8655 dispersion modelling results are expressed as $ou_E m^{-3}$ and compared against the criteria set
 8656 for *North Brabant*.

8657

8658 These hedonic weighted odour units can be very well used to identify sources with a similar
 8659 concentration inside a facility but with different offensiveness.

8660

8661 7.5. Calculating odour impact from intermittent sources and 8662 non-static receptors

8663

8664 If there are situations where particular meteorological or emission conditions occur relatively
8665 infrequently, special consideration should be given to whether the result of odour impact
8666 obtained is a good and representative environmental indicator of a nuisance. Some
8667 examples of situations where an expert assessment of representativeness would be required
8668 are as follows:

8669

8670 a) **Intermittent sources:** If a source produces short-term peaks in odorant emissions at a
8671 particular time of the day, this may lead to a significantly higher odour exposure that occurs
8672 only during that limited period of the day at specific locations. Even though the exposure
8673 criteria are met, there could be significant complaints due to a high odour concentration
8674 during a short period.

8675

8676 b) **non-static receptors:** When regular wind patterns during the day exist, as can be the
8677 case in coastal land-sea breezes, the situation can arise that a particular location is exposed
8678 predictably and with higher probability at a particular time of the day (typically in the early
8679 morning or evening, when the wind direction reverses). These exposure events are,
8680 therefore, more likely to correlate with periods when people return home from work and
8681 would like to enjoy leisure time. Therefore, The exposure criteria may underestimate the
8682 potential for nuisance impact on residents at that location.

8683

8684

8685 7.5.1 Calculation of odour exposure by intermittent / discontinuous / 8686 seasonal sources. 8687

8688 Sources are considered Intermittent when they produce:

- 8689 1. Short-term peaks in odorant emissions at a particular time of the day (for example,
8690 because of loading/unloading or cleaning operations) or
- 8691 2. Odorant emissions a few hours every day (e.g., plants operating 6 hours a day) or in
8692 certain seasons (e.g., fisheries).

8693 In these cases, calculating odour exposure might be challenging because most odour criteria
8694 are based on hourly percentiles of a year, considering that the odour source emits
8695 continuously throughout the time.

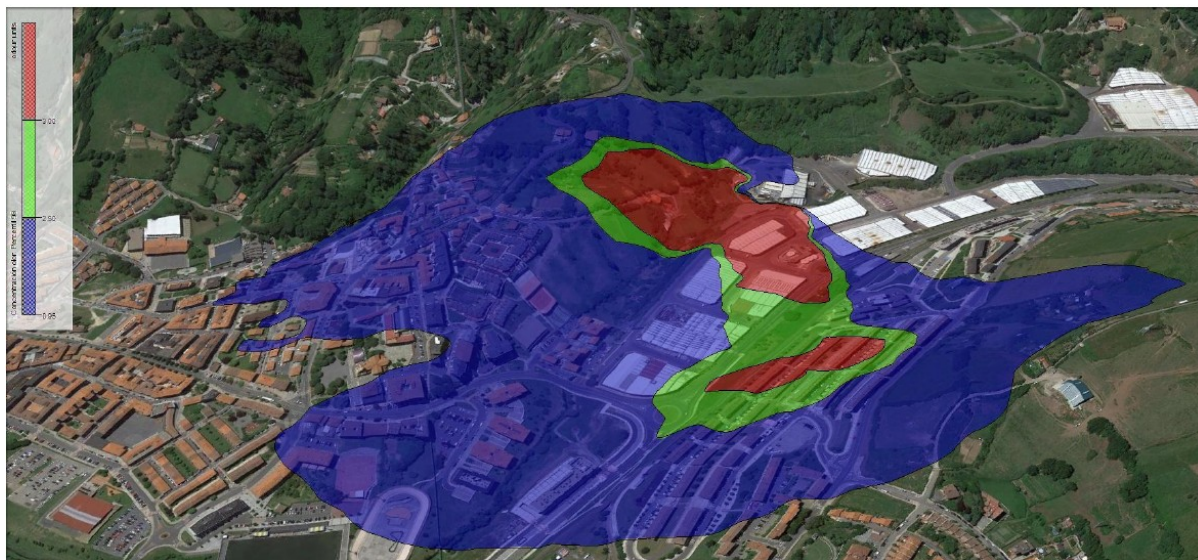
8696 Therefore, different approaches could be taken, the main ones:

- 8697 1. To model odour exposure as a percentile of the hours of the year
- 8698 2. To model odour exposure as a percentile of the working hours
- 8699 3. To calculate odour load/dose and compare it with the odour load/dose of a regular
8700 plant working 24/7/365.

8701 The first approach has a few limitations as plants that emit short-term high-odour emission

8702 rates will produce impact provided the right conditions, independently of the source working
8703 only a few hours.

8704 The following Figure 7-16 shows the odour impact of an animal byproduct rendering plant
8705 located in Spain that operated only 6 hours daily, usually during the morning. This plant had
8706 a record of many years of odour complaints.



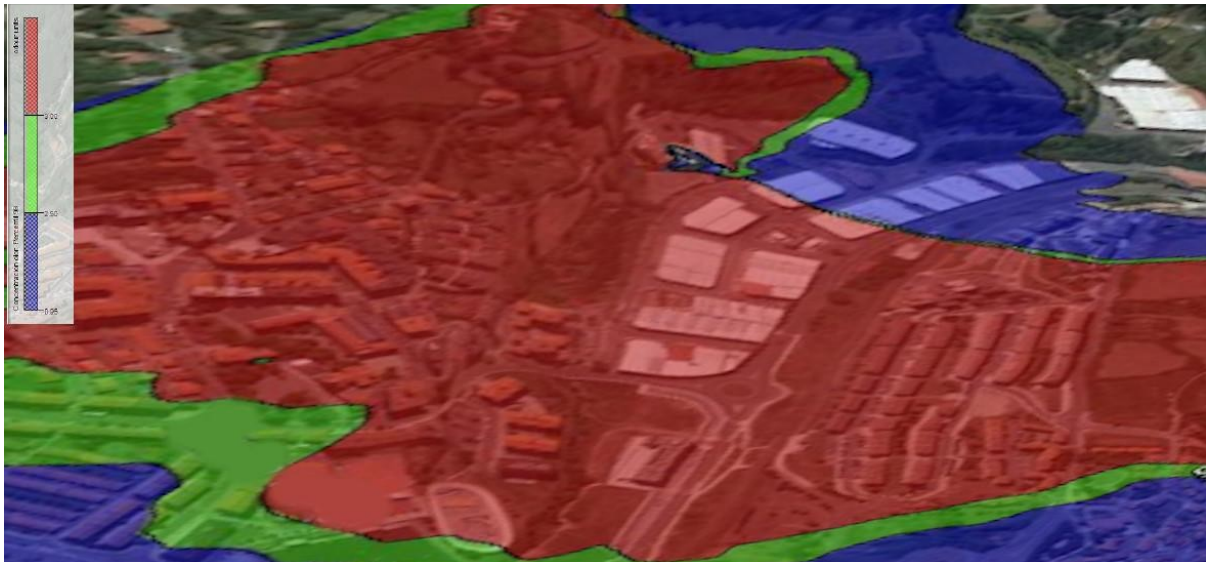
8707

8708 **Figure 7-16** P98 Odour isopleths of a year of an animal by-product plant when modelling 6
8709 hours of emissions daily (175 hours of the 8760 hours of the year) (Courtesy of Ambiente et
8710 Odora).

8711 The contours showed no impact by calculating the percentile 98 of the year's hours. The
8712 model used in this case was CALPUFF. The blue, green and red area shows a P₉₈ of 1, ou_E.

8713 Thus, the first approach of modelling odour exposure as a percentile of the year's hours did
8714 not reflect the reality of the complaints at that time. This plant still had a record of many
8715 years of odour complaints.

8716 Therefore a second approach was taken. That is, the modeller used only the 6 hours of the
8717 morning the plant was working. The result is shown in the following Figure 7-17.



8718

8719 **Figure 7-17** Odour isopleths of an animal by-product plant when modelling 6 hours of
 8720 emissions daily and calculating the P98 of these 6 hours of emission (44 hours of 2190
 8721 hours of the year) (Courtesy of Ambiente et Odora)

8722 The impact, in this case, is shown as much higher.

8723 Unfortunately, the odour impact criteria set for different legislations are based on hourly
 8724 percentiles of the year. Therefore the results of this exercise could not be compared with any
 8725 existing level set in any guideline or regulation, as they are all based on continuous emitting
 8726 sources.

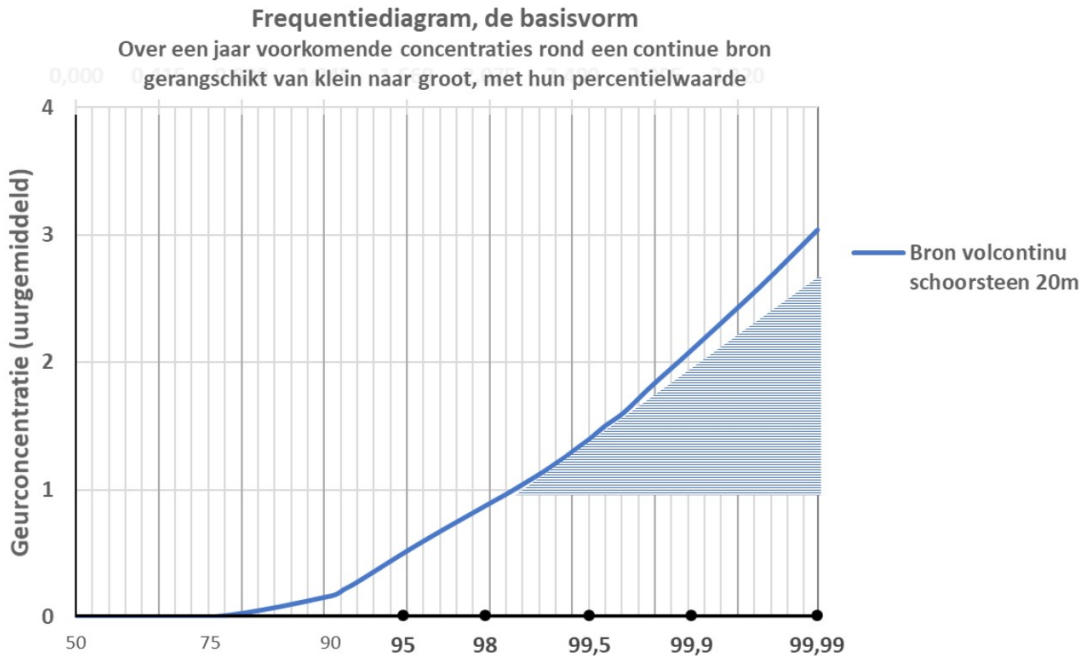
8727 This is the main limitation of modelling only a few hours of the day.

8728 In addition, percentiles have many limitations, reflecting only a set of maximum
 8729 concentrations at a given number of hours a year.

8730 Intermittent sources, like the one of this animal byproduct plant, will produce impact even
 8731 though a certain percentile shows that it does not.

8732 The concept of *odour load* or *odour dose* is being discussed in the working group revising
 8733 the Dutch standard NTA 9065 (Diaz et al., 2020). The way to express the odour load is
 8734 through diagrams of frequency distributions such as the one below (Figure 7-18).

8735



8736

8737 **Figure 7-18** Odour dose as obtained representing the odour concentration (Y-axis) at
8738 different percentiles (X-axis) in a receptor (Courtesy of Hugo van Belois).

8739 The *odour dose or load* would correspond with the yearly total number of hours X with an
8740 odour concentration Y above the detection value.

8741 The Y axis shows the odour concentration on a linear scale. The X-axis shows the total
8742 number of hours of the year represented in the form of percentiles. For example, 95, 98,
8743 99.5, and 99.9 percentiles correspond with the maximum concentrations above one odour
8744 unit obtained considering 438, 175, 44 and 9 hours of the year, respectively.

8745 The total odour load would be the area of the graph corresponding with the odour
8746 concentration above the detection limit (1 odour unit).

8747

8750

7.7. Online calculation of odour impact

8751

7.7.1 Real time odour plumes

8752 In principle, a “real-time” atmospheric modelling system tailored for a specific plant needs
8753 the definition of these components: a simulation domain, an emission scenario and
8754 meteorological information. Strictly speaking, “real-time” could be a wrong term because
8755 acquiring data and using them to perform calculations requires time, even though a short
8756 one. It should be better to use the term *nowcasting*, which refers to predictions in the very
8757 near future (i.e., minutes).

8758

8759 The extension of the simulation domain is defined once for the worst impact expected from
8760 the plant, and the geophysical information is processed and stored within the system. For
8761 example, a simulation system based on CALMET/CALPUFF (Scire et al., 2000a, 2000b)
8762 must include, at minimum, topography and land use for each meteorological grid. This
8763 information must not be renewed at any simulation; it is part of the system setup. The
8764 specification of sensible receptors must also be done in the setup phase.

8765

8766 Concerning the emissions, they include both static and dynamic information. Static
8767 information includes source coordinates, stack heights, diameters and geometrical variables
8768 of other source types. This information does not vary with time unless new sources are
8769 added, or existing ones are modified or removed. The dynamic information is related to the
8770 emissions. Major stacks within large plants typically mount *Automatic Measuring Systems*
8771 (AMS), which are composed of hardware (e.g., gas analysers, sampling systems,
8772 thermometers) and software for data acquisition and storage.

8773

8774 AMSs provide in real-time volume flow rate, emission temperature, and concentration of
8775 each pollutant of interest. Among the pollutants monitored by AMSs, there could be some
8776 odorants, such as H₂S, VOC or other compounds such as CH₄, that is odourless, but it is
8777 often related to the odour emission of a landfill. In other cases, the signal provided by an
8778 IOMS might also be used.

8779

8780 Meteorological information may derive from a monitoring station - or more stations -
8781 installed within or near the plant. Moreover - even though this paragraph describes “real-
8782 time” applications - sometimes it is useful to adopt a prognostic regional model such as
8783 WRF (Skamarock et al., 2008) to get the current hour meteorological data. Indeed, the data
8784 forecasted by the prognostic model a few hours ago (the past) are used for the current
8785 hour (the present), they are not used for the next hours (the future). Therefore, the model
8786 is not used to forecast the odour plume. Meteorological fields obtained from WRF or other
8787 prognostic models can be spatially refined through diagnostic models (e.g., CALMET).
8788 Adopting prognostic models for real-time simulations is particularly useful when there are
8789 no representative meteorological stations close to the plant, in particular vertical profiles
8790 able to represent the atmospheric flow at upper levels.

8791

8792 These three components (domain, emissions, meteorology) must communicate through a
8793 suitable software system, often a web-based one. The results will be the concentration
8794 values at the sensitive and gridded receptors.

8795

8796 When emissions do not arrive from stacks (e.g., fugitive emissions from flanges, valves, etc.,
8797 of a refinery or tanks of a WWTP), and/or a specific pollutant cannot be measured by an
8798 AMS (e.g. an odorant) or by an IOMS (odour), the situation is more complicated. Emissions
8799 may depend on the meteorological variables, such as wind speed and/or wind direction (e.g.,
8800 Bellasio and Bianconi, 2022). The simulation system may include a sort of feedback in order
8801 to improve the quality of the simulation. For example, an IOMS may be placed downwind
8802 over the plant fence line and measure an odour concentration equal to C_{EN} . If the model
8803 concentration corresponding to the position of the IOMS and calculated with an initial
8804 emission E is C_M , the model must run again with a new emission equal to $E_{NEW} = E * C_{EN}/C_M$.
8805 This is the simplest situation when a single source is present; the real situations may be
8806 more complicated.

8807

8808 Uvezzi et al. (2022) conducted a short review of real-time odour dispersion modelling. They
8809 identified three main scientific works on the topic: Chirmata et al. (2015), Giveleta et al.
8810 (2012) and Burgués et al. (2021). Chirmata et al. (2015) applied their methodology to an
8811 Agadir (Morocco) industrial plant. They integrated the data of six IOMSs and those
8812 measured by some meteorological stations; odour concentration maps in real-time were
8813 obtained using the AERMOD dispersion model. Givelet et al. (2012) applied their system to
8814 a Waste Methaisaation Facility in Montpellier (France). The system was composed of
8815 dedicated sensors and IOMSs, together with an air dispersion model, allowing to get the
8816 odour map in real-time. The software generated warning messages when the odour
8817 concentration exceeded a specific threshold. Finally, the system of Burgués et al. (2021) is
8818 based on small drones specifically designed for real-time odour monitoring. The system was
8819 applied to a WWTP facility in Spain. The drones were equipped with more than twenty
8820 different sensors; the signal was sent in real-time to a base station, and the data were
8821 visualised both as text and as an odour concentration map.

8822

8823 There is also some commercial software available for real-time odour dispersion simulation.
8824 For example, AMS, Atmospheric Modelling System (Enviroware srl), Nose Vision 360
8825 (Arianet), Prolor (Ambiente et Odora), EnviroSuite (Envirosuite Ltd), Meteosim (Meteosim),
8826 Total Odour Management System, TOM (Osmotech srl) and SmartPlume (The Synergy
8827 Group).

8828 7.7.2 Forecasting odour impact

8829 This tool could be useful for industrial activities provided that they can control their emission
8830 using operative actions, such as a decrease or delay in the production of a unit or an
8831 increase of the efficiency of the odour abatement system. This can be done, for example, by
8832 using more chemicals or increasing the fan's speed to favour the plume's dispersion.

8833 Odour forecasting requires the same system components needed for determining real-time
8834 odour plumes. On the one hand, odour forecasting is even simpler than nowcasting
8835 because, for example, the feedback procedure to adjust emissions is not required since it

8836 cannot be done. On the other hand, while nowcasting could be done by “simply” using the
8837 data of a meteorological station, forecasting odour impact necessarily requires using a
8838 prognostic meteorological model such as WRF. For example, a modelling system for odour
8839 forecasting has been described by Cartelle et al. (2016). Thanks to wind speed and direction
8840 availability, these systems also allow forecasts of wind-dependent odour emissions (e.g.,
8841 Bellasio and Bianconi, 2022) and use them to feed the dispersion model.

8842 7.8. Role of electronic olfaction devices to test the performance 8843 of odour dispersion models.

8844

8845 There is a need to investigate the role of Electronic Olfaction devices, better known as
8846 *Instrumental Odour Monitoring Systems* (IOMS), in evaluating model performance. However,
8847 it is unclear if, at this stage, these devices are reliable enough to serve as monitors of odour
8848 in ambient air.

8849

8850 IOMSs work better when located near odour sources (Bax et al., 2020) or at the fenceline
8851 (Bax et al., 2021; Cangialosi et al., 2021) due to the high odour concentrations usually found
8852 there. Unfortunately, they cannot be used to evaluate the performance of a dispersion
8853 model. Commercially available IOMSs may struggle at distances over 1 km from the source.
8854 Odour concentration in ambient air is usually tens to a few hundred European odour units. At
8855 those relatively low odour concentrations, IOMS performance is limited.

8856

8857 Although many IOMS manufacturers claim that their devices can measure odours, there is a
8858 need to standardise those claims. The *European Committee on Standardisation* (CEN) have
8859 tried to standardise the use of these devices, but no text has been produced (Harreveld,
8860 2022). Some national Standards on IOMSs include the Dutch NTA 9055:2012, the German
8861 VDI/VDE 3518 Part 3 or the Italian UNI 11761:2019.

8862

8863 In addition, there are other developments related to IOMSs, such as the three initiatives
8864 carried out by IEEE: IEEE P2520.2.1 Standard for Machine Olfaction Devices and Systems
8865 Used for General Outdoor Odor Monitoring, IEEE P2520.4.1 Standard for Performance of
8866 Machine Olfaction Devices and Systems for Chemical Manufacture, and IEEE P2520.1
8867 Standard for Baseline Performance for Odor Analysis Devices and Systems.

8868

8869 More research is needed to compare the results of a dispersion model with that measured
8870 with an IOMS.

8871 7.8.1 Evaluation of performance according to EN 16841 part 1

8872

8873 EN 16841 part 1 deals with the measurement of odours using the so-called grid method.
8874 This methodology uses assessors brought to different points in a grid to determine if odours
8875 are present in those points (see Chapter [4.4.1. Ambient air measurement to characterise
8876 odour exposure: grid method](#)).

8877

8878 The unit of measurement of odours is the “odour hour” .

8879

8880 According to EN 16841 part 1, the odour hour is obtained by a single measurement when
8881 the percentage of the odour time reaches or exceeds 10% by convention.

8882

8883 At the end of a minimum of 6 months of data collection, there will be 13 measurements at
8884 each point of the grid. After a year, there will be 26 measurements. At each measurement
8885 point, an assessor inhales every 10 seconds and records if he/she perceives an odour. After
8886 10 minutes, there will be 60 observations. If in 6 of these 60 observations (10%) an odour is
8887 detected, the result is expressed as one odour hour.

8888

8889 Therefore, for 6 months, there will be 13 recordings of the presence/absence of odour (of a
8890 certain quality) for 10 minutes. That is, of the 4830 hours of a half year, there will be only 13
8891 that will be used in each point of the grid after 6 months. Or, to be more precise, of 26280
8892 packages of 10-min data, only 13 packages will be used to check model performance.

8893

8894 This is not much data to check model performance, so it is difficult that EN 16841 part 1
8895 could be used to evaluate model performance.

8896

8897 7.8.2 Evaluation of performance according to EN 16841 part 2

8898

8899 Evaluation according to EN 16841 part 2 is more suitable for checking dispersion model
8900 performance. Part 2 of this standard deals with measuring odour in ambient air using the
8901 plume method (for more details, see Chapter [4.4.2. Ambient air measurement of odours by
8902 using the plume method](#)).

8903

8904 One of the important points of this methodology is that it needs Gaussian-like conditions to
8905 carry out the plume measurement. That means that model performance can be carried out
8906 with the plume measurement but only with constant turbulence conditions (no changing
8907 dispersion class) during one measurement cycle. The atmospheric stability is specified by
8908 indicating the Monin-Obukhov length LM, which can be measured by a 3D ultrasonic
8909 anemometer. EN 16841 part 2 prescribes that the Monin-Obukhov length (LM) shall be
8910 under -150 m or above 250 m. Also, turbulence classes should be slightly stable, neutral or
8911 slightly unstable (for example, Pasquill C or D or part of B and E).

8912

8913 Unfortunately, odour impact usually occurs when there are calm or low wind conditions (Diaz
8914 et al. 2014), so model performance will not be carried out under these conditions using EN
8915 16841 part 2.

8916

8917 A typical example of using the plume method for assessing dispersion modelling
8918 performance is the Uttenweiler experiment mentioned in Chapter [5.7.1. Examples of
8919 validation with odour measurements](#).

8920 7.9. References

8921 Arianet. Nose Vision 360. (2022). Monitoraggio integrato in tempo reale dell'odore generato
8922 da un impianto di trattamento delle acque. *Ingegneria Dell'Ambiente*, 9(1), 70–71.

- 8923 Armand, P., Olry, C., Albergel, A., Duchenne, C., & Moussafir, J. (2013, May). Development
8924 and application of RETRO-SPRAY a backward atmospheric transport and dispersion model
8925 at the regional and urban scale. In 15th International conference on Harmonisation within
8926 Atmospheric dispersion Modelling for Regulatory Purposes, Harmo (Vol. 15, pp. 789-793).
- 8927 Bächlin, W.; Rühling, A.; Lohmeyer, A. 2002. Bereitstellung von validierungs-daten für
8928 geruchsausbreitungs-modelle-naturmessungen. (Baden-Württemberg, Germany).
- 8929 Bax, C., Sironi, S., & Capelli, L. (2020). Definition and Application of a Protocol for Electronic
8930 Nose Field Performance Testing: Example of Odor Monitoring from a Tire Storage Area.
8931 *Atmosphere*, 11(4), 426. <https://doi.org/10.3390/atmos11040426>
- 8932 Bax C., Lotesoriere B., Capelli L., 2021. IOMS for the real-time monitoring of odour
8933 concentration at a msw landfill, 9th IWA Odours & VOC/Air Emission Conference, Bilbao,
8934 Spain, www.olores.org.
- 8935 Bellasio R, Bianconi R. A Heuristic Method for Modelling Odour Emissions from Open Roof
8936 Rectangular Tanks. *Atmosphere*. 2022; 13(3):367. <https://doi.org/10.3390/atmos13030367>
- 8937 Bianconi R., Mosca S. and Graziani G. (1999) PDM: A Lagrangian particle model for
8938 atmospheric dispersion. European Commission. EUR 17721 EN, 63 pp.
- 8939 Bilsen I. and De Fré R. (2008), Sniffing team measurements in Flanders: Code of Good
8940 Practice. *Water Practice and Technology*, June 2009, 4 (2) wpt2009027; DOI:
8941 10.2166/wpt.2009.027. presented at the 3rd IWA International Conference on Odour &
8942 VOCs in September 2008.
- 8943 Bilsen I., De Fré R. and Bosmans S. (2009). Code van Goede Praktijk: Bepalen van de geur-
8944 verspreiding door middel van snuffelploegmetingen (Code of Good Practice: Determination
8945 of the odour dispersion by means of sniffing team measurements), VITO, Mol, Belgium.
- 8946 Bisignano, A., Trini Castelli, S., Malguzzi, P. (2020). Development and Verification of a New
8947 Meteo-Dispersive Modelling System for Accidental Releases in the Italian Territory: SMART.
8948 In: Mensink, C., Gong, W., Hakami, A. (eds) *Air Pollution Modeling and its Application XXVI*,
8949 pp. 77-81. ITM 2018. Springer Proceedings in Complexity. Springer, Cham.
8950 https://doi.org/10.1007/978-3-030-22055-6_13
- 8951 Bonafè, G., Bellasio, R., & Bianconi, R. (2016). The LAPMOD_SA Modelling System for
8952 Source Attribution. In *Air Pollution Modeling and its Application XXIV* (pp. 357-361).
8953 Springer, Cham.
- 8954 Brancher, M., Griffiths, K. D., Franco, D., & de Melo Lisboa, H. (2017). A review of odour
8955 impact criteria in selected countries around the world. *Chemosphere*, 168, 1531-1570.
- 8956 Burgués, J., Esclapez, M. D., Doñate, S., & Marco, S. (2021). RHINOS: A lightweight
8957 portable electronic nose for real-time odor quantification in wastewater treatment plants.
8958 *IScience*, 24(12), 103371.
- 8959 Cangialosi F, Fornaro A., De Santis G., Detection of gas leakage from landfills using optical
8960 gasimaging coupled with fence monitoring system of odour by IOMS: A case study,
8961 IWA2021 Conference, Bilbao, Spain, www.olores.org.
- 8962 Capelli L., Dentoni L., Sironi S., Guillot JM., Experimental Approach for the Validation of
8963 Odour Dispersion Modelling, *Chemical Engineering Transactions*, Vol. 30 2012.
8964

- 8965 Carslaw, D. C., and K. Ropkins. 2012. "openair — An R package for air quality data
8966 analysis." *Environmental Modelling & Software* 27–28 (0): 52–61.
8967 <https://doi.org/10.1016/j.envsoft.2011.09.008>.
- 8968 Cartelle D., J.M. Vellon, A. Rodriguez, D. Valino, J.A. Gonzalez, C. Casas, & F. Carrera-
8969 Chapela. (2016). Prolor: A modelling approach for environmental odor forecast. *Chemical*
8970 *Engineering Transactions*, 54, 229–234. <https://doi.org/10.3303/CET1654039>
- 8971 Chiapello, I., Bergametti, G., Chatenet, B., Bousquet, P., Dulac, F., & Soares, E. S. (1997).
8972 Origins of African dust transported over the northeastern tropical Atlantic. *Journal of*
8973 *Geophysical Research: Atmospheres*, 102man (D12), 13701-13709.
- 8974 Chirmata, A., Ichou, I. A., & Page, T. (2015). A continuous electronic nose odor monitoring
8975 system in the city of Agadir Morocco. *Journal of Environmental Protection*, 6(01), 54.
- 8976 Chunrong Jia, Jim Holt, Herb Nicholson, Jody Edward Browder, Xianqiang Fu, Xinhua Yu,
8977 Ronné Adkins, Identification of origins and influencing factors of environmental odor
8978 episodes using trajectory and proximity analyses, *Journal of Environmental Management*,
8979 Volume 295, 2021, 113084, ISSN 0301-4797
- 8980 Cressman G .P "An operational objective analysis system" *Monthly Weather Review* , Vol
8981 87, No 10 Oct 1959, pp 367-374
- 8982 C. Diaz, C. Izquierdo, A. Antón. Is it possible to set a universal odour limit? NOSE 2020
8983 conference.
- 8984 Diaz C., Cartelle D., Barclay J., 2014, Revision of Regulatory Dispersion Models, an
8985 Important Key in Environmental Odour Management, 1st International Seminar of Odours in
8986 the Environment, Santiago, Chile, www.olores.org Accessed July 2022
8987 ([https://www.olores.org/en/techniques/dispersion-modelling/359-revision-of-regulatory-](https://www.olores.org/en/techniques/dispersion-modelling/359-revision-of-regulatory-dispersion-models-an-important-key-in-environmental-odour-management)
8988 [dispersion-models-an-important-key-in-environmental-odour-management](https://www.olores.org/en/techniques/dispersion-modelling/359-revision-of-regulatory-dispersion-models-an-important-key-in-environmental-odour-management))
- 8989 EN 16841-1: 2017-03 Ambient air - Determination of odour in ambient air by using field
8990 inspection - Part 1: Grid method; German version EN 16841-1:2016.
- 8991 EN 16841-2: 2017-03 Ambient air - Determination of odour in ambient air by using field
8992 inspection - Part 2: Plume method; German version EN 16841-2:2016.
- 8993 Elbern, H., Strunk, A., Schmidt, H., & Talagrand, O. (2007). Emission rate and chemical
8994 state estimation by 4-dimensional variational inversion. *Atmospheric Chemistry and Physics*,
8995 7(14), 3749-3769.
- 8996 EnviroSuite Ltd. Odowatch (2022). <https://envirosuite.com/parameters/odour-management>
8997 (last visited: November 2022).
- 8998 Enviroware (2022). Atmospheric Modelling System. .
8999 <https://www.enviroware.com/projects/ams/>
- 9000 Exponent (2023) CALPUFF Modeling System. <http://www.src.com/> (Accessed March 2023).
- 9001 Ferrarese, S., & Trini Castelli, S. (2019). Detection of CO2 source areas using two
9002 lagrangian particle dispersion models, at regional scale and long range. In 19th International
9003 Conference On Harmonisation Within Atmospheric Dispersion Modelling For Regulatory
9004 Purposes, Harmo 2019 (pp. 1-5).

- 9005 Fleming Z.L., Monks P.S. and Manning A.J. (2012) Review: Untangling the influence of air-
9006 mass history in interpreting observed atmospheric composition. *Atmospheric Research*, 1-
9007 39. doi:10.1016/j.atmosres.2011.09.009
- 9008 Flesch, T. K., Wilson, J. D., & Yee, E. (1995). Backward-time Lagrangian stochastic
9009 dispersion models and their application to estimate gaseous emissions. *Journal of Applied*
9010 *Meteorology and Climatology*, 34(6), 1320-1332.
- 9011 Gallego, E., Alarcon, M., Roca, F.J., Perales, J.F., Soriano, C, Guardino, X., "Identification of
9012 the origin of odour episodes through social participation, chemical control (DT-GC/MS) and
9013 numerical modelling", *Atmospheric Environment*,42, 8150-8160 (2008)
- 9014 Givelet, A., Lazarova, V., Kelly, R., & Dauthuille, P. (2012). The NOSE Platform®: A Real-
9015 Time Solution to Forecast & Monitor Nuisance Odours. *Chemical Engineering Transactions*,
9016 30, 253-258.
- 9017 Gurney, K. R., Law, R. M., Denning, A. S., Rayner, P. J., Baker, D., Bousquet, P., ... & Yuen,
9018 C. W. (2002). Towards robust regional estimates of CO₂ sources and sinks using
9019 atmospheric transport models. *Nature*, 415(6872), 626-630.
- 9020 Henry R.P., Chang Y., Spiegelman C.H. (2002) Locating nearby sources of air pollution by
9021 nonparametric regression of atmospheric concentrations on wind direction. *Atmospheric*
9022 *Environment*, Vol. 36, n. 13, 2237-2244.
- 9023 Hourdin, F., & Issartel, J. P. (2000). Sub-surface nuclear tests monitoring through the CTBT
9024 Xenon Network. *Geophysical research letters*, 27(15), 2245-2248.
- 9025 Hourdin, F., & Talagrand, O. (2006). Eulerian backtracking of atmospheric tracers. I: Adjoint
9026 derivation and parametisaation of subgrid-scale transport. *Quarterly Journal of the Royal*
9027 *Meteorological Society: A journal of the atmospheric sciences, applied meteorology and*
9028 *physical oceanography*, 132(615), 567-583.
- 9029 Hutchinson, M., Oh, H., & Chen, W. H. (2017). A review of source term estimation methods
9030 for atmospheric dispersion events using static or mobile sensors. *Information Fusion*, 36,
9031 130-148.
- 9032 Janicke Consulting (2019) Dispersion Model LASAT Version 3.4. Reference Book
- 9033 Jiang, K.; Kaye, R. Comparison study on portable wind tunnel system and isolation chamber
9034 for determination of VOCs from areal sources. *Water Sci. Technol.* 1996, 34, 583–589.
- 9035 Kopacz, M., Jacob, D. J., Henze, D. K., Heald, C. L., Streets, D. G., & Zhang, Q. (2009).
9036 Comparison of adjoint and analytical Bayesian inversion methods for constraining Asian
9037 sources of carbon monoxide using satellite (MOPITT) measurements of CO columns.
9038 *Journal of Geophysical Research: Atmospheres*, 114(D4).
- 9039 Kwiatkowski K., Both R., Sucker K., 2021, Determination of hedonic odour effect based on
9040 polarity profiles. 9th IWA Odour& VOC/Air Emission Conference, Bilbao, Spain,
9041 www.olores.org.
- 9042
- 9043 Li J., Li W., Geng J., Zhai Z., Yang W. (2017) "Determination of the hedonic odour tone in
9044 China and the behavior curve of ammonia" *Austrian Contributions to Veterinary*
9045 *Epidemiology*. Vol. 9, 7-14.
- 9046 Li, J., Zou, K., Li, W., Wang, G., & Yang, W. (2019). Olfactory characterisaation of typical

- 9047 odorous pollutants part I: Relationship between the hedonic tone and odor concentration.
9048 Atmosphere, 10(9), 524.
- 9049 Mensink C. and Cosemans G. (2005) Quantification of diffuse sources of PM10 in regulatory
9050 hot spot regions in Flanders. 11th Conf. On Harmonisation within Atmospheric Dispersion
9051 Modelling for Regulatory Purposes, 205-209.
- 9052 Olfasense GmbH, Ortellium 2022. [https://www.olfasense.com/odour-measurement-](https://www.olfasense.com/odour-measurement-equipment/instruments/ortellium-dispersion-modelling/)
9053 [equipment/instruments/ortellium-dispersion-modelling/](https://www.olfasense.com/odour-measurement-equipment/instruments/ortellium-dispersion-modelling/) (Last visited: November 2022)
- 9054 Osmotech srl. Total Odour Management System (TOM) (2022). [https://osmotech.it/total-](https://osmotech.it/total-odour-management-system-tom/)
9055 [odour-management-system-tom/](https://osmotech.it/total-odour-management-system-tom/) (Last visited: November 2022).
- 9056 Pisso, I., Sollum, E., Grythe, H., Kristiansen, N. I., Cassiani, M., Eckhardt, S., Arnold, D.,
9057 Morton, D., Thompson, R. L., Groot Zwaaftink, C. D., Evangeliou, N., Sodemann, H.,
9058 Haimberger, L., Henne, S., Brunner, D., Burkhardt, J. F., Fouilloux, A., Brioude, J., Philipp, A.,
9059 Seibert, P., and Stohl, A. (2019). The Lagrangian particle dispersion model FLEXPART
9060 version 10.4, Geosci. Model Dev., 12, 4955–4997, [https://doi.org/10.5194/gmd-12-4955-](https://doi.org/10.5194/gmd-12-4955-2019)
9061 [2019](https://doi.org/10.5194/gmd-12-4955-2019), 2019.
- 9062 Platt, N., & DeRiggi, D. (2012). Comparative investigation of source term estimation
9063 algorithms using fusion field trial 2007 data: linear regression analysis. International Journal
9064 of Environment and Pollution, 48(1-4), 13-21.
- 9065 Prolor (2014). <https://www.prolor.net/> (Last visited: November 2022.)
- 9066 Pudykiewicz, J. A. (1998). Application of adjoint tracer transport equations for evaluating
9067 source parameters. Atmospheric environment, 32(17), 3039-3050.
- 9068 Region Lombardy. D.g.r. 15 Febbraio 2012–n. IX/3018. Determinazioni Generali in Merito
9069 Alla Caratterizzazione Delle Emissioni Gassose in Atmosfera Derivanti da Attività a Forte
9070 Impatto Odorigeno; Region Lombardy: Milan, Italy, 2012. (In Italian)
- 9071 Ramos Pablo, Cartelle David, y Diaz Carlos, 2017, Gestión de episodios de olor mediante
9072 sistemas de participación ciudadana y cálculo de retrotrayectorias de aire, IV Conferencia
9073 Internacional sobre gestión de Olores y COVs en el Medio Ambiente, Valladolid, España,
9074 www.olors.org
- 9075 Roca, F.J., Gallego, E., Perales, J.F., Guardino, X., “Simultaneous evaluation of odor
9076 episodes and air quality. Methodology to identify air pollutants and their origin combining
9077 chemical analysis (TD-GC/MS), social participation and mathematical simulations
9078 techniques“ Air Quality in the 21 st Century, pp. 139-209, ISBN 978-1-60456-793-9
9079 NovaPublishers, NY, (2008)
- 9080 Scire, J. S., Robe, F. R., Fernau, M. E., & Yamartino, R. J. (2000a). A user’s guide for the
9081 CALMET Meteorological Model. Earth Tech, USA, 37.
- 9082 Scire, J. S., Strimaitis, D. G., & Yamartino, R. J. (2000b). A user’s guide for the CALPUFF
9083 dispersion model. Earth Tech, Inc, 521, 1-521.
- 9084 Skamarock, W. C., Klemp, J. B., Dudhia, J., Gill, D. O., Barker, D. M., Wang, W., & Powers,
9085 J. G. (2008). A description of the Advanced Research WRF version 3. NCAR Technical
9086 note-475+ STR.
- 9087 The Synergy Group. SmartPlume.. <https://en.tsgenvironmental.com/post/the-power-of-time->

- 9088 in-your-hand-with-smart-plume (Last visited: November 2022).
- 9089 Sofiev, M., Siljamo, P., Valkama, I., Ilvonen, M., Kukkonen, J. (2006). A dispersion
9090 modelling system SILAM and its evaluation against ETEX data, *Atmospheric Environment*
9091 40, 674–685.
- 9092 Sprenger, M. & Wernli, H. (2015). The LAGRANTO Lagrangian analysis tool – version 2.0,
9093 *Geosci. Model Dev.*, 8, 2569–2586, <https://doi.org/10.5194/gmd-8-2569-2015>.
- 9094 Stein, A. F., Draxler, R. R., Rolph, G. D., Stunder, B. J. B., Cohen, M. D., & NGAN, F.
9095 (2015). NOAA's HYSPLIT Atmospheric Transport and Dispersion System. *Bulletin of the*
9096 *American Meteorological Society*, 96 (12). 2059-2077, doi:/10.1175/BAMS-D-14-00110.1.
- 9097 Stohl, A., and P. Seibert (1998). Accuracy of trajectories as determined from the
9098 conservation of meteorological tracers. *Q. J. Roy. Met. Soc.* 124, 1465-1484
- 9099 Thompson, R. L., Ishijima, K., Saikawa, E., Corazza, M., Karstens, U., Patra, P. K., ... &
9100 Bousquet, P. (2014). TransCom N₂O model inter-comparison–Part 2: Atmospheric
9101 inversion estimates of N₂O emissions. *Atmospheric Chemistry and Physics*, 14(12), 6177-
9102 6194.
- 9103 Tinarelli, G., Anfossi, D., Castelli, S. T., Bider, M., & Ferrero, E. (2000). A new high
9104 performance version of the Lagrangian particle dispersion model SPRAY, some case
9105 studies. In *Air pollution modelling and its application XIII* (pp. 499-507). Springer, Boston,
9106 MA.
- 9107 Tinarelli, G., Uboldi, F., & Carlino, G. (2018). Source term estimation using an adjoint model:
9108 a comparison of two different algorithms. *International Journal of Environment and Pollution*,
9109 64(1-3), 209-229.
- 9110 Trini Castelli S., Tinarelli G., Uboldi F., Malguzzi P. and Bonasoni P. (2021) Developments of
9111 SPRAY Lagrangian particle dispersion model for tracing the origin of odour nuisance. *Air*
9112 *Pollution modelling and its Application XXVII*, C. Mensink and O. Jorba Casellas (eds.)
9113 Springer Proceedings in Complexity, Springer International Publishing Switzerland, in press.
- 9114 Uvezzi G., Invernizzi M., Sironi S. 2022 Real-Time Odour Dispersion Modelling for Industrial
9115 Sites Application: State of the Art and Future Perspectives. *Chemical Engineering*
9116 *Transactions* 95: 133–38. <https://doi.org/10.3303/CET229502>
- 9117 Van Broeck G., Van Langenhove H. and Nieuwejaers B. (2001). Recent odour regulation
9118 developments in Flanders: ambient odour quality standards based on dose-response
9119 relationships. *Water Science and Technology*, 44, 103-110. Presented at the 1st IWA
9120 International Conference on Odour & VOCs in March 2001.
- 9121 Van Broeck G. and Van Elst T. (2003), The way to a sustainable odour policy in Flanders.
9122 Paper presented at the 2nd IWA International Conference on Odour & VOCs in September
9123 2003.
- 9124 Van Elst T., Delva J., 2016, The european standard prEN 16841-2 (determination of odour in
9125 ambient air by using field inspection: plume method): a review of 20 year experience with the
9126 method in Belgium, *Chemical Engineering Transactions*, 54, 175-180.
- 9127 van Harreveld, Anton P., 2021, The long and winding road of CEN/TC264/WG41 developing
9128 a standard for validating Instrumental Odour Measurement Systems. 9th IWA Odour &

- 9129 VOC/Air Emission Conference, Bilbao, Spain, link accessed July 2022 (
9130 [https://www.olores.org/en/techniques/instrumental-odour-monitoring-o-sensors/1190-the-](https://www.olores.org/en/techniques/instrumental-odour-monitoring-o-sensors/1190-the-long-and-winding-road-of-cen-tc264-wg41-developing-a-standard-for-validating-instrumental-odour-measurement-systems)
9131 [long-and-winding-road-of-cen-tc264-wg41-developing-a-standard-for-validating-instrumental-](https://www.olores.org/en/techniques/instrumental-odour-monitoring-o-sensors/1190-the-long-and-winding-road-of-cen-tc264-wg41-developing-a-standard-for-validating-instrumental-odour-measurement-systems)
9132 [odour-measurement-systems](https://www.olores.org/en/techniques/instrumental-odour-monitoring-o-sensors/1190-the-long-and-winding-road-of-cen-tc264-wg41-developing-a-standard-for-validating-instrumental-odour-measurement-systems)).
- 9133 VDI 3883 (2017) Part 4: "Effects and assessment of odours - Processing odour complaints"
9134 Beuth Verlag GmbH, Berlin
- 9135 VDI 3940 Part 3:2010-01 Measurement of odour impact by field inspection - Determination
9136 of odour intensity and hedonic odour tone, Beuth Verlag GmbH, Berlin
- 9137 VDI 3940 Blatt 5:2013-11 Measurement of odour impact by field inspection - Determination
9138 of odour intensity and hedonic odour tone - Instructions and examples of use
- 9139 Yu K.N., Cheung Y.P., Cheung T., Henry R.P. (2004) Identifying the impact of large urban
9140 airports on local air quality by non-parametric regression. Atmospheric Environment, Vol. 38,
9141 n. 27, 4501-4507.
- 9142 Zarra T., Naddeo V., Giuliani S., Belgiorno V. (2010). Optimisation of field inspection method
9143 for odour impact assessment. Chemical Engineering Transactions, vol. 23, p. 93-98, ISSN:
9144 1974-9791. <https://doi.org/10.3303/CET1123016>.
- 9145 Zarra T., Belgiorno V., Naddeo V. (2021). Environmental odour nuisance assessment in
9146 urbanized area: Analysis and comparison of different and integrated approaches.
9147 Atmosphere, Volume 12, Issue 6, 690. <https://doi.org/10.3390/atmos12060690>
9148
9149
9150

9151 8. Reporting

9152 8.1. Introduction

9153 An odour modelling report aims to show the potential impact on a certain area, including at
9154 sensitive receptors, of the emissions from an odour source or sources.

9155 The methodology and results in an odour report should be presented in a way that can be
9156 understood by the reader, which could include plant managers, regulators or complainants.
9157 Several publicly available guidelines exist and these set out minimum requirements for
9158 dispersion modelling, data analysis, and reporting. Example guidance documents include
9159 those from regulatory authorities such as UK EA 2021, EPA NSW 2022, Eusko Jauraritza
9160 2012, Oregon 2022, NZ ME 2004 and SEA 2023.

9161 Minimum information in a report can include a location map, a list of odour emission sources,
9162 a summary of applicable odour regulations, an explanation of the meteorological data and
9163 dispersion model used, emission rates and parameters adopted, modelled domain,
9164 receptors, surface characteristics, and terrain and building treatments.

9165 Some guidelines require other, more detailed specific information in the report, such as
9166 estimating the model uncertainty or performing a sensitivity analysis. Additional requirements
9167 can include model input parameters and settings or sometimes text outputs of input files as
9168 an appendix.

9169 While there is general information detailing the requirements for general air quality
9170 assessment reports, some differences make reporting odour challenging. For example,
9171 examining model uncertainty is challenging when odour concentration in ambient air is
9172 usually below the threshold of the reference methodology for measuring odours in a
9173 laboratory (dynamic olfactometry). Other standards dealing with measuring odour in ambient
9174 air (EN 16841) either do not have a significant number of odour records (EN 16841 part 1),
9175 or they use modelling the other way around to calculate the odour emission rate of a source
9176 by using reverse modelling (EN 16841 part 2), as explained in chapter 7.2.

9177 In addition, Instrumental Odour Monitoring Systems (IOMS) are not, at this stage, suitable
9178 for evaluating model performance.

9179 The following sections will describe the minimum and recommended information to be
9180 considered when preparing a report assessing odour exposure using dispersion modelling.

9181 8.2. Report structure

9182 8.2.1 Cover Page

9183 The cover page should include the Project Title, the author(s) of the report, the version
9184 number and the date that the report was issued. The cover page should also include the
9185 name of the company or person the report was prepared for.

9186 The report's index (Table of contents) should be included immediately after the cover page.
 9187 A list of Figures, Tables, metrics of conversion and Acronyms and Abbreviations can also be
 9188 included if required.

9189 8.2.2 Introduction

9190 The introduction should give a general description of the facility, such as the company name,
 9191 proponents involved in the project, the proposed use or modification to that use, including
 9192 activities on site that may emit odours, and the potential receptors of odour impact. Data
 9193 that could be included are shown in Table 8-1 below.

9194 The introduction should include information on the selection of the methodology and the
 9195 scenarios implemented.

9196

9197 **Table 8-1** Requirements to be described in the introduction

Elements	Description
Project Name	The title of the facility or proposed project must be stated
Proponents	The name of the entities or individuals involved during the entire phases of the project (e.g., corporation, partnership, single proprietorship, etc.).
Project Location	The location where the site is situated. Include the geographical coordinates and location map.
Project Type	Project classification defined during implementation that specifies essential project attributes.
Status of the operation	Specify if the project is new, or an expansion of the existing plant.
Dispersion Model Type	The considerations in selecting the dispersion model must be briefly justified (e.g., Gaussian-based, Lagrangian-based, etc.)
Contact person and details	The name of the responsible person must be included here and necessary contact information.

9198

9199

9200 8.2.3. Regulatory requirements

9201 The report should summarise the regulations, documents or guidelines used as references
 9202 to perform the assessment. The requirements could include local or international legislation,
 9203 policies, guidelines or technical specifications.

9204 Table 8-2 below provides a list of elements that could be reported.

9205

9206 **Table 8-2** Elements to be considered in reporting

Elements	Description
Definition of the law, guideline, ordinance, etc.	This element has to briefly report the scope, aims and general provisions. Moreover, implementing rules and regulations (IRR) must also be included.
Responsible authorities	The relevant government agencies must be introduced, which can be at the regional level, state, country and/or an internationally recognised organisation.
Parameters or variables regulated	This includes some specific needed parameters such as peak concentrations and the method suggested to calculate them starting from modelling results, if not directly available (by, for example, applying a peak to mean ratio). The extent of applicability of the law must be emphasised, particularly to the parameter being regulated. If a specific law or guidance does not apply to the facility, an indication of the most appropriate best practice guidelines should be included.
Odour Impact Criteria (OIC)	OIC selected for the project.

9207

9208 8.2.4. Project description

9209 This section should present all of the information about the project that is relevant to the
 9210 assessment of odour emissions and their potential impact on the surrounding area. In
 9211 particular, information should be provided about the nature and type of activities performed
 9212 at the facility and how the emissions are generated, released and dispersed from the facility.

9213 The section should be organised into subsections, each including the elements detailed

9214 below.

9215 8.2.4.1. Site location and affected area

9216 This subsection should provide a site location map and details of the area in which the
9217 project is located. The subsection should:

- 9218 ● identify sensitive receptors in the area of the project and within the potential zone of
9219 impact;
- 9220 ● describe the topography near the site and the land uses in the surrounding areas;
9221 and
- 9222 ● describe ambient air quality and other potential odour sources in the immediate
9223 vicinity of the site and consider the risks of cumulative impacts within the potential
9224 zone of impact.

9225 A scale location plan should be provided which shows:

- 9226 ● layout of the site which clearly shows all relevant odour sources;
- 9227 ● site boundary;
- 9228 ● relevant sensitive receptors; and
- 9229 ● topography.

9230

9231 8.2.4.2. Facility, plant, and process description

9232 This subsection should describe the plant activities and the processes performed at the
9233 facility. In particular, the details of the activities performed and how they may affect the
9234 release of emissions and their dispersion in the atmosphere should be included. As a
9235 minimum, a description of the site's operations in simple language should be included.

9236 Table 8-3 presents a list of process information that could be included in this subsection.

9237 **Table 8-3** Requirements to be considered in the discussion of the facility

Elements	Description
Process flow diagram	This should clearly show all unit operations carried out
Production data	Details of batch and/or continuous processes to be presented to include duration of operation for each distinct cycle where relevant
Production rate	The rate of material processed (tonnes/hour), rate of items processed per hour for general manufacturing processes or other indicators of process activity should be stated.

Operating information The operational hours and consideration of any seasonal variations in activity should be stated.

Odour sources

The report should include odour emitting sources including area and stationary sources. A description of each source including what the source does should be included. Commentary should also be included if specific assumptions relating to management measures are required, for example equipment failure and or maintenance requirements.

Treatment and abatement of emissions

If proposed or required, the report should include details of odour control systems and essential operating information for these systems. This could include a description of the control system, with particular regard to any fugitive emission capture (e.g. hooding, ducting), treatment (for example, scrubbers, bag filters) and discharge systems (for example, stacks). Any performance guarantees or other information regarding the performance of the systems which the report relies upon should be included.

9238

9239 All potential sources of odour, including the source type (point, area, diffuse, passive, etc.),
9240 the physical and location features and dimensions and the emission characteristics of each
9241 identified source should be provided. There should be sufficient information provided to allow
9242 a reader to reconstruct the assessment or at least understand what occurs on site.

9243 8.2.5. Model selection and setup

9244 This section should present all of the information about model selection and its application.

9245 The section could be organised into subsections, each bearing the elements described
9246 below.

9247 8.2.5.1. Dispersion model selection and assumptions

9248 This subsection shall include details of the modelling methodology, including reasons for the
9249 selection of the dispersion model. The section should identify any specific local, regional or
9250 national regulatory and/or best practice requirements. For example, in some countries, the
9251 Regulatory Authority may have a preferred or recommended model for specific
9252 assessments, which should be identified if relevant in the report. If the recommended model
9253 is not being used, the reasons for this choice and for selecting the model that has been
9254 applied should be explained.

9255 8.2.5.2. Dispersion model application

9256

9257 **Assessment scenarios**

9258 This section should report and describe the scenarios that are investigated. For example, a
 9259 study may consider specific sources of odour emissions at a facility, such as the wastewater
 9260 treatment plant or specific active sources, which could include a particular process at a site
 9261 which may only operate for a limited period each day.

9262 The section should describe what scenarios were assessed and the reasons for selecting
 9263 those scenarios.

9264 **Topographical and terrain data**

9265 This section should describe the topographical features of the site and the surrounding area
 9266 in terms of a description of data sources and/or graphical representations. The applicability
 9267 of the dispersion model should be discussed having regard to the local terrain. The
 9268 subsection could include a review of the relevant information that may have been obtained
 9269 during site assessment (e.g., mapping, field surveys, odour sampling) to generate data
 9270 presented through topographical maps, aerial photographs, 3-dimensional contour plots, 2-
 9271 dimensional cross-sections between odour sources and receptors. GIS software can be a
 9272 useful tool to present this information especially where cadastral information is required to be
 9273 included.

9274 **Simulation Domain**

9275 This section should describe the position and extent of the computational domain, with the
 9276 identification and location of possible sensitive receptors inside, receptor grid location and
 9277 resolution. Justifications should be included for any receptors that are not included in the
 9278 assessment.

9279 The domain could be described in terms of its extent and coordinates, and/or graphically.

9280 **Meteorological Data**

9281 This subsection should describe the type and location of data sources for meteorology,
 9282 which can include data from meteorological stations or meteorological models.

9283 Justifications should be provided with regard to representative local data, any software used
 9284 for the processing of meteorological data, and the representative wind rose. Justifications
 9285 should be provided as to why the year(s) modelled are representative of meteorology in the
 9286 area.

9287 The meteorological data at the site should be fully described, including:

- 9288 ● description of the techniques used to prepare the meteorological data into a format
 9289 for use in the dispersion modelling;
- 9290 ● detailed discussion of the prevailing dispersion meteorology at the site. The report
 9291 should include wind rose diagrams and an analysis of wind speed, wind direction,
 9292 stability class, mixing height and ambient temperature. If rainfall or other parameters

- 9293 influence emissions, these should also be discussed; and
 9294 ● a description of the results of model switches and settings, quality assurance and
 9295 quality control checks on the meteorological data used in the dispersion modelling.

9296 It is important that the meteorological data are either a representative set of measurements
 9297 or that prognostic model results are validated against nearby weather station data. While not
 9298 always required, the input files can be provided as an annex to the report, or the report can
 9299 offer to make the input and outputs available for peer review if required.

9300 **Emission Data**

9301 This section should describe the characteristics of each emission source. A table of the
 9302 required input data to allow the emissions to be estimated construction and execution of the
 9303 dispersion model should be included.

9304 The emission inventory data should include the following information:

- 9305 ● A detailed discussion of the methodology used to calculate the expected odour
 9306 emission rates for each source with references to the source of the information and
 9307 the methodologies used for sampling and measurement;
- 9308 ● a table showing source release parameters (for example, temperature, exit velocity,
 9309 stack dimensions and emission rates);
- 9310 ● Subject to the source type, a summary that includes:
 - 9311 ○ the hours of operation of the facility,
 - 9312 ○ whether the process or activity is batch or continuous in nature,
 - 9313 ○ whether emissions vary as a function of process conditions (e.g temperature,
 9314 pressure etc.), production rate, the hour of the day, week, month or season,
 9315 meteorological variables (e.g. wind speed, ambient temperature, humidity,
 9316 atmospheric stability class and rainfall), feedstock, and animal age or feed
 9317 type.

9318

9319 **8.2.6. Presentation of the odour impact assessment results**

9320 Odour impact reports should, as a minimum, include odour contours with the applicable
 9321 criteria and also receptor concentrations predicted using discrete receptors. For figures, it is
 9322 preferable to include a caption that details the scenario, model used, criteria adopted,
 9323 averaging time, percentile and the author.

9324 The post-processing of relevant percentile values has to be reported, with the addition of the
 9325 local level of background odour concentration from other sources, when these
 9326 concentrations are required by local legislation. For example, in Germany, a maximum
 9327 allowable odour level of 2% of the background concentration is allowed for new activities
 9328 (TA-Luft, 2021).

9329 The results of odour dispersion modelling shall be interpreted using the necessary air quality
 9330 objectives or other relevant criteria, guidelines, and standards. The results should be
 9331 explained in a concise manner that can be easily understood by the reader. If the contours
 9332 are inconsistent with terrain information, the cause of this should be discussed. For example,
 9333 a tall stack that emits above a valley.

9334 Elements that could be included in a report are detailed in Table 8-4 below.

9335 **Table 8-4** Elements in reporting the results of odour dispersion modelling

General	Possible elements to report
	Supporting data for the input parameters and the factors affecting the variations
	A summary of receptor concentrations for each scenario
	Explanation of the accuracy and the limitations of the assessment (if relevant)
Presentation of Maps	Criteria
	Overlay the odour contours on a good quality base map.
	Clear perspective, scale, and content of the results, including sufficient contours to enable a reader to interpret the contours.
	Clear labels and/or legends
For Thematic Maps:	Present a clear legend that indicate the extent of odour pollution at various colour scale
For Isopleths Maps:	Appropriate number of concentration contours
Presentation of Tables	Criteria
	Key data in the report i.e. receptor concentration at specified averaging time and percentile
	Large datasets as appendix
Model Analysis and Interpretation	Criteria
	Locations of the high concentrations
	Consistency of high odour concentrations with meteorological conditions
	Robustness of the simulation with respect to important conditions, especially when using non-steady state meteorology
Estimation of model error and accuracy	Criteria
	Identify the reducible (input data and the model implementation) and inherent uncertainty (limitations of the selected model or approach)
Impact Assessment and Programs	Criteria

General	Possible elements to report
	Compliance with the relevant environmental standards
	The environmental and health impacts
	The mitigation measures for the identified impacts
	The different phases of the activities
	The documentations and other related reports

9336

9337

9338 In the following section, suggestions on the criteria to be adopted for the presentation of the
9339 results are provided.

9340 8.2.6.1. Odour impact assessment criteria - Data elaboration criteria

9341 As mentioned in Chapter 6, one way to quantitatively and qualitatively estimate an odour
9342 impact is by considering annoyance factors related to the *frequency*, *intensity*, *duration*,
9343 *offensiveness* of the odour emitted and the receptor's *sensitivity* (FIDOS).

9344 These factors usually lead to or are reflected in the definition of exposure limit values, a
9345 concept composed of the following aspects:

- 9346 ● **A limit concentration or threshold [C]: (intensity factor)** for different types of
9347 sources. Different limit concentrations are usually defined depending on their hedonic
9348 tone (offensive factor). Different limiting concentrations may also be defined for
9349 different land use types, such as industrial, commercial or residential (sensitivity
9350 factor).
- 9351 ● **A criterion of compliance with the limiting concentration over time** usually
9352 expressed as a percentile [p] (frequency factor). Different percentiles may be defined
9353 for different types of land use (sensitivity factor).
- 9354 ● **A criterion related to the average assessment time [t] (duration factor).**

9355 These three variables result in the following exposure limit values: C, p, t, where:

9356 **C: threshold concentration**, usually given in odour units [ou_E/m^3].

9357 **p: percentile of compliance.** For example, the 98th percentile means that the threshold
9358 concentration is met 98% of the time. That is, if the time is one year, this concentration is
9359 exceeded 175 hours per year.

9360 **t: assessment time**, typically between 0.1 s and 60 min. An average value for one hour is
9361 usually considered according to the possibilities offered by modelling tools.

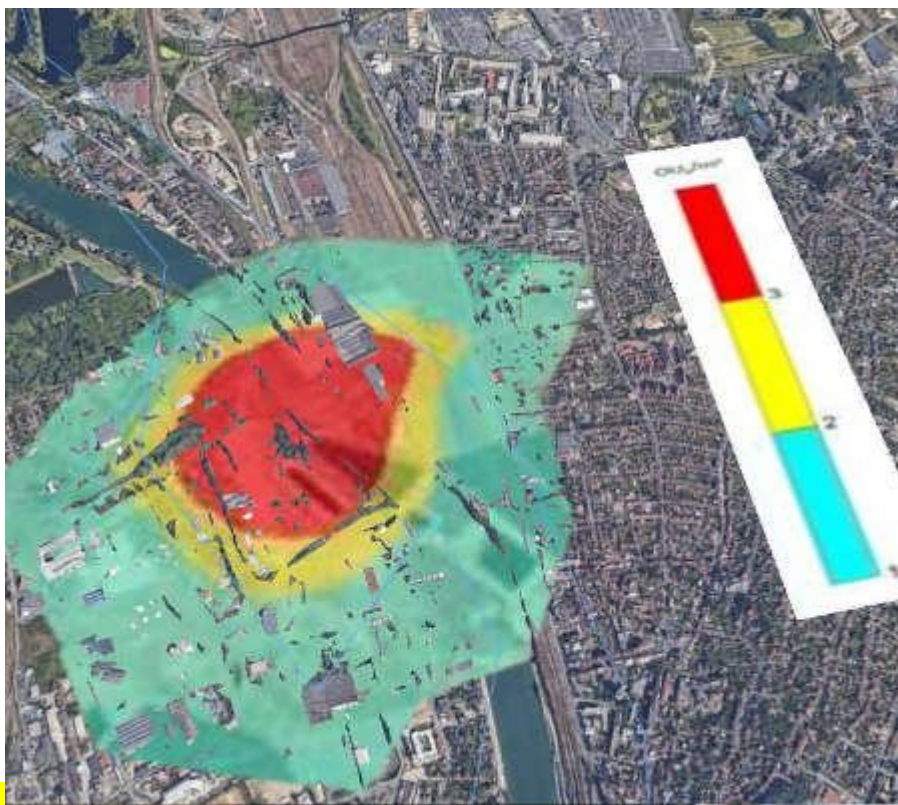
9362

9363 8.2.6.2. Criteria for odour exposure maps

9364 There are usually two ways of expressing odour exposure, by means of isopleths of
 9365 concentration and by using frequencies of perception.

9366 Approach 1) Quantification according to odour isoconcentration curves

9367 The modelling work allows the generation of graphs corresponding to maps that represent
 9368 the odour dispersion phenomenon associated with emission events and meteorological
 9369 conditions in the territorial context of the potential receptors (see Figure 8-1); these illustrate
 9370 lines that indicate the same odour concentration in the corresponding units (ou_E/m^3).



9371

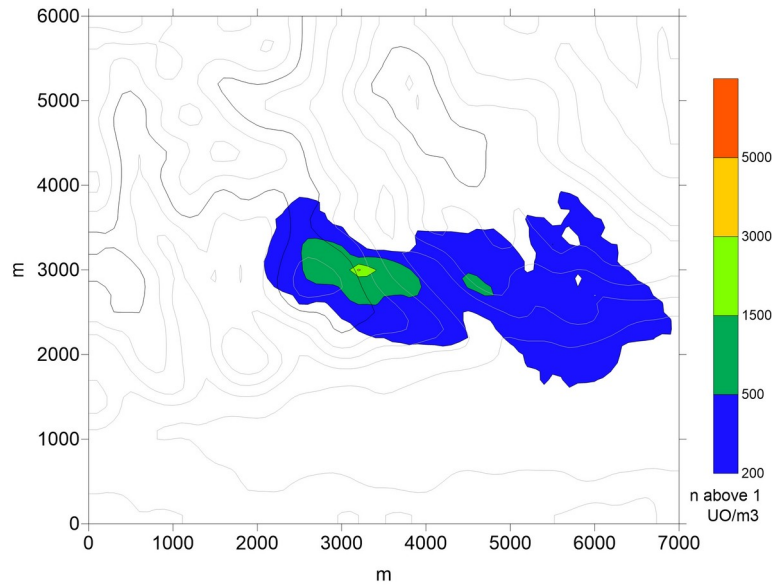
9372 **Figure 8-1** Representation of odour concentration isopleths for a 98th percentile (courtesy of
 9373 Ambiente et Odora)

9374 Approach 2) Quantification of odour perception frequency

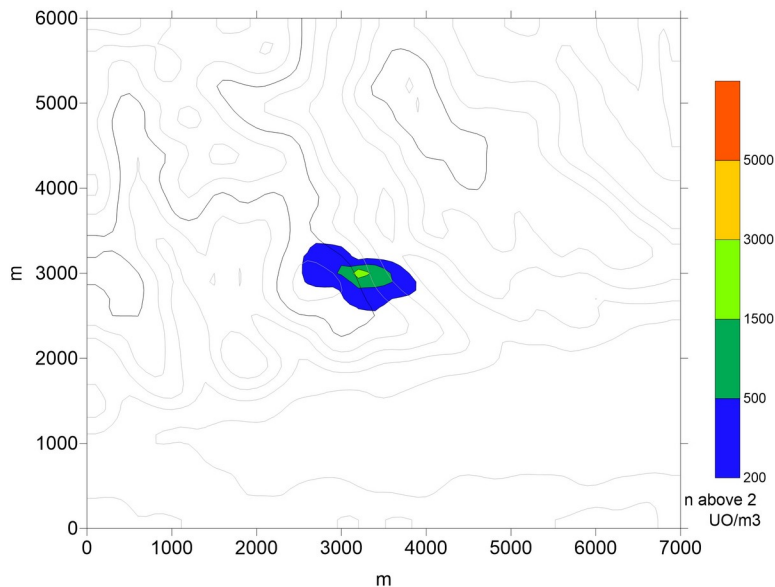
9375 Odour exposure is usually quantified in terms of the frequency of occurrence of hourly
 9376 average concentrations of a given odour above a defined threshold concentration.

9377 The criteria of maximum hourly impact, or worst-case condition, is not representative of the
 9378 total odour exposure at a receptor. A better approach is to use high percentiles, such as the
 9379 90th or 98th percentiles, at a specific odour concentration. This methodology allows
 9380 visualising the percentages of hours in which the value defined for 8,760 hours of a year is
 9381 exceeded. Figure 8-2 illustrates a graphical example.

9382



9383



9384

9385 **Figure 8-2** Example of representation of odour hourly frequencies, number of cases above 1
 9386 ou_E/m^3 (above) and above 2 ou_E/m^3 (below) during one year (courtesy of ARIANET)

9387 8.2.6.3. Criteria for quantification of odour exposure at receptors

9388 Deciding on the sensitive receptors that may be affected by odour impact is essential. In
 9389 some countries like Australia receptors are residences and workplaces. For example see
 9390 NSW EPA (2022) or DEHP (2021).

9391 There are two approaches to selecting the relevant receptors:

9392 **Approach 1)** Directly ask the potentially odour-impacting activity which receptors are the
 9393 most sensitive.

9394 **Approach 2)** Try to determine using an aerial photo, taking into account either the wind rose
 9395 or the outline of the odour isopleth contour, which receptors are the most relevant.

9396 The first approach is interesting because usually, the plant operators know where the odour
 9397 complaints come from. However, there is a risk that due to a conflict of interest, some

9398 receptors that may be relevant are not given to the modeller, so they do not appear in the
9399 report.

9400 Approach 2 is interesting because it allows an unbiased assessment of which receptors may
9401 be most exposed to odour impact. However, this methodology does not consider the
9402 sensitivity of the receptors, which is much better known by local people.

9403 Carrying out both approaches is suggested. The report should include a sentence describing
9404 which approach has been used by the modeller to select the different receptors.

9405 This handbook has defined the concepts of “receptor” and “sensitive receptors”. Both
9406 concepts, though related, are different.

9407 The *Institute of Air Quality Management* (IAQM) published in 2018 Guidance on the
9408 assessment of odour for planning. A series of matrices, similar to environmental impact
9409 matrices, are defined in this document to try to identify the most relevant sensitive receptors.
9410 However, this methodology has the same limitations as any impact matrix: it is subject to the
9411 personal judgement of the technician who prepares it and is therefore exposed to a usually
9412 high degree of subjectivity.

9413 In any case, it is advisable to set receptors in high-sensitivity areas. For example, the
9414 *Recommended Procedures for Air Quality Dispersion Modelling* recently published by the
9415 *Department of Environmental Quality of the State of Oregon* in 2022 recommends that
9416 discrete receptors should be placed in *sensitive areas such as schools or other child*
9417 *exposure areas*.

9418 The odour exposure at the receptors shall be indicated in a table; an example of a table is
9419 given below.

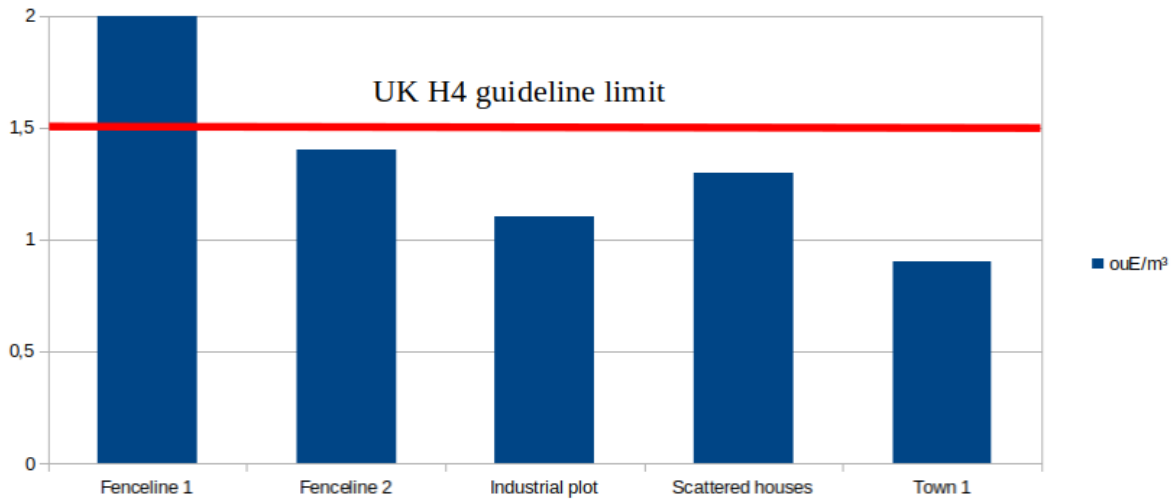
9420 **Table 8-5** Example of table with the location of receptors and odour concentrations
9421 calculated

Receptor	X UTM coordinate (m)	Y UTM coordinate (m)	Odour Concentration at P98 (ou _E /m ³)
Fenceline 1	250891	4239606	2.4
Fenceline 2	250892	4139448	1.4
Industrial plot	250890	4140006	1.1
Scattered houses	250893	4139880	1.3
Town 1	250891	4138769	0.9

9422 Unless a regulatory document states otherwise, the odour concentration in ambient air
9423 should only specify one decimal place when detailed at the receptors. Odour concentration
9424 in stacks and other emission sources should never contain decimals.

9425 Using tables helps indicate written values of odour concentration at receptors. However,
9426 when assessing compliance with a given odour impact criterion, using graphs can be more
9427 informative. An example is provided below in Figure 8-4.

9428



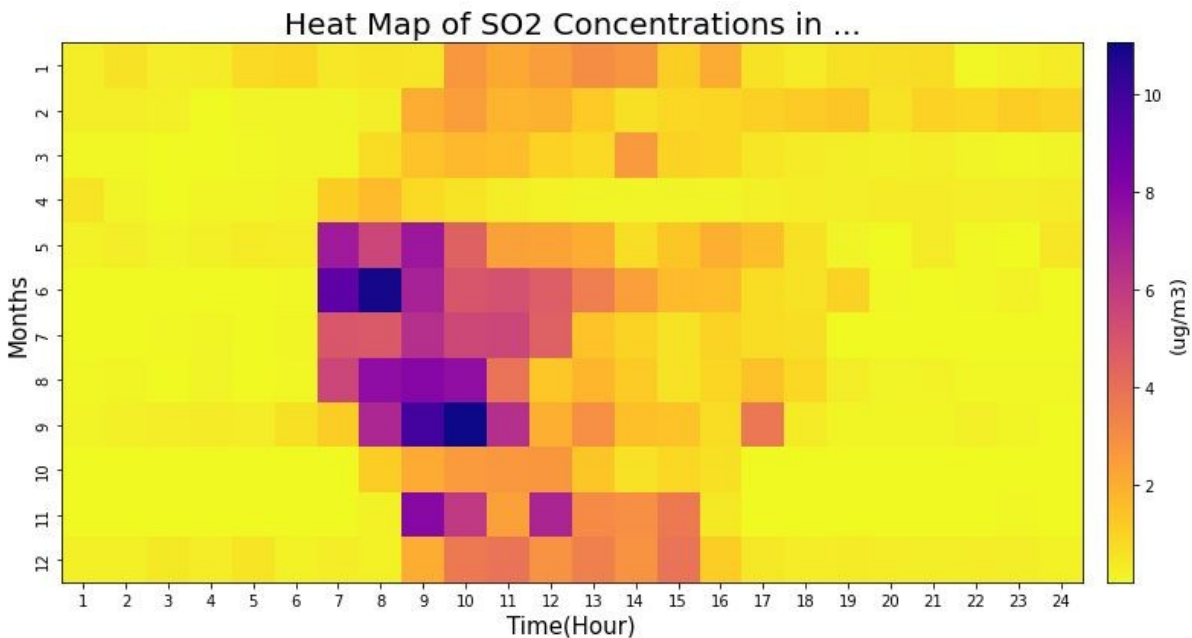
9429

9430 **Figure 8-3** Concentration at receptors and exposure criteria taken as reference (Courtesy of
 9431 Ambiente et Odora)

9432 There are other ways to express odour exposure at the receptors. For example, a graph
 9433 showing odour dose, such as the one in Chapter 7.5, could be adequate for intermittent
 9434 receptors.

9435 There are other ways to evaluate the impact on receptors. The following graph (Figure 8-4)
 9436 was carried out by plotting discrete receptor results using an AERMOD post-file with a one-
 9437 hour time interval during a year.

9438



9439

9440 **Figure 8-4** Hourly odorant SO₂ concentration of a year in a receptor close to an oil refinery.
 9441 (courtesy of José Junco, Epalife)

9442

9443 The graph above shows the months and hours of the year when the odorant impact is more
 9444 significant at a specific receptor.

9445 **8.3. References**

- 9446 EN 16841-1: 2017-03 Ambient air - Determination of odour in ambient air by using field
9447 inspection - Part 1: Grid method; German version EN 16841-1:2016.
- 9448 EN 16841-2: 2017-03 Ambient air - Determination of odour in ambient air by using field
9449 inspection - Part 2: Plume method; German version EN 16841-2:2016.
- 9450 DEHP (2021) Guideline: Odour Impact Assessment from Developments. Queensland
9451 Department of Environment and Heritage Protection, Brisbane.
- 9452 DWER, 2019: Odour emissions, Department of Water and Environmental Regulation
9453 (DWER), June 2019
- 9454 EPA NSW, State of New South Wales and the Environment Protection Authority. Approved
9455 Methods for the Modelling and Assessment of Air Pollutants in New South Wales, 2022,
9456 ISBN 978 1 922778 45 1
- 9457 Eusko Jaurlaritza 2012, Guidance on Good Practice Guide for the development of dispersion
9458 models, June 2012. Basque Government. Department of the Environment, Territorial
9459 Planning, Agriculture and Fisheries. Directorate of Environmental Planning
- 9460 IAQM, 2018 Guidance on the assessment of odour for planning, Institute of Air Quality
9461 Management (IAQM), 2018
- 9462 NZ ME, 2004. Ministry for the Environment. New Zealand, Good practice guide for
9463 atmospheric dispersion modelling, June 2004
- 9464
- 9465 Oregon 2022, Recommended Procedures for Air Quality Dispersion Modelling. March 2022.
9466 Air Quality Division Technical Services, Department of Environmental Quality, State of
9467 Oregon.
- 9468 SEA 2023, Guideline in the use of air quality models in the SEIA, Servicio de Evaluación
9469 Ambiental, Second Edition, Santiago, Chile, February 2023
- 9470 TA Luft. Technical Instructions on Air Pollution Control. 18 August 2021.
- 9471 UK EA 2021, UK Environment Agency and Department for Environment, Food & Rural
9472 Affairs. 2021. Environmental permitting: air dispersion modelling reports 1–8.
9473
- 9474

9475 Appendix A

9476 Note: All the URLs reported in this Appendix have been accessed on March 30, 2023

9477 **A. Raw meteorological data**

9478 Free meteorological data are made available in different countries, with different formats that
 9479 may require some processing to be used in dispersion models. The data listed below are
 9480 collected, managed and stored by different agencies or private citizens. Some quality control
 9481 operations are always suggested before using the data. The list is of course not complete,
 9482 because many other agencies may provide meteorological data, particularly at the local
 9483 level. Most of the links provided below refer to surface data (typically measured at 10 m
 9484 above ground level). The last two links refer to vertical profile data.

9485 **NOAA ISD (Integrated Surface Database)**

9486 Global hourly and synoptic observations compiled from numerous sources into a single
 9487 common ASCII format. Over 35,000 stations worldwide. Over 14,000 "active" stations are
 9488 updated daily. Data available since 1901 (few stations initially). Numerous parameters
 9489 included (e.g., wind speed and direction, wind gust, temperature, dew point, cloud data, sea
 9490 level pressure, altimeter setting, station pressure, present weather, visibility, precipitation
 9491 amounts for various time periods, snow depth, and other parameters). The WBAN/USAF
 9492 codes of the station(s) of interest must be known (see NOAA NCEI below).

9493 <https://www1.ncdc.noaa.gov/pub/data/noaa/>

9494 **NOAA ISD Lite**

9495 These data have been designed to be an easier-to-work-with subset of the larger ISD
 9496 dataset. They are represented with a modified timestamp which corresponds to the nearest
 9497 hour of actual observation. Sub-hourly observations present in the ISD have been removed.

9498 Each file contains eight meteorological variables represented in fixed-width format: Air
 9499 temperature (°C, multiplied by 10), Dew point temperature (°C, multiplied by 10), Sea level
 9500 pressure (hPa), Wind direction (degrees), Wind speed (m/s, multiplied by 10), Total cloud
 9501 cover (described by a code, see format documentation), One-hour accumulated liquid
 9502 precipitation (mm), Six-hour accumulated liquid precipitation (mm).

9503 <https://www1.ncdc.noaa.gov/pub/data/noaa/isd-lite/>

9504 **NOAA NCEI (National Centers for Environmental Information)**

9505 Meteorological data for the whole world. Stations can be graphically selected from a viewer,
 9506 then available data can be downloaded. This viewer is useful to identify the WBAN/USAF
 9507 codes for surface stations

9508 <https://www.ncei.noaa.gov/maps/hourly/>

9509 **SCRAM (Support Center for Regulatory Atmospheric Modelling) - USA**

9510 Available only for the USA and for the time interval 1984-1992. Useful for analysis of past
 9511 events. Available as .zip files containing *.dat ASCII files.

9512 <https://www.epa.gov/scram/scram-surface-meteorological-archived-data>

9513 **Iowa Environmental Mesonet (IEM)**

9514 Automated Surface/Weather Observing Systems (ASOS/AWOS) data for the whole world.

9515 http://mesonet.agron.iastate.edu/request/download.phtml?network=MN_ASOS

9516 **Meso West (USA)**

9517 Meteorological data measured in the USA. Directly downloadable from the web site. API
9518 service also available.

9519 <https://mesowest.utah.edu/>

9520 **Weather Underground**

9521 Thousands of stations are located around the world. Beware that many of these stations are
9522 managed by private citizens, therefore data must be critically checked before using in a
9523 dispersion model.

9524 <https://www.wunderground.com/wundermap>

9525 **ASOS 1-minute**

9526 Data consist of running 2-minute average winds, reported every minute. The maximum 5-
9527 second wind speed and the corresponding direction are also reported. Available from the
9528 year 2000 only for the USA.

9529 <https://www.ncei.noaa.gov/pub/data/asos-onemin/>

9530 **ASOS 5-minute**

9531 Wind data, cloud cover and other variables. Available from the year 2000 for the USA. The
9532 5-minute data consists of the 2-minute wind speeds reported every 5-minutes.

9533 <https://www.ncei.noaa.gov/pub/data/asos-fivemin/>

9534 **NDBC (National Data Buoy Center)**

9535 Measurements carried out by automatic buoys or by ships. Available for the current hour and
9536 for the past 12 hours. Both meteorological and waves-related variables are available.

9537 <https://www.ndbc.noaa.gov/>

9538 **GeoSphere Austria Data Hub (Austria)**

9539 National meteorological data for Austria. The data can be accessed freely via the web portal.

9540 <https://data.hub.zamg.ac.at/>

9541 **The Global Wind Atlas**

9542 The Global Wind Atlas is a free, web-based application with data to identify high-wind areas
9543 for wind power generation virtually anywhere in the world, and then perform preliminary
9544 calculations. The downloadable datasets are free. Users can also download high-resolution

9545 maps of the wind resource potential, for use in GIS tools, at the global, country, and first-
 9546 administrative unit (State/Province/etc.) level in the Download section. Information on the
 9547 datasets and methodology used to create the Global Wind Atlas can be found in the
 9548 Methodology and Datasets sections. The resource is also very useful for good graphical
 9549 representations of wind conditions in specific areas and has uses beyond the wind-energy
 9550 sector for which the tool was developed. Includes a link to the Global Solar Atlas where
 9551 information about solar irradiance is available.

9552 <https://globalwindatlas.info/en/about/introduction>

9553 **Online Environmental Data for State of Styria (Austria)**

9554 Meteorological data from stations operated by the Regional Government of Styria, Austria
 9555 plus elevation data can be downloaded freely here.

9556 <https://www.umwelt.steiermark.at/cms/ziel/2060750/DE/>

9557 **Chilean Meteorological Directorate - Climate Services (Chile)**

9558 Freely download one-minute data by month for automatic stations.

9559 <https://climatologia.meteochile.gob.cl/application/index/menuTematicoEmas>

9560 **China Meteorological Data Service Centre (China)**

9561 Fee-based service for surface and upper air station data throughout China.

9562 <https://data.cma.cn/en>

9563 **Copernicus Climate Data Store**

9564 This is a huge data repository operated by European Centre for Medium Range Weather
 9565 Forecast (ECMWF). Reanalysis data as well as land use and topographical data can be
 9566 obtained from this site. Must register for free to obtain access.

9567 <https://cds.climate.copernicus.eu#!/home>

9568 **MeteoNet (France)**

9569 MeteoNet is an open meteorological dataset created by METEO FRANCE, the French
 9570 national meteorological service. Their goal is to provide a clean and ready-to-use dataset for
 9571 Data Scientists who require weather data. The data spans over 3 years, 2016 to 2018, and
 9572 covers two geographical areas : the north-western and south-eastern quarters of France.

9573 <https://meteofrance.github.io/meteonet/english/data/summary/>

9574 **Climate Data Center - CDC (Germany)**

9575 The Climate Data Center of the German Meteorological Service (Deutscher Wetterdienst -
 9576 DWD) offers open access to a wide range of climate data.

9577 https://www.dwd.de/DE/klimaumwelt/cdc/cdc_node.html

9578 **Met Eireann (Ireland)**

9579 Met Eireann is the Irish Meteorological Service. Good datasets are available for a fee but

9580 the data has to be processed to a usable input format for dispersion models. There is also a
 9581 lot of free historical data for the various weather stations, including wind roses, rainfall,
 9582 temperature etc.

9583 <https://www.met.ie/>

9584 **Israel Meteorological Service - IMS (Israel)**

9585 Data for all of Israel may be obtained freely from this meteorological database. API service
 9586 available.

9587 https://ims.gov.il/en/data_gov

9588 **Yr.no (Norway)**

9589 Yr.no is a website and a mobile app for weather forecasting and dissemination of other types
 9590 of meteorological information hosted by the Norwegian Broadcasting Corporation in
 9591 collaboration with the Norwegian Meteorological Institute. Datasets are free but have to be
 9592 processed to get to usable data for dispersion modelling.

9593 <https://yr.no>

9594 **State Meteorological Agency (Spain)**

9595 In Spain, meteorological data generally is not free. A manual petition must be made to the
 9596 State Meteorological Agency (Agencia Estatal de Meteorología or AEMET). To get hourly
 9597 and sub hourly data from the 800 plus meteorological stations visit:

9598 <https://sede.aemet.gob.es/AEMET/es/GestionPeticones/nuevaSolicitud>

9599 **Open Data Euskadi - Basque Country (Spain)**

9600 In some other regions of Spain you may find free online meteorological data. For example,
 9601 here is data from the Euskadi region.

9602 <https://opendata.euskadi.eus/catalogo/-/estaciones-meteorologicas-lecturas-recogidas-en-2023/>
 9603

9604 **Agroclimatic Information Network of Andalusia - RIA (Spain)**

9605 The region of Andalusia offers free data from its 122 stations, but a manual petition is
 9606 required (no fee).

9607 https://www.juntadeandalucia.es/agriculturaypesca/ifapa/riaweb/web/inicio_estaciones

9608 **Agrometeorological service of Galicia (Spain)**

9609 Meteorological data for numerous stations in Galicia, Spain.

9610 http://servizos.meteogalicia.gal/agroMeteo/index.action?request_locale=es

9611 **Swedish Meteorological and Hydrological Institute (Sweden)**

9612 Here you may freely download meteorology, hydrology, and oceanographic data.
 9613 Meteorological observation station data includes hourly temperature, precipitation, wind, air
 9614 pressure, lightning, solar radiation, cloud cover and more.

9615 <https://www.smhi.se/data/meteorologi/ladda-ner-meteorologiska-observationer#param=airtemperatureInstant,stations=core>

9617 **Federal Office of Meteorology and Climatology MeteoSwiss (Switzerland)**

9618 SwissMetNet, the automatic measurement network of MeteoSwiss, comprises about 160
9619 automatic stations with a full measurement program. Data access is fee-based.

9620 <https://www.meteoswiss.admin.ch/weather/measurement-systems/land-based-stations/automatic-measurement-network.html>

9622 **ARPA Lombardia (Italy)**

9623 Meteorological data measured in Region Lombardy (Italy). They are delivered in your
9624 mailbox a few minutes after the request. They are easily-readable (CSV format) and
9625 available in different time-aggregations (daily, hourly, sub-hourly).

9626 <https://www.arpalombardia.it/Pages/Meteorologia/Richiesta-dati-misurati.aspx>

9627 **ARPA Emilia Romagna (Italy)**

9628 Meteorological data measured in Region Emilia Romagna (Italy). They are delivered in your
9629 mailbox a few minutes after the request. They are easily-readable (CSV, XLS, PDF formats)
9630 and available in different time-aggregations (daily, hourly, sub-hourly).

9631 <https://simc.arpae.it/dext3r/>

9632

9633 **ARPA Puglia (Italy)**

9634 Meteorological data measured in Region Puglia (Italy). Data available for selected years and
9635 stations in CSV format.

9636 <http://www.webgis.arpa.puglia.it/meteo/index.php>

9637 **Mareografico (Italy)**

9638 Meteorological data measured along the coastline of Italy.

9639 <https://www.mareografico.it/>

9640 **MeteoHub (Italy)**

9641 Meteorological observations coming from many regional networks plus forecast model data
9642 with spatial resolution up to 2.2 km distributed as open data. The download is available in
9643 BUFR and JSON format for observed data and in GRIB format for forecast data to registered
9644 users.

9645 <https://meteohub.mistralportal.it/app/datasets>

9646 **National Meteorological Service of Slovenia (Slovenia)**

9647 Meteorological data measured in Slovenia. Directly downloadable from the web site. Easily
9648 readable (CSV format). Available in different time-aggregations (daily, sub-hourly, more),

9649 hourly not available.

9650 <http://meteo.arso.gov.si/met/en/app/webmet/>

9651 **IGRA (Integrated Global Radiosonde Archive)**

9652 Radiosonde observations for standard, surface, tropopause, and significant pressure levels.
 9653 Over 2,700 stations worldwide. Over 1,000 "active" stations are updated daily. Data are
 9654 available since 1905 (only a few stations initially). Parameters include: pressure,
 9655 temperature, geopotential height, relative humidity, dew point, wind direction and speed,
 9656 elapsed time since launch.

9657 [https://www.ncdc.noaa.gov/data-access/weather-balloon/integrated-global-radiosonde-](https://www.ncdc.noaa.gov/data-access/weather-balloon/integrated-global-radiosonde-archive)
 9658 [archive](https://www.ncdc.noaa.gov/data-access/weather-balloon/integrated-global-radiosonde-archive)

9659 **RAOBS (NOAA/ESRL Radiosonde database)**

9660 The RAOBS site is an alternative to IGRA to get upper air meteorological data. It might be
 9661 used, for example, to download short time periods.

9662 <http://esrl.noaa.gov/raobs/>

9663

9664 **B. AERMOD-ready meteorological data**

9665 AERMOD is one of the preferred and recommended air quality dispersion models of the US
 9666 EPA. It is also widely used both in the US and in many countries of the world. The
 9667 preparation of reliable input meteorological data for AERMOD requires the use of other tools
 9668 (e.g., AERMET, AERSURFACE), the availability of raw meteorological data, and may be
 9669 time consuming. For all these reasons Table A.1 summarises many pre-processed
 9670 meteorological data prepared by regulatory agencies in the US and Canada. A link is
 9671 provided for each state or province. In some cases data can be directly downloaded from
 9672 the link, while in other cases they must be requested.

9673 **Table A.1.** USA States and Canadian Provinces that provide AERMOD-Ready
 9674 meteorological data

EPA Region / State	Air Agency Web Address	Availability
Region 1		
Connecticut	https://portal.ct.gov/DEEP/Air/Modeling/Dispersion	Download
Maine	https://www.maine.gov/dep/air/meteorology/metdata.html	Request
Massachusetts	https://www.mass.gov/how-to/air-quality-modeling-submittal-aq-mm	Request
New Hampshire	https://www.des.nh.gov/air/state-implementation-plans/modeling	Request
Rhode Island	https://dem.ri.gov/environmental-protection-bureau/air-resources/air-permits	No

EPA Region / State	Air Agency Web Address	Availability
Vermont	https://dec.vermont.gov/air-quality/permits/construction/impact-evaluation	Request
Region 2		
New Jersey	https://dep.nj.gov/boss/	Request
New York	https://www.dec.ny.gov/chemical/281.html	Request
Region 3		
Delaware	https://dnrec.alpha.delaware.gov/air/	No
District of Columbia	https://doee.dc.gov/air	No
Maryland	https://mde.maryland.gov/programs/Air/Pages/index.aspx	Request
Pennsylvania	https://www.dep.pa.gov/Business/Air/ARMDivision/Pages/default.aspx	No
Virginia	https://www.deq.virginia.gov/air/air-quality-monitoring-assessments/air-assessments	No
West Virginia	https://dep.wv.gov/daq/planning/Pages/AirModelingGroup.aspx	No
Region 4		
Alabama	https://adem.alabama.gov/programs/air/emissionsModeling.cnt	Request (fee)
Florida	https://floridadep.gov/air/air-business-planning/content/aermet-datasets-map	Download
Georgia	https://epd.georgia.gov/air-protection-branch-technical-guidance-0/air-quality-modeling/georgia-aermet-meteorological-data	Download
Kentucky	https://eec.ky.gov/Environmental-Protection/Air/Pages/Modeling%20and%20Meteorology.aspx	Download
Mississippi	https://www.mdeq.ms.gov/air/nsr-air-quality-modeling-2/met-data/	Download
North Carolina	https://deq.nc.gov/about/divisions/air-quality/air-quality-permits/modeling-meteorology/meteorological-data	Download
South Carolina	https://gis.dhec.sc.gov/aermod/ or https://scdhec.gov/environment/air-quality/air-dispersion-modeling-data	Download
Tennessee	https://www.tn.gov/environment/program-areas/apc-air-pollution-control-home/apc/air-quality-modeling.html	Request
Region 5		
Illinois	https://www2.illinois.gov/epa/topics/air-quality/Pages/default.aspx	Request

EPA Region / State	Air Agency Web Address	Availability
Indiana	https://www.in.gov/idem/airquality/modeling/	Download
Michigan	https://www.michigan.gov/egle/about/organization/air-quality/modeling-meteorology	Download
Minnesota	https://www.pca.state.mn.us/business-with-us/aermod-ready-meteorological-data	Download
Ohio	https://epa.ohio.gov/divisions-and-offices/air-pollution-control/reports-and-data/aermet-output-files-for-aermod-model-input	Download
Wisconsin	https://dnr.wisconsin.gov/topic/AirPermits/Modeling.html	Download
Region 6		
Arkansas	https://www.adeq.state.ar.us/air/permits/files.aspx	Download
Louisiana	https://deq.louisiana.gov/subhome/air	No
New Mexico	https://www.env.nm.gov/air-quality/modeling-publications/	Download
Oklahoma	https://www.deq.ok.gov/divisions/aqd/	Request
Texas	https://www.tceq.texas.gov/permitting/air/nav/datasets.html	Download
Region 7		
Iowa	https://www.iowadnr.gov/Environmental-Protection/Air-Quality/Modeling/Dispersion-Modeling	Download
Kansas	https://www.kdhe.ks.gov/333/Air-Permit-Modeling	Request
Missouri	https://dnr.mo.gov/air/business-industry/permit-modeling	No
Nebraska	http://dee.ne.gov/NDEQProg.nsf/AirHome.xsp	Request
Region 8		
Colorado	https://cdphe.colorado.gov/air-emissions/air-quality-modeling-guidance-for-permits	Request
Montana	https://deq.mt.gov/Air/	No
North Dakota	https://deq.nd.gov/AQ/Modeling/	No
South Dakota	https://danr.sd.gov/Environment/AirQuality/default.aspx	No
Utah	https://deq.utah.gov/air-quality/emissions-impact-assessment-guideline-preface	Download
Wyoming	https://deq.wyoming.gov/aqd/new-source-review/	Request
Region 9		
Arizona	https://www.azdeq.gov/node/2127	Download

EPA Region / State	Air Agency Web Address	Availability
California	https://ww2.arb.ca.gov/resources/documents/harp-aermod-meteorological-files	Download
Hawaii	https://health.hawaii.gov/cab/	Request
Nevada	https://ndep.nv.gov/air	Request
Region 10		
Alaska	https://dec.alaska.gov/air/air-permit/aermod-met-data/	Download
Idaho	https://www.deq.idaho.gov/permits/air-quality-permitting/	Request
Oregon	https://www.oregon.gov/deq/aq/cao/Pages/CAO-Risk-Assessment-Resources.aspx	Request
Washington	https://ecology.wa.gov/Air-Climate	No
Canadian Province		
Alberta	https://www.alberta.ca/meteorological-data-for-dispersion-models.aspx	Purchase
British Columbia	https://www2.gov.bc.ca/gov/content/environment/air-land-water/air/air-quality-management/modelling	No
Manitoba	https://www.gov.mb.ca/sd/environment_and_biodiversity/air_quality/air-emissions/index.html	No
New Brunswick	https://www2.gnb.ca/content/gnb/en/departments/elg/environment/content/air_quality.html	No
Newfoundland and Labrador	https://www.gov.nl.ca/ecc/env-protection/ics/	No
Northwest Territories	https://www.enr.gov.nt.ca/en/services/air-quality	No
Nova Scotia	https://novascotia.ca/nse/air/	No
Nunavut	https://www.gov.nu.ca/environment	No
Ontario	https://www.ontario.ca/page/map-regional-meteorological-and-terrain-data-air-dispersion-modelling	Download
Prince Edward Island	https://www.princeedwardisland.ca/en/information/environment-energy-and-climate-action/air-quality-permit	No
Quebec	https://www.environnement.gouv.qc.ca/air/criteres/index.htm	Download
Saskatchewan	https://environment-saskatchewan.hub.arcgis.com/datasets/aermod-input-file-download-by-location-explore?location=54.329076%2C-105.748273%2C6.20	Download
Yukon	https://yukon.ca/en/doing-business/permits-and-licensing/get-air-emissions-permit	No

9676 C. Geophysical data

9677 Geophysical data are important for using meteorological and dispersion models. The most
 9678 important variables are terrain elevation and land cover. Other variables, such as roughness
 9679 length, albedo and Bowen length may be determined from the land cover type. Typically
 9680 dispersion models have their own processors to manage these data. For example, AERMOD
 9681 manages elevation data through AERMAP and land cover data through AERSURFACE.
 9682 Similarly, the CALMET/CALPUFF system manages these data through the processors
 9683 TERREL, CTGPROC and MAKEGEO. Some geophysical data providers are listed in Table
 9684 A.2.

9685 **Table A.2. Geophysical data providers**
 9686
 9687

Web site	URL	Contents
Earth Explorer	https://earthexplorer.usgs.gov/	Terrain elevation, land cover and many other data. Requires a free account.
ESA/CCI ^[1]	http://maps.elie.ucl.ac.be/CCI/viewer/index.php	Land cover data at global level
MRLC ^[2]	https://www.mrlc.gov/viewer/	Land cover data for US
ESA Climate Data Dashboard	https://climate.esa.int/en/explore/access-climate-data/	Land cover and several climate data
CORINE Land Cover	https://land.copernicus.eu/pan-european/corine-land-cover	Land cover data for Europe
USGS National Map	https://apps.nationalmap.gov/	Terrain elevation and many other data for US
ALOS Global Digital Surface Model	https://www.eorc.jaxa.jp/ALOS/en/dataset/aw3d30/aw3d30_e.htm	Terrain elevation data (1 arc-second). Requires a free account.
National Lidar Dataset	https://en.wikipedia.org/wiki/National_Lidar_Dataset_(United_States)	Terrain elevation data for US
US Interagency Elevation Inventory	https://coast.noaa.gov/inventory/#	Terrain elevation data for US

CGIAR-CSI Consortium for Spatial Information	https://srtm.csi.cgiar.org/srtmdata/	Terrain elevation data
Vito	https://lcviewer.vito.be/download	Land cover
RCMRD GeoPortal	https://geoportal.rcmr.org/	Land cover for the Eastern and Southern Africa regions
Open Topography	https://portal.opentopography.org/dataCatalog	Terrain elevation data, tools, and software

9688

9689 D. Tools

9690 The following tools may be useful to manage the geophysical and meteorological data listed
9691 in the previous sections.

9692 Scripting and File Translation

9693 The most useful tools are probably scripting languages such as Perl (<https://www.perl.org/>)
9694 and Python (<https://www.python.org/>). They allow you to ingest a huge quantity of data and
9695 to process them as desired.

9696 GDAL (<https://gdal.org/>) is a translator library for raster and vector geospatial data formats.

9697 Some useful tools in R (<https://www.simularia.it/simulariatools/>). They are licensed as open
9698 source software and freely available on CRAN as R package or on GitHub at:
9699 (<https://github.com/Simularia/simulariatools>).

9700

9701 NCL (NCAR Command Language)

9702 An open source collection of scripts and tools for scientific data analysis. Supports NetCDF
9703 3/4, GRIB 1/2, HDF 4/5, HDF-EOS 2/5, shapefile, ASCII, binary.

9704 <https://www.ncl.ucar.edu/>

9705

9706 Metview

9707 Metview is a meteorological workstation application distributed by ECMWF that can take
9708 input data from a variety of sources, including: GRIB, BUFR, MARS (ECMWF's
9709 meteorological archive), ODB, ASCII, and NetCDF. Metview has excellent graphing
9710 capabilities.

9711 <https://confluence.ecmwf.int/display/METV/Metview>

9712

9713 **GIS Mapping Programs - Open Source**

9714 These are all free and open source geographic information systems which run under
 9715 Windows, Linux, or Mac OS/X. They allow users to load many layers of data and reproject
 9716 them as needed. Many plugins are available to carry out specific operations.

9717 **QGIS**

9718 <https://qgis.org/en/site/>

9719 **uDig**

9720 <http://udig.refrations.net/>

9721 **GeoDa**

9722 <http://udig.refrations.net/>

9723 **OrbisGIS**

9724 <http://orbisgis.org/>

9725 **SAGA - System for Automated Geoscientific Analyses**

9726 <https://saga-gis.sourceforge.io/en/index.html>

9727 **GRASS GIS**

9728 <https://grass.osgeo.org/Grass>

9729

9730 **Coordinate Converters**

9731 Many online tools are able to perform coordinate transformations, such as between geoids
 9732 or to/from UTM and Latitude-Longitude.

9733 <http://rcn.montana.edu/Resources/Converter.aspx>

9734 <https://mygeodata.cloud/cs2cs/>

9735 https://epsg.io/transform#s_srs=4326&t_srs=32616&x=-85.7284000&y=38.2546700

9736 <https://www.earthpoint.us/convert.aspx>

9737 <https://www.ngs.noaa.gov/NCAT/>

9738 <https://twcc.fr/en/#>

9739 **Grid Reference Finder (Ireland)**

9740 This site is a useful grid reference finder and co-ordinate inter-converter for Ireland. Datasets

9741 and access are free.

9742 <https://irish.gridreferencefinder.com/>

9743 And finally, here is one coordinate converter to download and run on a local computer

9744 <https://proj.org/about.html>

9745

9746 **Mapping Data and Viewers**

9747 **Copernicus Climate Data Store**

9748 A useful set of tools for plotting and analysing maps and data

9749 <https://cds.climate.copernicus.eu/cdsapp#!/toolbox>

9750 **Earth Data**

9751 A global multi-data source, requires free registration

9752 <https://www.earthdata.nasa.gov/>

9753 **Tailte Eireann (Ireland)**

9754 Tailte Eireann is a newly established Irish state agency which includes mapping and
9755 geodetic data for Ireland. There are fees payable for digital or paper mapping resources.

9756 <https://www.tailte.ie/>

9757 **The National Parks and Wildlife Service - NPWS (Ireland)**

9758 The NPWS mapping section offers a detailed mapping resource for ecologically sensitive
9759 sites in Ireland. Datasets are free.

9760 [https://dahg.maps.arcgis.com/apps/webappviewer/index.html?
9761 id=8f7060450de3485fa1c1085536d477ba](https://dahg.maps.arcgis.com/apps/webappviewer/index.html?id=8f7060450de3485fa1c1085536d477ba)

9762 **The Irish Environmental Protection Agency (Ireland)**

9763 The Irish Environmental Protection Agency mapping website presents a significant mapping
9764 resource for environmental professionals in Ireland. Datasets are free.

9765 <https://gis.epa.ie/EPAMaps/>

9766 **MICRODEM (download)**

9767 A useful mapping program to work with DEM, Land Cover, GeoPDF and other GIS data.

9768 <https://www.usna.edu/Users/oceano/pguth/website/microdem/microdem.htm>

9769

9770 **Wind Rose Generators**

9771 **cli-MATE**

9772 Multiple data type access, free account required

9773 <https://mrcc.purdue.edu/CLIMATE/>9774 **Iowa Environmental Mesonet (IEM)**9775 <https://mesonet.agron.iastate.edu/sites/locate.php>9776 **iWindsurf**

9777 Some simple wind data freely available, but more with a subscription

9778 <https://wx.iwindsurf.com/search/Victoria%20AU>9779 **Downloadable Excel wind rose generator**9780 [https://maps.cise.jmu.edu/public/wind/NewSBALPmapWebsite/Documents/](https://maps.cise.jmu.edu/public/wind/NewSBALPmapWebsite/Documents/WindRoseInstructions.pdf)9781 [WindRoseInstructions.pdf](https://maps.cise.jmu.edu/public/wind/NewSBALPmapWebsite/Documents/WindRoseInstructions.pdf)

9782

9783 **E. Prognostic Model Information**9784 The following are some of the more important meteorological models in use globally. Model
9785 information and numerical data are available from their webpages.9786 **North American Mesoscale Forecast System (NAM)**9787 Developed and operated by the U.S. National Centers For Environmental Prediction
9788 (NCEP).9789 <https://www.ncei.noaa.gov/products/weather-climate-models/north-american-mesoscale>9790 **Global Forecast System (GFS)**9791 Developed and operated by the U.S. National Centers For Environmental Prediction
9792 (NCEP).9793 <https://www.ncei.noaa.gov/products/weather-climate-models/global-forecast>

9794

9795 **Rapid Refresh (RAP)/Rapid Update Cycle (RUC)**9796 Developed and operated by the U.S. National Centers For Environmental Prediction
9797 (NCEP).9798 <https://www.ncei.noaa.gov/products/weather-climate-models/rapid-refresh-update>

9799

9800 **High Resolution Rapid Refresh (HRRR)**

9801 Developed and operated by the U.S. National Centers For Environmental Prediction

9802 (NCEP).

9803 <https://rapidrefresh.noaa.gov/hrrr/>

9804 **European Centre for Medium-Range Weather Forecasts - ECMWF (IFS)**

9805 Developed and operated by ECMWF.

9806 <https://www.ecmwf.int/en/forecasts/documentation-and-support/changes-ecmwf-model>

9807 **Consortium for Small-Scale Modelling (COSMO)**

9808 Developed and operated by Germany, Switzerland, Italy, Greece, Poland, Romania, Russia,
9809 and Israel.

9810 <https://www.cosmo-model.org/>

9811 **HARMONIE**

9812 Developed and operated by a consortium of meteorological institutes from Sweden, Norway,
9813 Denmark, Iceland, the Netherlands, Ireland, Spain, Estonia and Lithuania.

9814 <https://www.smhi.se/en/research/research-departments/climate-research-at-the-rossby-centre/harmonie-1.135580>

9816 **Unified Model (UM)**

9817 Developed and operated by Met Office UK.

9818 <https://www.metoffice.gov.uk/research/approach/modelling-systems/unified-model>

9819 **WRF Model**

9820 The WRF model was developed collaboratively by the National Center for Atmospheric
9821 Research (NCAR), the National Oceanic and Atmospheric Administration (represented by
9822 the National Centers for Environmental Prediction (NCEP) and the Earth System Research
9823 Laboratory), the U.S. Air Force, the Naval Research Laboratory, the University of Oklahoma,
9824 and the Federal Aviation Administration (FAA). It is operated by the University Corporation
9825 for Atmospheric Research (UCAR). WRF is the leading global numerical model, is in the
9826 public domain, and anyone may freely download the source code here:

9827 <https://www.mmm.ucar.edu/models/wrf>

9828 **WRF Portal**

9829 As indicated earlier in the Handbook, running the WRF model requires extensive computing
9830 resources (typically under Linux), thus the model is not realistically accessible for everyone.
9831 For those that do install and use the WRF model, the following portal is available to assist in
9832 program setup and execution:

9833 <https://esrl.noaa.gov/gsd/wrfportal/>

9834 **WRF Users Page**

9835 A Users Group has been established to facilitate an open exchange between users
9836 regarding questions and issues with the model:

9837 <https://www2.mmm.ucar.edu/wrf/users/>

9838 **Input Data to Initialise the WRF Model**

9839 **NCAR Research Data Archive**

9840 https://www2.mmm.ucar.edu/wrf/users/download/free_data.html

9841 **NOAA - NCEP Central Operations**

9842 <https://www.nco.ncep.noaa.gov/pmb/products/>

9843

9844 **Model Evaluation Tools**

9845 **The Atmospheric Model Evaluation Tool (AMET)**

9846 The AMET tool facilitates the evaluation of meteorological and air quality models. AMET is
 9847 designed to work with standard output formats of the Weather Research and Forecasting
 9848 (WRF) model (Dennis et al., 2010).

9849 <https://www.epa.gov/cmaq/atmospheric-model-evaluation-tool>

9850

9851 **MODEL EVALUATION TOOLS (MET)**

9852 MET is a highly-configurable, state-of-the-art suite of verification tools. It was developed by
 9853 the United States Air Force, the National Oceanic and Atmospheric Administration (NOAA),
 9854 and the National Center for Atmospheric Research (NCAR) using output from the Weather
 9855 Research and Forecasting (WRF) modelling system, but may be applied to the output of
 9856 other modelling systems as well.

9857 <https://dtcenter.org/community-code/model-evaluation-tools-met>

9858 **BOOT and ASTM Evaluation Procedures**

9859 The BOOT statistical model evaluation software package and a link to the ASTM procedure
 9860 are available from the website of The Initiative on Harmonisation within Atmospheric
 9861 Dispersion Modelling for Regulatory Purposes (HARMO). These two approaches to
 9862 statistical evaluation of models are discussed by Chang and Hanna (2004) and Olesen and
 9863 Chang (2010).

9864 <https://www.harmo.org/kit.php>

9865

9866 [1] CCI: Climate Change Initiative

9867 [2] MRLC: Multi Resolution Land Characteristics Consortium

9868